EMERGING
INFECTIOUS DISEASES®

Respiratory Infections

November 2020

EMERGING
INFECTIOUS DISEASES®

EDITOR-IN-CHIEF
D. Peter Drotman

On the Cover

John William Waterhouse (1849–1917), *A Tale from The Decameron,* **1916.** Oil on Canvas, 39.7 in x 62.5 in/101 cm x 159 cm. Lady Lever Art Gallery, National Museums, Liverpool.

Perspectives

Synopses

Research

Medscape
EDUCATION
ACTIVITY

2612

2777

EMERGING INFECTIOUS DISEASES®

Comment Letters

About the Cover

Etymologia

Online Report

Another Dimension

Research Letters

●DPDx

Diagnostic Assistance and Training in Laboratory Identification of Parasites

A free service of CDC available to laboratorians, pathologists, and other health professionals in the United States and abroad

Diagnosis from photographs of worms, histological sections, fecal, blood, and other specimen types

Expert diagnostic review

Formal diagnostic laboratory report

Submission of samples via secure file share

Visit the DPDx website for information on laboratory diagnosis, geographic distribution, clinical features, parasite life cycles, and training via Monthly Case Studies of parasitic diseases.

www.cdc.gov/dpdx
dpdx@cdc.gov

**U.S. Department of
Health and Human Services**
Centers for Disease
Control and Prevention

The Problem of Microbial Dark Matter in Neonatal Sepsis

Shamim A. Sinnar, Steven J. Schiff

Neonatal sepsis (NS) kills 750,000 infants every year. Effectively treating NS requires timely diagnosis and antimicrobial therapy matched to the causative pathogens, but most blood cultures for suspected NS do not recover a causative pathogen. We refer to these suspected but unidentified pathogens as microbial dark matter. Given these low culture recovery rates, many non–culture-based technologies are being explored to diagnose NS, including PCR, 16S amplicon sequencing, and whole metagenomic sequencing. However, few of these newer technologies are scalable or sustainable globally. To reduce worldwide deaths from NS, one possibility may be performing population-wide pathogen discovery. Because pathogen transmission patterns can vary across space and time, computational models can be built to predict the pathogens responsible for NS by region and season. This approach could help to optimally treat patients, decreasing deaths from NS and increasing antimicrobial stewardship until effective diagnostics that are scalable become available globally.

The term "microbial dark matter" refers to organisms that cannot easily be cultured under available laboratory conditions (*1*). The knowledge that microbial dark matter exists is not new; some of these organisms have been responsible for human infections throughout the history of microbiology. Indeed, Robert Koch himself recognized that the postulates he proposed to demonstrate causality between a microorganism and a disease were not fulfilled in several common diseases, including malaria and leprosy (*2*). One major reason was difficulty in cultivating the responsible organisms.

Difficult-to-isolate organisms continue to be responsible for serious human infections, such as leptospirosis, syphilis, and many others (*3,4*). In fact, organisms that cause even such relatively common and potentially deadly syndromes as neonatal sepsis (NS) often constitute microbial dark matter, not because they cannot in theory be cultured but because in actual cases of NS these organisms are rarely recovered and identified. Organisms that are known to commonly cause NS in some areas of the world include *Escherichia coli*, group B *Streptococcus*, *Klebsiella* spp., and *Staphylococcus aureus* (*5*). However, because in most cases of NS worldwide we do not identify the organisms involved, we often cannot determine optimal treatments for NS or design successful prevention strategies. This problem is compounded by the fact that the organisms known to be frequently associated with NS differ in different parts of the world (*5,6*).

The inability to properly diagnose or treat NS constitutes a substantial global health issue. NS affects ≈3 million neonates per year worldwide (*7*) and causes ≈750,000 deaths per year worldwide; rates of death are highest in sub-Saharan Africa (*8*). Children who do survive are at risk for deadly or debilitating sequelae, such as cerebral palsy, seizures, cognitive delays, respiratory disease (*9*), and postinfectious hydrocephalus (*10,11*). Thus, timely and effective treatment of NS is imperative to prevent death and reduce sequelae, but when the causative organisms cannot be determined, optimal medical management of NS is problematic.

Current State of Diagnosis in NS

Several studies illustrate the low organism recovery rates from NS cultures. One, a large retrospective study from the United Kingdom, found that the proportion of blood cultures positive for the putative pathogen in individual cases ranged from 0.8% at birth to 15% on day 7 of life (*12*). A recent study from rural Cambodia determined that only 2% of blood cultures from neonates were positive for a pathogen; 10% of those cultures—5 times as many—were positive for likely contaminants (*13*). Similarly, in the recent ANISA (Aetiology of Neonatal Infection in South Asia) study on the causes and incidence of community-acquired serious infections among young children in South Asia, in which blood cultures were obtained

Author affiliation: The Pennsylvania State University, University Park, Pennsylvania, USA

in a sterile manner from >4,800 infants with suspected bacterial infection, only 2.1% of cultures were true positives (*14*).

One reason for the low recovery rates is that, although blood cultures are the gold standard for discovering bacterial pathogens causing NS, their sensitivity can be extremely low (*15*). Blood culturing may fail to identify NS pathogens, in part because very low levels of bacteremia can cause symptoms in neonates (*9,16*), and in part because it is difficult to obtain sufficient blood for sensitive culture recovery from small neonates. Furthermore, even if the blood obtained does contain bacteria known to cause NS, these bacteria may not grow well in culture (*17*). In addition, nonbacterial pathogens that do not grow in common culture media can cause NS symptoms; these include viruses such as enteroviruses, rhinoviruses, and coronaviruses (*18,19*), fungi such as *Candida* sp. (*19*), and parasites such as *Plasmodium*, the agent responsible for malaria (*20*). Finally, any antimicrobial treatment administered before blood is collected further reduces the chances of recovering pathogens using culturing techniques (*15*).

This inability to identify pathogens in many cases has serious clinical implications. For most NS cases, clinicians must balance the opposing risks of undertreating a serious bacterial infection or using broad-spectrum antimicrobial drugs that may be unnecessary in many cases. Use of narrow-spectrum antimicrobial drugs without knowing the organisms responsible increases the risk of providing ineffective therapy, which is associated with increased risk for death, infectious complications, and treatment failure (*21*). On the other hand, routinely using broad-spectrum antimicrobial drugs when pathogens cannot be identified can drive antimicrobial resistance (*22*), which runs increasingly high in underresourced areas of the world (*23*). Antimicrobial stewardship is especially important in these communities due to limited access to the newer antimicrobial drugs needed to treat multidrug-resistant bacterial infections (*24,25*).

Moreover, because the epidemiology of NS varies worldwide (*6*), treatment decisions in a particular geographic location cannot be made simply on the basis of the pathogens recovered in other settings. For example, although group B *Streptococcus* is a leading cause of NS in Europe and North America, it does not seem to be a dominant cause of NS in many other regions of the world (*26*). Furthermore, recommendations that culture-negative NS be treated with short courses of narrow spectrum antimicrobials may not be appropriate for the low-resource settings where most NS cases occur (*5,22*).

Another issue complicating diagnosis and treatment is that NS can sometimes have polymicrobial causes (*27–29*). Polymicrobial infections tend to be more severe and harder to treat than monomicrobial infections (*27,30*). The true rate of polymicrobial NS might be higher than that reported in the studies cited because 1 organism may outcompete the others in culture and because of the detection difficulties detailed. This failure to identify all of the causal organisms may further contribute to inadequate treatment.

Limitations of Emerging Technologies for Detecting Pathogens

Because of the low recovery rate of cultures (*15*), there has been intense interest in developing alternative methods for diagnosing febrile illnesses, including NS (*9*). In theory, some of these newer technologies could be used to more effectively diagnose the causes of NS when a bacterial culture fails to yield results; that is, they could help to address the problem of microbial dark matter in NS diagnosis. All of these methods, however, have critical drawbacks.

One group of methods relies on targeted PCR to amplify and detect the DNA or RNA of specific organisms from body fluids such as blood or cerebrospinal fluid (CSF) (*31*). However, PCR-based assays can only detect the specific organisms that are targeted by the assay; thus, one cannot discover pathogens that were not expected a priori. This method would be most beneficial when the epidemiology of NS is already well-established for a particular population. A similar principle applies for detecting antimicrobial resistance genes; PCRs can uncover only the resistance genes that they are targeted to detect. Moreover, given that there are now thousands of known antimicrobial resistance genes, it would be very difficult to test for all of these genes individually using PCR, and it remains a challenge for qPCR. Furthermore, novel mutations conferring antimicrobial resistance would still be missed.

Another approach is 16S amplicon sequencing using PCR to amplify the common 16S ribosomal gene shared by all bacteria. DNA sequencing of this PCR product is then used to identify the specific bacteria (*32*). 16S amplicon techniques can, in theory, uncover bacterial pathogens in an unbiased manner. However, contamination from clinical collection, laboratory reagents, or the laboratory environment can dominate the sequencing results if pathogen sequences in the patient sample are present in very low concentrations (*31*), which is often the case in NS. Bacterial DNA can be present in minute quantities and therefore difficult to detect within the much

greater mass of contaminant bacterial DNA acquired during routine sequencing workflows (*32*).

Methods have been developed to remove some of this contamination, either during the sample preparation process before amplification and sequencing occur (*33,34*) or during the computational analysis after sequencing (*35*). In either case, suitable negative and positive controls are crucial for accurate analysis because blood from apparently healthy patients can harbor bacterial sequences (*36*). For NS studies, healthy NS-negative infants from similar environments would be ideal clinical controls, but blood and CSF from healthy infants are rarely sampled. Another control option would be age-matched infants whose blood and CSF samples were taken for reasons unrelated to NS, such as for elective surgery.

Yet another alternative for pathogen discovery is sequencing the bulk DNA or RNA, or both, contained in the sample. After filtering out the human DNA or RNA, remaining sequences can be analyzed to detect bacteria, viruses, fungi, and parasites (*37*). Some of these sequencing approaches include enrichment steps to increase the detection of viral sequences in an otherwise overwhelming background of host sequences (*38*). Sequencing total DNA and RNA is especially attractive for unbiased discovery of panmicrobial pathogens and can additionally detect polymicrobial infections. In theory, sequencing total DNA and RNA makes it possible to retrieve nucleic acid sequences from all pathogens, regardless of kingdom. Sequencing of total DNA can also detect antimicrobial resistance genes and therefore guide treatment (*39,40*). However, sequencing total DNA and RNA has its own challenges, including biases potentially being introduced during sample preparation and by inadequate depth of sequencing, as well as by the current absence of standardized software tools and pipelines for sequence analysis (*41,42*). In addition, issues with contamination and lack of suitable negative controls likewise apply to this method.

Although there are case reports of whole genome sequencing leading to actionable diagnosis in the face of negative blood cultures (*43,44*), these methods are not yet ready to be implemented in routine diagnostics. The more complex sequencing techniques, though effective in certain cases, remain research laboratory endeavors at the moment. Even if some of these sequencing-based assays could be incorporated into a diagnostic workflow, the high cost, technical optimization required, and bioinformatic and statistical expertise needed to analyze complex sequencing data currently make this technology impractical, even in high-resource settings. Therefore, unbiased pathogen discovery technology is at present neither scalable nor sustainable on a global level and remains difficult to implement effectively in the resource-poor countries where incidence and death from NS are highest.

Moving Forward in Neonatal Sepsis Diagnosis

Until lower-cost solutions can be disseminated, pathogen discovery requiring costly and sophisticated technology might need to be performed at research laboratories or specialized institutions remote from clinical centers, which means that discovery cannot be done effectively in real time. Therefore, reducing neonatal death worldwide from infections caused by microbial dark matter might require a paradigm shift.

Population-wide discovery of NS pathogens may be a way forward. Hundreds of blood or CSF samples with proper controls can be collected from regional treatment sites and analyzed by sophisticated sequencing methods at separate pathogen discovery centers. Population-wide results defining the probabilistic distributions of likely pathogens by location could then be used to inform the most effective treatment strategies, including antimicrobial choices, at the point of care. In other words, clinicians would better know which organisms would be the most likely to cause NS in their patient population and, therefore, which antimicrobials from their often limited choices would most effectively treat the NS. Such knowledge would increase clinicians' ability to optimize treatment and reduce illness and death from NS. We call this approach predictive personalized public health.

If pathogen transmission patterns were stable across time, discovering the organisms causing NS would only need to be done once. However, the pathogens responsible for NS may differ by season, akin to the seasonally varying distribution of pathogens responsible for diseases such as cholera, malaria, and melioidosis (*45–47*). Therefore, being able to predict the pathogens most likely responsible for NS, or any other syndromic disease, based on the season as well as the patient's geographic location would be ideal. Predictive computational models of the diseases in question could be developed to identify the most likely pathogens for a specific region at a specific time of year. Combined with data on a pathogen's resistance to specific antimicrobial drugs, this approach could optimize the use of broad- versus narrow-spectrum antimicrobial drugs to improve both treatment outcomes and antimicrobial stewardship.

The feasibility of initiating such an organism discovery and modeling approach has been recently

shown in Uganda. Over the past few decades, in thousands of cases of infant postinfectious hydrocephalus resulting from neonatal sepsis, CSF samples have failed to yield any positive cultures (*10*; S.J. Schiff, unpub. data). However, more recently, advanced genomic techniques were used to identify a difficult-to-culture novel bacterial strain, *Paenibacillus thiaminolyticus* Mbale (*48*), and demonstrate frequent co-infection with human herpesvirus 5 (cytomegalovirus) in many of these infants with postinfectious hydrocephalus (*49*). Spatial GPS data demonstrated that, compared to control cases, the bacterial infections were localized to the swampy regions north and south of the banks of Lake Kyoga (p<0.03), whereas the cytomegalovirus infections were distributed widely (*49*). The statistically significant spatial discrimination of infection locations by GPS demonstrated in these cases, combined with an established association of rainfall with infant postinfectious hydrocephalus in Uganda (*50*), highlights the substantial potential for predictive models to optimize point-of-care treatment.

In conclusion, for syndromic illnesses such as NS that are not linked to a specific pathogen, effective diagnostics to identify microbial dark matter and guide treatment are urgently needed. However, until point-of-care molecular diagnostics can be sustainably implemented in regions of the world with the greatest disease burden, alternative predictive treatment models such as the one we described may help to reduce illness and death.

About the Authors

Dr. Sinnar is an assistant professor in the Department of Medicine at The Pennsylvania State University. Her research focuses on the diagnostics, epidemiology, and immunology of infant hydrocephalus and neonatal sepsis.

Dr. Schiff is Brush Chair Professor of Engineering and Professor of Engineering Science and Mechanics, Neurosurgery, and Physics, and member of the Centers for Neural Engineering and Infectious Disease Dynamics at The Pennsylvania State University. His research interests include epilepsy, hydrocephalus, sustainable health engineering and global health.

References

1. Lok C. Mining the microbial dark matter. Nature. 2015;522:270–3. https://doi.org/10.1038/522270a
2. Evans AS. Causation and disease: the Henle-Koch postulates revisited. Yale J Biol Med. 1976;49:175–95.
3. Adler B, de la Peña Moctezuma A. *Leptospira* and leptospirosis. Vet Microbiol. 2010;140:287–96. https://doi.org/10.1016/j.vetmic.2009.03.012
4. Radolf JD, Deka RK, Anand A, Šmajs D, Norgard MV, Yang XF. *Treponema pallidum*, the syphilis spirochete: making a living as a stealth pathogen. Nat Rev Microbiol. 2016;14:744–59. https://doi.org/10.1038/nrmicro. 2016.141
5. Zea-Vera A, Ochoa TJ. Challenges in the diagnosis and management of neonatal sepsis. J Trop Pediatr. 2015;61:1–13. https://doi.org/10.1093/tropej/fmu079
6. Waters D, Jawad I, Ahmad A, Lukšić I, Nair H, Zgaga L, et al. Aetiology of community-acquired neonatal sepsis in low and middle income countries. J Glob Health. 2011;1:154–70.
7. Fleischmann-Struzek C, Goldfarb DM, Schlattmann P, Schlapbach LJ, Reinhart K, Kissoon N. The global burden of paediatric and neonatal sepsis: a systematic review. Lancet Respir Med. 2018;6:223–30. https://doi.org/10.1016/S2213-2600(18)30063-8
8. Ranjeva SL, Warf BC, Schiff SJ. Economic burden of neonatal sepsis in sub-Saharan Africa. BMJ Glob Health. 2018;3:e000347. https://doi.org/10.1136/bmjgh-2017-000347
9. Sinha M, Jupe J, Mack H, Coleman TP, Lawrence SM, Fraley SI. Emerging technologies for molecular diagnosis of sepsis. Clin Microbiol Rev. 2018;31:e00089-17. https://doi.org/10.1128/CMR.00089-17
10. Warf BC. Hydrocephalus in Uganda: the predominance of infectious origin and primary management with endoscopic third ventriculostomy. J Neurosurg. 2005;102(Suppl 1):1–15. https://doi.org/10.3171/ped.2005.102.1.0001
11. Dewan MC, Rattani A, Mekary R, Glancz LJ, Yunusa I, Baticulon RE, et al. Global hydrocephalus epidemiology and incidence: systematic review and meta-analysis. J Neurosurg. 2019;130:1065–79. https://doi.org/10.3171/2017.10.JNS17439
12. Blackburn RM, Muller-Pebody B, Planche T, Johnson A, Hopkins S, Sharland M, et al. Neonatal sepsis—many blood samples, few positive cultures: implications for improving antibiotic prescribing. Arch Dis Child Fetal Neonatal Ed. 2012;97:487–8. https://doi.org/10.1136/archdischild-2012-302261
13. Labuda SM, Te V, Var C, Iv Ek N, Seang S, Bazzano AN, et al. Neonatal sepsis epidemiology in a rural province in southeastern Cambodia, 2015–2017. Am J Trop Med Hyg. 2019;100:1566–8. https://doi.org/10.4269/ajtmh.18-0739
14. Saha SK, Schrag SJ, El Arifeen S, Mullany LC, Shahidul Islam M, Shang N, et al. Causes and incidence of community-acquired serious infections among young children in south Asia (ANISA): an observational cohort study. Lancet. 2018;392:145–59. https://doi.org/10.1016/S0140-6736(18)31127-9
15. Iroh Tam PY, Bendel CM. Diagnostics for neonatal sepsis: current approaches and future directions. Pediatr Res. 2017;82:574–83. https://doi.org/10.1038/pr.2017.134
16. Stranieri I, Kanunfre KA, Rodrigues JC, Yamamoto L, Nadaf MIV, Palmeira P, et al. Assessment and comparison of bacterial load levels determined by quantitative amplifications in blood culture-positive and negative neonatal sepsis. Rev Inst Med Trop São Paulo. 2018;60:e61. https://doi.org/10.1590/s1678-9946201860061

17. Schiff SJ, Kiwanuka J, Riggio G, Nguyen L, Mu K, Sproul E, et al. Separating putative pathogens from background contamination with principal orthogonal decomposition: evidence for *Leptospira* in the Ugandan neonatal septisome. Front Med (Lausanne). 2016;3:22. https://doi.org/10.3389/fmed.2016.00022

18. Ronchi A, Michelow IC, Chapin KC, Bliss JM, Pugni L, Mosca F, et al. Viral respiratory tract infections in the neonatal intensive care unit: the VIRIoN-I study. J Pediatr. 2014;165:690–6. https://doi.org/10.1016/j.jpeds.2014.05.054

19. Simonsen KA, Anderson-Berry AL, Delair SF, Davies HD. Early-onset neonatal sepsis. Clin Microbiol Rev. 2014;27:21–47. https://doi.org/10.1128/CMR.00031-13

20. Ekanem AD, Anah MU, Udo JJ. The prevalence of congenital malaria among neonates with suspected sepsis in Calabar, Nigeria. Trop Doct. 2008;38:73–6. https://doi.org/10.1258/td.2007.005274

21. Hsu J-F, Chu S-M, Huang Y-C, Lien R, Huang H-R, Lee C-W et al. Predictors of clinical and microbiological treatment failure in neonatal bloodstream infections. Clin Micro Infect. 2015;21:482.e9–17. https://doi.org/10.1016/j.cmi.2015.01.009

22. Klingenberg C, Kornelisse RF, Buonocore G, Maier RF, Stocker M. Culture-negative neonatal sepsis—at the crossroad between efficient sepsis care and antimicrobial stewardship. Front Pediatr. 2018;6:285. https://doi.org/10.3389/fped.2018.00285

23. Le Doare K, Bielicki J, Heath PT, Sharland M. Systematic review of antibiotic resistance rates among gram-negative bacteria in children with sepsis in resource-limited countries. J Pediatric Infect Dis Soc. 2015;4:11–20. https://doi.org/10.1093/jpids/piu014

24. Cox JA, Vlieghe E, Mendelson M, Wertheim H, Ndegwa L, Villegas MV, et al. Antibiotic stewardship in low- and middle-income countries: the same but different? Clin Microbiol Infect. 2017;23:812–8. https://doi.org/10.1016/j.cmi.2017.07.010

25. Laxminarayan R, Matsoso P, Pant S, Brower C, Røttingen J-A, Klugman K, et al. Access to effective antimicrobials: a worldwide challenge. Lancet. 2016;387:168–75. https://doi.org/10.1016/S0140-6736(15)00474-2

26. Madrid L, Seale AC, Kohli-Lynch M, Edmond KM, Lawn JE, Heath PT, et al. Infant group B streptococcal disease incidence and serotypes worldwide: systematic review and meta-analyses. Clin Infect Dis. 2017;65(suppl 2):S160–72. https://doi.org/10.1093/cid/cix656

27. Faix RG, Kovarik SM. Polymicrobial sepsis among intensive care nursery infants. J Perinatol. 1989;9:131–6.

28. Kumhar GD, Ramachandran V, Gupta P. Bacteriological analysis of blood culture isolates from neonates in a tertiary care hospital in India. J Health Popul Nutr. 2002:343–7.

29. Nizet V, Klein JO. Bacterial sepsis and meningitis. In: Remington JS, Klein JO, Wilson CB, Nizet V, Maldonado YA, editors. Infectious diseases of the fetus and newborn. 7th ed. Philadelphia: Elsevier Saunders; 2011. p. 222–75.

30. Pammi M, Zhong D, Johnson Y, Revell P, Versalovic J. Polymicrobial bloodstream infections in the neonatal intensive care unit are associated with increased mortality: a case-control study. BMC Infect Dis. 2014;14:390. https://doi.org/10.1186/1471-2334-14-390

31. Pammi M, Flores A, Leeflang M, Versalovic J. Molecular assays in the diagnosis of neonatal sepsis: a systematic review and meta-analysis. Pediatrics. 2011;128:e973–85. https://doi.org/10.1542/peds.2011-1208

32. Rutanga JP, Van Puyvelde S, Heroes A-S, Muvunyi CM, Jacobs J, Deborggraeve S. 16S metagenomics for diagnosis

33. Chang S-S, Hsu H-L, Cheng J-C, Tseng C-P. An efficient strategy for broad-range detection of low abundance bacteria without DNA decontamination of PCR reagents. PLoS One. 2011;6:e20303. https://doi.org/10.1371/journal.pone.0020303

34. Humphrey B, McLeod N, Turner C, Sutton JM, Dark PM, Warhurst G. Removal of contaminant DNA by combined UV-EMA treatment allows low copy number detection of clinically relevant bacteria using pan-bacterial real-time PCR. PLoS One. 2015;10:e0132954. https://doi.org/10.1371/journal.pone.0132954

35. Davis NM, Proctor DM, Holmes SP, Relman DA, Callahan BJ. Simple statistical identification and removal of contaminant sequences in marker-gene and metagenomics data. Microbiome. 2018;6:226. https://doi.org/10.1186/s40168-018-0605-2

36. Nikkari S, McLaughlin IJ, Bi W, Dodge DE, Relman DA. Does blood of healthy subjects contain bacterial ribosomal DNA? J Clin Microbiol. 2001;39:1956–9. https://doi.org/10.1128/JCM.39.5.1956-1959.2001

37. Lefterova MI, Suarez CJ, Banaei N, Pinsky BA. Next-generation sequencing for infectious disease diagnosis and management: a report of the Association for Molecular Pathology. J Mol Diagn. 2015;17:623–34. https://doi.org/10.1016/j.jmoldx.2015.07.004

38. Briese T, Kapoor A, Mishra N, Jain K, Kumar A, Jabado OJ, et al. Virome capture sequencing enables sensitive viral diagnosis and comprehensive virome analysis. MBio. 2015;6:e01491–15. https://doi.org/10.1128/mBio.01491-15

39. Arango-Argoty G, Garner E, Pruden A, Heath LS, Vikesland P, Zhang L. DeepARG: a deep learning approach for predicting antibiotic resistance genes from metagenomic data. Microbiome. 2018;6:23. https://doi.org/10.1186/s40168-018-0401-z

40. Bossé JT, Li Y, Rogers J, Fernandez Crespo R, Li Y, Chaudhuri RR, et al. on behalf of the BRaDP1T Consortium. Whole genome sequencing for surveillance of antimicrobial resistance in *Actinobacillus pleuropneumoniae*. Front Microbiol. 2017;8:311. https://doi.org/10.3389/fmicb.2017.00311

41. Byron SA, Van Keuren-Jensen KR, Engelthaler DM, Carpten JD, Craig DW. Translating RNA sequencing into clinical diagnostics: opportunities and challenges. Nat Rev Genet. 2016;17:257–71. https://doi.org/10.1038/nrg.2016.10

42. Conesa A, Madrigal P, Tarazona S, Gomez-Cabrero D, Cervera A, McPherson A, et al. A survey of best practices for RNA-seq data analysis. Genome Biol. 2016;17:13. https://doi.org/10.1186/s13059-016-0881-8

43. Wilson MR, Naccache SN, Samayoa E, Biagtan M, Bashir H, Yu G, et al. Actionable diagnosis of neuroleptospirosis by next-generation sequencing. N Engl J Med. 2014;370:2408–17. https://doi.org/10.1056/NEJMoa1401268

44. Wylie KM, Blanco-Guzman M, Wylie TN, Lawrence SJ, Ghobadi A, DiPersio JF, et al. High-throughput sequencing of cerebrospinal fluid for diagnosis of chronic *Propionibacterium acnes* meningitis in an allogeneic stem cell transplant recipient. Transpl Infect Dis. 2016;18:227–33. https://doi.org/10.1111/tid.12512

45. Rebaudet S, Sudre B, Faucher B, Piarroux R. Environmental determinants of cholera outbreaks in inland Africa: a systematic review of main transmission foci and propagation routes. J Infect Dis. 2013;208(suppl 1):S46–54. https://doi.org/10.1093/infdis/jit195

46. Reiner RC Jr, Geary M, Atkinson PM, Smith DL, Gething PW. Seasonality of *Plasmodium falciparum* transmission: a systematic review. Malar J. 2015;14:343. https://doi.org/10.1186/s12936-015-0849-2

47. Wiersinga WJ, Virk HS, Torres AG, Currie BJ, Peacock SJ, Dance DAB, et al. Melioidosis. Nat Rev Dis Primers. 2018;4:17107. https://doi.org/10.1038/nrdp.2017.107

48. Hehnly C, Zhang L, Paulson JN, Almeida M, von Bredow B, Wijetunge DS et al. Complete genome sequences of the human pathogen *Paenibacillus thiaminolyticus Mbale* and Type Strain *P. thiaminolyticus* NRRL B-4156. Micro Res Ann. 2020;9:e00181-20. https://doi.org/10.1128/MRA.00181-20

49. Paulson JN, Williams B, Hehnly C, Mishra N, Sinnar SA, Zhang L, et al. Paenibacillus infection with frequent viral coinfection contributes to postinfectious hydrocephalus in Ugandan infants. Sci Transl Med. 2020; 12:eaba0565.

50. Schiff SJ, Ranjeva SL, Sauer TD, Warf BC. Rainfall drives hydrocephalus in East Africa. J Neurosurg Pediatr. 2012;10:161–7. https://doi.org/10.3171/2012.5.PEDS11557

Address for correspondence: Shamim Sinnar, The University of Pennsylvania, 320 Millennium Science Complex, University Park, PA 16802, USA; email: shamimsinnar@gmail.com

June 2020
Prions

- Identifying and Interrupting Superspreading Events—Implications for Control of Severe Acute Respiratory Syndrome Coronavirus 2

- Risks Related to Chikungunya Infections among European Union Travelers, 2012–2018

- Manifestations of Toxic Shock Syndrome in Children, Columbus, Ohio, USA, 2010–2017

- Genomic Epidemiology of 2015–2016 Zika Virus Outbreak in Cape Verde

- Epidemiologic Changes of Scrub Typhus in China, 1952–2016

- Pharmacologic Treatments and Supportive Care for Middle East Respiratory Syndrome

- Distribution of Streptococcal Pharyngitis and Acute Rheumatic Fever, Auckland, New Zealand, 2010–2016

- Temporary Fertility Decline after Large Rubella Outbreak, Japan

- Radical Change in Zoonotic Abilities of Atypical BSE Prion Strains as Evidenced by Crossing of Sheep Species Barrier in Transgenic Mice

- Characterization of Sporadic Creutzfeldt-Jakob Disease and History of Neurosurgery to Identify Potential Iatrogenic Cases

- Failures of 13-Valent Conjugated Pneumococcal Vaccine in Age-Appropriately Vaccinated Children 2–59 Months of Age, Spain

- Statin Use and Influenza Vaccine Effectiveness in Persons ≥ 65 Years of Age, Taiwan

- Increased Risk for Carbapenem-Resistant *Enterobacteriaceae* Colonization in Intensive Care Units after Hospitalization in Emergency Department

- Antimicrobial Resistance in *Salmonella enterica* Serovar Paratyphi B Variant Java in Poultry from Europe and Latin America

- Invasive Group B *Streptococcus* Infections in Adults, England, 2015–2016

- Zoonotic Alphaviruses in Fatal and Neurologic Infections in Wildlife and Nonequine Domestic Animals, South Africa

- Effectiveness and Tolerability of Oral Amoxicillin in Pregnant Women with Active Syphilis, Japan, 2010–2018

- Endemic Chromoblastomycosis Caused Predominantly by *Fonsecaea nubica*, Madagascar

- Emergence of New Non–Clonal Group 258 High-Risk Clones among *Klebsiella pneumoniae* Carbapenemase–Producing *K. pneumoniae* Isolates, France

- Zoonotic Vectorborne Pathogens and Ectoparasites of Dogs and Cats in Eastern and Southeast Asia

- Multihost Transmission of *Schistosoma mansoni* in Senegal, 2015–2018

- Estimating Risk for Death from Coronavirus Disease, China, January–February 2020

- Epidemiology of Coronavirus Disease in Gansu Province, China, 2020

- Severe Acute Respiratory Syndrome Coronavirus 2 from Patient with Coronavirus Disease, United States

- Syphilis in Maria Salviati (1499–1543), Wife of Giovanni de' Medici of the Black Bands

- Yaws Disease Caused by *Treponema pallidum* subspecies pertenue in Wild Chimpanzee, Guinea, 2019

- Fatal Encephalitis Caused by Cristoli Virus, an Emerging Orthobunyavirus, France

- Increased Community-Associated *Clostridioides difficile* Infections in Quebec, Canada, 2008–2015

- Melioidosis in a Resident of Texas with No Recent Travel History, United States

- No Adaptation of the Prion Strain in a Heterozygous Case of Variant Creutzfeldt-Jakob Disease

EMERGING INFECTIOUS DISEASES®

To revisit the June 2020 issue, go to:
https://wwwnc.cdc.gov/eid/articles/issue/26/6/table-of-contents

Two Pandemics, One Challenge— Leveraging Molecular Test Capacity of Tuberculosis Laboratories for Rapid COVID-19 Case-Finding

Susanne Homolka,[1] Laura Paulowski,[1] Sönke Andres, Doris Hillemann, Ruwen Jou,
Gunar Günther, Mareli Claassens, Martin Kuhns, Stefan Niemann, Florian P. Maurer

In many settings, the ongoing coronavirus disease (COVID-19) pandemic coincides with other major public health threats, in particular tuberculosis. Using tuberculosis (TB) molecular diagnostic infrastructure, which has substantially expanded worldwide in recent years, for COVID-19 case-finding might be warranted. We analyze the potential of using TB diagnostic and research infrastructures for severe acute respiratory syndrome coronavirus 2 (SARS-CoV-2) testing. We focused on quality control by adapting the 12 Quality System Essentials framework to the COVID-19 and TB context. We conclude that diagnostic infrastructures for TB can in principle be leveraged to scale-up SARS-CoV-2 testing, in particular in resource-poor settings. TB research infrastructures also can support sequencing of SARS-CoV-2 to study virus evolution and diversity globally. However, fundamental principles of quality management must be followed for both TB and SARS-CoV-2 testing to ensure valid results and to minimize biosafety hazards, and the continuity of TB diagnostic services must be guaranteed at all times.

Author affiliations: National and Supranational Reference Centre for Mycobacteria, Research Centre Borstel, Borstel, Germany (S. Homolka, L. Paulowski, S. Andres, D. Hillemann, M. Kuhns, S. Niemann, F.P. Maurer); Molecular and Experimental Mycobacteriology Unit, Research Centre Borstel, Borstel (S. Homolka, S. Niemann); Diagnostic Mycobacteriology Unit, Research Centre Borstel, Borstel (L. Paulowski, S. Andres, D. Hillemann, M. Kuhns, F.P. Maurer); National Reference Laboratory of Mycobacteriology, Centres for Disease Control, Ministry of Health and Welfare, Taipei, Taiwan (R. Jou); University of Namibia School of Medicine, Windhoek, Namibia (G. Günther, M. Claassens); Inselspital, Bern University Hospital, University of Bern, Bern, Switzerland (G. Günther); German Center for Infection Research, Research Centre Borstel, Borstel (S. Niemann); University Medical Centre Hamburg-Eppendorf, Hamburg, Germany (F.P. Maurer)

The ongoing coronavirus disease (COVID-19) pandemic presents a massive challenge for healthcare systems globally (*1,2*). Rapid case-finding and patient isolation are crucial to limit transmission and avoid exceeding capacity limits of critical healthcare infrastructures. Therefore, the World Health Organization (WHO) (*3*) strongly advocates a large and rapid increase of global testing capacities to detect severe acute respiratory syndrome coronavirus 2 (SARS-CoV-2) RNA (*2,4*). This task is enormous, in particular in resource-poor settings without widespread availability of microbiological laboratories and, even more so, specialized virologic laboratories. For example, although other outbreaks such as the 2014–2016 Ebola epidemic in West Africa triggered substantial investments into surveillance and preparedness, many hospitals, clinics, and laboratories in sub-Saharan Africa were already operating at maximum capacity before the COVID-19 pandemic (*5*). Consequently, the WHO Joint External Evaluation reports suggest that the ability to respond to an international health hazard, such as the importation of an infectious disease like COVID-19, requires almost universal laboratory improvement across sub-Saharan Africa (*6*).

With one quarter of the world's population infected with bacteria belonging to the *Mycobacterium tuberculosis* complex (MTBC), tuberculosis (TB) still represents a major global health threat (*7*). Substantial efforts have been made to scale-up highly sensitive and specific molecular diagnostic systems in high- and low-resource settings, which greatly improved TB care globally (*8*). Strategies included programmatic implementation of (near) point-of-care, easy-to-handle testing systems, such as the cartridge-based

GeneXpert (Cepheid, https://www.cepheid.com) platform (*8,9*). In addition, high-throughput PCR instruments are in use mostly at large central laboratories, in particular those also offering HIV and hepatitis viral load testing (*10*). Because TB diagnosistic infrastructures offer high spatial coverage, preexisting supply chains and clinical networks, staff trained to work with airborne pathogens, and the availability of analytical and biosafety equipment, leveraging the potential of these systems for SARS-CoV-2 testing is tempting. In fact, guidance has recently been issued by WHO (*11*) and the Stop TB Partnership (*7*). However, although rapid action is needed, we believe that quality must not be sacrificed for speed. We examined what efforts are needed to allocate molecular testing capacity to SARS-CoV-2 case-finding and research in laboratories usually dealing with TB and how the essentials of quality control apply in this context.

Establishing SARS-CoV-2 Testing Capacity for Routine Patient Care

We studied the availability of SARS-CoV-2 assays on analytical platforms commonly used in TB laboratories of different service levels, that is, at the point of care, at peripheral testing sites, at intermediate laboratories, and at central laboratories (Appendix Table 1, https://wwwnc.cdc.gov/EID/article/26/11/20-2602-App1.pdf) (*12*). It is evident that these approaches differ considerably with respect to setting, sample throughput, and hands-on time. For designing a SARS-CoV-2 testing strategy for a TB laboratory, we suggest considering 5 aspects: availability of hardware and consumables, expected throughput, distance between sampling sites and the laboratory, available personnel and their qualification levels, and pricing. For example, clearly a rapid testing response would ideally rely on existing instruments. In this regard, using GeneXpert instruments, which are available at many TB laboratories, is an obvious consideration. In addition, the Xpert Xpress SARS-CoV-2 testing cartridge, which has received US Food and Drug Administration (FDA) emergency use approval, is available through the Global Drug Facility of the Stop TB Partnership, albeit with a lead time of several months and at a price of $19.80 USD, which might still be too high to allow high-throughput testing (*13,14*). Also, in many district laboratories, single 4-slot GeneXpert instruments are used for TB diagnostics, which will easily be overwhelmed by a community screening program for SARS-CoV-2, putting at risk both COVID-19 and TB response. Moreover, although prior experience with GeneXpert is beneficial, additional training on interpretation of the Xpert SARS-CoV-2 assay results will be required. For example, unlike Xpert MTB/RIF, the Xpert SARS-CoV-2 assay might yield a presumptive positive result calling for a reflex testing algorithm made available for such cases. Furthermore, in some low-resource settings, PCR-based tests are still only available at central laboratories far away from primary or secondary healthcare facilities. These potential complications would increase turnaround time even with a relatively quick and easy test. Laboratories intending to offer SARS-CoV-2 testing must therefore thoroughly evaluate whether the available instruments will meet current and expected demands. This task is challenging because sample numbers might quickly increase, for example, because of the dynamics of the epidemic or through changes in testing policies, or decrease, for example, because of additional laboratory capacity becoming available elsewhere.

Similar considerations apply to staffing resources. Although in-house PCRs are comparably cheap and flexible because PCR chemistry of different manufacturers can be used, they are technically more demanding to perform than cartridge-based tests. Rigorous process control and higher operator skill levels are required to minimize cross-contamination, sample mixups, and PCR failures. In contrast, cartridge-based systems offer ease of use and rapid results at the cost of being dependent on a single manufacturer for reagent resupplies and instrument maintenance. Because countries have been bidding against each other for limited test reagents, low-resource countries with limited local funding might have concerns about their ability to procure enough tests. WHO, together with the United Nations and other international organizations, have recently set up a Global Supply Chain Task Force to secure SARS-CoV-2 tests produced by several manufacturers at negotiated prices for low- and middle-income countries (*3*).

Consideration of changing testing demands for TB during the ongoing SARS-CoV-2 pandemic also is important. For instance, at a national reference laboratory level, we experienced a decrease in samples sent for culture-based TB testing during the 12-week period of mid-March through mid-June, whereas requests for molecular TB testing increased. This pattern is likely because peripheral laboratories focused their own capacities on SARS-CoV-2 PCRs. Laboratory managers tasked to allocate workforce to SARS-CoV-2 testing need to consider potentially changing TB testing demands to guarantee the uninterrupted availability of TB diagnostic services at all times.

Biosafety and the 12 Quality System Essentials

Achieving, maintaining, and improving accuracy, timeliness and reliability of test results are key deliverables of diagnostic laboratories. As is the case for TB, late or false-negative SARS-CoV-2 test results will lead to delays in or even preclude correct diagnosis, jeopardizing timely isolation and prevention of transmission. In turn, false-positive tests will waste public health resources, will lead to incorrect epidemiologic data, and might even lead to patient stigmatization. Quality control is a cornerstone of safe, consistent, reliable diagnostics, and many studies and frameworks outline the structure of quality-management systems suitable for diagnostic laboratories (15–18).

We used the laboratory quality-management system guidance issued jointly by WHO, the US Centers for Disease Control and Prevention, and the Clinical and Laboratory Standards Institute to deduce critical interventions and management tasks required to expand the diagnostic workflow of TB laboratories to SARS-CoV-2 testing in a quality-controlled manner (18). Based on International Organization for Standardization document 15189 and Clinical and Laboratory Standards Institute document GP26-A3, the 12 Quality System Essentials approach is centered on 12 interlinked topics: organization, personnel, equipment, purchasing and inventory, process control, information management, documents and records, occurrence management, assessment, process improvement, stakeholder service, and facilities and safety. All 12 topics have practical implications relevant to the context of successfully implementing SARS-CoV-2 testing in TB laboratories (Appendix Table 2). When considering the 12 Quality System Essentials, we found that making the necessary changes to the analytical workflow is just one piece in the puzzle. In fact, several additional steps are needed, ranging from staff training (e.g., on sample collection for COVID-19 testing, which differs from coaching patients to produce sputum, and the definition and review of meaningful quality indicators) to participation in SARS-CoV-2 proficiency testing and anticipation of strategies for management of nonconformities. Furthermore, biosafety procedures will need to be carefully scrutinized, and staff instructions will need to be adapted in a concise, practical, and easy-to-understand manner. Procedures such as performing virus propagation, virus isolation, or neutralization assays should be performed only by competent personnel under Biosafety Level 3 conditions, ruling out such work at peripheral laboratories and in many resource-poor settings. WHO has summarized its biosafety recommendations for working with SARS-CoV-2 (19).

Using TB Infrastructure for Research on SARS-CoV-2

Although research requiring propagative work with SARS-CoV-2 will likely be beyond the scope of most dedicated TB laboratories, even when equipped with fully operational Biosafety Level 3 facilities, the TB community is strongly influenced by progress in next-generation sequencing (NGS), a technology that is also in heavy demand for research on SARS-CoV-2. Prime examples for the application of NGS in the TB field are the prediction of drug resistance from genome sequencing of clinical isolates (which can potentially also be performed directly from clinical samples), evolutionary studies looking into the adaptation of MTBC strains in response to antibiotic treatment, and the use of genome sequencing to trace local, regional, and national transmission or for cross-border molecular surveillance (8,20–23). Over the past few years, the potential of NGS technologies to replace time-consuming and complex-to-perform phenotypic techniques for resistance testing of MTBC isolates became more evident (21,24). Accordingly, WHO has released a technical guide on the use of NGS for the detection of resistance-associated mutations in MTBC strains (25), and some countries, such as the United Kingdom, have already shifted their TB diagnostic and surveillance approach to NGS, including substantial investments in hardware and bioinformatics infrastructure (26). In addition, NGS facilities are increasingly established in settings with high TB prevalence, including implementation of laboratory workflows with data analysis pipelines and quality-control procedures, in line with the 12 Quality System Essentials (18). In parallel to workflow and infrastructure set up, intensive training of technical and academic personnel is ongoing, for example, through a network dedicated to the application of sequencing technologies for the fight against resistant TB in high-incidence settings (SeqMDR TB_NET), which supports the implementation of NGS technologies in Kyrgyzstan, Moldova, Namibia, Mozambique, and Eswatini (https://ghpp.de/en/projects/seqmdrtb-net). These sequencing capacities, which are embedded in local and international clinical and epidemiologic research networks, are in principle suited to address urgent research questions related to the COVID-19 epidemic, such as establishing key epidemiologic, clinical, and virologic characteristics of the pathogen and, in particular, defining its ability to spread in humans. Several sequencing protocols, such the ARTICnetwork nCoV-2019 protocol (https://artic.network/ncov-2019), have been developed for NGS of SARS-CoV-2 (27). Virus sequencing

has been used early in the epidemic to understand the origin, spread, and evolution of SARS-CoV-2 in different regions of the world as well as for outbreak investigations (*28–31*). SARS-CoV-2 sequences are also collected by online tools that enable a prospective monitoring of the virus spread and evolution on the global level. For example, 4,397 genomes sampled during December 2019–August 2020 are archived in the GISAID online hCoV-19 database (https://www.gisaid.org/epiflu-applications/next-hcov-19-app). Virus sequencing will be crucial in the next phase of the COVID-19 pandemic for population-based surveillance and control of viral transmission (e.g., by allowing a precise understanding of the regional spread of the virus in relation to time, place, human migration, and other determinants) (*32*).

Another important aspect is the influence of coinfection with TB (and also with HIV) on the epidemiologic, clinical, virologic and immunological trajectory of COVID-19, and vice versa, in high-incidence settings as we observe the collision of 3 global pandemics with unpredicted outcomes. Moreover, with a renewed global focus on active case-finding in TB programs, resources dedicated for COVID-19 community-based research, such as household contact tracing or seroprevalence surveys, could easily be linked to programs to test for TB as well, providing a gateway for training, capacity building, and future TB research. However, as is the case for the capacity of TB diagnostic services, careful planning and close collaboration between the TB, HIV, and COVID-19 research communities will be crucial not to overburden these infrastructures, especially in resource-poor settings. In addition, strong political will and support for research communities are essential, especially in low- and middle-income settings, to advocate for and allocate resources needed to investigate these coinciding pandemics.

Conclusion

TB laboratories can be an important resource to increase the global capacity for SARS-CoV-2 diagnostic testing and research. However, expanding their scope to the detection of a viral pathogen warrants careful planning. Challenges will be different for peripheral, intermediate, and central-level laboratories and can relate to any of the 12 Quality System Essentials we have outlined. Despite the availability of SARS-CoV-2 assays on all major molecular TB testing systems, careful capacity planning is crucial to match the local demand, operator skills, and funding available. Mitigating the risk for supply chain interruptions is another key management task, and

establishing >1 SARS-CoV-2 test is advisable to guarantee service continuity. The diagnostic industry is challenged to manufacture SARS-CoV-2 tests without deprioritizing production of reagents needed to test for TB, HIV, and malaria. In addition, concerns exist about TB case-finding and culture-based diagnostics being impaired by the ongoing SARS-CoV-2 pandemic, as has been shown in a rapid assessment by the Stop TB Partnership (*33*). Likewise, a recent modeling analysis showed a 70% drop in the probability of TB diagnosis per visit to a healthcare provider because of reduced laboratory capacity and availability of healthcare staff secondary to the COVID-19 pandemic in countries such as India, Kenya, and Ukraine (*34*). Consequently, although leveraging the globally available TB diagnostic and research infrastructures is a powerful strategy to increase SARS-CoV-2 testing capacity and to elucidate some of the open research questions that have arisen during the ongoing SARS-CoV-2 pandemic, care must be taken that TB services are not disrupted at any time during the COVID-19 response.

discussion on tuberculosis and COVID-19 research. F.P.M., a clinical microbiologist and head of the Supranational Reference Laboratory, was responsible for the overall project design. S.H., L.P., S.N., and F.P.M. wrote the manuscript. All authors approved the final version of the manuscript.

About the Authors

Dr. Homolka is a senior postdoctoral scientist at Research Centre Borstel whose primary research interests include the analysis of the host–pathogen interaction in tuberculosis. Dr. Paulowski is a senior postdoctoral scientist at Research Centre Borstel whose primary research interests include diagnostic mycobacteriology and the development of optimized diagnostic workflows.

References

1. Gates B. Responding to Covid-19—a once-in-a-century pandemic? N Engl J Med. 2020;382:1677–9. https://doi.org/10.1056/NEJMp2003762
2. World Health Organization. Coronavirus disease 2019. 2020 [cited 2020 May 6]. https://www.who.int/emergencies/diseases/novel-coronavirus-2019
3. WHO Health Emergencies Programme. COVID-19 supply chain system: requesting and receiving supplies. Health emergencies preparedness and response 2020. 2020 [cited 2020 May 6]. https://www.who.int/publications/m/item/covid-19-supply-chain-system-requesting-and-receiving-supplies
4. World Health Organization. COVID-19 strategy update (as of 14 April 2020). Geneva: The Organization; 2020 [cited 2020 May 6]. https://apps.who.int/iris/handle/10665/332019
5. Kapata N, Ihekweazu C, Ntoumi F, Raji T, Chanda-Kapata P, Mwaba P, et al. Is Africa prepared for tackling the COVID-19 (SARS-CoV-2) epidemic. Lessons from past outbreaks, ongoing pan-African public health efforts, and implications for the future. Int J Infect Dis. 2020;93:233–6. https://doi.org/ 10.1016/j.ijid.2020.02.049
6. World Health Organization. WHO African Region: JEE mission reports. 2020 Jan 8 [cited 2020 May 6]. https://www.who.int/ihr/procedures/mission-reports-africa
7. Stop TB Partnership. Considerations for selection of SARS-CoV-2 diagnostics and potential multiplexing: a perspective to ensure continuity of care for people with TB. 2020 [cited 2020 Apr 15]. http://stoptb.org/assets/documents/covid/Considerations%20for%20selection%20of%20SARS-CoV-2%20diagnostics.pdf
8. Dheda K, Gumbo T, Maartens G, Dooley KE, Murray M, Furin J, et al.; Lancet Respiratory Medicine Drug-Resistant Tuberculosis Commission Group. The Lancet Respiratory Medicine Commission: 2019 update: epidemiology, pathogenesis, transmission, diagnosis, and management of multidrug-resistant and incurable tuberculosis. Lancet Respir Med. 2019;7:820–6. https://doi.org/10.1016/S2213-2600(19)30263-2
9. Cepheid. Cepheid | Xpert® Xpress SARS-CoV-2 has received FDA Emergency Use Authorization. 2020 [cited 2020 May 6]. https://www.cepheid.com/coronavirus
10. World Health Organization. Considerations for adoption and use of multidisease testing devices in integrated laboratory networks. Geneva: The Organization; 2017 [cited 2020 May 6]. https://apps.who.int/iris/handle/10665/255693
11. World Health Organization. Tuberculosis and COVID-19. COVID-19: considerations for tuberculosis (TB) care. Geneva: The Organization; 2020 [cited 2020 May 6]. https://www.who.int/docs/default-source/documents/tuberculosis/infonote-tb-covid-19.pdf
12. World Health Organization. Laboratory services in TB control, part I: organization and management. Geneva: The Organization; 1998 [cited 2020 May 6]. https://apps.who.int/iris/bitstream/handle/10665/65942/WHO_TB_98.258_(part1).pdf
13. Treatment Action Group. Fair pricing for Cepheid Xpert Tests (COVID-19, HIV, TB, HCV). 2020 Apr 3 [cited 2020 May 12]. https://www.treatmentactiongroup.org/webinar/fair-pricing-for-cepheid-xpert-tests-covid-19-hiv-tb-hcv
14. Stop TB Partnership. GDF diagnostics catalog. Geneva: United Nations Office for Project Services; 2020 [cited 2020 May 6]. http://www.stoptb.org/assets/documents/gdf/drugsupply/GDFDiagnosticsCatalog.pdf
15. International Organization for Standardization. Medical laboratories: requirements for quality and competence. Geneva: The Organization; 2012 [cited 2020 May 6]. https://www.iso.org/obp/ui/#iso:std:iso:15189:ed-3:v2:en
16. International Organization for Standardization. ISO/IEC 17043:2010. Conformity assessment—general requirements for proficiency testing. Geneva: The Organization; 2010 [cited 2020 May 6]. https://www.iso.org/standard/29366.html
17. Fonseca L, Domingues JP. ISO 9001: 2015 edition—management, quality and value. Int J Qual Res. 2017;1:149–58.
18. World Health Organization. Laboratory quality management system: handbook. Geneva: The Organization; 2011 [cited 2020 May 6]. https://www.who.int/ihr/publications/lqms
19. World Health Organization. Laboratory biosafety guidance related to coronavirus disease 2019 (COVID-19): interim guidance. Geneva: The Organization; 2020 [cited 2020 May 6]. https://apps.who.int/iris/rest/bitstreams/1277819/retrieve
20. Merker M, Barbier M, Cox H, Rasigade JP, Feuerriegel S, Kohl TA, et al. Compensatory evolution drives multidrug-resistant tuberculosis in Central Asia. eLife. 2018;7:7. https://doi.org/10.7554/eLife.38200
21. Meehan CJ, Goig GA, Kohl TA, Verboven L, Dippenaar A, Ezewudo M, et al. Whole genome sequencing of *Mycobacterium tuberculosis*: current standards and open issues. Nat Rev Microbiol. 2019;17:533–45. https://doi.org/10.1038/s41579-019-0214-5
22. Gröschel MI, Walker TM, van der Werf TS, Lange C, Niemann S, Merker M. Pathogen-based precision medicine for drug-resistant tuberculosis. PLoS Pathog. 2018;14:e1007297. https://doi.org/10.1371/journal.ppat.1007297
23. Diel R, Kohl TA, Maurer FP, Merker M, Meywald Walter K, Hannemann J, et al. Accuracy of whole-genome sequencing to determine recent tuberculosis transmission: an 11-year population-based study in Hamburg, Germany. Eur Respir J. 2019;54:1901154. https://doi.org/10.1183/13993003.01154-2019
24. Allix-Béguec C, Arandjelovic I, Bi L, Beckert P, Bonnet M, Bradley P, et al.; CRyPTIC Consortium and the 100,000 Genomes Project. CRyPTIC Consortium and the 100,000 Genomes Project. Prediction of susceptibility to first-line tuberculosis drugs by DNA sequencing. N Engl J Med. 2018;379:1403–15. https://doi.org/10.1056/NEJMoa1800474
25. World Health Organization. The use of next-generation sequencing technologies for the detection of mutations associated with drug resistance in *Mycobacterium*

tuberculosis complex: technical guide. Geneva: The Organization; 2018 [cited 2020 May 6]. https://apps.who.int/iris/handle/10665/274443

26. Public Health England. England world leaders in the use of whole genome sequencing to diagnose TB. London: Public Health England; 2017 [cited 2020 May 6]. https://www.gov.uk/government/news/england-world-leaders-in-the-use-of-whole-genome-sequencing-to-diagnose-tb

27. Xiao M, Liu X, Ji J, Li M, Li J, Yang L, et al. Multiple approaches for massively parallel sequencing of SARS-CoV-2 genomes directly from clinical samples. Genome Med. 2020;12:57. https://doi.org/10.1186/s13073-020-00751-4

28. Forster P, Forster L, Renfrew C, Forster M. Phylogenetic network analysis of SARS-CoV-2 genomes. Proc Natl Acad Sci U S A. 2020;117:9241–3. https://doi.org/10.1073/pnas.2004999117

29. Wu F, Zhao S, Yu B, Chen YM, Wang W, Song ZG, et al. A new coronavirus associated with human respiratory disease in China. Nature. 2020;579:265–9. https://doi.org/10.1038/s41586-020-2008-3

30. Walker A, Houwaart T, Wienemann T, Vasconcelos MK, Strelow D, Senff T, et al. Genetic structure of SARS-CoV-2 reflects clonal superspreading and multiple independent introduction events, North-Rhine Westphalia, Germany, February and March 2020. Euro Surveill. 2020;25:25. https://doi.org/10.2807/1560-7917.ES.2020.25.22.2000746

31. Khan S, Siddique R, Shereen MA, Ali A, Liu J, Bai Q, et al. Emergence of a novel coronavirus, severe acute respiratory syndrome coronavirus 2: biology and therapeutic options. J Clin Microbiol. 2020;58:e00187–20.

32. Harilal D, Ramaswamy S, Loney T, Al Suwaidi H, Khansaheb H, Alkhaja A, et al. SARS-CoV-2 whole genome amplification and sequencing for effective population-based surveillance and control of viral transmission. Clin Chem. 2020 Apr 23 [Epub ahead of print]. https://doi.org/10.1128/JCM.00187-20

33. Stop TB Partnership. We did a rapid assessment: the TB response is heavily impacted by the COVID-19 pandemic. 2020 [cited 2020 May 10]. http://www.stoptb.org/news/stories/2020/ns20_014.html

34. Stop TB Partnership. The potential impact of the covid-19 response on tuberculosis in high-burden countries: a modelling analysis. Geneva: United Nations Office for Project Services; 2020 [cited 2020 May 6]. http://www.stoptb.org/assets/documents/news/Modeling%20Report_1%20May%202020_FINAL.pdf

Address for correspondence: Florian P. Maurer, National and Supranational Reference Centre for Mycobacteria, Research Centre Borstel, Leibniz Lung Centre, Parkallee 18, 23845 Borstel, Germany; email: fmaurer@fz-borstel.de

Measuring Timeliness of Outbreak Response in the World Health Organization African Region, 2017–2019

Benido Impouma, Maroussia Roelens, George Sie Williams, Antoine Flahault, Claudia Torres Codeço, Fleury Moussana, Bridget Farham, Esther L. Hamblion, Franck Mboussou, Olivia Keiser

Large-scale protracted outbreaks can be prevented through early detection, notification, and rapid control. We assessed trends in timeliness of detecting and responding to outbreaks in the African Region reported to the World Health Organization during 2017–2019. We computed the median time to each outbreak milestone and assessed the rates of change over time using univariable and multivariable Cox proportional hazard regression analyses. We selected 296 outbreaks from 348 public reported health events and evaluated 184 for time to detection, 232 for time to notification, and 201 for time to end. Time to detection and end decreased over time, whereas time to notification increased. Multiple factors can account for these findings, including scaling up support to member states after the World Health Organization established its Health Emergencies Programme and support given to countries from donors and partners to strengthen their core capacities for meeting International Health Regulations.

The World Health Organization (WHO) African Region, encompassing 47 member states (*1*), carries one of the heaviest burdens of public health crises globally, including health emergencies due to disease outbreaks and humanitarian events that potentially pose international public health threats (*2–4*). More than 100 major public health events are reported annually in the region (*5*), which means these countries need to strengthen their capacities for early detection, notification, and response to mitigate their effect.

Author affiliations: World Health Organization Regional Office for Africa, Brazzaville, Congo (B. Impouma, G. Williams, F. Moussana, B. Farham, E.L. Hamblion, F. Mboussou); Institute of Global Health, University of Geneva, Switzerland (M. Roelens, A. Flahault, O. Keiser); Fundacao Oswaldo Cruz Ringgold Standard Institution, Rio de Janeiro, Brazil (C.T. Codeço)

These capacities are defined by the legally binding International Health Regulations 2005 (IHR 2005), which requires signatory member states "to prevent, protect against, control and provide a public health response to the international spread of disease" (*6*).

Using the response to the 2014–2016 Ebola virus disease outbreak in West Africa as a model, WHO established the WHO Health Emergencies (WHE) Programme in 2016 to help member states gain capacities to prevent, prepare for, detect, report on, respond to, and recover from public health emergencies (*7*). WHE provides technical support for member states to set up strong disease surveillance programs for detecting public health events early and to enhance capacities for responding rapidly, which has resulted in an increased number of events being detected and reported by member states (*8*).

Evaluating the performance of outbreak detection, notification, and control activities in the WHO African Region, as well as understanding the factors associated with changes in the timeliness of response over time, could provide key insights into factors that enable or inhibit effective outbreak response, and provide guidance for identifying or refining adapted interventions to improve performance. Metrics have been proposed for objectively and quantitatively evaluating this performance by systematically capturing and analyzing data on timeliness for reaching key milestones in outbreak detection and response (*9*).

For this study, we quantitatively assessed outbreak response in the African Region by measuring the timeliness and associated factors of reaching 3 milestones in outbreak response—detection, notification, and end—to determine if progress has been achieved since 2017 in the African Region. Our results provide a baseline metric for assessing progress

towards improved disease surveillance and outbreak response in the region.

Methods

We undertook a retrospective study of responses to all substantiated disease outbreaks reported to WHO by member states in the African Region during 2017–2019. Outbreaks were reported using the Integrated Disease Surveillance and Response (IDSR) strategy. A substantiated outbreak was defined as one whose hazard was confirmed or in which the occurrence of human cases was clearly in excess of normal expectancy; that is, the epidemic threshold was reached or surpassed. The substantiated disease outbreaks constituted a subset of all the public health events reported to WHO, which also encompasses humanitarian and other health emergencies.

The primary data source was the public health event database maintained by the WHE Programme at the Regional Office for Africa, which contains all formally reported public health events in the African Region including those verified through epidemic intelligence activities. Variables captured include country name, event name, etiology, date of onset, date of detection, date of notification to WHO, date of end of outbreak, and total number of cases and deaths, as well as a short description of events. Two additional variables were derived from the public health event database: each country reporting an outbreak was assigned to the Central, West, Eastern, or Southern African subregion on the basis of the WHO intercountry support team structure (10), and disease category was assigned on the basis of either similarity in mode of transmission, type of etiologic agent, or diseases requiring the same type of public health intervention (e.g., vaccination).

We used secondary sources to complete missing data, including the WHO event management system, IDSR weekly bulletins produced by member states in the African Region, outbreak investigation and situation reports submitted to WHO via email, published articles in peer-reviewed scientific journals, and the World Development Indicators database. The event management system is an online central repository for all globally reported events that may constitute a public health risk to countries through the international spread of disease or that may require a coordinated international response as required by IHR 2005 regulations (11). The World Development Indicators database is the World Bank's compilation of cross-country data on development, providing internationally comparable statistics on global development and the fight against poverty (12). We extracted data from

the database for 2017–2019 for selected variables that could influence our outcomes of interest (13): income level, population density, health expenditure as a percentage of gross domestic product, the percentage of internally displaced population, and the refugee population living in the countries in which the outbreaks occurred. We chose these predictor variables guided by available theoretical and empirical literature to determine how well our results agree with those of other published studies concerning these predictors and also to identify what is unique to the African Region.

Humanitarian emergencies and other public health events reported to WHO that did not constitute a disease outbreak were initially excluded because we could not estimate key milestone dates and their end dates did not necessarily depend on timely implementation of public health response given the context in which they occurred. Only substantiated disease outbreaks were selected for the study. Before analyzing the outcomes of interest, for each variable we discarded data from any outbreaks missing key milestone dates, while retaining data from that outbreak in other analyses that did not involve variables with missing data (14). We calculated the proportion of outbreaks sampled across each variable subcategory (e.g., by income level) and compared them with the proportion in all outbreaks to ensure representativeness and make inferences.

We adapted the definition of milestones used by Chan et al. (15). We chose 4 key dates from each outbreak to determine milestones for the analysis: dates of onset, detection, notification, and end of outbreak. For date of onset we used the reported date of symptom onset for the first case found by the investigators. For date of detection we used the date on which national authorities were alerted to the outbreak. For date of notification we used the date the event was first reported to WHO by a member state. For date of end we used either the date when a country declared an outbreak to have ended, or a defined length of time over which no new cases were reported. As a proxy, we used twice the maximum incubation period from the date of recovery or death for the last case. We chose this definition to ensure that disease transmission was no longer occurring and the outbreak was over.

We measured time to detection as the number of days between the dates of onset (first reported case) and detection, time to notification as the number of days between the dates of detection and notification, and time to end as the number of days between the dates of onset and end of the outbreak. A total of 29 events that began but had not ended during the study

period were right censored from the study on December 31, 2019.

We performed univariable and multivariable Cox proportional hazards regression analyses in 3 separate models to assess the rates of change over time to outbreak detection, notification, and end. Predictor variables were outbreak start year, WHO African subregion, income, number of refugees, percentage of internally displaced population, current health expenditure as percentage of gross domestic product, population density, and disease category. Each outbreak milestone was treated independently.

We computed the median time and interquartile range (IQR) for the time to reach each of the milestones for all the outbreaks included in the study, then stratified results by year of outbreak start, WHO Africa subregion (Central, West, Eastern, or Southern), and disease category (food/waterborne, vaccine-preventable, vectorborne, viral hemorrhagic fever, or others). We used the World Bank's classification of countries' economies (16) to stratify results by income level (low vs. middle and high). We used median values (i.e., in-country value for each variable compared with median value for that variable for all African Region countries) to stratify results by number of refugees (low or high), percentage of internally displaced population (low or high), current health expenditure as percentage of gross domestic product (low or high), and population density (low or high). The results are indicated as hazard ratios (HR) with 95% CIs. An HR >1 indicates improvement in the time to each of the milestones, whereas an HR <1 signals a regression in the time to each milestone. R version 3.5.2 (https://www.r-project.org) was used for statistical analysis and ESRI ArcGIS Desktop 10.6.1 (https://desktop.arcgis.com) for mapping of outbreaks included in our study.

Results

Of the 348 substantiated public health events reported to WHO in the African Region from 2017 to 2019, we selected 296 disease outbreaks for the study. Key milestone dates were often missing, and therefore we only included 184 (62%) events for time to detection, 232 (78%) events for time to notification, and 201 (68%) events for time to end (Figure 1). The percentage of events included in the study for each outcome of interest slightly decreased from 2017 through 2019, after exclusion of outbreaks with missing data, across each year (Tables 1, 2).

Events meeting our selection criteria occurred in 41 out of 47 WHO member states in the African
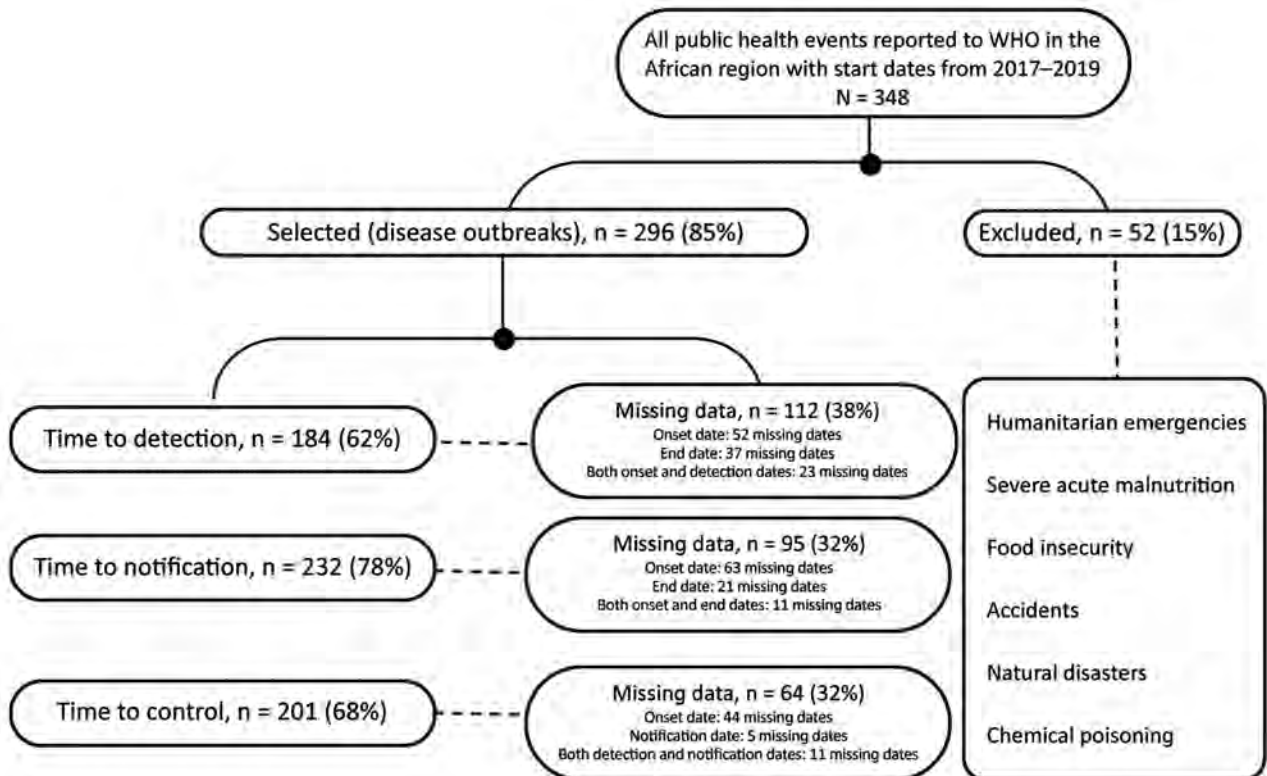
Figure 1. Exclusion criteria used to select subset of substantiated disease outbreaks reported to the WHO African Region, 2017–2019. WHO, World Health Organization.

Table 1. Median time to progression for 3 outbreak milestones (detection, notification, and end) by predictor variables, WHO African Region, 2017–2019*

Categories	Total no.†	Time to detection (*15*)		Time to notification (*15*)		Time to end (*15*)	
		No. (%)‡	Median (IQR)	No. (%)‡	Median (IQR)	No. (%)‡	Median (IQR)
Income (*16*)							
Low	156	107 (68.6)	9 (2–27)	127 (81.4)	3 (0–8)	109 (53.2)	86 (37–169)
Middle and high	140	77 (55.0)	8 (2–29)	105 (75.0)	2 (0–8)	92 (44.9)	54 (24–155)
WHO subregion (*10*)							
Eastern/Southern	133	78 (58.6)	6 (1–23)	96 (72.2)	3 (0–9)	96 (46.8)	70 (30–148)
Western	102	74 (72.5)	10 (5–28)	88 (86.3)	2 (0–6)	37 (18.0)	68 (29–158)
Central	61	32 (52.5)	16 (3–33)	48 (78.7)	2 (0–9)	68 (33.2)	136 (50–221)
Outbreak start date§ (*15*)							
2017	103	75 (72.8)	14 (6–37)	87 (84.5)	1 (0–5)	62 (30.2)	131 (67–237)
2018	101	62 (61.4)	7 (1–27)	83 (82.2)	3 (0–14)	72 (35.1)	67 (25–144)
2019	87	47 (54.0)	4 (1–11)	62 (71.3)	4 (1–9)	67 (32.7)	45 (22–90)
No. refugees from elsewhere (*13*)							
Low¶	199	129 (64.8)	8 (3–28)	160 (80.4)	2 (0–8)	133 (64.9)	69 (25–166)
High¶	97	55 (56.7)	8 (1–28)	72 (74.2)	3 (0–9)	68 (33.2)	84 (43–147)
IDP, % population (*13*)							
Low¶	212	139 (65.6)	7 (2–23)	170 (80.2)	3 (0–8)	145 (70.7)	60 (25–126)
High¶	84	45 (53.6)	17 (2–37)	62 (73.8)	2 (0–9)	56 (27.3)	153 (65–227)
Disease category							
Food/waterborne	74	47 (63.5)	2 (0–7)	54 (73.0)	3 (0–6)	60 (29.3)	82 (24–154)
Vectorborne	48	24 (50.0)	7 (1–24)	34 (70.8)	3 (0–24)	31 (15.1)	138 (48–232)
Viral hemorrhagic fever	56	41 (73.2)	9 (6–17)	49 (87.5)	1 (0–4)	37 (18.0)	47 (28–82)
Vaccine-preventable	85	49 (57.6)	28 (8–50)	67 (78.8)	2 (0–15)	52 (25.4)	90 (52–175)
Other	33	23 (69.7)	11 (4–18)	28 (84.8)	5 (1–10)	21 (10.2)	42 (17–146)
Current health expenditure, % GDP (*13*)							
Low¶	162	99 (61.1)	11 (3–21)	126 (77.8)	2 (0–9)	112 (54.6)	79 (35–167)
High¶	134	85 (63.4)	7 (2–21)	106 (79.1)	3 (0–8)	89 (43.4)	77 (27–155)
Population density (*13*)							
Low¶	201	121 (60.2)	11 (3–31)	157 (78.1)	2 (0–9)	131 (63.9)	76 (36–191)
High¶	95	63 (66.3)	6 (2–18)	75 (78.9)	2 (0–5)	70 (34.1)	77 (21–130)

*GDP, gross domestic product; IDP, internally displaced persons; IQR, interquartile range.
†Total number based on records of total outbreaks meeting selection criteria (total for each modality = 296).
‡Numbers based on records of total outbreaks minus those with key missing dates (n [detection] = 184, n [notification] = 132, n [end] = 201 for each modality). Percentages are figured as no. in category/total number × 0.01.
§Five dates missing in initial dataset.
¶Low indicates < median, high indicates > median of in-country value for variable compared with that value for all countries in the African region.

Region. Uganda registered the highest number of events (n = 21); The Gambia, Rwanda, and Seychelles registered the fewest (n = 1). São Tomé and Príncipe, Guinea-Bissau, Gabon, Equatorial Guinea, Eritrea, and Eswatini did not report any disease outbreak with a start date during the study period (Figure 2). Cholera (18.6%) was the most frequently reported outbreak disease, followed by measles (11.1%), dengue fever (7.8%), Crimean-Congo hemorrhagic fever (7.4%), poliomyelitis (5.7%), and meningococcal disease (5.4%) (Table 2).

Overall Duration of Key Milestones
We found an overall median time of 8 (IQR 2–28) days for time to detection, 3 (IQR 0–9) days for time to notification, and 77 (IQR 33–165) days for time to end. When analyzed by disease category, vaccine-preventable diseases had the longest median time to detection of 28 (IQR 8–50) days, whereas food/waterborne diseases had the shortest at 2 (IQR 0–7) days. The longest median time to end was 138 (IQR 48–232) days for vectorborne diseases and the shortest was 42 (IQR 17–146)

days for diseases in the others category. Median times for these and the other stratifying variables—income, WHO African subregion, number of refugees, internally displaced population, current health expenditure, and population density—are shown in Table 1.

Changes in Duration of Key Milestones over Time
Overall, the median time to end of outbreaks improved, decreasing from 131 (IQR 67–237) days in 2017 to 67 (IQR 25–144) days in 2018 and to 45 (IQR 22–90) days in 2019 (Table 1). The median time to detection decreased from 14 (IQR 6–37) days in 2017 to 7 days (IQR 1–27) days in 2018 and to 4 (IQR 1–11) days in 2019. The median time to notification increased over time from 1 (IQR 0–5) days in 2017 to 3 (IQR 0–14) days in 2018 and to 4 (IQR 1–9) days in 2019.

The multivariable Cox proportional hazards models confirmed the improvement of the time to detection during 2017–2019, time to end from 2017 through 2018, and the increase in time to notification during 2017–2019 (Table 3). The other variable associated with time to detection and end was the disease

category. HRs for time to detection decreased by 54% (HR 0.46, 95% CI 0.29–0.73) and time to end by 47% (HR 0.53, 95% CI 0.34–0.83) for vaccine-preventable diseases compared with food/waterborne diseases.

Discussion

Early detection and rapid response to outbreaks greatly contributed to reducing the illness and death rates during these events. Timeliness of response is an essential element of surveillance systems (17,18). Systematically capturing and analyzing the timeliness of key milestones in outbreak detection and response can also provide critical information to public health decision makers and stakeholders on progress made towards implementing IHR requirements. Our analyses explored trends in the timeliness of detection, notification, and end of outbreaks over 3 years (2017–2019) in the WHO African Region and predictor variables that could explain changes. Overall, the findings showed a decrease in the median time to detection and end of outbreaks over the years, signaling an improvement in capacities in these areas. In contrast, the median time to notification increased.

Our finding of overall improvement in time to detection of outbreaks in the African Region was consistent with 2 other studies, although the period studied, geography, and variables analyzed differed (15,19). In our study, the disease category was associated with differences in time to detection. Time to clinical diagnosis and laboratory confirmation of a disease affect time to detection. The median time to detection of food/waterborne disease outbreaks was found to be shorter than for other disease categories. Our final dataset contained a high number of food/waterborne diseases, with outbreaks of cholera the most frequent. Cholera has a relatively short incubation period compared with other diseases and the potential to spread rapidly, causing large-scale outbreaks (20). The main approach to clinical diagnosis and surveillance of cholera has been the use of the case definitions (21) contained in the IDSR guidelines. The scale-up of IDSR in recent years (22), coupled with the short incubation period, contribute to early detection of outbreaks of cholera. In addition, laboratory capacities for confirming *Vibrio cholerae,* particularly in cholera-prone settings, have improved (23),

Table 2. Number and frequency of disease outbreaks selected for the study on timeliness of outbreak milestones in the WHO African Region, 2017–2019

Outbreaks	Disease category	No. (%) outbreaks
Cholera	Food/waterborne	55 (18.6)
Measles	Vaccine-preventable	33 (11.1)
Dengue fever	Vectorborne	23 (7.8)
Crimean-Congo hemorrhagic fever	Viral hemorrhagic fever	22 (7.4)
Poliomyelitis (circulating vaccine-derived poliovirus type2)	Vaccine-preventable	17 (5.7)
Meningococcal disease	Vaccine-preventable	16 (5.4)
Lassa fever	Viral hemorrhagic fever	15 (5.1)
Anthrax	Other	13 (4.4)
Monkeypox	Other	12 (4.1)
Rift Valley fever	Viral hemorrhagic fever	12 (4.1)
Yellow fever	Vaccine-preventable	11 (3.7)
Malaria	Vectorborne	10 (3.4)
Plague	Vectorborne	6 (2.0)
Chikungunya	Vectorborne	6 (2.0)
Hepatitis E	Food/waterborne	5 (1.7)
Ebola virus disease	Viral hemorrhagic fever	5 (1.7)
Typhoid fever	Food/waterborne	4 (1.4)
Acute bloody diarrhea	Food/waterborne	4 (1.4)
Pertussis	Vaccine-preventable	3 (1.0)
Food--borne	Food/waterborne	3 (1.0)
Listeriosis	Food/waterborne	2 (0.7)
Influenza A(H1N1)	Other	2 (0.7)
Rubella	Vaccine-preventable	2 (0.7)
Aflatoxicosis	Food/waterborne	2 (0.7)
Guinea worm disease	Other	2 (0.7)
Marburg	Viral hemorrhagic fever	2 (0.7)
Leishmaniasis	Vectorborne	2 (0.7)
Botulism	Food/waterborne	1 (0.3)
Adverse effect following immunization	Other	1 (0.3)
Hepatitis A	Vaccine-preventable	1 (0.3)
Rotavirus	Vaccine-preventable	1 (0.3)
Zika virus disease	Vectorborne	1 (0.3)
Diphtheria	Vaccine-preventable	1 (0.3)
Scabies	Other	1 (0.3)
Total		296 (100.0)
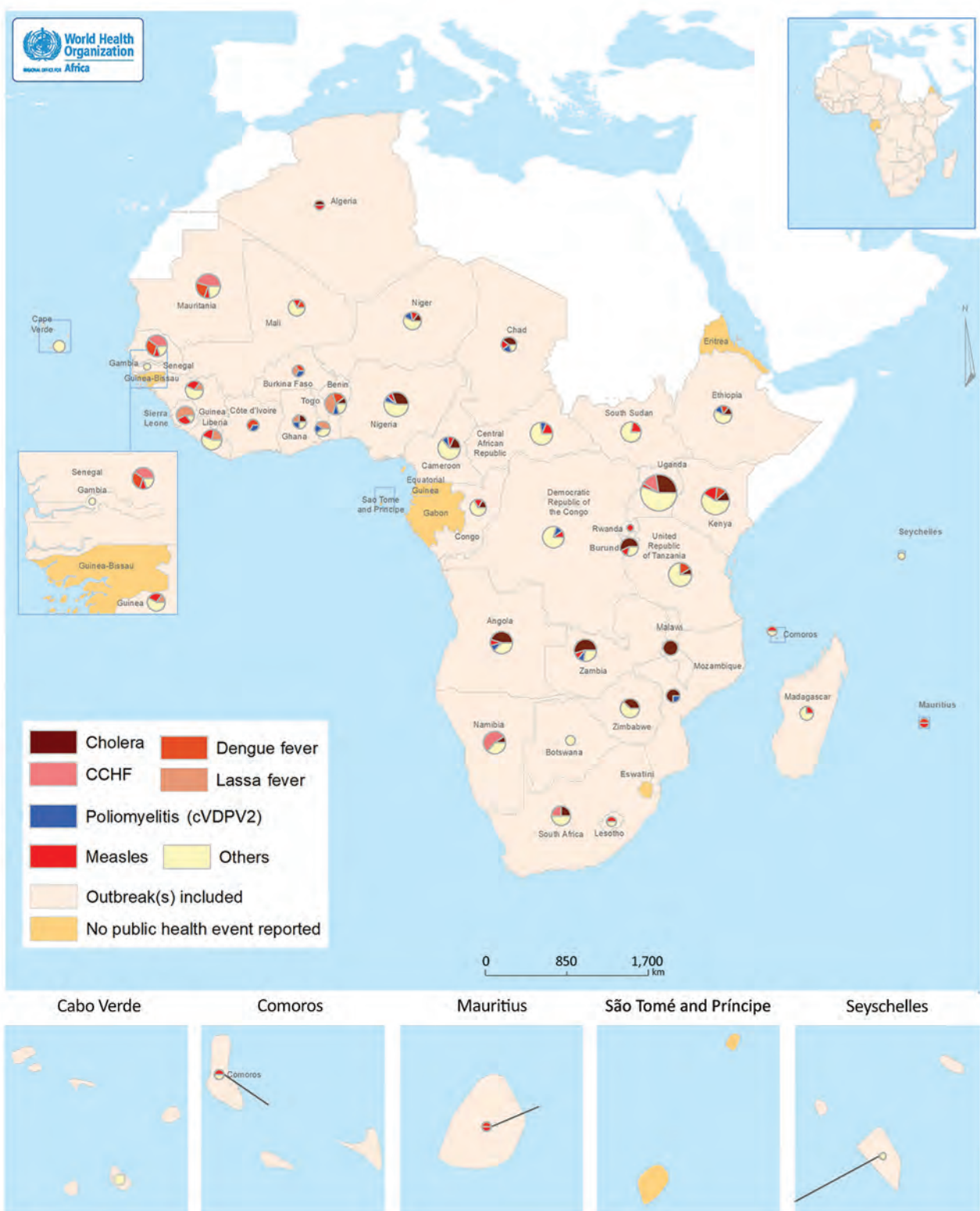
Figure 2. Geographic distribution of substantiated disease outbreaks selected in study of timeliness of key outbreak milestones in the WHO African Region, 2017–2019. CCHF, Crimean-Congo hemorrhagic fever; WHO, World Health Organization. cVDPV2, circulating vaccine-derived poliovirus type 2

reducing the time needed to confirm outbreaks. However, challenges remain, as surveillance and diagnostic capacities across member states vary and serious gaps exist (*24*).

The lower hazard ratio for time to detection of vaccine-preventable diseases compared with food/waterborne diseases could be explained in the context of the outbreak threshold for these diseases and how they are monitored. The IDSR outbreak threshold for cholera is one confirmed case while most vaccine-preventable diseases require several cases over a period of time to reach the epidemic threshold (*21*). Cholera outbreaks, therefore, are more likely to generate a quick alarm. Furthermore, monitoring of diseases reaching an outbreak threshold in the region continues to be performed mainly through indicator-based surveillance that relies on structured weekly IDSR reports from health facilities. This

structure could likely result in delays in early detection of vaccine-preventable disease outbreaks because this system captures only those cases from people visiting a health facility. Event-based surveillance systems are designed to address this limitation by capturing reports from a wide variety of sources. For example, introducing community event-based surveillance contributed to increased reporting of suspected cases of measles in Liberia, leading to early detection of measles outbreaks (*25*). However, event-based surveillance is not yet well developed in most countries in the region and there remain major gaps in its implementation (*22*).

No other predictor variable had a notable association with time to detection. Differences in national income levels and health expenditures by country GDP could provide plausible explanations for variations in the efficiency of health systems (*26*), with higher

Table 3. Results of multivariable Cox proportional hazard regression analysis of substantiated outbreaks by predictor variables, WHO African Region, 2017–2019*

Categories	Total no.†	Time to detection (*15*)	Time to notification (*15*)	Time to end (*15*)
Income (*16*)				
Low	156	Referent	Referent	Referent
Middle and high	140	1.01 (0.68–1.52)	1.11 (0.71–1.73)	1.07 (0.78–1.73)
Significance		p = 0.5147	p = 0.6289	p = 0.1513
WHO subregion (*10*)				
Eastern and Southern	133	Referent	Referent	Referent
Western	102	1.02 (0.52–1.46)	0.84 (0.47–1.50)	0.94 (0.56–1.54)
Central	61	0.81 (0.49–1.38)	1.13 (0.65–1.97)	0.55 (0.33–0.90)
Significance		p = 0.0427	p = 0.6784	p = 0.0608
Outbreak start date‡ (*15*)				
2017	103	Referent	Referent	Referent
2018	101	1.68 (1.16–2.34)	0.46 (0.31–0.70)	1.57 (1.08–2.27)
2019	87	2.59 (1.71–3.94)	0.40 (0.25–0.64)	0.94 (0.63–1.43)
Significance		p = 0.0000	p = 0.0000	p = 0.0182
No. refugees from elsewhere (*13*)				
Low‡	199	Referent	Referent	Referent
High‡	97	1.61 (0.96–2.70)	0.82 (0.45–1.48)	0.80 (0.48–1.33)
Significance		p = 0.2017	p = 0.8066	p = 0.0236
IDP, % population (*13*)				
Low‡	212	Referent	Referent	Referent
High‡	84	1.01 (0.64–2.70)	1.38 (0.85–2.23)	0.70 (0.47–1.04)
Significance		p = 0.8446	p = 0.2843	p = 0.0163
Disease category (*13*)				
Food/waterborne	74	Referent	Referent	Referent
Vectorborne	48	0.59 (0.34–1.03)	1.18 (0.63–2.22)	0.89 (0.54–1.45)
Viral hemorrhagic fever	56	0.40 (0.25–0.66)	1.57 (0.89–2.77)	1.20 (0.75–1.91)
Vaccine-preventable	85	0.46 (0.29–0.73)	1.19 (0.69–2.05)	0.53 (0.34–0.83)
Other	33	0.44 (0.34–1.05)	0.91 (0.47–1.78)	1.45 (0.85–2.46)
Significance		p = 0.0023	p = 0.4704	p = 0.0014
Current health expenditure, % GDP (*13*)				
Low§	162	Referent	Referent	Referent
High§	134	1.11 (0.75–1.65)	0.93 (0.58–1.49)	1.02 (0.69–1.51)
Significance		p = 0.5415	p = 0.7700	p = 0.9354
Population density (*13*)				
Low§	201	Referent	Referent	Referent
High§	95	1.10 (0.74–1.61)	0.98 (0.64–1.49)	0.96 (0.67–1.38)
Significance		p = 0.6555	p = 0.9258	p = 0.8251

*GDP, gross domestic product; IDP, internally displaced persons; IQR, interquartile range.
†Numbers, based on records of total outbreaks meeting selection criteria (total for each modality = 296).
‡Five dates missing in initial dataset.
§Low indicates ≤ median, high indicates > median of in-country value for variable compared with that value for all countries in the African region.

expenditures possibly leading to capacities gained for detecting outbreaks faster, even though we did not find any significant association (p>0.05) with the time to detection in this study. Also, delayed detection in the Central African subregion could be partly attributed to protracted humanitarian crises resulting from armed conflicts that have plagued many countries in this subregion (27,28). Notwithstanding, our study also did not find a significant association (p>0.05).

Other than outbreak start year, none of the predictor variables had a statistically significant association (p>0.05) with the time to notification. Rapid notification is aimed at preventing or limiting the international spread of diseases and avoiding disruption to international trade (29). Under this guideline, member states need to notify WHO within 24 hours of assessment of any event in their territory "that may constitute a public health emergency of international concern" (6). Reversing the increase over the years in time to notification will require continuous engagement with member states and capacity building for the national IHR focal points. Initiatives such as the open-access online "Global Health Security, Solidarity, and Sustainability through the International Health Regulations" course (30) may help enhance this capacity.

Many countries in the WHO African Region continue to experience recurrent disease outbreaks. Lessons gained from each outbreak response have helped to improve response to subsequent outbreaks, a possible reason for the reduction in time to end. The lower HR for controlling outbreaks of vaccine-preventable diseases compared with food/waterborne disease outbreaks may reflect challenges associated with vaccine acquisition, uptake, and access, particularly in hard-to-reach areas.

Our list of predictor variables was not exhaustive and several other factors may have influenced the improvement in time to detection and time to end, for example, the roles of WHE and other high-level initiatives and partnerships. WHE's enhanced use of a digital disease detection approach through media monitoring platforms such as Hazard Detection and Risk Assessment and Epidemic Intelligence from Open Sources (31–33) has expanded the window of opportunity for capturing event-based surveillance information. In 2018, about one quarter of the events in the African Region were verified by member states and reported to WHO following media monitoring activities undertaken at the Regional Office for Africa (34). In addition, several other high-level initiatives have been undertaken in the aftermath of the 2014–2016 Ebola outbreak to bolster global capacities for preparedness and response to infectious disease outbreaks (35).

There are 3 main limitations of the study. First, key milestone dates were missing in some of the reports sent to WHO, which excluded some outbreaks from the analysis. This omission may have had some effect on the findings, although efforts were made to ensure that the sample was representative of the study population of events (Appendix, https://wwwnc.cdc.gov/EID/article/26/11/19-1766-App1.pdf). Second, the number of outbreaks considered in our analysis is not an exhaustive list of all the outbreaks that occurred in the region. Only those reported to WHO by member states on the basis of IHR (2005) requirements, using the Annex 2 decision instrument (36), were included in the study. Third, the application of right censoring at the end of the study may have affected the results, especially for time to end of outbreaks in 2019, although the difference is unlikely to be substantial because relatively few events were right censored.

In spite of these limitations, our study shows that outbreak metrics can be collected and measured to allow countries to monitor the timeliness of outbreak detection and response and provides an estimate of improvement of outbreak detection and end over time. The next step is to enable countries to set up systems in which these measurements are routinely collected, analyzed, and used to improve surveillance and response interventions.

In conclusion, our study has established that the use of simple, easy-to-collect, and verifiable metrics is key to monitoring the timeliness of outbreak detection and response in the WHO African Region. The findings of improvement in early outbreak detection and rapid control over the studied period should be interpreted within the context of the variations and multiple factors that influence these outcomes. Further studies could shed better light on these variations within the member states, and across subregions and disease categories. The momentum needs to be sustained and member states supported in building capacities for early detection, notification, and rapid control of outbreaks. It is equally necessary to support member states to enable them to track key milestones systematically for continuous measurement of outbreak response performance.

About the Author

Dr. Impouma is program manager of Health Emergency Information & Risk Assessment for the WHO Health Emergencies Programme within the Regional Office for Africa. His primary research interests include prevention and control of infectious disease outbreaks, global public health, monitoring and evaluation, and health information systems.

References

1. World Health Organization Regional Office for Africa. WHO African Region country offices [in French] [cited 2019 Feb 17]. https://www.afro.who.int/countries
2. World Health Organization. The African regional health report: the health of the people. 2017 [cited 2019 Feb 13]. https://www.who.int/bulletin/africanhealth/en/
3. Impouma B, Archer BN, Lukoya OC, Hamblion EL, Fall IS. World Health Organization Regional Office for Africa weekly bulletin on outbreaks and other emergencies. Emerg Infect Dis. 2018;24:1394–5.
4. Lopez AD, Mathers CD, Ezzati M, Jamison DT, Murray CJ. Global and regional burden of disease and risk factors,2001: systematic analysis of population health data. Lancet. 2006; 367:1747–57. https://doi.org/10.1016/S0140-6736(06)68770-9
5. World Health Organization Regional Office for Africa. WHO Health Emergencies Programme [cited 2019 Apr 16]. https://www.afro.who.int/about-us/programmes-clusters/who-health-emergencies-programme
6. World Health Organization. International Health Regulations (2005): areas of work for implementation. Geneva: World Health Organization; 2007 [cited on 15 November 2019]. http://apps.who.int/iris/bitstream/10665/69770/1/WHO_CDS_EPR_IHR_2007.1_eng.pdf
7. World Health Assembly, 69. Reform of WHO's work in health emergency management: WHO Health Emergencies Programme report by the Director-General. World Health Organization [cited 2019 Feb 17]. https://apps.who.int/iris/handle/10665/252688
8. World Health Organization Regional Office for Africa. The compendium of short reports on selected outbreaks in the WHO African Region 2016–2018. 2018 [cited 2019 Dec 11]. https://www.afro.who.int/publications/compendium-short-reports-selected-outbreaks-who-african-region-2016-2018
9. Smolinski MS, Crawley AW, Olsen JM. Finding outbreaks faster. Heal Secur. 2017;15:215–20. PubMed https://doi.org/10.1089/hs.2016.0069
10. World Health Organization Regional Office for Africa. Organizational structure [cited 2019 Oct 21]. https://www.afro.who.int/about-us/organizational-structure
11. World Health Organization. WHO event management for international public health security: operational procedures. Working document. Geneva: World Health Organization; 2008 [cited 2019 Mar 4]. https://www.who.int/csr/HSE_EPR_ARO_2008_1.pdf?ua=1
12. World Bank world development indicators [cited 2019 Oct 21]. http://datatopics.worldbank.org/world-development-indicators/
13. World Bank world development indicators databank [cited 2019 Oct 21]. https://databank.worldbank.org/source/world-development-indicators
14. Roth PL. Missing data: a conceptual review for applied psychologists. Pers Psychol. 1994;47:537–60. https://doi.org/10.1111/j.1744-6570.1994.tb01736.x
15. Chan EH, Brewer TF, Madoff LC, Pollack MP, Sonricker AL, Keller M, et al. Global capacity for emerging infectious disease detection. Proc Natl Acad Sci U S A. 2010;107: 21701–6. https://doi.org/10.1073/pnas.1006219107
16. World Bank country and lending groups: data [cited 2019 Oct 15]. https://datahelpdesk.worldbank.org/knowledgebase/articles/906519-world-bank-country-and-lending-groups
17. World Health Organization. Communicable disease surveillance and response systems. Epidemic and pandemic alert and response. Geneva: World Health Organization; 2006 [cited on 15 November 2019]. http://www.who.int/csr/resources/publications/surveillance/WHO_CDS_EPR_LYO_2006_2/en/
18. Calba C, Goutard FL, Hoinville L, Hendrikx P, Lindberg A, Saegerman C, et al. Surveillance systems evaluation: a systematic review of the existing approaches. BMC Public Health. 2015;15:448. https://doi.org/10.1186/s12889-015-1791-5
19. Kluberg SA, Mekaru SR, McIver DJ, Madoff LC, Crawley AW, Smolinski MS, et al. Global capacity for emerging infectious disease detection, 1996–2014. Emerg Infect Dis. 2016;22:E1–6. https://doi.org/10.3201/eid2210.151956
20. Kuna A, Gajewski M. Cholera—the new strike of an old foe. Int Marit Health. 2017;68:163–7. https://doi.org/10.5603/IMH.2017.0029
21. World Health Organization. Technical guidelines for integrated disease surveillance and response in the African region. Geneva: World Health Organization; 3rd edition. 2019 [cited DATE]. https://www.afro.who.int/publications/technical-guidelines-integrated-disease-surveillance-and-response-african-region-third
22. Fall IS, Rajatonirina S, Yahaya AA, Zabulon Y, Nsubuga P, Nanyunja M, et al. Integrated Disease Surveillance and Response (IDSR) strategy: current status, challenges and perspectives for the future in Africa. BMJ Glob Health. 2019;4:e001427. https://doi.org/10.1136/bmjgh-2019-001427
23. Munier A, Njanpop-Lafourcade BM, Sauvageot D, Mhlanga RB, Heyerdahl L, Nadri J, et al. The African cholera surveillance network (Africhol) consortium meeting, 10–11 June 2015, Lomé, Togo. BMC Proc. 2017;11(Suppl 1):1–8. https://doi.org/10.1186/s12919-016-0068-z
24. Ganesan D, Gupta S Sen, Legros D. Cholera surveillance and estimation of burden of cholera. Vaccine. 2020;38:A13–7. https://doi.org/10.1016/j.vaccine.2019.07.036
25. Nagbe T, Williams GS, Rude JM, Flomo S, Yeabah T, Fallah M, et al. Lessons learned from detecting and responding to recurrent measles outbreak in Liberia post Ebola-epidemic 2016–2017. Pan Afr Med J. 2019;33(Suppl 2):7. https://doi.org/10.11604/pamj.supp.2019.33.2.17172
26. Sun D, Ahn H, Lievens T, Zeng W. Evaluation of the performance of national health systems in 2004–2011: an analysis of 173 countries. PLoS One. 2017;12:e0173346. https://doi.org/10.1371/journal.pone.0173346
27. ReliefWeb. Central African Republic: humanitarian response plan, January–December 2019. 2019. https://reliefweb.int/report/central-african-republic/central-african-republic-humanitarian-response-plan-january-december
28. World Health Organization Regional Office for Africa. Weekly bulletin on outbreaks and other emergencies, week 34. 2018 [cited on 24 August 2019]. https://apps.who.int/iris/handle/10665/274276
29. Simons H, Patel D. International Health Regulations in practice: focus on yellow fever and poliomyelitis. Hum Vaccin Immunother. 2016;12:2690–3. https://doi.org/10.1080/21645515.2016.1218100

30. Global Health Security, Solidarity and sustainability through the International Health Regulations [cited 2019 Dec 10]. https://www.coursera.org/learn/international-health-regulations

31. Enderlein U, Regmi J. Strengthening public health: making the case for mass gatherings. Public Health Panorama. 2018;4:67–71.

32. World Health Organization Regional Office for Europe. World Youth Day 2016 [cited 2019 Feb 17]. https://www.euro.who.int/en/countries/poland/news/news/2016/08/world-youth-day-2016

33. Barboza P. Epidemic Intelligence from Open Sources (EIOS) [cited 2019 Feb 17]. http://www.oie.int/eng/BIOTHREAT2017/Presentations/6.2_BARBOZA-presentation.pdf

34. Mboussou F, Ndumbi P, Ngom R, Kassamali Z, Ogundiran O, Van Beek J, et al. Infectious disease outbreaks in the African region: overview of events reported to the World Health Organization in 2018. Epidemiol Infect. 2019;147:e299. https://doi.org/10.1017/S0950268819001912

35. Ravi SJ, Snyder MR, Rivers C. Review of international efforts to strengthen the global outbreak response system since the 2014–16 West Africa Ebola epidemic. Health Policy Plan. 2019;34:47–54. https://doi.org/10.1093/heapol/czy102

36. World Health Organization. WHO guidance for the use of annex 2 of the International Health Regulations (2005). Geneva: World Health Organization; 2008 http://www.who.int/ihr/revised_annex2_guidance.pdf

Address for correspondence: Benido Impouma, WHO Regional Office for Africa, B.P. 06 Cité du Djoué, Brazzaville, Congo; email: impoumab@who.int

Challenges to Achieving Measles Elimination, Georgia, 2013–2018

Nino Khetsuriani, Ketevan Sanadze, Rusudan Chlikadze, Nazibrola Chitadze,
Tamar Dolakidze, Tamta Komakhidze, Lia Jabidze, Shahin Huseynov,
Myriam Ben Mamou, Claude Muller, Khatuna Zakhashvili, Judith M. Hübschen

Controlling measles outbreaks in the country of Georgia and throughout Europe is crucial for achieving the measles elimination goal for the World Health Organization's European Region. However, large-scale measles outbreaks occurred in Georgia during 2013–2015 and 2017–2018. The epidemiology of these outbreaks indicates widespread circulation and genetic diversity of measles viruses and reveals persistent gaps in population immunity across a wide age range that have not been sufficiently addressed thus far. Historic problems and recent challenges with the immunization program contributed to outbreaks. Addressing population susceptibility across all age groups is needed urgently. However, conducting large-scale mass immunization campaigns under the current health system is not feasible, so more selective response strategies are being implemented. Lessons from the measles outbreaks in Georgia could be useful for other countries that have immunization programs facing challenges related to health-system transitions and the presence of age cohorts with historically low immunization coverage.

The country of Georgia, along with the other member states of the European Region (EUR) of the World Health Organization (WHO), is committed to achieving the goal of eliminating measles and rubella (*1,2*). However, the resurgence of measles in EUR

Author affiliations: Centers for Disease Control and Prevention, Atlanta, Georgia, USA (N. Khetsuriani); CDC South Caucasus Office, Tbilisi, Georgia (N. Khetsuriani); National Center for Disease Control and Public Health, Tbilisi (K. Sanadze, R. Chlikadze, N. Chitadze, T. Dolakidze, T. Komakhidze, L. Jabidze, K. Zakhashvili); South Caucasus Field Epidemiology and Laboratory Training Program, Tbilisi (T. Komakhidze); World Health Organization European Regional Office, Copenhagen, Denmark (S. Huseynov, M. Ben Mamou); World Health Organization European Regional Reference Laboratory for Measles and Rubella, Luxembourg Institute of Health, Esch-sur-Alzette, Luxembourg (C. Muller, J.M. Hübschen)

since 2018 resulted in record-high numbers of cases and reestablished endemic transmission in some countries that had previously eliminated measles (*3,4*). Georgia is among the 12 EUR countries that have endemic transmission of measles and continues to experience periodic outbreaks (*4,5*).

Routine childhood immunization against measles was introduced in Georgia in 1966, resulting in reduction of incidence (Figure 1) (*5,6*). However, the excessive expansion of the list of contraindications to vaccination in the Soviet Union during the 1980s resulted in substantial immunity gaps (*7,8*). The immunization program deteriorated dramatically in the 1990s, during the first years after Georgia regained independence, but improved in the 2000s. Combined measles-mumps-rubella (MMR) vaccine (recommended at 12 months and 5 years of age) was successfully introduced in 2004. However, the accumulation of susceptible persons in cohorts born during the mid-1980s through the 1990s led to a series of measles outbreaks. A large-scale outbreak during 2004–2005 affected a wide age range, including older children and young adults (*5*). A nationwide measles-rubella supplementary immunization activity (SIA) in 2008, targeting the population 6–27 years of age, achieved only 50% coverage because of unjustified vaccine safety concerns (*9*). Another large-scale outbreak of measles occurred during 2013–2015 and was followed by the outbreak that began in 2017. Here, we review the status of measles in Georgia during 2013–2018, highlight challenges to achieving the elimination goal, and discuss approaches to address these problems.

Methods

We reviewed measles surveillance data from the Georgia national surveillance system. National guidelines for measles surveillance, revised in 2017 (*10*; Appendix, https://wwwnc.cdc.gov/EID/article/26/11/20-0259-App1.pdf), follow WHO regional recommendations. Healthcare providers report suspected measles

Figure 1. Incidence of measles (reported cases/1 million population), Georgia, 1958–2018. Second dose of measles vaccine was in the national immunization schedule during 1985–1993 but only 1982, 1983, and 1987 birth cohorts were vaccinated because of a lack of vaccine; the second dose was reintroduced in 1997 (*5*). MMR, measles-mumps-rubella vaccine; MR, measles-rubella vaccine; SIA, supplementary immunization activity.

cases to district public health centers, which report the cases to the national Electronic Infectious Disease Surveillance System and conduct case investigation and response. The National Center for Disease Control and Public Health (NCDC) is responsible for the national level analysis and provides overall guidance. Case-based data on suspected measles cases are reported electronically each month to EUR. Laboratory testing is conducted by the National Measles and Rubella Laboratory at NCDC or, in rare cases, by private laboratories. Virus characterization is performed at the Regional Reference Laboratory in Luxemburg Institute of Health and at the National Measles and Rubella Laboratory. Measles virus sequences are reported to WHO through the Measles Nucleotide Surveillance (MeaNS) database (*11,12*).

We reviewed basic epidemiologic data for cases reported during 2013–2018 and conducted a detailed analysis of cases reported during 2013–2014, including descriptive epidemiology, occupational status, patterns of transmission, and costs to the public health system. An analysis of measles transmission across age groups was performed for a subset of cases for which the age group of the source (adult vs. child) could be determined from the Electronic Infectious Disease Surveillance System. We obtained information on expenses associated with outbreak response (costs of vaccine and personnel) from NCDC and population data from Georgia's National Statistics Agency.

We obtained information on administrative MMR vaccine coverage from NCDC, supplemented

by independent estimates from a coverage survey that we conducted in 2015–2016 (*13*; Appendix). In this survey, we estimated immunization coverage (nationwide and in 3 largest cities [Tbilisi, Batumi, and Kutaisi]) for the first MMR vaccine dose (MMR1) and the second MMR vaccine dose (MMR2) among children age-eligible to receive routine vaccinations in 2014 (2009 and 2013 birth cohorts). We estimated both coverage at the time of the survey and timely coverage by standard ages (MMR1 by age 24 months and MMR2 by age 72 months). We obtained additional information on the state of the immunization program in Georgia from WHO and GAVI (https://www.gavi.org) assessment reports. Additional details on epidemiologic methods are given in the Appendix.

The activities described in this report were determined by CDC to represent nonresearch. Therefore, institutional review board review was not applicable.

Results

Measles Epidemiology, 2013–2015

Descriptive Epidemiology
A total of 11,495 measles cases were reported in Georgia during 2013–2015 (7,872 in 2013, 3,192 in 2014, and 431 in 2015) (Table 1; Figure 1; Appendix Figure), compared with 30 cases in 2012. The outbreak began in early 2013, and cases occurred predominantly among adults in Tbilisi, the capital city. The outbreak

Table 1. Epidemiologic characteristics of reported measles case-patients, Georgia, 2013–2018*

Characteristic	Reported measles cases, no. (%)		
	2013–2015 outbreak	2016	2017–2018 outbreak
Total cases	11,495 (100.0)	14 (100.0)	2,295 (100.0)
Final case classification category			
Laboratory-confirmed	1220 (10.6)	5 (35.7)	1,748 (76.1)
Epidemiologically linked	466 (4.1)	0 (0)	112 (4.9)
Clinically compatible	9,809 (85.3)	9 (64.3)	435 (19.0)
Sex			
M	6,000 (52.4)	8 (57.1)	1133 (49.4)
F	5,457 (47.6)	6 (42.9)	1162 (50.6)
Age group, y			
<1	1,130 (9.8)	4 (28.7)	229 (10.0)
1–4	1,707 (14.9)	6 (42.9)	321 (14.0)
5–9	962 (8.4)	0 (0)	167 (7.3)
10–14	751 (6.5)	1 (7.1)	174 (7.6)
15–19	1,286 (11.2)	0 (0)	164 (7.1)
20–24	1,707 (14.8)	1 (7.1)	302 (13.2)
25–29	1,750 (15.2)	1 (7.1)	304 (13.2)
30–39	1,546 (13.5)	0 (0)	441 (19.2)
40–49	477 (4.1)	0 (0)	143 (6.2)
≥50	179 (1.6)	1 (7.1)	50 (2.2)
No. doses of measles-containing vaccine received			
0	3,972 (34.6)	7 (50.0)	981 (42.7)
≥1	1,346 (11.7)	4 (28.7)	183 (8.0)
1	1,020 (8.9)	4 (28.7)	123 (5.4)
2	326 (2.8)	0 (0)	60 (2.6)
Unknown	6,177 (53.7)	3 (21.3)	1131 (49.3)
Region			
Tbilisi	5,364 (47.0)	7 (50.0)	864 (37.6)
Achara	270 (2.4)	4 (28.7)	380 (16.6)
Guria	87 (0.8)	0 (0)	50 (2.2)
Imereti	742 (6.5)	0 (0)	469 (20.4)
Kakheti	610 (5.3)	1 (7.1)	36 (1.6)
Kvemo Kartli	1,159 (10.2)	0 (0)	87 (3.8)
Mtskheta-Mtianeti	286 (2.5)	1 (7.1)	29 (1.2)
Racha-Lechkhumi-Kvemo Svaneti	83 (0.7)	0 (0)	13 (0.6)
Samegrelo-Zemo-Svaneti	1,200 (10.5)	1 (7.1)	289 (12.6)
Samtskhe-Javakheti	83 (0.7)	0 (0)	28 (1.2)
Shida Kartli	1,509 (13.2)	0 (0)	36 (1.6)
Abkhazia	27 (0.2)	0 (0)	14 (0.6)

*Sex was not reported for 34 cases during 2013–2015. Region was not specified for 75 cases during 2013–2015. For Abkhazia, currently outside Georgia Government control, only cases treated in healthcare facilities in the government-controlled areas are reported.

spread rapidly, affecting all regions by April and continued until mid-2015 (Figure 2). Tbilisi accounted for 47.0% of reported cases. The regions with the highest cumulative incidence per 1 million population during 2013–2015 were Shida Kartli (5,725) and Tbilisi (4,863), whereas Samtskhe-Javakheti (513) and Guria (763) had the lowest incidence.

Cases occurred across a wide age range (0–73 years; median 19 years), but most cases (60.4%) were among those ≥15 years of age (Table 1). The incidence was highest among children <1 year of age, followed by the 1–4-year- and 15–29-year age groups (Figures 3, 4). Almost 90% of the cases were in unvaccinated persons (34.6%) or those who had an unknown immunization status (53.7%); 8.9% had received 1 dose of measles-containing vaccine, and 2.8% had received 2 doses (Table 1). Distribution of cases by age group and immunization status by case-classification category are given in Figures 5–7.

Approximately one third (3,930 [34.3%]) of the 11,477 case-patients with hospitalization status reported were hospitalized. Hospitalizations were most common among unvaccinated persons (40.9% were hospitalized), followed by persons with unknown immunization status (33.5%), and were least common (18.6%) among recipients of ≥1 dose of measles-containing vaccine (p<0.001 by χ^2 test). Complications were reported for 1,883 (16.4%) cases, most commonly pneumonia (1,328 cases [11.6%]) and diarrhea (587 cases [5.1%]). Encephalitis was reported in 9 (0.1%) cases. Adverse outcomes of pregnancy occurred in 5 cases (premature delivery in 3 cases and miscarriage in 2 cases). Four measles-related deaths occurred (case-fatality ratio 0.3/1,000 cases). Three of the fatal cases (in persons 11 months, 4 years, and 19 years of age) were in unvaccinated persons, and 1 was in a 36-year-old person with unknown immunization status.

Figure 2. Incidence of measles (reported cases/1 million population), by region, Georgia, 2013 (A), 2014 (B), and 2015 (C). Rates for Abkhazia, currently outside government control, could not be calculated because of incomplete surveillance and lack of reliable population data.
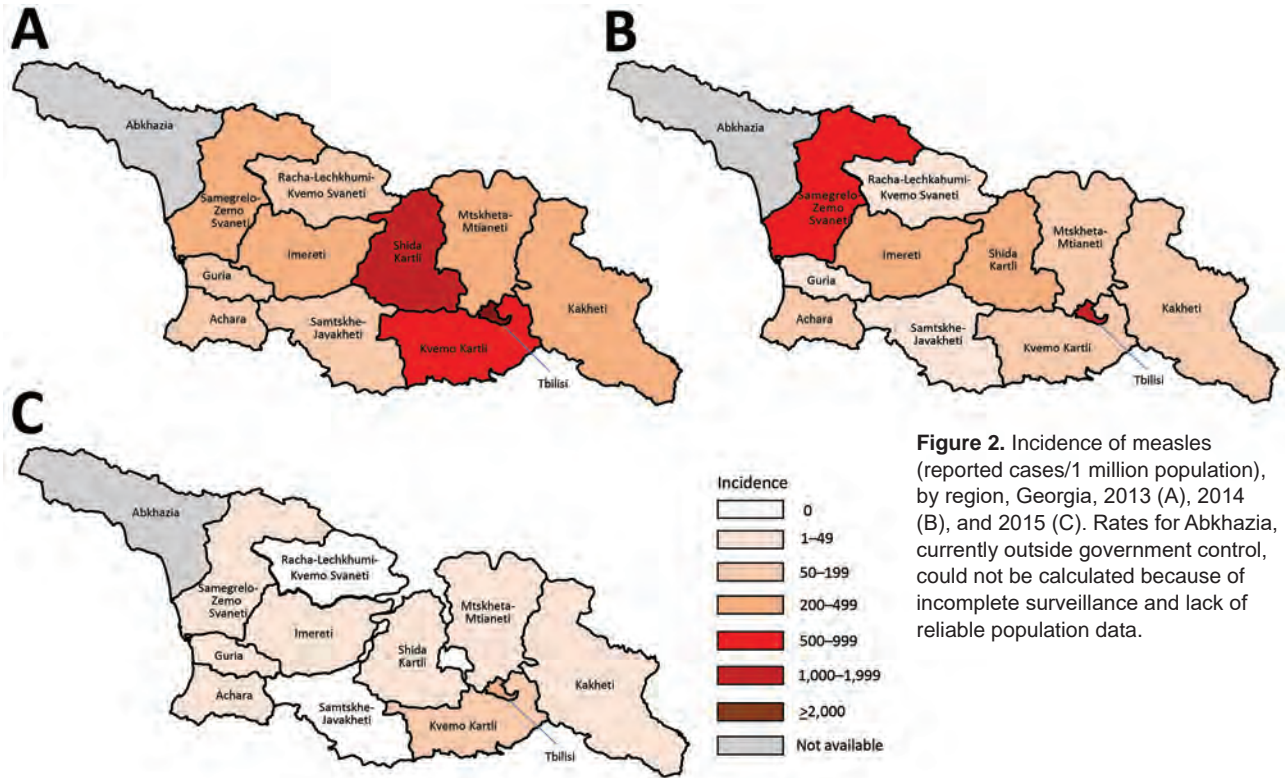
Molecular Epidemiology

Molecular characterization of 93 measles viruses detected during 2013–2015, mostly in eastern Georgia, identified a single genotype (D8) with 9 different sequence variants (8 belonged to the Frankfurt-Main lineage, and 1 was identical to the Villupuram named strain) (Figure 8). The Frankfurt-Main variant (cluster 1) was the predominant strain associated with the outbreak (n = 74). This strain, first detected in Tbilisi in February 2013, became widespread during 2013–2014 but was not seen in 2015. Cluster 2 was represented by 5 strains from the Frankfurt-Main lineage (4 identical ones and 1 with 1 nucleotide difference) detected during February–April 2014. Another cluster of 4 sequences from March 2014 also differed from the Frankfurt-Main variant by 1 nucleotide (cluster 3). The July 2013 strain from Gagra (cluster 4) (in Abkhazia, currently outside Georgia government control) was clearly distinct from all other strains in the Frankfurt-Main lineage and most likely represents a separate introduction. Three other sequences, which differed from the Frankfurt-Main variant by 1 nucleotide each, were also identified (clusters 5–7). The lack of identical sequences from elsewhere in GenBank suggests that these strains could have evolved locally from the main Frankfurt-Main variant. Six sequences (1 from
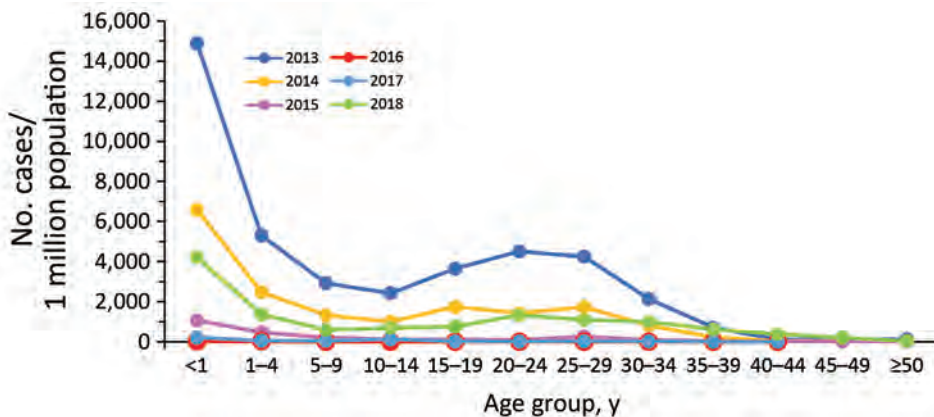
Figure 3. Incidence of measles (reported cases/1 million population), by age group and year, Georgia, 2013–2018.

Figure 4. Reported measles cases during 2013–2015 and 2016–2018 and cumulative incidence (cases/1 million population) for 2013–2018, by birth year and eligibility to MCVs, Georgia. Children born during 2014–2017 gradually became eligible for the first dose of measles-mumps-rubella vaccine (MMR) by 2018 as the respective birth cohorts turned 1 year old. Children born during 2009–2013 were <5 years of age in 2013, at the start of 2013–2015 outbreak, and were either too young to be vaccinated (2013 cohort) or were eligible for the first dose of MMR vaccine only (2009–2012 cohorts), but gradually became eligible for the second dose of MMR vaccine by 2018, as the respective birth cohorts turned 5 years old. The 1981–2008 birth cohorts were eligible to 2 doses of MCV (measles vaccine, measles-rubella vaccine or MMR) through routine program, several supplementary immunization activities, or both. The 1959–1980 cohorts were eligible for 1 dose of measles vaccine through routine vaccination or catch-up immunizations conducted at the time of vaccine introduction. MCV, measles-containing vaccine.
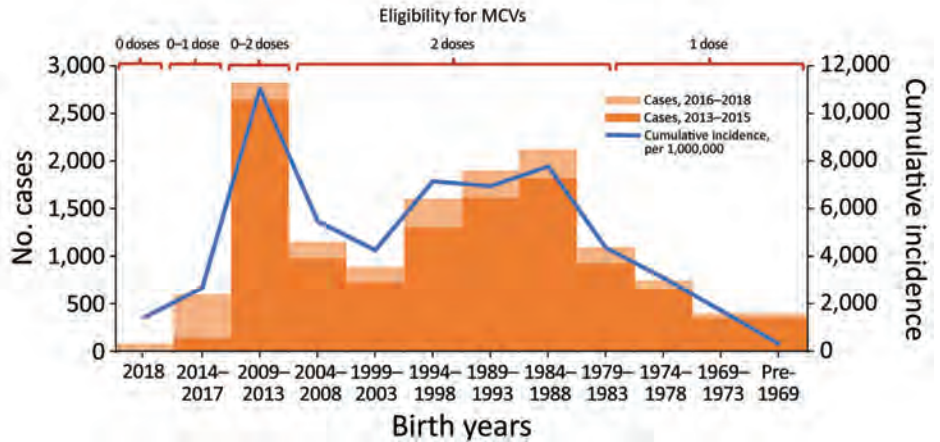
April 2014 and all 5 sequences from March–December 2015) were identcal to the Villupuram variant (cluster 8), representing ≥1 separate introduction.

Virus Transmission across Age Groups

Among the 1,157 cases during 2013–2014 for which the age group of measles source was determined, the source of transmission in most cases (67.2%) was an adult (defined as ≥15 years of age) (Table 2), but the distribution of adult and child sources varied by the age of cases (p<0.001). Cases in adults were significantly more likely than those in children to have another adult as the source of infection (81.5% vs. 51.7%; odds ratio 4.0, 95% CI 3.0–5.2; p<0.001). Adult sources accounted for >50% of the cases among adults, infants <1 year of age, and older children (10–14 years of age), whereas young children (1–9 years of age) contracted measles primarily from other children (Table 2).

Population Groups Affected

Information on patient occupation was reported for 6,441 (58.2%) cases during 2013–2014. Almost half (48.1%) of them occurred among children not attending daycare (21.6%) or adults not working regularly outside the home (26.5%) (Table 3). Schoolchildren accounted for 17.5%, college students for 5.2%, and children attending daycare for 4.2% of the cases. Persons involved in direct customer service accounted for 7.5% of the cases. Healthcare facility (HCF) employees and medical or nursing students accounted for 3.9% of the cases, whereas 5.7% of the cases occurred among military or police.

Transmission associated with HCFs was observed in 123 cases linked to 30 different clusters, which also involved an additional 53 cases for which transmission occurred outside an HCF. The settings for HCF-associated transmission included major
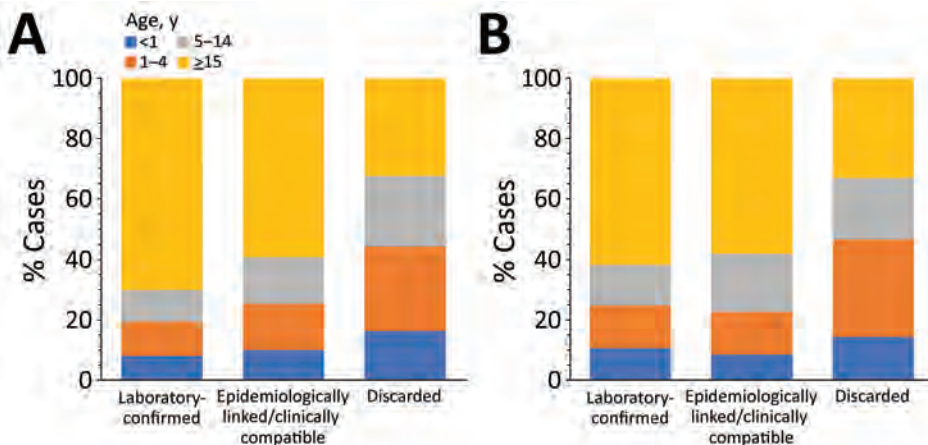
Figure 5. Age distribution of suspected measles case-patients, by final case classification category, Georgia, 2013–2018. A) Cases reported during 2013–2015. B) Cases reported during 2016–2018.
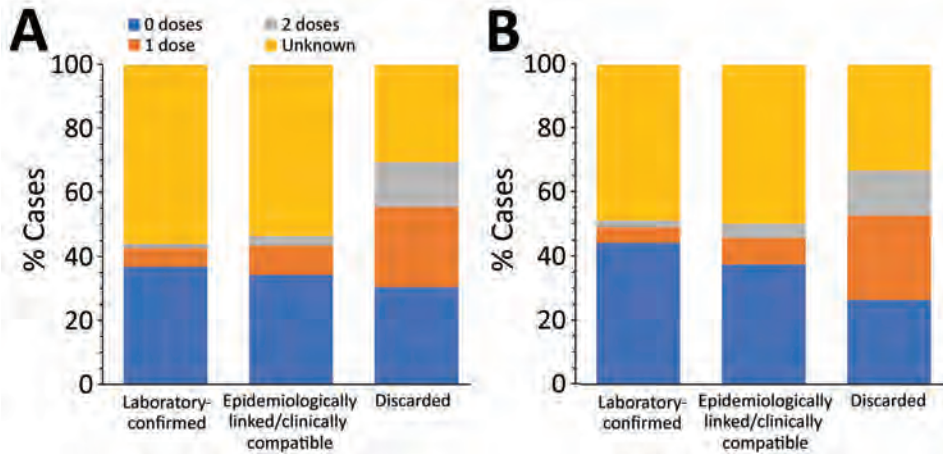
Figure 6. Vaccination status of suspected measles case-patients, by final case classification category, Georgia, 2013–2018. A) Cases reported during 2013–2015. B) Cases reported during 2016–2018.

pediatric hospitals in Tbilisi, ambulance services, a cardiology clinic, infectious disease hospitals, a military hospital, and dental clinics.

Outbreak Response and Cost
The outbreak response activities and additional funds were mandated by the Prime Minister and the Minister of Health of Georgia. During 2013–2015, a total of

272,000 additional doses of MMR vaccine were procured. The immunization response included contact vaccination and offering MMR vaccine free of charge for all unvaccinated children <7 years of age, initially in Tbilisi, then nationwide. Subsequently, the eligible age group was expanded to those ≥30 years of age. Targeted special groups included healthcare workers and military personnel. Vaccine uptake was generally
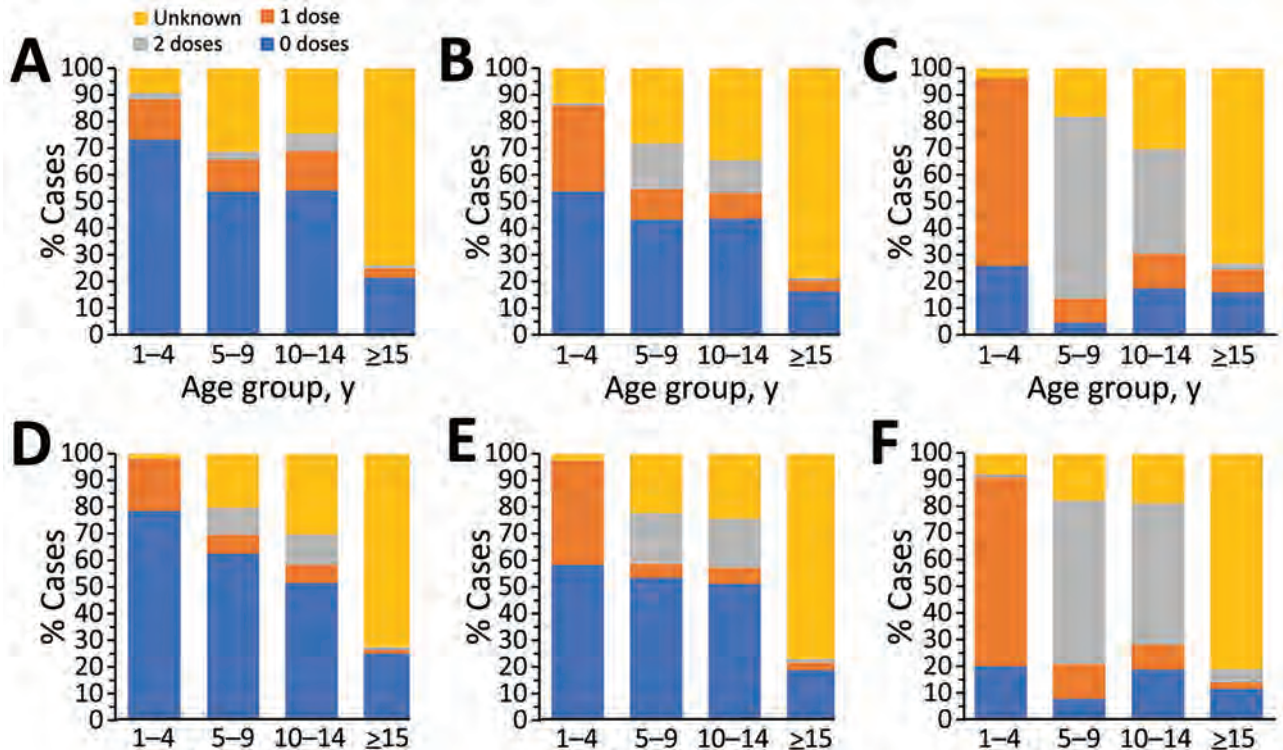
Figure 7. Vaccination status of suspected measles cases, by age group and final case classification category, Georgia, 2013–2015 and 2016–2018. A) Laboratory-confirmed cases reported during 2013–2015 (n = 1,220). B) Epidemiologically linked or clinically compatible cases reported during 2013–2015 (n = 10,275). C) Discarded cases during 2013–2015 (n = 289). D) Laboratory-confirmed cases reported during 2016–2018 (n = 1,753). E) Epidemiologically linked or clinically compatible cases reported during 2016–2018 (n = 556). F) Discarded cases during 2016–2018 (n = 608). Children <1 year of age, too young to be eligible for measles-mumps-rubella vaccination, are excluded.
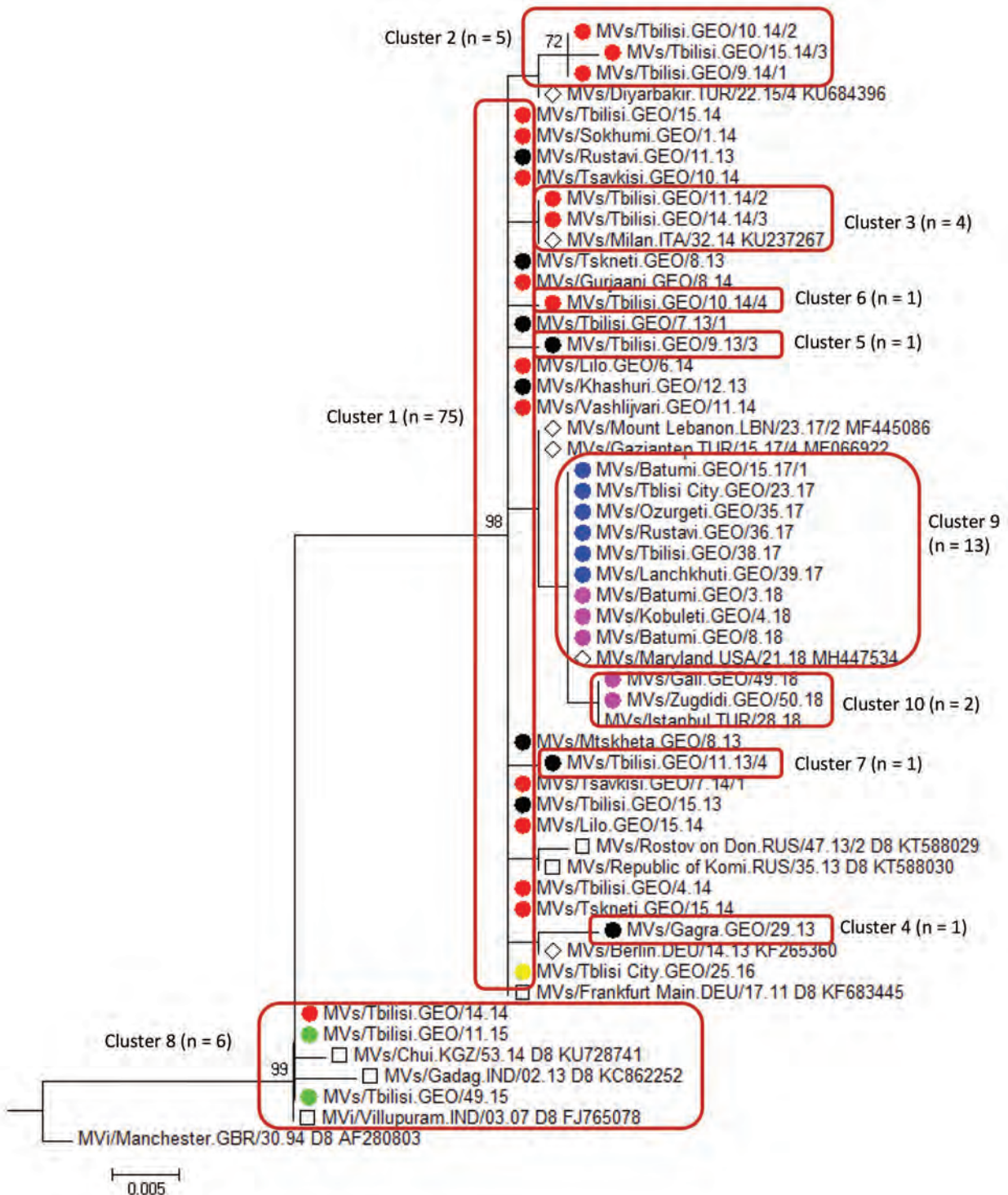
Figure 8. Genetic diversity of measles virus strains identified in Georgia, 2013–2018. Genotype D8 cluster of a phylogenetic tree is based on 450 nt of the measles virus nucleoprotein gene. The Kimura 2-parameter model and the neighbor-joining method in MEGA7 (*14*) were used, and only bootstrap values >70 are shown. The closest matches of the Georgia sequence variants identified by BLAST (https://blast.ncbi.nlm.nih.gov/Blast.cgi) are marked with a diamond; named strains of genotype D8 are marked with a square. For identical sequences, only the oldest and the most recent strains found in a certain location in a certain year are shown. The total number of sequences identified in each cluster are included in parentheses. Year of virus detection is indicated by colored circles: black for 2013, red for 2014, green for 2015, yellow for 2016, blue for 2017, pink for 2018. Scale bar indicates genetic distance, calculated based on the Kimura 2-parameter model, measured in nucleotide substitutions per site.

Table 2. Measles transmission sources for adult and child case-patients, by age group of measles case-patients, Georgia, 2013–2014*

Age of measles case-patients	Age group of measles source, no. (%)	
	Adult (>15 y)	Child (<15 y)
All ages, n = 1,157	778 (67.2)	379 (32.8)
Children <15 y, n = 545	282 (51.7)	263 (48.3)
<1 y, n = 151	118 (78.2)	33 (21.8)
<6 mo, n = 48	43 (89.6)	5 (10.4)
1–14 y, n = 394	164 (41.6)	230 (58.4)
1–4 y, n = 168	69 (41.1)	99 (58.9)
5–9 y, n = 112	35 (31.3)	77 (68.7)
10–14 y, n = 114	60 (52.6)	54 (47.4)
Adults >15 y, n = 612	496 (81.1)	116 (18.9)
15–19 y, n = 158	117 (74.1)	41 (25.9)
20–24 y, n = 145	128 (88.3)	17 (11.7)
25–29 y, n = 127	108 (85.0)	19 (15.0)
>30 y, n = 182	143 (78.6)	39 (21.4)

*Includes 1,157 cases reported during 2013–-2014 for which the age group of the measles transmission source (adults age >15 y vs. children age <15 y) could be established from the available surveillance data.

low (except among the military); 170,000 doses (62.5% of the available doses) were administered (85,000 doses to children 2–14 years of age, 41,000 doses to adults 15–29 years of age, 7,000 doses to healthcare workers, and 37,000 doses to contacts of measles case-patients and military personnel). Because of the substantial numbers of cases among the military, military personnel were considered potentially exposed or at high risk for exposure and vaccinated under the contacts category.

The total direct cost of additional vaccines and salaries for public health personnel during 2013–2015 was $720,000 (USD), of which $663,000 (92%), including $245,000 provided by the US government, was used for purchasing vaccines. The average direct cost per measles case for the public health system during this outbreak was $63.

Measles Epidemiology, 2016–2018
Only 14 cases were reported in 2016 (Table 1), including a 3-case cluster in Tbilisi in June. The measles virus identified from that cluster was Frankfurt-Main, identical to the main outbreak strain circulating during 2013–2014 (cluster 1) (Figure 8). The 26-month interval since the last detection of this strain (in 2014) suggests a new introduction rather than continued transmission.

Ninety-six measles cases were reported in 2017 (Table 1), 92 (95.8%) of which occurred during August–December. The first 2 laboratory-confirmed cases occurred in April, 7 months after the previous laboratory-confirmed case. An outbreak of 16 cases during August–September began in Guria and was notable for its very high proportion of cases linked to HCF-associated transmission (13 cases [81.3%]), including 3 cases among healthcare workers. Measles activity further increased in late 2017, starting with school-based outbreaks in 2 districts of Achara and subsequently spreading to the regional capital Batumi. In 2017, Achara (65 cases) and neighboring region Guria (13 cases) accounted for 78 (81.3%) of cases in Georgia.

Table 3. Occupations of reported measles case-patients, Georgia, 2013–2014

Occupation of case-patients	No. (%)
Adult not working outside the home	1,704 (26.5)
Unemployed	1,011 (15.7)
Housewife	693 (10.8)
Child not attending daycare	1,392 (21.6)
School student (all grades)	1,127 (17.5)
Customer services (e.g., employees of banks, stores, casinos, restaurants)	484 (7.5)
Military or law enforcement	369 (5.7)
Military	239 (3.7)
Law enforcement	130 (2.0)
College or vocational school student	334 (5.2)
Child attending daycare	271 (4.2)
Healthcare facility employee or medical student	250 (3.9)
Healthcare facility employee	209 (3.2)
Medical student	41 (0.6)
Government or office worker	141 (2.2)
Other	369 (5.7)
Total with occupation information reported	6,441 (100)

The outbreak expanded in 2018, resulting in 2,199 reported cases (Table 1; Figures 1, 3, 9; Appendix Figure). During 2017–2018, the 4 regions with the highest cumulative incidence (cases/1 million population) , Achara (1,119), Imereti (911), Samegrelo-Zemo Svaneti (894), and Tbilisi (760), accounted for 2,002 (87.3%) cases. Two unvaccinated case-patients (ages 11 months and 16 years) died in 2018. The age distribution and immunization status of case-patients during 2017–2018 was comparable to the 2013–2015 period (Table 1; Figures 5–7). As seen during 2013–2015, most affected groups in 2016–2018 included birth cohorts too young to be vaccinated or age-eligible for MMR1 only, as well as young adults born during the 1980s and 1990s (Figure 4).

Measles virus sequences from 2017–2018 (n = 15) were detected across 8 regions and belonged to genotype D8. Thirteen identical strains (cluster 9) (Figure 8) detected during April 2017–February 2018 differed by 2 nucleotides from cluster 1, the predominant strain during 2013–2014. The other 2 identical sequences from December 2018 (cluster 10) were 1 nucleotide different from the rest of the 2018 strains and were identical to a virus identified earlier (July 2018) in Turkey (Figure 8).

Outbreak response activities included intensifying contact tracing and case-finding, enhancing surveillance and testing, reviewing immunization records of children in affected areas, and offering MMR vaccine free of charge to contacts and unvaccinated and undervaccinated persons <40 years of age. During 2017–2018, approximately 60,000 additional doses of vaccine were procured, and 47,000 doses were administered as part of the outbreak response. In November 2018, Georgia's healthcare law was amended to make routine childhood immunizations mandatory (*15*). In early 2019, the policy of mandatory MMR vaccination for certain occupational groups, including healthcare workers, was introduced (*16*). The National Strategic Plan for Measles and Rubella Elimination was developed and is pending government approval.

Immunization Coverage

The administrative coverage fluctuated over time and mostly remained below the national target (95%) (Figure 10). However, in 2015 and 2017, reported MMR1 coverage reached 95%–96% and MMR2 coverage reached 90%–91%. In 2018, coverage for both doses exceeded 95% for the first time (98% for MMR1 and 96% for MMR2).

A coverage survey conducted during 2015–2016 demonstrated that by the time of the survey, 89% of children born in 2013 and 93% of children born in 2009 had received MMR1; and 76% of children born in 2009 had received MMR2 (Figure 11). Timely coverage was lower, particularly in the 2009 cohort,
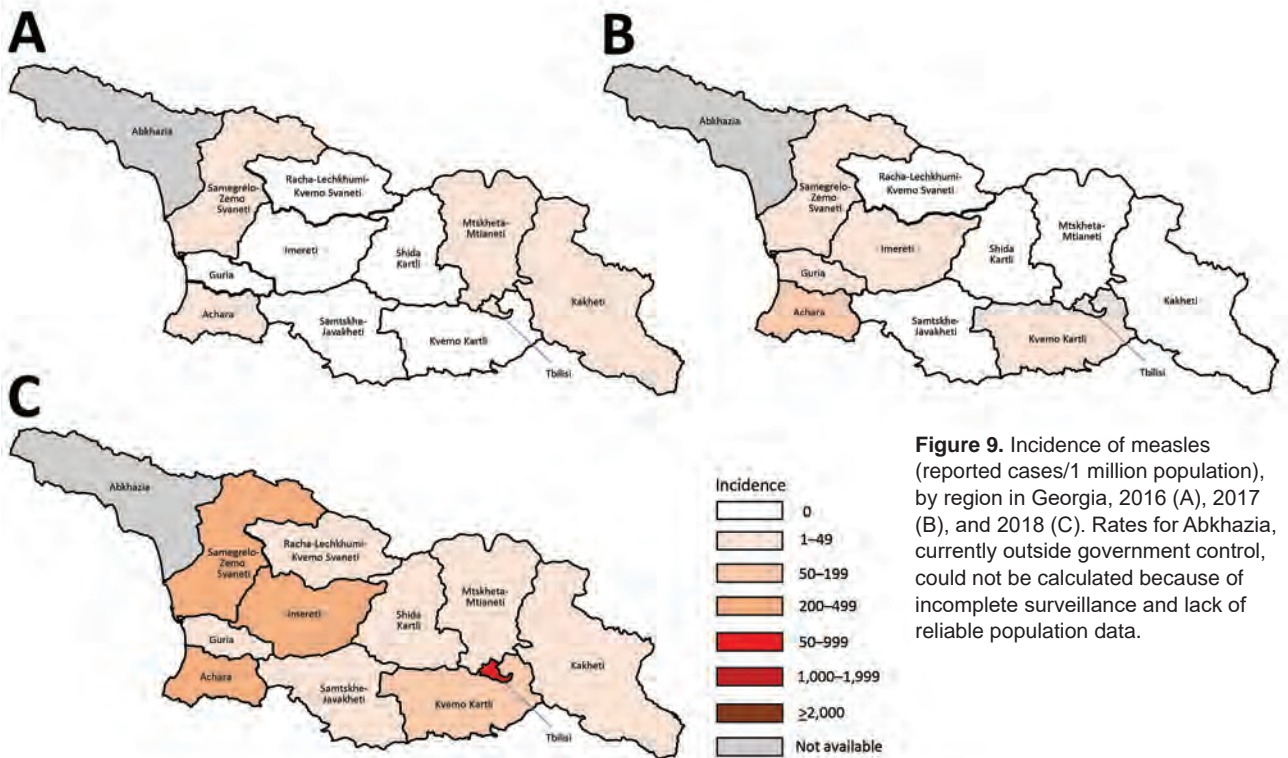
Figure 9. Incidence of measles (reported cases/1 million population), by region in Georgia, 2016 (A), 2017 (B), and 2018 (C). Rates for Abkhazia, currently outside government control, could not be calculated because of incomplete surveillance and lack of reliable population data.

Incidence
- 0
- 1–49
- 50–199
- 200–499
- 50–999
- 1,000–1,999
- ≥2,000
- Not available
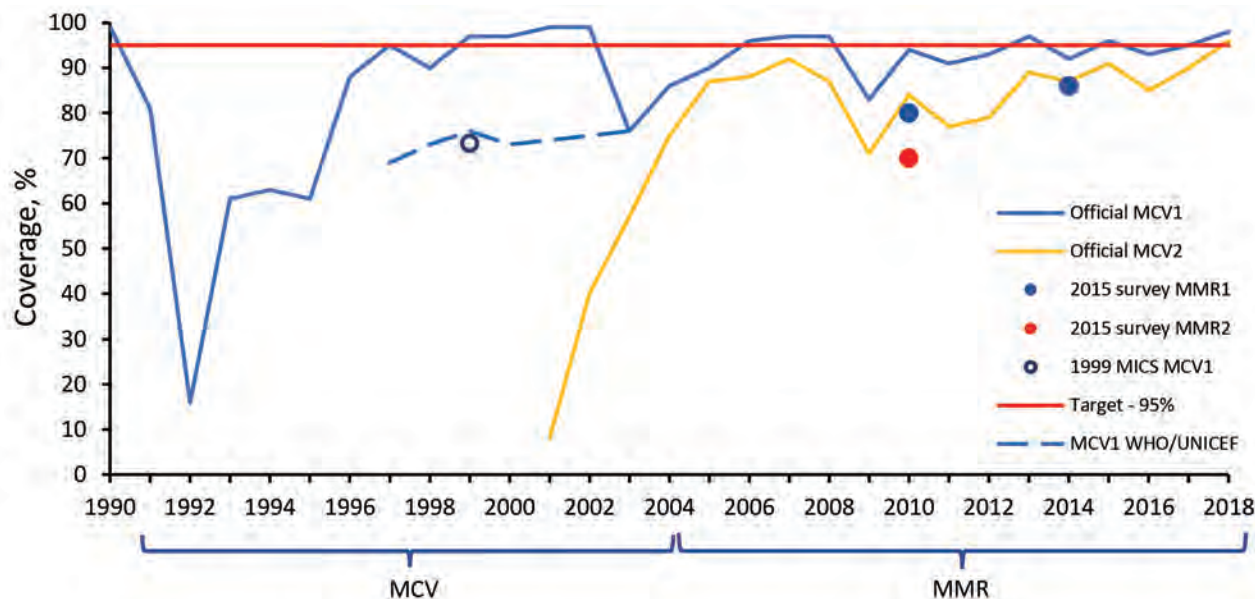
Figure 10. Immunization coverage with measles-containing vaccines in Georgia, 1990–2018. WHO/UNICEF estimates are included for 1997–2003, when official estimates were unreliable because of uncertainty in population numbers. WHO/UNICEF estimates are in agreement with the official estimates from 2003 to present. MCV, measles-containing vaccine; MCV1, first dose of MCV; MCV2, second dose of MCV; MICS, Multiple Indicator Cluster Survey; MMR, measles-mumps-rubella vaccine; MMR1, first dose of MMR; MMR2, second dose of MMR; WHO/UNICEF, World Health Organization/United Nations Children's Fund.

highlighting the problem with delayed vaccinations, although MMR1 coverage by age 24 months improved from 80% in the 2009 cohort to 86% in the 2013 cohort. Timely MMR2 coverage in the 2009 cohort was 70%. Geographic variations were particularly notable for the 2009 cohort, with substantially higher coverage in Batumi than in other sites. MMR1 coverage in the 2013 cohort was lowest in Kutaisi. MMR2 coverage was low in all sites except Batumi (Figure 11).

Main Performance Indicators for Measles Surveillance
During 2013–2017, the discarded case rates ranged from a high of 4.5/100,000 population in 2013 to a low of 1.2/100,000 population in 2016; the >2.0/100,000 population WHO target for this indicator was met only in 2013. Geographic variations were observed, with consistently low discarded case rates in some regions. In 2018, surveillance quality improved substantially, with a discarded case rate of 13.6/100,000 population nationwide and >2/100,000 population in all regions. The >80% target for timeliness of case investigation (1) was consistently met; during 2013–2018, case investigation was initiated within 48 hours of notification for >95% of suspected measles cases. The rate of laboratory investigation of cases (1) has improved substantially, from 13.3% during 2013–2015 to 79.6% in 2016 and 84.6% during 2017–

2018, resulting in a decline in the proportion of clinically compatible cases among all measles cases from 85.3% during 2013–2015 to 19.0% during 2017–2018. Comparison of age distribution and vaccination status of suspected measles cases by final classification category indicated relatively minor differences between laboratory-confirmed cases and those classified as epidemiologically linked or clinically compatible; however, cases in all these categories differed substantially from discarded cases, which had lower proportions of adults and higher proportions of vaccinated persons (Figures 5–7). The highest proportions of unvaccinated cases were observed in the laboratory-confirmed category among children 1–4 years of age (who were age-eligible for MMR1 only), whereas the highest proportions of vaccinated children were observed among epidemiologically linked or clinically compatible cases in children 5–14 years of age (who were age-eligible for both MMR1 and MMR2) (Figure 7). In contrast, in the discarded category, most case-patients <15 years of age were vaccinated; 1-dose recipients were predominately children 1–4 years of age and 2-dose recipients children 5–14 years of age. The similarities between different categories of measles cases and their clear differences from discarded cases during large-scale outbreaks provide additional reassurance regarding the quality of measles surveillance in Georgia.

Discussion

Measles epidemiology in Georgia during 2013–2018 shows widespread circulation and genetic diversity of measles viruses and points to persistent gaps in population immunity across a wide age range that have not been sufficiently addressed by interventions undertaken so far (5,9). Measles in Georgia is associated with substantial economic costs, disease, and deaths; its effects extend beyond the acute illness, as suggested by the recently demonstrated high risk for subacute sclerosing panencephalitis after measles outbreaks in Georgia (17).

Cases among children highlight challenges with routine immunization services. Previous suboptimal MMR1 coverage and vaccination delays, primarily because of unwarranted contraindications (13), likely contributed to the high incidence of measles among children. Although most children receive MMR vaccine, vaccination often happens years after the recommended ages, widening the window of susceptibility, particularly among those age-eligible to MMR1 only.

High incidence among adults and <1-year-old infants results from continued susceptibility among persons born in the 1980s and 1990s (Figure 4) and is consistent with the results of a serosurvey conducted in Georgia immediately after the 2013–2015 outbreak (18), which demonstrated residual seronegativity to measles above the 7% susceptibility threshold needed for preventing outbreaks (19) among young adults. Seronegativity was 10.1% among persons 18–24 years of age, including 14.5% among college students and 8.0% among those 24–29 years of age (18). Analysis of measles transmission patterns demonstrated the important role of adults in virus circulation, suggesting that the adult population could potentially maintain measles transmission in Georgia. Along with widespread susceptibility among adults, small birth cohorts and the generally small number of children in households in Georgia (20) could have contributed to this finding.

Our findings highlight the urgent need to address population susceptibility across all age groups in Georgia. To improve immunity among children, ongoing catch-up immunization of unvaccinated and undervaccinated children should be accelerated, along with further strengthening routine immunization services. Educational efforts promoting awareness among parents and healthcare providers should be intensified to address needless delays attributable to unwarranted contraindications. Effective communication and stakeholder coordination will be needed to ensure the successful implementation of legislation endorsing mandatory childhood vaccinations in Georgia (15). Implementing mandatory MMR vaccination of certain occupational groups (16) and expanding this policy to include all college students could considerably reduce measles transmission among adults in high-risk settings, including HCFs, which have been a substantial contributor to outbreaks. However, reaching susceptible persons in the general adult population who account for a large proportion of cases, remains extremely challenging. The unsuccessful measles-rubella SIA conducted in 2008 (9) was a missed opportunity to close historic immunity gaps in Georgia. Conducting large-scale SIAs in Georgia's present healthcare environment is not feasible because of the lack of defined catchment areas or populations, the voluntary nature of patient registration with HCFs, the lack of mechanisms or motivation for providers to identify and offer vaccinations to unregistered persons, and difficulties in locating historic records to ascertain vaccination status of adults. In addition, acceptance of mass
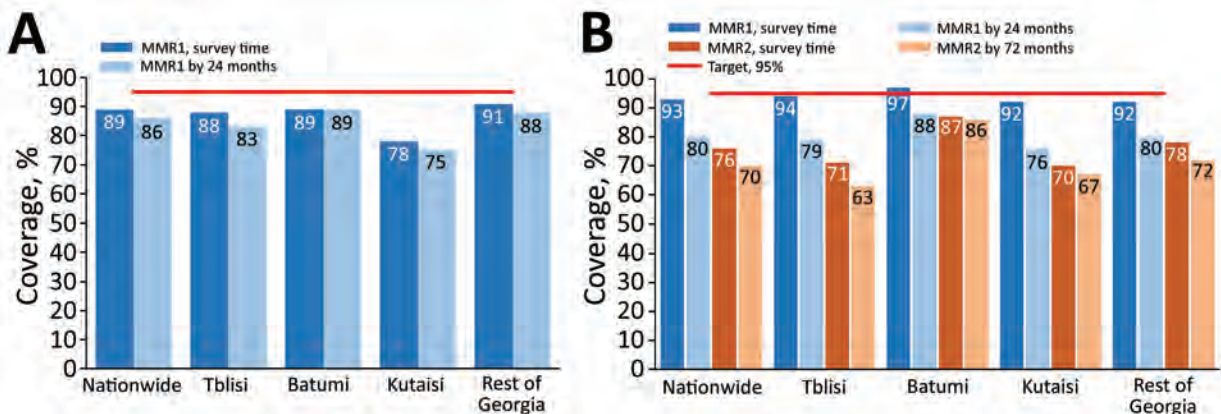
Figure 11. Coverage with the first and the second doses of measles-mumps-rubella vaccine, according to an immunization coverage survey, Georgia, 2015–2016. A) 2013 birth cohort. B). 2009 birth cohort. MMR, measles-mumps-rubella vaccine; MMR1, first dose of MMR; MMR2, second dose of MMR.

immunizations among healthcare providers and public health professionals has been low since the SIA in 2008 (*9*). Under these circumstances, more selective and targeted efforts to control measles outbreaks are being implemented. The result of these efforts will depend primarily on the level of public acceptance. The suboptimal uptake of MMR vaccine among adults indicates the need for interventions to generate vaccine demand.

Information provided by the measles surveillance system is critical for guiding outbreak responses and documenting virus transmission. Measles surveillance in Georgia currently meets most performance indicators. Further improving the quality of case and outbreak investigations will help ensure that all chains of transmission are promptly identified and followed up.

Improved molecular surveillance, notwithstanding certain temporal and geographic gaps, helped demonstrate that virus introductions and local evolution likely contributed to continued transmission. At least 2 variants of measles virus (the main outbreak strain [cluster 1] and the strain in cluster 8) have likely established long-term ($\geq$12 months) transmission in Georgia during the 2013–2015 outbreak, but their circulation has been interrupted since then. Cluster 9, detected during April 2017–February 2018, possibly represents a new introduction. Given the slow rate of measles virus evolution (*21*) and a very low level of measles activity in 2016, the 2-nucleotide difference from the Frankfurt-Main strain probably would not have emerged over the 9-month period since its last detection in Georgia. Cluster 9 strains also might have circulated for $\geq$12 months, but no virus specimens were collected during March–November 2018 (the peak of the outbreak), preventing definitive conclusion.

Controlling measles outbreaks throughout EUR is crucial for achieving the regional elimination goal. The experience in Georgia demonstrates that without adequate and timely response, substantial susceptibility to measles can persist in settings with historically suboptimal coverage even after large-scale outbreaks, thus leaving room for future outbreaks. A similar pattern was observed in Ukraine and in Bosnia and Herzegovina, where, in the absence of appropriate response, the historically underimmunized birth cohorts were affected by repeated outbreaks of measles (*22–27*). In contrast, those countries in the former Soviet Union and Eastern Europe that successfully implemented wide-age SIAs, achieved elimination or substantial reduction of measles incidence for prolonged periods (*4,28,29*). However, implementing traditional SIAs is not feasible in many middle- and high-income countries of EUR. Lessons learned from Georgia could be useful for other countries with immunization systems facing similar challenges related to health-system transitions and the presence of age cohorts or population groups with historically low coverage.

About the Author

Dr. Khetsuriani is a medical epidemiologist at the Global Immunization Division, Center for Global Health, Centers for Disease Control and Prevention. Her current research interests are focused on vaccine-preventable diseases and immunizations, primarily in the European Region. In the past, the fields of her interest also included enteroviruses and other picornaviruses, encephalitis, respiratory viruses, asthma, and allergies.

References

1. World Health Organization. Eliminating measles and rubella. Framework for the verification process in the WHO European Region. 2014 [cited 2019 Oct 2]. http://www.euro.who.int/__data/assets/pdf_file/0009/247356/Eliminating-measles-and-rubella-Framework-for-the-verification-process-in-the-WHO-European-Region.pdf
2. World Health Organization Regional Committee for Europe. Resolution EUR/RC60/R12 on renewed commitment to elimination of measles and rubella and prevention of congenital rubella syndrome by 2015 and sustained support for polio-free status in the WHO European Region. Copenhagen: World Health Organization Regional Office for Europe; 2010 [cited 2019 Oct 2]. http://www.euro.who.int/__data/assets/pdf_file/0016/122236/RC60_eRes12.pdf

3. Patel MK, Dumolard L, Nedelec Y, Sodha SV, Steulet C, Gacic-Dobo M, et al. Progress toward regional measles elimination—worldwide, 2000–2018. MMWR Morb Mortal Wkly Rep. 2019;68:1105–11. https://doi.org/10.15585/mmwr.mm6848a1

4. World Health Organization. Eighth Meeting of the European Regional Verification Commission for Measles and Rubella Elimination. 2019 Jun 12–14. Warsaw, Poland [cited 2019 Oct 2]. http://www.euro.who.int/__data/assets/pdf_file/0019/413236/8th-RVC-Report.pdf

5. Doshi S, Khetsuriani N, Zakhashvili K, Baidoshvili L, Imnadze P, Uzicanin A. Ongoing measles and rubella transmission in Georgia, 2004–05: implications for the national and regional elimination efforts. Int J Epidemiol. 2009;38:182–91. https://doi.org/10.1093/ije/dyn261

6. World Health Organization. Disease incidence series—measles [cited 2019 Oct 2]. http://apps.who.int/immunization_monitoring/globalsummary/timeseries/tsincidencemeasles.html

7. Tatochenko V, Mitjushin IL. Contraindications to vaccination in the Russian Federation. J Infect Dis. 2000;181(Suppl 1):S228–31. https://doi.org/10.1086/315567

8. Khetsuriani N, Imnadze P, Dekanosidze N. Diphtheria epidemic in the Republic of Georgia, 1993–1997. J Infect Dis. 2000;181(Suppl 1):S80–5. https://doi.org/10.1086/315544

9. Khetsuriani N, Imnadze P, Baidoshvili L, Jabidze L, Tatishili N, Kurtsikashvili G, et al. Impact of unfounded vaccine safety concerns on the nationwide measles-rubella immunization campaign, Georgia, 2008. Vaccine. 2010; 28:6455–62. https://doi.org/10.1016/j.vaccine.2010.07.043

10. Ministry of Labor, Health, and Social Welfare of Georgia. National guidelines for measles, rubella, and congenital rubella syndrome surveillance and outbreak control. Tbilisi, 2017 [in Georgian] [cited 2019 Oct 3]. http://ncdc.ge/Pages/User/News.aspx?ID=71654a22-1b85-4ecf-ade3-fbdf8668113a

11. Rota PA, Brown K, Mankertz A, Santibanez S, Shulga S, Muller CP, et al. Global distribution of measles genotypes and measles molecular epidemiology. J Infect Dis. 2011;204(Suppl 1):S514–23. https://doi.org/10.1093/infdis/jir118

12. Santibanez S, Hübschen JM, Ben Mamou MC, Muscat M, Brown KE, Myers R, et al. Molecular surveillance of measles and rubella in the WHO European Region: new challenges in the elimination phase. Clin Microbiol Infect. 2017;23:516–23. https://doi.org/10.1016/j.cmi.2017.06.030

13. Khetsuriani N, Wannemuehler K, Geleishvili M, Komakhidze T. Final report—immunization coverage survey in Georgia, 2015–2016. Tbilisi (Georgia): US Centers for Disease Control and Prevention, Ministry of Labor, Health,and Social Affairs of Georgia; 2017. pp.1–58 [cited 2020 Apr 12]. https://www.ncdc.ge/Pages/User/Documents.aspx?ID=1d6e5458-6504-4e5c-88a1-e547b79d5b47&language=en-US

14. Kumar S, Stecher G, Tamura K. MEGA7: Molecular Evolutionary Genetics Analysis Version 7.0 for Bigger Datasets. Mol Biol Evol. 2016;33:1870–4. https://doi.org/10.1093/molbev/msw054

15. The Law of Georgia on Health Care, as amended 14 November, 2018 [in Georgian] [cited 2019 Oct 2]. https://matsne.gov.ge/ka/document/view/29980

16. Minister of Internally Displaced Persons from the Occupied Territories, Labor, Health, and Social Affairs of Georgia. Decree No. 01–6/N: on approval of the list of occupations subject to mandatory preventive immunizations [in Georgian]. 2019 Jan 2 [cited 2019 Oct 2]. https://www.moh.gov.ge/uploads/files/2019/Failebi/30.01.2019-2.pdf

17. Khetsuriani N, Sanadze K, Abuladze M, Tatishvili N. High risk of subacute sclerosing panencephalitis following measles outbreaks in Georgia. Clin Microbiol Infect. 2020;26:737–42.

18. Khetsuriani N, Chitadze N, Russell S, Ben Mamou M. Measles and rubella seroprevalence among adults in Georgia in 2015: helping guide the elimination efforts. Epidemiol Infect. 2019;147:e319. https://doi.org/10.1017/S0950268819002048

19. Funk S, Knapp JK, Lebo E, Reef SE, Dabbagh AJ, Kretsinger K, et al. Combining serological and contact data to derive target immunity levels for achieving and maintaining measles elimination. BMC Med. 2019;17:180. https://doi.org/10.1186/s12916-019-1413-7

20. National Statistics Office of Georgia (GEOSTAT). 2014 general population census—main results, general information [cited 2019 Oct 2]. http://census.ge/files/results/Census_release_ENG.pdf

21. Beaty SM, Lee B. Constraints on the genetic and antigenic variability of measles virus. Viruses. 2016;8:109. https://doi.org/10.3390/v8040109

22. Spika JS, Aidyralieva C, Mukharskaya L, Kostyuchenko NN, Mulders M, Lipskaya G, et al. Measles outbreak in the Ukraine, 2005–2006. Euro Surveill. 2006;11:E060309.1.

23. Velicko I, Müller LL, Pebody R, Gergonne B, Aidyralieva C, Kostiuchenko N, et al. Nationwide measles epidemic in Ukraine: the effect of low vaccine effectiveness. Vaccine.2008; 26:6980–5. https://doi.org/10.1016/j.vaccine.2008.09.012

24. Ministry of Health of Ukraine, Public Health Center. Operational data on the incidence of measles: September 26, 2019 [in Ukrainian] [cited 2019 Oct 3]. https://phc.org.ua/news/kir-ne-vidstupae-ediniy-nadiyniy-zakhist-vakcinaciya-0

25. World Health Organization. Immunization, vaccines, and biologicals. Data, statistics, and graphics. Case-series [2019 Oct 3]. http://www.who.int/immunization/monitoring_surveillance/data

26. World Health Organization. Reported incidence time series—measles cases, Bosnia and Herzegovina [2019 Oct 21]. https://apps.who.int/immunization_monitoring/globalsummary/incidences?c=BIH%20=%20BIH%20cases%20of%20VPDs

27. Salimović-Bešić I, Šeremet M, Hübschen JM, Hukić M, Tihić N, Ahmetagić S, et al. Epidemiologic and laboratory surveillance of the measles outbreak in the Federation of Bosnia and Herzegovina, February 2014–April 2015. Clin Microbiol Infect. 2016;22:563.e1–7. https://doi.org/10.1016/j.cmi.2016.02.005

28. World Health Organization. Seventh Meeting of the European Regional Verification Commission for Measles and Rubella Elimination (RVC). 2018 Jun 13–15. Paris, France [cited 2019 Oct 2]. http://www.euro.who.int/__data/assets/pdf_file/0008/378926/7th-RVC-Meeting-Report-FINAL.pdf

29. Khetsuriani N, Deshevoi S, Goel A, Spika J, Martin R, Emiroglu N. Supplementary immunization activities to achieve measles elimination: experience of the European Region. J Infect Dis. 2011;204(Suppl 1):S343–52. https://doi.org/10.1093/infdis/jir074

Phage-Mediated Immune Evasion and Transmission of Livestock-Associated Methicillin-Resistant *Staphylococcus aureus* in Humans

Raphael N. Sieber, Tinna R. Urth, Andreas Petersen, Camilla H. Møller, Lance B. Price,
Robert L. Skov, Anders R. Larsen, Marc Stegger,[1] and Jesper Larsen[1]

Medscape EDUCATION ACTIVITY

In support of improving patient care, this activity has been planned and implemented by Medscape, LLC and Emerging Infectious Diseases. Medscape, LLC is jointly accredited by the Accreditation Council for Continuing Medical Education (ACCME), the Accreditation Council for Pharmacy Education (ACPE), and the American Nurses Credentialing Center (ANCC), to provide continuing education for the healthcare team.

Medscape, LLC designates this Journal-based CME activity for a maximum of 1.00 **AMA PRA Category 1 Credit(s)™**. Physicians should claim only the credit commensurate with the extent of their participation in the activity.

Successful completion of this CME activity, which includes participation in the evaluation component, enables the participant to earn up to 1.0 MOC points in the American Board of Internal Medicine's (ABIM) Maintenance of Certification (MOC) program. Participants will earn MOC points equivalent to the amount of CME credits claimed for the activity. It is the CME activity provider's responsibility to submit participant completion information to ACCME for the purpose of granting ABIM MOC credit.

All other clinicians completing this activity will be issued a certificate of participation. To participate in this journal CME activity: (1) review the learning objectives and author disclosures; (2) study the education content; (3) take the post-test with a 75% minimum passing score and complete the evaluation at http://www.medscape.org/journal/eid; and (4) view/print certificate. For CME questions, see page 2796.

Release date: October 16, 2020; Expiration date: October 16, 2021

Learning Objectives

Upon completion of this activity, participants will be able to**:**

- Describe the impact of IEC- and *tarP*-harboring phages on household transmission of LA-MRSA in the North Denmark Region during 2004–2011, according to whole-genome sequencing and epidemiologic investigations

- Determine the association of IEC- and *tarP*-harboring phages in LA-MRSA in the North Denmark Region during 2004–2011 with spread in the general population, according to an analysis of all Danish patients who had an episode of LA-MRSA infection during 2007–2018

- Identify clinical and public health implications of the effect of IEC- and *tarP*-harboring phages on household transmission of LA-MRSA in the North Denmark Region during 2004–2011, and of their association with spread into the general population

CME Editor

Dana C. Dolan, BS, Copyeditor, Emerging Infectious Diseases. *Disclosure: Dana C. Dolan, BS, has disclosed no relevant financial relationships.*

CME Author

Laurie Barclay, MD, freelance writer and reviewer, Medscape, LLC. *Disclosure: Laurie Barclay, MD, has disclosed no relevant financial relationships.*

Authors

Disclosures: **Raphael N. Sieber, PhD; Tinna Urth, MPH; Andreas Petersen, PhD; Camilla Møller, MD, PhD; Lance B. Price, PhD; Robert L. Skov, MD; Anders Larsen, PhD; Marc Stegger, PhD;** and **Jesper Larsen, PhD,** *have disclosed no relevant financial relationships.*

Author affiliations: Statens Serum Institut, Copenhagen, Denmark (R.N. Sieber, T.R. Urth, A. Petersen, C.H. Møller, R.L. Skov, A.R. Larsen, M. Stegger, J. Larsen); Translational Genomics Research Institute, Flagstaff, Arizona, USA (L.B. Price, M. Stegger); George Washington University, Washington, DC, USA (L.B. Price)

[1]These senior authors contributed equally to this article.

Livestock-associated methicillin-resistant *Staphylococcus aureus* (LA-MRSA) can acquire phage-encoded immune modulators, such as the immune evasion cluster (IEC), which protects bacteria from components of the human innate immune system, and the enzyme TarP, which protects against antibody-mediated immune recognition. We used whole-genome sequencing and epidemiologic investigations to study the effects of IEC- and *tarP*-harboring phages on household transmission of LA-MRSA in North Denmark Region during 2004–2011. We reviewed information about all patients throughout Denmark who experienced LA-MRSA infection during 2007–2018 to determine whether IEC is associated with increased spread into the general population. Horizontal acquisition of IEC in the human host was associated with increased household transmission of LA-MRSA and spillover into the community and healthcare settings, whereas we found no evidence to suggest that IEC-positive LA-MRSA isolates have become self-sustainable in the general population. By contrast, TarP did not seem to influence household transmission of LA-MRSA.

Livestock-associated methicillin-resistant *Staphylococcus aureus* (LA-MRSA) clonal complex (CC) 398 is a major cause of zoonotic disease in Denmark and several other countries in Europe that have industrial pig production (*1–3*). In Denmark, the prevalence of LA-MRSA CC398 in pig farms increased from 3.5% in 2008 to ≈90% in 2018, when LA-MRSA CC398 accounted for 21% of all human MRSA infections (*3*). Most LA-MRSA CC398 infections occur in young and otherwise healthy livestock workers and their household contacts (*3–5*). Although LA-MRSA CC398 seems to be poorly adapted for human-to-human transmission (*6*), it is nonetheless able to spread to and cause serious illness and even death in elderly and immunocompromised persons in community and healthcare settings (*3–5*).

S. aureus uses a diverse range of immune-evasive strategies to maintain a lifelong relationship with the human host, many of which are encoded on phages and other mobile genetic elements (*7*). Of note, human *S. aureus* clones harbor a genetic element, the immune evasion cluster (IEC), on a 44-kb ΦSa3int prophage that is stably integrated into the *hlb* gene on the bacterial chromosome (*8,9*). The IEC element encodes ≥1 immune modulators, including staphylococcal complement inhibitor, chemotaxis inhibitory protein of staphylococci, staphylokinase, staphylococcal enterotoxin A, and staphylococcal enterotoxin P, which interact specifically with components of the human innate immune system (*7*). LA-MRSA CC398 isolates are descendants of a human variant of *S. aureus* CC398 but

have lost the ΦSa3int prophage and the associated IEC element in connection with the host switch event (*10*); this change provides a potential explanation for the observed relatively low human-to-human transmissibility of LA-MRSA CC398 (*6*). However, some studies have shown that LA-MRSA CC398 might be capable of readapting to the human host through acquisition of phage-encoded immune modulators. For example, a Denmark study showed that 6% of human LA-MRSA CC398 isolates collected during 2004–2011 harbored the IEC element, whereas a more recent study revealed that 40% of LA-MRSA CC398 isolates from pigs in Denmark produce another phage-encoded immune modulator enzyme known as TarP, which enables *S. aureus* to subvert antibody-mediated immune recognition by altering a dominant cell surface epitope known as wall teichoic acids (WTA) (*3,11*).

These earlier findings raise important questions about the source and dynamics of phages encoding IEC and TarP in LA-MRSA CC398 and their role in host adaptation. In this study, we sequenced and compared a collection of epidemiologically well-characterized LA-MRSA CC398 isolates from humans and pigs in North Denmark Region to determine their population structure and the contribution of IEC and TarP to household transmission. We also used national surveillance data to further investigate whether IEC plays a role during spread of LA-MRSA CC398 into the community and healthcare settings.

Data used in this study were collected as part of the national MRSA surveillance program, as approved by the Danish Data Protection Agency (protocol no. 2001-14-0021). The National Committee on Health Research Ethics waived the need for approval and informed consent because data and biologic material were fully anonymized and collected in compliance with national legislation on statutory notification of MRSA in humans.

Methods

Study Population

North Denmark Region (≈7,900 km²) is a semirural area in northwest Denmark that had a population of ≈580,000 persons and ≈3 million pigs in 2011 (http://www.statbank.dk). We identified the study population using surveillance data collected by the regional infection control staff in North Denmark Region; it included all patients colonized or infected with LA-MRSA CC398 during 2004–2011, as well as all their household contacts who tested negative during the same period. We interviewed all of these persons to obtain relevant information, including sex, age, livestock contact,

residential address, and workplace, and assigned each to 1 of 3 categories: livestock-exposed persons (direct contact); household contacts of livestock-exposed persons (indirect contact); and persons not connected to livestock production (no contact). We defined livestock-exposed persons as primary cases in their households, and the index person as the primary case in households with no connection to livestock production.

Study Isolates and Data Aggregation

The study isolates comprised 96 human LA-MRSA CC398 isolates from North Denmark Region collected by regional infection control staff during 2004–2011 and 45 LA-MRSA CC398 isolates collected from pigs (1 isolate per farm) in North Denmark Region in 2014 (Appendix 1 Table 1, https://wwwnc.cdc.gov/EID/article/26/11/20-1442-App1.xlsx). The human isolates have been characterized previously for *spa* type, presence of IEC, and antimicrobial susceptibilities (*3*); the pig isolates originated from a study investigating the population structure and dynamics of LA-MRSA CC398 in the pig population in Denmark (*12*). We used whole-genome sequencing and bioinformatics analyses to study the phylogenetic distribution, genetic diversity, and host association of IEC-harboring and *tarP*–harboring prophages among the 141 study isolates (Appendix 2, https://wwwnc.cdc.gov/EID/article/26/11/20-1442-App2.pdf).

Analysis of National Surveillance Data

MRSA has been notifiable in Denmark since November 2006. As part of the national MRSA surveillance program, local clinical microbiology departments perform *S. aureus* identification and antimicrobial susceptibility testing and submit all confirmed MRSA isolates to the National Reference Laboratory for Antimicrobial Resistance at Statens Serum Institut (Copenhagen, Denmark), which collects patient information from general practitioners and assesses the *spa* type or the clonal complex and the presence or absence of the IEC element. The following data are collected for each case: sex, age, livestock contact, residential address, indication for testing (screening or infection), and hospitalization dates. Cases without direct or indirect livestock contact are defined as healthcare-onset (HO) if the culture is obtained ≥48 hours after admission; healthcare-associated community-onset (HACO) if the person has had contact with the healthcare setting within the preceding 12 months or the culture is obtained within the first 48 hours after admission; or community-onset (CO) if no other criteria are met. For this study, we retrieved the following information about all patients in Denmark who had an episode of LA-MRSA CC398

infection during January 2007–December 2018 (n = 1,545): sex; age; direct, indirect, or no livestock contact; location of disease onset (e.g., HO, HACO, or CO); and presence or absence of the IEC element in the corresponding LA-MRSA CC398 isolate. We calculated the excess number of clinical cases due to increased spread of IEC-positive isolates into a given patient group of interest as the total number of cases in the patient group of interest multiplied by the difference between the proportion of IEC-positive isolates in the patient group of interest (the sink) and the patient group with direct contact to livestock (the source).

Statistical Analysis

We used Fisher exact test to analyze categorical data and Student t test to analyze continuous data (GraphPad Prism version 5; GraphPad, https://www.graphpad.com). We reported prevalence differences between different groups as prevalence ratios (PRs) and 95% CIs. The significance level was set at α = 0.05.

Results

Study Population

A total of 96 patients were colonized or infected with LA-MRSA CC398 in North Denmark Region during 2004–2011, including 67 primary cases and 29 secondary cases from 65 households. A total of 71 household contacts tested negative. The 67 primary cases comprised 57 persons with direct animal contact, 2 with indirect animal contact, and 8 with no animal contact. Those with direct animal contact included 44 pig farm employees from 42 households and 23 animal farms (2 households each contained 2 pig farm employees), 3 mink farm employees from 3 households and animal farms, 1 cattle farm employee, 1 turkey farm employee, 1 pig veterinarian, 3 lorry drivers transporting pigs from 3 households, 2 pig abattoir workers from 2 households, and 2 craftsmen working in pig stables from 2 households. Persons with indirect contact were from 2 households (a wife and a child of pig farm employees who were never tested), and those with no contact were from 8 households.

Distribution of IEC and *tarP* in LA-MRSA CC398

Most of the human isolates collected from persons living in the same household clustered together, with an average pairwise single-nucleotide polymorphism (SNP) distance of 5.9 (range 0–18 SNPs) and were genotypically homogeneous with respect to presence of specific IEC-harboring and *tarP*-harboring prophages (Appendix 2 Figure). Furthermore, human isolates from different households connected to the same animal farm

also tended to cluster together but were genotypically more diverse than isolates from the same household (19.6 SNPs [range 0–156 SNPs] in different households versus 6.7 SNPs [range 0–18 SNPs] in the same household; p = 0.027). Pig isolates collected from unique farms were widely distributed across the phylogeny; the average pairwise SNP distance was 95.4 (range 3–224 SNPs).

We identified IEC in 20 isolates, which clustered within a closely related clade (Appendix 2 Figure). The IEC-harboring ΦSa3int prophages could be divided into 6 variants (I–VI) and 5 phylogenetic clusters (A–E) on the basis of their phylogenetic relationship, IEC type, and chromosomal integration site (Table 1; Figure 1). Each of the 6 ΦSa3int variants was unique to isolates from a single household. The 6 households comprised 4 pig farm employees (ΦSa3int-I–IV), a pig veterinarian (ΦSa3int-V), and a mink farm employee (ΦSa3int-VI), and their household contacts (Table 1). We also detected ΦSa3int-VI in 3 pig isolates that were closely related to the isolates from the mink farm employee's household; the prophage was furthermore highly similar to ΦSa3int-V present in the isolate from the pig veterinarian but integrated into a different part of the chromosome (Table 1).

We identified the *tarP* gene in 45 isolates, which were more widely distributed across the phylogeny than the IEC-positive isolates (Appendix 2 Figure). Analysis of the genetically linked *int* genes showed that *tarP* was carried on 5 different prophages (ΦSa1int, ΦSa3int, ΦSa7int, ΦSa9int, and a prophage with an untypeable *int* gene hereafter referred to as ΦUT1). BLASTN searches (https://blast.ncbi.nlm.nih.gov/Blast.cgi) showed that the *int* gene in ΦUT1 was 100% identical to the *int* gene in the bovine *S. aureus* phage ΦDW2 (GenBank accession no. KJ140076). We found Φ*tarP*-Sa9int exclusively in pig isolates (n = 15), whereas the other *tarP*-harboring prophages were identified in 25 human isolates from 16 households and in 5 pig isolates.

IEC was more prevalent in human isolates (17/96; 18%) than in pig isolates (3/45; 6.7%), although the difference was not statistically significant (PR 2.66, 95% CI 0.90–8.26; p = 0.12). By contrast, *tarP* was significantly less prevalent in human isolates (25/96; 26%) than in pig isolates (20/45; 44%) (PR 0.59, 95% CI 0.37–0.95; p = 0.034). The IEC element in the 3 pig isolates was genetically linked to *tarP* on ΦSa3int-V and ΦSa3int-VI (Table 1; Appendix 2 Figure).

Role of IEC and *tarP* during Household Transmission of LA-MRSA CC398 in North Denmark Region

Household transmission of LA-MRSA CC398 was based on detection of secondary cases of colonization or infection with isolates that were closely related and genotypically indistinguishable from the isolate of the primary case. Households consisting of 1 person (n = 26) and households with ≥2 persons reporting direct animal contact (n = 2) were excluded from both analyses. In addition, 1 household with a mixed population of IEC-positive and IEC-negative isolates was excluded from the corresponding analysis.

IEC-positive isolates were present in 14% (5/36) of the eligible households. Secondary transmission occurred more often in IEC-positive households (4/5; 80%) than in IEC-negative households (10/31; 32%), although the difference was not statistically significant (PR 2.48, 95% CI 1.04–4.64; p = 0.064). The proportion of secondary cases was significantly higher in IEC-positive households (65%; 11/17) than in IEC-negative households (22%; 16/74) (PR 2.99, 95% CI 1.65–5.12; p = 0.0010). Isolates carrying *tarP* were present in 32% (12/37) of the eligible households. We

Table 1. Distribution of IEC-harboring ΦSa3int prophages among livestock-associated methicillin-resistant *Staphylococcus aureus* CC398 isolates from North Denmark Region, Denmark*

Variant	Phylogenetic cluster†	IEC type	Integration site‡	*tarP*	Isolate origin	Household ID	Farm ID
I	A	B	0723–0724	–	1 pig farm employee and 4 household members	H02	F01
II	B	E	2238	–	1 pig farm employee and 1 household member	H30	F01
III	C	B	2059 (*hlb*)	–	1 pig farm employee and 3 household members	H63	F04
IV	D	B	2591 (*cidA*)	–	1 pig farm employee	H51	F07
V	E	F	2059 (*hlb*)	+	1 pig veterinarian	H46	None
VI	E	F	2644	+	1 mink farm employee and 3 household members	H49	F21
	E	F	2644	+	Pig	NA	A
	E	F	2644	+	Pig	NA	B
	E	F	2644	+	Pig	NA	C

*Allocation of ΦSa3int prophages into variants (ΦSa3int-I to ΦSa3int-VI) was based on their phylogenetic relationship, IEC type, and chromosomal integration site. CC, clonal complex; ID, identification; IEC, immune evasion cluster; NA, not applicable; –, negative, +, positive.
†Phylogenetic clusters are illustrated in Figure 1.
‡Numbers refer to annotated genes in reference strain S0385 (GenBank accession no. NC_017333).
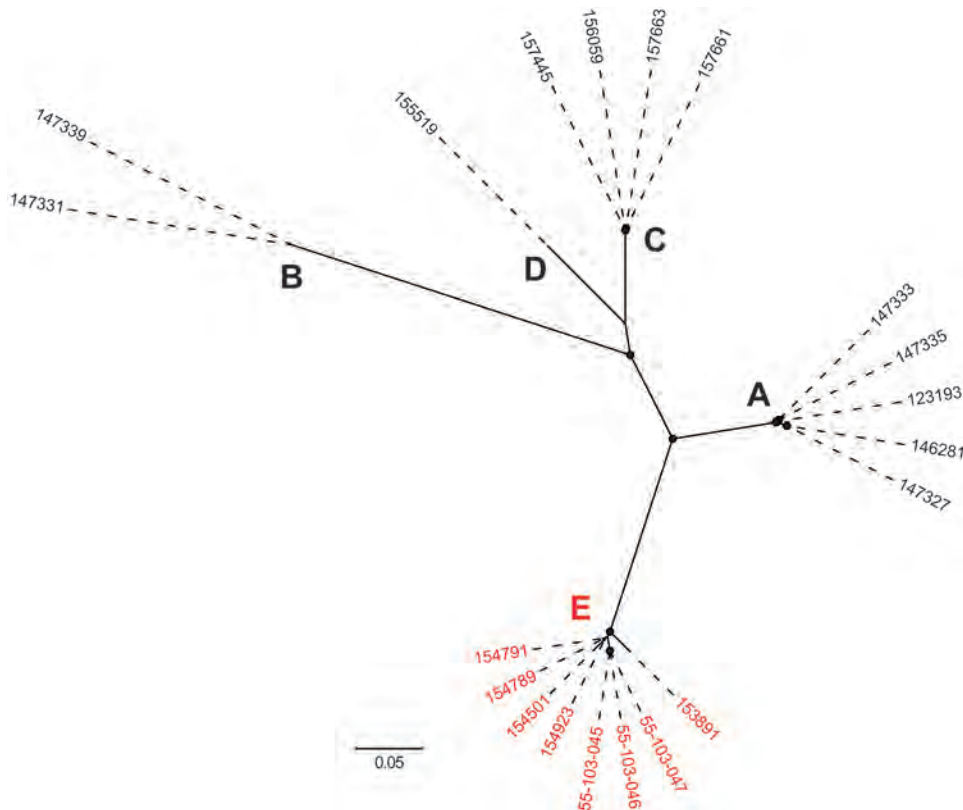
Figure 1. Maximum-likelihood phylogeny showing the genetic diversity of the 20 IEC-harboring ΦSa3int prophages identified in livestock-associated methicillin-resistant *Staphylococcus aureus* CC398 isolates from North Denmark Region, Denmark. Capital letters indicate phylogenetic clusters (A–E). Red text indicates ΦSa3int prophages harboring both IEC and *tarP* (cluster E). The phylogeny was estimated for 795 high-quality core SNPs. Filled circles at nodes indicate bootstrap values >90%. Scale bar represents number of nucleotide substitutions per variable site.

saw no differences in occurrence of secondary transmission between *tarP*-positive households (5/12; 42%) and *tarP*-negative households (9/25; 36%) (PR 1.16, 95% CI 0.47–2.55; p = 1.00) or in the proportion of secondary cases between *tarP*-positive households (10/33; 30%) and *tarP*-negative households (17/62; 27%) (PR 1.28, 95% CI 0.65– 2.42; p = 0.48). The average number of household contacts per household, excluding the primary case, did not differ significantly between IEC-positive (3.4; range 2–5) and IEC-negative households (2.4; range 1–7; p = 0.17) or between *tarP*-positive (2.8; range 1–7) and *tarP*-negative households (2.5; range, 1–5; p = 0.62). These findings indicate that IEC, but not *tarP*, facilitates household transmission of LA-MRSA CC398.

Prevalence of IEC among LA-MRSA CC398 Isolates in Persons with No Livestock Contact

We investigated whether IEC also plays a role during spread of LA-MRSA CC398 in the general population, on the assumption that persons with direct livestock contact serve as the source of transmission to their household contacts (i.e., persons with indirect livestock contact) and into the local community, through which the bacterium is transmitted into healthcare settings. The analysis included 1,545 isolates from patients in 4 groups: patients with direct livestock contact (n = 727); patients with indirect livestock contact (n = 256); patients with CO infection (n = 383); and patients with HO/HACO infection (n = 179). The results showed that the proportion of IEC-positive isolates increased along this hypothetical transmission chain, from 3.4% in patients with direct contact to livestock to 6.3% (PR 1.82, 95% CI 0.99–3.31; p = 0.068) in patients with indirect contact to livestock, 7.1% (PR 2.05, 95% CI 1.21–3.46; p = 0.010) in patients with CO infection, and 11% (PR 3.25, 95% CI 1.85–5.65; p = 0.0001) in patients with HO/HACO infection (Table 2). The excess number of clinical cases attributable to increased spread of IEC-positive isolates ranged from 7 (2.8%) among persons with indirect livestock contact to 14 in both the community (3.6%) and healthcare (7.7%) settings (Table 2). These findings demonstrate an association of IEC with increased human-to-human transmission and excess disease burden of LA-MRSA CC398.

If IEC-positive isolates become fixed (i.e., self-sustainable) in the general population, we expect their proportion to increase over time in patients with CO and HO/HACO infections, compared with patients with direct contact to livestock. However, although the number of LA-MRSA CC398 infections increased in all 4 patient groups during 2007–2018 (Figure 2,

Table 2. Patient characteristics and presence of IEC among livestock-associated methicillin-resistant *Staphylococcus aureus* CC398 cases and isolates, North Denmark Region, Denmark*

Patient group	No. isolates	Male:female ratio	Median age, y (range)	% IEC	No. IEC-related excess cases (% all cases)	Prevalence ratio (95% CI)	p value
Patients with livestock contact							
Direct contact	727	3.2	33 (0–93)	3.4	Referent	Referent	Referent
Indirect contact	256	0.59	22 (0–91)	6.3	7 (2.8)	1.82 (0.99–3.31)	0.068
Patients with CO infection	383	1.0	52 (0–98)	7.1	14 (3.6)	2.05 (1.21–3.46)	0.010
Patients with HO/HACO infection	179	1.1	66 (0–97)	11	14 (7.7)	3.25 (1.85–5.65)	0.0001

*CC, clonal complex; CO, community-onset; HACO, healthcare-associated community-onset; HO, healthcare-onset; IEC, immune evasion cluster.

panel A), the prevalence ratio of IEC-positive isolates among patients with CO and HO/HACO infections either decreased or remained relatively stable over the years (Figure 2, panel B).

Discussion

Successful spread of *S. aureus* in humans depends upon the bacterium's ability to survive and multiply in newly colonized persons. For example, *S. aureus* must compete with other bacteria and avoid the innate and adaptive immune defenses of the skin and nasal environments. In this study, we have shown that acquisition of IEC, but not *tarP*, is associated with increased household transmission of LA-MRSA CC398 and excess spread into the community and healthcare settings. The findings should be interpreted with some caution because of the small number of households and cases analyzed, and more follow-up studies should be done to further evaluate the relative contribution of IEC and other risk factors, such as household size (*13*), to the spread of LA-MRSA CC398 in humans.

Animal and human studies have shown that IEC is ubiquitous in human *S. aureus* clones, whereas it is consistently absent in livestock-associated *S. aureus* clones (*9,10*). Staphylococcal complement inhibitor and other IEC-encoded immune modulators have human-specific activities toward central components of the innate immune response, such as neutrophils and complements, and are produced in both healthy carriers and patients with *S. aureus* infection (*14–16*). Our findings suggest that IEC promotes survival of *S. aureus* in the human host, which in turn is expected to increase the likelihood of human-to-human transmission.

Nonetheless, the disease burden of IEC-positive LA-MRSA CC398 isolates in the community and healthcare settings remains relatively low in Denmark. We saw no suggestion that they will become fixed in the general population; van Alen et al. reached the same conclusion after finding a low, albeit slightly increasing, prevalence of IEC among LA-MRSA CC398 isolates from hospital patients during 2000–2015, ranging from 1.1% during 2000–2006 to 3.9% during 2007–2015 (*17*). Research indicates several possible reasons why IEC-positive LA-MRSA CC398 isolates have not become self-sustainable in humans. First, our findings showed that the 20 IEC-positive isolates from North Denmark Region clustered within a closely related clade, indicating that not all LA-MRSA CC398 isolates have the same ability to acquire ΦSa3int phages. Second, a recent study (*18*) has shown that LA-MRSA CC398 carries substitutions at the usual attachment site (*att*B) located within the *hlb* gene, which interferes with phage integration and might explain why ΦSa3int phages often integrate into other genomic regions than
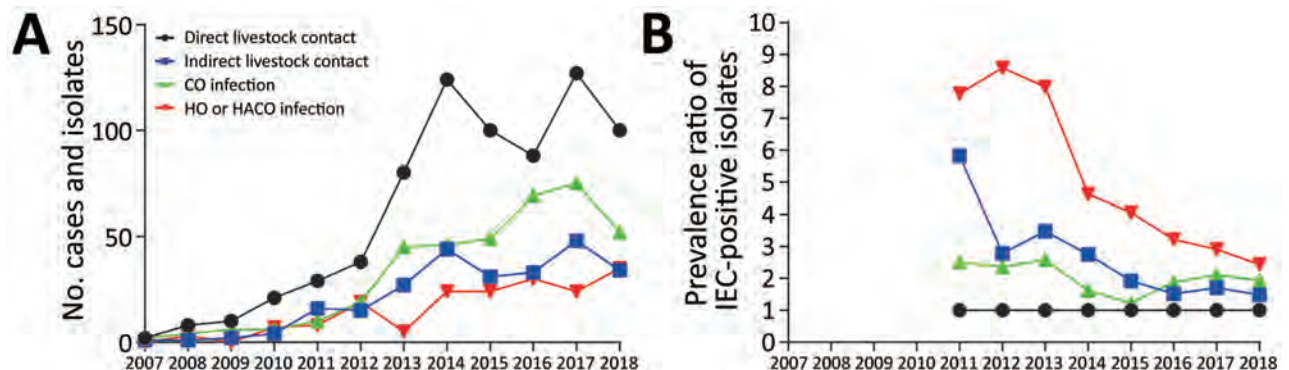
Figure 2. Temporal trends of livestock-associated methicillin-resistant *Staphylococcus aureus* infections in Denmark. A) Annual number of cases and isolates. B) Proportion of IEC-positive isolates in patients with indirect livestock contact, CO, and HO/HACO infection compared with patients who had direct contact with livestock. Data are shown as prevalence ratios (5-year rolling averages). CO, community-onset; HACO, healthcare-associated community-onset; HO, healthcare-onset; IEC, immune evasion cluster.

the *hlb* gene in LA-MRSA CC398 through recombination between the phage attachment site (*att*P) and alternative *att*B sites, as demonstrated in our study and others (*17–19*). Third, it is possible that LA-MRSA CC398 has undergone other genetic changes, in addition to losing the IEC-harboring ΦSa3int prophage during the human-to-animal host switch event, that are beneficial in the livestock reservoir but detrimental in the human host. For example, LA-MRSA CC398 isolates from Denmark have acquired several mobile genetic elements encoding resistance to a wide range of the most frequently used antimicrobial drugs in pigs, including β-lactams, aminoglycosides, macrolides, tetracyclines, and zinc (*12*), which are likely to exert a fitness cost outside the livestock reservoir (*20*). This possibility is supported by our recent finding that LA-MRSA CC398 isolates from hospital patients carry far fewer antimicrobial resistance genes of veterinary importance than LA-MRSA CC398 isolates from pigs (*21*).

The widespread distribution of IEC among human *S. aureus* clones, the phylogenetic clustering of IEC-harboring ΦSa3int prophages in LA-MRSA CC398 isolates from the same household, and the low prevalence of IEC in LA-MRSA CC398 isolates from pigs suggest that acquisition of IEC by LA-MRSA CC398 mainly occurs through transfer of ΦSa3int phages from human *S. aureus* donors circulating in households. In support of this view, we found little evidence for phage transfer or transmission of IEC-positive isolates between pigs and humans. An exception was a possible transmission chain involving 3 IEC-positive isolates from pigs and 4 isolates from a mink farm employee and his household members and a possible phage transfer event between this cluster of isolates and an isolate from a pig veterinarian. Of note, the IEC-harboring ΦSa3int prophage found in the 3 pig isolates also encoded TarP, thus raising the possibility that IEC can be passively maintained in the pig population by co-selection for other traits.

TarP-mediated protection against anti-WTA antibodies did not seem to influence household transmission of LA-MRSA CC398 in our study despite the fact that anti-staphylococcal antibodies are present at high levels in serum and nasal secretions of both persistent *S. aureus* carriers and noncarriers (*15,16*). Instead, there is evidence that the much more widely distributed staphylococcal protein A (SpA), which is produced by all known human and livestock-associated *S. aureus* clones, is sufficient for escaping the adaptive immune response. SpA contains several immunoglobulin-binding domains capable of binding both the Fcγ of IgG antibodies and the Fab of V_H3-idiotype antibodies, thereby limiting opsonophagocytosis and broad-spectrum antibody responses to other secreted and surface-bound antigens during *S. aureus* colonization and infection (*22–30*).

In summary, our study suggests that acquisition of IEC, but not *tarP*, is associated with increased household transmission of LA-MRSA CC398 and spillover into the community and healthcare settings, which might also explain why IEC is widespread among human *S. aureus* clones. Despite these findings, the attributable disease burden remains relatively low in Denmark, and we found no evidence to suggest that they have become self-sustainable in the general population. However, the dynamic nature of *S. aureus* genome evolution and host adaptability, as documented here and elsewhere, underscores the need for continued surveillance at the human–animal interface to detect evolutionary as well as epidemiologic changes that affect public health.

About the Author

Dr. Sieber is a research associate in infectious diseases at Statens Serum Institut, Copenhagen. His research interests are the evolution of opportunistic pathogens and their epidemiology.

References

1. van Cleef BA, Monnet DL, Voss A, Krziwanek K, Allerberger F, Struelens M, et al. Livestock-associated methicillin-resistant *Staphylococcus aureus* in humans, Europe. Emerg Infect Dis. 2011;17:502–5. https://doi.org/10.3201/eid1703.101036
2. Danish Integrated Antimicrobial Resistance Monitoring and Research Programme. DANMAP 2018: use of antimicrobial agents and occurrence of antimicrobial resistance in bacteria from food animals, food, and humans in Denmark. 2019 Sep [cited 2020 Mar 9]. https://www.danmap.org/-/media/arkiv/projekt-sites/danmap/danmap-reports/danmap-2018/danmap_2018.pdf
3. Kinross P, Petersen A, Skov R, Van Hauwermeiren E, Pantosti A, Laurent F, et al.; European Human LA-MRSA Study Group. Livestock-associated meticillin-resistant *Staphylococcus aureus* (MRSA) among human MRSA

isolates, European Union/European Economic Area countries, 2013. Euro Surveill. 2017;22:16-00696. https://doi.org/10.2807/1560-7917.ES.2017.22.44.16-00696

4. Larsen J, Petersen A, Sørum M, Stegger M, van Alphen L, Valentiner-Branth P, et al. Meticillin-resistant *Staphylococcus aureus* CC398 is an increasing cause of disease in people with no livestock contact in Denmark, 1999 to 2011. Euro Surveill. 2015;20:30021. https://doi.org/10.2807/1560-7917.ES.2015.20.37.30021

5. Larsen J, Petersen A, Larsen AR, Sieber RN, Stegger M, Koch A, et al.; Danish MRSA Study Group. Emergence of livestock-associated methicillin-resistant *Staphylococcus aureus* bloodstream infections in Denmark. Clin Infect Dis. 2017;65:1072–6. https://doi.org/10.1093/cid/cix504

6. Hetem DJ, Bootsma MC, Troelstra A, Bonten MJ. Transmissibility of livestock-associated methicillin-resistant *Staphylococcus aureus.* Emerg Infect Dis. 2013;19:1797–802. https://doi.org/10.3201/eid1911.121085

7. Thammavongsa V, Kim HK, Missiakas D, Schneewind O. Staphylococcal manipulation of host immune responses. Nat Rev Microbiol. 2015;13:529–43. https://doi.org/10.1038/nrmicro3521

8. Bae T, Baba T, Hiramatsu K, Schneewind O. Prophages of *Staphylococcus aureus* Newman and their contribution to virulence. Mol Microbiol. 2006;62:1035–47. https://doi.org/10.1111/j.1365-2958.2006.05441.x

9. Richardson EJ, Bacigalupe R, Harrison EM, Weinert LA, Lycett S, Vrieling M, et al. Gene exchange drives the ecological success of a multi-host bacterial pathogen. Nat Ecol Evol. 2018;2:1468–78. https://doi.org/10.1038/s41559-018-0617-0

10. Price LB, Stegger M, Hasman H, Aziz M, Larsen J, Andersen PS, et al. *Staphylococcus aureus* CC398: host adaptation and emergence of methicillin resistance in livestock. MBio. 2012;3:e00305-11. https://doi.org/10.1128/mBio.00305-11

11. Gerlach D, Guo Y, De Castro C, Kim SH, Schlatterer K, Xu FF, et al. Methicillin-resistant *Staphylococcus aureus* alters cell wall glycosylation to evade immunity. Nature. 2018;563:705–9. https://doi.org/10.1038/s41586-018-0730-x

12. Sieber RN, Skov RL, Nielsen J, Schulz J, Price LB, Aarestrup FM, et al. Drivers and dynamics of methicillin-resistant livestock-associated *Staphylococcus aureus* CC398 in pigs and humans in Denmark. MBio. 2018;9:e02142-18. https://doi.org/10.1128/mBio.02142-18

13. Di Ruscio F, Guzzetta G, Bjørnholt JV, Leegaard TM, Moen AEF, Merler S, et al. Quantifying the transmission dynamics of MRSA in the community and healthcare settings in a low-prevalence country. Proc Natl Acad Sci U S A. 2019;116:14599–605. https://doi.org/10.1073/pnas.1900959116

14. Rooijakkers SH, Ruyken M, Roos A, Daha MR, Presanis JS, Sim RB, et al. Immune evasion by a staphylococcal complement inhibitor that acts on C3 convertases. Nat Immunol. 2005;6:920–7. https://doi.org/10.1038/ni1235

15. Verkaik NJ, de Vogel CP, Boelens HA, Grumann D, Hoogenboezem T, Vink C, et al. Anti-staphylococcal humoral immune response in persistent nasal carriers and noncarriers of *Staphylococcus aureus.* J Infect Dis. 2009;199:625–32. https://doi.org/10.1086/596743

16. Verkaik NJ, Lebon A, de Vogel CP, Hooijkaas H, Verbrugh HA, Jaddoe VW, et al. Induction of antibodies by *Staphylococcus aureus* nasal colonization in young children. Clin Microbiol Infect. 2010;16:1312–7. https://doi.org/10.1111/j.1469-0691.2009.03073.x

17. van Alen S, Ballhausen B, Kaspar U, Köck R, Becker K. Prevalence and genomic structure of bacteriophage phi3 in human-derived livestock-associated methicillin-resistant *Staphylococcus aureus* isolates from 2000 to 2015. J Clin Microbiol. 2018;56:e00140–18. https://doi.org/10.1128/JCM.00140-18

18. Tang Y, Nielsen LN, Hvitved A, Haaber JK, Wirtz C, Andersen PS, et al. Commercial biocides induce transfer of prophage Φ13 from human strains of *Staphylococcus aureus* to livestock CC398. Front Microbiol. 2017;8:2418. https://doi.org/10.3389/fmicb.2017.02418

19. Kraushaar B, Hammerl JA, Kienöl M, Heinig ML, Sperling N, Dinh Thanh M, et al. Acquisition of virulence factors in livestock-associated MRSA: lysogenic conversion of CC398 strains by virulence gene-containing phages. Sci Rep. 2017;7:2004. https://doi.org/10.1038/s41598-017-02175-4

20. Andersson DI, Hughes D. Antibiotic resistance and its cost: is it possible to reverse resistance? Nat Rev Microbiol. 2010;8:260–71. https://doi.org/10.1038/nrmicro2319

21. Sieber RN, Larsen AR, Urth TR, Iversen S, Møller CH, Skov RL, et al. Genome investigations show host adaptation and transmission of LA-MRSA CC398 from pigs into Danish healthcare institutions. Sci Rep. 2019;9:18655. https://doi.org/10.1038/s41598-019-55086-x

22. Forsgren A. Significance of protein A production by staphylococci. Infect Immun. 1970;2:672–3. https://doi.org/10.1128/IAI.2.5.672-673.1970

23. Björk I, Petersson BA, Sjöquist J. Some physiochemical properties of protein A from *Staphylococcus aureus.* Eur J Biochem. 1972;29:579–84. https://doi.org/10.1111/j.1432-1033.1972.tb02024.x

24. Potter KN, Li Y, Capra JD. Staphylococcal protein A simultaneously interacts with framework region 1, complementarity-determining region 2, and framework region 3 on human V_H3-encoded Igs. J Immunol. 1996;157:2982–8.

25. Graille M, Stura EA, Corper AL, Sutton BJ, Taussig MJ, Charbonnier JB, et al. Crystal structure of a *Staphylococcus aureus* protein A domain complexed with the Fab fragment of a human IgM antibody: structural basis for recognition of B-cell receptors and superantigen activity. Proc Natl Acad Sci U S A. 2000;97:5399–404. https://doi.org/10.1073/pnas.97.10.5399

26. Goodyear CS, Silverman GJ. Death by a B cell superantigen: in vivo V_H-targeted apoptotic supraclonal B cell deletion by a staphylococcal toxin. J Exp Med. 2003;197:1125–39. https://doi.org/10.1084/jem.20020552

27. Falugi F, Kim HK, Missiakas DM, Schneewind O. Role of protein A in the evasion of host adaptive immune responses by *Staphylococcus aureus.* MBio. 2013;4:e00575-13. https://doi.org/10.1128/mBio.00575-13

28. Pauli NT, Kim HK, Falugi F, Huang M, Dulac J, Henry Dunand C, et al. *Staphylococcus aureus* infection induces protein A-mediated immune evasion in humans. J Exp Med. 2014;211:2331–9. https://doi.org/10.1084/jem.20141404

29. Sun Y, Emolo C, Holtfreter S, Wiles S, Kreiswirth B, Missiakas D, et al. Staphylococcal protein A contributes to persistent colonization of mice with *Staphylococcus aureus.* J Bacteriol. 2018;200:e00735–17. https://doi.org/10.1128/JB.00735-17

30. Chen X, Sun Y, Missiakas D, Schneewind O. *Staphylococcus aureus* decolonization of mice with monoclonal antibody neutralizing protein A. J Infect Dis. 2019;219:884–8. https://doi.org/10.1093/infdis/jiy597

Address for correspondence: Jesper Larsen, Department of Bacteria, Parasites and Fungi, Statens Serum Institut, Artillerivej 5, DK-2300 Copenhagen S, Denmark; email: JRL@ssi.dk

Validated Methods for Removing Select Agent Samples from Biosafety Level 3 Laboratories

Alexandria E. Kesterson, John E. Craig, Lara J. Chuvala, Henry S. Heine

The Federal Select Agent Program dictates that all research entities in the United States must rigorously assess laboratory protocols to sterilize samples being removed from containment areas. We validated procedures using sterile filtration and methanol to remove the following select agents: *Francisella tularensis*, *Burkholderia pseudomallei*, *B. mallei*, *Yersinia pestis*, and *Bacillus anthracis*. We validated methanol treatment for *B. pseudomallei*. These validations reaffirm safety protocols that enable researchers to keep samples sufficiently intact when samples are transferred between laboratories.

The Federal Select Agent Program (FSAP), which is jointly administered by the Centers for Disease Control and Prevention and the US Department of Agriculture, designates high-risk organisms and guidelines for their safe handling. FSAP defines Tier 1 select agents as organisms that have the potential to be used as biological weapons (*1*). These organisms might infect humans, important agricultural species of plant and animal origin, or both. Various safety and security measures prevent these organisms from being inadvertently released into the environment or obtained by persons without authorized access. For example, researchers can handle these organisms only within Biosafety Level (BSL) 3 or -4 laboratories. Transfer of these agents into, out of, or between laboratories must be well-documented to ensure the safety of the public and research personnel (*1*, *2*). In 2015, failures in the sample removal protocols led the US Army to inadvertently ship live *Bacillus anthracis* spores to several laboratories in the United States and other countries (*3*). *B. anthracis* is a Tier 1 select agent and therefore subject to the rules of FSAP. These samples were thought to have been inactivated by radiation, but lapses in protocol resulted in incomplete sterility (*3*). Afterward, the FSAP created additional regulations and guidance on how

samples potentially containing select agents could be removed from BSL-3 and -4 laboratories.

FSAP requires that each inactivation or sterility method for sample removal be individually tested and validated, ensuring that these methods account for assay variability and technical limits of detection (*2*). The new guidance requires the entity developing the procedure to assess the risk that live material will remain in an inactivated sample (*2*). The FSAP recognizes that checking the sterility of all samples is impossible, but laboratories should minimize the risk for a viable select agent remaining within a sample believed to be inactivated. In addition, if an entity changes an already validated procedure, the entity must revalidate that procedure (*2*). Entities might develop their procedures from commonly accepted practices or from methods described in the literature (*2*). The entity must then use the appropriate controls to validate the effectiveness of the procedure. We defined the term validate to mean that a protocol, if followed exactly, renders select agent–containing samples sterile at the bacterial concentrations stated and that the sterility verification procedures identify protocol failures.

Our laboratory at the University of Florida (Orlando, FL, USA) evaluates therapeutics for the Tier 1 select agents *Francisella tularensis*, *Burkholderia pseudomallei*, *B. mallei*, *Yersinia pestis*, and *Bacillus anthracis*. We frequently conduct studies in which serum, plasma, bronchoalveolar lavage (BAL) fluid, or spent media must be transferred from the BSL-3 to the BSL-2 laboratory to conduct specific assays. These samples must be sufficiently intact so that we can evaluate drug, cytokine, chemokine, or enzyme levels and other host or bacterial components of interest. In most instances, chemical inactivation of the samples is not advisable. We selected 0.2-μm centrifuge filtration as the most effective method to sterilize small volumes of select agent–containing samples while maintaining other components in the samples. We describe and validate a standardized method using several different matrices.

Measuring the intracellular levels of antimicrobial drugs in the BAL fluid is sometimes necessary to determine the amount of compound penetrating the site of infection within the cell. When it is necessary to measure the intracellular concentration, we treat the BAL cell pellet and the BAL fluid as 2 independent samples. Because the cell pellet sample cannot be filtered, we describe an additional procedure for removing BAL cell pellets from the containment laboratory.

Materials and Methods

Biosafety

We tested all protocols in a BSL-3 laboratory at the University of Florida, which is registered and licensed with the Centers for Disease Control and Prevention and the Animal and Plant Health Inspection Service, US Department of Agriculture, to conduct select agent research. The containment laboratory uses a high-efficiency particulate air filter to decontaminate discharged air. All staff must don facility-dedicated scrubs, Tyvek suits (Dupont, https://www.dupont.com), respiratory protection, double gloves, and shoe covers. All bacterial work is performed in a class II Biosafety cabinet, and all waste is removed using pass-through autoclaves.

Bacterial Strains and Growth Conditions

We used the following strains from the Biodefense and Emerging Infections Resource Repository: *B. anthracis* (Ames), *Y. pestis* (CO92), *F. tularensis* (SchuS4), *B. pseudomallei* (1026b), and *B. mallei* (China 7). We isolated *B. anthracis* spores according to Leighton and Doi (*4*) and maintained the spores in refrigerated sterile water at $\approx 1 \times 10^{10}$ CFU/mL. We verified this concentration by serial dilution in sterile water onto sheep blood agar plates as previously stated (*5*).

We cultured *Y. pestis* CO92 from frozen stock on sheep blood agar (Becton Dickinson, https://www.bd.com) and incubated it for 48 h at 28°C. We then removed colonies from the stock plate and suspended them in 1 mL heart infusion broth (Becton Dickinson). We added this suspension to 100 mL heart infusion broth containing 2 mL 10% xylose (Indofine, https://indofinechemical.com). We incubated this mixture in a 500 mL flask with agitation for 18–24 h.

We then cultured *B. mallei* China 7 and *B. pseudomallei* 1026b from frozen stock vials on tryptic soy agar and incubated them at 35°C for 24–48 h to generate a stock plate of each strain. We selected 2–3 colonies from each incubated stock plate and inoculated them in brain heart infusion (BHI) broth (Becton Dickinson) overnight culture. We then incubated the cultures at 35°C with agitation for 16–20 h.

We also cultured *F. tularensis* SchuS4 from frozen stock onto chocolate agar (Becton Dickinson) and incubated it at 35°C for 48 h. We selected colonies from the agar plate and used them to inoculate a BHI culture containing 2% Isovitalex (Becton Dickinson). We incubated this culture for 18–20 h at 35°C with agitation.

Matrices

We tested the filtration protocol with murine lung BAL fluid, serum, plasma, and the listed culture mediums (Table 2). For the spore preparation, we used BHI as the culture media. We purchased the murine serum, plasma, and BAL from BioreclamationIVT (https://bioivt.com). We used mouse plasma from Balb/c mice collected in sodium citrate–containing tubes and pooled across sex. We also used mouse BAL and serum from Balb/c mice and pooled across sex.

Test Sample Preparation

All matrices had a final volume of 2 mL. We selected test sample starting concentrations that exceeded the maximum published bacterial concentrations (Table 1). We established a conversion factor for each species on the basis of serial dilution plate counts and optical density (OD) measurements at 600 nm (H. Heine, unpub. data). We used these conversion factors to determine the concentrations of overnight cultures and spore preparations. *Y. pestis* had a conversion factor of 5.34×10^8 CFU/OD, *B. mallei* and *B. pseudomallei* 1.57×10^9 CFU/OD, and *F. tularensis* 3.89×10^{10} CFU/OD.

Table 1. Maximum bacterial concentrations of select agents in tissues of infected mice*

Agent (reference)	Lung, per g	Cell pellet, per mL BAL	Blood, per mL	Overnight culture, per mL
	Source of samples, bacterial load			
Bacillus anthracis (*5,6*)	$<10^8$	Not tested	$<10^4$	10^8
Yersinia pestis (*7*)	$<10^{10}$	Not tested	$<10^6$	10^9
Burkholderia mallei (*8–11*)	$<10^9$†	Not tested	$<10^4$	10^9
Burkholderia pesudomallei (*11,12*)	$<10^8$	10^5‡	$<10^5$	10^9
Francisella tularensis (*13*)	10^7	Not tested	$<10^5$	10^9

*BAL, bronchoalveolar lavage.
†References (*7*) and (*8*) use a different strain of *B. mallei*
‡Value determined through in-house testing of lung samples.

For *B. anthracis* Ames strain, we prepared spores and spiked the different matrices. We used 20 μL of the spore preparation for BAL and culture medium samples. We diluted the spore preparation 1:1000 and used 20 μL of the diluted solution to spike each serum and plasma sample (Table 2).

We prepared test samples for *Y. pestis* from the incubated 100 mL broth culture. We took an OD reading from serially diluted broth culture and conversion factors to determine the culture concentration. We centrifuged 20 mL of this culture at 3,500 × *g* for 15 min. We then resuspended this pellet in 2 mL of BAL fluid (Table 2). We repeated the process for the culture medium. We inoculated serum and plasma samples with a uncentrifuged overnight culture (Table 2).

We prepared *B. mallei* test samples from the overnight broth cultures incubated previously. We prepared BAL fluid test samples by centrifuging 2 mL overnight broth culture at 3,500 rpm for 15 min and then resuspending the pellet in 2 mL BAL fluid. We inoculated serum and plasma with an overnight culture that had been diluted 1:100, then added 20 μL to each matrix (Table 2). We inoculated culture medium by centrifuging 20 mL of the overnight culture then suspending the pellet in 2 mL of culture media (Table 2).

We prepared *B. pseudomallei* test samples for culture medium as stated for *B. mallei* and *Y. pestis* using the conversion factor. We prepared BAL fluid samples by adding 200 μL overnight culture to 1.8 mL BAL fluid (Table 2). We inoculated serum and plasma with 20 μL of overnight culture that was first diluted 1:10 (Table 2).

We prepared *F. tularensis* samples for culture medium with a final concentration of 2% Isovitalex. We took an OD reading and used the conversion factor to concentrate samples appropriately. We centrifuged 20 mL of an overnight culture and resuspended it in

culture medium with 2% Isovitalex. We spiked serum and plasma samples with 20 μL of an overnight culture that was first diluted 1:10 and inoculated BAL fluid with 20 μL of an overnight culture (Table 2).

Methanol Test Sample Preparation

Test samples, positive controls, and the negative control of BAL fluid for the methanol treatment procedure all had a final volume of 500 μL. We used stock plates to grow bacteria, then selected colonies and suspended them in 3 mL of sterile water for injection (GE Healthcare, https://www.gehealthcare.com). We took an OD reading at 600 nm on a spectrophotometer (ThermoFisher Scientific, https://www.thermofisher.com) using a 1 cm² cuvette (ThermoFisher Scientific). We converted this value to an approximate CFU per milliliter value using a conversion factor as stated in test sample preparation. We calculated the total volume needed to spike each sample so that each sample would have 2×10^6 CFU (Table 2).

Filtration Procedure

We conducted all filtration test procedures in triplicate for each matrix type. For negative controls, we used uninoculated matrix samples. For positive controls, we used 100 μL of unfiltered inoculated test samples suspended in broth culture medium. We then placed 450 μL of each test sample into a clean 0.2 μm PALL Nanosep Bio-Inert centrifuge filter (Pall Corporation, https://www.pall.com) with a sterile microcentrifuge tube. In accordance with the manufacturer's recommendations, we centrifuged the filters for 3 min at 14,000 × *g*. We then transferred the filtrate to a clean tube and sealed it to prevent secondary contamination. We emphasize that the filtrate collection tubes should not be sealed with the same cap used to close the centrifuge filter before spinning

Table 2. Preparation of select agents in different matrices*

Agent	CFU/mL (matrix)	BAL fluid	Serum and plasma, μL	Culture	BAL cell pellet
Bacillus anthracis	10^{10} (spore prep†)	20 μL	20§	20 μL	NT
Yersinia pestis	10^9 (overnight culture)	Resuspend pellet¶	20	Resuspend pellet¶	NT
Burkholderia mallei	10^9 (overnight culture)	Resuspend pellet#	20**	Resuspend pellet††	NT
Burkholderia pseudomallei	10^9 (overnight culture)	200 μL + 1.8 mL BAL	20‡‡	Resuspend pellet§§	2×10^6 CFU
Francisella tularensis	10^9 (overnight culture‡)	20 μL	20¶¶	Resuspend pellet##	NT

*BAL, bronchoalveolar lavage; NT, not tested.
†Spores for aerosol challenge were maintained in sterile water and diluted to the nebulizer-challenge concentration of »1×10^{10} CFU/mL.
‡All broth cultures will require a 2% supplement with Isovitalex (Becton Dickinson, https://www.bd.com) to obtain growth of *F. tularensis*.
§Dilute spore prep 1:1000; transfer 20 μL to serum and plasma.
¶Centrifuge 20 mL of overnight culture, resuspend pellet in 2 mL BAL fluid or culture media.
#Centrifuge 2 mL of overnight culture, resuspend in 2 mL BAL fluid.
**Dilute overnight culture 1:100; transfer 20 μL to BAL fluid.
††Centrifuge 20 mL of overnight culture, resuspend pellet in 2 mL culture media.
‡‡Dilute overnight culture 1:10 transfer 20 μL to serum or plasma.
§§Centrifuge 20 mL of overnight culture, resuspend pellet in 2 mL culture media.
¶¶Dilute overnight culture 1:10 transfer 20 μL to BAL fluid.
##Centrifuge 20 mL of overnight culture, resuspend pellet in 2 mL culture media.

Table 3. Sterility of select agent samples after sterile filtration and methanol procedure*‡

Agent (reference)	Positive serum	Positive plasma	Positive BAL	Positive overnight culture	Positive BAL cell pellet
Bacillus anthracis	0/3	0/3	0/3	0/3	NT
Yersinia pestis	0/3	0/3	0/3	0/3	NT
Burkholderia mallei	0/3	0/3	0/3	0/3	NT
Burkholderia pesudomallei	0/3	0/3	0/3	0/3	0/3
Francisella tularensis (*14*)	0/6	0/6	1/6†	1/6†	NT

*BAL, bronchoalveolar lavage; NT, not tested.
†Negative result caused by contaminated tube cap.
‡Total success rate for filtration: 97%

because this cap could be contaminated with residual unfiltered sample and thus might yield false positive outcomes. We then suspended the filtrate in 4.5 mL BHI and incubated it at 35°C for 2 d. We incubated the positive controls in the same manner. After 48 h, we checked the tubes for turbidity and plated 5 × 200 μL samples onto the appropriate media. We incubated these samples at 35°C for an additional 7 d to ensure complete sterility. We considered this method to be validated only if all 3 replicates of all matrices were sterile in both broth and agar medium. Any failure, defined here as positive growth on agar or in broth media, prompted a review of the procedures. Once we determined the cause of the failure, we made the appropriate adjustments and reconducted the procedure in 3 replicates.

Methanol Procedure

We centrifuged BAL fluid for 5 min at 5,000 × *g*. We removed the supernatant and decontaminated it using the filtration procedure detailed in the previous section. We suspended the pellet in 500 μL of 80% methanol (ThermoFisher Scientific) and incubated it for 10 min. We placed 10% of this sample into 9.5 mL Dey-Engley neutralization broth (D/E media) (Becton Dickinson) and incubated it at 35°C for 5 d. After 5 d, we plated 200 μL of the D/E media onto 5 agar plates specific to each bacterial species and incubated them at 35°C for an additional 2 d.

For positive controls, we used D/E media inoculated with bacteria and D/E media with 80% methanol added to the same volume as the test sample (50 μL of 80% methanol into 9.5 mL D/E media). We incubated this tube for 10 min and then inoculated it with bacteria. We also used growth media specific to each bacterial species as positive controls. For negative controls, we used uninoculated D/E media and D/E media inoculated with methanol treated bacteria.

Results

After following the described procedures, we observed that all samples (except 1) were sterilized in broth culture after 48 h incubation. The samples remained sterile after plating on agar medium incubated for 7 d (Table 3). We determined that the test sample that had not been sterilized had sustained secondary contamination from the centrifuge filter unit cap. The PALL centrifuge filters are supplied as a filter and tube unit; they do not come with sterile secondary caps. To avoid secondary contamination, we transferred the filtrate to a clean tube immediately after spinning. We also observed that all samples were sterilized after treatment with 80% methanol and after incubation in broth culture for 5 d. The samples remained sterile on agar after an additional 2 d incubation.

Discussion

Validating sterility procedures is a time-intensive and costly necessity for removing select agent samples from BSL-3 laboratories. Researchers can streamline this process by publishing validated methods in peer-reviewed journals.

We described and validated reproducible procedures for select agent sample removal. However, researchers should ascertain that none of their sample is lost because of binding to the filter material. In this study, we checked 100% of the sample as a proof of concept, although we recognize the impossibility of incubating 100% of the sample to ensure sterility during actual experiments. Our laboratory now samples 10% of the filtrate to verify successful disinfection. We have found that these filters have an approximate failure rate of 0.1%; however, other researchers such as Dauphin et al. have found a failure rate closer to 3% (*14*). The differences in failure rates, variety of available filter membranes, and new methods of sterilization showcase the need for clear, detailed, and reproducible published methods.

About the Author

Ms. Kesterson is a doctoral candidate in biomedical sciences at the University of Florida. Her research interests include bacterial host pathogen interaction and antimicrobial countermeasures for biothreat pathogens and their associated immune responses.

References

1. US Department of Health and Human Services. Biosafety in microbiological and biomedical laboratories, 5th ed. Washington (DC): The Department; 2009.

2. Centers for Disease Control and Prevention; Animal and Plant Health Inspection Service. Guidance on the Inactivation or Removal of Select Agents or Toxins for Future Use. 2018 [cited 2019 Aug 4]. https://www.selectagents.gov/irg-intro.html

3. US Government Accountability Office. Actions Needed to Improve Management of DOD's Biosafety and Biosecurity Program. 2018 [cited 2019 Aug 4]. https://www.gao.gov/products/GAO-18-422

4. Leighton TJ, Doi RH. The stability of messenger ribonucleic acid during sporulation in *Bacillus subtilis*. J Biol Chem. 1971;246:3189–95.

5. Heine HS, Shadomy SV, Boyer AE, Chuvala L, Riggins R, Kesterson A, et al. Evaluation of combination drug therapy for treatment of antibiotic-resistant inhalation anthrax in a murine model. Antimicrob Agents Chemother. 2017;61:e00788–17. https://doi.org/10.1128/AAC.00788-17

6. Heine HS, Bassett J, Miller L, Hartings JM, Ivins BE, Pitt ML, et al. Determination of antibiotic efficacy against *Bacillus anthracis* in a mouse aerosol challenge model. Antimicrob Agents Chemother. 2007;51:1373–9. https://doi.org/10.1128/AAC.01050-06

7. Heine HS, Chuvala L, Riggins R, Hurteau G, Cirz R, Cass R, et al. Natural history of *Yersinia pestis* pneumonia in aerosol-challenged BALB/c mice. Antimicrob Agents Chemother. 2013;57:2010–5. https://doi.org/10.1128/AAC.02504-12

8. Judy BM, Whitlock GC, Torres AG, Estes DM. Comparison of the in vitro and in vivo susceptibilities of *Burkholderia mallei* to Ceftazidime and Levofloxacin. BMC Microbiol. 2009;9:88. https://doi.org/10.1186/1471-2180-9-88

9. Mott TM, Johnston RK, Vijayakumar S, Estes DM, Motamedi M, Sbrana E, et al. Monitoring therapeutic treatments against *Burkholderia* infections using imaging techniques. Pathogens. 2013;2:383–401. https://doi.org/10.3390/pathogens2020383

10. Moustafa DA, Scarff JM, Garcia PP, Cassidy SKB, DiGiandomenico A, Waag DM, et al. Recombinant salmonella expressing *Burkholderia mallei* LPS O antigen provides protection in a murine model of melioidosis and glanders. PLoS One. 2015;10:e0132032. https://doi.org/10.1371/journal.pone.0132032

11. Lafontaine ER, Zimmerman SM, Shaffer TL, Michel F, Gao X, Hogan RJ. Use of a safe, reproducible, and rapid aerosol delivery method to study infection by *Burkholderia pseudomallei* and *Burkholderia mallei* in mice. PLoS One. 2013;8:e76804. https://doi.org/10.1371/journal.pone.0076804

12. Tan GG, Liu Y, Sivalingam SP, Sim S-H, Wang D, Paucod J-C, et al. *Burkholderia pseudomallei* aerosol infection results in differential inflammatory responses in BALB/c and C57Bl/6 mice. J Med Microbiol. 2008;57:508–15. https://doi.org/10.1099/jmm.0.47596-0

13. Heine HS, Chuvala L, Riggins R, Cirz R, Cass R, Louie A, et al. Natural history of *Francisella tularensis* in aerosol-challenged BALB/c mice. Antimicrob Agents Chemother. 2016;60:1834–40. https://doi.org/10.1128/AAC.02887-15

14. Dauphin LA, Bowen MD. A simple method for the rapid removal of *Bacillus anthracis* spores from DNA preparations. J Microbiol Methods. 2009;76:212–4. https://doi.org/10.1016/j.mimet.2008.10.009

Address for correspondence: Henry Heine, Institute for Therapeutic Innovation, University of Florida, 6550 Sanger Rd, Orlando, FL 32827, USA; email: henry.heine@medicine.ufl.edu

Epidemiology of COVID-19 Outbreak on Cruise Ship Quarantined at Yokohama, Japan, February 2020

Expert Taskforce for the COVID-19 Cruise Ship Outbreak[1]

To improve understanding of coronavirus disease (CO-VID-19), we assessed the epidemiology of an outbreak on a cruise ship, February 5–24, 2020. The study population included persons on board on February 3 (2,666 passengers, 1,045 crew). Passengers had a mean age of 66.1 years and were 55% female; crew had a mean age of 36.6 years and were 81% male. Of passengers, 544 (20.4%) were infected, 314 (57.7%) asymptomatic. Attack rates were highest in 4-person cabins (30.0%; n = 18). Of crew, 143 (13.7%) were infected, 64 (44.8%) asymptomatic. Passenger cases peaked February 7, and 35 had onset before quarantine. Crew cases peaked on February 11 and 13. The median serial interval between cases in the same cabin was 2 days. This study shows that severe acute respiratory syndrome coronavirus 2 is infectious in closed settings, that subclinical infection is common, and that close contact is key for transmission.

On January 30, 2020, the director-general of the World Health Organization (WHO) declared the outbreak of a novel coronavirus disease (COVID-19) a public health emergency of international concern (*1*). Three days later, health authorities in Hong Kong alerted health authorities in Japan that a COVID-19 case was confirmed in Hong Kong on February 1 in a patient who had developed symptoms on January 19 and disembarked from a cruise ship en route to Yokohama, Japan, on January 25. The ship had initiated its voyage from Yokohama on January 20 and visited ports in Japan, Hong Kong, Vietnam, and Taiwan before returning to Yokohama.

Authorities in Japan ordered the captain of the ship to remain at Yokohama port upon arrival, with no persons allowed to disembark. At that time, 2,666 passengers and 1,045 crew members were on board,

Author affiliation: National Institute for Infectious Diseases, Shinjuku-ku, Tokyo, Japan

totaling 3,711 persons. On February 3, health authorities in Japan reviewed logs at the onboard clinic for symptomatic (febrile or respiratory) patients and obtained respiratory specimens from them. On February 5, severe acute respiratory syndrome coronavirus 2 (SARS-CoV-2) was detected through real-time reverse transcription PCR (rRT-PCR) in 1 of these specimens.

At 7:00 AM on February 5, all persons on board were ordered to remain in their cabins for 14 days and were informed that this period could be extended if they had had close contact with someone who had a confirmed case. As of March 8, a total of 696 COV-ID-19 cases had been reported from this ship (*2*). Our objective was to characterize the epidemiology of this cruise ship outbreak to improve global understanding of COVID-19 and inform response measures for the global outbreak.

Design and Methods

We used descriptive and analytical statistics to conduct this epidemiologic assessment of quarantine measures aboard the ship during February 5–24, 2020, including all persons aboard the ship during that time. The assessment was approved by the institutional review board at the National Institute of Infectious Diseases, Tokyo.

Persons on the ship included all 3,711 persons (crew and passengers) registered with the cruise ship owner as being on board on February 3, 2020, when the ship arrived at Yokohama. Beginning on February 5, passengers were quarantined in their cabins with their cabinmates. Passenger cabin capacity ranged from 1 to 4 persons. Passengers, organized by deck and section, were allowed a 60-minute period on an exterior deck each day, during which they were instructed to wear masks, refrain from touching anything, and maintain a

1-meter distance from others. Monitors observed these periods. After each group came a 30-minute period in which the areas were disinfected. Room cleaning was suspended. Food and clean linens were delivered to cabin doors by crew, and dirty dishes and linens were picked up at cabin doors by crew. Clean services and dirty services were performed by separate groups of the crew.

Crew members were ordered to remain in their cabins except to perform essential duties. Depending on the job and rank, crew cabin capacity ranged from 1 to 4 persons. Health authorities from Japan distributed personal protective equipment to crew members and instructed them on proper use.

On February 7, authorities provided thermometers to passengers and instructed them to check body temperature regularly. Thermometers were also distributed to the crew, although not to every member, and crew members were requested to monitor body temperature. A fever call center was established inside the ship; persons on board were asked to call the center if they had a temperature $\geq37.5°C$. A respiratory specimen was obtained from any person with fever or respiratory symptoms. Specimens were tested for SARS-CoV-2 by rRT-PCR (3). Any person with a positive rRT-PCR specimen was defined as having COVID-19; these persons disembarked and were transferred to an isolation facility in Japan.

Cabinmates of confirmed case-patients were classified as close contacts, and their 14-day observation period was reset on the last day of contact with the case-patient. Any close contact with a positive test result was considered a case-patient; these persons disembarked and were taken to an isolation facility. A negative test result allowed the person to remain on board in quarantine. Because of the limited availability of laboratories with the capacity to test for SARS-CoV-2 early in this outbreak, only symptomatic close contacts were tested initially. As laboratory capacity in Japan increased, the testing strategy changed to include, first, all contacts of case-patients, then all passengers (beginning with older age groups), and then all crew. Any person on board who developed serious illness, including non–COVID-19 conditions (such as myocardial infarction), was taken off the ship, sent to a healthcare facility, and tested for SARS-CoV-2. To be released from quarantine, a person had to complete a 14-day observation period without being defined as a close contact during the period, pass medical screening for fever and respiratory symptoms at the end of the 14-day period, and obtain ≥1 negative test result (and no positive result) during the 14-day period.

Primary data sources for this article included rRT-PCR results, information from the ship manifest (age, sex, country of passport, cabin number, and classification as passenger or crew), and symptom data (presence or absence of symptoms, onset date, and severe outcomes) recorded at the time of respiratory specimen collection or through standard public health follow-up of cases. A confirmed case of COVID-19 was defined as an illness in any person on board the ship during the study period who had 1 positive rRT-PCR result for SARS-CoV-2, independent of symptoms. A symptomatic case was defined as one with the presence of COVID-19 related symptoms, such as fever or cough, at the time of respiratory specimen collection.

We classified countries of origin according to the passport country listed in the ship manifest. We then used number of cases reported to WHO as of February 5 (4) to group countries as having 0 cases reported, 1–5 cases, or >5 cases reported.

We calculated descriptive statistics and used denominators based on the ship manifest as of February 5. Because of the different natures of the quarantines for passengers and crew, we analyzed them, for most analyses, as separate populations. A series interval of 4 days (Nishiura HL, unpub. data, https://doi.org/10.1101/2020.02.03.20019497) was used to assign secondary or tertiary case status within cabins: secondary cases had to have onset dates ≥4 days after primary cases, and tertiary cases had onset days ≥4 days after secondary cases.

To conduct spatial analysis, we analyzed the spatial distribution of confirmed cases across decks. We used the assigned cabin numbers of passengers and crew members for mapping. We used the date of illness onset, if known. If the date of onset was unknown or the patient was asymptomatic, we subtracted the mean delay from illness onset to diagnosis (3 days) from the date of confirmation and set it this as the date of illness onset. To calculate attack rates by cabin occupancy, we removed from the analyses 110 passengers who stayed in crew cabins.

This assessment focused on providing additional epidemiologic characteristics of COVID-19, a new infectious disease with high public health risk. It was granted institutional review board approval with the use of simplified informed consent procedures at the National Institute of Infectious Diseases.

Results

The study population included 2,666 passengers and 1,045 crew members. The mean age of passengers was 66.1 years, and 55% were female. Most (84%) passengers' country of origin had reported >5 COVID-19

cases by February 5. The mean age of the crew was 36.6 years, and 19% were female. Most crew (69%) had countries of origin that had reported 1–5 COVID-19 cases as of February 5, and 19% of crew members' countries of origin had reported zero cases.

During the study period, 544 (20.4%) of the passengers were defined as case-patients (Table 1). Passenger case-patients averaged 67.9 years of age (SD ±12.0). Among case-patients, 314 (57.7%) were asymptomatic, 33 had nonfatal severe outcomes, and 7 died. Attack rates among passengers were highest among those who stayed in 4-person cabins (30.0%; n = 18), followed by 3-person cabins (22.0%; n = 27), 2-person cabins (20.6%; n = 491), and 1-person cabins (8%; n = 6).

Among crew, 143 (13.7%) were defined as case-patients. Crew case-patients averaged 37.7 years of age (SD ±9.0). Among these, 64 (44.8%) were asymptomatic; none had fatal or nonfatal severe outcomes.

Figure 1 displays the number of cases by date of onset for the study period for cases with an available onset date (in 127 passengers and 51 crew). Symptomatic cases among passengers peaked on February 7. Another 35 passenger cases had onset dates before February 5. Cases among crew peaked on February 11 and 13.

Figure 2 shows the spatial snapshot of COVID-19 cases during February 13–16, 2020. Infected passengers were observed across different decks, and there was no identifiable aggregation or large-scale clustering by deck or zone. Crew decks produced a diffusive pattern, although a large number of cases was observed among restaurant staff on deck 3.

Table 2 presents cases among passengers and crew according to symptom presentation. For passengers, there were more asymptomatic than symptomatic cases for all age groups except for those 20–29 and 80–89 years of age. For crew, higher proportions of symptomatic cases were observed among all age groups except those 40–49 years of age, for which they were similar.

Among 26 pairs of passenger cases that occurred in the same cabin, 9 (35%) had a serial interval of 5 days or greater. Three of these occurred in 3- or 4-person cabins. The median interval for these cases was 2 days (range 0–25 days; interquartile range 2–4 days). In the two 4-person cabins in which multiple cases were reported, 1 had serial intervals of 1, 3, and 0 days between the first and second, second and third, and third and fourth cases. The other had intervals of 5 days between the first and second and 6 days between second and third cases. Among crew members, 6 pairs of cases were identified in the same cabins, with serial intervals of 0, 1, 2, 3, 4, and 5 days.

Discussion

Over 20 days, 22% of a cruise ship population of 3,711 was detected to have been infected with SARS-CoV-2. More than half of all case-patients were asymptomatic at the time of respiratory specimen collection. Passenger cases typically had onset dates earlier than crew cases, and many cases had onset dates before the ship's arrival in Yokohama. Infection by that time was spread across multiple decks without spatial clustering. Passengers 10–29 years of age had similar infection rates to those 60–99 years of age. Passengers were more likely to be infected than crew and more likely to present asymptomatically than crew. Attack rates increased with increasing cabin occupancy.

Table 1. Characteristics of persons aboard quarantined cruise ship, Japan, February 5–24, 2020

	No. (%) persons			
	Passengers, n = 2,666		Crew, n = 1,045	
Characteristic	Cases, n = 544; 20.4%	Noncases, n = 2,122; 79.6%	Cases, n = 143; 13.7%	Noncases, n = 902; 86.3%
Age group				
0–9	1 (6.3)	15 (93.8)	0	0
10–19	5 (22.7)	17 (77.3)	0	1 (100)
20–29	9 (18.4)	40 (81.6)	29 (9.7)	269 (90.3)
30–39	7 (11.9)	52 (88.1)	55 (14.9)	315 (85.1)
40–49	4 (5.5)	69 (94.5)	41 (15.8)	219 (84.2)
50–59	49 (16.2)	253 (83.8)	17 (17.3)	81 (82.7)
60–69	177 (19.4)	734 (80.6)	1 (5.6)	17 (94.4)
70–79	239 (23.7)	769 (76.3)	0	0
80–89	51 (23.7)	164 (76.3)	0	0
90–99	2 (18.2)	9 (81.8)	0	0
Sex				
M	245 (20.6)	944 (79.4)	112 (13.3)	731 (86.7)
F	299 (20.2)	1,178 (79.8)	31 (15.3)	171 (84.7)
No. cases reported from country of origin as of Feb 5				
0	11 (15.1)	62 (84.9)	27 (13.5)	173 (86.5)
1–5	62 (17.5)	293 (82.5)	10 (13.9)	617 (86.1)
>5	471 (21.0)	1767 (79.0)	16 (12.5)	112 (87.5)
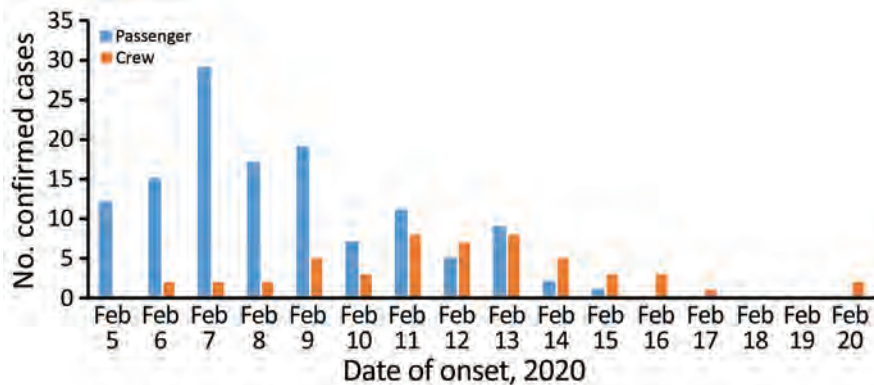
Figure 1. Number of coronavirus disease cases aboard cruise ship quarantined in Japan, by date of symptom onset, February 5–20, 2020 (n = 178). The graph displays the number of cases by symptom onset date for the cases for which onset date was available for passengers and crew members. Cases without a recorded symptom onset date were excluded.

Recent modeling on controlling COVID-19 outbreaks with isolation alone has shown that isolation alone is insufficient, even if contract tracing reaches nearly 100%; thus, additional public health interventions would be needed to control and halt an outbreak (5). Because of the nature of the ship, individual isolation of passengers and crew was not possible, and some crew members were required to continue essential services and ship functions. Thus, the quarantine measures should not have been expected to stop transmission completely. Nevertheless, a modeling study has suggested that the basic reproduction rate (R_0) during the outbreak aboard this ship was 4 times higher than that for Wuhan, China, during its outbreak and that 79% of the population aboard would have been infected if not for the intervention (6). A second modeling study suggested that the R_0 early in the outbreak would have produced
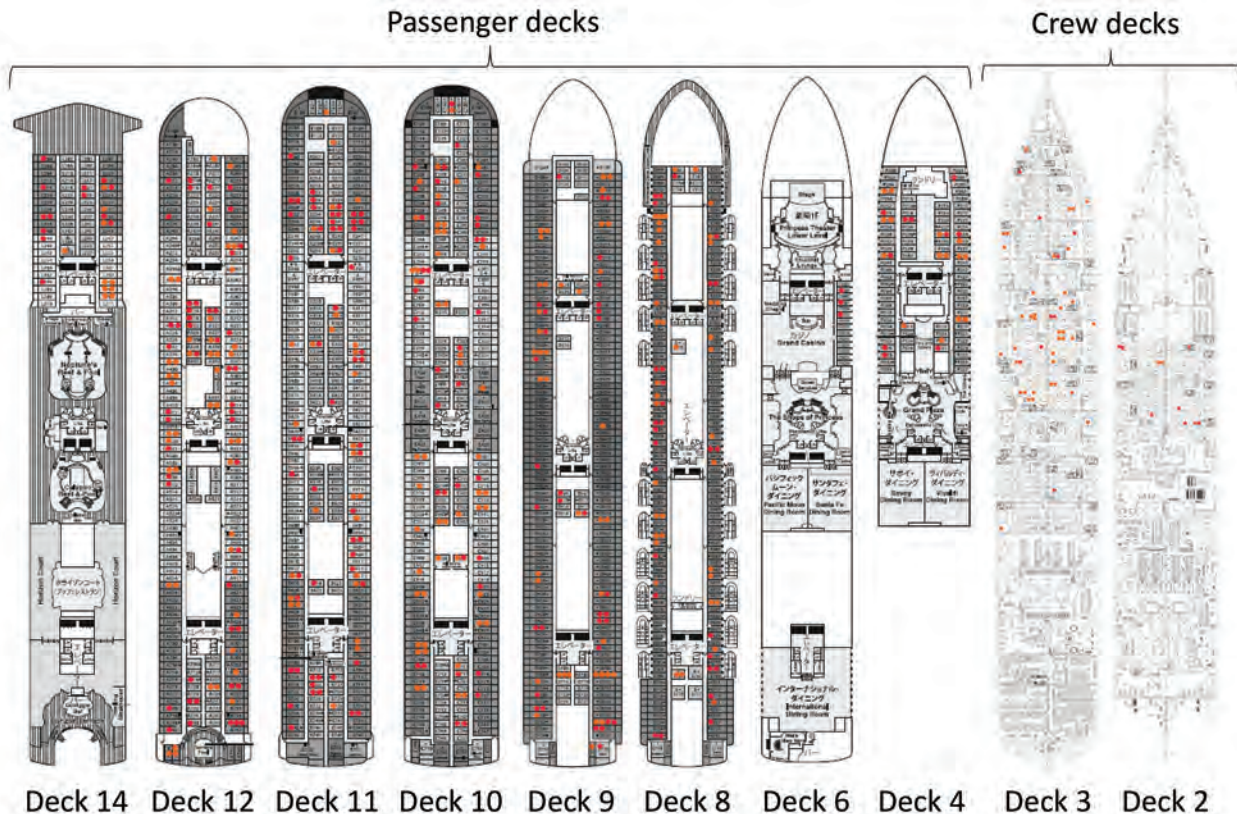
Figure 2. Spatial mapping of coronavirus disease cases aboard cruise ship quarantined in Japan, by deck, February 3–25, 2020. The ship had 18 decks (i.e., floors). Decks 4–14 contained cabin rooms for passengers; decks 2 and 3 were for crew. Red dots indicate the latest cases in cabins (i.e., cases with illness onset starting February 13–16 or infected but asymptomatic persons whose samples tested positive by real-time reverse transcription PCR from February 16 onward. Orange dots represent cases in passengers or crew who appeared to be infected before those periods.

Table 2. Symptomatic and asymptomatic cases among passengers and crew aboard quarantined cruise ship, by age group, Japan

Age group, y	No. (%) persons			
	Passengers		Crew	
	Symptomatic	Asymptomatic	Symptomatic	Asymptomatic
0–9	0	1 (100)	0	0
10–19	2 (40.0)	3 (60.0)	0	0
20–29	7 (77.8)	2 (22.2)	18(62.1)	11(37.9)
30–39	2 (28.6)	5 (71.4)	30(54.5)	25(45.5)
40–49	1 (25.0)	3 (75.0)	20(48.8)	21(51.2)
50–59	19 (38.8)	30 (61.2)	11(64.7)	6(35.3)
60–69	75 (42.4)	102 (57.6)	0	1(100)
70–79	95 (39.7)	144 (60.3)	0	0
80–89	27 (52.9)	24 (47.1)	0	0
90–99	2 (100)	0	0	0
Total	230 (42.3)	314 (57.7)	79 (55.2)	64 (44.8)

1,514 cases, and that a reduction by 50% would have resulted in 758 total cases, which is higher than the observed number of cases on board.

As the models and our findings have pointed out, there was substantial infection on board the ship before arrival in Yokohama (*7*). The index case that was reported by Hong Kong authorities was more likely an indicator case; that is, the first detected case among many infected persons. Dates of onset for passengers included in this assessment stretch back to January 20. Onboard clinic fever data (Appendix Figure 1, https://wwwnc.cdc.gov/EID/article/26/11/20-1165-App1.pdf) similarly showed an increasing trend since the beginning of the voyage. Most early infections occurred among passengers; given that crew dates of onset peaked on February 11 and 13, it is reasonable to assume that transmission from passengers to crew occurred, on average, 7 days earlier, on February 4 or 6, just before and just after quarantine began.

Spatial clustering was not identified on a specific deck or zone, and transmission does not seem to have spread to neighboring cabins, implying that droplet or contact transmission to nearby cabins was not the major mode of infection. Risk of infection did increase with cabin occupancy, but a relatively small proportion of cases in the same cabin had ≥4 days between their onsets, implying a common source of infection. Beyond that, however, the major transmission routes might include a common source outside the cabin and aerosolized fomite or contact transmission across different deck levels. One review of human coronaviruses, which did not include SARS-CoV-2, has shown that they can persist on inanimate surfaces up to 9 days but can be inactivated by surface disinfection procedures within 1 minute (*8*). Given recent reports of outbreaks of COVID-19 in conferences, live music houses, and religious gatherings, a common source event is justified. Such an event in the days before the quarantine would

explain both the spatial distribution and the temporal distribution of symptomatic cases.

A key finding of this assessment was the high proportion of cases with asymptomatic infection. No other study has identified such rates. A large study of COVID-19 cases reported 1% asymptomatic cases (*9*). Nevertheless, in this population, every person was tested; thus, it may be representative of the true picture of infection and transmission for COVID-19 (Appendix Figure 2). If such is the case, then the proportion of fatal and severe cases (1.0%) is much lower than that reported globally (*2,7,9–11*). It is noteworthy that two thirds of the ship population was ≥60 years of age. This finding also implies that, given the current number of fatal and severe cases globally, there is substantial underdetection or underreporting of infection.

As described elsewhere (*12*), it is difficult to know whether these cases were truly asymptomatic, presymptomatic, or postsymptomatic. We reclassified ≈30 asymptomatic cases as symptomatic after learning through follow-up that the case-patients had developed symptoms. Some authors have suggested that presymptomatic transmission is possible (*13,14*). A high proportion of asymptomatic cases will pose serious challenges to understanding and controlling the global outbreak. Contact tracing will struggle to find chains of transmission, infected persons will pass through entry and exit screening posts, and seemingly healthy persons may infect vulnerable ones.

Several key considerations limit the findings in our study. First, throughout the study period, persons on board permanently disembarked for many reasons: confirmed cases, medical emergencies, family members with medical emergencies, country-assisted repatriations, and completion of quarantine requirements. Thus, the true denominators shrank over time, which may result in overestimating the true proportion of infected persons. Second, initial

data collection was limited by the emergency nature of the response. For many of the early cases, symptom onset dates were obtained retrospectively. The differential approach to obtaining these data may introduce bias in comparing the prequarantine and quarantine periods. Third, laboratory testing was initially limited to symptomatic cases and close contacts but then expanded to include all passengers and crew. Thus, asymptomatic infection early in the study period may have been underestimated if these asymptomatic case-patients cleared their viral loads before being tested. Fourth, we are aware of ≥9 persons who tested negative while on board the ship and positive after being released. It is difficult to know for certain if these results were caused by false negatives, false positives, infections developing between the 2 tests, or an increased viral load between the 2 tests. Nevertheless, we cannot rule out that some infections may have gone undetected, which would underestimate the true proportion of infected persons. Fifth, 89 asymptomatic passengers were repatriated by chartered flights before receiving rRT-PCR tests. Some of them were confirmed positive after repatriation, but we could not incorporate their results into this study. It is thus possible that our findings underestimate the true proportion of affected persons, though the difference is not expected to be large.

Moving forward, we propose 4 key steps. First, public health authorities should adapt their response strategies to reflect the high proportion of asymptomatic cases found here. Second, the scientific community should investigate transmission routes other than person-to-person droplets. Third, the scientific community should conduct serologic surveys and shedding experiments to understand the role of asymptomatic infection and pre- and postsymptomatic phases of symptomatic infection on transmission. Fourth, the international maritime community should begin dialogue with national governments (especially quarantine and health sectors) to discuss the feasibility of quarantining large passenger ships.

As of March 8, 2020, all passengers and crew had disembarked from the ship, which was sanitized afterward. Public health measures may have prevented >2,000 COVID-19 cases, and quarantine prevented case-patients from being released into the community. The findings from this complex emergency, in one of the few populations to have been completely tested by rRT-PCR for SARS-CoV-2, imply that the virus is highly infectious, especially in a closed environment, but that it results in a lower proportion of fatal cases than previously reported.

Members of the Expert Taskforce for the COVID-19 Cruise Ship Outbreak: Hajime Kamiya, Infectious Disease Surveillance Center, National Institute of Infectious Diseases; Hiroyuki Fujikura, Field Epidemiology Training Program, National Institute of Infectious Diseases; Ikuko Doi, Field Epidemiology Training Program, National Institute of Infectious Diseases; Kensaku Kakimoto, Field Epidemiology Training Program, National Institute of Infectious Diseases; Motoi Suzuki, Infectious Disease Surveillance Center, National Institute of Infectious Diseases; Tamano Matsui, Infectious Disease Surveillance Center, National Institute of Infectious Diseases; Tomimasa Sunagawa, Infectious Disease Surveillance Center, National Institute of Infectious Diseases; Takuri Takahashi, Infectious Disease Surveillance Center, National Institute of Infectious Diseases; Takuya Yamagishi, Infectious Disease Surveillance Center, National Institute of Infectious Diseases; Anita Samuel, Infectious Disease Surveillance Center, National Institute of Infectious Diseases; Naganori Nao, Department of Virology 3, National Institute of Infectious Diseases; Ikuyo Takayama, Influenza Virus Research Center, National Institute of Infectious Diseases; Shinji Saito, Influenza Virus Research Center, National Institute of Infectious Diseases; Hideki Asanuma, Influenza Virus Research Center, National Institute of Infectious Diseases; Tsutomu Kageyama, Influenza Virus Research Center, National Institute of Infectious Diseases; Kiyoko Okamoto, Infectious Disease Surveillance Center, National Institute of Infectious Diseases; Makoto Ohnishi, National Institute of Infectious Diseases; Takaji Wakita, National Institute of infectious Diseases; Natalie M. Linton, Graduate School of Medicine, Hokkaido University; Keita Yoshii, Graduate School of Medicine, Hokkaido University; Tetsuro Kobayashi, Graduate School of Medicine, Hokkaido University; Abdi Rahman Mahamud, World Health Organization; Matthew M. Griffith, World Health Organization.

References

1. World Health Organization. WHO news room, 2020 Jan 30 [cited 2020 March 3]. https://www.who.int/news-room/detail/30-01-2020-statement-on-the-second-meeting-of-the-international-health-regulations-(2005)-emergency-committee-regarding-the-outbreak-of-novel-coronavirus-(2019-ncov)
2. World Health Organization. Coronavirus disease 2019 (COVID-19) situation report—47; 2020 [cited 2020 March 8]. https://www.who.int/docs/default-source/coronaviruse/situation-reports/20200307-sitrep-47-covid-19.pdf?sfvrsn=27c364a4_2
3. Shirato K, Nao N, Katano H, Takayama I, Saito S, Kato F, et al. Development of genetic diagnostic methods for detection for novel coronavirus 2019(nCoV-2019) in Japan. Jpn J Infect Dis. 2020;73. https://doi.org/10.7883/yoken.JJID.2020.061
4. World Health Organization. Novel coronavirus (2019-ncov) situation report—19—erratum; 2020 [cited 2020 Mar 8]. https://www.who.int/docs/default-source/coronaviruse/situation-reports/20200205-sitrep-16-ncov.pdf
5. Hellewell J, Abbott S, Gimma A, Bosse NI, Jarvis CI, Russell TW, et al.; Centre for the Mathematical Modelling of Infectious Diseases COVID-19 Working Group. Feasibility of controlling COVID-19 outbreaks by isolation of cases and contacts. Lancet Glob Health. 2020;8:e488–96. https://doi.org/10.1016/S2214-109X(20)30074-7
6. Rocklöv J, Sjödin H, Wilder-Smith A. COVID-19 outbreak on the Diamond Princess cruise ship: estimating the epidemic potential and effectiveness of public health countermeasures. J Travel Med. 2020;27:taaa030. https://doi.org/10.1093/jtm/taaa030
7. National Institute of Infectious Diseases. Field briefing: Diamond Princess COVID-19 cases; 2020 [cited 2020 Mar 9]. https://www.niid.go.jp/niid/en/2019-ncov-e/9407-covid-dp-fe-01.html
8. Kampf G, Todt D, Pfaender S, Steinmann E. Persistence of coronaviruses on inanimate surfaces and their inactivation with biocidal agents. J Hosp Infect. 2020;104:246–51. https://doi.org/10.1016/j.jhin.2020.01.022
9. Wu Z, McGoogan JM. Characteristics of and important lessons from the coronavirus disease 2019 (COVID-19) outbreak in China: summary of a report of 72 314 cases from the Chinese Center for Disease Control and Prevention. JAMA. 2020;323:1239. https://doi.org/10.1001/jama.2020.2648
10. Novel Coronavirus Pneumonia Emergency Response Epidemiology Team. The epidemiological characteristics of an outbreak of 2019 novel coronavirus (COVID-19)—China, 2020 [in Chinese] China CDC Weekly. 2020;2:1–10.
11. Li Q, Guan X, Wu P, Wang X, Zhou L, Tong Y, et al. Early transmission dynamics in Wuhan, China, of novel coronavirus-infected pneumonia. N Engl J Med. 2020;382:1199–207.
12. National Institute of Infectious Diseases. Field briefing update, 2020 Feb 21 [cited 2020 Feb 26]. https://www.niid.go.jp/niid/en/2019-ncov-e/9417-covid-dp-fe-02.html
13. Tong Z-D, Tang A, Li K, Li P, Wang H, Yi J, et al. Potential presymptomatic transmission of SARS-CoV-2, Zhejiang Province, China, 2020. Emerg Infect Dis. 2020;26:1052–4. https://doi.org/10.3201/eid2605.200198
14. Rothe C, Schunk M, Sothmann P, Bretzel G, Froeschl G, Wallrauch C, et al. Transmission of 2019-nCoV infection from an asymptomatic contact in Germany. N Engl J Med. 2020;382:970–1. https://doi.org/10.1056/nejmc2001468
15. World Health Organization. Coronavirus disease 2019 (COVID-19) situation report—29; 2020 [cited 2020 Aug 12]. https://www.who.int/docs/default-source/coronaviruse/situation-reports/20200811-covid-19-sitrep-204.pdf?sfvrsn=1f4383dd_2

Address for correspondence: Hajime Kamiya, National Institute for Infectious Diseases, 1-chōme-23-1 Toyama, Shinjuku City, Tokyo 162-0052, Japan; email: hakamiya@niid.go.jp

Analysis of SARS-CoV-2 Transmission in Different Settings, Brunei

Liling Chaw, Wee Chian Koh, Sirajul Adli Jamaludin, Lin Naing, Mohammad Fathi Alikhan, Justin Wong

We report the transmission dynamics of severe acute respiratory syndrome coronavirus 2 (SARS-CoV-2) across different settings in Brunei. An initial cluster of SARS-CoV-2 cases arose from 19 persons who had attended the Tablighi Jama'at gathering in Malaysia, resulting in 52 locally transmitted cases. The highest nonprimary attack rates (14.8%) were observed from a subsequent religious gathering in Brunei and in households of attendees (10.6%). Household attack rates from symptomatic case-patients were higher (14.4%) than from asymptomatic (4.4%) or presymptomatic (6.1%) case-patients. Workplace and social settings had attack rates of <1%. Our analyses highlight that transmission of SARS-CoV-2 varies depending on environmental, behavioral, and host factors. We identify red flags for potential superspreading events, specifically densely populated gatherings with prolonged exposure in enclosed settings, persons with recent travel history to areas with active SARS-CoV-2 infections, and group behaviors. We propose differentiated testing strategies to account for differing transmission risk.

Cases of coronavirus disease (COVID-19) have escalated since the disease was initially reported on December 31, 2019. A rapid response by the global scientific community has described many aspects of the causative agent, severe acute respiratory syndrome coronavirus 2 (SARS-CoV-2). Estimates suggest a basic reproduction number of 2–3 in the early stages of the outbreak (1), which can be valuable in assessing the spread of the virus but obscures individual heterogeneity in the level of infectivity among persons and in different settings (2,3). Early reports suggest that superspreading events (SSEs) might play a role in the explosive propagation of SARS-CoV-2 (4). Targeted approaches that reduce the likelihood

Author affiliations: Universiti Brunei Darussalam, Jalan Tungku Link, Brunei (L. Chaw, L. Naing); Centre for Strategic and Policy Studies, Jalan Pasar Baru Gadong, Brunei (W.C. Koh); Ministry of Health, Bandar Seri Begawan, Brunei (S.A. Jamaludin, M.F. Alikhan, J. Wong)

of SSEs are contingent on the environmental, behavioral, and host factors that drive transmission and the most effective interventions to control those factors. To address these factors, we report an analysis of a transmission chain in Brunei that resulted from an international SSE.

Brunei is a small, well-connected country in Southeast Asia with a population of 459,500 (5). Brunei has multiple land borders and limited state capacity to manage large-scale outbreaks (6). Multigeneration households are common and social interactions center on strong family and religious relationships (7,8). These characteristics make Brunei particularly vulnerable to outbreaks and the rapid progression of clusters to widespread community transmission (9).

A COVID-19 case was detected in Brunei on March 9, after a 4-day religious gathering, Tablighi Jama'at, in neighboring Kuala Lumpur, Malaysia. The Tablighi Jama'at gathering in Malaysia has been recognized as an SSE and had >16,000 attendees, including international participants (10). Tablighi is an apolitical Islamic movement with adherents from >200 countries. Tablighi adherents usually gather at annual international events lasting several days where they participate in communal prayers, meals, and speeches. In Malaysia, the participants stayed and slept at the mosque, and several of them were deputized to cook and clean. Seventy-five persons from Brunei attended this event. Of the 135 confirmed cases in Brunei reported by the first week of April, 71 (52.6%) cases had an epidemiologic link to this event (Figure 1).

Because SARS-CoV-2 is a novel infection in a naive population, an outbreak investigation of this event can provide insights into its transmission dynamics and the effectiveness of outbreak control measures. Brunei's thorough contact tracing provides a rare opportunity to study the epidemiologic and transmission characteristics of SARS-CoV-2 in different community settings.
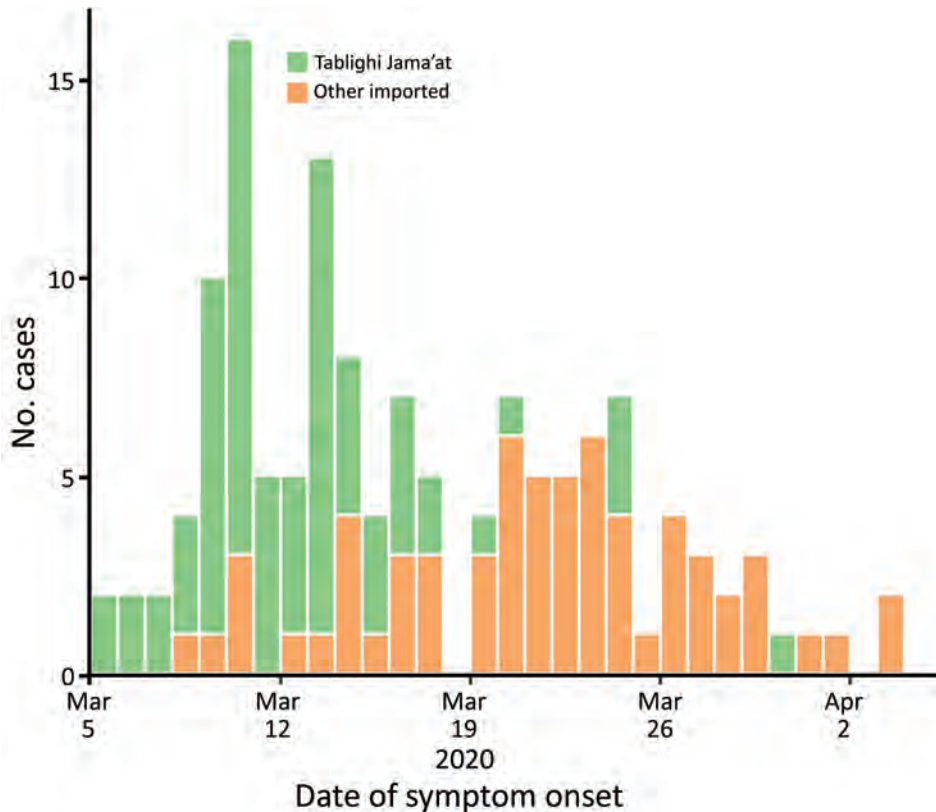
Figure 1. Epidemic curve for the first 135 cases of coronavirus disease (COVID-19) in Brunei Darussalam by cluster groups. Tablighi Jama'at cases were related to a religious gathering in Kuala Lumpur, Malaysia, during February 28–March 1, 2020.

Methods

Surveillance and Case Identification

Brunei's Ministry of Health (MoH) is responsible for communicable disease surveillance and implemented testing criteria for suspected COVID-19 cases on January 23, 2020. Initially, only persons with acute respiratory symptoms and history of travel to a high-risk area were tested for SARS-CoV-2. Over the next several weeks, the program expanded to include contacts of a confirmed case, regardless of symptoms; persons with pneumonia admitted to an inpatient healthcare facility; and persons with acute respiratory illness treated at a health facility for the second time within 14 days. On March 21, MoH started testing and isolating all travelers and returning residents. On March 25, MoH introduced SARS-CoV-2 sampling at selected sentinel health centers to test persons with influenza-like symptoms, and on April 7, MoH implemented mandatory random screening for selected groups of foreign workers.

MoH defined a confirmed COVID-19 case as a person who tested positive for SARS-CoV-2 through real-time reverse transcription PCR (RT-PCR) testing on a nasopharyngeal (NP) swab specimen (*11*). The first positive case in Brunei was detected on March 9 in a person who met the testing criteria by having a fever and cough and having recently traveled to Kuala Lumpur.

Epidemiologic Investigation

Under the Infectious Disease Act, MoH conducted epidemiologic investigations and collected data for each case and close contact by using the World Health Organization's first few cases protocol (*12*). The first identified case-patient was interviewed for demographic characteristics, clinical symptoms, travel history, activity mapping, and contact history. Once MoH identified the case-patient's participation at the Tablighi event in Malaysia, they identified several other persons from Brunei who also had participated at the event. We subsequently obtained the details of all participants from Brunei.

NP swabs were collected from all identified participants and tested with RT-PCR. Persons who tested positive were admitted to the National Isolation Centre (NIC). Persons who tested negative were quarantined for 14 days after their return to Brunei at a designated community quarantine facility, where they were screened for symptoms and body temperature daily. Persons who had symptoms develop at the NIC were retested. Activity mapping of confirmed cases was conducted, and contact tracing was initiated.

We defined a close contact as any person living in the same household as a confirmed case-patient or someone who had been within 1 m of a confirmed case-patient in an enclosed space for >15 minutes (*13*). We identified secondary cases through interviews and checked cellular phone data when information on contacts was uncertain. NP swabs from all close contacts of confirmed case-patients were tested by using RT-PCR. Persons who tested positive were admitted to the NIC and persons who tested negative were placed under home quarantine for 14 days from their last exposure to the confirmed case-patient. Public health workers monitored the compliance and health status of persons under home quarantine daily through video calls or face-to-face assessments. Persons who had symptoms develop during home quarantine were retested.

Clinical Management

All confirmed case-patients were treated and isolated at the NIC and monitored until recovery. We obtained clinical information on case histories, including any prior treatment by health services, clinical examination, and laboratory and radiological results, from digital inpatient records on the national health information system database. In addition, we collected information on each case-patient's oral history to ascertain whether they had symptoms ≤14 days before diagnosis. Case-patients were discharged from the NIC after 2 consecutive negative specimens collected ≥24 hours apart.

Case-Patients

We categorized cases into 2 groups: primary cases were in persons presumably infected at the Tablighi event in Malaysia and nonprimary cases were in persons who had an epidemiologic link to a primary case but did not attend the Tablighi event in Malaysia. For each case-patient, we recorded symptom status and classified them as follows: symptomatic patients reported having symptoms during or before NP swab collection; presymptomatic patients reported having symptoms after NP sampling but during admission to the NIC; and asymptomatic patients reported no symptoms during NP swab collection or admission to the NIC.

Close Contacts

We classified close contacts into 5 groups or settings: household, relatives, workplace, social, and a local religious gathering. We defined household contacts as persons living in the same household and further classified them by their relationship to a case-patient (spouse, child, or other, which included other familial relationships or housekeepers living in the household). We defined relatives as persons related to a case-patient who lived outside the household, workplace contacts as persons encountered at a workplace or school, and social contacts as those encountered during travel or at social events. We defined contacts from a local religious gathering as persons who attended a local Tablighi event in Brunei on March 5; the event ran throughout the night, and participants stayed all night. Such small local weekly gatherings usually take place among Tablighi adherents in their home countries.

Data Analysis

We used χ^2, Fisher exact, or Mann-Whitney tests to compare groups of primary and nonprimary cases, as appropriate. We calculated the incubation period from dates of exposure and symptom onset, when these were clear. We calculated serial interval by subtracting the date of symptom onset of an infectee (secondary case) from the date of symptom onset of the infector (primary case); we only included symptomatic and presymptomatic infector–infectee pairs for which epidemiologic links were clear.

We calculated the attack rate for each setting by dividing the number of positive contacts by the total number of close contacts. To identify risk factors for infection, we applied a log-binomial regression analysis to estimate the risk ratio for gender, age, and setting. We performed further stratification to assess differences in the symptom status of infectors across settings. We estimated the 95% CI by using the normal-approximation method, or the binomial method if the count was <5.

We calculated the mean observed reproductive number (R) and distribution of personal reproductive numbers in each setting by using the number of close contacts infected by each primary case-patient. We estimated the 95% CI by using a Poisson distribution (*14*).

We conducted all analyses by using Excel (Microsoft, https://www.microsoft.com) and R version 3.6.3 (*15*). We considered p<0.05 statistically significant. We obtained ethical approval from the University Research Ethics Committee, Universiti Brunei Darussalam (approval no. UBD/OAVCR/UREC/Apr2020–05).

Results

Epidemiologic Characteristics

Among 75 persons from Brunei who attended the Tablighi event in Malaysia, 19 tested positive for SARS-CoV-2; 52 local close contacts also tested positive, bringing the total cluster size to 71. We analyzed

the epidemiologic links in this cluster by generation in the transmission chain and case-patient symptom status. We noted 32 (45.1%) cases in generation 1, 15 (21.1%) in generation 2, and 5 (7.0%) in generation 3 (Figure 2).

We also analyzed the demographic and clinical characteristics of case-patients in the cluster (Table 1). The median age was 33.0 years (interquartile range [IQR] 21–50 years), 46 (64.8%) case-patients were male and 25 (35.2%) female, and 5 (7.1%) had preexisting chronic conditions. Compared with nonprimary case-patients, primary case-patients were much older, and most were men. Most (55/71; 77.4%) persons with diagnosed COVID-19 were immediately admitted to the NIC within 5 days of symptom onset or NP swab collection (data not shown).

Many case-patients were presymptomatic (22/71; 31.0%) or asymptomatic (9/71; 12.7%) and 40 (56.3%) case-patients reported symptoms during contact tracing investigation. The most reported symptoms were fever, cough, and sore throat. Only 1 (1.4%) case was critical and 2 (2.8%) were severe.

We calculated the incubation period from 8 case-patients who had confirmed epidemiologic links and had attended the March 5 religious gathering in Brunei. By using March 5 as the exposure date, the median incubation period was 4.5 days (range 1–11 days; IQR 2.75–5.5 days). Based on 35 symptomatic infector–infectee pairs, the serial interval was 4.26 days (SD ±4.27 days; range -4 to 17 days). Among the 35 symptomatic infector–infectee pairs, 4 (11.4%) had negative serial interval values. We noted that the serial interval distribution resembled a normal distribution (Appendix Figure 1, https://wwwnc.cdc.gov/EID/article/26/11/20-2263-App1.pdf).

Transmission Characteristics
Among 1,755 close contacts of the COVID-19 cluster among Tablighi members in Brunei, 52 local transmissions were detected, giving an overall nonprimary attack rate of 2.9% (95% CI 2.2%–3.8%). We excluded case 121 (Figure 2) from the analysis because the case-patient was not detected during contact tracing. The highest attack rates were among spouses (41.9%
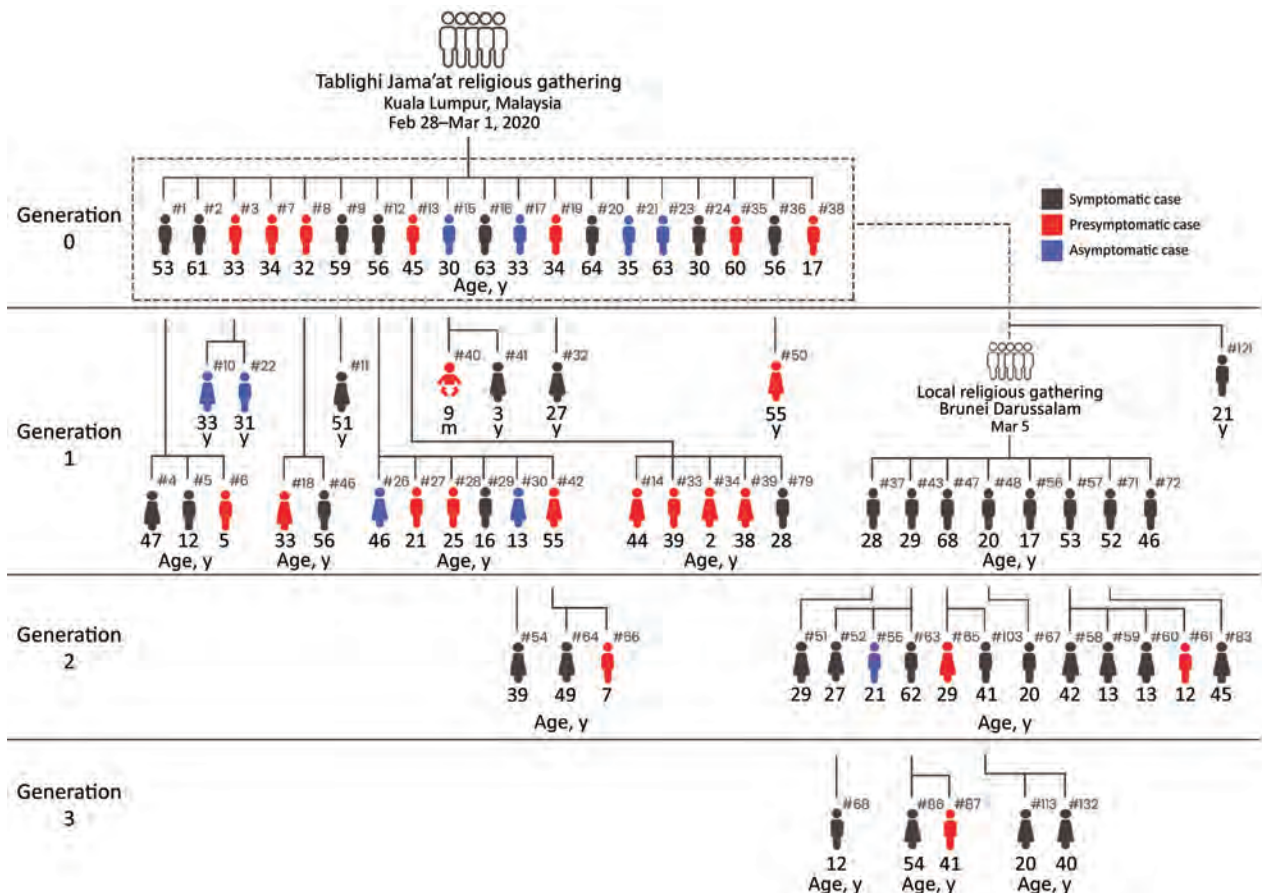
Figure 2. A cluster of coronavirus disease cases in Brunei Darussalam. Epidemiologic links are illustrated by generation and symptomatic status. Generation 0 occurred among attendees of a Tablighi Jama'at gathering in Kuala Lumpur, Malaysia, during February 28–March 1, 2020. Generations 1, 2, and 3 occurred in Brunei. #, case number.

Table 1. Demographic and clinical characteristics of cases in a cluster of coronavirus disease among a Tablighi Jama'at community, Brunei

Characteristics	Overall, n = 71	Primary cases, n = 19	Nonprimary cases, n = 52	p value
Median age, y (IQR)	33.0 (21–50)	35.0 (33– 59.5)	29.0 (20–46)	0.009
Range	0.75–68	17–64	0.75–68	
Age group, y				
0–9	4 (5.6)	0 (0.0)	4 (5.6)	0.002
10–19	9 (12.7)	1 (1.4)	8 (11.3)	
20–29	16 (22.5)	1 (1.4)	15 (21.1)	
30–39	14 (19.7)	8 (11.3)	6 (8.5)	
40–49	10 (14.1)	1 (1.4)	9 (12.7)	
50–59	11 (15.5)	3 (4.2)	8 (11.3)	
60–69	7 (9.9)	5 (7.0)	2 (2.8)	
Sex				
F	25 (35.2)	0 (0.0)	25 (48.1)	<0.001
M	46 (64.8)	19 (100)	27 (51.9)	
Underlying conditions				
Obesity	4 (5.6)	2 (10.5)	2 (3.8)	0.289
Heart disease	4 (5.6)	3 (15.8)	1 (1.9)	0.056
Respiratory disease	5 (7.0)	2 (10.5)	3 (5.8)	0.605
Cancer	1 (1.4)	1 (5.3)	0 (0.0)	0.268
Diabetes mellitus	5 (7.0)	3 (15.8)	2 (3.8)	0.115
Symptom status				
Symptomatic	40 (56.3)	8 (42.1)	32 (61.5)	0.265
Median time from symptom onset to diagnosis, d (range; IQR)	4.0 (0–15; 2–6)	3.5 (0–7; 2.75–6)	4.0 (1–15; 2–6.25)	0.746
Presymptomatic	22 (31.0)	7 (36.8)	15 (28.8)	
Median time from symptom to and NP swab collection, d (range; IQR)	0 (–7 to –1; –2.5 to 0)	0 (–1 to 1; 0–1)	0 (–7 to 1; –3 to 0)	0.034
Asymptomatic	9 (12.7)	4 (21.1)	5 (9.5)	
Symptoms ever reported				
Fever	42 (59.2)	9 (47.4)	33 (63.5)	0.343
Cough	42 (59.2)	14 (73.7)	28 (53.8)	0.218
Runny nose	25 (35.2)	7 (36.8)	18 (34.6)	1.000
Sore throat	42 (59.2)	9 (47.4)	33 (63.5)	0.342
Disease severity				
Asymptomatic	9 (12.7)	4 (21.1)	5 (9.6)	0.278
Mild	52 (73.2)	12 (63.2)	40 (76.9)	
Moderate	7 (9.9)	2 (10.5)	5 (9.6)	
Severe or critical	3 (4.2)	1 (5.3)	2 (3.9)	

*Values are no. (%) except as indicated. IQR, interquartile range; NP, nasopharyngeal.

[95% CI 24.1%–60.7%]), attendees of a local religious gathering (14.8% [95% CI 7.1%–27.7%]), and children (14.1% [95% CI 7.8%–23.8%]). The overall household attack rate was 10.6% (95% CI 7.3%–15.1%).

Multiple log-binomial regression analyses revealed that the type of close contact was the only statistically significant variable (p<0.001; Table 2). Compared with social contacts, spouses of positive case-patients had the highest adjusted risk ratio for infection (45.2 [95% CI 16.8–156.1]), their children had a risk ratio of 14.1 (95% CI 4.8–51.5), and attendees of the local religious gathering had a risk ratio of 15.6 (95% CI 4.8–59.9).

Attack rates also differed by symptom status of the infector (Table 3; Appendix Table). In households where the infectors were symptomatic, attack rates were higher (14.4%) than in households in which the infectors were asymptomatic (4.4%) or presymptomatic (6.1%). We could not calculate the attack rate for attendees of the local religious gathering because the 3 primary cases at the event had different symptom statuses and we could not ascertain how transmission occurred. In the household setting, symptomatic case-patients had 2.7 times the risk of transmitting SARS-CoV-2 to their close contacts, compared with asymptomatic and presymptomatic case-patients (crude risk ratio 2.66 [95% CI 1.12–6.34]; Table 3).

The mean observed R was highest (2.67) among attendees of the local religious gathering. Observed R was 0.67 (95% CI 0.44–0.96) for household members (Table 4). The observed R distribution for the household setting was skewed toward 0 (Appendix Figure 2), and 71.4% (20/28 positive contacts) of household infections were from 16.7% (7/42) of possible links to primary cases.

Discussion

We characterized a cluster of COVID-19 cases in Brunei among attendees of the Tablighi Jama'at in Malaysia, an SSE that led to an epidemic in Brunei. Our

Table 2. Risk factors for severe acute respiratory syndrome coronavirus 2 infection among close contacts, Brunei*

Characteristics	Total, n = 1,755	Positive, n = 51	Attack rate, % (95% CI)	Crude risk ratio (95% CI)†	Adjusted risk ratio (95% CI)‡
Sex					
M	913	24	2.6 (1.7–3.9)	Referent	Referent
F	842	27	3.2 (2.2–4.7)	1.22 (0.71–2.11)	1.23 (0.69–2.27)
Age group					
0–9	267	4	1.5 (0.4–3.8)§	Referent	Referent
10–19	163	8	4.9 (2.3–9.8)	3.28 (1.05–12.12)	1.92 (0.63–7.03)
20–29	364	13	3.6 (2.0–6.2)	2.38 (0.85–8.39)	1.91 (0.70–6.61)
30–39	441	6	1.4 (0.6–3.1)	0.91 (0.26–3.53)	0.85 (0.24–3.38)
40–49	255	9	3.5 (1.7–6.8)	2.36 (0.78–8.61)	1.95 (0.63–7.32)
50–59	174	8	4.6 (2.2–9.2)	3.07 (0.98–11.36)	1.84 (0.58–7.05)
≥60	83	3	3.6 (0.8–10.2)§	2.41 (0.48–10.74)	1.00 (0.20–4.51)
Types of close contact					
Social	445	4	0.9 (0.2–2.3)§	Referent	Referent
Relatives	144	5	3.5 (1.3–8.3)	3.86 (1.04, 15.43)	**4.13 (1.10–16.51)**
Local religious gathering	54	8	14.8 (7.1–27.7)	16.48 (5.38–60.13)	**15.60 (4.81–59.87)**
Workplace or school	848	6	0.7 (0.3–1.6)	0.79 (0.23–3.07)	0.79 (0.23–3.10)
Household					
Child	85	12	14.1 (7.8–23.8)	15.71 (5.62–55.16)	**14.09 (4.79–51.54)**
Spouse	31	13	41.9 (24.1–60.7)	46.65 (17.77–158.39)	**45.20 (16.76–156.12)**
Others¶	148	3	2.0 (0.4–5.8)§	2.26 (0.45–10.2)	2.23 (0.44–10.0)

*Bold text indicates statistically significant value.
†Calculated by using simple log-binomial regression.
‡Calculated by using multiple log-binomial regression (sex, p = 0.485; age group, p = 0.339; types of close contact, p<0.001).
§For counts <5, calculated by using binomial 95% CI.
¶Others include siblings, parents, housekeepers, or relatives, such as grandparents and grandchildren.

analysis revealed several key findings. First, SSEs play a major role in SARS-CoV-2 transmission. Second, transmission variability is high across different settings. Third, transmission varies between symptomatic, asymptomatic, and presymptomatic persons. Our findings highlight the potential for silent chains of transmission.

Within this cluster, 38% of all cases were among participants at an SSE: 19 (26.7%) from the Tablighi event in Malaysia and 8 (11.3%) from a local religious gathering. Of note, 19/75 persons from Brunei who attended the Tablighi event in Malaysia tested positive for SARS-CoV-2. Assuming a representative sample, this suggests an attack rate of 25% and implies that >4,000 of the ≈16,000 participants at the event in Malaysia might have been infected. Moreover, we found that the highest overall nonprimary attack rate

(14.8%) and mean observed R (2.67) were from a local religious gathering, which were higher than the attack rate (10.6%) and mean observed R (0.67) for the household setting. These observations suggest that mass gatherings facilitate SARS-CoV-2 transmission.

During this investigation, we identified several common characteristics at both the local religious gathering and the event in Malaysia (10). First, large numbers of attendees gathered in an enclosed area for a prolonged time. Second, some attendees had a history of recent travel; the Tablighi event in Malaysia drew participants from across the world and ≥3 attendees of the local religious gathering had recently returned from Malaysia. Third, the gatherings included communal sleeping areas, sharing of toilet facilities, and shared dining. We propose that these 3 characteristics are hallmarks for an SSE for

Table 3. Attack rates in different settings stratified by symptom status of the primary case of severe acute respiratory syndrome coronavirus 2, Brunei*

Setting and symptom status	Total, n = 1,701	Positive, n = 43	Attack rate, % (95% CI)	Crude risk ratio (95% CI)†	p value
Household					
Asymptomatic or presymptomatic	111	6	5.4 (1.2–9.6)	Referent	
Symptomatic	153	22	14.4 (8.8–19.9)	**2.66 (1.12–6.34)**	0.027
Nonhousehold‡					
Asymptomatic or presymptomatic	580	9	1.6 (0.5–2.6)	Referent	
Symptomatic	857	6	0.7 (0.1–1.3)	0.45 (0.16–1.26)	0.129
Overall					
Asymptomatic or presymptomatic	691	15	2.2 (1.1–3.3)	Referent	
Symptomatic	1,010	28	2.8 (1.8–3.8)	1.28 (0.69–2.37)	0.439

*Bold text indicates statistically significant value.
† Calculated by using simple log-binomial regression.
‡Includes visits to relatives, workplace, and social settings. The local religious gathering is excluded because 3 primary cases at the event had varying symptom status and we could not ascertain how transmission occurred.

Table 4. Characteristics and mean observed reproductive number for each setting in which infection of severe acute respiratory syndrome coronavirus 2 occurred, Brunei

Setting	No. nonprimary cases	Proportion of links with nonzero infections	Total no. of close contacts	Contacts traced per case	Range of setting size	Mean observed reproductive number (95% CI)
Household	28	0.36	264	9.4	1–13	0.67 (0.44–0.96)
Relatives	5	0.11	144	28.8	1–26	0.26 (0.09–0.61)
Workplace	6	0.20	848	141.3	1–202	0.24 (0.09–0.52)
Social	4	0.16	445	111.3	1–179	0.16 (0.04–0.41)
Local religious gathering	8	1.00	54	6.8	54*	2.67 (NA)*
Overall	51	0.37	1,755	34.4	1–220	0.94 (0.70–1.24)

*Indicates only a single event, so no range for setting size or calculated 95% CI are available. NA, not applicable.

SARS-CoV-2 transmission. Health authorities can use these characteristics as red flags in their risk assessment and mitigation strategies for preventing and detecting high-risk activities, including mass gatherings, and in other institutional settings, such as care homes, prisons, and dormitories.

To a lesser degree, our observations on the within-household transmission are similar to those observed for the 2 religious gatherings. Among 16 household contacts who subsequently became first generation cases, 10 (62.5%) were from just 3 primary cases. However, even within similar settings, we can expect wide variability in transmission patterns. This observation supports our finding of a moderately high household attack rate but an observed R of <1, suggesting that transmission is driven by a relatively small number of cases (2). High attack rates in spouses and children reflect intimate relationships with a high degree of interaction, close proximity, and in the case of the spouse, sleeping in the same room. Concordant with our SSE findings, we suggest that encounters among groups that involve close proximity in enclosed settings for prolonged times (≥1 night) are a main driver of SARS-CoV-2 transmission.

Our overall nonprimary attack rate result of 10.6% in the household setting is comparable to other studies that used contract tracing datasets (16; H.-Y. Cheng et al. unpub. data, https://www.medrxiv.org/content/10.1101/2020.03.18.20034561v1; L. Luo et al., unpub. data, https://www.medrxiv.org/content/10.1101/2020.03.24.20042606v1; Q. Bi et al. unpub. data, https://www.medrxiv.org/content/10.1101/2020.03.03.20028423v3). A study near Wuhan, China (17), reported a higher attack rate of 16.3%, but they detected 56.2% of cases >5 days after persons began having symptoms. By contrast, 77.4% of cases in our study were detected and patients were isolated ≤5 days of symptom onset, suggesting that early case isolation can reduce the attack rate. The Brunei MoH's strategy of aggressive testing of contacts might have contributed to reduced attack rates among household members.

We noted a low nonprimary attack rate (<1%) and mean observed R (<0.3) for workplace and social settings. Moderate physical distancing was implemented in Brunei following the identification of this cluster, but community quarantine and lockdown were not implemented. Public services and businesses remained open and no internal movement restrictions were imposed in the country.

Combined with our observations on the role of SSEs in driving SARS-CoV-2 transmission, we suggest that areas with limited community transmission can avoid full lockdown measures that adopt a blunt approach of restricting all movement. Instead, such areas can use a more targeted approach that combines case isolation, contact tracing, and moderate levels of physical distancing and takes into account the red flags for mass gatherings we identified. However, this approach is resource intensive and only feasible in communities with sufficient public health capacity. The high proportion of asymptomatic persons suggests that even with best efforts at contact tracing, the potential for widespread community transmission is clear. Once SARS-CoV-2 is established in a location, its suppression requires implementation of broader physical distancing measures (18,19). Nonetheless, effective contact tracing and case isolation approaches have been shown to control COVID-19 during the early stage of outbreaks (20). In addition, modeling studies using data from South Korea showed that less extreme physical distancing measures can help suppress an outbreak (21).

We identified several environmental settings and behavioral factors that potentially account for higher attack rates observed in mass gatherings and households. To assess the effect of host factors in driving transmission, we compared the nonprimary attack rate in symptomatic, asymptomatic, and presymptomatic persons, considering the high proportion of asymptomatic (12.7%) and presymptomatic (31.0%) case-patients. Case reports of presumptive asymptomatic and presymptomatic SARS-CoV-2 transmission have been published (22,23), but few observational studies quantify such transmissions.

A study from Ningbo, China, analyzed the overall attack rates between symptomatic and asymptomatic COVID-19 case-patients and did not find major differences between the 2 groups (*24*). Another study reinterpreted the same data and theorized that SARS-CoV-2 could be more transmissible from symptomatic than asymptomatic persons under certain conditions (*25*). In fact, our overall crude risk ratio for symptomatic case-patients showed no statistically significant difference compared with asymptomatic or presymptomatic case-patients (Table 3; Appendix Table). However, we suggest this finding masks the true picture in transmissibility when different settings are taken into account.

We did not find statistically significant differences in the attack rate for nonhousehold settings, which usually practice some form of nonpharmaceutical interventions (NPI), such as taking medical leave for persons with moderate or severe symptoms. In addition, some physical distancing likely would be practiced by contacts of persons with visible symptoms. However, our findings suggest that transmission occurs more frequently at the household level where such physical distancing and control measures are less practical. We observed that the household attack rate for symptomatic persons (14.4%) is higher than that of asymptomatic (4.1%) or presymptomatic (6.1%) persons, suggesting that presence of symptoms is a host factor in driving transmission.

The higher household attack rate observed among symptomatic case-patients suggests that testing for contacts of symptomatic persons should be prioritized, especially in low resource areas. Nonetheless, the attack rates we observed for asymptomatic (4.4%) and presymptomatic (6.1%) case-patients were not negligible and our findings have several implications for high resource areas with greater testing capacity. First, it strengthens the argument for testing household contacts in the absence of symptoms. Second, some flexibility should be permitted in the surveillance system because the high proportion of asymptomatic case-patients poses challenges for rapid detection and isolation. Thus, we recommend that moderate levels of physical distancing should be implemented even in countries with highly developed testing and tracing capacities. Third, proactive testing of travelers, attendees of red flag events, and persons housed in institutional settings might be necessary to contain COVID-19 spread.

This study has several limitations. First, because we conducted a retrospective study based on a contact tracing dataset, determination of the index case and direction of transmission could be uncertain, particularly because a substantial proportion of case-patients were asymptomatic. Moreover, we did not account for outside sources of infection, so setting-specific attack rates could have been overestimated even though no community transmission has been detected in Brunei. Viral sequencing can confirm homology between the strains infecting index and secondary cases across the various settings but was not conducted for all cases. Second, we have not accounted for other potential environmental factors, such as the relative household size, time spent at home with others, air ventilation, and transmission from fomites. Third, we do not have information on NPIs practiced by close contacts; presumably, persons would take precautions during an outbreak. Fourth, case-patients reported their symptom status during NP swab collection, which we assumed to be reflective of their condition when their close contacts were exposed; however, this might not be true for all cases. Finally, the generalizability of our results is limited because there was no community transmission, the small number of cases, and the lack of cases in communal settings, such as residential care facilities and dormitories.

The main strength of our study is the availability of a complete contact tracing dataset at the national level. Because all case-contacts were tested, we believe our study more accurately describes SARS-CoV-2 transmission than studies in which only symptomatic case-contacts were tested.

In conclusion, our analysis highlights the variability of SARS-CoV-2 transmission across different settings and the particular role of SSEs. We identify red flags for potential SSEs and describe environmental, behavioral, and host factors that drive transmission. Overall, we provide evidence that a combination of case isolation, contact tracing, and moderate physical distancing measures can be an effective approach for SARS-CoV-2 containment.

About the Author

Dr. Chaw is a lecturer at the Pengiran Anak Puteri Rashidah Sa'adatul Bolkiah Institute of Health Sciences, Universiti Brunei Darussalam, Bandar Seri Begawan. Her primary research interests include the burden and transmission dynamics of infectious diseases, particularly for acute respiratory diseases.

References

1. Kucharski AJ, Russell TW, Diamond C, Liu Y, Edmunds J, Funk S, et al; Centre for Mathematical Modelling of Infectious Diseases COVID-19 working group. Early dynamics of transmission and control of COVID-19: a mathematical modelling study. Lancet Infect Dis. 2020; 20:553–8. https://doi.org/10.1016/S1473-3099(20)30144-4
2. Liu Y, Eggo RM, Kucharski AJ. Secondary attack rate and superspreading events for SARS-CoV-2. Lancet. 2020;395:e47. https://doi.org/10.1016/S0140-6736(20)30462-1
3. Stein ML, van der Heijden PGM, Buskens V, van Steenbergen JE, Bengtsson L, Koppeschaar CE, et al. Tracking social contact networks with online respondent-driven detection: who recruits whom? BMC Infect Dis. 2015;15:522. https://doi.org/10.1186/s12879-015-1250-z
4. Frieden TR, Lee CT. Identifying and interrupting super-spreading events–implications for control of severe acute respiratory syndrome coronavirus 2. Emerg. Emerg Infect Dis. 2020;26:1059–66. https://doi.org/10.3201/eid2606.200495
5. Department of Economic Planning and Development. Mid-year population estimates for Brunei Darussalam, 2019 [cited 2020 Apr 22]. http://www.deps.gov.bn/SitePages/Population.aspx
6. Wong J, Koh WC, Alikhan MF, Abdul Aziz ABZ, Naing L. Responding to COVID-19 in Brunei Darussalam: lessons for small countries. J Glob Health. 2020;10:010363. https://doi.org/10.7189/jogh.10.010363
7. Ahmad N. Attitudes towards family formation among young adults in Brunei Darussalam. Pakistan Journal of Women's Studies. Alam-e-Niswan. 2018;25:15–34. https://doi.org/10.46521/pjws.025.01.0052
8. Ahsan Ullah AKM, Ahmad Kumpoh AA-Z. Diaspora community in Brunei: culture, ethnicity and integration. Diaspora Studies. 2019;12:14–33. https://doi.org/10.1080/09739572.2018.1538686
9. Cabore JW, Karamagi HC, Kipruto H, Asamani JA, Droti B, Seydi ABW, et al. The potential effects of widespread community transmission of SARS-CoV-2 infection in the World Health Organization African Region: a predictive model. BMJ Glob Health. 2020;5:e002647. https://doi.org/10.1136/bmjgh-2020-002647
10. Che Mat NF, Edinur HA, Abdul Razab MKA, Safuan S. A single mass gathering resulted in massive transmission of COVID-19 infections in Malaysia with further international spread. J Travel Med. 2020;27:taaa059. https://doi.org/10.1093/jtm/taaa059
11. Wong J, Koh WC, Momin RN, Alikhan MF, Fadillah N, Naing L. Probable causes and risk factors for positive SARS-CoV-2 test in recovered patients: Evidence from Brunei Darussalam. J Med Virol. 2020 Jun 19 [Epub ahead of print] https://doi.org/10.1002/jmv.26199
12. World Health Organization. The First Few X (FFX) Cases and contact investigation protocol for 2019-novel coronavirus (2019-nCoV) infection, version 2. Geneva: The Organization; 2020. [cited 2020 May 1]. https://www.who.int/docs/default-source/coronaviruse/20200129-generic-ffx-protocol-2019-ncov.pdf
13. World Health Organization. Global surveillance for COVID-19 caused by human infection with COVID-19 virus: interim guidance, 20 March 2020. Geneva: The Organization; 2020 [cited 2020 Jun 30]. https://www.who.int/publications/i/item/global-surveillance-for-human-infection-with-novel-coronavirus-(2019-ncov)
14. Liu Y, Gayle AA, Wilder-Smith A, Rocklöv J. The reproductive number of COVID-19 is higher compared to SARS coronavirus. J Travel Med. 2020;27:taaa021. https://doi.org/10.1093/jtm/taaa021
15. R Core Team. R: A language and environment for statistical computing. Vienna: R Foundation for Statistical Computing; 2020.
16. Jing Q-L, Liu M-J, Zhang Z-B, Fang L-Q, Yuan J, Zhang A-R, et al. Household secondary attack rate of COVID-19 and associated determinants in Guangzhou, China: a retrospective cohort study. Lancet Infect Dis. 2020 Aug 21 [Epub ahead of print]. https://doi.org/10.1016/S1473-3099(20)30471-0
17. Li W, Zhang B, Lu J, Liu S, Chang Z, Cao P, et al. The characteristics of household transmission of COVID-19. Clin Infect Dis. 2020 Apr 17 [Epub ahead of print]. https://doi.org/10.1093/cid/ciaa450
18. Sjödin H, Wilder-Smith A, Osman S, Farooq Z, Rocklöv J. Only strict quarantine measures can curb the coronavirus disease (COVID-19) outbreak in Italy, 2020. Euro Surveill. 2020;25:2000280. https://doi.org/10.2807/1560-7917.ES.2020.25.13.2000280
19. Lau H, Khosrawipour V, Kocbach P, Mikolajczyk A, Schubert J, Bania J, et al. The positive impact of lockdown in Wuhan on containing the COVID-19 outbreak in China. J Travel Med. 2020;27:taaa037. https://doi.org/10.1093/jtm/taaa037
20. Hellewell J, Abbott S, Gimma A, Bosse NI, Jarvis CI, Russell TW, et al.; Centre for the Mathematical Modelling of Infectious Diseases COVID-19 Working Group. Feasibility of controlling COVID-19 outbreaks by isolation of cases and contacts. Lancet Glob Health. 2020;8:e488–96. https://doi.org/10.1016/S2214-109X(20)30074-7
21. Park SW, Sun K, Viboud C, Grenfell BT, Dushoff J. Potential role of social distancing in mitigating spread of coronavirus disease, South Korea. Emerg Infect Dis. 2020 Aug 21 [Epub ahead of print]. https://doi.org/10.3201/eid2611.201099
22. Wei WE, Li Z, Chiew CJ, Yong SE, Toh MP, Lee VJ. Pre-symptomatic Transmission of SARS-CoV-2 - Singapore, January 23-March 16, 2020. MMWR Morb Mortal Wkly Rep. 2020;69:411–5. https://doi.org/10.15585/mmwr.mm6914e1
23. Qian G, Yang N, Ma AHY, Wang L, Li G, Chen X, et al. COVID-19 transmission within a family cluster by presymptomatic carriers in China. Clin Infect Dis. 2020;71:861–2. https://doi.org/10.1093/cid/ciaa316
24. Chen Y, Wang AH, Yi B, Ding KQ, Wang HB, Wang JM, et al. Epidemiological characteristics of infection in COVID-19 close contacts in Ningbo city [in Chinese]. Zhonghua Liu Xing Bing Xue Za Zhi. 2020;41:667–71. https://doi.org/10.3760/cma.j.cn112338-20200304-00251
25. He D, Zhao S, Lin Q, Zhuang Z, Cao P, Wang MH, et al. The relative transmissibility of asymptomatic COVID-19 infections among close contacts. Int J Infect Dis. 2020;94:145–7. https://doi.org/10.1016/j.ijid.2020.04.034

Address for correspondence: Liling Chaw, PhD; PAPRSB Institute of Health Sciences, Universiti Brunei Darussalam, Jalan Tungku Link Gadong BE1410, Brunei Darussalam; email: liling.chaw@ubd.edu.bn

Case-Control Study of Use of Personal Protective Measures and Risk for SARS Coronavirus 2 Infection, Thailand

Pawinee Doung-ngern, Rapeepong Suphanchaimat, Apinya Panjangampatthana,
Chawisar Janekrongtham, Duangrat Ruampoom, Nawaporn Daochaeng, Napatchakorn Eungkanit,
Nichakul Pisitpayat, Nuengruethai Srisong, Oiythip Yasopa, Patchanee Plernprom, Pitiphon Promduangsi,
Panita Kumphon, Paphanij Suangtho, Peeriya Watakulsin, Sarinya Chaiya, Somkid Kripattanapong,
Thanawadee Chantian, Emily Bloss, Chawetsan Namwat, Direk Limmathurotsakul

We evaluated effectiveness of personal protective measures against severe acute respiratory disease coronavirus 2 (SARS-CoV-2) infection. Our case-control study included 211 cases of coronavirus disease (COVID-19) and 839 controls in Thailand. Cases were defined as asymptomatic contacts of COVID-19 patients who later tested positive for SARS-CoV-2; controls were asymptomatic contacts who never tested positive. Wearing masks all the time during contact was independently associated with lower risk for SARS-CoV-2 infection compared with not wearing masks; wearing a mask sometimes during contact did not lower infection risk. We found the type of mask worn was not independently associated with infection and that contacts who always wore masks were more likely to practice social distancing. Maintaining ≥1 m distance from a person with COVID-19, having close contact for ≤15 minutes, and frequent handwashing were independently associated with lower risk for infection. Our findings support consistent wearing of masks, handwashing, and social distancing to protect against COVID-19.

Author affiliations: Ministry of Public Health, Nonthaburi, Thailand
(P. Doung-ngern, R. Suphanchaimat, A. Panjangampatthana,
C. Janekrongtham, D. Ruampoom, N. Daochaeng, N. Eungkanit,
N. Pisitpayat, N. Srisong, O. Yasopa, P. Plernprom,
P. Promduangsi, P. Kumphon, P. Suangtho, P. Watakulsin,
S. Chaiya, S. Kripattanapong, T. Chantian, C. Namwat); Thailand
Ministry of Public Health–US Centers for Disease Control and
Prevention Collaboration, Nonthaburi (E. Bloss); Mahidol
University, Bangkok, Thailand (D. Limmathurotsakul); University
of Oxford, Oxford, United Kingdom (D. Limmathurotsakul)

Evaluation of the effectiveness of mask-wearing to protect healthy persons in the general public from infection with severe acute respiratory syndrome coronavirus 2 (SARS-CoV-2), the causative agent of coronavirus disease (COVID-19), is urgently needed (*1,2*). On February 27, 2020, during the early stages of the COVID-19 outbreak, the World Health Organization (WHO) announced that wearing a mask of any type was not recommended for asymptomatic persons (*3*). The rationale at that time was to avoid unnecessary cost, procurement burden, and a false sense of security (*3*). Several systematic reviews found no conclusive evidence to support widespread use of masks in public settings to protect against respiratory infectious diseases, such as influenza and severe acute respiratory syndrome (SARS) (*4–6*). However, China, South Korea, Japan, Thailand, and other countries in Asia have recommended the use of face masks among the general public since early in the COVID-19 pandemic (*7*). Evidence suggests that persons with COVID-19 can have a presymptomatic period, during which they can be contagious and transmit SARS-CoV-2 to others before symptoms develop (*8*). These findings led to a change in recommendations from the US Centers for Disease Control and Prevention on April 4, 2020, that advised all persons wear a cloth face covering when in public (*9*). On April 6 and June 5, 2020, WHO updated its advice on the use of masks for the general public and encouraged countries that issue the recommendations to conduct research on this topic (*8*).

Thailand has been implementing multiple measures against transmission of SARS-CoV-2 since the beginning of the outbreak (*10,11*). The country established thermal screening at airports on January 3, 2020, and detected an early case of COVID-19 outside China in a traveler from Wuhan, China, arriving at Bangkok Suvarnabhumi airport on January 8, 2020 (*10*). Thailand uses Surveillance and Rapid Response Teams (SRRTs), together with village health volunteers, to conduct contact tracing, educate the public about COVID-19, and monitor close contacts of persons with COVID-19 in quarantine (*11*). SRRTs are epidemiologic teams trained to conduct surveillance, investigations, and initial control of communicable diseases, such as SARS and influenza (*12,13*). More than 1,000 district-, provincial-, and regional-level SRRTs are working on COVID-19 contact tracing in Thailand.

By February 2020, public pressure to wear masks in Thailand was high. However, medical masks became difficult for the public to procure, and the government categorized medical masks as price-controlled goods. When the Ministry of Public Health (MoPH) designated COVID-19 a dangerous communicable disease, according to the Communicable Disease Act of 2015, government officials were empowered to quarantine case-contacts and close venues (*14,15*). On March 3, MoPH recommended public use of cloth face masks (*16*). On March 18, schools, universities, bars, nightclubs, and entertainment venues were closed (*17*). On March 26, when the country was reporting ≈100–150 new COVID-19 cases per day, the government declared a national state of emergency, prohibited public gatherings, and enforced wearing of face masks by all persons on public transport (*18*). On April 21, MoPH announced 19 new PCR-confirmed COVID-19 cases, bringing the total number of cases to 2,811 (*18*). Given the lack of evidence, we sought to evaluate the effectiveness of mask-wearing, handwashing, social distancing, and other personal protective measures against SARS-CoV-2 infection in public in Thailand.

Methods

Study Design
We conducted a retrospective case-control study by drawing persons with COVID-19 cases and noninfected controls from a cohort of contact tracing records of the central SRRT team at the Department of Disease Control (DDC), MoPH, Thailand. We included contact investigations of 3 large COVID-19 clusters in nightclubs, boxing stadiums, and a state enterprise office in Thailand.

Contacts were defined by DDC as persons who had activities with or were in the same location as a person with confirmed COVID-19 (*19,20*). The main aim of contact tracing was to identify and evaluate contacts, perform reverse transcription PCR (RT-PCR) diagnostic tests, and quarantine high-risk contacts, as defined by the MoPH (Appendix, https://wwwnc.cdc.gov/EID/article/26/11/20-3003-App1.pdf). RT-PCR was performed at laboratories certified for COVID-19 testing by the National Institute of Health of Thailand (*19,20*). Data on risk factors associated with SARS-CoV-2 infection, such as type of contact and use of mask, were recorded during contact investigations, but data sometimes were incomplete.

The central SRRT performed contact investigations for clusters of >5 PCR-confirmed COVID-19 cases from the same location within a 1-week period (*19,20*). We used these data to identify contacts who were asymptomatic during March 1–31, 2020. We used all available contact tracing records of the central SRRT in the study.

We telephoned contacts during April 30–May 27, 2020, and asked details about their contact with a COVID-19 index patient, such as dates, locations, duration, and distance of contact. We asked whether contacts wore a mask during the contact with the index patient, the type of mask, and the frequency of wearing a mask, which we defined as compliance with mask-wearing. We asked whether and how frequently contacts washed their hands while with the index patient. We asked whether contacts performed social distancing and whether they had physical contact with the COVID-19 index patient. If they did not know, or could not remember, contact with the index patient, we asked whether they had contact with other persons at the location. We asked whether the contact shared a cup or a cigarette with other persons in the place they had contact or had highest risk for contact with the index patient and whether the COVID-19 index patient, if known to the respondent, had worn a mask (Appendix, Additional Methods). We also asked, and verified by using DDC records, whether and when the contacts had symptoms and when COVID-19 was diagnosed.

For our study, we defined cases as asymptomatic contacts who later tested positive for SARS-CoV-2, on the basis of RT-PCR results available by April 21, 2020. We defined controls as asymptomatic contacts who did not have positive test results for SARS-CoV-2 by April 21, including those who tested negative and those who were not tested. We defined asymptomatic contacts as persons who had contact with or were in

the same location as a symptomatic COVID-19 patient and had no symptoms of COVID-19 on the first day of contact. We defined index patients as persons identified from contact tracing data as the potential source of SARS-CoV-2 infection; cases (as defined above) also could be index patients. We defined primary index patients as persons whose probable sources of infection were before the study period, March 1–31; for whom we were not able to identify the source of infection; or whose probable sources of infection were outside the contact tracing data included in the study. We defined high-risk exposure as that which occurred when persons lived in the same household as a COVID-19 patient; had a direct physical contact with a COVID-19 patient; were ≤1 m from a COVID-19 patient for >15 minutes; or were in the same closed environment, such as a room, nightclub, stadium, or vehicle, ≤1 m from a COVID-19 patient for >15 minutes.

We used 21 days after March 31 as a cutoff date based on evidence that most persons with COVID-19 likely would develop symptoms within 14 days (21) and that it could take ≤7 additional days for symptomatic persons under contact investigation to go to a healthcare facility and be tested for COVID-19. Our study follows the STROBE guidelines (22).

Statistical Analysis
To include only initially asymptomatic contacts in the study, we excluded persons who reported having symptoms of COVID-19 at the time of initial contact with an index patient. Because our study focused on the risk for infection in the community, we excluded contacts whose contact locations were healthcare facilities. We also excluded primary index patients if they were the first to have symptoms at the contact investigation location, had symptoms since the first day of visiting the location, or were the origin of infection based on the contact investigation.

We estimated secondary attack rates by using the percentage of new cases among asymptomatic contacts with high-risk exposure to enable comparison with other studies. We estimated odds ratios (ORs) and 95% CIs for associations between developing COVID-19 and factors evaluated. We used logistic regression with random effects for location and for index patients nested in the same location. If an asymptomatic contact had contact with ≥1 symptomatic COVID-19 index patient, the interviewer identified the index patient as the symptomatic COVID-19 patient with the closest contact. The percentage of missing values for the variable indicating whether the index patients wore a mask was 27%; thus, we

did not include this variable in our analyses. For other variables, we assumed that missing values were missing at random and used imputation by chained equations (23,24). We created 10 imputed datasets and the imputation model included the case-control indicator and variables used in the multivariable models, including sex, age group, contact place, shortest distance of contact, duration of contact at ≤1 m, sharing dishes or cups, sharing cigarettes, handwashing, mask-wearing, and compliance with mask-wearing. We developed the final multilevel mixed-effect logistic regression models on the basis of previous knowledge and a purposeful selection method (25; Appendix, Additional Analyses). Because of collinearity between mask use and mask type, we conducted a separate analysis including mask type in the multilevel mixed-effects logistic regression model for SARS-CoV-2 infection. We also tested a predefined interaction between mask type and compliance with mask-wearing (Appendix, Additional Analyses).

To clarify patterns of behavior and factors related to compliance with mask-wearing, we used multinomial logistic regression models and the imputed dataset to estimated OR and 95% CI for associations between 3 mask-wearing compliance categories, never, sometimes, or all the time; and for other practices, including handwashing and social distancing during the contact period. We used logistic regression to estimate p values for pairwise comparisons.

To estimate the proportional reduction in cases that would occur if exposure to risk factors was reduced, we estimated the population attributable fraction by using the imputed dataset and a direct method based on logistic regression, as described previously (26,27; Appendix, Additional Analyses). We performed all analyses by using Stata version 14.2 (StataCorp, https://www.stata.com) and R version 4.0.0 (R Foundation for Statistical Computing, https://www.r-project.org).

Results

Characteristics of the Cohort Data
The contact tracing records of the central SRRT included 1,716 persons who had contact with or were in the same location as a person with diagnosed COVID-19 in an investigation of 3 large clusters (Figure 1). Overall, 18 primary index patients were identified: 11 from the nightclub cluster, 5 from the boxing stadiums cluster, and 2 from the state enterprise office cluster. Timelines of primary index patients from the 3 clusters varied (Appendix Figures
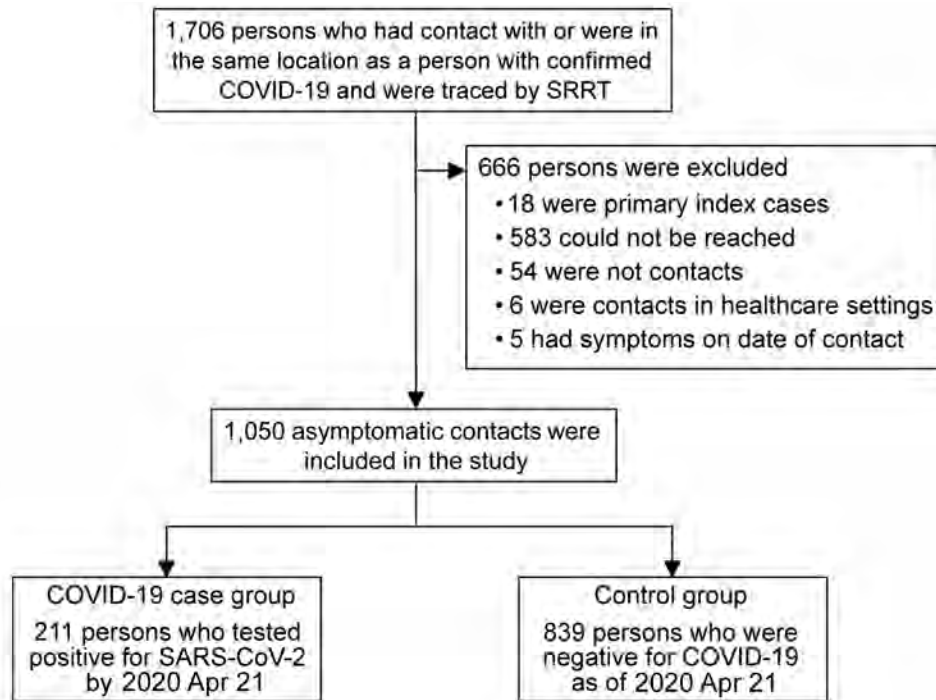
Figure 1. Flow diagram in case-control study of severe acute respiratory syndrome coronavirus 2 infections and contacts, Thailand, March–April 2020. COVID-19, coronavirus disease; SARS-CoV-2, severe acute respiratory syndrome coronavirus 2; SRRT, Surveillance and Rapid Response Team of Ministry of Public Health.

1–3); we excluded the 18 primary index patients from our analyses.

Characteristics of Cases and Controls

After interviewing each contact by phone and applying the exclusion criteria (Figure 1), our analysis included 1,050 asymptomatic persons who had contact with or were in the same location as a symptomatic COVID-19 index patient during March 1–31, 2020. The median age of persons included was 38 years (IQR 28–51 years); 55% were male, and 45% were female (Table 1). Most (61%; n = 645) asymptomatic contacts included in the study were associated with the boxing stadiums cluster, 36% (n = 374) were related to the nightclub cluster, and 3% (n = 31) were related to the state enterprise office cluster. Overall, 890 (84.8%) contacts were considered to have high-risk exposure.

Among 1,050 asymptomatic contacts included in our analysis, 211 (20.1%) tested positive for SARS-CoV-2 by April 21, 2020, and were classified as cases; 839 (79.9%) never tested positive and were controls. Of the 211 cases, 195 (92.4%) had high-risk exposures and 150 (71.1%) had symptoms before COVID-19 diagnosis by RT-PCR (Appendix). The last date that a COVID-19 case was detected was April 9, 2020. Among the 839 controls, 695 (82.8%) had high-risk exposures and 719 (85.7%) were tested by PCR at least once.

Among asymptomatic contacts included in the study, 228 had contact with a COVID-19 index patient at nightclubs, 144 at boxing stadiums, and 20 at the state enterprise office (Figure 2). The others had contacts with a COVID-19 index patient at workplaces (n = 277), households (n = 230), and other places (n = 151). Among 890 asymptomatic contacts with high-risk exposures included in the study, the secondary attack rate from boxing stadiums was 86% (111/129), the secondary attack rate for nightclubs was 18.2% (34/187), the household secondary attack rate was 16.5% (38/230), the workplace secondary attack rate was 4.9% (10/205), and the secondary attack rate at other places was 1.4% (2/139).

Bivariate Analyses

Our analysis showed risk for SARS-CoV-2 infection was negatively associated with personal protective measures (Table 1). Crude odds ratio (OR) for infection was 0.08 (95% CI 0.02–0.31) for those maintaining a distance of ≥ 1 m from a COVID-19 patient; 0.13 (95% CI 0.04–0.46) for those whose duration of contact was ≤ 15 minutes; 0.41 (95% CI 0.18–0.91) for those who performed handwashing sometimes; 0.19 (95% CI 0.08–0.46) for those who washed hands often; and 0.16 (95% CI 0.07–0.36) for those wearing a mask all the time during contact with a COVID-19 patient. We noted a higher risk for SARS-CoV-2 infection among persons sharing dishes or cups (OR 2.71; 95% CI 1.48–4.94) and sharing cigarettes (OR 6.12; 95% CI 2.12–17.72) with other persons in general, not necessarily including a COVID-19 patient. In the bivariate model, type of mask was associated with risk for infection (p = 0.003).

Multivariable Analyses

We found a negative association between risk for SARS-CoV-2 infection and maintaining a distance of ≥1 m from a COVID-19 patient (adjusted odds ratio [aOR] 0.15; 95% CI 0.04–0.63); duration of contact ≤15 minutes (aOR 0.24; 95% CI 0.07–0.90); handwashing often (aOR 0.33; 95% CI 0.13–0.87); and wearing a mask all the time during contact with a COVID-19 patient (aOR 0.23; 95% CI 0.09–0.60) (Table 1). Wearing masks sometimes during contact with a COVID-19 patient was not statistically significantly associated with lower risk for infection (aOR 0.87; 95% CI 0.41–1.84). Sharing cigarettes with other persons was associated with higher risk for infection (aOR 3.47; 95% CI 1.09–11.02).

Compliance with mask-wearing during contact with a COVID-19 patient was strongly associated

Table 1. Factors associated with coronavirus disease among persons followed through contract tracing, Thailand, March–April 2020*

Factors	COVID-19 cases, no. (%), N = 211†	Controls, no. (%), N = 839†	Crude odds ratio (95% CI)‡	p value	Adjusted odds ratio (95% CI)‡	p value
Sex	n = 211	n = 838				
F	65 (30.8)	404 (48.2)	Referent	0.52	Referent	0.37
M	146 (69.2)	434 (51.8)	0.83 (0.47–1.46)		0.76 (0.41–1.41)	
Age group, y	n =211	n = 829				
≤15	6 (2.8)	49 (5.9)	0.65 (0.17–2.48)	0.29	0.57 (0.15–2.21)	0.21
>15–40	94 (44.5)	435 (52.5)	Referent		Referent	
>40–65	98 (46.4)	302 (36.4)	1.65 (0.91–2.97)		1.77 (0.94–3.32)	
>65	13 (6.2)	43 (5.0)	1.29 (0.33–5.07)		0.97 (0.22–4.24)	
Contact place§	n = 211	n = 839				
Nightclub	35 (16.6)	193 (23.0)	NA	NA	NA	NA
Boxing stadium	125 (59.2)	19 (2.3)				
Workplace	11 (5.2)	286 (34.0)				
Household	38 (18.0)	192 (22.9)				
Others	2 (0.9)	149 (17.8)				
Shortest distance of contact	n = 197	n = 809				
Physical contact	132 (67.0)	292 (36.1)	Referent	0.001	Referent	0.02
≤1 m without physical contact	61 (30.9)	335 (41.4)	0.76 (0.43–1.35)		1.09 (0.58–2.07)	
>1 m	4 (2.0)	182 (22.5)	0.08 (0.02–0.31)		0.15 (0.04–0.63)	
Duration of contact within 1 m	n = 199	n = 801				
>60 min	180 (90.4)	487 (60.8)	Referent	0.003	Referent	0.09
>15–60 min	14 (7.0)	162 (20.2)	0.53 (0.24–1.17)		0.67 (0.29–1.55)	
≤15 min	5 (2.5)	152 (19.0)	0.13 (0.04–0.46)		0.24 (0.07–0.90)	
Sharing dishes or cups¶	n = 210	n = 837				
N	125 (59.5)	576 (68.8)	Referent	0.001	Referent	0.39
Y	85 (40.5)	261 (31.2)	2.71 (1.48–4.94)		1.33 (0.70–2.54)	
Sharing cigarettes#	n = 209	n = 836				
N	196 (93.8)	824 (98.6)	Referent	0.001	Referent	0.03
Y	13 (6.2)	12 (1.4)	6.12 (2.12–17.72)		3.47 (1.09–11.02)	
Handwashing**	n = 210	n = 826				
None	44 (20.9)	121 (14.6)	Referent	<0.001	Referent	0.045
Sometimes	114 (54.3)	333 (40.3)	0.41 (0.18–0.91)		0.34 (0.14–0.81)	
Often	52 (24.8)	372 (45.0)	0.19 (0.08–0.46)		0.33 (0.13–0.87)	
Type of mask††	n = 211	n = 834				
None	102 (48.3)	500 (60.0)	Referent	0.003	–	–
Nonmedical masks only	25 (11.8)	77 (9.2)	0.78 (0.32–1.90)			
Nonmedical and medical	12 (5.7)	48 (5.8)	0.46 (0.13–1.64)			
Medical mask only	72 (34.1)	209 (25.0)	0.25 (0.12–0.53)			
Compliance with mask-wearing††	n = 210	n = 823				
Not wearing a mask	102 (48.6)	500 (60.7)	Referent	<0.001	Referent	0.006
Wearing a mask sometimes	79 (37.6)	125 (15.2)	0.75 (0.37–1.52)		0.87 (0.41–1.84)	
Always wearing a mask	29 (13.8)	198 (24.1)	0.16 (0.07–0.36)		0.23 (0.09–0.60)	

*NA, not applicable; COVID-19, coronavirus disease.
†Data not available for all cases and controls for all factors.
‡Crude and adjusted odds ratios were estimated using logistic regression with random effects for location and for index patient nested within the same location.
§The state enterprise office was included as a workplace. Others included restaurants, markets, malls, religious places, and households of index patients or other persons in persons not living in that household. Location was included in the model as a random effect variable.
¶Sharing multiserving dishes and using communal serving utensils to portion food individually was not categorized as sharing dishes.
#Included sharing electronic cigarettes and any vaping devices.
**Included washing with soap and water, and by using alcohol-based solutions.
††Wearing masks incorrectly, such as not covering both nose and mouth, was considered the same as not wearing a mask for analyses. Crude odds ratios of wearing mask and of each factor evaluated were estimated using logistic regression with random effects for location and for index patient nested within the same location to take into account clustering; therefore, the crude odds ratios are not equal to dividing of the odds in the case group by the odds in the control group.

with lower risk for infection in the multivariable model. Because of collinearity with mask-wearing compliance, we did not include mask type in the final model. We included mask type in a separate multivariable model and found type of mask was not independently associated with infection (p = 0.54) (Appendix Table 1). We found no evidence of effect modification between mask type and mask-wearing compliance.

Association Between Mask-Wearing Compliance and Other Social Distancing Practices

Because mask-wearing throughout the contact period was negatively associated with COVID-19, we
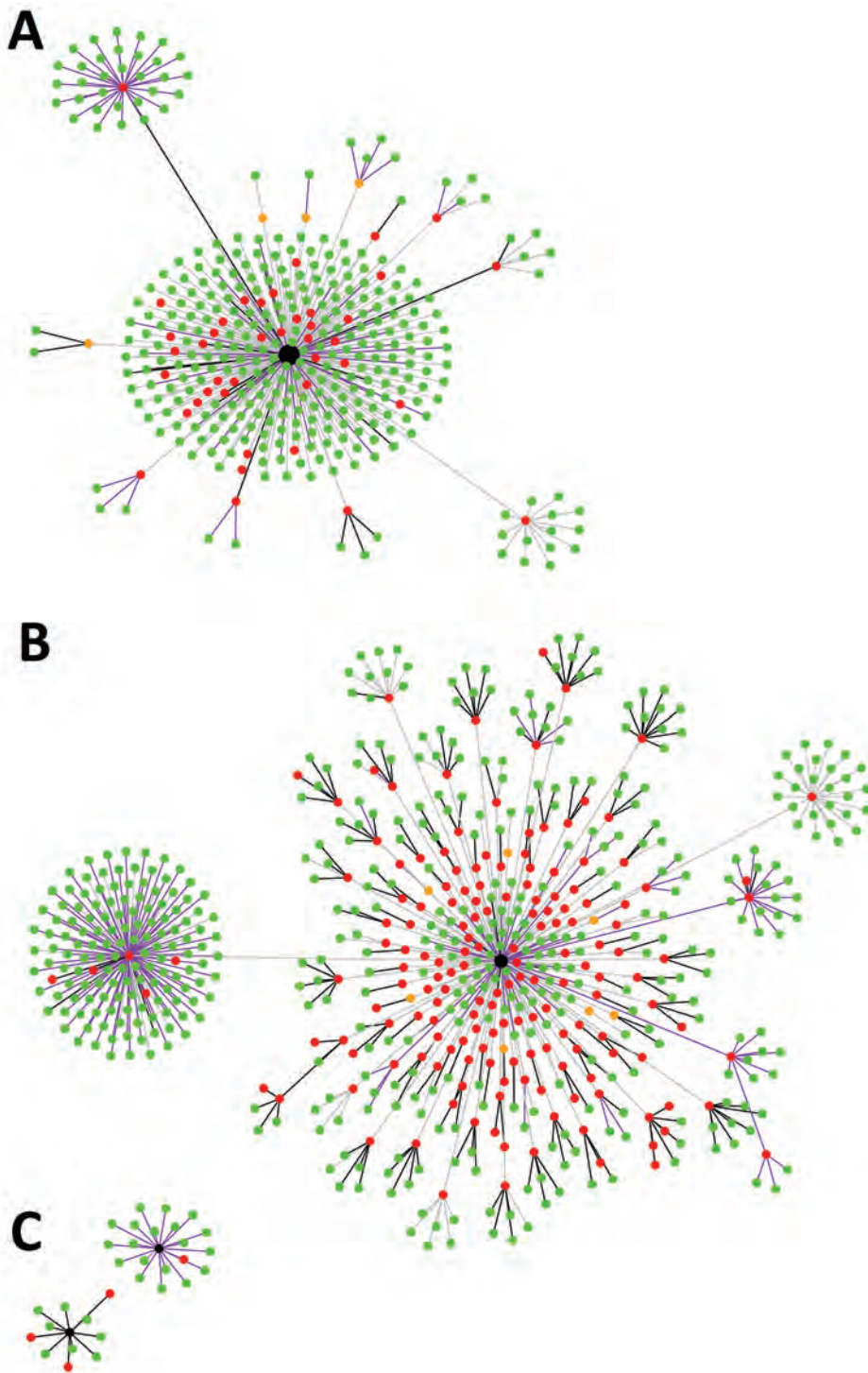
Figure 2. Development and transmission of severe acute respiratory syndrome coronavirus 2 among asymptomatic contacts, Thailand, March–April 2020. Clusters indicate coronavirus disease (COVID-19) contacts from nightclubs (A); boxing stadiums (B), and the state enterprise office (C). Black nodes represent primary index patients, red dots cases (contacts of primary index patients who had COVID-19), green dots noninfected controls, and orange dots patients with confirmed COVID-19 who could not be contacted by the study team. Black lines represent household contacts, purple lines contacts at workplaces, and gray lines contacts at other locations.

further explored characteristics of participants to ascertain whether wearing a mask produced a potential false sense of security. We found that during the contact period, 25% of persons who wore masks all the time reported maintaining ≥1 m distance from contacts compared with 18% of persons who did not wear a mask (pairwise p = 0.03). In addition, persons who wore masks all the time were more likely to report duration of contact ≤15 minutes (26% vs. 13% for those who did not wear a mask; pairwise p<0.001) and washing hands often (79% vs. 26% for those who did not wear a mask; pairwise p<0.001) (Table 2). We found that 43% of persons who wore masks sometimes were likely to wash their hands often compared with those who did not wear masks (26%; pairwise p<0.001), but they were more likely to have physical contact (50% vs. 42%; pairwise p = 0.03) and report duration of contact >60 minutes

(75% vs. 67%; pairwise p = 0.04) compared with those who did not wear masks.

Discussion

Our findings provide evidence that mask-wearing, handwashing, and social distancing are independently associated with lower risk for SARS-CoV-2 infection in the general public in community settings in Thailand. We observed that wearing masks throughout the period of exposure to someone infected with SARS-CoV-2 was associated with lower risk for infection, but wearing masks only sometimes during the period was not. This evidence supports recommendations to wear masks consistently and correctly at all times in public (2,7–9).

The effectiveness of mask-wearing we observed is consistent with previous studies, including a randomized-controlled trial showing that consistent face

Table 2. Factors associated with compliance of mask wearing among coronavirus disease cases and controls, Thailand, March–April 2020*

Factors	Not wearing masks, no. (%), n = 602	Sometimes wearing masks, no. (%), n = 204	Always wearing masks, no. (%), n = 227	p value†
Sex	n = 601	n = 204	n = 227	
F	277 (46.1)	75 (36.8)	112 (49.3)	0.03
M	324 (53.9)	129 (63.2)	115 (50.7)	
Age group, y	n = 594	n = 204	n = 225	
≤15	45 (7.6)	5/204 (2%)	3/225 (1%)	<0.001
>15–40	269 (45.3)	117/204 (57%)	132/225 (59%)	
>40–65	236 (39.7)	76/204 (37%)	84/225 (37%)	
>65	44 (7.4)	6/204 (3%)	6/225 (3%)	
Contact places‡	n = 602	n = 204	n = 227	
Nightclub	84 (14.0)	51 (25.0)	91 (40.1)	<0.001
Boxing stadium	48 (8.0)	66 (32.4)	29 (12.8)	
Workplace	178 (29.6)	46 (22.5)	64 (28.2)	
Household	167 (27.7)	27 (13.2)	33 (14.5)	
Others	125 (20.7)	14 (6.9)	10 (4.4)	
Shortest distance of contact	n = 588	n = 191	n = 212	
Physical contact	246 (41.8)	96 (50.3)	76 (35.8)	0.005
≤1 m without physical contact	238 (40.5)	70 (36.6)	83 (39.1)	
>1 m	104 (17.7)	25 (13.1)	53 (25.0)	
Duration of contact within 1 m	n = 590	n = 190	n = 205	
>60 min	396 (67.1)	143 (75.3)	121 (59.0)	<0.001
>15–60 min	120 (20.3)	23 (12.1)	30 (14.6)	
≤15 min	74 (12.5)	24 (12.6)	54 (26.3)	
Sharing dishes or cups§	n = 601	n = 203	n = 226	
N	361 (60.1)	130 (64.0)	200 (88.5)	<0.001
Y	240 (39.9)	73 (36.0)	26 (11.5)	
Sharing cigarettes¶	n = 600	n = 202	n = 226	
N	586 (97.7)	194 (96.0)	223 (98.7)	0.29
Y	14 (2.3)	8 (4.0)	3 (1.3)	
Handwashing#	n = 594	n = 203	n = 224	
None	142 (23.9)	16 (7.9)	6 (2.7)	<0.001
Sometimes	298 (50.2)	99 (48.8)	42 (18.8)	
Often	154 (25.9)	88 (43.3)	176 (78.6)	

*Data not available for all cases and controls for all factors. Wearing masks incorrectly, such as not covering both nose and mouth, was considered the same as not wearing a mask for analyses.
†p values were estimated by using univariable multinomial logistic regression models. Missing values were imputed using the imputation model.
‡The state enterprise office was included as a workplace. Others included restaurants, markets, malls, religious places, and households of index patients or other persons but not living together (e.g., persons not living in that household).
§Sharing multiserving dishes and using communal serving utensils to portion food individually was not categorized as sharing dishes.
¶Included sharing electronic cigarettes and any vaping devices.
#Included washing with soap and water, and by using alcohol-based solutions.

mask use reduced risk for influenza-like illness (*28*), 2 case-control studies that found that mask-wearing was associated with lower risk for SARS infection (*29,30*), and a retrospective cohort study that found that mask-wearing by index patients or family members at home was associated with lower risk for SARS-CoV-2 infection (*31*). Previous studies found use of surgical masks or similar 12–16-layer cotton reusable masks demonstrated protection against coronavirus infection in the community (*32*), but we did not observe a difference between wearing nonmedical and medical masks in the general population. Our results suggest that wearing nonmedical masks in public can potentially reduce transmission of SARS-CoV-2. Another study found perception of risk of developing COVID-19 can increase a person's likelihood of wearing a medical mask in nonmedical settings (T.D. Huynh, unpub. data, https://www.medrxiv.org/content/10.1101/2020.03.26.20044388v1). However, given supply shortages, medical masks should be reserved for use by healthcare workers.

We found a negative association between risk for SARS-CoV-2 infection and social distancing, consistent with previous studies that found that ≥ 1 m physical distancing was associated with a large protective effect and distances of >2 m could be more effective (*32*). Our findings on effectiveness of hand hygiene also were consistent with reports in previous studies (*33*).

In this study, secondary attack rates at different venues varied widely. The household secondary attack rate in our study (16.5%) is comparable with ranges reported previously (11%–23%) (*34,35*), and relatively high compared with workplaces (4.9%) and other settings (1.4%). Although quarantine measures can be challenging and sometimes impractical, household members should immediately separate a person who develops symptoms of COVID-19; the sick person should stay in a specific room; use a separate bathroom, if possible; and not share dishes, cups, and other utensils (*36*). All household members should wear masks, frequently wash their hands, and perform social distancing to the extent possible (*37*).

The high number of COVID-19 cases associated with nightclub exposures in Bangkok is comparable to a COVID-19 outbreak associated with the Itaewon nightclub cluster in Seoul, South Korea, during May 2020 (*38*), in which persons visited several nightclubs in the same area during a short period of time. The secondary attack rate in boxing stadiums was high (86%) but similar to a cluster of COVID-19 cases associated with a football match in Italy during February 2020 (*39*). The secondary attack rate of COVID-19 at a choir practice in the United States was reported to be 53.3%–86.7% (*40*). Secondary attack rates in public gathering places with high densities of persons shouting and cheering, such as football and boxing stadiums, are still uncertain but appear to be high.

Clear and consistent public messaging from policy makers likely can prevent a false sense of security and promote compliance with social distancing in Thailand. We found that those who wore masks throughout the time they were exposed to a COVID-19 patient also were more likely to wash their hands and perform social distancing. Traditional and social media outlets can support public health responses by working with governments to provide consistent, simple, and clear messages (*41*). In Thailand, daily briefings from the Centre for COVID-19 Situation Administration provided clear, consistent messages on social distancing, how to put on a mask, and how to wash hands, which might have improved public confidence with the recommendations. Consistent public messages on how to wear masks correctly also are needed, particularly for those who wear masks sometimes or incorrectly, such as not covering both nose and mouth. We found that persons who only intermittently wore masks during exposure also did not practice social distancing adequately.

Our study has several limitations. First, because our findings were based on contacts related to 3 major COVID-19 clusters in Thailand during March 2020, they might not be generalizable to all settings. Second, estimated ORs were conditioned on reported contact with index patients; our study did not evaluate or consider the probability of having contact with other infected persons in the community, which could have occurred. Third, because only 89% of controls were tested, those not tested could have been infected; therefore, cases might have been missed in persons with mild or no symptoms or who did not report symptoms or seek care or testing. Nonetheless, we believe that misclassification likely was minimal because those who were not tested with RT-PCR were low-risk contacts; the small number likely would not change our main findings and recommendations on personal protective measures. Fourth, identifying every potential contact can be nearly impossible because some persons might have had contact with >1 COVID-19 patient. Hence, our estimated secondary attack rates among contacts with high-risk exposure could be overestimated or underestimated. Fifth, population attributable fraction is based on several assumptions, including causality, and should be interpreted with caution (*42,43*). Finally, findings were subject to

common biases of retrospective case-control studies, including memory bias, observer bias, and information bias (*44*). To reduce potential biases, we used structured interviews in which each participant was asked the same set of defined questions.

As many countries begin to relax social distancing measures, our findings provide evidence supporting consistent mask-wearing, handwashing, and adhering to social distancing recommendations to reduce SARS-CoV-2 transmission in public gatherings. Wearing nonmedical masks in public could help slow the spread of COVID-19. Complying with all measures could be highly effective; however, in places with a high population density, additional measures might be required.

Clear and consistent public messaging on personal protective recommendations is essential, particularly for targeting those who wear masks intermittently or incorrectly. Our data showed that no single protective measure was associated with complete protection from COVID-19. All measures, including mask-wearing, handwashing, and social distancing, can increase protection against COVID-19 in public settings.

This article was preprinted at https://www.medrxiv.org/content/10.1101/2020.06.11.20128900.

About the Author
Dr. Pawinee Doung-ngern is the head of Communicable Disease Unit, Bureau of Epidemiology, Department of Disease Control, Ministry of Public Health, Thailand. Her primary research interests include the public health and epidemiology of communicable diseases.

References
1. Greenhalgh T, Schmid MB, Czypionka T, Bassler D, Gruer L. Face masks for the public during the covid-19 crisis. BMJ. 2020;369:m1435. https://doi.org/10.1136/bmj.m1435
2. Cheng KK, Lam TH, Leung CC. Wearing face masks in the community during the COVID-19 pandemic: altruism and solidarity. Lancet. 2020 April 16 [Epub ahead of print]. https://doi.org/10.1016/S0140-6736(20)30918-1
3. World Health Organization. Rational use of personal protective equipment for coronavirus disease (COVID-19): interim guidance, 27 February 2020 [cited 2020 Jun 23]. https://apps.who.int/iris/handle/10665/331215
4. Long Y, Hu T, Liu L, Chen R, Guo Q, Yang L, et al. Effectiveness of N95 respirators versus surgical masks against influenza: A systematic review and meta-analysis. J Evid Based Med. 2020;13:93–101. https://doi.org/10.1111/jebm.12381
5. Cowling BJ, Zhou Y, Ip DK, Leung GM, Aiello AE. Face masks to prevent transmission of influenza virus: a systematic review. Epidemiol Infect. 2010;138:449–56. https://doi.org/10.1017/S0950268809991658
6. Jefferson T, Del Mar CB, Dooley L, Ferroni E, Al-Ansary LA, Bawazeer GA, et al. Physical interventions to interrupt or reduce the spread of respiratory viruses. Cochrane Database Syst Rev. 2011; (7):CD006207. https://doi.org/10.1002/14651858.CD006207.pub4
7. Feng S, Shen C, Xia N, Song W, Fan M, Cowling BJ. Rational use of face masks in the COVID-19 pandemic. Lancet Respir Med. 2020;8:434–6. https://doi.org/10.1016/S2213-2600(20)30134-X
8. World Health Organization. Advice on the use of masks in the context of COVID-19: interim guidance, 5 June 2020 [cited 2020 Jun 23]. https://apps.who.int/iris/handle/10665/332293
9. US Centers for Disease Control and Prevention. Coronavirus disease 2019 (COVID-19): how to protect yourself and others [cited 2020 Jun 23]. https://www.cdc.gov/coronavirus/2019-ncov/prevent-getting-sick/prevention.html
10. Okada P, Buathong R, Phuygun S, Thanadachakul T, Parnmen S, Wongboot W, et al. Early transmission patterns of coronavirus disease 2019 (COVID-19) in travellers from Wuhan to Thailand, January 2020. Euro Surveill. 2020;25. https://doi.org/10.2807/1560-7917.ES.2020.25.8.2000097
11. Department of Disease Control, Ministry of Public Health, Thailand. Coronavirus disease (COVID-19): situation reports 2020 [cited 2020 Jun 23]. https://ddc.moph.go.th/viralpneumonia/eng/situation.php
12. Chunsuttiwat S. Response to avian influenza and preparedness for pandemic influenza: Thailand's experience. Respirology. 2008;13:S36–40. https://doi.org/10.1111/j.1440-1843.2008.01256.x
13. Putthasri W, Lertiendumrong J, Chompook P, Tangcharoensathien V, Coker R. Capacity of Thailand to contain an emerging influenza pandemic. Emerg Infect Dis. 2009;15:423–32. https://doi.org/10.3201/eid1503.080872
14. Bangkok Post. Tougher Covid-19 measures take effect Sunday. 2020 Feb 29 [cited 2020 Jun 23]. https://www.bangkokpost.com/thailand/general/1868439/tougher-covid-19-measures-take-effect-sunday
15. World Health Organization, Thailand. Coronavirus disease 2019 (COVID-19) WHO Thailand situation report–11: 29 Feb 2020 [cited 2020 Jun 23]. https://www.who.int/docs/default-source/searo/thailand/20200229-tha-sitrep-11-covid-19-final.pdf

16. Channel News Asia. 'Better than nothing': Thailand encourages cloth masks amid surgical mask shortage. 12 Mar 2020 [cited 2020 Jun 23]. https://www.channelnewsasia.com/news/asia/coronavirus-thailand-cloth-masks-surgical-shortage-covid-19-12530896

17. Bangkok Post. Cabinet approves plans to close schools, postpone Songkran. 2020 Mar 17 [cited 2020 Jun 23]. https://www.bangkokpost.com/thailand/general-al/1880635/cabinet-approves-plans-to-close-schools-postpone-songkran

18. World Health Organization, Thailand. Coronavirus disease 2019 (COVID-19) WHO Thailand situation report–59: 21 April 2020 [cited 2020 Jun 23]. https://www.who.int/docs/default-source/searo/thailand/2020-04-21-tha-sitrep-59-covid19-new-template-final.pdf

19. Department of Disease Control, Ministry of Public Health, Thailand. Coronavirus disease 2019: COVID-19, updated on 3 March 2020 [cited 2020 Jun 23]. https://ddc.moph.go.th/viralpneumonia/file/guidelines/G_Invest_03_2.pdf

20. Department of Disease Control, Ministry of Public Health, Thailand. Coronavirus disease 2019: COVID-19, updated on 23 March 2020 [cited 2020 Jun 23]. https://ddc.moph.go.th/viralpneumonia/file/g_srrt/g_srrt_250363.pdf

21. Lauer SA, Grantz KH, Bi Q, Jones FK, Zheng Q, Meredith HR, et al. The incubation period of coronavirus disease 2019 (COVID-19) from publicly reported confirmed cases: estimation and application. Ann Intern Med. 2020;172: 577–82. https://doi.org/10.7326/M20-0504

22. Vandenbroucke JP, von Elm E, Altman DG, Gøtzsche PC, Mulrow CD, Pocock SJ, et al.; STROBE Initiative. Strengthening the reporting of observational studies in epidemiology (STROBE): explanation and elaboration. PLoS Med. 2007;4:e297. https://doi.org/10.1371/journal.pmed.0040297

23. van Buuren S, Boshuizen HC, Knook DL. Multiple imputation of missing blood pressure covariates in survival analysis. Stat Med. 1999;18:681–94. https://doi.org/10.1002/(SICI)1097-0258(19990330)18:6<681::AID-SIM71>3.0.CO;2-R

24. Raghunathan T, Lepkowski J, Hoewyk J, Solenberger P. A multivariate technique for multiply imputing missing values using a sequence of regression models. Surv Methodol. 2001;27:85–95.

25. Bursac Z, Gauss CH, Williams DK, Hosmer DW. Purposeful selection of variables in logistic regression. Source Code Biol Med. 2008;3:17. https://doi.org/10.1186/1751-0473-3-17

26. Azimi SS, Khalili D, Hadaegh F, Yavari P, Mehrabi Y, Azizi F. Calculating population attributable fraction for cardiovascular risk factors using different methods in a population based cohort study. J Res Health Sci. 2015;15:22–7.

27. Rückinger S, von Kries R, Toschke AM. An illustration of and programs estimating attributable fractions in large scale surveys considering multiple risk factors. BMC Med Res Methodol. 2009;9:7. https://doi.org/10.1186/1471-2288-9-7

28. MacIntyre CR, Cauchemez S, Dwyer DE, Seale H, Cheung P, Browne G, et al. Face mask use and control of respiratory virus transmission in households. Emerg Infect Dis. 2009;15:233–41. https://doi.org/10.3201/eid1502.081166

29. Wu J, Xu F, Zhou W, Feikin DR, Lin CY, He X, et al. Risk factors for SARS among persons without known contact with SARS patients, Beijing, China. Emerg Infect Dis. 2004;10:210–6. https://doi.org/10.3201/eid1002.030730

30. Lau JT, Tsui H, Lau M, Yang X. SARS transmission, risk factors, and prevention in Hong Kong. Emerg Infect Dis. 2004;10:587–92. https://doi.org/10.3201/eid1004.030628

31. Wang Y, Tian H, Zhang L, Zhang M, Guo D, Wu W, et al. Reduction of secondary transmission of SARS-CoV-2 in households by face mask use, disinfection and social distancing: a cohort study in Beijing, China. BMJ Glob Health. 2020;5:e002794. https://doi.org/10.1136/bmjgh-2020-002794

32. Chu DK, Akl EA, Duda S, Solo K, Yaacoub S, Schünemann HJ, et al.; COVID-19 Systematic Urgent Review Group Effort (SURGE) study authors. Physical distancing, face masks, and eye protection to prevent person-to-person transmission of SARS-CoV-2 and COVID-19: a systematic review and meta-analysis. Lancet. 2020;395:1973–87. https://doi.org/10.1016/S0140-6736(20)31142-9

33. Jefferson T, Del Mar C, Dooley L, Ferroni E, Al-Ansary LA, Bawazeer GA, et al. Physical interventions to interrupt or reduce the spread of respiratory viruses: systematic review. BMJ. 2009;339:b3675. https://doi.org/10.1136/bmj.b3675

34. Bi Q, Wu Y, Mei S, Ye C, Zou X, Zhang Z, et al. Epidemiology and transmission of COVID-19 in 391 cases and 1286 of their close contacts in Shenzhen, China: a retrospective cohort study. Lancet Infect Dis. 2020;20:911–9. https://doi.org/10.1016/S1473-3099(20)30287-5

35. Jing Q-L, Liu M-J, Yuan J, Zhang Z-B, Zhang A-R, Dean NE, et al. Household secondary attack rate of COVID-19 and associated determinants. Lancet Infect Dis. 2020 Jun 17 [Epub ahead of print]. PubMed https://doi.org/10.1016/S1473-3099(20)30471-0

36. US Centers for Disease Control and Prevention. Coronavirus disease 2019 (COVID-19): what to do if you are sick [cited 2020 Jun 23]. https://www.cdc.gov/coronavirus/2019-ncov/if-you-are-sick/steps-when-sick.html

37. US Centers for Disease Control and Prevention. Coronavirus disease 2019 (COVID-19): households living in close quarters [cited 2020 Jun 23]. https://www.cdc.gov/coronavirus/2019-ncov/daily-life-coping/living-in-close-quarters.html

38. Kang CR, Lee JY, Park Y, Huh IS, Ham HJ, Han JK, et al.; Seoul Metropolitan Government COVID-19; Rapid Response Team (SCoRR Team). Coronavirus disease exposure and spread from nightclubs, South Korea. Emerg Infect Dis. 2020;26. https://doi.org/10.3201/eid2610.202573

39. Boccia S, Ricciardi W, Ioannidis JPA. What other countries can learn from Italy during the COVID-19 pandemic. JAMA Intern Med. 2020;180:927. https://doi.org/10.1001/jamainternmed.2020.1447

40. Hamner L, Dubbel P, Capron I, Ross A, Jordan A, Lee J, et al. High SARS-CoV-2 attack rate following exposure at a choir practice—Skagit County, Washington, March 2020. MMWR Morb Mortal Wkly Rep. 2020;69:606–10. https://doi.org/10.15585/mmwr.mm6919e6

41. Hopman J, Allegranzi B, Mehtar S. Managing COVID-19 in low- and middle-income countries. JAMA. 2020;323:1549. https://doi.org/10.1001/jama.2020.4169

42. Levine B. What does the population attributable fraction mean? Prev Chronic Dis. 2007;4:A14.

43. Mansournia MA, Altman DG. Population attributable fraction. BMJ. 2018;360:k757. https://doi.org/10.1136/bmj.k757

44. Kopec JA, Esdaile JM. Bias in case-control studies. A review. J Epidemiol Community Health. 1990;44:179–86. https://doi.org/10.1136/jech.44.3.179

Address for correspondence: Direk Limmathurotsakul, 420/6 Mahidol-Oxford Tropical Medicine Research Unit, Faculty of Tropical Medicine, Rajvithi Road, Bangkok 10400, Thailand; email: direk@tropmedres.ac

Transmission of SARS-CoV-2 During Long-Haul Flight

Nguyen Cong Khanh,[1] Pham Quang Thai,[1] Ha-Linh Quach, Ngoc-Anh Hoang Thi,
Phung Cong Dinh, Tran Nhu Duong, Le Thi Quynh Mai, Ngu Duy Nghia, Tran Anh Tu,
La Ngoc Quang, Tran Dai Quang, Trong-Tai Nguyen, Florian Vogt,[2] Dang Duc Anh[2]

To assess the role of in-flight transmission of severe acute respiratory syndrome coronavirus 2 (SARS-CoV-2), we investigated a cluster of cases among passengers on a 10-hour commercial flight. Affected persons were passengers, crew, and their close contacts. We traced 217 passengers and crew to their final destinations and interviewed, tested, and quarantined them. Among the 16 persons in whom SARS-CoV-2 infection was detected, 12 (75%) were passengers seated in business class along with the only symptomatic person (attack rate 62%). Seating proximity was strongly associated with increased infection risk (risk ratio 7.3, 95% CI 1.2–46.2). We found no strong evidence supporting alternative transmission scenarios. In-flight transmission that probably originated from 1 symptomatic passenger caused a large cluster of cases during a long flight. Guidelines for preventing SARS-CoV-2 infection among air passengers should consider individual passengers' risk for infection, the number of passengers traveling, and flight duration.

During the first 6 months of 2020, severe acute respiratory syndrome coronavirus 2 (SARS-CoV-2) spread to almost all countries and infected ≈4 million persons worldwide (*1*). Air travel is contributing to the extent and speed of the pandemic spread through the movement of infected persons (*2–4*); consequently, in March, many countries either completely halted or substantially reduced air travel.

Spread of SARS-CoV-2 across international borders by infected travelers has been well documented (*5,6*); however, evidence and in-depth assessment of the risk for transmission from infected passengers to other passengers or crew members during the course of a flight (in-flight transmission) are limited. Although the international flight industry has judged the risk for in-flight transmission to be very low (*7*), long flights in particular have become a matter of increasing concern as many countries have started lifting flight restrictions despite ongoing SARS-CoV-2 transmission (*8*).

The first case of coronavirus disease (COVID-19) in Vietnam was recorded on January 23, 2020; the patient was a visitor from Wuhan, China (*9*). On January 24, Vietnam suspended air travel from mainland China, Hong Kong, and Taiwan and, as the epidemic spread worldwide, gradually expanded travel bans, mandatory quarantine, and testing measures to incoming passengers from other countries (*10*).

In early March, when much of the global community was just beginning to recognize the severity of the pandemic, we detected a cluster of COVID-19 cases among passengers arriving on the same flight from London, UK, to Hanoi, Vietnam, on March 2 (Vietnam Airlines flight 54 [VN54]). At that time, importation of COVID-19 had been documented in association with 3 flights to Vietnam, including a cluster of 6 persons who had index cases and were evacuated from Wuhan; 6 secondary cases and resulted from virus transmission in Vietnam (*11*). No in-depth investigations among passengers on those flights were conducted, and no evidence indicated that transmission had occurred during the flights themselves.

Initial investigations of flight VN54 led us to hypothesize potential in-flight transmission originating from 1 symptomatic passenger in business class (the

[1]These first authors contributed equally to this article.

[2]These last authors contributed equally to this article.

probable index case). We subsequently launched an extensive epidemiologic investigation that involved testing and isolation/quarantine of all traceable passengers and crew members of the identified flight. Our objectives were to estimate the probability that transmission of SARS-CoV-2 occurred on the flight in question and to identify risk factors associated with transmission.

Methods

We defined cases of SARS-CoV-2 infection according to Vietnam Ministry of Health guidelines in place at the time of our investigation (12). Specifically, we suspected defined suspected flight-associated COVID-19 cases as passengers or crew members on board flight VN54 landing in Hanoi on March 2 who reported fever and cough, with or without shortness of breath, during March 1–16. We defined confirmed flight-associated COVID-19 cases as passengers or crew members on flight VN54, regardless whether signs or symptoms developed, who had positive SARS-CoV-2 real-time reverse transcription PCR results from nasopharyngeal swab samples (13). Flight-associated cases were considered to have very likely acquired infection on board VN54 and were hence classified as probable secondary cases in this analysis if the following 3 criteria were met: 1) they experienced signs/symptoms 2–14 days after arrival or if they were SARS-CoV-2 positive by PCR 2–14 days after arrival in the absence of signs/symptoms; 2) in-depth investigation did not reveal any potential exposure to SARS-CoV-2 before or after the flight during their incubation period; and 3) they had shared cabin space with the probable index case during the flight (14–17).

At the time of flight VN54 arrival, all passengers from COVID-19–infected areas, including the United Kingdom, had their body temperature screened by thermal imaging and were required to declare any COVID-19 symptoms; only passengers arriving from China, South Korea, Iran, or Italy were required to undergo SARS-CoV-2 testing and 14-day quarantine. At that time, the use of face masks was not mandatory on airplanes or at airports (18).

As soon as the travel history of the probable index case became evident, the passenger list and flight manifest for flight VN54 was obtained from the Bureau of Immigration and the Civil Aviation Administration and sent to all provincial Centers for Disease Control with instructions for local health staff to trace all passengers and crew members of flight VN54. All successfully traced passengers and

crew members were interviewed by use of a standard questionnaire, tested for SARS-CoV-2, and quarantined in designated facilities or at home. Any symptomatic person was isolated immediately until the test result was received. In-depth interviews were conducted with all persons with suspected or confirmed flight-associated cases; the specific focus was detecting any potential SARS-CoV-2 transmission events before and after the flight to investigate potential alternative scenarios for transmission other than during the flight. Furthermore, all persons with suspected or confirmed flight-associated cases were asked to identify persons with whom they had had close contact (<2 meter distance for >15 minutes) between arriving in Vietnam and the start of quarantine/isolation. These close contacts were also contacted, tested, and quarantined for 14 days. All persons in quarantine were checked twice daily for clinical signs/symptoms and fever; oropharyngeal swabs were collected on the day of admission, after 3–5 days, and on day 13, unless signs/symptoms developed, in which instance a specimen was collected immediately and the person was isolated and monitored until receipt of the test result.

Initial investigations of the probable index case generated our working hypothesis of in-flight transmission and guided further investigations. In particular, we investigated all possible exposures of all persons with flight-associated cases during their incubation period in relation to the timing of the flight, including locations where flight-associated cases may have crossed paths before and after the flight. To identify factors associated with in-flight infection risks, we calculated risk ratios and 95% CIs.

Results

Setting

Flight VN54 departed London at 11:10 AM local time on March 1, 2020, and arrived in Hanoi at 5:20 AM local time on March 2; the nonstop flight lasted about 10 hours. A total of 16 crew members and 201 passengers were on board. The 274 seats on the airplane were divided into business class (28 seats), premium economy class (35 seats), and economy class (211 seats); there were 4 toilets for business and premium economy classes and 5 for economy. The business class was exclusively reserved and separated from the premium economy and economy classes by a service/toilet area (Figure 1). Of the 201 passengers, 21 occupied business (75% seats occupied), 35 premium economy (100%), and 145 economy (67%) seats (Figure 1). Two meals were served, and flight attendants
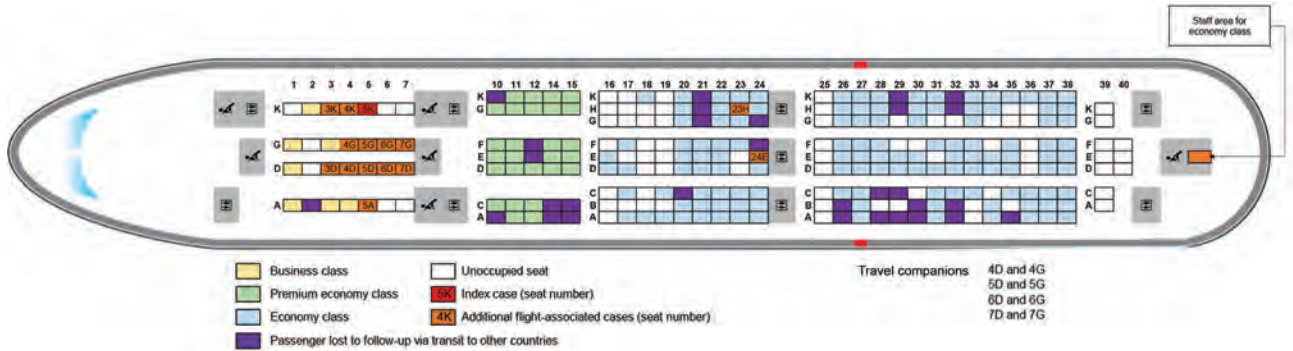
Figure 1. Seating location of passengers on Vietnam Airlines flight 54 from London, UK, to Hanoi, Vietnam, on March 2, 2020, for whom severe acute respiratory syndrome coronavirus 2 infection was later confirmed.

worked in 2 teams, 1 for the business and premium economy sections and 1 for the economy section.

Investigation of Probable Index Case

A 27-year-old businesswoman from Vietnam, whom we identified as the probable index case (hereafter case 1), had been based in London since early February. Our case investigations supplemented by information obtained from media reports indicated that she had traveled to Italy on February 18 with her sister, who was later confirmed to be SARS-CoV-2–positive in London, and back to London on February 20 to stay with her sister for another 2 nights. On February 22, case 1 and her sister returned to Milan, Italy, and subsequently traveled to Paris, France, for the yearly Fashion Week before returning back to London on February 25. They continued to reside in London until February 29, when case 1 started to experience a sore throat and cough while attending meetings and visiting entertainment hubs with friends. On March 1, she boarded flight VN54. She was seated in business class and continued to experience the sore throat and cough throughout the flight. Her signs and symptoms (fever, sore throat, fatigue, and shortness of breath) progressed further after arrival, and she self-isolated at her private residence in Hanoi and had contact with household personnel only. On March 5, she sought care at a local hospital in Hanoi, where an oropharyngeal swab sample was taken and tested; SARS-CoV-2 infection was confirmed by real-time reverse transcription PCR on March 6. On March 7, three of her household personnel received positive SARS-CoV-2 results, as did a friend of hers, whom she had visited in London on February 29, on March 10.

Case Finding and Epidemiologic Investigations

By March 10, all 16 (100%) of the flight crew and 168 (84%) of the passengers who remained in Vietnam had been traced; 33 (16%) passengers had already transited to other countries. We were able to quarantine, interview, and collect swab specimens for PCR testing from all passengers and crew members who remained in Vietnam. Passengers and crew had traveled on to 15 provinces in Vietnam, ranging from Lao Cai and Cao Bang in the north to Kien Giang in the south.

Through these efforts, we identified an additional 15 PCR-confirmed COVID-19 cases, 14 among passengers and 1 among crew members, resulting in a total of 16 confirmed flight-associated cases. Ages of affected persons ranged from 30 to 74 years (median 63.5 years); 9 (>50%) were male, and 12 (75%) were of British nationality (Table 1). Of the 15 persons with flight-associated cases, 12 (80%) had traveled in business class with case 1, and 2 travelers (cases 14 and 15) and 1 flight attendant (case 16) had been in economy class (Figure 1). Among persons in business class, the attack rate was 62% (13/21). Among passengers seated within 2 meters from case 1, which we approximated in business class to be ≤2 seats away, 11 (92%) were SARS-CoV-2–positive compared with 1 (13%) located >2 seats away (risk ratio 7.3, 95% CI 1.2–46.2) (Table 2). Of the 12 additional cases in business class, symptoms subsequently developed in 8 (67%); median symptom onset was 8.8 days (interquartile range 5.8–13.5) after arrival (Figure 2). None of the additional cases showed COVID-19 symptoms while on board VN54. All 12 additional cases in business class met the definition of probable secondary cases.

Our investigation did not reveal strong evidence supporting potential SARS-CoV-2 exposure either before or after the flight for any of the additional persons with flight-associated cases other than having traveled on the same flight as case 1 (Appendix, https://wwwnc.cdc.gov/EID/article/26/11/20-3299-App1.pdf). There were 4 traveling companion couples on board, and individuals within each couple

Table 1. Descriptive epidemiology for 217 passengers and crew on Vietnam Airlines flight 54 from London, UK, to Hanoi, Vietnam, March 2, 2020*

Passenger/crew information	Positive for SARS-CoV-2 by PCR, no. (%)†	Negative for SARS-CoV-2 by PCR, no. (%)
Total	16 (7.4)	201 (92.6)
Age, y		
<18	0	3 (2)
18-49	3 (19)	89 (44)
50-64	4 (25)	80 (40)
>65	9 (56)	29 (14)
Sex		
M	9 (56)	98 (49)
F	7 (44)	103 (51)
Nationality		
British	12 (75)	133 (66)
Vietnamese	3 (19)	31 (15)
Other	1 (6)	37 (18)
Seating location		
Business class	13 (81)	8 (4)
Premium economy class	0	35 (17)
Economy class	2 (13)	143 (71)
Crew members	1 (6)	15 (8)

*Median age, y (interquartile range) was 63.5 (56.0–67.5) for those who were SARS-CoV-2 positive and 51.5 (32.0–60.0) for those who were SARS-CoV-2 negative. SARS-CoV-2, severe acute respiratory syndrome coronavirus 2.
†including the probable index case.

sat next to each other in business class. None of the couples or individual cases traveled or stayed with another couple or individual case before the flight or after arrival in Vietnam. Of these case-pairs, 3 (6 persons) were positive for SARS-CoV-2 on the same date: 6 days after arrival in Vietnam.

Among >1,300 close contacts of VN54 passengers and crew members, 5 confirmed cases were identified, 3 of whom were household personnel linked to case 1. The timing of last contact of the remaining 2 confirmed close contacts with their respective flight-associated cases suggests that infection of the flight-associated cases occurred at the same time and that time of infection coincided with the time of the flight (Appendix).

Discussion

Among the 217 passengers and crew members on a direct flight from London to Hanoi in early March 2020, we identified a cluster of 16 laboratory-confirmed COVID-19 cases. In-depth epidemiologic investigations strongly suggest that 1 symptomatic passenger (case 1) transmitted SARS-CoV-2 infection during the flight to at least 12 other passengers in business class (probable secondary cases).

Case 1 was the only symptomatic person on board and was the only person with a flight-associated case who had established contact with a person with a confirmed case (her sister) during her incubation period. The incubation periods for all persons with confirmed flight-associated cases overlapped with the timing of the flight (Figure 2). Our interviews did not reveal that any of the additional persons with flight-associated cases had been exposed to SARS-CoV-2 before or after the flight during their incubation periods other than having taken the same flight as case 1, nor did they suggest exposure for any of the 4 travel companion couples after the flight (Appendix). Similar intervals between arrival and positive SARS-CoV-2 test results among 3 case-pairs suggest a common exposure event rather than subsequent infection from one partner to the other. Last, we found a clear association between sitting in close proximity to case 1 and risk for infection (Table 2).

In the absence of genomic analysis, we were unable to completely rule out alternative transmission routes. However, all persons with flight-associated cases departed from the United Kingdom (none transited from other countries); and until the departure date of flight VN54, only 23 COVID-19 cases had

Table 2. Risk for SARS-CoV-2 infection by seating location among business class passengers on Vietnam Airlines flight 54 from London, UK, to Hanoi, Vietnam, March 2, 2020*

Seating location in relation to index case	Positive for SARS-CoV-2 by PCR, no. (%)†	Negative for SARS-CoV-2 by PCR, no. (%)	Relative risk	Risk ratio (95% CI)
≤2 seats away	11 (92)	1 (13)	0.9	7.3 (1.2–46.2)
>2 seats away	1 (8)	7 (88)	0.1	

*SARS-CoV-2, severe acute respiratory syndrome coronavirus 2.
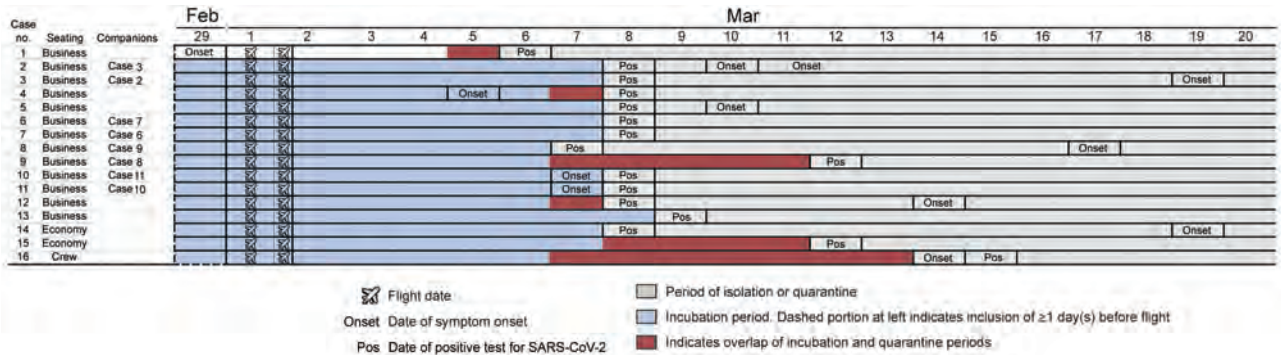†Excluding the index case.

Figure 2. Epidemiologic and clinical timeline for passengers on Vietnam Airlines flight 54, from London, UK, to Hanoi, Vietnam, March 2, 2020, for whom SARS-CoV-2 infection was later confirmed. Because the flight arrived quite early in the morning (5:20 AM), we considered the remainder of the day (19 h) to be the day of arrival. Case 14 traveled with a companion who was tested but negative for SARS-CoV-2 infection. SARS-CoV-2, severe acute respiratory syndrome coronavirus 2.

been recorded in the United Kingdom. Although testing had not been implemented on a large scale nationwide at that time (19), community transmission in the United Kingdom was not yet widely established (20), making the presence of multiple persons on board incubating the illness unlikely. Similarly, for case 4, who reported having visited India before the United Kingdom during his incubation period, the possibility of preflight transmission remains slim because by March 1, only 3 cases of COVID-19 had been reported in India, although testing in India was still limited (20–22). Furthermore, none of the 30 colleagues of case 4, who shared the same preflight travel history but were all seated in economy class, were infected (Appendix).

We consider local transmission after arrival in Vietnam unlikely. As of March 1, 2020, only 16 cases of COVID-19 had been reported in Vietnam, and 17 days had passed since the last reported case (case 1 reported here became Vietnam case no. 17) (18). At that time, 1,593 persons had tested negative for SARS-CoV-2 infection in Vietnam, and according to official policy at that time, another 10,089 contacts and travelers returning from COVID-19–affected areas overseas were under preemptive quarantine directly at the time of arrival. In early March 2020, there was no evidence of community transmission of SARS-CoV-2 in Vietnam (18). We also note that cases 3 and 14 experienced symptom onset 17 days after flight VN54. Whether these cases reflect unusually long incubation periods or symptoms caused by conditions other than COVID-19 is unknown.

The most likely route of transmission during the flight is aerosol or droplet transmission from case 1, particularly for persons seated in business class (23). Contact with case 1 might also have occurred outside the airplane at the airport, in particular among

business class passengers in the predeparture lounge area or during boarding. Although Vietnam Airlines keeps business class passengers separated from economy class passengers during most procedures before and during the flight, contact with the 2 economy class cases might have occurred after arrival during immigration or at baggage claim. We also note that 2 passengers, in the seats between the 2 cases in economy class, were lost to follow-up. Whether either of these passengers could represent a separate index case in economy class is unknown.

The role of fomites and on-board surfaces such as tray tables and surfaces in toilets remains unknown. For example, airline crew often use business class toilets while on board, which might explain the case among the crew serving in economy class, for whom no other potential source of infection could be established. Of note, the temporal sequence of symptom onset among cases in economy class and the crew member serving in economy class also allows for the possibility of a second inflight transmission event, independent of the cluster in buisness class (Figure 2).

Our study has several limitations. First, we did not have genomic sequencing data available to support our hypothesis of in-flight transmission. However, the conclusiveness and unambiguity of our in-depth epidemiologic upstream and downstream investigations coupled with extensive laboratory testing make us confident of our main findings. Second, we lacked detailed data on activities of the cases while on board (e.g., movements or seat changes, use of toilets, or sharing meals), which might have enabled us to pinpoint the precise route of transmission. Third, our assessment of passengers' preflight exposure to other confirmed cases relied on interviews only. Fourth, we had no data available on individual

passenger use of face masks while on board, which would have enabled a more refined risk analysis. Face masks were neither recommended nor widely used on airplanes in early March, in particular not among travelers from Europe (24–26), who constituted the majority of passengers on flight VN54. Last, given the delay between arrival and confirmation of the probable index case, no environmental samples could be collected from the airplane.

Our findings have several implications for international air travel, especially because several countries have resumed air travel despite ongoing SARS-CoV-2 transmission. First, thermal imaging and self-declaration of symptoms have clear limitations, as demonstrated by case 1, who boarded the flight with symptoms and did not declare them before or after the flight. Second, long flights not only can lead to importation of COVID-19 cases but also can provide conditions for superspreader events. It has been hypothesized that a combination of environmental factors on airplanes (humidity, temperature, air flow) can prolong the presence of SARS-CoV-2 in flight cabins (27). No evidence indicated that the regular air conditioning and exchange system on flight VN54 were malfunctioning. The number of probable secondary cases detected in our study is on the upper end of hypothesized estimations for SARS-CoV-2 transmission on airplanes in the absence of face mask use, although the movement of aerosols and droplets in the specific conditions of a flight cabin remains poorly understood (27). A study of a COVID-19 cluster with 16 infected flight passengers from Singapore in February 2020 identified only 1 instance of potential in-flight transmission (28). In-flight transmission has been hypothesized but not substantiated sufficiently in a non–peer-reviewed report of a cluster of 10 flight-associated cases in China in February (N. Yang et al., unpub. data, https://www.medrxiv.org/content/10.1101/2020.03.28.20040097v1.full.pdf). In January 2020, no secondary cases were detected after a 15-hour flight to Canada with a symptomatic person with COVID-19 on board (29), although contact tracing and monitoring were limited (30). Similar results with similar limitations have been reported from flights arriving in France (31,32) and Thailand (33) in January and February. All of these studies limited contact tracing to passengers within 2 rows of the index cases, which could explain why secondary flight-related transmission was not detected by those studies.

The latest guidance from the international air travel industry classifies the in-flight transmission risk as very low (34) and recommends only the use of face masks without additional measures to increase physical distance on board, such as blocking the middle seats (7,35). Our findings challenge these recommendations. Transmission on flight VN54 was clustered in business class, where seats are already more widely spaced than in economy class, and infection spread much further than the existing 2-row (36) or 2 meters (37) rule recommended for COVID-19 prevention on airplanes and other public transport would have captured. Similar conclusions were reached for SARS-CoV superspreader events on a flight in 2003, in which a high risk for infection was observed for passengers seated farther than 3 rows from the index case (4). This finding also concurs with transmission patterns observed for influenza virus (38) and is generally in line with the mounting evidence that airborne transmission of SARS-CoV-2 is a major yet underrecognized transmission route (39,40).

Our findings call for tightened screening and infection prevention measures by public health authorities, regulators, and the airline industry, especially in countries where substantial transmission is ongoing (37). Making mask wearing obligatory and making hand hygiene and cough etiquette standard practice while on board and at airports seems an obvious and relatively simple measure (27). Blocking middle seats, currently recommended by the airline industry (7,35), may in theory prevent some in-flight transmission events but seems to be insufficient to prevent superspreading events. Also, systematic testing, quarantine policies, or both, for inbound passengers at arrival might be justified for countries with low levels of community transmission, high risk for case importation, and limited contact tracing capacity (5). In Vietnam, for example, as a result of this investigation, national policy was changed toward mandatory testing at arrival irrespective of departure location and 14-day quarantine irrespective of test result or clinical signs/symptoms (41). This policy change eliminated the need for resource-intensive contact tracing of flight passengers altogether and enabled detection of another 106 cases among ≈5,000 passengers on 44 flights until all international flights were halted on March 28. However, given the logistic and economic implications of such policies, developing a quick and reliable point-of-care test that covers the entire infectious period remains paramount.

We conclude that the risk for on-board transmission of SARS-CoV-2 during long flights is real and has the potential to cause COVID-19 clusters of substantial size, even in business class–like settings with spacious seating arrangements well beyond the established distance used to define close contact on

airplanes. As long as COVID-19 presents a global pandemic threat in the absence of a good point-of-care test, better on-board infection prevention measures and arrival screening procedures are needed to make flying safe.

About the Author

Dr. Khanh is an epidemiologist at the Department of Communicable Diseases Control, National Institute of Hygiene and Epidemiology. He is a member of Rapid Response Team of Vietnam's National Steering Committee for COVID-19 Prevention and Control. His research interests include epidemiology of viral and bacterial respiratory infectious diseases and zoonotic diseases including COVID-19, severe acute respiratory syndrome, avian influenza (H5N1), and seasonal influenza.

References

1. World Health Organization. Coronavirus disease (COVID-19) situation reports [cited 2020 Jul 8]. https://www.who.int/emergencies/diseases/novel-coronavirus-2019/situation-reports
2. Grout A, Howard N, Coker R, Speakman EM. Guidelines, law, and governance: disconnects in the global control of airline-associated infectious diseases. Lancet Infect Dis. 2017;17:e118–22. https://doi.org/10.1016/S1473-3099(16)30476-5
3. Hsu CI, Shih HH. Transmission and control of an emerging influenza pandemic in a small-world airline network. Accid Anal Prev. 2010;42:93–100. https://doi.org/10.1016/j.aap.2009.07.004
4. Olsen SJ, Chang HL, Cheung TYY, Tang AFY, Fisk TL, Ooi SPL, et al. Transmission of the severe acute respiratory syndrome on aircraft. N Engl J Med. 2003;349:2416–22. https://doi.org/10.1056/NEJMoa031349
5. Myers JF, Snyder RE, Porse CC, Tecle S, Lowenthal P, Danforth ME, et al.; Traveler Monitoring Team. Identification and monitoring of international travelers during the initial phase of an outbreak of COVID-19—California, February 3–March 17, 2020. MMWR Morb Mortal Wkly Rep. 2020;69:599–602. https://doi.org/10.15585/mmwr.mm6919e4
6. Gostic K, Gomez ACR, Mummah RO, Kucharski AJ, Lloyd-Smith JO. Estimated effectiveness of symptom and risk screening to prevent the spread of COVID-19. eLife. 2020;9:e55570. https://doi.org/10.7554/eLife.55570
7. Richard M. Safely restarting aviation: ACI and IATA joint approach [cited 2020 Jul 8]. https://www.iata.org/contentassets/5c8786230ff34e2da406c72a52030e95/safely-restart-aviation-joint-aci-iata-approach.pdf
8. European Commission. Commission recommends gradual lifting of travel restrictions [cited 2020 Jul 8]. https://ec.europa.eu/commission/presscorner/detail/en/ip_20_1035
9. Phan LT, Nguyen TV, Luong QC, Nguyen TV, Nguyen HT, Le HQ, et al. Importation and human-to-human transmission of a novel coronavirus in Vietnam. N Engl J Med. 2020;382:872–4. https://doi.org/10.1056/NEJMc2001272
10. Shira D. COVID-19 in Vietnam: travel updates and restrictions [cited 2020 Jul 8]. https://www.vietnam-briefing.com/news/covid-19-vietnam-travel-updates-restrictions.html
11. Le TQM, Takemura T, Moi ML, Nabeshima T, Nguyen LKH, Hoang VMP, et al. Severe acute respiratory syndrome coronavirus 2 shedding by travelers, Vietnam, 2020. Emerg Infect Dis. 2020;26:1624–6. https://doi.org/10.3201/eid2607.200591
12. Vietnam Ministry of Health. Decision 343/QD-BYT regarding guidelines for surveillance, prevention and control of novel pneumonia disease caused by nCoV [in Vietnamese]. 2020 Feb 7 [cited 2020 Jul 8]. https://moh.gov.vn/ web/dich-benh/huong-dan-chuyen-mon/-/asset_publisher/NxZAa8ST2KXb/content/quyet-inh-so-343-q-byt-ngay-07-02-2020-ve-viec-ban-hanh-huong-dan-tam-thoi-giam-sat-va-phong-chong-benh-viem-uong-ho-hap-cap-do-chung-moi-cua-vi-rut-c
13. Corman VM, Landt O, Kaiser M, Molenkamp R, Meijer A, Chu DKW, et al. Detection of 2019 novel coronavirus (2019-nCoV) by real-time RT-PCR. Euro Surveill. 2020;25:2000045. https://doi.org/10.2807/1560-7917.ES.2020.25.3.2000045
14. Dietz L, Horve PF, Coil DA, Fretz M, Eisen JA, Van Den Wymelenberg K. 2019 Novel coronavirus (COVID-19) pandemic: built environment considerations to reduce transmission. mSystems. 2020;5:e00245–20. https://doi.org/10.1128/mSystems.00245-20
15. Wang J, Du G. COVID-19 may transmit through aerosol. Ir J Med Sci. 2020 Mar 24 [Epub ahead of print].
16. Yu ITS, Li Y, Wong TW, Tam W, Chan AT, Lee JHW, et al. Evidence of airborne transmission of the severe acute respiratory syndrome virus. N Engl J Med. 2004;350:1731–9. https://doi.org/10.1056/NEJMoa032867
17. World Health Organization. Transmission of SARS-CoV-2: implications for infection prevention precautions [cited 2020 Aug 10]. https://www.who.int/news-room/commentaries/detail/transmission-of-sars-cov-2-implications-for-infection-prevention-precautions
18. Vietnam Ministry of Health. COVID-19 updates in Vietnam [in Vietnamese] [cited 2020 May 1]. https://ncov.moh.gov.vn/
19. Department of Health and Social Care. Coronavirus (COVID-19) in the UK: UK summary [cited 2020 Jul 13]. https://coronavirus.data.gov.uk/
20. World Health Organization. Situation report-67 HIGHLIGHTS [cited 2020 Jun 5]. https://www.who.

int/docs/default-source/coronaviruse/situation-reports/20200327-sitrep-67-covid-19.pdf?sfvrsn=b65f68eb_4

21. Government of India. #IndiaFightsCorona COVID-19 in India, corona virus tracker [cited 2020 Jul 13]. https://www.mygov.in/covid-19/

22. Indian Council of Medical Research. SARS-CoV-2 (COVID-19) testing status [cited 2020 Jul 13]. https://www.icmr.gov.in/

23. van Doremalen N, Bushmaker T, Morris DH, Holbrook MG, Gamble A, Williamson BN, et al. Aerosol and surface stability of SARS-CoV-2 as compared with SARS-CoV-1. N Engl J Med. 2020;382:1564–7. https://doi.org/10.1056/NEJMc2004973

24. Elachola H, Ebrahim SH, Gozzer E. COVID-19: Facemask use prevalence in international airports in Asia, Europe and the Americas, March 2020. [Internet]. Travel Med Infect Dis. 2020;35:101637. https://doi.org/10.1016/j.tmaid.2020.101637

25. Sunjaya AP, Jenkins C. Rationale for universal face masks in public against COVID-19. Respirology. 2020;25:678–9. https://doi.org/10.1111/resp.13834

26. Keshtkar-Jahromi M, Sulkowski M, Holakouie-Naieni K. Public masking: an urgent need to revise global policies to protect against COVID-19. Am J Trop Med Hyg. 2020;102:1160–1. https://doi.org/10.4269/ajtmh.20-0305

27. Jayaweera M, Perera H, Gunawardana B, Manatunge J. Transmission of COVID-19 virus by droplets and aerosols: a critical review on the unresolved dichotomy. Environ Res. 2020;188:109819. https://doi.org/10.1016/j.envres.2020.109819

28. Chen J, He H, Cheng W, Liu Y, Sun Z, Chai C, et al. Potential transmission of SARS-CoV-2 on a flight from Singapore to Hanghzou, China: an epidemiological investigation. Travel Med Infect Dis. 2020;36:101816. https://doi.org/10.1016/j.tmaid.2020.101816

29. Silverstein WK, Stroud L, Cleghorn GE, Leis JA. First imported case of 2019 novel coronavirus in Canada, presenting as mild pneumonia. Lancet. 2020;395:734. https://doi.org/10.1016/S0140-6736(20)30370-6

30. Schwartz KL, Murti M, Finkelstein M, Leis JA, Fitzgerald-Husek A, Bourns L, et al. Lack of COVID-19 transmission on an international flight. CMAJ. 2020;192:E410. https://doi.org/10.1503/cmaj.75015

31. Eldin C, Lagier JC, Mailhe M, Gautret P. Probable aircraft transmission of Covid-19 in-flight from the Central African Republic to France. Travel Med Infect Dis. 2020;35:101643. https://doi.org/10.1016/j.tmaid.2020.101643

32. Bernard Stoecklin S, Rolland P, Silue Y, Mailles A, Campese C, Simondon A, et al.; Investigation Team. First cases of coronavirus disease 2019 (COVID-19) in France: surveillance, investigations and control measures, January 2020. Euro Surveill. 2020;25:2000094. https://doi.org/10.2807/1560-7917.ES.2020.25.6.2000094

33. Okada P, Buathong R, Phuygun S, Thanadachakul T, Parnmen S, Wongboot W, et al. Early transmission patterns of coronavirus disease 2019 (COVID-19) in travellers from Wuhan to Thailand, January 2020. Euro Surveill. 2020;25:2000097. https://doi.org/10.2807/1560-7917.ES.2020.25.8.2000097

34. International Air Transport Association. IATA calls for passenger face covering and crew masks [cited 2020 Jul 8]. https://www.iata.org/en/pressroom/pr/2020-05-05-01/

35. Richard M. Biosecurity for air transport a roadmap for restarting aviation v.2 [cited 2020 Jul 8]. https://www.iata.org/contentassets/4cb32e19ff544df590f3b70179551013/roadmap-safely-restarting-aviation.pdf

36. Stover Hertzberg V, Weiss H. On the 2-row rule for infectious disease transmission on aircraft. Ann Glob Health. 2016;82:819–23. https://doi.org/10.1016/j.aogh.2016.06.003

37. World Health Organization. Operational considerations for managing COVID-19 cases or outbreak in aviation: interim guidance, 18 Mar 2020 [cited 2020 Jul 8]. https://apps.who.int/iris/handle/10665/331488

38. Leitmeyer K, Adlhoch C. Review article: influenza transmission on aircraft. Epidemiology. 2016;27:743–51. https://doi.org/10.1097/EDE.0000000000000438

39. Yao M, Zhang L, Ma J, Zhou L. On airborne transmission and control of SARS-Cov-2. Sci Total Environ. 2020;731:139178. https://doi.org/10.1016/j.scitotenv.2020.139178

40. Morawska L, Milton DK. It is time to address airborne transmission of COVID-19. Clin Infect Dis. 2020 Jul 6: ciaa939. Epub ahead of print. https://doi.org/10.1093/cid/ciaa939

41. Ha BTT, Ngoc Quang L, Mirzoev T, Tai NT, Thai PQ, Dinh PC. Combating the COVID-19 epidemic: experiences from Vietnam. Int J Environ Res Public Health. 2020;17:3125. https://doi.org/10.3390/ijerph17093125

Address for correspondence: Cong-Khanh Nguyen, Department of Communicable Diseases Control, National Institute of Hygiene and Epidemiology, 1 Yersin St, Hai Ba Trung District, Hanoi 100000, Vietnam; email: nck@nihe.org.vn

Endotheliopathy and Platelet Dysfunction as Hallmarks of Fatal Lassa Fever

Lucy E. Horton,[1] Robert W. Cross,[1] Jessica N. Hartnett, Emily J. Engel, Saori Sakabe, Augustine Goba, Mambu Momoh, John Demby Sandi, Thomas W. Geisbert, Robert F. Garry, John S. Schieffelin, Donald S. Grant, Brian M. Sullivan

Lassa fever (LF) causes multisystem disease and has a fatality rate <70%. Severe cases exhibit abnormal coagulation, endothelial barrier disruption, and dysfunctional platelet aggregation but the underlying mechanisms remain poorly understood. In Sierra Leone during 2015–2018, we assessed LF patients' day-of-admission plasma samples for levels of proteins necessary for coagulation, fibrinolysis, and platelet function. P-selectin, soluble endothelial protein C receptor, soluble thrombomodulin, plasminogen activator inhibitor 1, ADAMTS-13, von Willebrand factor, tissue factor, soluble intercellular adhesion molecule 1, and vascular cell adhesion molecule 1 were more elevated in LF patients than in controls. Endothelial protein C receptor, thrombomodulin, intercellular adhesion molecule 1, plasminogen activator inhibitor 1, D-dimer, and hepatocyte growth factor were higher in fatal than nonfatal LF cases. Platelet disaggregation occurred only in samples from fatal LF cases. The impaired homeostasis and platelet dysfunction implicate alterations in the protein C pathway, which might contribute to the loss of endothelial barrier function in fatal infections.

Lassa fever (LF) is an acute viral hemorrhagic fever endemic to West Africa, where ≈300,000–500,000 cases/year occur and mortality rates are high (1). Humans primarily are infected from exposure to excreta from the rodent host, Natal multimammate mouse (*Mastomys natalensis*). Pregnant women especially are susceptible to severe disease; infection during pregnancy usually leads to spontaneous abortion (2). The high rates illness and death, lack of vaccines or approved treatments, and potential to cause a public health emergency led to the US Centers for Disease Control and Prevention to classify LF as a category A bioterrorism agent (https://emergency.cdc.gov/agent/agentlist-category.asp) and the World Health Organization to classify LF as a priority disease (https://www.who.int/dg/priorities).

Early clinical manifestations and symptoms of LF often are nonspecific and easily confused with other diseases prevalent in the endemic region, such as malaria and typhoid fever. Consequently, patients often are not admitted for LF treatment until symptoms are severe and they have failed other therapies. Bleeding at mucous membranes and edema generally are seen in the most severe cases (3,4), but bleeding diathesis reportedly was common during a recent outbreak in Nigeria (4). Overt hemorrhage is rare, mostly limited to the mucosal surfaces, and not severe enough to cause shock. Pathologic changes seen on autopsy lack major cell and tissue injury but include signs of pleural effusion, pulmonary edema, ascites, and gastrointestinal mucosa bleeding (5,6), all indications of systemic vascular leakage. Severely ill LF patients often have mild to moderate thrombocytopenia, but rarely have platelet counts <100,000/µL (7). Thrombocytopenia is a common feature of hemorrhagic fevers and vascular permeability disorders (8), but the decrease in platelet counts in acute LF is not low enough to cause spontaneous hemorrhage.

LF could be characterized as a disease of enhanced vascular permeability but the underlying

[1]These authors contributed equally to this article.

pathophysiology remains ambiguous. Because gross signs of endotheliopathy and vascular leakage are restricted mostly to severe LF cases, we hypothesized that differences in hemostatic markers between fatal and nonfatal cases found in day-of-admission plasma samples could be prognostic and elucidate changes in hemostasis during LF. We identified differences in markers of endothelial activation and injury between fatal and nonfatal cases that indicate disruption of the protein C pathway and endothelial stress in fatal LF.

Materials and Methods

Subjects

The study was conducted at the Lassa Laboratory at the Kenema Government Hospital (KGH) in Sierra Leone during 2015–2018. Patients with diagnosed acute LF met clinical criteria (9). We confirmed LF by detecting Lassa fever virus (LASV) antigen (LASV-Ag) by using ReLASV Pan-Lassa Antigen (Zalgen Labs, https://www.zalgen.com) or by detecting Lassa-specific IgM (LASV IgM) by using ReLASV Pan-Lassa IgG/IgM (Zalgen Labs) ELISA tests. All human subjects provided written informed consent before inclusion in the study. The study was approved by the institutional review boards of the Scripps Research Institute (approval no. 17-6972), Tulane University

Figure 1. Clinical features suggestive of vascular permeability in patients with Lassa fever, Sierra Leone, 2015–2018. Patients with acute LF who had ≥2 signs or symptoms indicating vascular permeability at the time of admission were more likely to have fatal outcomes based on multiple logistic regression compared with patients who had no of symptoms vascular permeability (p = 0.0335). Case-fatality rates associated with various signs and symptoms are shown at the top and violin plot depicting the number of persons in each category at the bottom (median value indicated by dotted vertical lines). CFR, case-fatality rate; E, generalized edema; MB, mucosal membrane bleeding; RS, respiratory symptoms, such as cough or pulmonary edema.

(approval no. 09-00419), and the Sierra Leone Ethics and Scientific Review Committee.

Clinical Information

Blood was collected in EDTA tubes, processed within 6 hours, and stored at -20°C until analysis. Clinical data, including blood chemistries, liver function tests, and blood counts were obtained when feasible by using Piccolo Xpress (Abaxis, https://www.abaxis.com) and manual complete blood counts. Clinical outcomes data was incomplete and survival status was not known for patients not admitted to the viral hemorrhagic fever ward or transferred to another medical facility.

Biosafety

Samples were brought to the Lassa Laboratory from the Lassa ward in secondary containers. Staff performing experiments in the laboratory wore full personal protective equipment, including Tyvec suits, N95 masks, face shields, gloves, and boots. Infectious samples were handled in Biosafety cabinets.

ELISAs

We assessed plasma samples by using commercially available kits. For plasminogen activator inhibitor 1 (PAI-1) we used Human Serpin E1/PAI-1 Quantikine ELISA Kit (R&D Systems, https://www.rndsystems.com) or Human PAI-1 Platinum Kit (eBioscience, https://www.thermofisher.com). We used Human t-Plasminogen Activator/tPA Quantikine ELISA Kit (R&D Systems) to measure tissue plasminogen activator (tPA). We used Human Thrombomodulin/BDCA-3 Quantikine ELISA Kit (R&D Systems) or Human Thrombomodulin ELISA Kit (Innovative Research Inc., https://www.innov-research.com) to measure thrombomodulin (THBD) and Human Thrombin-Antithrombin Complex ELISA Kit (Abcam, https://www.abcam.com) to measure thrombinantithrombin (TAT) complexes. To assess endothelial protein C receptor (EPCR) we used Human EPCR DuoSet ELISA Kit (R&D Systems), for D-dimer we used Human D-Dimer ELISA Kit (Abcam), for a disintegrin and metalloproteinase with a thrombospondin type 1 motif, member 13 (ADAMTS-13) we used Human ADAMTS13 Quantikine ELISA Kit (R&D Systems), for P-selectin we used Human CD62P ELISA Kit (Abcam), for hepatocyte growth factor (HGF) we used Human HGF Quantikine ELISA Kit (R&D Systems), for von Willebrand factor (vWF) we used vWF Human ELISA Kit (ThermoFisher, https://www.thermofisher.com), and for tissue factor we used Human Coagulation Factor III/Tissue Factor Quantikine ELISA Kit (R&D Systems).

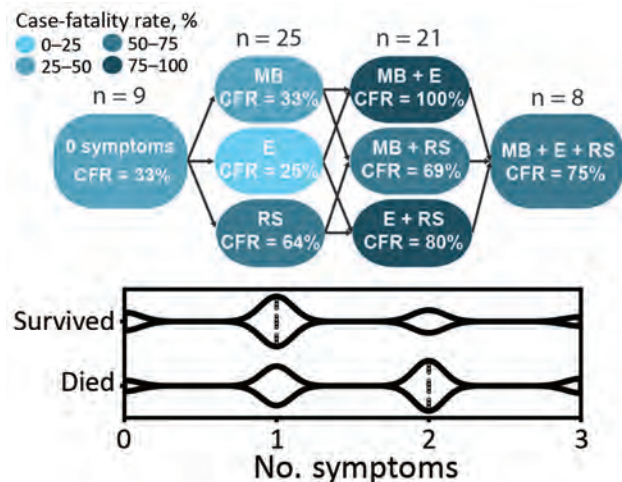**Table.** Characteristics and clinical and laboratory findings of patients in a study of Lassa fever fatality, Sierra Leone during 2015–2018*

Characteristics	All Lassa fever cases, n = 98	Outcomes		Non–LF febrile controls, n = 7
		Survived, n = 23	Died, n = 51	
Mean age, y (range)	23 (1–75)	20 (3–29)	25 (1–75)	24 (3–60)
Sex				
F	64 (65.3)	18 (78.3)	29 (56.8)	2 (22.2)
M	34 (34.7)	5 (21.7)	22 (43.1)	5 (71.4)
Clinical findings	n = 70	n = 23	n = 34	n = 9
Bleeding symptoms				
Bleeding gums	5 (7.1)	2 (8.7)	2 (5.9)	1
Epistaxis	4 (5.7)	1 (4.3)	2 (5.9)	1
Blood in stool	6 (8.6)	3 (13.0)	3 (8.8)	0
Blood in vomit	6 (8.6)	2 (8.7)	4 (11.8)	2
Injected conjunctiva	11 (15.7)	2 (8.7)	7 (20.6)	0
Bleeding hematoma	1 (1.4)	0	1 (2.9)	0
Blood in sputum	6 (8.6)	1 (4.3)	4 (11.8)	0
Blood in urine	3 (4.3)	2 (8.7)	1 (2.9)	1
Vaginal bleeding	3 (4.3)	1 (4.3)	2 (5.9)	1
Other bleeding	6 (8.6)	2 (8.7)	2 (5.9)	0
Edema	21 (30.0)	6 (26)	12 (35.3)	0
Other clinical symptoms				
Cough	45 (64.3)	15 (65.2)	24 (70.6)	6 (66.7)
Fever	54 (77.1)	16 (69.6)	30 (88.2)	0
Rash	2 (2.9)	0	2 (5.9)	1 (11.1)
Headache	60 (85.7)	20 (87)	28 (82.4)	6 (66.7)
Vomiting	37 (52.9)	11 (47.8)	20 (58.8)	5 (55.6)
Diarrhea	32 (45.7)	8 (34.8)	24 (70.6)	1 (11.1)
Jaundice	6 (8.6)	0	0	1 (11.1)
Laboratory findings, mean (±SD)				
AST, U/L	439 (±689)	423 (±651.7)	717 (±777)	76 (±78)
ALT, U/L	455 (±556)	246 (±463)	707 (±540)	41 (±35)
Alkaline phosphatase, U/L	220 (±269)	106 (±87)	313 (±339)	157 (±108)
Total bilirubin, mg/dL	1.18 (±1.38)	0.95 (±1.41)	1.44 (±1.54)	4.12 (±0.59)
Total protein, g/L	6.7 (±1.8)	7.1 (±10.0)	6.2 (±1.7)	7.3 (±0.5)
Creatinine, mg/dL	1.85 (±2.12)	0.88 (±0.40)	2.75 (±2.70)	0.5 (±0.26)
BUN, mg/dL	24 (±32)	10 (±5)	31 (±27)	17 (±11)

*Values are no. (%) except as indicated. ALT, alanine aminotransferase; AST, aspartate aminotransferase; BUN, blood urea nitrogen; LF, Lassa fever.

Platelet Aggregation Studies

Cryopreserved plasma samples were dialyzed in phosphate-buffered saline by using a 100 kDa or 1 MDa pore membrane (Spectra-Por Float-A-Lyzer; Sigma-Aldrich, https://www.sigmaaldrich.com) to remove EDTA and mixed 1:1 with platelet rich plasma collected from a healthy subject. Light transmission aggregation was performed on a Chrono-Log 450 (Chrono-Log, https://www.chronolog.com) aggregometer by using AGGRO/LINK 8 software (Chrono-Log). To initiate platelet aggregation, we used 5 μM adenosine diphosphate and incubated for 1 min.

Statistical Analyses

We performed statistical analyses by using Prism (GraphPad Software, https://www.graphpad.com) and Excel (Microsoft Corporation, https://www.microsoft.com) software. We used a 1-way analysis of variance Kruskal-Wallis test for comparing ≥3 variables to determine whether group values were due to random sampling. Then, we subjected these data to Dunn's multiple comparisons test to detect statistically significant differences between groups. We used Mann-Whitney tests when we assessed only 2 variables. We used linear regressions to find the best fit curve and Spearman correlations to find correlations between 2 variables. We used multiple logistical regression for some data (Figure 1) and considered p<0.05 statistically significant.

Results

The biorepository at the KGH contains samples from consented patients admitted and not admitted to the Lassa ward, but clinical information and outcomes were not available for all samples used. LF was diagnosed in patients with symptoms plus a positive ELISA result indicating either LASV-Ag or LASV-specific IgM, as previously described (*9*). We collected clinical data and plasma samples from 98 LF patients, 33 non–LF febrile controls (NLFCs), and 13 healthy controls (HCs) and summarized demographic information, outcomes, and LASV-Ag or IgM status for patients whose data were available (Table).

Severe LF is characterized by facial and pulmonary edema, pleural effusions, and ascites, indicating profound vascular dysfunction. To a lesser extent,

patients also might exhibit petechiae and mucosal membrane bleeding, which suggest dysregulation of the coagulation or fibrinolytic systems (7). Patients who died during our study more frequently had edema, bleeding at mucous membranes, and respiratory signs, including cough or hemoptysis, than patients who survived (Table). Patients who had >2 symptoms suggestive of vascular permeability had higher case-fatality rates than patients with <2 symptoms (Figure 1).

Coagulation Markers

To characterize hemostatic changes in LF patients, we measured levels of proteins essential to hemostasis and compared these results with plasma from NLFCs and HCs. The procoagulant enzyme, thrombin, contributes to the formation of hemostatic clots by converting fibrinogen into fibrin, but thrombin also induces endothelial permeability (10). THBD, a cofactor located on the surface of endothelial cells, binds thrombin and changes its specificity from a procoagulant enzyme to an anticoagulant enzyme. THBD-bound thrombin activates protein C into activated protein C (APC). APC then inhibits further thrombin formation by inactivating factors Va and VIIIa. When the THBD ectodomain is cleaved from the transmembrane stack, soluble THBD (sTHBD) can be detected in plasma and is associated with endothelial cell activation and vascular dysfunction (11). We noted much higher levels of sTHBD (mean 11.18 ng/mL) in LF patients than in HCs (mean 0.48 ng/mL; p = 0.0084), consistent with generation of endothelial stress factors in LF-infected patients (Figure 2, panel A). Samples from fatal LF cases also had more elevated sTHBD levels (mean 18.94 ng/mL) than samples from LF survivors (mean 1.78 ng/mL; p = 0.0239), indicating
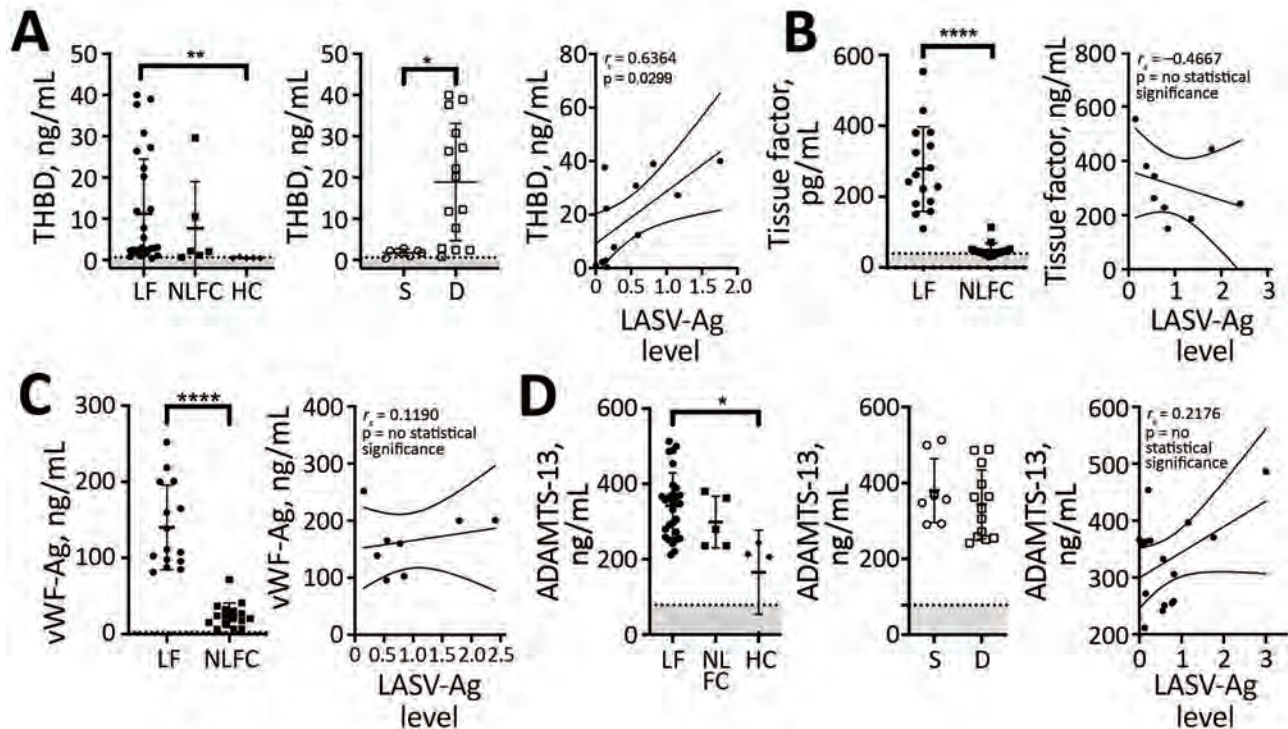

Figure 2. Laboratory findings for coagulation markers for patients with acute LF, NLFCs, and HCs, Sierra Leone, 2015–2018. A) Soluble thrombomodulin is elevated in LF and predicts fatal outcomes (Kruskal-Wallis p = 0.0002 across all groups). Levels of soluble THBD were statistically significantly higher (**p = 0.0084) in acute LF cases (n = 28) than in HCs (n = 5); patients who died (n = 15) had higher levels of soluble THBD than those who survived (n = 7; *p = 0.0239); and we noted a positive correlation between soluble THBD and LASV-Ag levels (n = 12). B) Tissue factor was statistically significantly elevated (****p<0.0001) in acute fatal LF cases (n = 16) compared with NLFC (n = 16), but no statistically significant correlation was found between TF and LASV-Ag levels in LF patients. C) vWF Ag levels were statistically significantly elevated (****p<0.0001) in acute fatal LF patients (n = 15) compared with NLFC (n = 16), but no statistically significant correlation was found between vWF and LASV-Ag levels in LF patients. D) Plasma levels of ADAMTS-13 were statistically significantly different between groups (Kruskal-Wallis p = 0.0155). Levels of ADAMTS-13 were statistically significantly higher (*p = 0.0292) in patients with acute LF (n = 28) compared with HCs (n = 4). No differences were seen between those who died (n = 13) versus those who survived (n = 8), nor was a statistically significant correlation found between ADAMTS-13 and LASV-Ag in LF patients. Limits of detection are indicated by dashed lines and gray shading below. Error bars show SDs; horizontal lines indicate means. D, died; HC, healthy control; LF, Lassa fever; LASV-Ag, Lassa fever virus antigen; NLFC, non-LF febrile control; S, survived; THBD, thrombomodulin; vWF, von Willebrand factor; vWF-Ag, von Willebrand factor antigen.
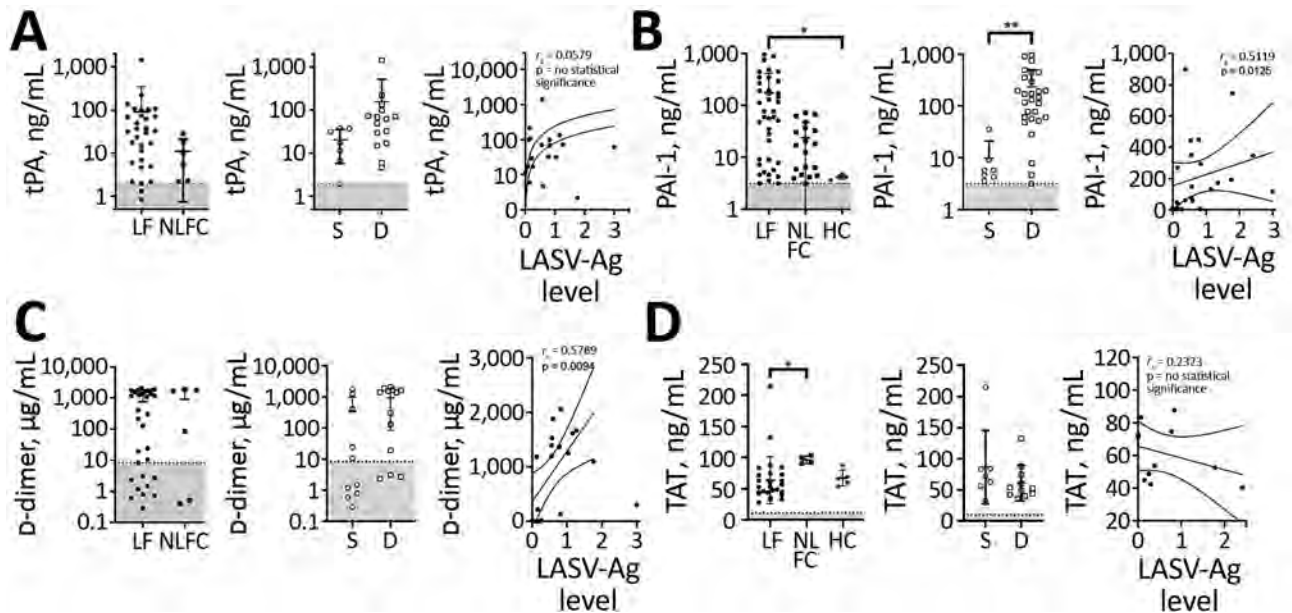
Figure 3. Laboratory findings for fibrinolysis markers for patients with acute LF, NLFCs, and healthy controls HCs, Sierra Leone, 2015–2018. A) Levels of tPA were not statistically significantly different between groups (Kruskal-Wallis p = 0.0516); no differences in tPA were observed between LF (n = 31) and NLFC (n = 6), or between patients who survived (n = 7) and patients who died (n = 15). B) PAI-1 levels predict fatal outcomes (Kruskal-Wallis p<0.0001 across all groups); PAI-1 was statistically significantly elevated (*p = 0.0145) in patients with acute LF (n = 40) compared with HCs (n = 5); patients who died (n = 28) had higher levels of PAI-1 (**p = 0.0031) than those who survived (n = 7); statistically significant positive correlation was observed between PAI-1 and LASV antigen in LF patients (n = 23). C) D-dimer levels in plasma were not statistically significantly different between groups (Kruskal-Wallis p = 0.2167); no difference in D-dimer levels were observed between LF (n = 32) and NLFC (n = 6), nor between patients who died (n = 13) and those who survived (n = 10); and a statistically significant positive correlation was observed between D-dimer levels and LASV antigen in LF patients (n = 19). D) No increased levels of TAT were observed between LF (n = 26) and HC (n = 5) (*p value), nor between patients who survived (n = 7) and died (n = 11), and no statistically significant correlation was observed between TAT levels and LASV-Ag in LF patients (n = 11). Limits of detection are indicated by dashed lines and gray shading below. Error bars show SDs; horizontal lines indicate means. D, died; HC, healthy control; LF, Lassa fever; LASV-Ag, Lassa fever virus antigen; NLFC, non-LF febrile control; PAI-1, plasminogen activator inhibitor 1; S, survived; TAT, thrombinantithrombin complexes; THBD, thrombomodulin; tPA, tissue plasminogen activator.

that advanced vascular dysfunction is associated with fatality (Figure 2, panel A). We also found a positive correlation between LASV-Ag levels and sTHBD in LF patients (Spearman ρ [r_s] = 0.6364; p = 0.0299).

Next, we measured levels of tissue factor (TF), the key initiator of coagulation in severe systemic infections that lead to sepsis (12). TF, a transmembrane glycoprotein, triggers the extrinsic coagulation cascade by binding factors VIIa and X and facilitating thrombin generation when exposed on the surface of the vascular endothelium at a site of injury (13). Circulating TF in microparticles can be released from leukocytes, endothelial cells, and platelets (14). Because hyperactivation of the TF system has been observed in sepsis (15) and disseminated intravascular coagulation (DIC), we measured soluble TF in plasma and found much higher levels (mean 278 pg/mL) among fatal LF cases than NLFCs (mean 48.8 pg/mL; p<0.0001) (Figure 2, panel B), but we did not find a correlation between TF and antigen levels among LF patients.

The endothelium constitutively releases low molecular weight vWF multimers. High molecular weight vWF multimers are released by activated platelets and endothelium and are highly biologically active and necessary for platelet adhesion, aggregation, and initiation of fibrin clot formation. We did not have specific equipment needed to measure high molecular weight vWF multimers, but we measured total vWF antigen (vWF-Ag) by ELISA and found vWF-Ag levels were statistically significantly higher (mean 140.2 ng/mL) in fatal LF cases than in NLFCs (mean 24.58 ng/mL; p<0.0001). vWF levels in LF patients did not correlate with LASV-Ag levels (Figure 2, panel C).

We also measured levels of ADAMTS-13, the metalloprotease that degrades high molecular weight vWF multimers. Degradation of vWF can lead to increased bleeding because high molecular weight vWF multimers are critical for homeostasis (16). We found increased ADAMTS-13 levels (mean 342.4 ng/mL) in
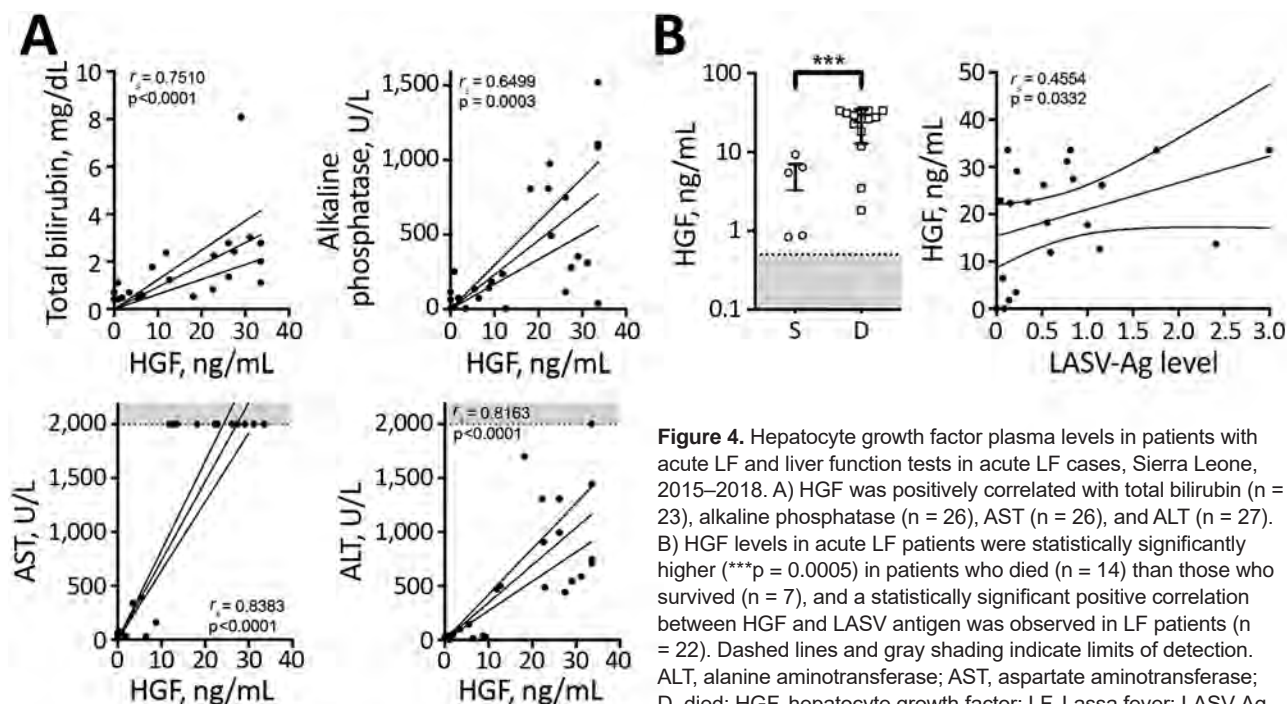
Figure 4. Hepatocyte growth factor plasma levels in patients with acute LF and liver function tests in acute LF cases, Sierra Leone, 2015–2018. A) HGF was positively correlated with total bilirubin (n = 23), alkaline phosphatase (n = 26), AST (n = 26), and ALT (n = 27). B) HGF levels in acute LF patients were statistically significantly higher (***p = 0.0005) in patients who died (n = 14) than those who survived (n = 7), and a statistically significant positive correlation between HGF and LASV antigen was observed in LF patients (n = 22). Dashed lines and gray shading indicate limits of detection. ALT, alanine aminotransferase; AST, aspartate aminotransferase; D, died; HGF, hepatocyte growth factor; LF, Lassa fever; LASV-Ag, Lassa fever virus antigen; S, survived.

LF patients compared with HCs (mean 165.5 ng/mL; p<0.0292) (Figure 2, panel D), suggesting high molecular weight vWF multimers also might be decreased, especially in the microvasculature where shear stress enhances the availability of vWF cleavage sites. However, we did not observe differences in ADAMTS-13 levels between LF patients who survived (mean 379.8 ng/mL) and those who died (mean 343.6 ng/mL). We also found no statistically significant correlation between LASV-Ag levels and ADAMTS-13 (Figure 2, panel D).

Fibrinolysis Markers
We also sought to determine changes in the fibrinolysis cascade. tPA, an enzyme that activates the zymogen plasminogen into the enzyme plasmin, dissolves fibrin clots and is inhibited by PAI-1. tPA levels trended higher (mean 90.7 pg/mL) in LF patients than NLFCs (median 11.04 pg/mL) but did not reach statistical significance (Figure 3, panel A). PAI-1 levels were much higher (mean 175.8 ng/mL) in LF patients than in HCs (mean 4.20 ng/mL; p = 0.0145). We also found a statistically significant positive correlation between LASV-Ag and PAI-1 (r_s = 0.5119; p = 0.0125) (Figure 3, panel B). tPA has a short half-life in circulation; elevated tPA levels might not represent active tPA but tPA–PAI-1 complexes, which are not distinguished by our ELISA.

Only PAI-1 was statistically significantly higher in patients with fatal LF (p = 0.0031) (Figure 3, panel B).

Increased fibrinolysis leads to the production of fibrin degradation products, such as D-dimers. We noted elevated D-dimers in ≈50% of LF patients and NLFCs, but we found no statistically significant differences between the groups. However, among LF patients, we found a statistically significant positive correlation between LASV-Ag levels and D-dimers (r_s = 0.5789; p = 0.0094) (Figure 3, panel C). Increased D-dimer is onej parameter used to determine DIC, which has been controversial in LF. Diagnosing DIC can be complex and requires measuring several parameters, including platelet count, prothrombin time, fibrin degradation products, and fibrinogen level, but we could not measure these with the available samples. Elevated TAT complexes are a common feature of DIC but do not indicate DIC when measured alone. TAT levels in LF patients were not elevated (mean 63.83 ng/mL) compared with HCs (mean 67.35 ng/mL) but were statistically significantly lower than levels in NLFCs (mean 96.64 ng/mL; p = 0.0349). We did not detect differences between TAT in LF survivors (median 71.47 ng/mL) and LF deaths (median 52.59 ng/mL), nor did we find a correlation between LASV-Ag antigen levels and TAT (Figure 2, panel D). We observed high baseline TAT values in HCs, but the levels were not different from baseline values

reported in other studies that used the same ELISA kit (17,18), indicating differences in standard values could be assay specific.

Elevated plasma HGF has correlated with severe coagulopathy, including DIC (19). During acute LF, we noted that HGF correlated with markers of liver damage, including total bilirubin (r_s = 0.7510; p<0.0001), alkaline phosphatase (r_s = 0.6499; p = 0.0003), aspartate transaminase (r_s = 0.8383; p<0.0001), and alanine transaminase (r_s = 0.8163; p<0.0001) (Figure 4, panel A). However, HGF alone was a better marker of fatal LF; the mean HGF in survivors was 3.27 ng/mL compared with 23.73 ng/mL in patients who died (p = 0.0005) (Figure 4, panel B). We also found that levels of HGF positively correlated with levels of LASV-Ag (r_s = 0.4554; p = 0.0332).

Endothelial Activation

EPCR promotes generation of APC by the thrombin–thrombomodulin complex by recruiting protein C to the endothelial surface (20). APC, when associated with the EPCR on endothelial cells, signals through protease-activated receptor 1 (PAR-1) to stabilize endothelial barrier function through an increase in tight junctions, antiapoptotic signals, and suppression of inflammatory cytokines (21–23). We measured soluble EPCR (sEPCR) to assess whether this pathway is altered during LF. We found no statistically significant differences in sEPCR levels between analyzed groups (Figure 4, panel A), but we observed a statistically significant positive correlation between plasma concentrations of sTHBD and sEPCR (r_s = 0.7351; p = 0.0003). When analyzed by outcome, we only observed this correlation in fatal LF cases (r_s = 0.9167; p = 0.0013; Figure 5, panel B).

Damage to the endothelial barrier causes exposure and secretion of platelet agonists, including collagen and vWF. P-selectin is found on the plasma membrane of platelets after activation, but an alternatively spliced P-selectin isoform lacking the transmembrane domain also is released from endothelial cells and platelet α granules upon activation (24,25). Plasma levels of soluble P-selectin are elevated during DIC, systemic thrombosis, and platelet consumption (26–29). We found higher levels of soluble P-selectin (mean 129.7 ng/mL) in LF patients than HCs (mean 20.34 ng/mL), but not statistically significant differences (p<0.05), nor did we find a statistically significant correlation between levels of P-selectin and LASV-Ag (Figure 6, panel A).

Activated endothelia release intracellular adhesion molecule 1 (ICAM-1) and vascular cell adhesion molecule 1 (VCAM-1) (30,31). We measured soluble ICAM-1 (sICAM-1) and soluble VCAM-1 (sVCAM-1) and found LF patients had statistically significantly higher levels of both markers (mean sICAM-1 829.1 ng/mL; mean sVCAM-1 4,388 ng/mL) compared with HCs (mean sICAM-1 633.5 ng/mL, p<0.0001; mean sVCAM-1 2,517 ng/mL, p = 0.0127) (Figure 6, panels B, C). We also observed statistically significant differences in sICAM-1 levels between HCs and fatal LF cases (mean sICAM-1 1,015 ng/mL; p = 0.0001) (Figure 4, panel B), but not with sVCAM-1 (Figure 6, panel C). We found no statistically significant correlation between sICAM-1 or sVCAM-1 and LASV-Ag (Figure 6, panels B, C).

Platelet Dysfunction

An inhibitor of platelet aggregation has been observed in the plasma of patients with severe LF and Argentine hemorrhagic fever, which is caused by the arenavirus Junin (7,32,33). The inhibition is platelet extrinsic and aggregation inhibition can be observed in plasma–platelet mixing experiments by using either autologous platelets from the acute case or platelets from healthy persons. We observed the same

Figure 5. Soluble endothelial protein C receptor plasma levels in patients with acute LF, NLFCs, and HCs, Sierra Leone, 2015–2018. A) EPCR is not statistically significantly different across groups (Kruskal-Wallis p = 0.0889). Error bars show SDs; horizontal lines indicate means. B) EPCR plasma levels correlated with soluble thrombomodulin in patients with acute LF. Patients with higher levels of soluble THBD tended to have higher levels of EPCR (n = 19). When analyzed by survival, a statistically significant positive correlation was found only in fatal LF cases (n = 9). Dashed lines and gray shading indicate limits of detection. D, died; EPCR, endothelial protein C receptor; HC, healthy control; LF, Lassa fever; NLFC, non-LF fever febrile control; THBD, thrombomodulin.
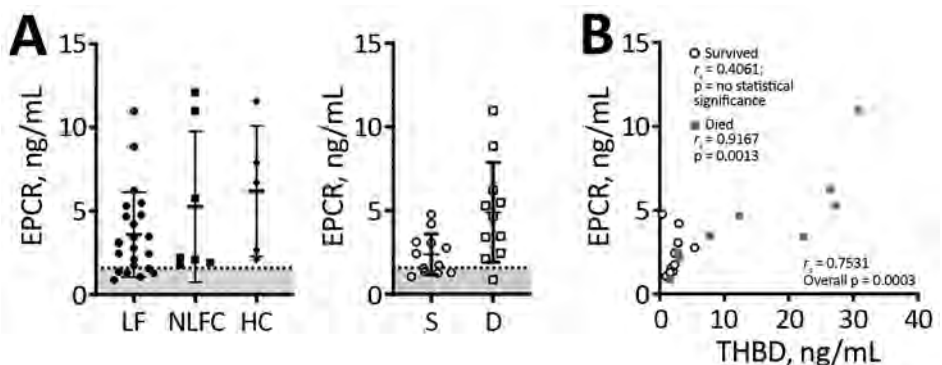
phenomenon in a mouse model of lethal arenavirus infection (*37*). We performed platelet aggregometry on a 1:1 mix of platelet-rich plasma from a healthy person collected in citrated tubes and dialyzed plasma from LF patients. EDTA inhibits platelet aggregation. KGH biorepository samples were collected in EDTA. Therefore, we dialyzed plasma used in aggregation assays to remove EDTA. Our unpublished observations in mice indicate EDTA can be dialyzed out of the plasma while retaining the inhibitory function of the platelet aggregation inhibitor.

Plasma samples varied in their turbidity and we could not reliably compare aggregation curves between samples. However, when platelets are agonized by ADP in the presence of the inhibitor, a characteristic disaggregation curve is observed (*32–34*). Platelet aggregation and subsequent disaggregation after ADP addition is independent of sample turbidity (Figure 7, panel A). Thus, we assessed the relative difference between peak aggregation and total aggregation 4 min after ADP addition. Platelet disaggregation only occurred in samples from fatal LF cases (Figure 7, panel B).

Discussion

We identified differences in plasma markers between nonfatal and fatal LF that imply loss of homeostasis, alterations in the protein C pathway, and platelet dysfunction likely contribute to weakened endothelial barriers observed in fatal LF cases. The increased

Figure 6. P-selectin and adhesion molecule levels in patients with acute LF, NLFCs, and healthy controls (HCs), Sierra Leone, 2015–2018. A) Differences in soluble P-selectin (CD62P) were statistically significant (Kruskal-Wallis p = 0.0358), but we found no statistically significant differences when comparing groups to each other using Dunn's multiple comparisons test (left, middle); no statistically significant correlation was observed between P-selectin and LASV-Ag levels (n = 15). B) Statistically significant differences in soluble ICAM levels were noted across all groups (Kruskal-Wallis p<0.0001). ICAM was statistically significantly elevated (****p<0.0001) in acute LF (n = 34) compared with HCs (n = 41) and NLFCs (n = 44; **p = 0.0036). No statistically significant correlation was found between ICAM and LASV antigen (n = 14) C) Statistically significant differences in soluble VCAM levels were observed across all groups (Kruskal-Wallis p = 0.0052). VCAM was statistically significantly elevated (*p = 0.0127) in acute LF (n = 34) compared with HCs (n = 41). No statistically significant differences were observed in acute LF patients who survived (n = 6) compared with those who died (n = 21) and no statistically significant correlation was found between VCAM and LASV-Ag (n = 14). Limits of detection are indicated by dashed lines and gray shading below. Error bars show SDs; horizontal lines indicate means. D, died; HC, healthy controls; ICAM, intercellular adhesion molecule; LF, Lassa fever; LASV, Lassa fever virus; LASV-Ag, Lassa fever virus antigen; NLFC, non–LF febrile controls; S, survived; VCAM, vascular cell adhesion molecule.
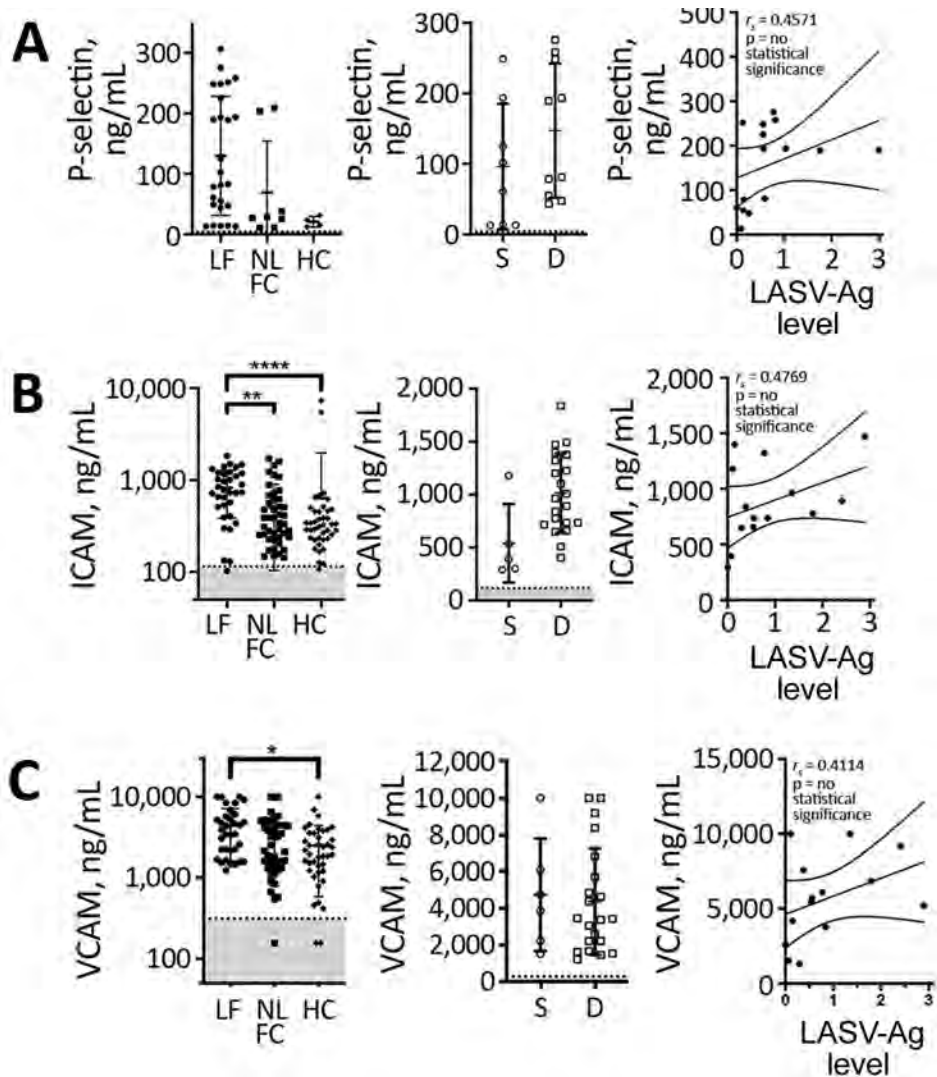
Figure 7. Representative platelet aggregometry performed on a 1:1 mix of platelet-rich plasma from a healthy control (HC) participant and platelet-poor plasma dialyzed to remove EDTA from either healthy controls or acute Lassa fever (LF) patients, Sierra Leone, 2015–2018. Aggregation was stimulated by addition of 5 μmol ADP. Plasma from fatal LF cases caused a decrease in aggregation at 4 min compared with peak aggregation, but plasma from LF survivor and non–LF febrile controls (NLFCs) showed no disaggregation by 4 min. A) Percent aggregation over 4 min. B) Aggregation at 4 min divided by the maximum aggregation in assays by using plasma from 14 fatal LF cases, 7 nonfatal LF cases, and 5 NLFC cases. Only assays using plasma from fatal cases showed disaggregation by the experimental endpoint. Error bars shows SD; horizontal lines indicate means. HC, healthy control; LF, Lassa fever; NLFC, non-LF febrile control.
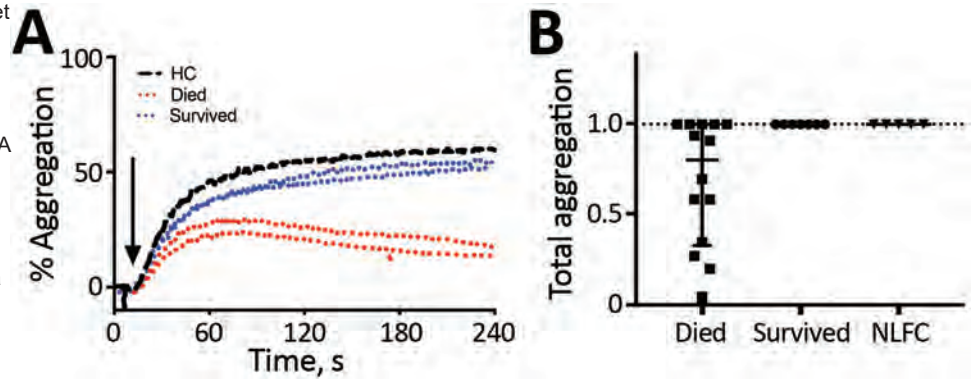
sTHBD we noted in fatal LF is consistent with vascular dysfunction seen in fatal LF cases. The concomitant increase in sEPCR suggests endothelial expression of both receptors of the protein C pathway were affected, pointing toward a potential impaired ability of the endothelium to generate APC and mediate APC cellular function, which includes stabilizing endothelial barrier function.

APC and EPCR also can inhibit NLRP3 inflammasome and apoptosis, which could contribute to Lassa-induced immunopathology. Studies show elevated interleukin 1 beta during later stages of LASV infection in cynomologous macaques (35), but this and other markers of inflammasome activation have not been well characterized during human infection. Recombinant APC (rAPC) therapy has had mixed results. After initial positive preclinical results (36), rAPC was ineffective in treating sepsis (37). However, rAPC given to Zaire ebolavirus–infected primates delayed death by several days (38). Because we could not measure expression of THBD and EPCR on the surface of endothelial cells, we do not know whether the signaling capacity of the APC-EPCR-PAR-1 pathway changes during LF.

Other mechanisms for disruption of endothelial barrier function have been proposed and also might play a role in LF. LASV can alter the biosynthesis of its cellular receptor, α-dystroglycan (39) and disrupt endothelial connections to the extracellular matrix by displacing laminin (40–42). Immune-mediated targeting of infected endothelial cells causes the pulmonary vascular permeability observed in our mouse model of lethal arenavirus infection (34,43). Cytokine storm has been implicated as a mechanism of capillary leak, but tumor necrosis factor α, a cytokine responsible for increasing vascular permeability, rarely has been observed in plasma of animal arenavirus models (35,44) or human LF cases (45–47).

Diseases that manifest as systemic endothelial dysfunction, such as LF, lead to disruption in homeostasis through exposure of TF, triggering coagulation cascade and platelet activation on the basal side of the endothelium. Observation of a platelet aggregation inhibitor only in fatal cases implies this factor is a potential contributor to the bleeding and vascular permeability characteristic of severe, fatal disease. In response to ADP and collagen, platelets exposed to the aggregation inhibitor begin to aggregate normally (32; Figure 8, panel A), indicating platelet activation is maintained. However, the initial aggregation is followed by disaggregation, suggesting an inhibition of platelet degranulation. Release of platelet granule contents is necessary for the second wave of platelet activation that sustains aggregation. The contents of these granules also are vital for coagulation, angiogenesis, wound repair, and inflammation; thus, inhibition of their release can have systemic effects.

Prior studies concluded coagulation dysfunction and DIC are not features of acute LF (48,49). We observed D-dimers and tPA trending higher, but these indicators of changes in fibrinolysis were not statistically significant. Moreover, we could not determine whether patients had DIC by the standardized diagnostic scoring system (50). Nevertheless, a positive correlation between increased D-dimers and LASV-Ag without an increase in TAT complexes suggest an atypical coagulation dysfunction. However, our data support pathologic activation of coagulation indicated by increased circulating TF, sTHBD, and vWF. Presence of a platelet aggregation inhibitor

might complicate coagulation dysfunction during LF further by disrupting or weakening active thrombus formation, leading to changes in blood coagulation parameters that appear similar to DIC but without thrombus formation in the microvasculature. Biochemical identification of the inhibitor and imaging studies to identify microthrombi in the vasculature of animals and humans could help clarify whether, and to what extent, DIC occurs during severe LF.

Our studies provide a comprehensive analysis of coagulation and endotheliopathy in human LF cases. These data only offer a snapshot of hemostatic changes; we cannot rule out resolution of dysregulated hemostasis in nonfatal LF patients before admission.

Figure 8. Working model of endothelial barrier function during time-of-admission for Lassa fever showing differences in function between healthy endothelium, and endothelium in nonfatal and fatal Lassa fever, Sierra Leone during 2015–2018. A) Healthy endothelium; resting platelets circulate and lower molecular weight vWF multimers are constitutively secreted by the endothelium. B) Endothelium barrier function in non-fatal Lassa fever. 1) Immune mediated damage near infected endothelial cells leads to collagen exposure, fibrin deposition, platelet activation, endothelial activation, and release of ultra-high molecular weight vWF from endothelial cells and platelets. Functional coagulation and platelet responses lead to endothelial repair. 2) Endothelial surface bound thrombomodulin and EPCR lead to activation of protein C; PAR-1 activation strengthens endothelial tight junctions, increases endothelial survival, and dampens the inflammatory response. C) Endothelium barrier function in fatal Lassa fever. 3) Increased endothelial infection has been observed in fatal LF cases. Increased immune infiltrates likely stress the endothelial barrier and lead to increased endothelial activation, evidenced by increased soluble ICAM, P-selectin, and EPCR. 4) Ultra-high molecular weight vWF multimers are broken down by ADAMTS-13, likely leading to the increased vWF ELISA signal observed during fatal LF. 5) Increases in soluble thrombomodulin and EPCR likely leave less surface bound forms, inhibiting the ability of endothelial cells to activate cytoprotective pathways through PAR-1 and increasing their susceptibility to immune mediated destruction. 6) Our in vitro aggregation studies show that platelets in the presence of the aggregation inhibitor become activated and change shape in response to platelet agonists but fail to maintain the aggregated state. These data are consistent with the inhibition of the release of α or dense granules or their contents, thereby inhibiting certain aspects of primary hemostasis, clot formation, and endothelial repair. 7) The state of fibrinolysis during fatal LF is unclear. Increased PAI-1 suggests an inhibition of fibrinolysis, but D-dimers and other FDPs are only formed during plasmin mediated breakdown of fibrin. Likely, increased platelet activation leads to an increase of total fibrin formation. Platelet dysfunction can lead to weaker hemostatic plugs which then leave fibrin more susceptible to cleavage by plasmin. APC, activated protein C; EC, endothelial cell; EPCR, endothelial protein C receptor; FDP, fibrin degradation product; ICAM, intercellular adhesion molecule; LASV, Lassa fever virus; PAI-1, plasminogen activator inhibitor 1; PAR-1, protease-activated receptor 1; plasminogen activator inhibitor 1; THBD, thrombomodulin; vWF, von Willebrand factor.
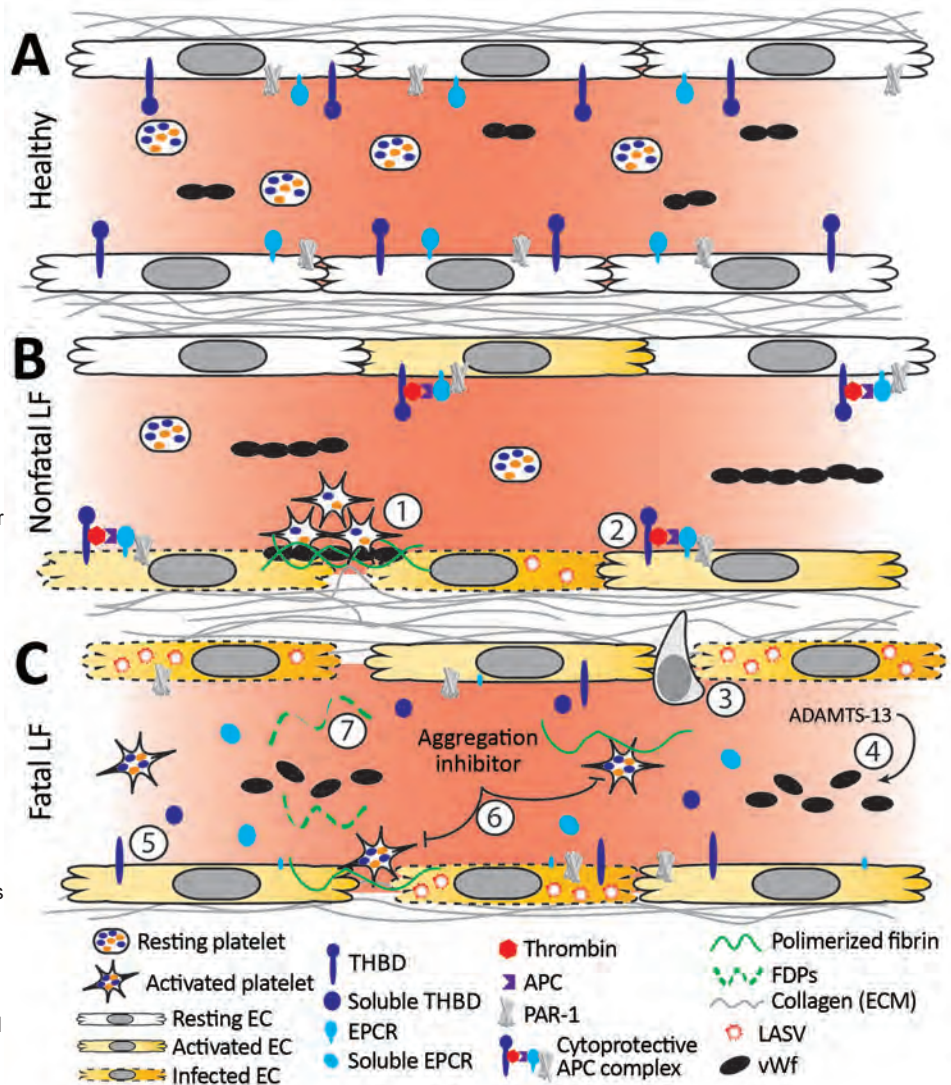
Certain clinical and epidemiologic information, such as date of symptom onset and outcomes for patients not admitted to the Lassa ward, was not available. Moreover, unavailability of samples and ELISA kits in Sierra Leone limited more extensive analyses of our data, specifically in cases in which analytes trended but did not reach statistical significance. More robust patient data and sample collection could help define hematological dysfunction during disease progression and correlate these markers with signs, such as facial and pulmonary edema.

In conclusion, we propose a model in which immunopathology causes disruption to the endothelial barrier (Figure 8). The combination of endothelial damage and an inability to repair it could contribute to the vascular permeability observed in most severe LF cases. In addition, the cytoprotective APC pathway and platelet aggregation, mechanisms that normally protect and maintain endothelial cell integrity, are disrupted during LASV infection. Further studies incorporating serial samples and samples collected earlier in the disease course are needed in animal models and humans to elucidate the molecular mechanisms underlying vascular dysfunction during severe LF. However, our data forms a basis for investigation into specific pathways that could provide targets of intervention to minimize the effects of host immunopathology and enable the immune system adequate time to clear the virus.

About the Author

Dr. Horton is an infectious diseases physician at the University of California, San Diego. Her research interests include emerging and re-emerging infectious diseases, refugee health, and tropical medicine.

References

1. Ogbu O, Ajuluchukwu E, Uneke CJ. Lassa fever in West African sub-region: an overview. J Vector Borne Dis. 2007;44:1–11.
2. Price ME, Fisher-Hoch SP, Craven RB, McCormick JB. A prospective study of maternal and fetal outcome in acute Lassa fever infection during pregnancy. BMJ. 1988;297:584–7. https://doi.org/10.1136/bmj.297.6648.584
3. McCormick JB, King IJ, Webb PA, Johnson KM, O'Sullivan R, Smith ES, et al. A case-control study of the clinical diagnosis and course of Lassa fever. J Infect Dis. 1987;155:445–55. https://doi.org/10.1093/infdis/155.3.445
4. Shehu NY, Gomerep SS, Isa SE, Iraoyah KO, Mafuka J, Bitrus N, et al. Lassa fever 2016 outbreak in Plateau State, Nigeria–the changing epidemiology and clinical presentation. Front Public Health. 2018;6:232. https://doi.org/10.3389/fpubh.2018.00232
5. Edington GM, White HA. The pathology of Lassa fever. Trans R Soc Trop Med Hyg. 1972;66:381–9. https://doi.org/10.1016/0035-9203(72)90268-4
6. Bausch DG, Sesay SS, Oshin B. On the front lines of Lassa fever. Emerg Infect Dis. 2004;10:1889–90. https://doi.org/10.3201/eid1010.IM1010
7. Fisher-Hoch S, McCormick JB, Sasso D, Craven RB. Hematologic dysfunction in Lassa fever. J Med Virol. 1988;26:127–35. https://doi.org/10.1002/jmv.1890260204
8. Zapata JC, Cox D, Salvato MS. The role of platelets in the pathogenesis of viral hemorrhagic fevers. PLoS Negl Trop Dis. 2014;8:e2858. https://doi.org/10.1371/journal.pntd.0002858
9. Shaffer JG, Grant DS, Schieffelin JS, Boisen ML, Goba A, Hartnett JN, et al.; Viral Hemorrhagic Fever Consortium. Lassa fever in post-conflict Sierra Leone. PLoS Negl Trop Dis. 2014;8:e2748. https://doi.org/10.1371/journal.pntd.0002748
10. Esmon CT, Esmon NL, Harris KW. Complex formation between thrombin and thrombomodulin inhibits both thrombin-catalyzed fibrin formation and factor V activation. J Biol Chem. 1982;257:7944–7.
11. Ishii H, Majerus PW. Thrombomodulin is present in human plasma and urine. J Clin Invest. 1985;76:2178–81. https://doi.org/10.1172/JCI112225
12. van Gorp EC, Suharti C, ten Cate H, Dolmans WM, van der Meer JW, ten Cate JW, et al. Review: infectious diseases and coagulation disorders. J Infect Dis. 1999;180:176–86. https://doi.org/10.1086/314829
13. Chu AJ. Tissue factor, blood coagulation, and beyond: an overview. Int J Inflamm. 2011;2011:1–29. https://doi.org/10.4061/2011/367284

14. van der Poll T. Tissue factor as an initiator of coagulation and inflammation in the lung. Crit Care. 2008;12(Suppl 6):S3. https://doi.org/10.1186/cc7026

15. Bu X, Zhang X, Cao W. The expression of plasminogen activator inhibitor-1 (PAI-1) gene in human astrocytomas [in Chinese]. Zhonghua Bing Li Xue Za Zhi. 1998;27:433–5.

16. Sadler JE. Biochemistry and genetics of von Willebrand factor. Annu Rev Biochem. 1998;67:395–424. https://doi.org/10.1146/annurev.biochem.67.1.395

17. Oklu R, Sheth RA, Wong KHK, Jahromi AH, Albadawi H. Neutrophil extracellular traps are increased in cancer patients but does not associate with venous thrombosis. Cardiovasc Diagn Ther. 2017;7(Suppl 3):S140–9. https://doi.org/10.21037/cdt.2017.08.01

18. Hyacinth HI, Adams RJ, Greenberg CS, Voeks JH, Hill A, Hibbert JM, et al. Effect of chronic blood transfusion on biomarkers of coagulation activation and thrombin generation in sickle cell patients at risk for stroke. PLoS One. 2015;10:e0134193. https://doi.org/10.1371/journal.pone.0134193

19. Chung S, Kim JE, Kim JY, Lee DS, Han KS, Kim HK. Circulating hepatocyte growth factor as an independent prognostic factor of disseminated intravascular coagulation. Thromb Res. 2010;125:e285–93. https://doi.org/10.1016/j.thromres.2010.01.046

20. Esmon CT, Owen WG. Identification of an endothelial cell cofactor for thrombin-catalyzed activation of protein C. Proc Natl Acad Sci U S A. 1981;78:2249–52. https://doi.org/10.1073/pnas.78.4.2249

21. Griffin JH, Zlokovic BV, Mosnier LO. Activated protein C: biased for translation. Blood. 2015;125:2898–907. https://doi.org/10.1182/blood-2015-02-355974

22. Mohan Rao LV, Esmon CT, Pendurthi UR. Endothelial cell protein C receptor: a multiliganded and multifunctional receptor. Blood. 2014;124:1553–62. https://doi.org/10.1182/blood-2014-05-578328

23. Mosnier LO, Zlokovic BV, Griffin JH. The cytoprotective protein C pathway. Blood. 2007;109:3161–72. https://doi.org/10.1182/blood-2006-09-003004

24. Ishiwata N, Takio K, Katayama M, Watanabe K, Titani K, Ikeda Y, et al. Alternatively spliced isoform of P-selectin is present in vivo as a soluble molecule. J Biol Chem. 1994;269:23708–15.

25. Dunlop LC, Skinner MP, Bendall LJ, Favaloro EJ, Castaldi PA, Gorman JJ, et al. Characterization of GMP-140 (P-selectin) as a circulating plasma protein. J Exp Med. 1992;175:1147–50. https://doi.org/10.1084/jem.175.4.1147

26. Ferroni P, Martini F, Riondino S, La Farina F, Magnapera A, Ciatti F, et al. Soluble P-selectin as a marker of in vivo platelet activation. Clin Chim Acta. 2009;399:88–91. https://doi.org/10.1016/j.cca.2008.09.018

27. Mosad E, Elsayh KI, Eltayeb AA. Tissue factor pathway inhibitor and P-selectin as markers of sepsis-induced non-overt disseminated intravascular coagulopathy. Clin Appl Thromb Hemost. 2011;17:80–7. https://doi.org/10.1177/1076029609344981

28. Chong BH, Murray B, Berndt MC, Dunlop LC, Brighton T, Chesterman CN. Plasma P-selectin is increased in thrombotic consumptive platelet disorders. Blood. 1994;83:1535–41. https://doi.org/10.1182/blood.V83.6.1535.1535

29. Connolly-Andersen AM, Sundberg E, Ahlm C, Hultdin J, Baudin M, Larsson J, et al. Increased thrombopoiesis and platelet activation in hantavirus-infected patients. J Infect Dis. 2015;212:1061–9. https://doi.org/10.1093/infdis/jiv161

30. Leeuwenberg JF, Smeets EF, Neefjes JJ, Shaffer MA, Cinek T, Jeunhomme TM, et al. E-selectin and intercellular adhesion

31. molecule-1 are released by activated human endothelial cells in vitro. Immunology. 1992;77:543–9.

31. Videm V, Albrigtsen M. Soluble ICAM-1 and VCAM-1 as markers of endothelial activation. Scand J Immunol. 2008; 67:523–31. https://doi.org/10.1111/j.1365-3083.2008.02029.x

32. Cummins D, Fisher-Hoch SP, Walshe KJ, Mackie IJ, McCormick JB, Bennett D, et al. A plasma inhibitor of platelet aggregation in patients with Lassa fever. Br J Haematol. 1989;72:543–8. https://doi.org/10.1111/j.1365-2141.1989.tb04321.x

33. Cummins D, Molinas FC, Lerer G, Maiztegui JI, Faint R, Machin SJ. A plasma inhibitor of platelet aggregation in patients with Argentine hemorrhagic fever. Am J Trop Med Hyg. 1990;42:470–5. https://doi.org/10.4269/ajtmh.1990.42.470

34. Oldstone MBA, Ware BC, Horton LE, Welch MJ, Aiolfi R, Zarpellon A, et al. Lymphocytic choriomeningitis virus clone 13 infection causes either persistence or acute death dependent on IFN-1, cytotoxic T lymphocytes (CTLs), and host genetics. Proc Natl Acad Sci U S A. 2018;115:E7814–23. https://doi.org/10.1073/pnas.1804674115

35. Hensley LE, Smith MA, Geisbert JB, Fritz EA, Daddario-DiCaprio KM, Larsen T, et al. Pathogenesis of Lassa fever in cynomolgus macaques. Virol J. 2011;8:205. https://doi.org/10.1186/1743-422X-8-205

36. Bernard GR, Vincent JL, Laterre PF, LaRosa SP, Dhainaut JF, Lopez-Rodriguez A, et al.; Recombinant human protein C Worldwide Evaluation in Severe Sepsis (PROWESS) study group. Efficacy and safety of recombinant human activated protein C for severe sepsis. N Engl J Med. 2001;344:699–709. https://doi.org/10.1056/NEJM200103083441001

37. Ranieri VM, Thompson BT, Barie PS, Dhainaut JF, Douglas IS, Finfer S, et al.; PROWESS-SHOCK Study Group. Drotrecogin alfa (activated) in adults with septic shock. N Engl J Med. 2012;366:2055–64. https://doi.org/10.1056/NEJMoa1202290

38. Hensley LE, Stevens EL, Yan SB, Geisbert JB, Macias WL, Larsen T, et al. Recombinant human activated protein C for the postexposure treatment of Ebola hemorrhagic fever. J Infect Dis. 2007;196(Suppl 2):S390–9. https://doi.org/10.1086/520598

39. Rojek JM, Campbell KP, Oldstone MB, Kunz S. Old World arenavirus infection interferes with the expression of functional alpha-dystroglycan in the host cell. Mol Biol Cell. 2007;18:4493–507. https://doi.org/10.1091/mbc.e07-04-0374

40. Cao W, Henry MD, Borrow P, Yamada H, Elder JH, Ravkov EV, et al. Identification of alpha-dystroglycan as a receptor for lymphocytic choriomeningitis virus and Lassa fever virus. Science. 1998;282:2079–81. https://doi.org/10.1126/science.282.5396.2079

41. Kunz S, Sevilla N, McGavern DB, Campbell KP, Oldstone MB. Molecular analysis of the interaction of LCMV with its cellular receptor [alpha]-dystroglycan. J Cell Biol. 2001;155:301–10. https://doi.org/10.1083/jcb.200104103

42. Kunz S, Rojek JM, Perez M, Spiropoulou CF, Oldstone MB. Characterization of the interaction of lassa fever virus with its cellular receptor alpha-dystroglycan. J Virol. 2005;79:5979–87. https://doi.org/10.1128/JVI.79.10.5979-5987.2005

43. Baccala R, Welch MJ, Gonzalez-Quintial R, Walsh KB, Teijaro JR, Nguyen A, et al. Type I interferon is a therapeutic target for virus-induced lethal vascular damage. Proc Natl Acad Sci U S A. 2014;111:8925–30. https://doi.org/10.1073/pnas.1408148111

44. Baize S, Marianneau P, Loth P, Reynard S, Journeaux A, Chevallier M, et al. Early and strong immune responses are associated with control of viral replication and

recovery in Lassa virus-infected cynomolgus monkeys. J Virol. 2009;83:5890–903. https://doi.org/10.1128/JVI.01948-08

45. Schmitz H, Köhler B, Laue T, Drosten C, Veldkamp PJ, Günther S, et al. Monitoring of clinical and laboratory data in two cases of imported Lassa fever. Microbes Infect. 2002;4:43–50. https://doi.org/10.1016/S1286-4579(01)01508-8

46. Mahanty S, Bausch DG, Thomas RL, Goba A, Bah A, Peters CJ, et al. Low levels of interleukin-8 and interferon-inducible protein-10 in serum are associated with fatal infections in acute Lassa fever. J Infect Dis. 2001;183:1713–21. https://doi.org/10.1086/320722

47. Branco LM, Grove JN, Boisen ML, Shaffer JG, Goba A, Fullah M, et al. Emerging trends in Lassa fever: redefining the role of immunoglobulin M and inflammation in diagnosing acute infection. Virol J. 2011;8:478. https://doi.org/10.1186/1743-422X-8-478

48. Peters CJ, Liu CT, Anderson GW Jr, Morrill JC, Jahrling PB. Pathogenesis of viral hemorrhagic fevers: Rift Valley fever and Lassa fever contrasted. Rev Infect Dis. 1989;11(Suppl 4): S743–9. https://doi.org/10.1093/clinids/11.Supplement_4.S743

49. Kunz S. The role of the vascular endothelium in arenavirus haemorrhagic fevers. Thromb Haemost. 2009;102:1024–9. https://doi.org/10.1160/TH09-06-0357

50. Taylor FB Jr, Toh CH, Hoots WK, Wada H, Levi M; Scientific Subcommittee on Disseminated Intravascular Coagulation (DIC) of the International Society on Thrombosis and Haemostasis (ISTH). Towards definition, clinical and laboratory criteria, and a scoring system for disseminated intravascular coagulation. Thromb Haemost. 2001;86:1327–30. https://doi.org/10.1055/s-0037-1616068

Address for correspondence: Brian M. Sullivan, The Scripps Research Institute, 10550 N Torrey Pines Rd, IMM-6, La Jolla, California 92037, USA; email: bsully@scripps.edu

July 2020

Emerging Viruses

EMERGING INFECTIOUS DISEASES®

To revisit the July 2020 issue, go to:
https://wwwnc.cdc.gov/eid/articles/issue/26/7/table-of-contents

High Dengue Burden and Circulation of 4 Virus Serotypes among Children with Undifferentiated Fever, Kenya, 2014–2017

Melisa M. Shah, Bryson A. Ndenga, Francis M. Mutuku, David M. Vu,
Elysse N. Grossi-Soyster, Victoria Okuta, Charles O. Ronga, Philip K. Chebii, Priscilla Maina,
Zainab Jembe, Carren M. Bosire, Jael S. Amugongo, Malaya K. Sahoo, ChunHong Huang, Jenna Weber,
Sean V. Edgerton, Jimmy Hortion, Shannon N. Bennett, Benjamin A. Pinsky, A. Desiree LaBeaud

Little is known about the extent and serotypes of dengue viruses circulating in Africa. We evaluated the presence of dengue viremia during 4 years of surveillance (2014–2017) among children with febrile illness in Kenya. Acutely ill febrile children were recruited from 4 clinical sites in western and coastal Kenya, and 1,022 participant samples were tested by using a highly sensitive real-time reverse transcription PCR. A complete case analysis with genomic sequencing and phylogenetic analyses was conducted to characterize the presence of dengue viremia among participants during 2014–2017. Dengue viremia was detected in 41.9% (361/862) of outpatient children who had undifferentiated febrile illness in Kenya. Of children with confirmed dengue viremia, 51.5% (150/291) had malaria parasitemia. All 4 dengue virus serotypes were detected, and phylogenetic analyses showed several viruses from novel lineages. Our results suggests high levels of dengue virus infection among children with undifferentiated febrile illness in Kenya.

Author affiliations: Stanford University School of Medicine, Stanford, California, USA (M.M. Shah, D.M. Vu, E.N. Grossi-Soyster, M.K. Sahoo, C. Huang, J. Weber, J. Hortion, B.A. Pinsky, A.D. LaBeaud); Kenya Medical Research Institute, Kisumu, Kenya (B.A. Ndenga, V. Okuta, C.O. Ronga); Technical University of Mombasa, Mombasa, Kenya (F.M. Mutuku, C.M. Bosire, J.S. Amugongo); Msambweni County Referral Hospital, Msambweni, Kenya (P.K. Chebii, P. Maina); Diani Health Center, Ukunda, Kenya (Z. Jembe); California Academy of Sciences, San Francisco, California, USA (S.V. Edgerton, S.N. Bennett); École Normale Supérieure de Lyon, Lyon, France (J. Hortion)

Dengue virus (DENV) is a reemerging arbovirus with an expansive worldwide range (*1*). Recent modeling studies suggest wider dengue circulation in Africa than previously recognized (*2*). In addition, both major dengue vectors (*Aedes aegypti* and *Ae. albopictus* mosquitoes) are present in Africa (*3,4*). The true burden of dengue is likely underestimated because most infections are never accounted for among patients who have self-limited disease or are misdiagnosed as malaria (*2*).

Dengue viremia among returning travelers from Africa and scattered reports from individual countries suggest ongoing dengue circulation in Africa (*2*). Each DENV serotype (DENV-1, DENV-2, DENV-3, and DENV-4) is structured into major lineages referred to as genotypes which have been defined (*5–7*). Relatively few DENV sequences are available from Africa (Figure 1), and DENV-2 is the predominant serotype in Africa to date (*2*).

Isolation of DENV-1 and DENV-2 in Africa was made in Nigeria during 1968 (*8*). The first DENV-3 strains isolated from humans from Africa were reported from Mozambique during 1984 (*9*). Only 2 human DENV-4 sequences are publicly available from Africa, 1 from Senegal during 1986 and 1 from Angola during 2014 (*10*).

A laboratory-confirmed outbreak of dengue occurred in coastal Kenya during 1982, followed by a large dengue outbreak in northeastern Kenya during 2011 (*11,12*). Circulation of DENV-1, DENV-2, and DENV-3 was reported in northern and coastal Kenya during 2011–2014 (*13*).
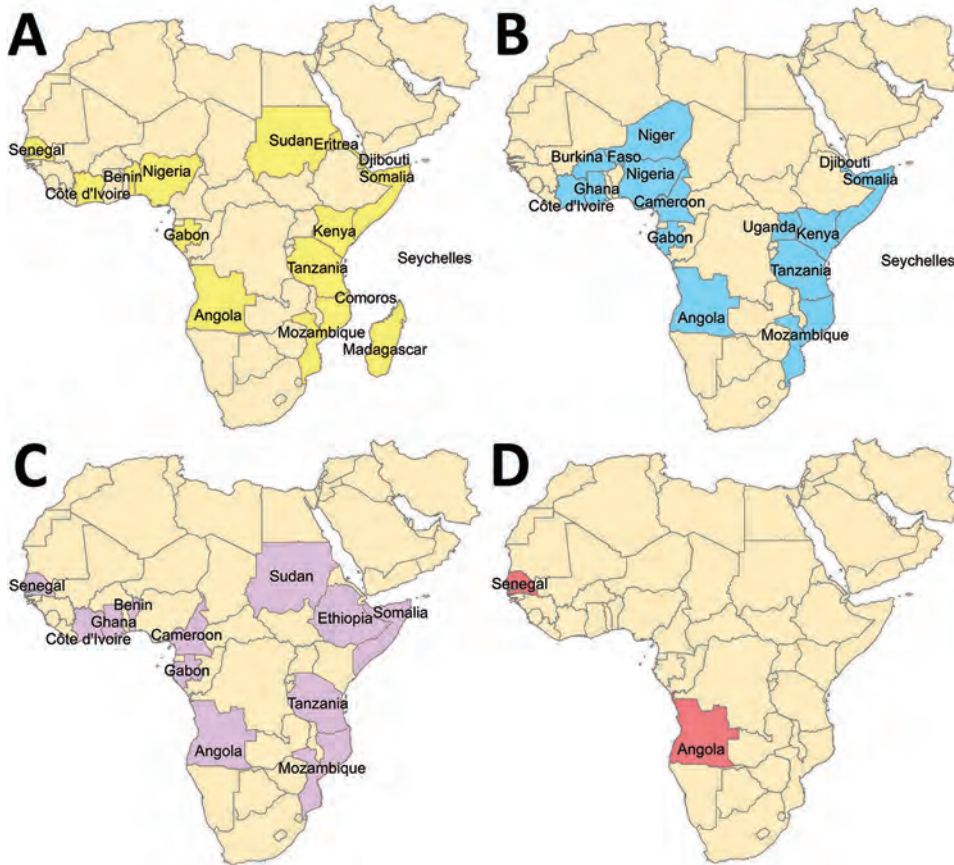
Figure 1. Countries in Africa (indicated by colors) for which dengue virus (DENV) sequences isolated from humans are available in GenBank. A) DENV-1, B) DENV-2, C) DENV-3, D) DENV-4. Further details on search strategy used for this map are available in Appendix Table 2 (https://wwwnc.cdc.gov/EID/article/26/11/20-0960-T2.App1.pdf).

Given the mounting evidence for dengue in Africa, we evaluated the presence of dengue viremia during 4 years of surveillance (2014–2017) among children with febrile illness in coastal and western Kenya by using a highly-sensitive, multiplexed, real-time reverse transcription PCR (rRT-PCR) and genomic sequencing. We report the clinical manifestations, associated factors, serotypes, and phylogenetic relationships.

Methods

Study Sites and Enrollment

Children in Kenya who had undifferentiated febrile illness from 4 outpatient clinics located in Chulaimbo, Kisumu, Msambweni, and Ukunda were enrolled during January 24, 2014–August 15, 2017 (Figure 2). The clinics in Chulaimbo (a rural setting) and Kisumu (an urban setting) are located near Lake Victoria in western Kenya. Msambweni District Hospital (a rural setting) and Ukunda/Diani Health Centre (an urban setting) are located in coastal Kenya. All clinics are operated by the Kenyan Ministry of Health. Each child 1–17 years of age who came for care (Monday–Friday) because of an acute febrile illness (defined as reported illness during the previous 14 days and current observed temper-

ature ≥38°C) and no localizing symptoms were recruited. Participants or their parents/guardians provided consent. We obtained detailed clinical histories and performed physical examinations. Comprehensive demographic and household data were recorded. Blood from each of the study participants was collected for serologic analysis, molecular testing, and malaria parasite smear. Data were stored in REDCap (*14*).

RNA Extraction and cDNA Synthesis

An aliquot of whole blood from each participant was collected in Kenya. RNA was extracted by using the GeneJET RNA Purification Kit (ThermoFisher Scientific, https://www.thermofisher.com), and purified RNA was synthesized into complementary DNA (cDNA) by using the Maxima H Minus First Strand cDNA Synthesis Kit (ThermoFisher Scientific) according to the manufacturers' instructions. All samples, including serum and cDNA, were shipped on dry ice and maintained at -80°C once received at Stanford University.

RT-PCR and Envelope Gene Sequencing

PCR was performed at the Stanford Clinical Virology Laboratory. The rRT-PCRs used in this study, including
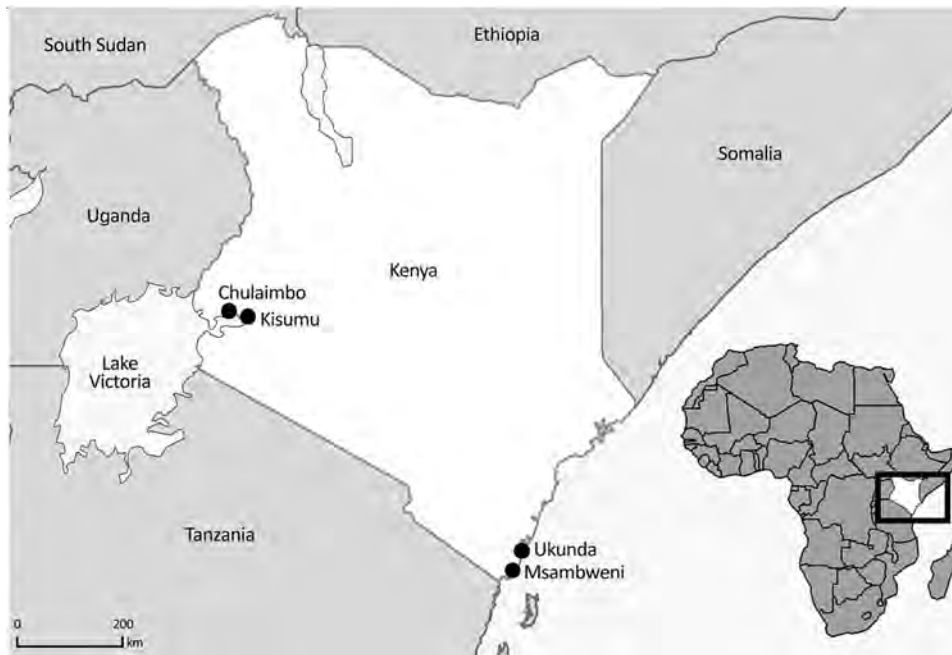
Figure 2. Study recruitment sites (black dots) for dengue burden and circulation of 4 virus serotypes among children with undifferentiated fever, Kenya, 2014–2017. Inset map shows location of Kenya in Africa.

a pan-DENV assay that detects all serotypes but does not distinguish between them, and a DENV serotyping assay, have been described (*15,16*). The pan-DENV assay uses primers and probes targeting RNaseP, which serves as an internal control. Specimens negative for DENV RNA with an internal control cycle threshold value >45 were considered to have failed extraction, cDNA generation, or PCR. Samples with cycle thresholds <35 by the pan-DENV assay or serotype-specific assay underwent sequencing attempts.

On the basis of the serotypes identified by rRT-PCR, serotype-specific envelope gene primers were used to generate amplicons for sequencing (Appendix Table 1, https://wwwnc.cdc.gov/EID/article/26/11/20-0960-App1.pdf). Each 25-μL reaction contained LongAmp Hot Start Taq 2× Master Mix (New England BioLabs, https://www.neb.com), 400 nmol/L of forward and reverse primers, 3% dimethyl sulfoxide, and 5 μL of cDNA. Amplification was performed in an Applied Biosystems Veriti 96-Well Thermal Cycler (ThermoFisher Scientific) by using the following cycling parameters: 94°C for 2 min; 40 cycles of 94°C for 30 s, 70°C for 1 s (ramp rate 20%), 55°C for 45 s (ramp rate 20%), and 65°C for 3 min, 20 s; and final extension for 10 min at 65°C. The PCR products were subjected to electrophoresis on a 1% agarose gel and visualized by staining with ethidium bromide. Dideoxynucleotide chain-termination sequencing (Sanger) was performed by Elim Biopharmaceuticals (https://www.elimbio.com) using the same primers used for amplification.

Whole-Genome Sequencing

Whole-genome sequencing was performed on a subset of convenience samples at the California Academy of Sciences' Center for Comparative Genomics (https://www.calacademy.org). cDNA was purified by using the Zymo Clean and Concentrator Kit (Zymo Research, https://www.zymoresearch.com). Library preparation was performed by using the Nextera XT DNA Library Preparation Kit (96 samples) and the Nextera XT Index Kit (96 indices, 384 samples) (both from Illumina, https://www.illumina.com) according to manufacturer's instructions with modifications: 3 ng of input cDNA with 4 μL index was used per reaction (rather than the suggested 1 ng input with 5 μL index because of low cDNA concentrations). Samples were tagged with a molecular identification tag. Libraries were quantified and assessed for quality on a BioAnalyzer (Agilent, https://www.agilent.com) before equimolar pooling for sequencing on the Illumina MiSeq platform using reagent run kits in series Nano, V2, and V3. Raw reads were uploaded by using CLC Genomics Workbench version 7.0.3 (https://www.qiagen.com) after being sorted by sample. DENV sample reads were mapped to complete, reference genome sequences downloaded from GenBank for each serotype. Virus consensus sequences were extracted in CLC Genomics Workbench version 7.0.3 and exported for phylogenetic analyses.

Serologic Tests

Serum samples obtained at each patient visit were tested by using an indirect IgG ELISA for flavivirus

IgG (17). An ELISA result positive for DENV IgG in serum was indicative of previous exposure. Participants who had DENV IgG at the febrile visit were identified as having past exposure to dengue. All samples were tested in duplicate.

Phylogenetic Analysis and Consensus Generation

Consensus sequences were deposited in GenBank under accession nos. MT076932–62. Multiple sequence alignment of both partial and complete genome sequences was performed by using the Multiple Alignment and Fast Fourier Transform plug-in in Geneious Prime 2020.0.5 (https://www.geneious.com). Reference genomes were selected to represent all genotype lineages and wide sampling of time periods focusing on sequences from Africa. To classify taxa, a maximum likelihood tree supported with maximum likelihood bootstrap replicates was inferred by using RAXML (https://raxml-ng.vital-it.ch) for each dengue serotype. Bootstrapping values were estimated starting with 100 replicates. The resulting trees were mid-point rooted to maintain consistency. Sylvatic strains were initially included to check for spillover, but then excluded from subsequent analyses to highlight differences in human-derived sequences.

Statistical Testing and Cartography

Complete cases with cDNA specimens available for DENV rRT-PCR were included. Univariate analysis and a χ^2 test for categorical variables and a *t*-test for continuous variables was used to compare participants on the basis of infection status with $\alpha = 0.05$. One-way analysis of variance was used for >2 group mean comparisons. A comprehensive GenBank search term (Appendix Table 2) was used to obtain a list of original, verified, human dengue sequences from Africa through February 19, 2020. Maps were made by using QGIS version 3.4.14 (https://qgis.org).

Ethics

The study protocol was approved by the Stanford University Institutional Review Board (IRB-31488) and Kenya Medical Research Institute Scientific and Ethical Review Unit in Kenya (protocol 2611). Participation in the study did not affect routine clinical evaluation and treatment provided by the Ministry of Health.

Results

During January 24, 2014–August 15, 2017, a total of 5,178 participants met eligibility for having an ongoing febrile illness without localization and documented body temperature ≥38°C when care was sought. Of eligible participants at clinics in the

western region, 72.4% consented to participate in the study; 97.2% from clinics in the coastal region consented. RNA extraction and cDNA synthesis were successful for 1,022 specimens that were shipped to the United States for DENV nucleic acid analysis. The mean number of illness days before seeking care was 2 days (range 1–14 days). The study included 11 participants who had 2 separate visits for febrile illness. Of the 1,022 specimens tested by using the internally controlled, pan-DENV rRT-PCR, 15.7% (160/1,022) showed negative results for extraction, cDNA production, or PCR on the basis of the internal control and absence of DENV nucleic acid amplification. Dengue viremia was observed in 41.9% (361/862) of samples that passed quality control, including 46.2% (255/552) from western Kenya and 34.2% (106/310) from coastal Kenya. Overall, 92.2% (333/361) were classified as primary infections (DENV IgG not present) and 3.9% (14/361) as secondary infections (DENV IgG present); 3.9% (14/361) lacked DENV IgG data because of sample unavailability.

We provide baseline characteristics for participants by clinical site (Table 1). The mean age of enrolled children from the coastal region was higher than that for children from the western region (6.7 years vs. 4.6 years; p<0.001). Overall, girls were less represented than boys (467/1,022, 45.7%), and this trend was consistent across sites (44.5% girls in the coastal region, 46.5% girls in the western region). Bednet use was higher in the coastal region than in the western region (94.8% vs. 69.7%; p<0.001). Children in the coastal region had lower household wealth, defined as having <3 of a domestic worker, bicycle, telephone, radio, motor vehicle, or television (64.5% vs. 54.8%; p = 0.003). The number of illness days before seeking care was lower in the coastal region than in the western region (2.3 vs. 3.1 days; p<0.001). Malaria smear positivity was lower in the coastal region than in the western region (47.1% vs. 56.8%; p = 0.006) (Table 1). A higher proportion of febrile children in the western region had dengue viremia than children in the coastal region (46.2% vs. 34.2%; p = 0.001). Participants from the coastal region were more likely to be positive for DENV IgG at the febrile visit than participants from the western region (19/420 4.5% vs. 7/568 1.2%; p = 0.003) (Table 1). The mean age was 11.0 years for participants who were positive for DENV IgG compared with 5.4 years for participants who were negative for DENV IgG at the febrile visit (p<0.001).

Mean age of children with DENV detected by rRT-PCR did not differ from all others (5.2 years vs. 5.6 years; p = 0.13) (Table 2). In children with and without dengue, mean body temperature, sex, and

Table 1. Characteristics of participants by geographic location in study of dengue burden and circulation of 4 virus serotypes among children with undifferentiated fever, Kenya, 2014–2017*

Characteristic	Coastal clinics (Msambweni and Ukunda), n = 422	Western clinics (Chulaimbo and Kisumu), n = 600	p value
Mean (SD) age, y	6.7 (4.4)	4.6 (2.9)	<0.001
Sex			
F	188 (44.5)	279 (46.5)	0.58
M	234 (55.5)	321 (53.5)	0.58
Always uses bednet	400 (94.8)	418 (69.7)	<0.001
Wealth index <3†	272 (64.5)	329 (54.8)	0.003
Mean (SD) no. illness days before seeking care	2.3 (0.72)	3.1 (1.9)	<0.001
Dengue viremic by rRT-PCR	106 (34.2)	255 (46.2)	0.001
DENV IgG present at febrile visit	19 (4.5)	7 (1.2)	0.003
Malaria smear positive	194 (47.1)	247 (56.8)	0.006

*Values are no. (%) unless indicated otherwise. DENV, dengue virus; rRT-PCR, real-time reverse transcription PCR.
†Defined as a household having <3 of the following: domestic worker, bicycle, telephone, radio, motor vehicle, and television.

malaria smear positivity were not different (Table 2). DENV viremic participants commonly reported headache (49.6%), poor appetite (46.8%), cough (45.7%), and joint pains (36.8%). Poor appetite was more often reported in dengue patients than in children without dengue (46.8% vs. 36.3%; p = 0.001). Antimicrobial drug prescriptions were significantly more common for children who had dengue viremia than for febrile patients without DENV (50.4% vs. 43.9%; p = 0.05). Antimalarial drug prescriptions were also more likely for DENV viremic patients (48.8% vs. 36.8%; p<0.001), although malaria smear positivity was not different between the groups (Table 2).

Among all 1,022 study participants, 419 (41.0%) were given an antimalarial. Malaria microscopy results were available for 847 (82.9%) participants; 441 (52.1%) were smear positive. Among study participants who had confirmed dengue and without malaria, 29/141 (20.6%) were given an antimalarial drug, 75/141 (53.2%) were given an antimicrobial drug, and 12/141 (8.5%) were given antimalarial and antimicrobial drugs. Fourteen (6.6%) of 213 participants who did not have dengue or malaria were given antimalarial and antimicrobial drugs.

Serotypes were obtained for 61.2% (221/361) of DENV-positive samples. Samples that were able to be serotyped had higher mean virus loads than untypeable samples (6.5 $\log_{10}$ cDNA copies/µL vs. 4.6 $\log_{10}$ cDNA copies/µL; p<0.001). Of the serotyped samples, 16.3% (36/221) were DENV-1, 47.5% (105/221) were DENV-2, 4.5% (10/221) were DENV-3, 4.5% (10/221) were DENV-4, and in 26.7% (59/221) ≥2 serotypes were identified. Among the 59 mixed infections, the most common was DENV-2/DENV-3 (59.3%, 35/59); a total of 26/35 occurred during July 2015. The other serotype combinations were DENV-1/DENV-2 (20/59, 33.9%) and DENV-1/DENV-4 (4/59, 6.8%). Patients infected with DENV-3 had highest virus loads, but participant

Table 2. Clinical characteristics of febrile children stratified by dengue viremia status in study of dengue burden and circulation of 4 virus serotypes among children with undifferentiated fever, Kenya, 2014–2017*

Characteristic	Participants with dengue viremia, n = 361	Participants without dengue viremia, n = 661	p value
Mean (SD) age, y	5.2 (3.4)	5.6 (3.9)	0.13
Mean (SD) temperature, °C	38.8 (0.6)	38.9 (0.7)	0.14
Mean (SD) no. illness days before seeking care	2.8 (1.6)	2.7 (1.5)	0.21
Sex			
F	168 (46.5)	299 (45.2)	0.74
M	193 (53.5)	362 (54.8)	0.74
Signs and symptoms			
Headache	179 (49.6)	326 (49.3)	0.99
Poor appetite	169 (46.8)	240 (36.3)	0.001
Cough	165 (45.7)	278 (42.1)	0.29
Joint pain	133 (36.8)	259 (39.2)	0.50
Nausea or vomiting	128 (35.5)	219 (33.1)	0.50
Chills	66 (18.3)	118 (17.9)	0.93
Abdominal pain	46 (12.7)	134 (20.3)	0.003
Diarrhea	42 (11.6)	68 (10.3)	0.58
Muscle aches	30 (8.3)	54 (8.2)	1.00
Malaria smear positive	150 (51.5)	291 (52.3)	0.88
DENV IgG present at febrile visit	14 (4.0)	12 (1.9)	0.07
Prescribed antimicrobial drugs	182 (50.4)	290 (43.9)	0.05
Prescribed antimalarial drugs	176 (48.8)	243 (36.8)	<0.001

*Values are no. (%) unless indicated otherwise. DENV, dengue virus.

Table 3. Characteristics of participants by DENV serotype in study of dengue burden and circulation of 4 virus serotypes among children with undifferentiated fever, Kenya, 2014–2017*

Characteristic	DENV-1, n = 36	DENV-2, n = 105	DENV-3, n = 10	DENV-4, n = 11	Mixed, n = 59	p value
Mean (SD) age, y	4.4 (2.8)	5.2 (3.3)	5.8 (3.9)	3.8 (1.6)	5.6 (3.3)	0.21
Mean (SD) viral load, $\log_{10}$ cDNA copies/µL	6.1 (2.5)	5.7 (2.2)	9.7 (3.8)	5.2 (2.7)	7.9 (1.8)	<0.001
Site						<0.001
Chulaimbo	5 (13.9)	53 (50.5)	2 (20.0)	1 (9.1)	26 (49.2)	
Kisumi	10 27.8)	28 (26.7)	7 (70.0)	10 (90.9)	25 (42.4)	
Msambweni	21 (58.3)	12 (11.4)	1 (10.0)	0	0	
Ukunda	0	12 (11.4)	0	0	0	
Mean (SD) no. illness days before seeking care	2.6 (1.6)	2.9 (1.9)	3.5 (1.5)	2.8 (1.47)	2.6 (1.3)	0.46
Malaria smear positive	18 (51.4)	42 (55.3)	3 (42.9)	4 (45.5)	23 (62.2)	0.78

*Values are no. (%) unless indicated otherwise. cDNA, complementary DNA; DENV, dengue virus.

age, number of illness days before seeking care, and malaria smear positivity rate did not differ by serotype (Table 3). In Ukunda (urban coastal region), only DENV-2 was identified. In Msambweni, DENV-1 was the most common serotype. DENV-2 was most common serotype in Kisumu. DENV-4 was found mostly in Kisumu; there were a few cases in Msambweni. We provide the distribution of dengue serotypes over the study period (Figure 3).

We provide phylogenetic relationships of 31 DENV sequences, including 7 whole genomes, from the current study (Figures 4–7). The samples span July 2014–June 2017 and are derived from participants in coastal and western Kenya. Both DENV-2 and DENV-3 were sequenced from 1 participant sample (MT076939 and MT076951). Many of the samples belong to genotypes that differ from existing reference sequences from Africa. One DENV-2 sample in genotype IV aligns near reference sequences from Malindi, Kenya, and other countries in Africa, and all other DENV-2 samples cluster in genotype I (Figure 5).

Discussion

Our study characterized the epidemiology of dengue among children with fever who came to clinics for outpatient care and the phylogenetic relationships of all 4 detected virus serotypes in Kenya. Of 1,022 febrile pediatric visits in western and coastal Kenya, >40% had evidence of dengue viremia. This unprecedented finding suggests an enormous burden of dengue fever among children with undifferentiated febrile illness in Kenya. The higher proportion of dengue in children from the western region than in children from the coastal region might be explained by a reported dengue outbreak in western Kenya during July 2014–June 2015 (18). Similar to previous findings showing 25% dengue viremia by RT-PCR for febrile patients in Kenya during 2011–2014 (13), the current study also identified a major proportion of febrile illness attributable to dengue. Similarly, Bhatt et al. estimated a burden of dengue disease in Africa similar to that in the Americas (>16% of the total global burden) (19). Our study supports the notion of an underrecognized dengue burden in Africa.
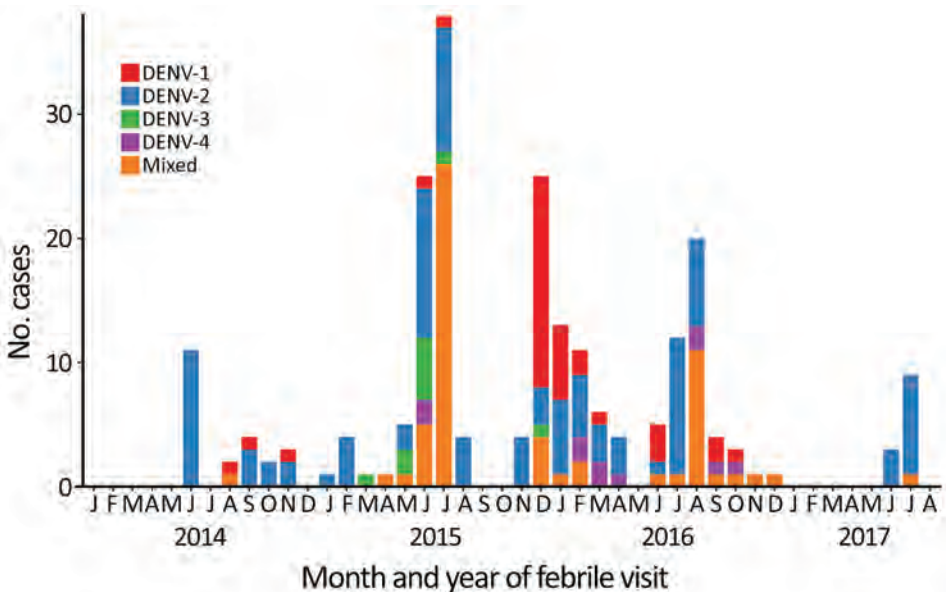
Figure 3. Dengue virus serotypes detected over time for children tested during a medical visit for fever, Kenya, 2014–2017. Data from 4 sites are included. DENV, dengue virus.

Our study identified circulation of multiple serotypes of DENV and adds valuable field strains to the public repository. Compilation of available DENV sequences from Africa into the phylogenetic analyses illustrates the dearth of sequences from Africa and is particularly evident for DENV-1 and

Figure 4. Maximum-likelihood phylogenetic tree for DENV-1 sequences from children with undifferentiated fever in Kenya, 2014–2017 (red), and reference sequences from other locations in Africa (blue) and elsewhere. Numbers at nodes represent bootstrap support values based on maximum-likelihood replicates. Genotypes are indicated at right. Scale bar indicates nucleotide substitutions per site. DENV, dengue virus.
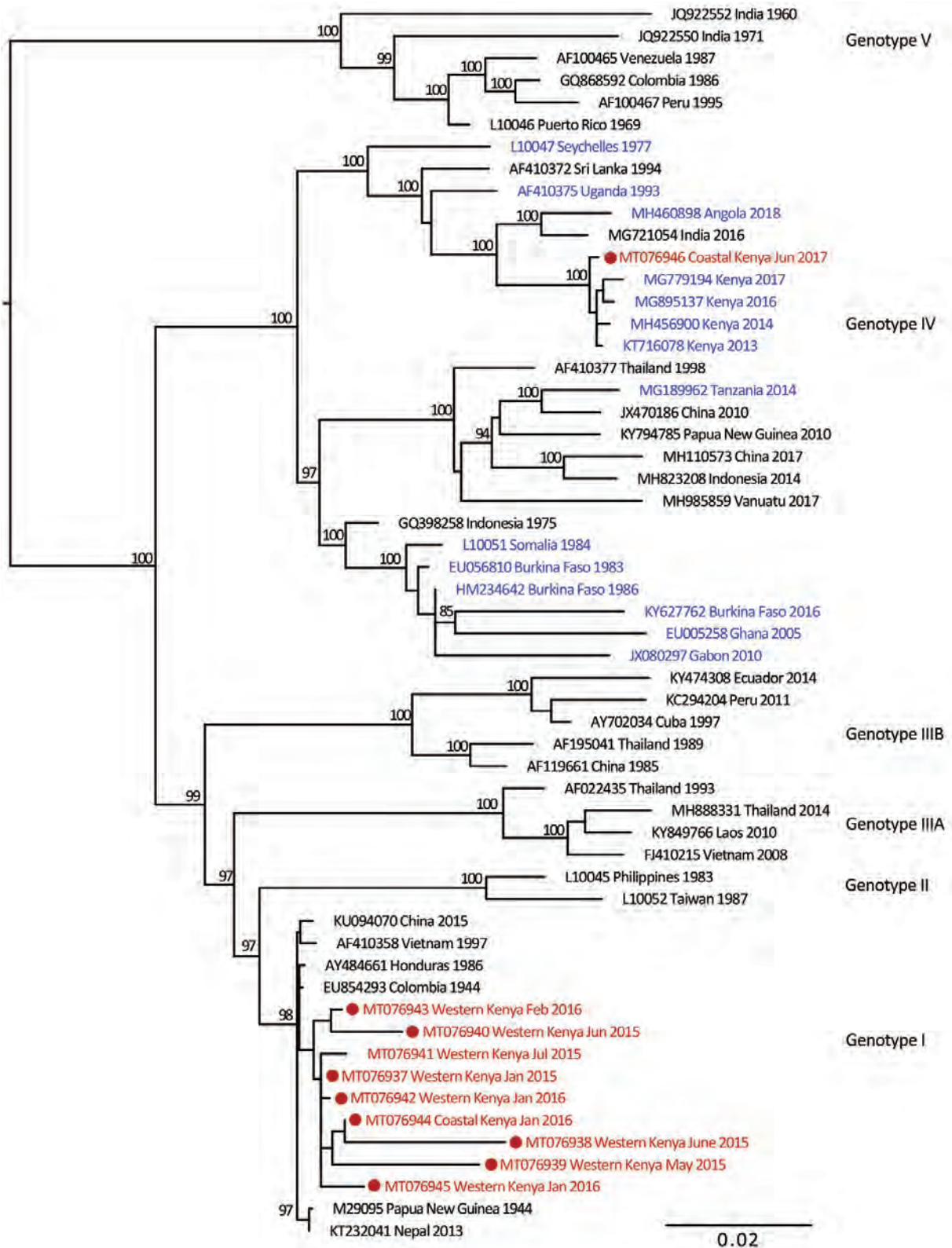
Figure 5. Maximum-likelihood phylogenetic tree for DENV-2 sequences from children with undifferentiated fever in Kenya, 2014–2017 (red), and reference sequences from other locations in Africa (blue) and elsewhere. Numbers at nodes represent bootstrap support values based on maximum-likelihood replicates. Genotypes are indicated at right. Scale bar indicates nucleotide substitutions per site. DENV, dengue virus.

DENV-4 (Figure 1). The DENV-1 samples align closely with a historical Thailand 1964 strain in genotype II. Although such a finding might suggest laboratory error or viral contamination, the Thailand 1964 strain is not a publicly available strain and has never been present in our laboratories. A DENV-1 strain in genotype II was curiously noted to cause human disease in Indonesia during 2012 and is similar to the Thailand 1964 strain (20). We postulate that viral strains related to the Thailand 1964 strain might be circulating at low levels in Kenya, but further surveillance for DENV-1 in other regions of Kenya and Africa is needed.

DENV-2 has been reported as the predominant serotype circulating in Africa (2). One study participant from coastal Kenya in June 2017 was infected with DENV-2 genotype IV, which clustered with previously reported DENV-2 sequences from Africa. However, 9 study samples from 2015 and 2016 clustered in genotype I and were related to sequences from China isolated during 2015 and Nepal during 2013. Commercial trade between Asia and Kenya has increased in recent years, and further sampling is needed to examine the role of such ties in the importation of dengue virus (21).

Several samples from western Kenya isolated during 2015 cluster in a DENV-3 lineage (genotype V, first documented in the Philippines in 1956). Samples from this lineage have been reported only rarely over the years, most recently in 2004 when they were recovered from human cases in Brazil (22). DENV-3 outbreaks and disease in returning travelers have been reported in Africa occurring within the genotype III (Indian) lineage, including the 2011 Mandera and 2013 coastal Kenya outbreaks (13,23). Observation of DENV-3 genotype V might indicate strains with low-level circulation endemically in eastern Africa or arrival by importation.

Of the 4 DENV serotypes, DENV-4 has been the least documented in Africa. During 2016, we documented a DENV-4 cluster in samples from western Kenya and in 1 sample from coastal Kenya. These serotypes group together in genotype II (Indonesia) in which related sequences come from the Americas and Asia. The recovery of DENV-4 sequences in our study was unexpected, in light of the paucity of DENV-4 documentation on the continent. Importation might be driver of dengue circulation in Kenya, but a clear source of DENV-4 introduction was not identified in this study. The findings suggest active DENV-4 circulation in eastern Africa for which robust surveillance is needed.

Human movement by modern transportation is a critical behavioral component underlying dengue cir-

culation (24,25). The current study raises the possibility that dengue circulation in Africa might be driven by importations of disease, rather than by endemic strains. The similarity of some study samples to those of studies from Asia and Southeast Asia could also reflect movement along trade routes. Further sampling in Africa is required to unravel how the study isolates fit within the global circulation of DENV genotypes and to delineate the role of human movement in dengue transmission.

We document DENV circulation in Kenya over a 4-year period interspersed with small outbreaks as described (17). This pattern of disease is not consistent with large-scale dengue outbreaks flanked by long periods of disease quiescence as described in some settings (26). Whether underlying host susceptibility and host dengue viremia determine such patterns is an interesting avenue for further study, especially since persons of African ancestry might be less susceptible to dengue (27,28). Primary DENV infections comprised most of our samples, but interpretation is limited because our study was not representative of the general population.

Although there is no question that DENV circulates in Kenya, it is worth noting that the level of dengue we detected was surprisingly high. In addition, the number of concomitant serotype infections was also high and unexpected. The high percentage of dengue we document in febrile samples could be the result of the highly sensitive rRT-PCR used in this study (16). Another consideration is that RNA extraction was performed on whole blood as opposed to serum. In a study of hospitalized patients, when serum was compared with whole blood for rRT-PCR testing, whole blood yielded higher levels of dengue viremia and increased the detectable viremic window to 9 days (29). Testing of whole blood might have enabled detection of low-level viremia that would otherwise have not been detected in serum or plasma samples.

Half of the study participants who had dengue viremia also had malaria parasitemia. Some participants might have had fevers driven by malaria infection with asymptomatic dengue, and others had dengue plus asymptomatic malaria (30). This distinction is essential because asymptomatic dengue infections provide a major reservoir for human-to-mosquito dengue transmission (19). The higher rates of antimalarial and antimicrobial drug prescriptions for dengue viremic participants suggest more severe disease in this group and supports dengue as the driver of acute illness.

Our results confirm results of previous studies that showed overtreatment and diagnosis of malar-
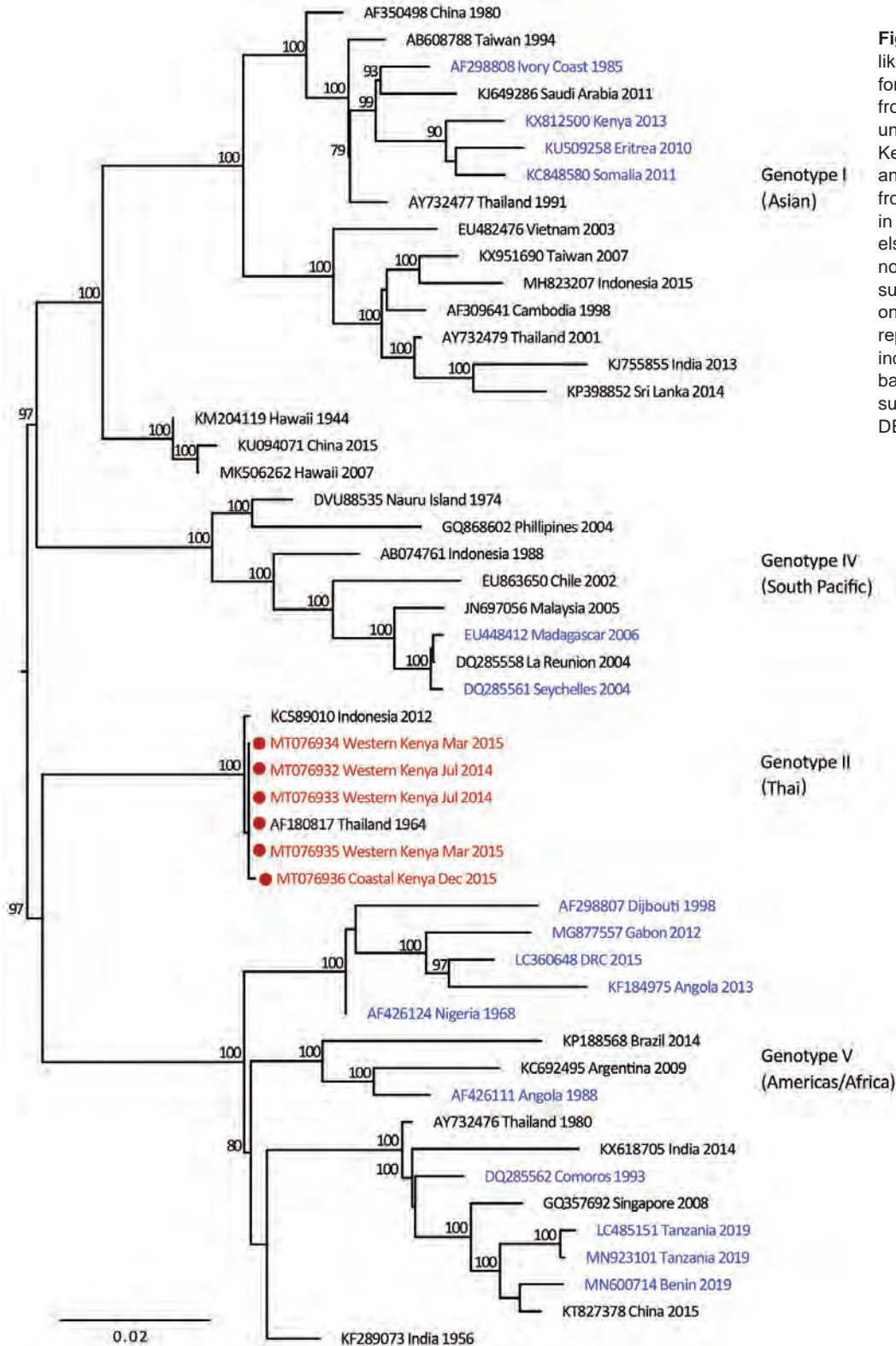
Figure 6. Maximum-likelihood phylogenetic tree for DENV-3 sequences from children with undifferentiated fever in Kenya, 2014–2017 (red), and reference sequences from other locations in Africa (blue) and elsewhere. Numbers at nodes represent bootstrap support values based on maximum-likelihood replicates. Genotypes are indicated at right. Scale bar indicates nucleotide substitutions per site. DENV, dengue virus.

ia parasitemia (*31,32*). Persons with dengue symptoms should receive antibacterial and antimalarial therapies in the absence of point-of-care diagnostics for dengue. The similar clinical manifestations for persons with and without dengue also make treatment decisions difficult. Antimicrobial drug use for undifferentiated fever is a common practice, given challenges in ensuring close follow-up, expectations for prescriptions, and practice norms in developing countries. The consequences of untreated bacterial infections can be fatal because of limited access to care, but development of drug resistance and treatment for

adverse effects must also be considered. Dedicated investments to develop a reliable dengue point-of-care diagnostic is urgently needed.

There are several limitations to this study. First, participants recruited were outpatients who had undifferentiated febrile illness and did not represent the general population. Studies designed to estimate dengue disease incidence and how febrile illness surveys can be extrapolated to estimate incidence are lacking. Sample testing by PCR occurred inconsistently throughout the study because of logistical considerations (availability of electricity, reliable

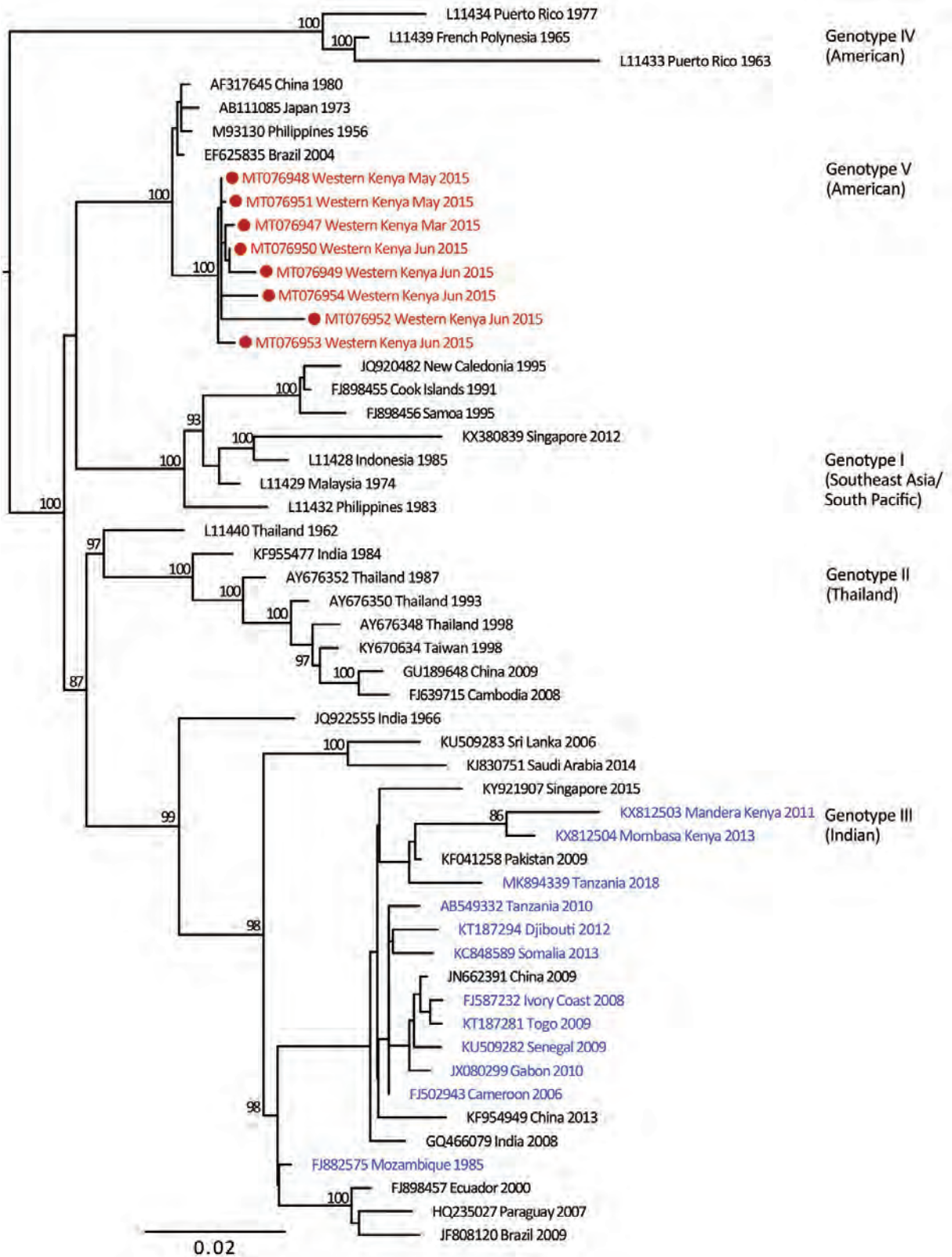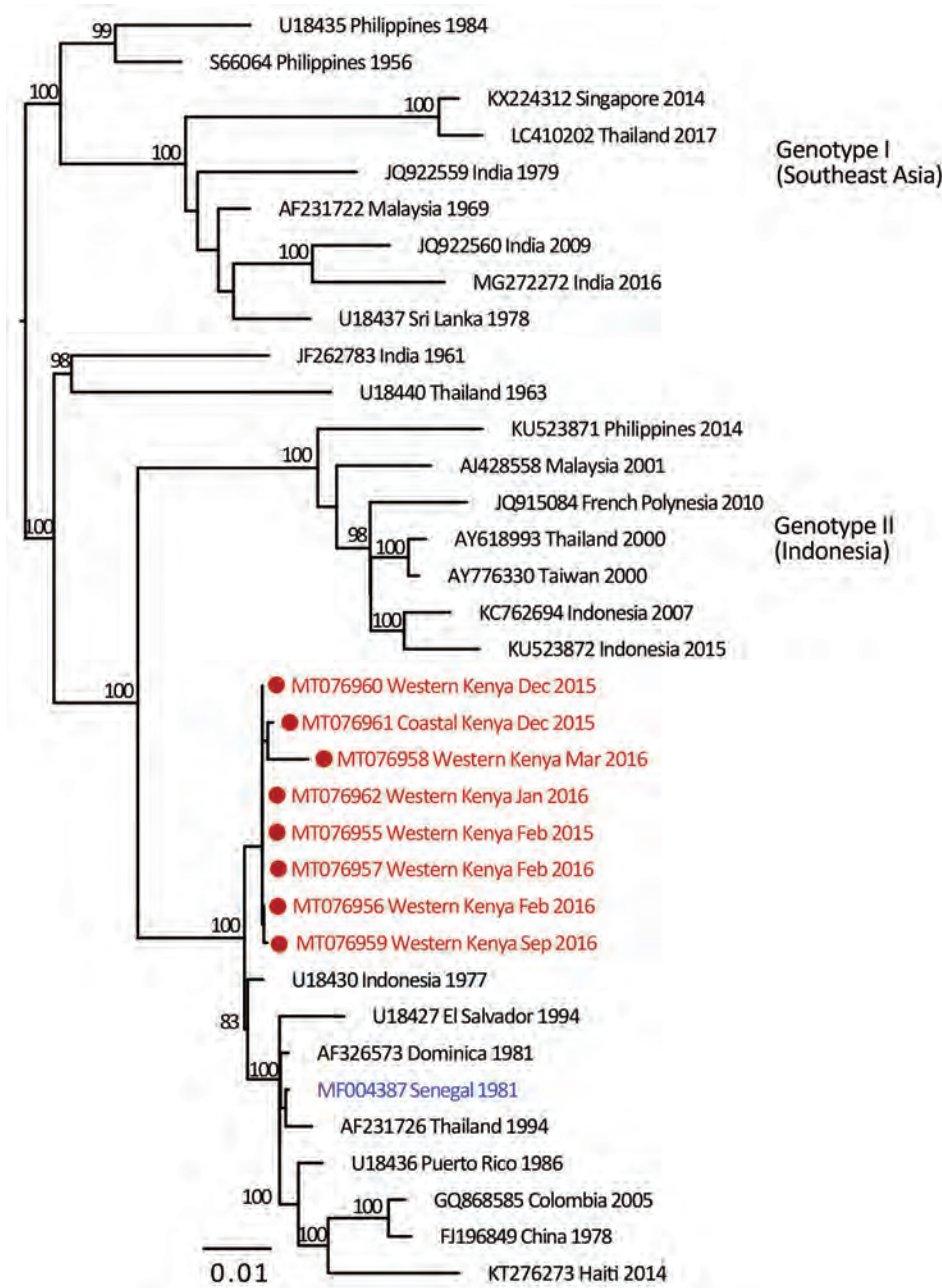**Figure 7.** Maximum-likelihood phylogenetic tree for DENV-4 sequences from children with undifferentiated fever in Kenya, 2014–2017 (red), and reference sequences from other locations in Africa (blue) and elsewhere. Numbers at nodes represent bootstrap support values based on maximum-likelihood replicates. Genotypes are indicated at right. Scale bar indicates nucleotide substitutions per site. DENV, dengue virus.

transportation, access to laboratory equipment, strikes among healthcare workers), and the possibility of sampling bias exists. In addition, a proportion of total samples failed quality control measures because of suboptimal handling of specimens, inefficient nucleic acid extraction, or the presence of inhibitors in the PCR. This study cannot detangle the role of malaria versus dengue in symptomatic illness. Given the descriptive focus of this study, the clinical and statistical interpretation is limited, and further studies are needed to account for confounding and effect modification.

Our study provides insights into the phylogeny of DENV serotypes in eastern Africa and raises many more unanswered questions and avenues for further research. Phylogenetic analysis of circulating DENVs is crucial to clarifying movement of dengue into and throughout Africa. Viral movement will help identify dengue hotspots and ultimately provide clearer targets for prevention efforts. In addition, serotype circulation to the level of genotype is needed for assessing and predicting the efficacy of dengue vaccines. The paucity of dengue surveillance studies and sequence data from Africa is striking. Dengue activity will likely continue to spread in Africa because of rapid land use change, climate change, urbanization, increased human travel, and international trade (*33*). Knowledge of the spatial–temporal dynamics of dengue circulation throughout Africa is critically needed to inform a coordinated public health response in an increasingly interconnected world.

About the Author

Dr. Shah is a postdoctoral researcher and infectious diseases fellow in the laboratory of A. Desiree LaBeaud, at Stanford University, Stanford, CA. Her research interests focus on how human movement and environmental conditions impact arbovirus disease transmission.

References

1. Wilson ME, Chen LH. Dengue: update on epidemiology. Curr Infect Dis Rep. 2015;17:457. https://doi.org/10.1007/s11908-014-0457-2
2. Amarasinghe A, Kuritsk JN, Letson GW, Margolis HS. Dengue virus infection in Africa. Emerg Infect Dis. 2011;17:1349–54.
3. Kraemer MU, Sinka ME, Duda KA, Mylne AQ, Shearer FM, Barker CM, et al. The global distribution of the arbovirus

vectors *Aedes aegypti* and *Ae. albopictus*. eLife. 2015;4:e08347. https://doi.org/10.7554/eLife.08347
4. Paupy C, Ollomo B, Kamgang B, Moutailler S, Rousset D, Demanou M, et al. Comparative role of *Aedes albopictus* and *Aedes aegypti* in the emergence of dengue and chikungunya in central Africa. Vector Borne Zoonotic Dis. 2010;10:259–66. https://doi.org/10.1089/vbz.2009.0005
5. Lanciotti RS, Gubler DJ, Trent DW. Molecular evolution and phylogeny of dengue-4 viruses. J Gen Virol. 1997;78:2279–84. https://doi.org/10.1099/0022-1317-78-9-2279
6. Lewis JA, Chang G-J, Lanciotti RS, Kinney RM, Mayer LW, Trent DW. Phylogenetic relationships of dengue-2 viruses. Virology. 1993;197:216–24. https://doi.org/10.1006/viro.1993.1582
7. Wang E, Ni H, Xu R, Barrett AD, Watowich SJ, Gubler DJ, et al. Evolutionary relationships of endemic/epidemic and sylvatic dengue viruses. J Virol. 2000;74:3227–34. https://doi.org/10.1128/JVI.74.7.3227-3234.2000
8. Carey DE, Causey OR, Reddy S, Cooke AR. Dengue viruses from febrile patients in Nigeria, 1964–68. Lancet. 1971;1:105–6. https://doi.org/10.1016/S0140-6736(71)90840-3
9. Gubler DJ, Sather GE, Kuno G, Cabral JR. Dengue 3 virus transmission in Africa. Am J Trop Med Hyg. 1986;35:1280–4. https://doi.org/10.4269/ajtmh.1986.35.1280
10. Saluzzo JF, Cornet M, Castagnet P, Rey C, Digoutte JP. Isolation of dengue 2 and dengue 4 viruses from patients in Senegal. Trans R Soc Trop Med Hyg. 1986;80:5. https://doi.org/10.1016/0035-9203(86)90182-3
11. Johnson BK, Musoke S, Ocheng D, Gichogo A, Rees PH. Dengue-2 virus in Kenya. Lancet. 1982;320:208–9. https://doi.org/10.1016/S0140-6736(82)91047-9
12. Obonyo M, Fidhow A, Ofula V. Investigation of laboratory confirmed dengue outbreak in north-eastern Kenya, 2011. PLoS One. 2018;13:e0198556. https://doi.org/10.1371/journal.pone.0198556
13. Konongoi L, Ofula V, Nyunja A, Owaka S, Koka H, Makio A, et al. Detection of dengue virus serotypes 1, 2 and 3 in selected regions of Kenya: 2011–2014. Virol J. 2016;13:182. https://doi.org/10.1186/s12985-016-0641-0
14. Harris PA, Taylor R, Thielke R, Payne J, Gonzalez N, Conde JG. Research electronic data capture (REDCap): a metadata-driven methodology and workflow process for providing translational research informatics support. J Biomed Inform. 2009;42:377–81. https://doi.org/10.1016/j.jbi.2008.08.010
15. Waggoner JJ, Abeynayake J, Sahoo MK, Gresh L, Tellez Y, Gonzalez K, et al. Comparison of the FDA-approved CDC DENV-1-4 real-time reverse transcription-PCR with a laboratory-developed assay for dengue virus detection and serotyping. J Clin Microbiol. 2013;51:3418–20. https://doi.org/10.1128/JCM.01359-13
16. Waggoner JJ, Gresh L, Mohamed-Hadley A, Ballesteros G, Davila MJ, Tellez Y, et al. Single-reaction multiplex reverse transcription PCR for detection of Zika, chikungunya, and dengue viruses. Emerg Infect Dis. 2016;22:1295–7. https://doi.org/10.3201/eid2207.160326
17. Hortion J, Mutuku FM, Eyherabide AL, Vu DM, Boothroyd DB, Grossi-Soyster EN, et al. Acute flavivirus and alphavirus infections among children in two different areas of Kenya, 2015. Am J Trop Med Hyg. 2019;100:170–3. https://doi.org/10.4269/ajtmh.18-0297
18. Vu DM, Mutai N, Heath CJ, Vulule JM, Mutuku FM, Ndenga BA, et al. Unrecognized dengue virus infections in children, western Kenya, 2014–2015. Emerg Infect Dis. 2017;23:1915–7. https://doi.org/10.3201/eid2311.170807

19. Bhatt S, Gething PW, Brady OJ, Messina JP, Farlow AW, Moyes CL, et al. The global distribution and burden of dengue. Nature. 2013;496:504–7. https://doi.org/10.1038/nature12060

20. Fahri S, Yohan B, Trimarsanto H, Sayono S, Hadisaputro S, Dharmana E, et al. Molecular surveillance of dengue in Semarang, Indonesia revealed the circulation of an old genotype of dengue virus serotype-1. PLoS Negl Trop Dis. 2013;7:e2354. https://doi.org/10.1371/journal.pntd.0002354

21. Busse M, Erdogan C, Mühlen H. China's impact on Africa: the role of trade, FDI and aid. Kyklos. 2016;69:228–62. https://doi.org/10.1111/kykl.12110

22. Araújo JM, Bello G, Schatzmayr HG, Santos FB, Nogueira RM, Araújo JM, et al. Dengue virus type 3 in Brazil: a phylogenetic perspective. Mem Inst Oswaldo Cruz. 2009;104:526–9. https://doi.org/10.1590/S0074-02762009000300021

23. Franco L, Di Caro A, Carletti F, Vapalahti O, Renaudat C, Zeller H, et al. Recent expansion of dengue virus serotype 3 in west Africa. Euro Surveill. 2010;15:19490.

24. Sessions OM, Khan K, Hou Y, Meltzer E, Quam M, Schwartz E, et al. Exploring the origin and potential for spread of the 2013 dengue outbreak in Luanda, Angola. Glob Health Action. 2013;6:21822. https://doi.org/10.3402/gha.v6i0.21822

25. Adams B, Kapan DD. Man bites mosquito: understanding the contribution of human movement to vector-borne disease dynamics. PLoS One. 2009;4:e6763. https://doi.org/10.1371/journal.pone.0006763

26. Stewart-Ibarra AM, Lowe R. Climate and non-climate drivers of dengue epidemics in southern coastal ecuador. Am J Trop Med Hyg. 2013;88:971–81. https://doi.org/10.4269/ajtmh.12-0478

27. Chacón-Duque JC, Adhikari K, Avendaño E, Campo O, Ramirez R, Rojas W, et al. African genetic ancestry is associated with a protective effect on dengue severity in Colombian populations. Infect Genet Evol. 2014;27:89–95. https://doi.org/10.1016/j.meegid.2014.07.003

28. Xavier-Carvalho C, Cardoso CC, de Souza Kehdy F, Pacheco AG, Moraes MO. Host genetics and dengue fever. Infect Genet Evol. 2017;56:99–110. https://doi.org/10.1016/j.meegid.2017.11.009

29. Klungthong C, Gibbons RV, Thaisomboonsuk B, Nisalak A, Kalayanarooj S, Thirawuth V, et al. Dengue virus detection using whole blood for reverse transcriptase PCR and virus isolation. J Clin Microbiol. 2007;45:2480–5. https://doi.org/10.1128/JCM.00305-07

30. Sow A, Loucoubar C, Diallo D, Faye O, Ndiaye Y, Senghor CS, et al. Concurrent malaria and arbovirus infections in Kedougou, southeastern Senegal. Malar J. 2016;15:47. https://doi.org/10.1186/s12936-016-1100-5

31. Reyburn H, Mbatia R, Drakeley C, Carneiro I, Mwakasungula E, Mwerinde O, et al. Overdiagnosis of malaria in patients with severe febrile illness in Tanzania: a prospective study. BMJ. 2004;329:1212. https://doi.org/10.1136/bmj.38251.658229.55

32. Hooft AM, Ripp K, Ndenga B, Mutuku F, Vu D, Baltzell K, et al. Principles, practices and knowledge of clinicians when assessing febrile children: a qualitative study in Kenya. Malar J. 2017;16:381. https://doi.org/10.1186/s12936-017-2021-7

33. Messina JP, Brady OJ, Golding N, Kraemer MU, Wint GR, Ray SE, et al. The current and future global distribution and population at risk of dengue. Nat Microbiol. 2019;4:1508–15. https://doi.org/10.1038/s41564-019-0476-8

Address for correspondence: Melisa M. Shah, Stanford University, Lane Bldg, Ste 134, 300 Pasteur Dr, Stanford, CA 94305-5107, USA; email: melisas@stanford.edu or melisa.shah@gmail.com

Systematic Review and Meta-Analyses of Incidence for Group B *Streptococcus* Disease in Infants and Antimicrobial Resistance, China

Yijun Ding, Yajuan Wang, Yingfen Hsia, Neal Russell, Paul T. Heath

We performed a systematic review and meta-analysis of the incidence, case-fatality rate (CFR), isolate antimicrobial resistance patterns, and serotype and sequence type distributions for invasive group B *Streptococcus* (GBS) disease in infants <1–89 days of age in China. We searched the PubMed/Medline, Embase, Wanfang, and China National Knowledge Infrastructure databases for research published during January 1, 2000–March 16, 2018, and identified 64 studies. Quality of included studies was assessed by using Cochrane tools. Incidence and CFR were estimated by using random-effects meta-analyses. Overall incidence was 0.55 (95% CI 0.35–0.74) cases/1,000 live births, and the CFR was 5% (95% CI 3%–6%). Incidence of GBS in young infants in China was higher than the estimated global incidence (0.49 cases/1,000 live births) and higher than previous estimates for Asia (0.3 cases/1,000 live births). Our findings suggest that implementation of additional GBS prevention efforts in China, including maternal vaccination, could be beneficial.

Group B *Streptococcus* (GBS; *Streptococcus agalactiae*) is a major cause of illness and death in young infants worldwide (*1–3*). A recent systematic review reported the global incidence to be 0.49 cases/1,000 live births (*4*). It is estimated that this incidence results in ≈90,000 deaths (uncertainty death range 36,000–169,000) in infants every year (*5*). Furthermore, ≈32% of infants who survive GBS meningitis have neurodevelopmental impairment 18 months after illness, including 18% who

have moderate-to-severe neurodevelopmental impairment (*6*). GBS is also a major cause of preterm delivery, stillbirths, and puerperal sepsis (*5,7*).

Screening pregnant women for GBS and offering intrapartum antimicrobial drug prophylaxis (IAP) to those who are found to be colonized, or have risk factors, has been widely implemented in many countries (*8*). However, the increased use of antimicrobial drugs has raised concerns regarding the emergence of resistance (*9*). Clindamycin and erythromycin resistance rates have increased greatly in the past 20 years (*10*) but might vary by geographic location (*10,11*). Knowledge of local antimicrobial drug resistance of GBS strains can contribute to optimal prophylactic and treatment strategies.

On the basis of the polysaccharide capsule, GBS strains are classified into 10 serotypes (*12*). A global review showed that serotype III was the most frequent isolate from infants who had invasive disease (*4*). Serotyping is of particular relevance to GBS vaccine development because most current candidates include serotype-specific polysaccharide–protein conjugate vaccines (*13*). An effective vaccine will need to prevent most infant disease, avoid the limitations of IAP, and cost-effective. Therefore, knowledge of prevalent serotypes will be relevant to country-specific decisions for vaccine implementation.

Evidence regarding the burden of invasive GBS disease in infants in China is limited. The recent systematic review found only 5 studies from China and estimated an incidence of 0.42 cases/1,000 live births for eastern Asia (*4*). This review was limited because it did not include publications in Mandarin Chinese and might not provide an accurate estimate of the burden of GBS disease in China. Therefore, we performed a systematic review and meta-analysis on

Author affiliations: Department of Neonatology, Beijing Children's Hospital, Capital Medical University, National Center for Children's Health, Beijing, China (Y. Ding, Y. Wang); Paediatric Infectious Diseases Research Group & Vaccine Institute, St. George's, University of London, London, UK (Y. Hsia, N. Russell, Paul T. Heath); Queen's University Belfast, Belfast, Northern Ireland, UK (Y. Hsia)

the incidence, case-fatality rate (CFR), isolate antimicrobial resistance (AMR) patterns, and serotype and sequence type distributions for invasive GBS disease cases in infants <1–89 days of age in China.

Methods

This systematic review was reported according to the Preferred Reporting Items for Systematic Reviews and Meta-Analyses guidelines (14). We focused on infants <1–89 days of age who had invasive GBS disease. We included studies that reported incidence and deaths associated with invasive disease, and antimicrobial drug resistance, serotypes, and multilocus sequence typing (MLST) of GBS isolates. Eligible studies were those published during January 1, 2000–March 16, 2018. The geographic scope of analysis was limited to China and included Taiwan, Hong Kong, and Macau.

Definitions

Invasive GBS disease was defined as a positive GBS culture from any normally sterile site accompanied with signs of clinical disease. Early onset of GBS (EO-GBS) was defined as isolation of GBS from infants ≤1–6 days after birth, and late onset of GBS (LOGBS) was defined as isolation of GBS from infants 7–89 days after birth. Incidence was defined as cases/1,000 live births (invasive GBS disease cases divided by live births at the respective hospital). CFR was defined as number of fatal GBS cases divided by total number of GBS cases. We categorized studies as prospective (data collected for the infant at admission and in hospital) and retrospective (data collected after the infant was discharged from a hospital).

In mainland China, hospitals were classified as primary, secondary, or tertiary institutions. A primary hospital is typically a township hospital that has <100 beds. These hospitals are tasked with providing preventive care, minimal healthcare, and rehabilitation services. Secondary hospitals tend to be affiliated with a medium-size city, county, or district and have >100 but <500 beds. These hospitals are responsible for providing comprehensive health services, as well as medical education and conducting research on a regional basis. Tertiary hospitals are comprehensive or general hospitals at the city, provincial, or national level that have >500 beds. These hospitals provide specialist health services, perform a larger role with regard to medical education and scientific research, and serve as medical hubs providing care to multiple regions.

Search Strategy and Selection Criteria

We searched the PubMed/Medline, Embase, China National Knowledge Infrastructure, and Wanfang med online databases for literature published during January 1, 2000–March 16, 2018. We used the search terms "Streptococcus Group B" or "Group B streptococcal" OR "Streptococcus agalactiae" (medical subject headings) AND "infant," "outcome," "death," "mortality," "case AND fatality AND rate" for English databases. We used search terms "Group B streptococcal" OR "Streptococcus agalactiae" OR "GBS" AND "infant" OR "neonatal" in Chinese for Chinese databases. We limited searches to China, including Taiwan, Hong Kong, and Macau. An additional search for serotype data used the search terms "Streptococcus Group B serotype" or "Group B streptococcal serotype" OR "Streptococcus agalactiae serotype" (medical subject headings) and was performed with the same limits as listed above. We provide the full search strategy (Appendix Tables 1, 2, https://wwwnc.cdc.gov/EID/article/26/11/18-1414-App1.pdf).

We used snowball searches of article reference lists, including reviews, to identify additional studies. Two independent reviewers (Y.D. and Y.H.) critically appraised each paper and discussed discrepancies with a third coauthor (P.H.). We screened titles and abstracts according to specified inclusion and exclusion criteria, and then selected the full texts, followed by the details as described below.

Inclusion and Exclusion Criteria

We included studies with original data on GBS invasive disease in infants <1–89 days of age, which had a population denominator (as the total number of live births at the respective hospital), CFR, serotype, or AMR. We provide full details of inclusion and exclusion criteria (Appendix Table 3).

Data Abstraction and Quality Assessment

Isolates obtained from all normally sterile sites (blood, cerebrospinal fluid [CSF], lung aspirate, and joint specimens) were included for incidence estimates. For AMR, serotype, and MLST data, only isolates obtained from blood or CSF cultures were included. The quality of included studies was assessed in accordance with the Cochrane Handbook (15), including 9 items considered essential for good reporting of prevalence studies. Two independent reviewers (Y.D. and Y.H.) critically appraised each study. Disagreements were resolved by discussion with the third reviewer (P.H.).

Statistical Analysis

We performed a meta-analysis by using Stata software version 14.0 (StataCorp, https://www.stata.

com) We estimated overall incidence, EOGBS, LOG-BS incidence, and CFR of GBS with random-effects meta-analyses by using the DerSimonian and Laird method. The Q test was performed to test heterogeneity between studies, and the I^2 was used to assess the degree of variation across studies. The level of heterogeneity was defined as low ($I^2 = 25\%$), moderate ($I^2 = 50\%$), and high ($I^2 = 75\%$) (*15*). When heterogeneity was high, we also performed subgroup analysis based on study design (retrospective and prospective), isolate type (blood, CSF, and all sterile sites), and age of onset (EOGBS and LOGBS). Sensitivity analysis was conduct by excluding studies from Taiwan, Hong Kong, and Macau. As we anticipated, different infectious disease patterns, antimicrobial drug resistance, and healthcare systems in these regions might affect the estimates of GBS incidence and CFR. Potential publication bias was assessed by using a funnel plot and the Egger regression test. Descriptive analysis was performed to investigate the distribution of serotype and MLST typing. Antimicrobial drug resistance rates were reported by median with interquartile intervals.

Results

Literature Search and Study Selection
We identified 704 published studies from database searches (407 from China National Knowledge Infrastructure, 139 from Wanfang, 147 from PubMed, and 9 from Embase). Two additional articles were identified from reference lists. A total of 64 articles met our inclusion criteria and search strategy (Figure 1). A total of 14 articles reported incidence, 56 articles reported CFR, 20 articles reported AMR, 4 articles reported serotype, and 2 articles reported MLST. We provide a full list of articles included (Appendix Table 4) and of articles excluded (Appendix Table 5). We provide the publication years of included studies (Appendix Figure 1).

Study Characteristics
Of the 64 studies included, 55 were from mainland China, 7 from Taiwan, 1 from Hong Kong, and 1 from Macau. On the basis of economic divisions, 92.2% (59/64) of studies were from eastern China, 2 each were from western and central China, and 1 was
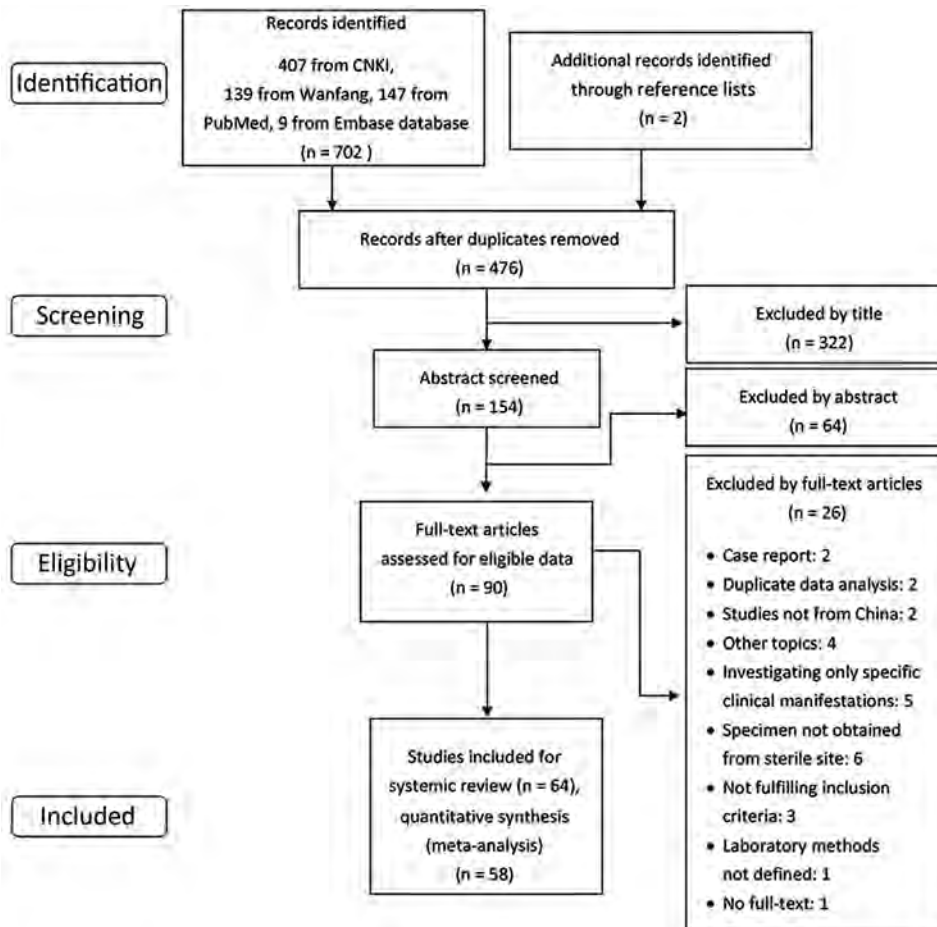
Figure 1. Process of study selection of systematic review and meta-analyses of incidence of group B *Streptococcus* disease in infants and antimicrobial resistance, China. CNKI, China National Knowledge Infrastructure.

from northeastern China. Among the 55 articles from mainland China, 45 were from tertiary hospitals, 9 from secondary hospitals, and 1 from a primary hospital. The 7 articles from Taiwan and the 1 article from Hong Kong were all from teaching hospitals, and the 1 article from Macau was from a general hospital. We provide the distribution of studies of invasive GBS disease reported in China by province (Figure 2).

Among the 14 studies reporting incidence, 13 were from eastern China, and 1 from western China. Six (42.9%) of 14 papers reported use of IAP, all from eastern China; 3 (50%) of 6 IAPs were based on screening. Of the 56 studies that reported CFRs, 52 articles were from eastern China and 2 each were from central and western China. A total of 20 studies reported AMR, 19 papers from eastern China and

1 from northeastern China. Serotypes were available from 4 studies, all of them from eastern China. Only 2 articles included data on MLST. We provide characteristics of included studies and outcome types (Table 1). We also provide the risk for bias of the studies (Appendix Figure 2).

Incidence of Invasive GBS Disease

Of the 14 relevant studies, 13 reported raw data on live births, which enabled a meta-analysis to be performed. Of 424,463 live births, 244 infants had invasive GBS disease at the age of 0–89 days; the pooled estimated incidence was 0.55 cases/1,000 live births (95% CI 0.35–0.74 case/1,000 live births). Significant heterogeneity was observed (p = 0.0001, I^2 = 85.4%) (Figure 3). Subgroup analyses were conducted to

Figure 2. Distribution of study locations in systematic review and meta-analyses of incidence of invasive group B *Streptococcus* disease, by province, China.
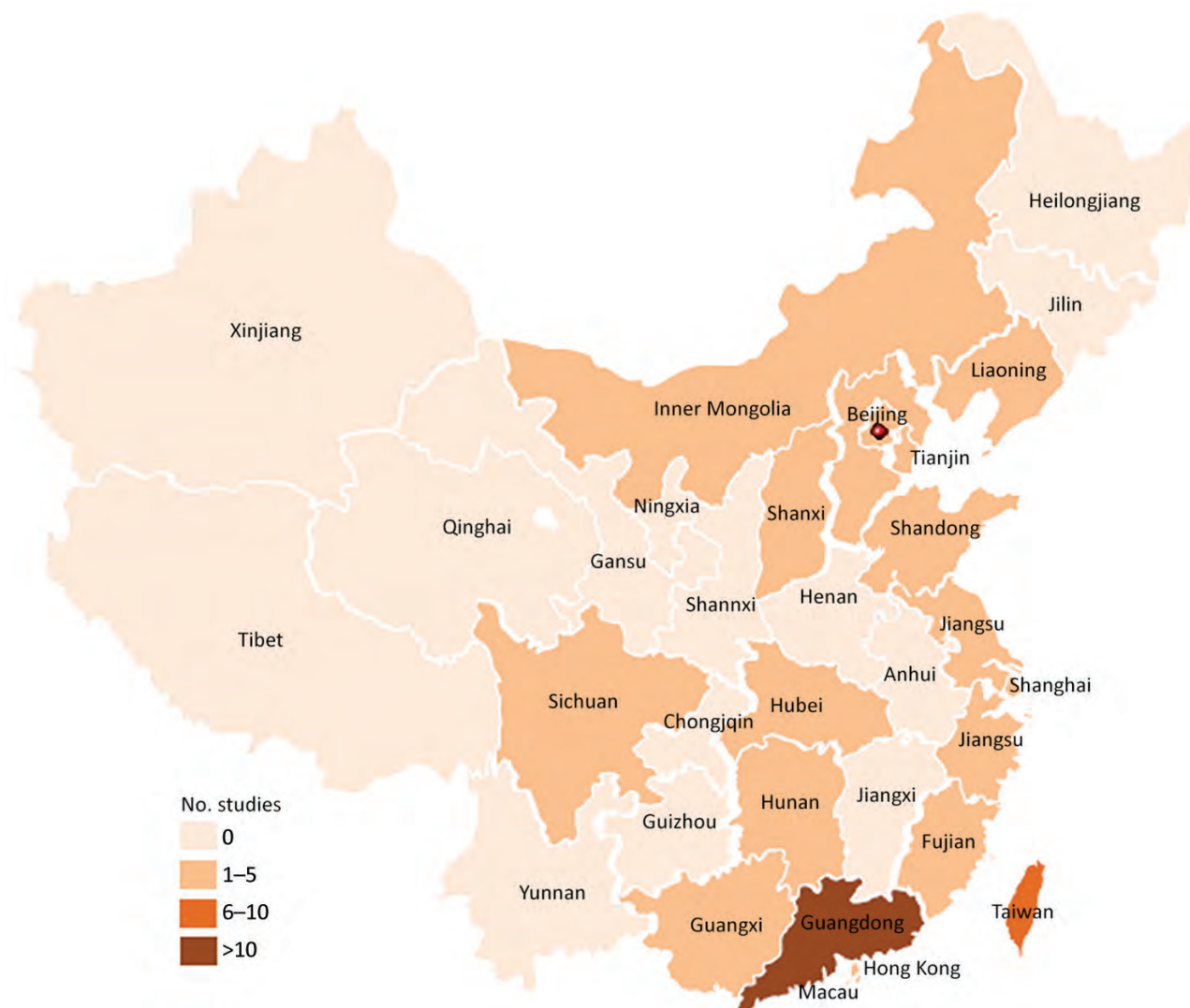
Table 1. Characteristics of included studies and outcome types for systematic review and meta-analyses of incidence of group B *Streptococcus* disease in infants, China*

Characteristic	Total, 64	Type and no. studies Incidence, 14	CFR, 56	AMR, 20	Serotypes, 4	MLST, 2
China						
Eastern	59	13	52	19	4	2
Central	2	0	2	0	0	0
Western	2	1	2	0	0	0
Northeastern	1	0	0	1	0	0
Hospital type						
Mainland China						
Tertiary	45	6	39	18	4	2
Secondary	9	3	9	2	0	0
Primary	1	0	1	0	0	0
Nonmainland China						0
Teaching	8	4	7	0	0	0
General	1	1	0	0	0	0
Study design						
Prospective	4	3	3	0	1	1
Retrospective	60	11	53	20	3	1
Reporting period, days						
Full, 0–89	53	11	46	16	4	2
Full EOGBS <1–6	7	3	6	2	0	0
Full LOGBS 7–89	4	0	4	2	0	0
Specimen type						
Blood only	25	5	18	8	2	0
CSF only	6	0	6	3	0	0
Blood and CSF	23	6	22	9	2	2
All sterile sites	4	3	3	0	0	0
Blood and CSF plus sputum or gastric fluid	6	0	7	0	0	0
IAP						
Any	10	6	9	3	1	1
None	4	0	3	2	0	0
Unknown	50	8	44	15	3	1

*AMR, antimicrobial resistance; CFR, case-fatality rate; CSF, cerebrospinal fluid; EOGBS, early onset group B *Streptococcus*; IAP, intrapartum antimicrobial drug prophylaxis; MLST, multilocus sequence typing; LOGBS, late onset group B *Streptococcus*.

assess heterogeneity by study design, isolate site, and age of onset. Among the 13 studies reporting raw data on live births, 11 studies distinguished early-onset and late-onset cases (n = 3 studies) born in a hospital. There were 133 cases of EOGBS for 352,574 live births, an incidence of 0.38 cases/1,000 live births (95% CI 0.25–0.51 cases/1,000 live births), and 33 cases of LOGBS for 168,849 live births, an incidence of 0.18 cases/1,000 live births (95% CI 0.11–0.25 cases/1,000 live births).We provide results of meta-analysis for LOGBS incidence (Appendix Figure 3), for EOGBA incidence (Appendix Figure 4), and for subgroup analyses (Appendix Table 6).

Sensitivity analysis was conducted to confirm the stability and liability of the meta-analysis by excluding data for Taiwan, Hong Kong, and Macau. This exclusion resulted in a pooled incidence of invasive GBS disease of 0.44 cases/1,000 live births (95% CI 0.25–0.63 cases/1,000 live births) for mainland China (Appendix Figure 5). According to the funnel plot and p value of the Eggers regression test (p = 0.069 [>0.05]), there was no visually apparent publication bias of included studies (Appendix Figure 6).

CFRs for GBS Invasive Disease

A total of 56 papers reported CFR data for infants <1–89 days of age. Of 1,439 infants with GBS invasive disease, 106 died. The overall pooled estimated CFR rate was 5.0% (95% CI 3.0%–6.0%). The EOGBS CFR was 6.0% (4.0%–8.0%), and LOGBS CFR was 4.0% (1.0%–6.0%). We provide results of meta-analysis for overall, EOGBS, and LOGBS CFRs (Appendix Figures 7, 8, and 9, respectively). Sensitivity analysis was conducted to confirm the stability and liability of the meta-analysis by including only studies from mainland China. The pooled estimated CFR was 4.0% (95% CI 2%.0%–6.0%) when data for only mainland China were included (Appendix Figure 5).

Antimicrobial Resistance

A total of 20 articles reported antimicrobial resistance for 598 GBS isolates. The highest prevalence of resistance was reported for tetracycline (median 98.0%, interquartile range [IQR] 80.0%–100%), followed by clindamycin (73.3%m IQR 62.6%–78.7%), erythromycin (64.4%, IQR 56.6%–75%), and ciprofloxacin (25.0%, IQR 9.1%–35.2%). There was no reported resistance to penicillin, ampicillin, vancomycin, or linezolid. For
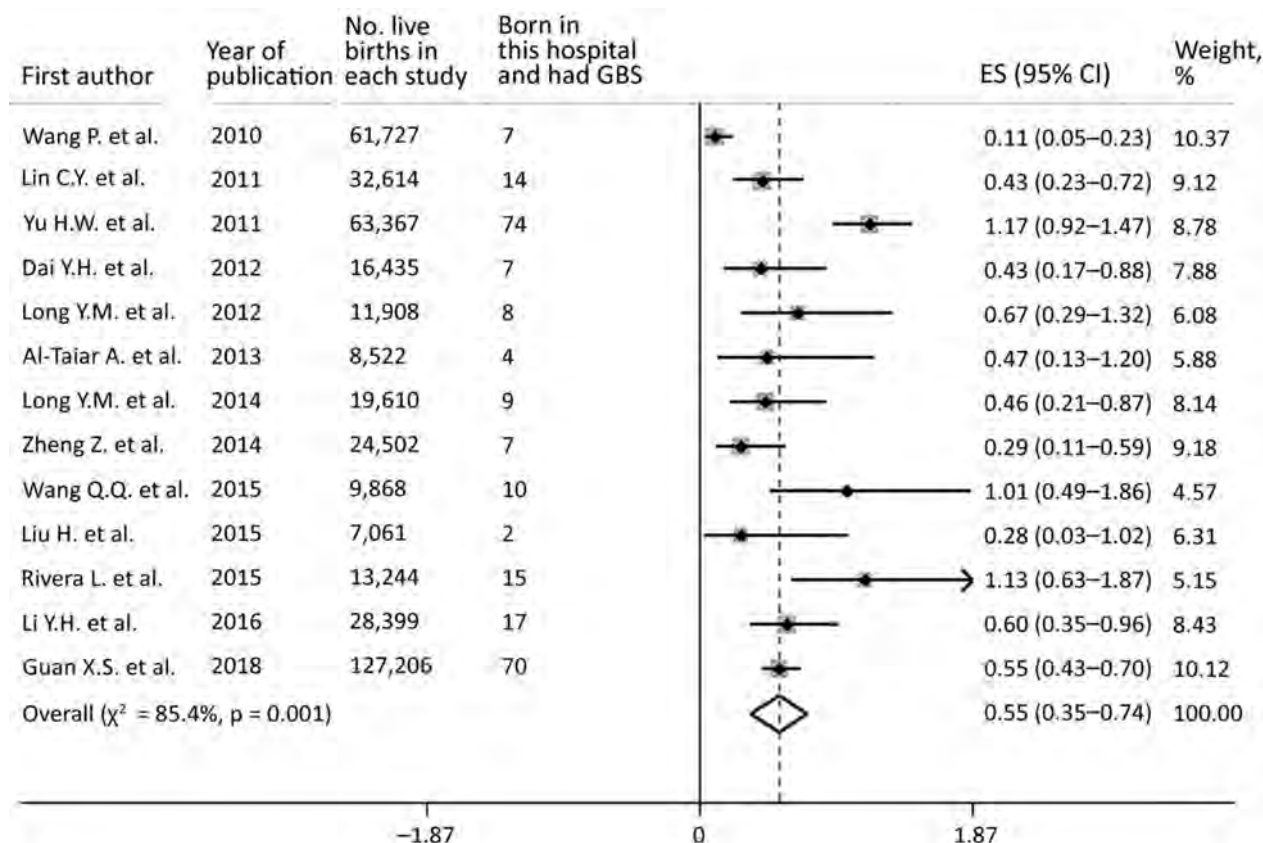
Figure 3. Overall incidence risk per 1,000 live births of invasive GBS disease in 13 infants <1–89 days of age, China. Vertical dashed line indicates a visual assessment of heterogeneity of the studies. If the vertical line can be drawn, forest plots indicate that all studies are similar enough to be included for meta-analysis. Error bars indicate 95% CIs. Reference details are provided in the Appendix (https://wwwnc.cdc.gov/EID/26/11/18-1414-App1.pdf). ES, effect size; GBS, group B *Streptococcus* disease.

ceftriaxone, the median prevalence of resistance was 0% (IQR 0%–60.0%), although 1 study reported 100% prevalence of resistance (1/1 isolates), and 1 study reported 80% resistance (12/15 isolates) (Table 2).

Serotype Distribution

Four studies included data on serotypes for 175 invasive GBS cases. All of these studies were from eastern China. Four serotypes (Ia, Ib, III, and V) accounted for 97% of invasive isolates. Serotype III was the most common (65%, 114/175), followed by Ib (16%, 27/175), Ia (10%, 18/175), and V (6%, 11/175). Two articles distinguished EO and LOGBS serotypes; there were 24 EOGBS isolates and 52 LOGBS isolates. Serotype III predominated in both EO (15/24, 63%) and LOGBS (40/52, 77%) (Appendix Figure 10).

MLST

Only 2 studies reported MLST. Of 76 isolates 15 sequence types (STs) were reported. A total of 89% (68/76) of strains belonged to 6 STs (ST17, ST12, ST23, ST1, ST19, and ST650). More than half (58%, 44/74) of

the samples were ST17, followed by ST12 (9%, 7/76) and ST23 (7%, 5/76); ST1, ST19, and ST650 each accounted for 5% (4/76).

Relationship between Serotype and MLST

Only 2/76 papers included data on serotype and MLST. A total of 80% (44/55) of serotype III strains were shown to be ST17, and 54% (7/13) of serotype Ib strains were ST12 (Appendix Table 7).

Discussion

The annual number of births in China ranged from 15.7 million to 17.8 million between 2001 and 2016 (*16*). Thus, with an estimated pooled incidence of 0.55 cases/1,000 live births (95% CI 0.35–0.74 cases/1,000 live births), there is a substantial burden of invasive GBS disease for infants in China. This incidence is also higher than that for all infants in the recent global review (0.49 cases/1,000 live births, 95% CI 0.43–0.56 cases/1,000 live births) and higher than that previously defined for eastern Asia (0.42 cases/1,000 live births) (*4*). Unlike most industrialized countries,

there are no national guidelines for GBS screening and prevention in China, although in 43% of studies from China, IAP was mentioned. However, there are no data on the extent to which IAP is currently used in China. Previous studies suggest that the low incidence of GBS infection for infants in Asia might be related to a lower rate of GBS colonization in pregnant women (*17*). A review of colonization identified 30 studies from China, which included 44,716 women, and showed an overall colonization rate of 11.3%. However, several studies from China reported much higher rates of GBS colonization (31%–36%) (*18,19*), suggesting substantial variability.

The CFR in our study (5.0%, 95% CI, 3.0%–6.0%) was lower than that estimated from the global review (8.4%, 95% CI 6.6%–10.2%) (*4*). Most of our data were for level-3 teaching hospitals in which use of antimicrobial drugs and standard of medical care might be higher, which might explain a lower mortality rate. We do not have information on birthweight and gestational age of infants with GBS disease with which we can compare with other settings; the CFR for preterm infants is known to be much higher (*1*).

The prevalence of resistance to clindamycin and erythromycin appear to be high in China. A study in Canada showed the prevalence of resistance to clindamycin was 4.5% and to erythromycin was 8% (*9*). In England and Wales, erythromycin resistance

in isolates causing disease in infants was 15% for EO disease and 13% for LO disease (*20*). In South Korea, the prevalence of resistance to erythromycin was 42.9%–51.8% and for clindamycin was 55.4% (*11,21*), suggesting that the prevalence might be much higher in Asia. This finding is consistent with a global systematic review (*22*) of GBS isolates causing colonization that reported a pooled prevalence of resistance of 25% for erythromycin and 27% for clindamycin, and notably higher prevalences in Asia (46% for erythromycin and 47% for clindamycin). A study of colonization of pregnant women in China also reported that most isolates were resistant to tetracycline (76.9%), erythromycin (72.1%) and clindamycin (66.4%) (*23*). Macrolide resistance in streptococci is caused mainly by a macrolide–specific efflux mechanism encoded by the *mef* A gene and ribosomal modification by a methylase associated with *erm* (erythromycin ribosome methylase) genes (*24,25*). Erythromycin resistance was associated mainly with *ermB* and *mef (A/E)* genes in China (*26,27*). The *erm(B)* and *erm(TR/A)* genes were the main macrolide-resistant genes in Spain and Canada (*9,25*), and *erm B* and *lnuB* genes were prevalent in South Korea (*28*).

Resistance to erythromycin and clindamycin presents a challenge for treatment and prophylaxis strategies because these antimicrobial drugs are often used for patients in China who are allergic to penicillin.

Table 2. Proportion of isolates demonstrating antimicrobial resistance in systematic review and meta-analyses of incidence of group B *Streptococcus* disease in infants, China*

Reference	Publication year	No. isolates	PEN	AMP	CFZ	CAX	VAN	LZD	CHL	ERY	TET	CIP	MXF	LVX	NIT	TGC
Zeng et al.	2013	11	0	0	NT	NT	0	0	NT	NT	100.0	9.1	9.1	9.1	0	0
Luo et al.	2013	15	0	0	NT	0	0	NT	NT	86.7	NT	NT	NT	0	NT	NT
Zheng et al.	2014	12	0	0	NT	NT	0	NT	NT	16.7	66.7	NT	NT	NT	NT	NT
Chen et al.	2014	16	0	0	NT	0	0	NT	NT	62.5	NT	25.0	NT	18.8	NT	NT
Zhu et al.	2014	13	0	10.0	0	100.0	38.5	0	100.0	100.0	NT	33.3	NT	8.3	0	NT
Fan et al.	2014	42	0	0	NT	NT	0	0	NT	69.1	73.8	NT	NT	38.1	NT	0
Wang et al.	2015	15	0	20.0	40.0	80.0	0	0	86.7	100.0	NT	26.7	NT	20.0	0	NT
Zhang et al.	2015	6	0	0	83.3	NT	0	0	NT	NT	NT	NT	NT	NT	NT	NT
Lei et al.	2015	20	NT	0	NT	NT	0	0	25.0	75.0	NT	80.0	NT	70.0	0	NT
Zhang et al.	2015	45	0	2.2	NT	NT	0	0	NT	42.2	93.3	0	0	0	NT	0
Cai et al.	2016	15	0	0	NT	NT	0	0	NT	46.7	100.0	NT	6.7	6.7	13.3	0
Zhao	2016	28	0	0	NT	0	0	3.6	NT	67.9	NT	NT	NT	42.9	NT	NT
Huang et al.	2016	49	NT	NT	NT	NT	NT	NT	NT	63.3	98.0	11.9	12.2	7.7	NT	NT
Liu et al.	2017	15	0	NT	NT	NT	0	NT	NT	NT	NT	NT	NT	NT	NT	NT
Zhang et al.	2017	55	0	0	NT	NT	0	0	NT	56.6	98.1	1.9	NT	NT	NT	NT
Zhang et al.	2017	15	6.7	0	NT	NT	0	0	NT	NT	80.0	73.3	73.3	60.0	0	0
Tan et al.	2017	20	0	0	NT	NT	0	0	NT	NT	100.0	16.7	NT	16.7	NT	0
Zhou et al.	2017	84	4.8	2.4	2.4	0	0	0	4.8	72.6	100.0	35.2	NT	36.9	0	NT
Zhao	2017	45	0	NT	NT	0	0	2.2	NT	64.4	NT	NT	NT	42.2	NT	NT
Guan et al.	2018	68	0	NT	NT	0	0	0	NT	57.4	95.6	NT	NT	5.9	NT	NT
Median	NA	NA	0	0	21.2	0	0	0	55.8	64.4	98.0	25.0	9.1	17.7	0	0
IQI 25%	NA	NA	0	0	0.6	0	0	0	9.8	56.6	80.0	9.1	3.3	6.9	0	0
IQI 75%	NA	NA	0	1.7	72.5	60.0	0	0	96.7	75.0	100	35.2	42.8	41.2	0	0

*Values are percentages. Reference details are provided in the Appendix (https://wwwnc.cdc.gov/EID/26/11/18-1414-App1.pdf). Green indicates a rate of AMR <25%; yellow 25%–50%; red >50%; 25%, and 75% refers to AMR interquartile interval of 25% and 75%. Amp, ampicillin; CFZ, cefazolin; CAX, ceftriaxone, CHL, chloramphenicol; CIP, ciprofloxacin; ERY, erythromycin; IQI, interquartile interval; LZD, linezolid; MXF, moxifloxacin; NA, not applicable; NIT, nitrofurantoin; NT, not tested; PEN, penicillin: TET, tetracycline; TGC, tigecycline; VAN, vancomycin.

However, GBS isolates were susceptible to penicillin, ampicillin, vancomycin, and linezolid, consistent with other reports (*9,21,22*). The apparent resistance to ceftriaxone is unusual and, as noted, the sample size for these 2 studies was small. Furthermore, because no details were provided on the methods used for testing the isolates, it is essential that this reported resistance is verified.

The serotype and MLST distribution of invasive GBS disease isolates in China is consistent with the global review (*4*); serotype III and ST17 are the most prevalent types (*21,29*). Therefore, our data suggest that a conjugate vaccine incorporating 5 serotypes (III, Ia, Ib, II, and V) could cover 97% of invasive GBS disease in infants <3 months of age in China.

Currently, there is limited evidence on the burden of GBS disease for infants in China. Our comprehensive review is a major addition to the literature because it includes a systematic review of studies in the Chinese language, as well as data on incidence, antimicrobial drug susceptibility, and MLST types.

There are several potential limitations to this study. First, major heterogeneity among studies was observed. Although potential sources of heterogeneity were explored by subgroup analyses, none of them sufficiently explain the heterogeneity. Sensitivity analysis suggests that the pooled estimated incidence and CFR was changed when Taiwan, Hong Kong, and Macau were excluded. This finding is plausible and might reflect the differences in healthcare systems compared with those of mainland China. Second, we did not search for unpublished studies, which could result in publication bias. Third, we were not able to assess the time of sample collection or the methods of collection, culture, and antimicrobial drug sensitivity testing. Fourth, there were limited data available on serotypes and MLST types; thus, meta-analysis was not possible. Fifth, for CFRs, we were only able to include patients who died in a hospital; thus, the true CFR might be higher.

The estimated burden of infant GBS disease in China is substantial, suggesting that implementation of additional prevention efforts could be beneficial. Interventions to be considered could include a coordinated national strategy for maternal GBS screening with administration of intrapartum antimicrobial drug prophylaxis, and, when available, maternal vaccination with an effective GBS vaccine. Further research to clarify the noted heterogeneity in infant GBS disease in China, as well as research to assess the acceptability, logistics, and cost-effectiveness of maternal GBS vaccination could help guide these efforts.

About the Author

Dr. Ding is a neonatologist at Beijing Children's Hospital, Capital Medical University, National Center for Children's Health, Beijing, China. Her primary research interest is infectious diseases.

References

1. Heath PT, Balfour G, Weisner AM, Efstratiou A, Lamagni TL, Tighe H, et al.; PHLS Group B Streptococcus Working Group. Group B streptococcal disease in UK and Irish infants younger than 90 days. Lancet. 2004;363:292–4. https://doi.org/10.1016/S0140-6736(03)15389-5
2. Sinha A, Russell LB, Tomczyk S, Verani JR, Schrag SJ, Berkley JA, et al.; GBS Vaccine Cost-Effectiveness Analysis in Sub-Saharan Africa Working Group. Disease burden of group B *Streptococcus* among infants in sub-Saharan Africa: a systematic literature review and meta-analysis. Pediatr Infect Dis J. 2016;35:933–42. https://doi.org/10.1097/INF.0000000000001233
3. Rivera L, Sáez-Llorens X, Feris-Iglesias J, Ip M, Saha S, Adrian PV, et al. Incidence and serotype distribution of invasive group B streptococcal disease in young infants: a multi-country observational study. BMC Pediatr. 2015;15:143. https://doi.org/10.1186/s12887-015-0460-2
4. Madrid L, Seale AC, Kohli-Lynch M, Edmond KM, Lawn JE, Heath PT, et al.; Infant GBS Disease Investigator Group. Infant group B streptococcal disease incidence and serotypes worldwide: systematic review and meta-analyses. Clin Infect Dis. 2017;65(suppl_2):S160–72. https://doi.org/10.1093/cid/cix656
5. Seale AC, Bianchi-Jassir F, Russell NJ, Kohli-Lynch M, Tann CJ, Hall J, et al. Estimates of the burden of group B streptococcal disease worldwide for pregnant women, stillbirths, and children. Clin Infect Dis. 2017;65(suppl_2):S200–19. https://doi.org/10.1093/cid/cix664
6. Kohli-Lynch M, Russell NJ, Seale AC, Dangor Z, Tann CJ, Baker CJ, et al. Neurodevelopmental impairment in children after group B streptococcal disease worldwide: systematic review and meta-analyses. Clin Infect Dis. 2017;65(suppl_2):S190–9. https://doi.org/10.1093/cid/cix663
7. Heath PT. An update on vaccination against group B streptococcus. Expert Rev Vaccines. 2011;10:685–94. https://doi.org/10.1586/erv.11.61
8. Le Doare K, O'Driscoll M, Turner K, Seedat F, Russell NJ, Seale AC, et al.; GBS Intrapartum Antibiotic Investigator Group. Intrapartum antibiotic chemoprophylaxis policies for the prevention of group B streptococcal disease worldwide: systematic review. Clin Infect Dis. 2017;65(suppl_2):S143–51. https://doi.org/10.1093/cid/cix654
9. de Azavedo JC, McGavin M, Duncan C, Low DE, McGeer A. Prevalence and mechanisms of macrolide

resistance in invasive and noninvasive group B *Streptococcus* isolates from Ontario, Canada. Antimicrob Agents Chemother. 2001;45:3504–8. https://doi.org/10.1128/AAC.45.12.3504-3508.2001

10. Castor ML, Whitney CG, Como-Sabetti K, Facklam RR, Ferrieri P, Bartkus JM, et al. Antibiotic resistance patterns in invasive group B streptococcal isolates. Infect Dis Obstet Gynecol. 2008;2008:727505. https://doi.org/10.1155/2008/727505

11. Yoon IA, Jo DS, Cho EY, Choi EH, Lee HJ, Lee H. Clinical significance of serotype V among infants with invasive group B streptococcal infections in South Korea. Int J Infect Dis. 2015;38:136–40. https://doi.org/10.1016/j.ijid.2015.05.017

12. Le Doare K, Heath PT. An overview of global GBS epidemiology. Vaccine. 2013;31(Suppl 4):D7–12. https://doi.org/10.1016/j.vaccine.2013.01.009

13. Nuccitelli A, Rinaudo CD, Maione D, Group B. Group B *Streptococcus* vaccine: state of the art. Ther Adv Vaccines. 2015;3:76–90. https://doi.org/10.1177/2051013615579869

14. Liberati A, Altman DG, Tetzlaff J, Mulrow C, Gøtzsche PC, Ioannidis JP, et al. The PRISMA statement for reporting systematic reviews and meta-analyses of studies that evaluate healthcare interventions: explanation and elaboration. BMJ. 2009;339:b2700. https://doi.org/10.1136/bmj.b2700

15. Higgins J, Green S. Cochrane handbook for systematic reviews of interventions version 5.1.0. The Cochrane Collaboration; 2011 [cited 2020 Aug 17]. https://handbook-5-1.cochrane.org

16. Su L, Yang X, Bai G, Fenglan L. Spatial inequality and regional difference of population birth rate in China. Journal of Chongqing University of Science and Technology. 2018;32:250–8.

17. Russell NJ, Seale AC, O'Driscoll M, O'Sullivan C, Bianchi-Jassir F, Gonzalez-Guarin J, et al.; GBS Maternal Colonization Investigator Group. Maternal colonization with group B *Streptococcus* and serotype distribution worldwide: systematic review and meta-analyses. Clin Infect Dis. 2017;65(suppl_2):S100–11. https://doi.org/10.1093/cid/cix658

18. Wang Y, He S. Correlation between the colonization of group B *Streptococcus* and the level of defensins in pregnant women in Hanzhong. Xiandai Jianyan Yixue Zazhi. 2013;28:87–9.

19. Wu J, Qian B. Resistance and genotype of B *Streptococcus* infected or colonized in perinatal pregnant woman. Chin Mod Doctor. 2017;55:12–15.

20. Lamagni TL, Keshishian C, Efstratiou A, Guy R, Henderson KL, Broughton K, et al. Emerging trends in the epidemiology of invasive group B streptococcal disease in England and Wales, 1991–2010. Clin Infect Dis. 2013;57:682–8. https://doi.org/10.1093/cid/cit337

21. Kang HM, Lee HJ, Lee H, Jo DS, Lee HS, Kim TS, et al. Genotype characterization of group B *Streptococcus* isolated from infants with invasive dDiseases in South Korea. Pediatr Infect Dis J. 2017;36:e242–7. https://doi.org/10.1097/INF.0000000000001531

22. Huang J, Li S, Li L, Wang X, Yao Z, Ye X. Alarming regional differences in prevalence and antimicrobial susceptibility of group B streptococci in pregnant women: a systematic review and meta-analysis. J Glob Antimicrob Resist. 2016;7:169–77. https://doi.org/10.1016/j.jgar.2016.08.010

23. Wang X, Cao X, Li S, Ou Q, Lin D, Yao Z, et al. Phenotypic and molecular characterization of *Streptococcus agalactiae* colonized in Chinese pregnant women: predominance of ST19/III and ST17/III. Res Microbiol. 2018;169:101–7. https://doi.org/10.1016/j.resmic.2017.12.004

24. Zhong P, Shortridge VD. The role of efflux in macrolide resistance. Drug Resist Updat. 2000;3:325–9. https://doi.org/10.1054/drup.2000.0175

25. Gonzalez JJ, Andreu A; Spanish Group for the Study of Perinatal Infection from the Spanish Society for Clinical Microbiology and Infectious Diseases. Multicenter study of the mechanisms of resistance and clonal relationships of *Streptococcus agalactiae* isolates resistant to macrolides, lincosamides, and ketolides in Spain. Antimicrob Agents Chemother. 2005;49:2525–7. https://doi.org/10.1128/AAC.49.6.2525-2527.2005

26. Yan Y, Hu H, Lu T, Fan H, Hu Y, Li G, et al. Investigation of serotype distribution and resistance genes profile in group B *Streptococcus* isolated from pregnant women: a Chinese multicenter cohort study. APMIS. 2016;124:794–9. https://doi.org/10.1111/apm.12570

27. Lu B, Chen X, Wang J, Wang D, Zeng J, Li Y, et al. Molecular characteristics and antimicrobial resistance in invasive and noninvasive group B *Streptococcus* between 2008 and 2015 in China. Diagn Microbiol Infect Dis. 2016;86:351–7. https://doi.org/10.1016/j.diagmicrobio.2016.08.023

28. Seo YS, Srinivasan U, Oh KY, Shin JH, Chae JD, Kim MY, et al. Changing molecular epidemiology of group B *Streptococcus* in Korea. J Korean Med Sci. 2010;25:817–23. https://doi.org/10.3346/jkms.2010.25.6.817

29. Imperi M, Gherardi G, Berardi A, Baldassarri L, Pataracchia M, Dicuonzo G, et al. Invasive neonatal GBS infections from an area-based surveillance study in Italy. Clin Microbiol Infect. 2011;17:1834–9. https://doi.org/10.1111/j.1469-0691.2011.03479.x

Address for correspondence: Yajuan Wang, Department of Neonatal Unit, Beijing Children's Hospital, Capital Medical University, National Center for Children's Health, No.56 Nan Lishi Rd, Beijing, China; email: cxswyj@vip.sina.com

Streptococcus pneumoniae Serotype 12F-CC4846 and Invasive Pneumococcal Disease after Introduction of 13-Valent Pneumococcal Conjugate Vaccine, Japan, 2015–2017

Satoshi Nakano, Takao Fujisawa, Yutaka Ito, Bin Chang, Yasufumi Matsumura,
Masaki Yamamoto, Shigeru Suga, Makoto Ohnishi, Miki Nagao

To prevent invasive pneumococcal disease (IPD), pneumococcal conjugate vaccines (PCVs) have been implemented in many countries; however, many cases of IPD still occur and can be attributable to nonvaccine serotypes of *Streptococcus pneumoniae*. In Japan, the number of IPD cases attributable to serotype 12F increased from 4.4% in 2015 to 24.6% in 2017 after 13-valent PCV was introduced. To clarify the associated genetic characteristics, we conducted whole-genome sequencing of 75 serotype 12F isolates. We identified 2 sequence types (STs) among the isolates: ST4846, which was the major type, and ST6945. Bayesian analysis suggested that these types diverged in ≈1942. Among serotype 12F-ST4846, we identified a major cluster, PC-JP12F, whose time of most recent common ancestor was estimated to be ≈2012. A phylogeographic analysis demonstrated that PC-JP12F isolates spread from the Kanto region, the most populated region in Japan, to other local regions.

S*treptococcus pneumoniae* is a common bacterial pathogen of children (*1*). To prevent pneumococcal infectious diseases, many countries have introduced 7-, 10-, and 13-valent pneumococcal conjugate vaccines (PCVs) (*2*), which have decreased the total number of invasive pneumococcal disease (IPD)

Author affiliations: Kyoto University Graduate School of Medicine, Kyoto, Japan (S. Nakano, Y. Matsumura, M. Yamamoto, M. Nagao); National Hospital Organization Mie National Hospital, Tsu, Japan (T. Fujisawa, S. Suga); Nagoya City University Graduate School of Medical Science, Nagoya, Japan (Y. Ito); National Institute of Infectious Diseases, Tokyo, Japan (B. Chang, M. Ohnishi)

cases globally. However, serotype shifts (i.e., increased identification of serotypes not in the PCV), were observed in areas in which PCVs were introduced (*3–6*); as a result, *S. pneumoniae* remains a major cause of bacterial infections, such as meningitis, pneumonia, and otitis media. In February 2010, PCV7 was licensed in Japan and was used on a voluntary basis until April 2013. During this period, the estimated rates of PCV7 vaccination for children <5 years of age increased from <10% in 2010 to 80%–90% in 2012 (*7*). In April 2013, use of PCV7 as a routine vaccine in Japan was approved, and in October 2013, vaccine for routine use was switched to PCV13.

To monitor the prevalence of different serotypes, sequence types (STs), and antimicrobial susceptibilities, we conducted a nationwide surveillance study of IPD and non-IPD cases in children in Japan during 2012–2017 (*8,9*). This passive nationwide surveillance was conducted by 254 medical institutions in Japan. During the first 3 years, 2012–2014, we detected decreased cases of PCV7 and PCV13 serotype pneumococcal infections and increased cases of serotype 24F IPD (*8*). During the next 3 years, 2015–2017, we detected markedly increased cases of serotype 12F IPD; 7 (4.4%) of 161 IPD isolates in 2015, 23 (13.9%) of 166 IPD isolates in 2016, and 42 (24.6%) of 171 IPD isolates in 2017 were classified as serotype 12F, although only 1 isolate classified as serotype 12F was detected during 2012–2014. Consequently, serotype 12F became the most prevalent serotype isolated from patients with IPD in 2017 in Japan (*9*). The mean age of these 73 IPD patients was 40.9 (range 3–126) months. Throughout the period, only 3 non-IPD serotype 12F isolates

were detected out of a total of 231 non-IPD isolates. To clarify ST prevalence, penicillin-binding protein (PBP) profiles, resistance genes, and pili detection, we conducted whole-genome sequencing analysis of the serotype 12F isolates recovered in Japan. In addition, we used Bayesian-based phylogenetic analysis to investigate the dynamics of the spread.

Materials and Methods

Bacterial Isolates
From 23 of 47 prefectures in Japan, we obtained 1 serotype 12F IPD isolate in 2013 and 72 IPD and 3 non-IPD isolates during 2015–2017. Of the 76 isolates, 1 did not grow from the stock medium; we thus analyzed all 75 remaining isolates. We tested the antimicrobial susceptibility of the isolates to penicillin, cefotaxime, meropenem, erythromycin, and levofloxacin by using the broth microdilution method according to the Clinical and Laboratory Standards Institute guidelines (*10*). We used the MIC interpretive criteria for meningitis for this study.

Basic Whole-Genome Sequencing Protocol
We extracted total genomic DNA and prepared sequence libraries by using a QIAamp DNA Mini Kit (QIAGEN, https://www.qiagen.com) and a Nextera XT DNA Library Preparation Kit (Illumina, https://www.illumina.com). We multiplexed and sequenced the samples by using an Illumina NextSeq system for 300 cycles (2 × 150-bp paired-end). The resulting sequences were assembled by using SPAdes version 3.13.1 (*11*). Mapping was performed by using Burrows-Wheeler Aligner version 0.7.17 (*12*) with *S. pneumoniae* strain ASP0581 (serotype 12F-ST4846, National Center for Biotechnology Information reference sequence NZ_AP019192.2) (*13*). Isolates with a mapping depth <20.0 were excluded from subsequent analysis. Multilocus sequence typing was performed by extracting all alleles from the assembled contigs by using BLAST+ version 2.6.0 (*14*) and a reference sequence of *S. pneumoniae* G54 (GenBank accession no. NC_011072.1). A clonal complex was defined as a group of STs sharing 5 of 7 loci in the multilocus sequence typing results.

PBP Typing, Antimicrobial Resistance Genes, Pilus Detection, and Global Pneumococcal Sequence Cluster Identification
We assigned PBP transpeptidase domain type numbers to the extracted pbp*1a*, *2b*, and *2x* transpeptidase domain sequences of the examined isolates. The type numbers originated from previously published US Centers for Disease Control and Prevention PBP types (*15–18*). PBP types that had not been previously published in the US Centers for Disease Control and Prevention database were labeled with the prefix JP (e.g., *pbp1a*-JP1). Some of these original PBP types from Japan had been previously published (*19–21*). We detected *ermB*, *ermTR*, *mefA*, *mefE*, *tetM*, *tetO*, *rrgA-1* (pili1), and *pitB-1* (pili2) genes and searched for mutations and insertions/deletions within the *folA* and *folP* genes in the assembled contigs by following the standards published in a previous study (*15*). In addition, we assigned Global Pneumococcal Sequence Cluster (GPSC) numbers (*22*) and detected *tet*(S/M) by using Pathogenwatch (https://pathogen.watch).

*Tn*916-like Integrative and Conjugative Element Analysis and *cps* Locus Comparison
We extracted the sequences of *Tn*916-like integrative and conjugative elements (ICEs) from the assembled contigs by using BLAST+ (https://blast.ncbi.nlm.nih.gov/Blast.cgi) and the *Enterococcus faecalis Tn*916 reference sequence (GenBank accession no. U09422.1). The analyzed sequences were annotated by using Prokka version 1.13.7 (*23*), and the structures of the regions were analyzed manually by using the Artemis Comparison Tool (*24*). In addition, we created a phylogenetic tree for the Tn916 region by using RAxML-ng version 0.9.0 (*25*). To obtain a phylogenetic tree of the *cps* locus, we mapped the trimmed reads to the serotype 12F *cps* locus reference sequence (GenBank accession no. CR931660.1) and obtained a phylogenetic tree by using RAxML (*26*).

Recombination Site Detection and Phylogenetic Tree Construction
We constructed a phylogenetic tree by using Genealogies Unbiased By recomBinations In Nucleotide Sequences (Gubbins) version 2.2.1 (*27*). We mapped the obtained short reads to a the complete *S. pneumoniae* ASP0581 reference sequence (GenBank accession no. NZ_AP019192.2) (*13*) and input the aligned sequences into Gubbins, which identifies recombination events by using an algorithm that iteratively identifies loci containing increased densities of base substitutions while concurrently constructing a phylogeny based on the putative point mutations outside of these regions.

Core-Genome Analysis
To clarify the differences in the genomic contents of the various clades, we used Prokka version 1.13.7 (*23*), Roary version 3.12.0 (*28*), and Scoary version 1.6.16 (*29*) to perform core-genome analysis. We

defined genes that were exclusively found in a cluster at p<0.01, obtained with the Fisher exact test followed by the Bonferroni correction, as being specific to the cluster.

Bayesian Analysis

We reconstructed a tree and obtained dates of the ancestors or nodes of the ST4846 and ST6945 clades by using the Bayesian Markov chain Monte Carlo framework. For this analysis, we performed recombination predictions by using the same protocol as described for all serotype 12F isolates. Final single-nucleotide polymorphism (SNP) alignments without recombination regions were used as the input dataset for BEAST version 1.10.4 (30). For the phylogeographic analysis, we used BEAUti (30) to additionally specify a symmetric discrete trait phylogeographic model by using a Bayesian stochastic search variable selection framework (31) as a metric for comparing geographic signals between datasets. We calculated Bayes factors indicating the transmission support by using SpreadD3 version 0.9.6 (32); consistent with convention, support was defined as a Bayes factor >3 (Appendix, https://wwwnc.cdc.gov/EID/article/26/11/20-0087-App1.pdf).

Results

STs and Antimicrobial Susceptibilities

Among the serotype 12F isolates recovered in Japan, we identified 2 STs: ST4846 (n = 59), which was the major ST, and ST6945 (n = 16), which was a double-locus variant of ST4846. Penicillin MICs for all serotype 12F isolates were ≤0.25 µg/mL. Of 59 ST4846 isolates, penicillin MICs for 16 isolates were ≤0.06 (susceptible), for 42 were ≤0.12 (resistant), and for 1 was ≤0.25 (resistant) (Table). Penicillin MICs for all but 1 of the 16 ST6945 isolates were ≤0.06 (susceptible). Of the 74 serotype 12F isolates, cefotaxime MICs for 69 isolates were ≤0.06 (susceptible), and meropenem MICs for 74 isolates were ≤0.06 (susceptible). For most isolates, erythromycin MICs were >128 (resistant, 71/74 isolates) and levofloxacin MICs were ≤1 (susceptible, 74/74 isolates).

Whole-Genome Sequencing Statistics

The average (± SD) number of contigs was 55.8 (± 15.6), N50 (shortest contig length needed to cover 50% of the genome) was 69,627 (± 12,462), and mapping depth was 106.1 (± 36.1) (Appendix Tables 1, 2). One isolate had a mapping depth of 17.5 and was therefore excluded from the study.

PBP Typing, Antimicrobial Resistance Genes, and Pilus Detection

All serotype 12F isolates contained *pbp1a*-37 (Figure 1; Appendix Table 1). All ST4846 isolates had *pbp2b*-JP14, and all ST6945 isolates contained *pbp2b*-4. We found 14 aa differences between *pbp2b*-JP14 and *pbp2b*-4. With regard to *pbp2x*, 55 of 58 ST4846 isolates had *pbp2x*-JP27 and all ST6945 isolates contained *pbp2x*-23. We found 19 aa differences between *pbp2x*-JP27 and *pbp2b*-23. In total, 55 of 58 ST4846 isolates had *pbp1a*:*pbp2b*:*pbp2x*, which equals 37:JP14:JP27, and all 16 ST6945 isolates contained *pbp1a*:*pbp2b*:*pbp2x*, which equals 37:4:23. All serotype 12F isolates had *tetM* and *ermB* with the exception of 3 ST6945 isolates that had only *tetM*. Of 58 ST4846 isolates, 52 carried the *folA* I100L mutation, but this mutation was not found in any of the ST6945 isolates. In addition, all ST4846 isolates had *folP* insertions, and none of the ST6945 isolates had mutations in this gene. None of the serotype 12F isolates carried *tetO*, *tet*(S/M), *ermTR*, *mefA/E*, Pili1, or Pili2. All serotype 12F isolates were assigned to GPSC334. Three isolates of GPSC334 were present in the GPSC database: 1 serotype 3 ST6945 isolate from Hong Kong and 2 serotype 12F isolates, ST1820 and ST1527, from Poland. Those 3 isolates were clustered into the ST6945 cluster in a subsequent recombination site-censored phylogenetic tree (Appendix Figure 1).

Tn916-like ICE Structure and cps Locus Analysis

All serotype 12F isolates tested in this study had a *Tn*916-like ICE with *tetM*, which encodes tetracycline resistance. Of 58 ST4846 isolates, 57 had *Tn*6002 (33), which was found in a previous study to be one of the most common *Tn*916-like ICEs containing erythromycin-resistance cassettes between open reading frames

Table. Antimicrobial susceptibilities of *Streptococcus pneumoniae* serotype 12F isolates recovered in Japan, 2017*

Sequence type	No. isolates	MIC, µg/mL										
		Penicillin			Cefotaxime			Meropenem	Erythromycin		Levofloxacin	
		≤0.06	0.12	0.25	≤0.06	0.12	0.25	≤0.06	≤0.06	>128	0.5	1
4846	59	16	42	1	54	3	2	59	0	59	4	55
6945	16	15	1	0	16	0	0	16	3	13	0	16

*Susceptibility categories were based on Clinical and Laboratory Standard 2015 antimicrobial susceptibility testing standards for *S. pneumoniae* (10). If categories for meningitis are available, they are shown. The standards are penicillin ≤0.06 susceptible, ≥0.12 resistant; cefotaxime ≤0.5 susceptible, 1.0 intermediate, ≥2 resistant; meropenem ≤0.25 susceptible, 0.5 intermediate, ≥1.0 resistant; erythromycin ≤0.25 susceptible, 0.5 intermediate, >1.0 resistant; levofloxacin ≤2.0 susceptible, 4.0 intermediate, ≥8.0 resistant.

19 and 20 of *Tn*916 (*34*). We did not obtain a completely connected contig throughout the whole length of the *Tn*916-like ICE region for another ST4846 isolate. With regard to ST6945 isolates, we did not obtain completely connected contigs throughout the whole length of the *Tn*916-like ICE region. However, 13 of 16 ST6945 isolates had *ermB* insertions at the same position within the partial *Tn*916-like ICE as ST4846 isolates. The phylogenetic tree that was created by using the *cps* locus sequences generated a ST6945-specific clade that included all ST6945 isolates (Appendix Figure 2).

Recombination Site Prediction, Phylogenetic Tree Construction, and Bayesian Analysis

When we constructed a recombination site censored phylogenetic tree of all serotype 12F isolates after

Figure 1. Recombination-free maximum-likelihood tree of *Streptococcus pneumoniae* serotype 12F-CC4846 isolates in Japan, created by using Gubbins (*27*). Two clusters were generated: 1 comprised only sequence type (ST) 4846 isolates and the other comprised only ST6945 isolates. All isolates had *pbp1a*-13. The *pbp2x* type "others" included *pbp2x*-JP23, *pbp2x*-JP58, and *pbp2x*-JP59. The geographic locations of the described regions in this figure are shown in the Appendix (https://wwwnc.cdc.gov/EID/article/26/11/20-0087-App1.pdf). The numbers on the branches indicate bootstrap values. SNP, single-nucleotide polymorphism; ST, sequence type.

recombination site prediction by using Gubbins (Figure 1; Appendix Figure 3), the tree identified 2 clusters composed exclusively of the ST4846 and ST6945 isolates. The average value of the pairwise SNP distances between isolates of the 2 clusters was 391, and the *r/m* value (average recombination to mutation rate) of the ST4846 clade was 0.3213 and of the ST6945 clade was 0.9639. One of the recombination sites overlapped with part of the nucleotide sequence of *pbp2b* (Appendix Figure 4). In addition, another recombination site overlapped with part of the *pbp2x* nucleotide sequence (Appendix Figure 4). No recombination site was found in the *cps* locus. We then performed a Bayesian analysis to estimate the time of most recent common ancestor (TMRCA) of the serotype 12F-CC4846 isolates by using BEAST. This analysis showed that serotype 12F-CC4846 in Japan arose in ≈1942 (95% highest posterior density [HPD] 1914–1963) (Appendix Figures 5, 6). In addition, 71 genes were unique to ST4846 isolates and 71 other genes were unique to ST6945 isolates. Although 16 of the 71 genes that were unique to ST6945 isolates did not exist in *S. pneumoniae* ASP0581, none of the 142 gene regions overlapped with the recombination regions predicted by Gubbins. We next used BEAST to estimate the TMRCA of the serotype 12F-ST4846 isolates based on only those belonging to the ST4846 clade. This analysis suggested that a common ancestor for our serotype 12F-ST4846 isolates arose in ≈2005 (95% HPD 2002–2009) (Figure 2; Appendix Figure) and generated 2 clades; the major clade (n = 44; 2015, 5/7 isolates; 2016, 17/23 isolates; 2017, 23/42 isolates), PC-JP12F, which arose in ≈2012 (95% HPD 2011–2013), had 5 genes that were lacking in the other ST4846 isolates (Appendix Table 3). This result indicated that the isolates included in the PC-JP12F clade spread rapidly in Japan; therefore, we conducted a phylogeographic analysis of the isolates to clarify the transmission over time. This analysis revealed 5 statistically supported (Bayes factor >3) routes of transmission between 6 discrete regions in Japan (Figure 3). All of the supported transmission routes originated from the Kanto region, which is the central populated region of Japan, and spread to all 5 other local regions. The highest support was obtained for transmission from the Kanto region to the Tokai region (Bayes factor 197.2), which is contiguous to the Kanto region.

The TMRCA of serotype 12F-ST6945 isolates, estimated by using only ST6945 isolates, was 1997 (95% HPD 1925–2005; Appendix Figure 8). The phylogenetic tree of the *Tn*916-like ICE region generated ST6945-specific and PC-JP12F–specific clades (Appendix Figure 9). In addition, all *ermB*-negative ST6945 isolates created a subclade within the ST6945-specific clade.
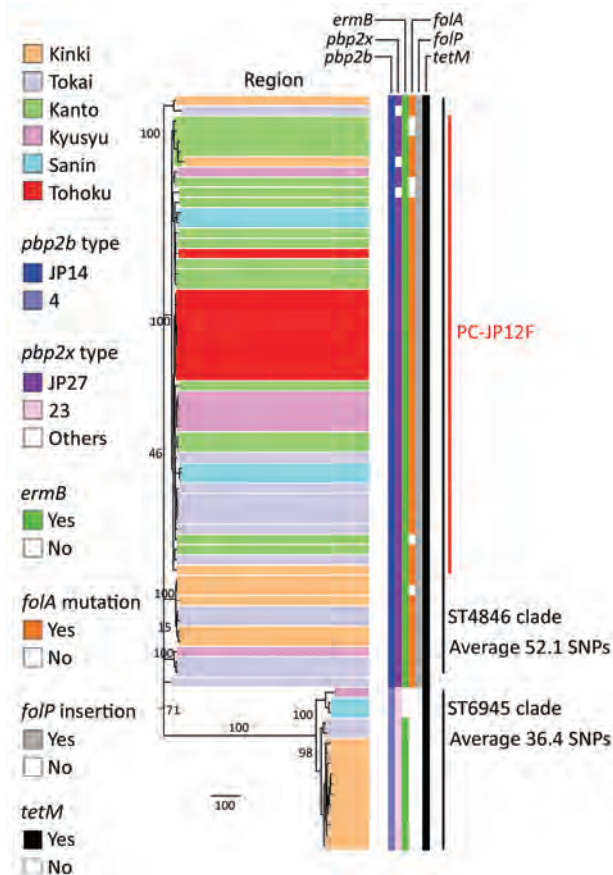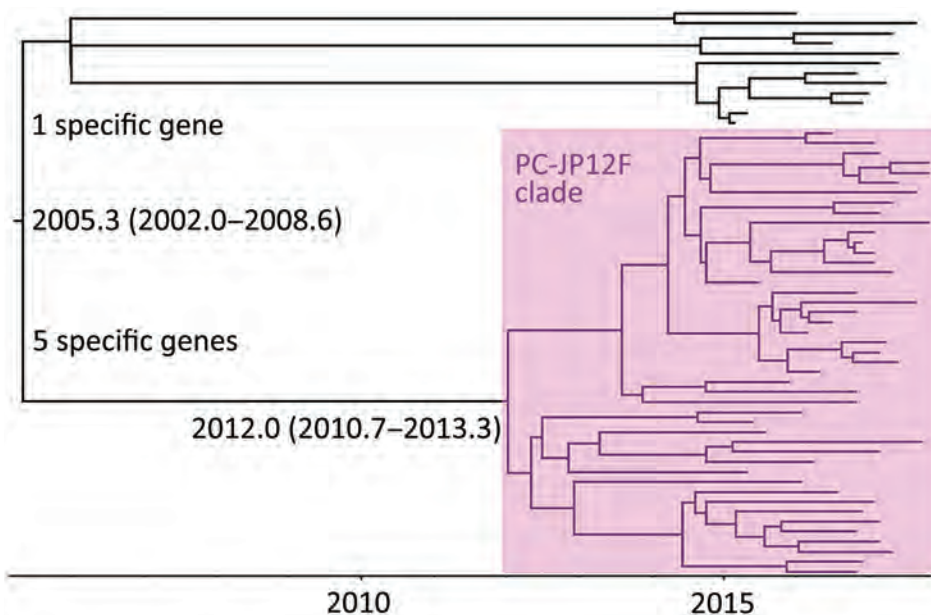
Figure 2. Maximum-clade credibility tree of *Streptococcus pneumoniae* sequence type (ST) 4846 clade isolates. The times of the most recent common ancestor are shown on the tree with 95% highest posterior density. This clade appeared to diversify in ≈2005, and the tree included 1 major clade, the PC-JP12F clade (pink shading), whose time of most recent common ancestor was ≈2012.0.

Discussion

In our nationwide surveillance study of pneumococcal disease in children, conducted in Japan during 2012–2017, we detected a rapid increase in serotype 12F IPD. Thus, we performed a whole-genome sequencing–based molecular analysis to clarify the associated genomic characteristics and their dynamics. We found 2 lineage STs within the serotype 12F isolates recovered in Japan: ST4846, which was the major sequence type, and ST6945, which was a double-locus variant of ST4846. To investigate whether these 2 STs had the same ancestor, we compared their genetic characteristics by whole-genome sequencing. According to the STs and the finding that both ST4846 and ST6945 isolates belonged to GPSC334, these isolates appear to be closely related. Although this GPSC334 was a minor cluster in the original study and the isolates from East Asia used in the study were limited (*22*), the average pairwise SNP distance between the 2 ST isolates was 391; this value is reasonable based on the evidence that the ST4846 and ST6945 isolates belonged to the same sequence cluster in the original study. However, we found several genetic differences between the 2 lineage STs, such as differences in the PBP profile, the prevalence of *folA* mutations and *folP* insertions, the Tn*916* structure, and the *cps* locus sequences. In addition, we found 142 genetic differences between the 2 STs in the core-genome analysis. In general, *S. pneumoniae* is a paradigm for recombination, and in our study, we certainly identified recombination sites, particularly in the ST6945 cluster. Therefore, we believe that these recombination events caused the discrepancy after its divergence in ≈1942.

Of note, recombination sites were not identified in the *cps* locus although the phylogenetic tree for the *cps* locus generated ST-specific clades. Considering that the process of evolving from a common ancestor to 2 distinctive clades is a result of randomly accumulated mutations, recombination events, or both, there might be ST-specific genetic backgrounds that influenced the dynamics of the *cps* region.

We found a major clade within the ST4846 isolates (i.e., PC-JP12F clade) that seemed to spread rapidly in Japan. Bayesian analysis suggested that this clade arose in ≈2012. This estimation showed a narrow 95% HPD, and we therefore believe that this estimated date was reliable. Thus, the rapid spread and high prevalence of serotype 12F-CC4846 in Japan appeared be mainly caused by this strain. In addition, the phylogeographic analysis suggested the route of transmission of this strain, which mainly involved spread from the Kanto region to other local regions. The Kanto region has 7 prefectures, including Tokyo, the capital of Japan, which contains ≈35% of the population of Japan and is thus the most populated of all regions in Japan. In general, in the phylogeographic analysis, Bayes factors >100 indicate decisive, 30–100 indicate very strong, 10–30 indicate strong, and 3–10 indicate substantial support for a model (*35*). Therefore, we believe that the determined transmission routes in Japan (i.e., from the urban region to countryside regions) were reasonable and reliable.

To date, 3 studies have demonstrated outbreaks of serotype 12F-CC4846 in Japan during 2016–2018 (*36–38*). Of the 3 outbreaks, 2 can be attributed to ST4846 isolates that occurred in the Chiba Prefecture
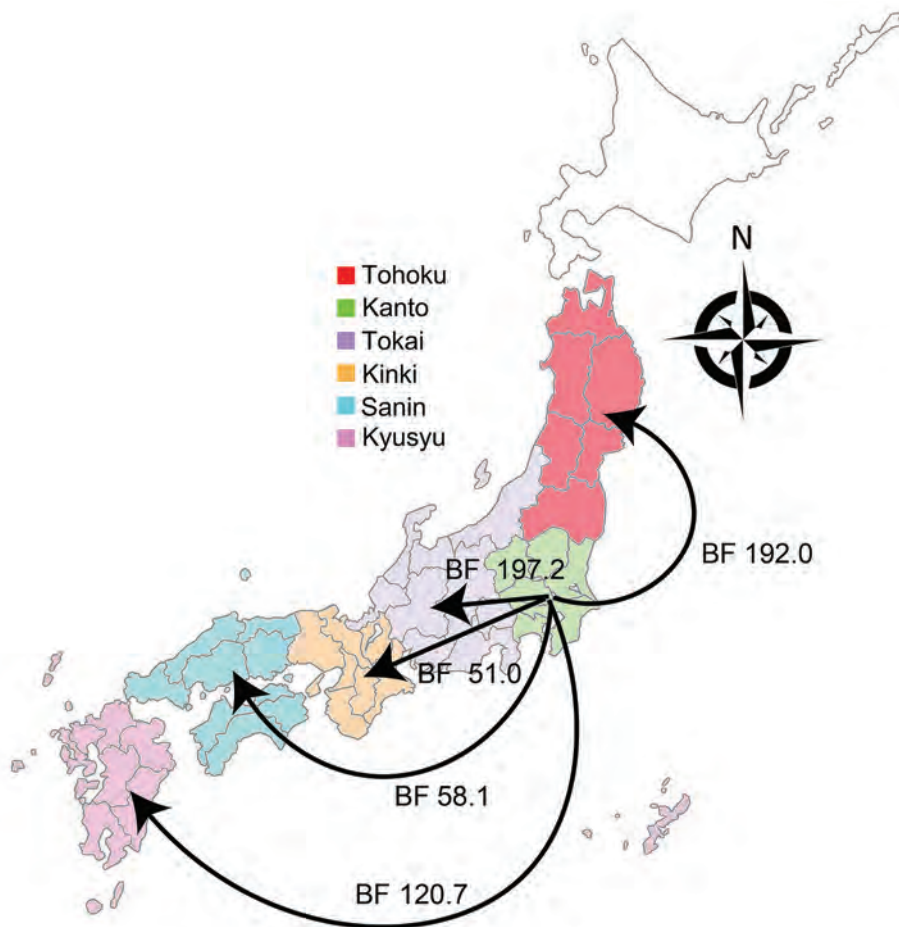
Figure 3. Bayesian phylogeography of *Streptococcus pneumoniae* serotype 12F isolates in the PC-JP12F clade between 6 discrete regions in Japan after the PC-JP12F clade arose. BFs indicate the transmission support; consistent with convention, support was defined as BF>3. Arrows indicate transmission direction. BF, Bayes factors.

in the Kanto region and in the Yamagata Prefecture in the Tohoku region. The other outbreak was attributable to ST6945 isolates in the Hyogo Prefecture in the Kinki region; in our study, ST6945 isolates were also recovered in the Kinki region (Figure 1). In addition, Shimbashi et al. reported that although the data were obtained from a pneumococcal surveillance study among adults, the ST6945 isolates were recovered in the Tokai, Kyusyu, and Tohoku regions during 2015–2017 (*39*). Given these findings, the serotype 12F-ST4846 isolates had already spread throughout Japan, and the serotype 12F-ST6945 isolates were still limited to several small regions but had already started spreading in Japan.

Serotype 12F isolates were recovered mainly from patients with IPD, including outbreak cases, in many areas globally after the introduction of PCV13 (*40–43*); several studies have demonstrated that serotype 12F is associated with high morbidity and mortality rates (*37,44*). The STs of serotype 12F isolates in different countries exhibit differences, which indicates that prevalence of these serotype

12F isolates was not the result of global but rather of regional clonal spread. In addition, Gladstone et al. and Balsells et al. found invasiveness to be relatively higher for serotype 12F pneumococci than for other serotypes (*22,45*). Of note, according to the GPSC database (*22*), all serotype 12F isolates are susceptible or mildly resistant to penicillin (MIC ≤0.12), similar to the results obtained for the isolates included in our study. Therefore, it is unlikely that antibiotic pressure caused the spread in Japan and other regions. Considering these findings, serotype 12F should exhibit high invasiveness and probably has the potential to be transmitted efficiently and thus cause an outbreak or regional spread. With regard to this issue, the mechanism underlying the rapid spread and high invasiveness of serotype 12F strains should be determined in future studies.

In this study, we identified the structures of *Tn*916-like ICEs in serotype 12F-CC4846. Most serotype 12F-ST4846 isolates contained *Tn*6002, which was also widely detected in serotype 15A-CC63 isolates in Japan (*19,20*). The phylogenetic tree of the

*Tn*916-like ICE region suggested that the origins of the *Tn*916-ICE region in PC-JP12F isolates might differ from those of the other serotype 12F-CC4846 isolates. However, we should note that the genetic difference might be caused by mapping errors (i.e., the choice of reference sequence). In Japan, the macrolide resistance rate was >90% (*9*); thus, further studies on *Tn*916-like ICEs, including its epidemiology, transmission mechanism, and functions that influence the dynamics of pneumococci, are needed.

We note some limitations of this study. First, we tested pneumococcal isolates that were collected in a nationwide surveillance study during 2012–2017. However, all isolates were recovered during 2015–2017, except for 1 that was recovered in 2013. Therefore, this short sampling period might affect the molecular clock analysis (i.e., TMRCA estimation). The TMRCAs of the serotype 12F-CC4846 isolates (Appendix Figure 5) and ST6945 (Appendix Figure) had very broad 95% HPDs. Therefore, we believe that longer samplings are needed to more accurately estimate the dates. In contrast, the TMRCA of ST4846 was estimated with a narrow 95% HPD. Thus, we believe that the results of the date estimations and the subsequent analyses (Figure 2) were robust and reliable.

In conclusion, we found rapid spread of serotype 12F-CC4846 isolates among patients with IPD in Japan after the introduction of PCV13. The results identified ST4846 and ST6945 (double-locus variant of ST4846) lineages for the serotype 12F-CC4846 isolates in Japan, but many genetic differences were found between the 2 lineages. Bayesian analysis identified a major cluster within the ST4846 isolates (PC-JP12F cluster). This PC-JP12F cluster arose in ≈2012 and rapidly spread from the Kanto region to countryside regions. As we showed in this study, *S. pneumoniae* serotype 12F lineages could have the potential to spread rapidly; therefore, we should monitor the trend of the lineages when they are detected.

Acknowledgments

About the Author

Dr. Nakano is an infectious disease physician working at the Department of Infection Control and Prevention, Kyoto University Hospital, Kyoto, Japan. He is also an assistant professor in the Department of Clinical Laboratory Medicine, Kyoto University Graduate School of Medicine. His research interests focus on infectious diseases and clinical microbiology, including molecular epidemiology.

References

1. Wahl B, O'Brien KL, Greenbaum A, Majumder A, Liu L, Chu Y, et al. Burden of *Streptococcus pneumoniae* and *Haemophilus influenzae* type b disease in children in the era of conjugate vaccines: global, regional, and national estimates for 2000-15. Lancet Glob Health. 2018;6:e744–57. https://doi.org/10.1016/S2214-109X(18)30247-X
2. Geno KA, Gilbert GL, Song JY, Skovsted IC, Klugman KP, Jones C, et al. Pneumococcal capsules and their types: past, present, and future. Clin Microbiol Rev. 2015;28:871–99. https://doi.org/10.1128/CMR.00024-15
3. Waight PA, Andrews NJ, Ladhani NJ, Sheppard CL, Slack MP, Miller E. Effect of the 13-valent pneumococcal conjugate vaccine on invasive pneumococcal disease in England and Wales 4 years after its introduction: an observational cohort study. Lancet Infect Dis. 2015;15:629. https://doi.org/10.1016/S1473-3099(15)70044-7
4. Abat C, Raoult D, Rolain JM. Dramatic decrease of *Streptococcus pneumoniae* infections in Marseille, 2003-2014. Eur J Clin Microbiol Infect Dis. 2015;34:2081–7. https://doi.org/10.1007/s10096-015-2455-1
5. Camilli R, D'Ambrosio F, Del Grosso M, Pimentel de Araujo F, Caporali MG, Del Manso M, et al.; Pneumococcal Surveillance Group. Impact of pneumococcal conjugate vaccine (PCV7 and PCV13) on pneumococcal invasive diseases in Italian children and insight into evolution of pneumococcal population structure. Vaccine. 2017;35(35 Pt B):4587–93. https://doi.org/10.1016/j.vaccine.2017.07.010
6. Moore MR, Link-Gelles R, Schaffner W, Lynfield R, Holtzman C, Harrison LH, et al. Effectiveness of 13-valent pneumococcal conjugate vaccine for prevention of invasive pneumococcal disease in children in the USA: a matched case-control study. Lancet Respir Med. 2016;4:399–406. https://doi.org/10.1016/S2213-2600(16)00052-7
7. Chiba N, Morozumi M, Shouji M, Wajima T, Iwata S, Ubukata K; Invasive Pneumococcal Diseases Surveillance Study Group. Changes in capsule and drug resistance of pneumococci after introduction of PCV7, Japan, 2010-2013. Emerg Infect Dis. 2014;20:1132–9. https://doi.org/10.3201/eid2007.131485
8. Nakano S, Fujisawa T, Ito Y, Chang B, Suga S, Noguchi T, et al. Serotypes, antimicrobial susceptibility, and molecular epidemiology of invasive and non-invasive *Streptococcus pneumoniae* isolates in paediatric patients after the introduction of 13-valent conjugate vaccine in a nationwide surveillance study conducted in Japan in 2012-2014. Vaccine. 2016;34:67–76. https://doi.org/10.1016/j.vaccine.2015.11.015
9. Nakano S, Fujisawa T, Ito Y, Chang B, Matsumura Y, Yamamoto M, et al. Nationwide surveillance of paediatric invasive and non-invasive pneumococcal disease in Japan after the introduction of the 13-valent conjugated

vaccine, 2015–2017. Vaccine. 2020;38:1818–24. https://doi.org/10.1016/j.vaccine.2019.12.022

10. Clinical and Laboratory Standards Institute. Performance standards for antimicrobial susceptibility testing; twenty-fifth informational supplement. CLSI document M100–S25. Wayne (PA): The Institute; 2015.

11. Bankevich A, Nurk S, Antipov D, Gurevich AA, Dvorkin M, Kulikov AS, et al. SPAdes: a new genome assembly algorithm and its applications to single-cell sequencing. J Comput Biol. 2012;19:455–77. https://doi.org/10.1089/cmb.2012.0021

12. Li H, Durbin R. Fast and accurate short read alignment with Burrows-Wheeler transform. Bioinformatics. 2009;25:1754–60. https://doi.org/10.1093/bioinformatics/btp324

13. Chang B, Morita M, Lee KI, Ohnishi M. Complete genome sequence of a sequence type 4846 *Streptococcus pneumoniae* serotype 12F strain isolated from a meningitis case in Japan. Microbiol Resour Announc. 2019 Mar 14;8:e01632-18).

14. Altschul SF, Gish W, Miller W, Myers EW, Lipman DJ. Basic local alignment search tool. J Mol Biol. 1990;215:403–10. https://doi.org/10.1016/S0022-2836(05)80360-2

15. Metcalf BJ, Gertz RE Jr, Gladstone RA, Walker H, Sherwood LK, Jackson D, et al.; Active Bacterial Core surveillance team. Strain features and distributions in pneumococci from children with invasive disease before and after 13-valent conjugate vaccine implementation in the USA. Clin Microbiol Infect. 2016;22:60.e9–29. https://doi.org/10.1016/j.cmi.2015.08.027

16. Metcalf BJ, Chochua S, Gertz RE Jr, Li Z, Walker H, Tran T, et al.; Active Bacterial Core surveillance team. Using whole genome sequencing to identify resistance determinants and predict antimicrobial resistance phenotypes for year 2015 invasive pneumococcal disease isolates recovered in the United States. Clin Microbiol Infect. 2016;22:1002.e1–8. https://doi.org/10.1016/j.cmi.2016.08.001

17. Li Y, Metcalf BJ, Chochua S, Li Z, Gertz RE Jr, Walker H, et al. Penicillin-binding protein transpeptidase signatures for tracking and predicting β-lactam resistance levels in *Streptococcus pneumoniae*. MBio. 2016;7:e00756-16. https://doi.org/10.1128/mBio.00756-16

18. Centers for Disease Control and Prevention. Minimum inhibitory concentrations predicted by the penicillin binding protein [cited 2020 Aug 17]. https://www.cdc.gov/streplab/pneumococcus/mic.html

19. Nakano S, Fujisawa T, Ito Y, Chang B, Matsumura Y, Yamamoto M, et al. Spread of meropenem-resistant *Streptococcus pneumoniae* serotype 15A-ST63 clone in Japan, 2012–2014. Emerg Infect Dis. 2018;24:275–83. https://doi.org/10.3201/eid2402.171268

20. Nakano S, Fujisawa T, Ito Y, Chang B, Matsumura Y, Yamamoto M, et al. Whole-genome sequencing analysis of multidrug-resistant serotype 15A *Streptococcus pneumoniae* in Japan and the emergence of a highly resistant serotype 15A-ST9084 clone. Antimicrob Agents Chemother. 2019;63:e02579-18. https://doi.org/10.1128/AAC.02579-18

21. Nakano S, Fujisawa T, Ito Y, Chang B, Matsumura Y, Yamamoto M, et al. Penicillin-binding protein typing, antibiotic resistance gene identification, and molecular phylogenetic analysis of meropenem-resistant *Streptococcus pneumoniae* serotype 19A-CC3111 strains in Japan. Antimicrob Agents Chemother. 2019;63:e00711–9. https://doi.org/10.1128/AAC.00711-19

22. Gladstone RA, Lo SW, Lees JA, Croucher NJ, van Tonder AJ, Corander J, et al.; Global Pneumococcal Sequencing Consortium. International genomic definition of pneumococcal lineages, to contextualise disease, antibiotic

resistance and vaccine impact. EBioMedicine. 2019;43:338–46. https://doi.org/10.1016/j.ebiom.2019.04.021

23. Seemann T. Prokka: rapid prokaryotic genome annotation. Bioinformatics. 2014;30:2068–9. https://doi.org/10.1093/bioinformatics/btu153

24. Carver T, Berriman M, Tivey A, Patel C, Böhme U, Barrell BG, et al. Artemis and ACT: viewing, annotating and comparing sequences stored in a relational database. Bioinformatics. 2008;24:2672–6. https://doi.org/10.1093/bioinformatics/btn529

25. Kozlov AM, Darriba D, Flouri T, Morel B, Stamatakis A. RAxML-NG: a fast, scalable and user-friendly tool for maximum likelihood phylogenetic inference. Bioinformatics. 2019;35:4453–5. https://doi.org/10.1093/bioinformatics/btz305

26. Stamatakis A. RAxML version 8: a tool for phylogenetic analysis and post-analysis of large phylogenies. Bioinformatics. 2014;30:1312–3. https://doi.org/10.1093/bioinformatics/btu033

27. Croucher NJ, Page AJ, Connor TR, Delaney AJ, Keane JA, Bentley SD, et al. Rapid phylogenetic analysis of large samples of recombinant bacterial whole genome sequences using Gubbins. Nucleic Acids Res. 2015;43:e15. https://doi.org/10.1093/nar/gku1196

28. Page AJ, Cummins CA, Hunt M, Wong VK, Reuter S, Holden MT, et al. Roary: rapid large-scale prokaryote pan genome analysis. Bioinformatics. 2015;31:3691–3. https://doi.org/10.1093/bioinformatics/btv421

29. Brynildsrud O, Bohlin J, Scheffer L, Eldholm V. Rapid scoring of genes in microbial pan-genome-wide association studies with Scoary. Genome Biol. 2016;17:238. https://doi.org/10.1186/s13059-016-1108-8

30. Drummond AJ, Rambaut A. BEAST: Bayesian Evolutionary Analysis by Sampling Trees. BMC Evol Biol. 2007;7:214. https://doi.org/10.1186/1471-2148-7-214

31. Lemey P, Rambaut A, Drummond AJ, Suchard MA. Bayesian phylogeography finds its roots. PLOS Comput Biol. 2009;5:e1000520. https://doi.org/10.1371/journal.pcbi.1000520

32. Bielejec F, Baele G, Vrancken B, Suchard MA, Rambaut A, Lemey P. SpreaD3: interactive visualization of spatiotemporal history and trait evolutionary processes. Mol Biol Evol. 2016;33:2167–9. https://doi.org/10.1093/molbev/msw082

33. Brenciani A, Bacciaglia A, Vecchi M, Vitali LA, Varaldo PE, Giovanetti E. Genetic elements carrying *erm*(B) in *Streptococcus pyogenes* and association with *tet*(M) tetracycline resistance gene. Antimicrob Agents Chemother. 2007;51:1209–16. https://doi.org/10.1128/AAC.01484-06

34. Schroeder MR, Stephens DS. Macrolide resistance in *Streptococcus pneumoniae*. Front Cell Infect Microbiol. 2016;6:98. https://doi.org/10.3389/fcimb.2016.00098

35. Adam DC, Scotch M, MacIntyre CR. Bayesian phylogeography and pathogenic characterization of smallpox based on *HA, ATI*, and *CrmB* genes. Mol Biol Evol. 2018;35:2607–17. https://doi.org/10.1093/molbev/msy153

36. Ohkusu M, Takeuchi N, Ishiwada N, Ohkusu K. Clonal spread of serotype 12F ST4846 *Streptococcus pneumoniae*. J Med Microbiol. 2019;68:1383–90. https://doi.org/10.1099/jmm.0.001047

37. Ikuse T, Habuka R, Wakamatsu Y, Nakajima T, Saitoh N, Yoshida H, et al. Local outbreak of *Streptococcus pneumoniae* serotype 12F caused high morbidity and mortality among children and adults. Epidemiol Infect. 2018;146:1793–6. https://doi.org/10.1017/S0950268818002133

38. Nakanishi N, Yonezawa T, Tanaka S, Shirouzu Y, Naito Y, Ozaki A, et al. Assessment of the local clonal

spread of *Streptococcus pneumoniae* serotype 12F caused invasive pneumococcal diseases among children and adults. J Infect Public Health. 2019;12:867–72. https://doi.org/10.1016/j.jiph.2019.05.019

39. Shimbashi R, Chang B, Tanabe Y, Takeda H, Watanabe H, Kubota T, et al.; Adult IPD Study Group. Epidemiological and clinical features of invasive pneumococcal disease caused by serotype 12F in adults, Japan. PLoS One. 2019;14:e0212418. https://doi.org/10.1371/journal.pone.0212418

40. Linkevicius M, Cristea V, Siira L, Mäkelä H, Toropainen M, Pitkäpaasi M, et al. Outbreak of invasive pneumococcal disease among shipyard workers, Turku, Finland, May to November 2019. Euro Surveill. 2019;24:1900681. https://doi.org/10.2807/1560-7917.ES.2019.24.49.1900681

41. González-Diaz A, Camara J, Ercibengoa M, Cercenado E, Larrosa N, Quesada MD, et al. Emerging non-13-valent pneumococcal conjugate vaccine (PCV13) serotypes causing adult invasive pneumococcal disease in the late-PCV13 period in Spain. Clin Microbiol Infect. 2020;26:753–9. https://doi.org/10.1016/j.cmi.2019.10.034

42. Golden AR, Baxter MR, Davidson RJ, Martin I, Demczuk W, Mulvey MR, et al. Comparison of antimicrobial resistance patterns in *Streptococcus pneumoniae* from respiratory and blood cultures in Canadian hospitals from 2007–16. J Antimicrob Chemother. 2019;74(Suppl_4):iv39–iv47. https://doi.org/10.1093/jac/dkz286

43. Valdarchi C, Dorrucci M, Mancini F, Farchi F, Pimentel de Araujo F, Corongiu M, et al.; FIMMG Group. Pneumococcal carriage among adults aged 50 years and older with co-morbidities attending medical practices in Rome, Italy. Vaccine. 2019;37:5096–103. https://doi.org/10.1016/j.vaccine.2019.06.052

44. Deng X, Peirano G, Schillberg E, Mazzulli T, Gray-Owen SD, Wylie JL, et al. Whole-genome sequencing reveals the origin and rapid evolution of an emerging outbreak strain of *Streptococcus pneumoniae* 12F. Clin Infect Dis. 2016;62:1126–32. https://doi.org/10.1093/cid/ciw050

45. Balsells E, Dagan R, Yildirim I, Gounder PP, Steens A, Muñoz-Almagro C, et al. The relative invasive disease potential of *Streptococcus pneumoniae* among children after PCV introduction: a systematic review and meta-analysis. J Infect. 2018;77:368–78. https://doi.org/10.1016/j.jinf.2018.06.004

Address for correspondence: Satoshi Nakano, Kyoto University Hospital, 54 Kawahara-cho, Syogoin, Sakyo-ku, Kyoto, 606-8507, Japan; email: snakano@kuhp.kyoto-u.ac.jp

etymologia revisited

Streptococcus
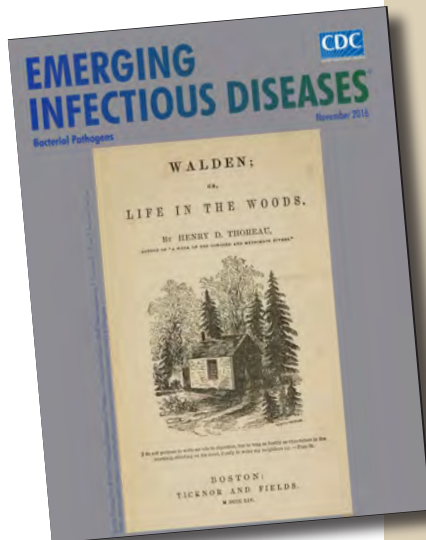
Originally published in November 2016

From the Greek *streptos* ("chain") + *kokkos* ("berry"), streptococcal diseases have been known since at least the 4th century BCE when Hippocrates described erysipelas (Greek for "red skin"). The genus *Streptococcus* was named by Austrian surgeon Theodor Billroth, who in 1874 described "small organisms as found in either isolated or arranged in pairs, sometimes in chains" in cases of erysipelas or wound infections. Over subsequent decades, as microscopy and staining techniques improved, many different researchers characterized the bacteria now known as *Streptococcus pyogenes* (Lancefield group A β-hemolytic streptococcus), *S. pneumoniae*, and other species.

Source: Majno G, Joris I. Billroth and Penicillium. Rev Infect Dis. 1979; 1:880–4. http://dx.doi.org/10.1093/clinids/1.5.880

https://wwwnc.cdc.gov/eid/article/22/11/et-2018_article

Nowcasting (Short-Term Forecasting) of Influenza Epidemics in Local Settings, Sweden, 2008–2019

Armin Spreco, Olle Eriksson, Örjan Dahlström, Benjamin John Cowling,
Matthew Biggerstaff, Gunnar Ljunggren, Anna Jöud, Emanuel Istefan, Toomas Timpka

The timing of influenza case incidence during epidemics can differ between regions within nations and states. We conducted a prospective 10-year evaluation (January 2008–February 2019) of a local influenza nowcasting (short-term forecasting) method in 3 urban counties in Sweden with independent public health administrations by using routine health information system data. Detection-of-epidemic-start (detection), peak timing, and peak intensity were nowcasted. Detection displayed satisfactory performance in 2 of the 3 counties for all nonpandemic influenza seasons and in 6 of 9 seasons for the third county. Peak-timing prediction showed satisfactory performance from the influenza season 2011–12 onward. Peak-intensity prediction also was satisfactory for influenza seasons in 2 of the counties but poor in 1 county. Local influenza nowcasting was satisfactory for seasonal influenza in 2 of 3 counties. The less satisfactory performance in 1 of the study counties might be attributable to population mixing with a neighboring metropolitan area.

Reliable forecasts of the timing and spatial spread of influenza during seasons and pandemics can meaningfully advance the timing of public health communication campaigns and implementation of resource allocation in healthcare (*1*). Different types of influenza forecast methods have been developed and applied to support public health response (*2*). However, although modelers have shown considerable interest in developing infectious disease forecasts, the readiness in the public health community for applying these predictions has been lacking (*3*). One reason for this discrepancy might be that national public health policies for response to infectious disease outbreaks often assign the responsibility for healthcare resource allocation to local health authorities (i.e., county and municipality governments). For geographic and infrastructural reasons, the timing of the spatial spread of influenza can differ substantially between these administrative units within nations and states. Therefore, a need exists for influenza forecasting methods that harmonize with policy-making responsibilities at local government levels and that are more relevant for public health practitioners.

Another reason for the poor uptake of forecasting methods might be a lack of prospective evaluations of their reliability. To address this issue, the US Centers for Disease Control and Prevention (CDC) has run the Forecast the Influenza Season Collaborative Challenge (FluSight) since the 2013–14 influenza season to prospectively evaluate different methods and data

Author affiliations: Linköping University Department of Health, Medicine, and Caring Sciences, Linköping, Sweden (A. Spreco, E. Istefan, T. Timpka); Center for Health Services Development, Region Östergötland, Linköping (A. Spreco, T. Timpka); Linköping University Department of Computer and Information Science, Linköping (O. Eriksson, T. Timpka); Linköping University Department of Behavioral Sciences and Learning, Linköping (Ö. Dahlström); World Health Organization Collaborating Centre for Infectious Disease Epidemiology and Control, The University of Hong Kong School of Public Health, Hong Kong (B.J. Cowling); Centers for Disease Control and Prevention, Atlanta, Georgia, USA (M. Biggerstaff); Karolinska Institutet Department of Neurobiology, Care Sciences, and Society, Huddinge, Sweden (G. Ljunggren); Public Health Care Services Committee Administration, Region Stockholm, Stockholm, Sweden (G. Ljunggren); Lund University Faculty of Medicine, Department of Laboratory Medicine, Division of Occupational and Environmental Medicine, Lund, Sweden (A. Jöud); Lund University Faculty of Medicine, Clinical Sciences, Division of Orthopedics, Lund (A. Jöud); Scania University Hospital Department for Research and Development, Lund (A. Jöud)

sources for influenza forecasting at the national, regional, and (starting in the 2017–18 influenza season) state level (*4*). At the local (county and municipality) level, however, few corresponding prospective evaluations based on routine health system data have been reported. Short-term forecasting is denoted as nowcasting (*5*). Recently, a prospective 5-year appraisal of a local nowcasting method (*6*) in a county in Sweden (county population ≈460,000) indicated promising results with regard to detection of the local start of the epidemic, prediction of peak timing, and prediction of peak intensity (*7*). The appraisal concluded that a longer prospective evaluation was needed to ascertain the validity of the results and that data from larger urban counties were required to draw reliable conclusions about generalizability.

In this article, we describe a prospective 10-year evaluation of this local influenza nowcasting method in 3 urban counties (population 1.3–2.2 million) in Sweden. The evaluation period included 1 pandemic (2009) and 9 seasonal influenza epidemics.

Methods

Study Design
We used an open cohort design based on the total population in 3 urban counties: Stockholm County (population 2,231,000), West Gothia County (population 1,649,000), and Scania County (population 1,304,000) (Figure 1). We used retrospective data from January 1, 2008, through June 30, 2009, and prospective data from July 1 through February 28, 2019, from 2 sources in the countywide health information system: daily numbers of clinically diagnosed influenza cases (Figure 2) and daily syndromic chief complaint data from a telenursing service (Figure 3) (*6,7*). The clinical influenza case data were used to detect the local start of the epidemic and prediction of its peak intensity, and the syndromic data were used to predict the peak timing. Existing evidence of a strong association between the clinical influenza case data and syndromic chief complaint data from the telenursing service was used in this nowcasting method (*8,9*). Because of a change of system, no syndromic chief complaint data were available for Stockholm County. Syndromic data from West Gothia County were therefore used to predict the peak timing for Stockholm County.

Timeliness was used as a performance metric for detection of the local start of the epidemic and the peak-timing prediction; the correct identification of intensity category on a 5-grade scale (i.e., nonepidemic, low, medium, high, and very high) was used

for peak-intensity prediction. The study design was approved by the Regional Research Ethics Board in Linköping (approval no. 2012/104-31).

Figure 1. Three regions analyzed in study of nowcasting for influenza epidemics in local settings, Sweden. Black indicates Stockholm County, red West Gothia County, gray Scania County. Included in the map is the island Zeeland (Sjaelland) (which is neighboring to Scania County). Blue indicates the city of Copenhagen (population 2 million) (on the island in the left lower corner of the figure).
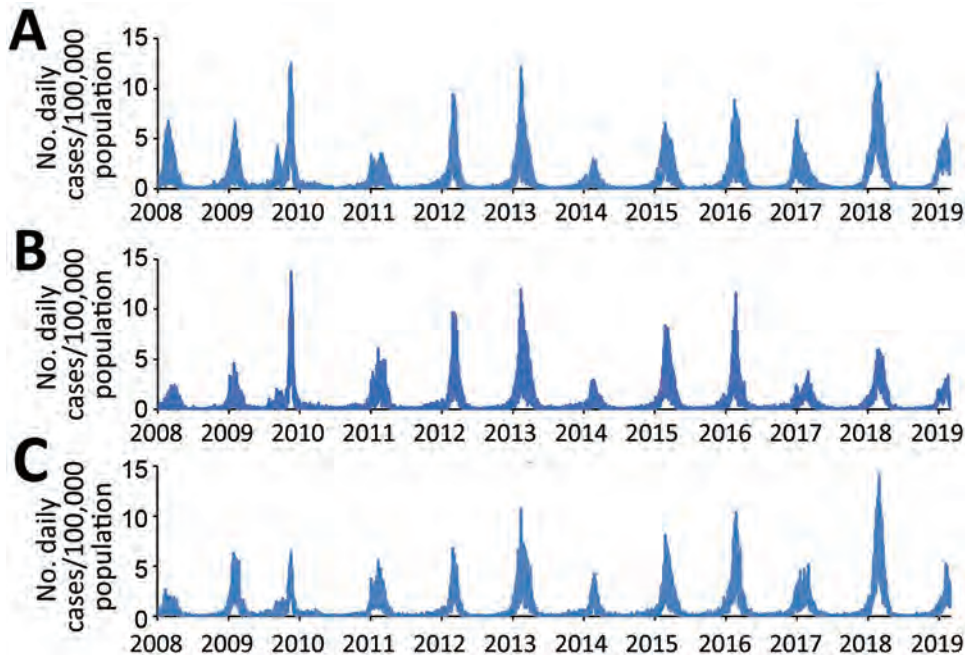
Figure 2. Daily numbers of influenza-diagnosis cases per 100,000 population, January 1, 2008–February 28, 2019, in Stockholm County (upper graph), West Gothia County (middle graph), and Scania County (lower graph), Sweden.

Definitions

Influenza cases were identified by using codes from the International Classification of Diseases, 10th Revision, for influenza (J10.0, J10.1, J10.8, J11.0, J11.1, J11.8) (*10*) as recorded in the local electronic health data repository. Only influenza diagnoses in the first coding position were used. Influenza-related telenursing call cases were identified by using the chief complaint codes associated with influenza symptoms. The symptoms used were fever, cough, and headache. These data were downloaded from the electronic patient record systems to the electronic health data repository twice daily.

The intensity level defining the start of a local epidemic (i.e., the intensity that determines the endpoint for the detection function) was set to 6.3 influenza-diagnosis cases/100,000 population recorded during a floating 7-day period in the countywide health information system (*6*). This level was chosen by inspecting the epidemic curves of previous local influenza epidemics. A recent comparison of influenza intensity levels in Europe estimated a similar level (6.4 influenza-diagnosis cases/week/100,000 population) for the 2008–09 seasonal influenza in Sweden (*11*). The optimal alerting threshold before each epidemic was decided by calculating the sensitivity and the specificity for the previous nonpandemic influenza seasons and studying them on a receiver operating characteristic curve (*6*). The calculation of the specificity was based on all days in the nonepidemic period (i.e., before the limit of 6.3 influenza-diagnosis cases/100,000 during a floating 7-day period occur), and the calculation of the sensitivity was based on the days in the epidemic period (i.e., from when the limit of 6.3 influenza-diagnosis cases/100,000 during a floating 7-day period has occurred). Peak timing was defined as the day when the highest number of influenza-diagnosis cases were documented in the countywide electronic patient record. Peak intensity was defined as the number of influenza-diagnosis cases that had been documented at peak timing.

Method Application

Technical details concerning the 3 functions of nowcasting have been described previously (*6*; Appendix, https://wwwnc.cdc.gov/EID/article/26/11/20-0448-App1.pdf). The functions are detecting the start of the influenza season or pandemic and forecasting the peak day and peak intensity. Once the epidemic has been detected using the clinical influenza data, the syndromic telenursing data are used to detect when it decreases, that being the indication for the peak. Because changes in clinical influenza data have been found to occur 14 days after corresponding changes in syndromic data, the peak timing in the clinical influenza data are forecasted to occur 14 days after the peak in the syndromic data. Finally, the peak intensity is forecasted by using the clinical influenza data. Syndromic data have a higher amplitude, and the relationship between syndromic data and clinical influenza data are not necessarily constant between seasons. Therefore, the clinical data were used to

predict the intensity once the peak day is predicted with the help of syndromic data.

To calibrate the detection component of the nowcasting method, we retrospectively determined weekday effects on recording of influenza-diagnosis cases and a baseline alert threshold by using the retrospective data. These data were collected from January 1, 2008, through June 30, 2009, including 2 nonpandemic influenza seasons (2007–08 and 2008–09). To determine weekday effects, data from the entire retrospective data collection period were used. To determine the initial alert threshold, only data from the seasonal influenza in 2008–09 were used. The 2007–08 seasonal influenza could not be used for this purpose because the season had started before January 1, 2008. Throughout the study period, the calibration data were updated after every seasonal influenza (i.e., no updates of the threshold after the 2009 pandemic outbreak). The detection algorithm was thus applied to the next epidemic by using the revised threshold determined in the updated retrospective dataset.

Before the 2010–11 seasonal influenza, no updates were performed because the set of retrospective data remained the same (i.e., it contained data from the 2008–09 seasonal influenza but excluded pandemic data). For the 2011–12 seasonal influenza, the threshold was updated by using retrospective data from the 2008–09 and 2010–11 seasonal influenza. For the 2012–13 seasonal influenza, the threshold was updated by using retrospective data from the 2008–09, 2010–11, and 2011–12 seasonal influenza, and so on. The weekday effects were assumed to be relatively constant over time in the local detection analyses and were therefore not updated after every seasonal influenza.

The set of retrospective data from the seasonal influenza in 2007–08 and in 2008–09 were also used to initially calibrate peak-timing prediction for West Gothia County and Scania County. The dataset was used to decide the grouping of chief complaints with the largest correlation strength and longest lead time from telenursing data to influenza-diagnosis data (10,11). For both counties, the best performing telenursing chief complaint was fever (among children and adults), and the most favorable lead time was 14 days. When the peak timing had been determined, the second component of the local prediction module was applied to influenza-diagnosis data from the corresponding epidemics to find the peak intensity on the predicted peak day (6). Regarding weekday effects on local prediction, the same calculation was applied and the same grouping of chief complaints and lead time were used throughout the study.

Metrics and Interpretations

On the basis of the utility of the nowcasting method in local healthcare settings, the maximum tolerable timeliness error for detection and peak-timing predictions was set to 11 days (≈1.5 weeks). Method performance was defined to be excellent if the absolute value of the timeliness error was <3 days, good if it was 4–7 days, tolerable if it was 8–11 days, and poor if it was >12 days. For the interpretation of peak intensity predictions, the intensity level categories

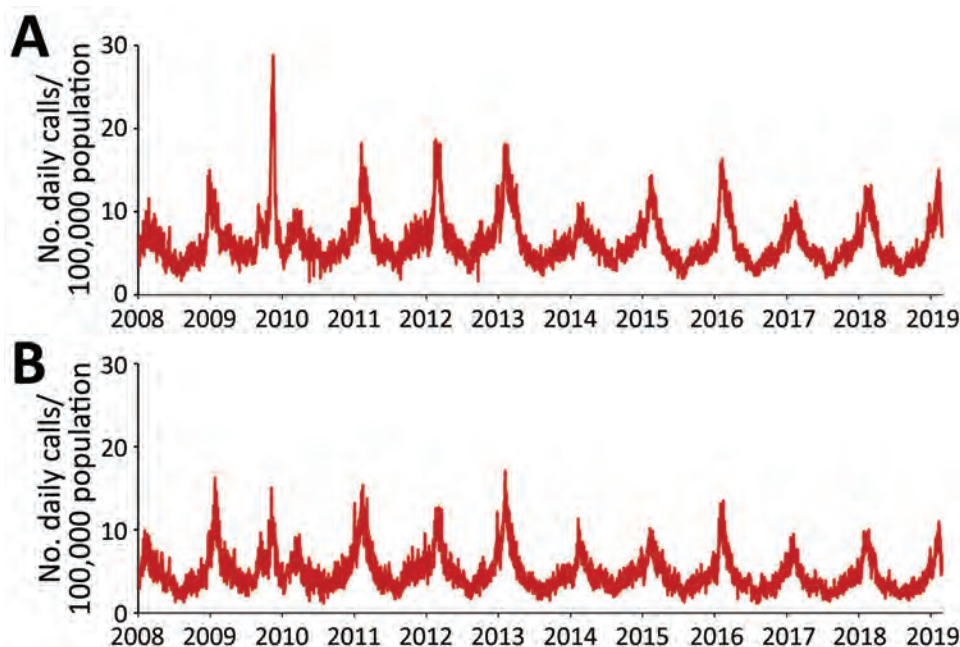

Figure 3. Daily numbers of telenursing calls attributable to fever (among children and adults) per 100,000 population, January 1, 2008–February 28, 2019, in West Gothia County (upper graph) and Scania County (lower graph), Sweden.

(nonepidemic <0.9, low 0.9, medium 2.4, high 5.5, and very high intensity level 7.9 cases/day/100,000 population) identified using the moving epidemic method for the reference influenza season 2008–09 in Sweden (*11*) were used. If the predicted peak intensity fell into the same category as the recorded peak intensity, the prediction was considered excellent. If the predicted peak intensity did not fall into the same intensity category, the predicted peak was considered good if it was up to 10% above or below the threshold for the recorded peak intensity category, tolerable if the predicted peak was 10%–20% above or below the threshold for the recorded peak intensity category, and poor otherwise. When assessing series of nowcasts, the performance of a sequence of nowcasts was considered satisfactory if all separate forecasts were assessed as excellent, good, or tolerable, and poor otherwise.

Results

Local Detection
The date of the actual start of the epidemic phase for the 10 influenza epidemics differed by 2–27 days between the 3 counties (Table 1). The detection component of the local nowcasting method showed good or excellent performance in all counties under surveillance for 6 of the 9 nonpandemic influenza seasons and in 2 out of 3 counties under surveillance for the 3 remaining seasons. Twice the poor alerts were issued too soon and once belatedly. The detection performance was good during the 2009 influenza A(H1N1) pandemic in 2 of 3 counties (Stockholm and West Gothia) and poor in 1 county (Scania).

Local Prediction
For the 2009 influenza pandemic, the performance of the peak-timing prediction was poor in all 3 study counties (Table 2). The peak-timing prediction was also poor for the 2010–11 seasonal, when influenza A(H1N1) and B viruses were circulating. Thereafter, the predictions were tolerable for the 2011–12 seasonal influenza, when influenza A(H3N2) virus was circulating, and good to excellent for the remaining influenza seasons, with the exception of the poor peak-timing predictions for Scania County for the 2016–17 and 2017–18 influenza seasons, with influenza A(H3N2) virus circulating in 2016–17 and influenza A(H3N2) and B in 2017–18.

The prediction of the peak-intensity level was poor for the 2009 influenza pandemic in all 3 study counties (Table 2). For seasonal influenza, in 2 of the study counties (Stockholm and West Gothia) the

predictions were tolerable to excellent for all seasons, except for the 2018–19 season with influenza A(H1N1) in Stockholm. In 1 county (Scania), the peak-intensity predictions were poor for 5 of the 9 influenza seasons: 2010–11 with influenza A(H1N1) and B, 2011–12 with influenza A(H3N2), 2014–15 with influenza A(H3N2) and B, 2015–16 with influenza A(H1N1) and B, and 2017–18 with influenza A(H3N2) and B circulating.

Discussion
Epidemic forecasts for large administrative areas (e.g., nations or states) might not be sufficiently informative for local response to epidemics if sizable variations in disease transmission patterns exist between the smaller administrative areas (e.g., counties) with independent local healthcare governance that they contain (*12*). The importance of taking the local context into regard in epidemic forecasting has been further emphasized during the current coronavirus pandemic (*13*). In our prospective 10-year evaluation of local nowcasting in 3 urban counties, the start of the influenza seasons included differed by up to 27 days and the peak intensity by >1 intensity level among the counties, whereas the time-of-peak differences were small. The purpose of the evaluated local detection function was to allow hospitals and primary healthcare centers time to prepare for management of influenza patients (e.g., by preparing intensive care unit resources or postponing some elective procedures). This component showed satisfactory performance in all 3 counties. The peak-timing prediction function was aimed at informing the local authorities when the peak has occurred and that health service routines soon can be permitted to return to normal. This component showed satisfactory performance from the 2011–12 influenza season onward. Predictions of peak timing were made 8–10 days before the peak and were +7 days accurate in most cases. This finding contrasts with the current practices in the study counties, where the peak of an influenza season is retrospectively determined from surveillance data ≈10–14 days after it has occurred. The nowcasting of peak-intensity level was aimed at warning the local authorities about high-intensity influenza transmission and the potential need for social distancing measures (e.g., closure of kindergartens). This component provided satisfactory information for influenza seasons in 2 out of 3 study counties (Stockholm and West Gothia).

Although the evaluated nowcasting method is automated to run on routinely collected healthcare data, the accuracy of the nowcasts depends on the

Table 1. Performance of the detection algorithm displayed with alert thresholds updated by using data from previous nonpandemic influenza seasons in evaluation of nowcasting for detection and prediction of local influenza epidemics, Sweden, 2008–2019

Influenza virus activity	Updated* alert threshold, cases/day/100,000 population†	Timeliness‡	Start according to method	Actual start§	Interpretation
2008–09 A(H3N2), initial retrospective data					
Stockholm	0.63				
West Gothia	0.73				
Scania	0.25				
2009 A(H1N1)					
Stockholm	0.63	−5	2009 Aug 24	2009 Aug 19	Good
West Gothia	0.73	−6	2009 Sep 3	2009 Aug 28	Good
Scania	0.25	18	2009 Aug 13	2009 Aug 31	Poor
2010–11 A(H1N1) and B¶					
Stockholm	0.63	−7	2010 Dec 30	2010 Dec 23	Good
West Gothia	0.73	−12	2011 Jan 9	2010 Dec 28	Poor
Scania	0.25	2	2010 Dec 23	2010 Dec 25	Excellent
2011–12 A(H3N2)					
Stockholm	0.59	2	2012 Jan 22	2012 Jan 24	Excellent
West Gothia	0.43	1	2012 Jan 31	2012 Feb 1	Excellent
Scania	0.27	23	2012 Jan 9	2012 Feb 1	Poor
2012–13 A(H3N2), A(H1N1), and B					
Stockholm	0.51	−6	2013 Jan 3	2012 Dec 28	Good
West Gothia	0.44	0	2012 Dec 29	2012 Dec 29	Excellent
Scania	0.28	0	2012 Dec 27	2012 Dec 27	Excellent
2013–14 A(H3N2), A(H1N1), and B					
Stockholm	0.52	0	2014 Jan 30	2014 Jan 30	Excellent
West Gothia	0.37	1	2014 Jan 27	2014 Jan 28	Excellent
Scania	0.35	0	2014 Jan 28	2014 Jan 28	Excellent
2014–15 A(H3N2) and B					
Stockholm	0.52	−6	2015 Jan 13	2015 Jan 7	Good
West Gothia	0.39	0	2015 Jan 17	2015 Jan 17	Excellent
Scania	0.35	7	2015 Jan 16	2015 Jan 23	Good
2015–16 A(pH1N1) and B					
Stockholm	0.52	0	2016 Jan 2	2016 Jan 2	Excellent
West Gothia	0.47	16	2015 Dec 28	2016 Jan 13	Poor
Scania	0.34	0	2015 Dec 16	2015 Dec 16	Excellent
2016–17 A(H3N2)					
Stockholm	0.34	−2	2016 Dec 1	2016 Nov 29	Excellent
West Gothia	0.31	−2	2016 Dec 17	2016 Dec 15	Excellent
Scania	0.31	0	2016 Dec 10	2016 Dec 10	Excellent
2017–18 A(H3N2) and B					
Stockholm	0.38	0	2017 Dec 12	2017 Dec 12	Excellent
West Gothia	0.44	4	2017 Dec 30	2018 Jan 3	Good
Scania	0.34	5	2017 Dec 22	2017 Dec 27	Good
2018–19 A(pH1N1)					
Stockholm	0.36	−7	2018 Dec 18	2018 Dec 5	Good
West Gothia	0.40	−6	2018 Dec 28	2018 Dec 22	Good
Scania	0.34	5	2018 Dec 27	2019 Jan 1	Good

*Threshold updated after every seasonal influenza (i.e., no updates after pandemic outbreaks).
†Threshold determined using clinical influenza-diagnosis data.
‡Positive value means that the algorithm issued an alarm before the local epidemic had started; negative value means that the alarm was raised after the start of the epidemic.
§Actual start is the date when the retrospectively calculated intensity level reached the predefined threshold for start of an epidemic (6.3 influenza-diagnosis cases/100,000 population recorded during a floating 7-day period) (7,11).
¶No update of threshold before this seasonal influenza because the previous outbreak was a pandemic.

stability of the data supply and information infrastructure over time. The method does not require influenza cases to be confirmed by a laboratory as long as data recording remains relatively stable. Nonetheless, some observations can be made about the sensitivity of the local nowcasts to contextual factors. In Sweden, vaccination adapted to the current circulating strains is made available free-of-cost to the elderly and risk groups before every influenza season. However, in the case of the 2009 influenza A(H1N1) pandemic, a national vaccination campaign was implemented, covering the entire population. This intervention probably influenced the nowcasting performance during the corresponding period. Looking only at the performance for seasonal influenza, we observed outcomes in 1 of the 3 study counties (Scania) that raise concerns about vulnerability of the nowcasts to sociodemographic dynamics (14). Malmö (population 450,000; capital of

Scania County, Sweden) and Copenhagen (population 2 million; capital of Denmark) are connected by a bridge providing for daily commuting between the metropolitan areas, and their labor markets are closely integrated. The epidemic situation in the highly cosmopolitan Copenhagen region might have had a stronger influence on influenza epidemics in Scania County than the epidemic situation in the neighboring regions had on the other study counties. By structured introduction, evaluation, and modification of prediction models that use additional data sources and statistical methods, local nowcasting can be adapted also to

communities with unusual characteristics (*15,16*). This evidence-based strategy means that our method can be incrementally adapted to modeling of, for instance, local rural or semirural communities in which residents commute extensively to a neighboring city that is not included in the model.

Some possible limitations exist in terms of the design of this prospective evaluation that require attention. First and foremost, whether the framework used to interpret the nowcasting performance is adequate from the local health authority perspective should be assessed. Regarding the time-of-peak

Table 2. Performance of peak-timing and peak-intensity predictions from evaluation of nowcasting for detection and prediction of local influenza epidemics, Sweden, 2008–2019

Influenza virus activity	Time-to-peak*				Peak-intensity category, cases/day/100,000 population†§		
	Prediction date	Predicted	Error	Interpretation	Predicted	Factual	Interpretation
2009 A(H1N1)							
Stockholm	2009 Sep 13	8	56	Poor	Medium (5.0)	Very high (12.4)	Poor
West Gothia	2009 Sep 13	8	56	Poor	Low (2.2)	Very high (13.7)	Poor
Scania	2009 Sep 25	10	42	Poor	Low (1.4)	High (6.4)	Poor
2010–11 A(H1N1) and B							
Stockholm	2011 Jan 14	10	28	Poor	Medium (3.4)	Medium (3.5)	Excellent
West Gothia	2011 Jan 14	10	14	Poor	Medium (4.3)	High (6.1)	Tolerable
Scania	2011 Jan 10	11	22	Poor	Medium (2.9)	High (5.5)	Poor
2011–12 A(H3N2)							
Stockholm	2012 Feb 27	8	−8	Tolerable	High (7.4)	Very high (9.4)	Good
West Gothia	2012 Feb 27	8	−8	Tolerable	High (7.8)	Very high (9.6)	Good
Scania	2012 Feb 27	8	−8	Tolerable	Medium (4.0)	High (6.8)	Poor
2012–13 A(H3N2), A(H1N1), and B							
Stockholm	2013 Feb 10	8	−7	Good	Very high (10.3)	Very high (12.2)	Excellent
West Gothia	2013 Feb 10	8	−7	Good	Very high (10.3)	Very high (11.9)	Excellent
Scania	2019 Feb 8	10	−7	Good	High (7.3)	Very high (10.7)	Good
2013–14 A(H3N2), A(H1N1), and B							
Stockholm	2014 Feb 16	8	−7	Good	Medium (2.7)	Medium (3.0)	Excellent
West Gothia	2014 Feb 16	8	−7	Good	Medium (3.5)	Medium (2.9)	Excellent
Scania	2014 Feb 17	8	−1	Excellent	Medium (3.2)	Medium (4.2)	Excellent
2014–15 A(H3N2) and B							
Stockholm	2015 Feb 22	8	6	Good	Medium (4.5)	High (6.5)	Tolerable
West Gothia	2015 Feb 22	8	6	Good	Very high (7.9)	Very high (8.3)	Excellent
Scania	2015 Feb 14	9	0	Excellent	Medium (3.9)	Very high (8.1)	Poor
2015–16 A(H1N1) and B							
Stockholm	2016 Feb 7	8	0	Excellent	High (6.7)	Very high (8.2)	Tolerable
West Gothia	2016 Feb 7	8	7	Good	High (7.6)	Very high (11.6)	Good
Scania	2016 Feb 6	9	7	Good	Medium (4.3)	Very high (10.4)	Poor
2016–17 A(H3N2)							
Stockholm	2017 Jan 1	8	−7	Good	Very high (8.2)	High (6.8)	Good
West Gothia	2017 Feb 12	8	7	Good	Medium (3.3)	Medium (3.7)	Excellent
Scania	2017 Feb 5	8	14	Poor	Medium (4.2)	Medium (5.1)	Excellent
2017–18 A(H3N2) and B							
Stockholm	2018 Feb 18	8	−7	Good	Very high (14.4)	Very high (11.6)	Excellent
West Gothia	2018 Feb 18	8	0	Excellent	Medium (5.2)	High (5.9)	Good
Scania	2018 Feb 4	8	14	Poor	Medium (4.2)	Very high (14.0)	Poor
2018–19 A(H1N1)							
Stockholm	2019 Feb 3	8	0	Excellent	Very high (14.4)	High (6.2)	Poor
West Gothia	2019 Feb 3	8	7	Good	Medium (4.0)	Medium (3.4)	Excellent
Scania	2019 Feb 3	8	−7	Good	Medium (2.8)	Medium (5.2)	Excellent

*Time-to-peak (days) determined using syndromic telenursing data. Positive value means that the peak was predicted to be reached before the actual peak occurs, whereas negative value means that the peak is predicted after the actual peak occurs.
†Peak-intensity category determined using clinical influenza-diagnosis data.
§Using clinical influenza data (Table 1; https://wwwnc.cdc.gov/EID/article/26/11/20-0448-T1.htm), the start of the epidemic was detected on December 27. On February 1, using syndromic data, the peak in clinical influenza data was forecasted to occur 8 days later (February 9), but the peak actually occurred on February 2 (7 days earlier than forecasted). Also, on February 1, the clinical influenza data intensity was forecasted to be high.

predictions, the ongoing FluSight study uses weekly data (*4*), thus accepting forecasts made at a weekly resolution. The evaluation framework used to classify forecasts as excellent was at a higher temporal resolution (less than one half week). This boundary was defined from a county government perspective, where the attention is on local resource allocation (e.g., intensive-care unit facilities and hospital beds) for the care of influenza patients. In this situation, nowcasts that are off by days to weeks might have severe consequences for patients in need of these resources. Categories that are suitable for evaluation of usefulness in local response preparations might not be suitable for interpretation of utility in national or international response planning. These observations suggest that the requirements on the accuracy of peak-timing predictions are context-dependent and warrant further research. Concerning the predictions of peak intensity, evaluation of the peak-intensity forecasts indicated that 22% (6 of 27) of the seasonal influenza nowcasts were poor. Retrospectively documenting baseline and threshold values for influenza epidemics helps define whether an influenza epidemic has been different in intensity compared with previous seasons and thereby contributes to future preparedness planning (*17*,*18*). For the evaluation of intensity predictions in this study, we used the thresholds established using the moving epidemic method from the reference 2008–09 seasonal influenza season. To improve the validity of the assessments, annual updates of the threshold values using county-level data from previous seasons should be considered for future evaluations of local influenza nowcasting.

Longitudinal prospective evaluations might be needed to draw valid conclusions concerning the performance of local epidemic nowcasting, and inclusion of data from urban counties might be required for generalizability (*7*). We found in our study that the performance of seasonal influenza nowcasting was satisfactory during a 10-year period in 3 urban counties regarding local detection and peak-timing prediction performance. The predictions of the local peak-intensity level were satisfactory in 2 of the study counties but poorer in 1 county, possibly because of sudden sociodemographic changes. We conclude that the performance of the local nowcasting method was satisfactory for seasonal influenza. The results are of general interest for local healthcare planning during epidemics because the precision by which healthcare systems can adapt its resources to the management of infected patients in these situations affects the resource availability for all other patient groups.

About the Author

Dr. Spreco is a researcher in the field of syndromic surveillance at Linköping University and Region Östergötland, Sweden. His main research focus is on evaluation and development of algorithms for detection and prediction of infectious diseases.

References

1. Nsoesie EO, Brownstein JS, Ramakrishnan N, Marathe MV. A systematic review of studies on forecasting the dynamics of influenza outbreaks. Influenza Other Respir Viruses. 2014;8:309–16. https://doi.org/10.1111/irv.12226
2. Wu JT, Ho A, Ma ES, Lee CK, Chu DK, Ho PL, et al. Estimating infection attack rates and severity in real time during an influenza pandemic: analysis of serial cross-sectional serologic surveillance data. PLoS Med. 2011;8:e1001103. https://doi.org/10.1371/journal.pmed.1001103
3. Viboud C, Vespignani A. The future of influenza forecasts. Proc Natl Acad Sci U S A. 2019;116:2802–4. https://doi.org/10.1073/pnas.1822167116
4. Reich NG, Brooks LC, Fox SJ, Kandula S, McGowan CJ, Moore E, et al. A collaborative multiyear, multimodel assessment of seasonal influenza forecasting in the United States. Proc Natl Acad Sci U S A. 2019;116:3146–54. https://doi.org/10.1073/pnas.1812594116
5. Schmid F, Wang Y, Harou A. Nowcasting guidelines—a summary. Geneva: World Meteorological Organization; 2019 [cited 2019 Jul 15]. https://public.wmo.int/en/resources/bulletin/nowcasting-guidelines-%E2%80%93-summary
6. Spreco A, Eriksson O, Dahlström Ö, Cowling BJ, Timpka T. Integrated detection and prediction of influenza activity for real-time surveillance: algorithm design. J Med Internet Res. 2017;19:e211. https://doi.org/10.2196/jmir.7101
7. Spreco A, Eriksson O, Dahlström Ö, Cowling BJ, Timpka T. Evaluation of nowcasting for detecting and predicting local influenza epidemics, Sweden, 2009-2014. Emerg Infect Dis. 2018;24:1868–73. https://doi.org/10.3201/eid2410.171940
8. Timpka T, Spreco A, Dahlström Ö, Eriksson O, Gursky E, Ekberg J, et al. Performance of eHealth data sources in local influenza surveillance: a 5-year open cohort study. J Med Internet Res. 2014;16:e116. https://doi.org/10.2196/jmir.3099

9. Timpka T, Spreco A, Eriksson O, Dahlström Ö, Gursky EA, Strömgren M, et al. Predictive performance of telenursing complaints in influenza surveillance: a prospective cohort study in Sweden. Euro Surveill. 2014;19:20966. https://doi.org/10.2807/1560-7917.ES2014.19.46.20966

10. World Health Organization. International statistical classification of diseases and related health problems. 10th revision. Volume 2. Geneva: The Organization; 2010 [cited 2019 Jun 1]. https://www.who.int/classifications/icd/ICD10Volume2_en_2010.pdf

11. Vega T, Lozano JE, Meerhoff T, Snacken R, Beauté J, Jorgensen P, et al. Influenza surveillance in Europe: comparing intensity levels calculated using the moving epidemic method. Influenza Other Respir Viruses. 2015;9:234–46. https://doi.org/10.1111/irv.12330

12. Chen Y, Ong JHY, Rajarethinam J, Yap G, Ng LC, Cook AR. Neighbourhood level real-time forecasting of dengue cases in tropical urban Singapore. BMC Med. 2018;16:129. https://doi.org/10.1186/s12916-018-1108-5

13. García-Basteiro AL, Chaccour C, Guinovart C, Llupià A, Brew J, Trilla A, et al. Monitoring the COVID-19 epidemic in the context of widespread local transmission. Lancet Respir Med. 2020;8:440–2. https://doi.org/10.1016/S2213-2600(20)30162-4

14. Timpka T, Eriksson H, Gursky EA, Nyce JM, Morin M, Jenvald J, et al. Population-based simulations of influenza pandemics: validity and significance for public health policy.

Bull World Health Organ. 2009;87:305–11. https://doi.org/10.2471/BLT.07.050203

15. Soliman M, Lyubchich V, Gel YR. Complementing the power of deep learning with statistical model fusion: probabilistic forecasting of influenza in Dallas County, Texas, USA. Epidemics. 2019;28:100345. https://doi.org/10.1016/j.epidem.2019.05.004

16. Collins GS, Moons KGM. Reporting of artificial intelligence prediction models. Lancet. 2019;393:1577–9. https://doi.org/10.1016/S0140-6736(19)30037-6

17. Ly S, Arashiro T, Ieng V, Tsuyuoka R, Parry A, Horwood P, et al. Establishing seasonal and alert influenza thresholds in Cambodia using the WHO method: implications for effective utilization of influenza surveillance in the tropics and subtropics. Western Pac Surveill Response J. 2017;8:22–32. https://doi.org/10.5365/wpsar.2017.8.1.002

18. Rakocevic B, Grgurevic A, Trajkovic G, Mugosa B, Sipetic Grujicic S, Medenica S, et al. Influenza surveillance: determining the epidemic threshold for influenza by using the Moving Epidemic Method (MEM), Montenegro, 2010/11 to 2017/18 influenza seasons. Euro Surveill. 2019;24:1800042. https://doi.org/10.2807/1560-7917.ES.2019.24.12.1800042

Address for correspondence: Armin Spreco, Division for Public Health and Statistics, Region Östergötland, Linköping, Sweden SE-581 91 Linköping, Sweden; email: armin.spreco@liu.se

Azithromycin to Prevent Pertussis in Household Contacts, Catalonia and Navarre, Spain, 2012–2013

Josep Alvarez, Pere Godoy, Pedro Plans-Rubio, Neus Camps, Monica Carol,
Gloria Carmona, Ruben Solano, Cristina Rius, Sofia Minguell, Irene Barrabeig,
Maria R. Sala-Farré, Raquel Rodriguez, Manuel Garcia-Cenoz, Carmen Muñoz-Almagro,
Angela Dominguez, Transmission of Pertussis in Households Working Group[1]

We retrospectively assessed the effectiveness of azithromycin in preventing transmission of pertussis to a patient's household contacts. We also considered the duration between symptom onset in the primary patient and azithromycin administration. We categorized contacts into 4 groups: those treated within $\leq$7 days, 8–14 days, 15–21 days, and >21 days after illness onset in the primary patient. We studied 476 primary index patients and their 1,975 household contacts, of whom 4.5% were later identified as having pertussis. When contacts started chemoprophylaxis within $\leq$21 days after the primary patient's symptom onset, the treatment was 43.9% effective. Chemoprophylaxis started >14 days after primary patient's symptom onset was less effective. We recommend that contacts of persons with pertussis begin chemoprophylaxis within $\leq$14 days after primary patient's symptom onset.

A fter decades of decline (1,2) and despite high vaccination coverage, the incidence of pertussis has increased substantially in Catalonia, Spain (3,4); Spain (5); and other regions and countries with well-established epidemiologic surveillance systems (6).

Many researchers attribute this pattern to an increasingly waning immunity in persons vaccinated with the acellular vaccines currently used in most countries instead of the whole-cell vaccines used until the late 1990s (7–11).

The causative agent of pertussis, *Bordatella pertussis*, is mainly spread through household contacts (12,13). However, guidelines contain few measures to prevent intrahousehold transmission. Most guidelines recommend patient isolation, vaccination of children <7 years of age, and chemoprophylaxis for household members and other frequent contacts (14,15). Generally, guidelines recommend that household contacts begin chemoprophylaxis with a macrolide within 21 days after symptom onset in the index patient. However, evidence of its effectiveness in preventing transmission is limited (16,17). In addition, there is a lack of studies on the effectiveness of azithromycin, because studies on chemoprophylaxis for pertussis usually use erythromycin (18,19).

A study of pertussis patients in Catalonia and Navarre, 2 autonomous communities in Spain, assessed the overall effectiveness of azithromycin in preventing transmission among household contacts (20). After adjustment for age, sex, vaccination history, and relationship to the primary patient, chemoprophylaxis had an adjusted effectiveness of 62.1% in this study, consistent with the results of other studies (21). However, this study cohort (20) included 164 nonprimary index patients (i.e. patients with the first reported case of pertussis in a household, but not the first chronological case) and their 877 contacts, did not consider the duration between symptom onset in the primary patient and start of treatment, and did

not exclude co-primary and tertiary patients (who might not have been infected by the primary patient) (20). We assessed whether delays in chemoprophylaxis reduce its effectiveness.

Materials and Methods

The study cohort comprised the household contacts of primary index patients with pertussis detected by the Epidemiologic Surveillance Units (ESU) of Catalonia and Navarre from January 1, 2012, through December 31, 2013. We followed up on the household contacts 28 days after symptom onset in the index patient.

The index patient was the first patient with pertussis reported to the ESU in each household and the primary patient was the first patient with pertussis in each household, regardless of whether or when his or her case had been reported. In most situations, the index and primary patients were the same person; for our study, we excluded instances when the index and primary patients were different persons. The ESU prescribed the postexposure intervention for every index patient and their contacts. Our study included only patients with *B. pertussis* infection confirmed by culture or real-time PCR of nasopharyngeal samples. We categorized household contacts as persons regularly living in the same household or persons in the home for >2 hours during the transmission period (≤21 days after symptom onset in the primary patient or ≤5 days after the patient's start of treatment).

ESU staff conducted telephone interviews to gather information about each contact's age, sex, relationship to the index or primary patient, receipt of chemoprophylaxis and start date, vaccination history, and presence of pertussis symptoms (cough lasting ≥2 weeks, paroxysmal cough, posttussive vomiting, inspiratory stridor, and apnea). Staff collected vaccination statuses and laboratory results (i.e., culture assay, PCR) from the contacts' medical records and determined a person's vaccination status using the vaccination records of each autonomous community. We categorized each contact as fully vaccinated (≥4 doses of vaccine), incompletely vaccinated (<4 doses), unvaccinated (no dose), incompletely vaccinated because of age (i.e. children <18 months of age who had received recommended doses), and unvaccinated because of age (i.e. children <2 months of age). Because few contacts >18 years of age had vaccination records, we analyzed this variable only in contacts ≤18 years of age.

At 28 days after symptom onset in the primary patient, we categorized contacts as follows: healthy contact, no clinical symptoms of pertussis; primary patient, the first patient at a specific address (this might differ from the index patient, who had the first reported case); co-primary patient, symptom onset within ≤6 days of the primary patient; secondary patient, symptom onset within 7–28 days after the primary patient; and tertiary patient, symptom onset within >28 days after the primary patient. Before administering treatment, ESU staff took nasopharyngeal samples of each patient and their contacts with possible pertussis symptoms. We considered symptomatic contacts as patients when we confirmed their diagnosis by culture or real-time PCR or found an epidemiologic link (onset of symptoms ≤28 days later) with a laboratory-confirmed case.

We evaluated the characteristics of persons who did or did not receive chemoprophylaxis using χ^2 (for categorical variables) and Student *t*-test (for continuous variables). We then studied the effectiveness of chemoprophylaxis in preventing pertussis in persons classified as healthy contacts or secondary patients after 28 days of follow-up. We excluded co-primary and tertiary patients from the analysis because they might not have been infected by primary patients.

We calculated the effectiveness of azithromycin for 5 days using the formula effectiveness = (1 − relative risk) × 100. We considered effectiveness according to the duration between symptom onset in the primary patient and start of chemoprophylaxis. We classified this duration into 4 categories: 1–7 days, 8–14 days, 15–21 days, and >21 days after illness onset in the primary patient.

We used unconditional logistic regression to estimate effectiveness adjusted by vaccination status. We also assessed effectiveness according to the age of contacts (<1 year, 1 year, 2–3 years, 4–6 years, 7–10 years, 11–18 years, 19–40 years, and >40 years of age), degree of relationship (cohabitants vs. persons in the home >2 hours), and type of relationship with the primary index patient (mother, father, sibling, grandparent, spouse, child, and other). We analyzed the data using SPSS Statistics 18.0 (IBM, https://www.ibm.com), and Epi Info (Centers for Disease Control and Prevention, https://www.cdc.gov).

The Ethics Committee of the Hospital Sant Joan de Deu approved the study (code: PIC-79–11). All contacts and family members gave informed written consent to participate.

Results

From January 1, 2012, through December 31, 2013, the ESU detected 688 cases of pertussis, of which 524 (76.2%) were primary index cases. Of these, 476 (90.8%) case-patients had reported data on the administration and outcome of chemoprophylaxis for

2,051 contacts. We excluded 76 contacts because they were co-primary patients (65 persons) or tertiary patients (11 persons). Therefore, our final study consisted of 1,975 household contacts of 476 primary index patients (hereafter primary patients).

Of the 1,975 contacts we analyzed, 53.5% were female. The mean age was 33.9 (SD ± 20.5) years; 2.2% of contacts were <1 year of age (the most vulnerable group), 34.7% were 19–40 years of age, and 35.4% were >40 years of age. A total of 76.5% of contacts lived with the primary patient; 23.4% of contacts were mothers, 21.5% were fathers, and 19.6% were siblings of the primary patient (Table 1). Most of the 591 contacts ≤18 years of age were completely vaccinated (65.7% had received ≥4 doses and 6.1% were completely vaccinated in accordance with recommendations for their age).

Of the 1,720 (87.1%) contacts who received chemoprophylaxis, 1,266 (73.6%) were treated within ≤21 days after symptom onset of the primary patient: 309 (18%) were treated within ≤7 days, 544 (31.6%) within 8–14 days, 413 (24%) within 15–21 days, and 393 (22.8%) in >21 days. At 28 days after symptom onset in the primary patient, pertussis had developed in 4.5% of contacts, including 1% of those who had received chemoprophylaxis ≤7 days and 7.6% of those who received it >21 days after symptom onset in the primary patient (Figure). The 1,720 (87.1%) contacts

Table 1. Characteristics of household contacts of primary patients with pertussis, Catalonia and Navarre, Spain, 2012–2013

| Characteristic | Contacts* | Received chemoprophylaxis* | | p value† |
		Yes	No	
Total	1,975 (100)	1,720 (87.1)	255 (12.9)	
Sex				
M	919 (46.5)	797 (46.3)	122 (47.8)	0.64
F	1,056 (53.5)	923 (53.7)	133 (52.2)	
Age, y				
<1	44 (2.2)	41 (2.4)	3 (1.2)	0.67
1	33 (1.7)	33 (1.9)	0 (0.0)	
2–3	79 (4.0)	67 (3.9)	12 (4.7)	
4–6	132 (6.7)	120 (7.0)	12 (4.7)	
7–10	154 (7.8)	135 (7.8)	19 (7.5)	
11–18	149 (7.5)	131 (7.6)	18 (7.1)	
19–40	685 (34.7)	595 (34.6)	90 (35.3)	
>40	699 (35.4)	598 (34.8)	101 (39.6)	
Mean age, y (± SD)	33.9 (20.5)	33.4 (20.5)	37.3 (20.6)	0.005‡
Median age, y	36	36	39	
Type of household contact				
Household cohabitant	1,511 (76.5)	1,311 (76.2)	200 (78.4)	0.44
Other >2 h	464 (23.5)	409 (23.8)	55 (21.6)	
Relationship to primary patient				
Mother	463 (23.4)	400 (23.3)	63 (24.7)	0.69
Father	424 (21.5)	366 (21.3)	58 (22.7)	
Sibling	388 (19.6)	352 (20.5)	36 (14.1)	
Grandparent	281 (14.2)	248 (14.4)	33 (12.9)	
Child	19 (1.0)	15 (0.9)	4 (1.6)	
Spouse	26 (1.3)	20 (1.2)	6 (2.4)	
Other	374 (18.9)	319 (18.5)	55 (21.6)	
Vaccination status ≤18 y	591	527	64	
Fully vaccinated (≥4 doses)	388 (65.7)	349 (66.2)	39 (60.9)	0.36
Incomplete for age	36 (6.1)	35 (6.6)	1 (1.6)	
Incomplete	16 (2.7)	15 (2.8)	1 (1.6)	
Not vaccinated	24 (4.1)	21 (4.0)	3 (4.7)	
Too young for vaccination	5 (0.8)	4 (0.8)	1 (1.6)	
Not stated	122 (20.6)	103 (19.5)	19 (29.7)	
Chemoprophylaxis initiation, d§				
1–7	309 (15.6)	309 (18.0)	0	
8–14	544 (27.5)	544 (31.6)	0	
15–21	413 (20.9)	413 (24.0)	0	
>21	393 (19.9)	393 (22.8)	0	
Unknown	61 (3.1)	61 (3.5)	0	
No chemoprophylaxis	255 (12.9)	255 (14.8)	0	
Type of contact				
Healthy contact	1,886 (95.5)	1,645 (95.6)	241 (94.5)	0.44
Secondary case	89 (4.5)	75 (4.4)	14 (5.5)	

*Values are no. (%) except as indicated.
†p value for χ² test.
‡p value for Student t-test.
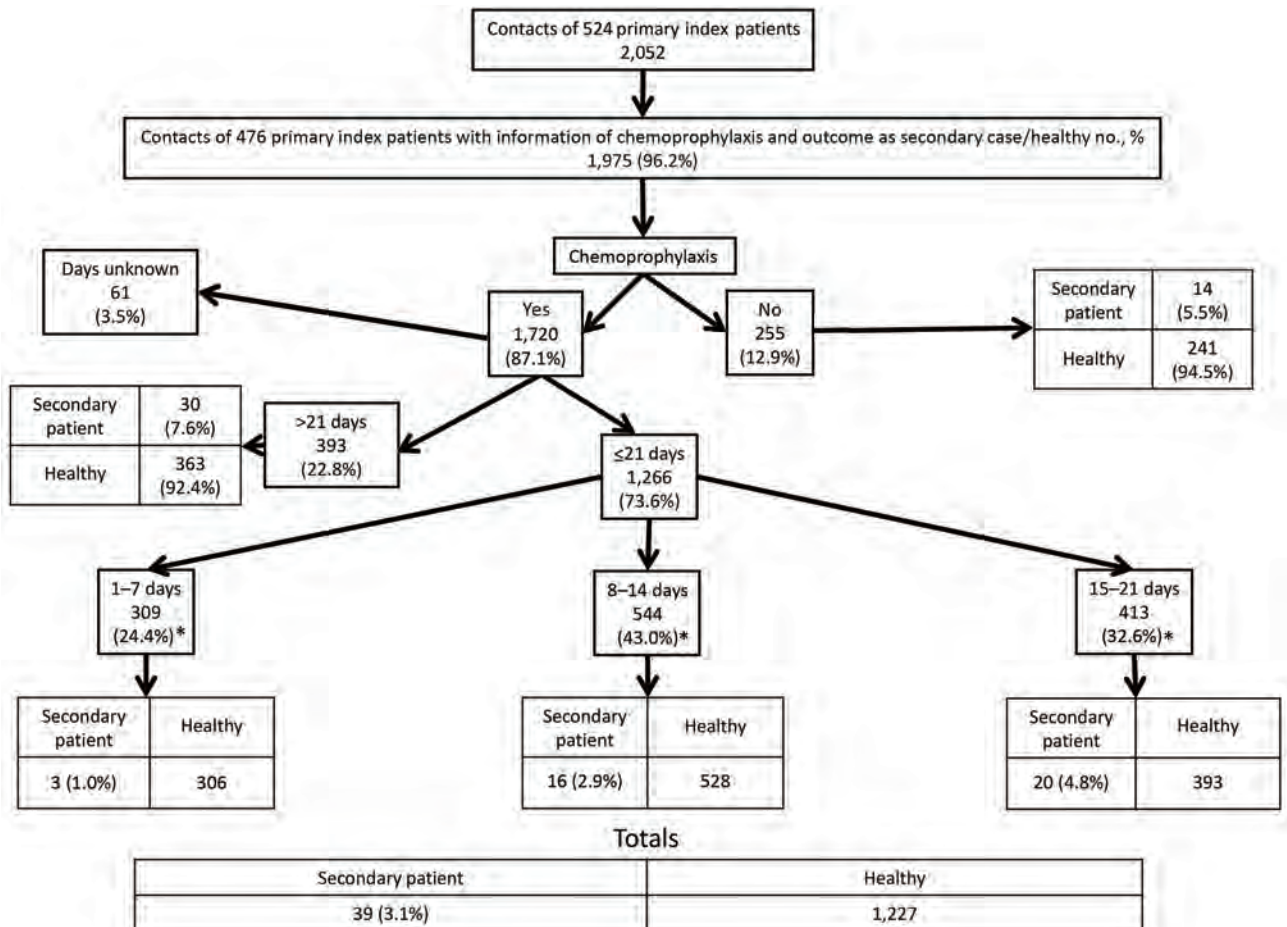§Days after symptom onset of the primary patient.

Figure. Flowchart of study of effectiveness of chemoprophylaxis in preventing pertussis transmission among household contacts of primary index patients, Catalonia and Navarre, Spain, 2012–2013. *Pooled data.

who received and 255 (12.9%) who did not receive chemoprophylaxis differed significantly only by mean age (33.4 vs. 37.3 years) and being a sibling of the primary patient (20.5% vs. 14.1%) (Table 1).

Chemoprophylaxis was 43.9% (95% CI –1.8% to 69.1%) effective when administered ≤21 days after symptom onset in the primary patient. Chemoprophylaxis was ineffective (–39.0% [95% CI –157.0% to 25.0%]) when administered after >21 days (Table 2).

Of contacts ≤18 years of age, 87.6% (298/340) received chemoprophylaxis, which was 44.1% (95% CI –42.2% to 77.7%) effective. Comparison of contacts ≤18 years of age who did and did not receive chemoprophylaxis within ≤21 days showed that chemoprophylaxis was 44.1% (95% CI –59.5% to 80.4%) effective in completely vaccinated persons (e4 doses) and 50% (95% CI –248.0% to 92.8%) effective in incompletely vaccinated persons. This difference was not significant, although the statistical power was very low (16% for completely vaccinated and 8% for unvaccinated persons) (Table 2).

Overall, in comparison with results for contacts who did not receive chemoprophylaxis, the treatment had an effectiveness of 82.3% (95% CI 39.1%–94.9%) for contacts who received it within ≤7 days, 46.4% (95% CI –8.1% to 73.4%) for those who received it within 8–14 days, and 11.8% (95% CI –71.5% to 54.6%) for those who received it within 15–21 days. When we adjusted the results by vaccination history, we found the reduction over time resembled the declining effectiveness (Table 3).

Discussion

Most guidelines recommend that contacts take chemoprophylaxis with azithromycin ≤21 days after symptom onset in the index patient (14,22–24). By only including primary index cases, our study more precisely assessed the effectiveness of chemoprophylaxis in preventing household transmission.

Chemoprophylaxis had an overall effectiveness of 43.9% (95% CI –1.8% to 69.1%), lower than the 62.1% found in the previous study in Catalonia and

Table 2. Effectiveness of chemoprophylaxis to prevent pertussis transmission among 1,975 household contacts, Catalonia and Navarre, Spain, 2012–2013

| Chemoprophylaxis timing for contacts* | No. contacts | Type of contact | | Effectiveness, % (95% CI) |
		Healthy contact, no. (%)	Secondary case-patient, no. (%)	
All	1,914	1831 (95.7)	64 (3.3)	
1–21 d	1,266	1,227 (96.9)	39 (3.1)	43.9 (−1.8 to 69.1)
>21 d	393	363 (92.4)	30 (7.6)	−39.0 (−157.0 to 25.0)
No chemoprophylaxis	255	241 (94.5)	14 (5.5)	Reference
Completely vaccinated				
1–21 d	248	233 (94.0)	15 (6.0)	44.1 (−59.5 to 80.4)
No chemoprophylaxis	37	33 (89.2)	4 (10.8)	Reference
Incompletely vaccinated				
1–21 d	50	45 (90.0)	5 (10.0)	50.0 (−248.0, 92.8)
No chemoprophylaxis	5	4 (80.0)	1 (20.0)	Reference

*No. days after symptom onset in primary patient whose contacts received chemoprophylaxis. Includes vaccination status of contacts ≤18 years of age.

Navarre (*20*). The effectiveness was highest when given during the first 7 days after symptom onset in the primary patient and fell significantly with increased treatment delays.

Our results reinforce the ineffectiveness (*14,24*) (–39.0% [95% CI –157.0% to 25.0%]) of administering chemoprophylaxis >21 days after symptom onset in the primary patient. Chemoprophylaxis also had a low effectiveness when administered after 14 days. Our results indicate that chemoprophylaxis should be started ≤14 days after symptom onset in the primary patient; however, this recommendation conflicts with the established clinical definition of pertussis, which describes a cough lasting ≥2 weeks (*22,25*). Therefore, we recommend that chemoprophylaxis should start immediately after the ESU is alerted to the possibility of pertussis, without waiting for a laboratory-confirmed diagnosis.

Perhaps because of the small number of persons in each category, effectiveness was not associated with age, vaccination status, degree of home contact, or relationship with the primary patient. However, confounding variables might influence the (lack of) association between vaccination status and chemoprophylaxis effectiveness; for example, vaccine effectiveness might wane in some age groups or be bolstered in persons not cohabiting (i.e., point contact instead of prolonged contact) with the primary patient. The effectiveness of chemoprophylaxis should be more closely investigated in children <1 year of age, in whom pertussis is particularly serious.

Our finding that azithromycin was ineffective when administered >14 days after symptom onset in the primary patient suggests that physicians should not initiate chemoprophylaxis after that time. This strategy might reduce costs, potential adverse effects, and risk for azithromycin resistance (*26–28*).

The limited effectiveness of chemoprophylaxis in reducing pertussis transmission highlights the importance of patient isolation until 21 days after symptom onset, or 5 days after treatment initiation (*22,24*). Furthermore, communities should strive for high vaccination coverage; physicians should review the vaccination status of contacts; and physicians should regularly update the vaccination schedule, as recommended by some guidelines (*22*). These measures are especially important when a patient with pertussis has contact with children <1 year of age; pregnant women; immunosuppressed persons; and persons with chronic diseases, such as asthma, cystic fibrosis, or congenital heart disease (*6*).

Our study was subject to several limitations. It lacked the statistical power to estimate the effectiveness of chemoprophylaxis in terms of contact age, degree of home contact, and relationship with the primary patient. We used self-reported data on treatment, so we cannot verify whether contacts complied with treatment. We also cannot rule out the possibility

Table 3. Effect of delay in chemoprophylaxis on preventing pertussis transmission among 1,975 household contacts, Catalonia and Navarre, Spain, 2012–2013

| Chemoprophylaxis for contacts, d* | No. contacts | Type of contact | | Effectiveness, % (95% CI) | Adjusted effectiveness, %† (95% CI) |
		Healthy contact, no. (%)	Secondary case-patient, no. (%)		
1–7	309	306 (99.0)	3 (1.0)	82.3 (39.1, 94.9)	89.0 (6.7, 98.7)
8–14	544	528 (97.1)	16 (2.9)	46.4 (−8.1 to 73.4)	37.2 (−114.9 to 75.4)
15–21	413	393 (95.2)	20 (4.8)	11.8 (−71.5 to 54.6)	2.8 (−171.3 to 65.2)
No chemoprophylaxis	255	241 (94.5)	14 (5.5)	Referent	

*No. days after symptom onset in primary patient whose contacts received chemoprophylaxis.
†Adjusted by vaccination status.

that undetected infected persons could have altered transmission dynamics. Finally, confirmatory laboratory testing was not conducted for 40.4% of secondary patients. However, we believe the probability of misclassification is very low.

In conclusion, our results show azithromycin chemoprophylaxis for pertussis had low effectiveness when initiated >14 days after symptom onset in the primary patient. Therefore, public health services should expedite chemoprophylaxis in homes where contacts of suspected patients have risk factors for this disease.

About the Author

Dr. Alvarez is head of the Epidemiological Surveillance Service, Catalonia Public Health Agency, Barcelona. His primary research interests are community-acquired Legionnaires' disease, tuberculosis, and the spread of pertussis in households.
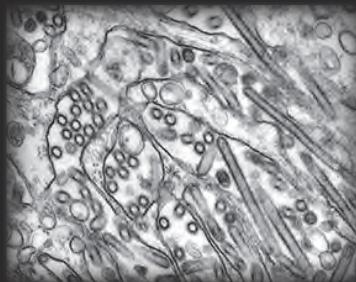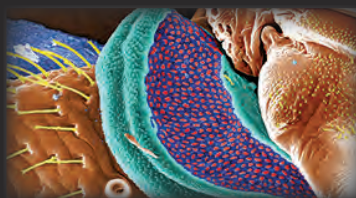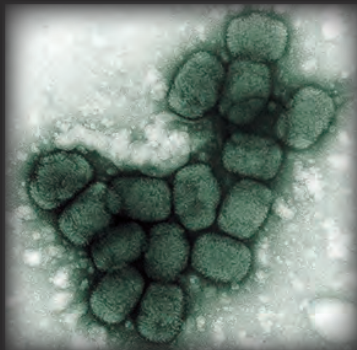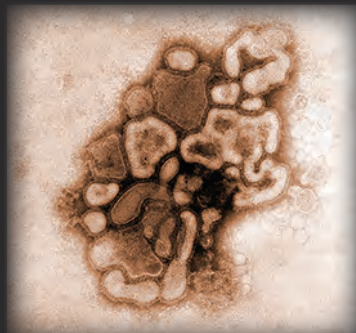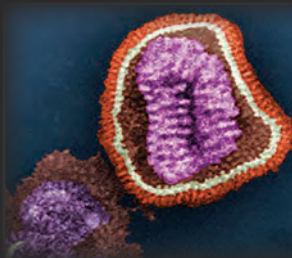
References

1. World Health Organization Strategic Advisory Group of Experts Pertussis Working Group. Background paper [cited 2020 Feb 9]. http://www.who.int/immunization/sage/meetings/2014/april/1_Pertussis_background_FINAL4_web.pdf?ua=
2. Tan T, Dalby T, Forsyth K, Halperin SA, Heininger U, Hozbor D, et al. Pertussis across the globe: recent epidemiologic trends from 2000 to 2013. Pediatr Infect Dis J. 2015;34:e222–32. https://doi.org/10.1097/INF.0000000000000795
3. Crespo I, Cardeñosa N, Godoy P, Carmona G, Sala MR, Barrabeig I, et al. Epidemiology of pertussis in a country with high vaccination coverage. Vaccine. 2011;29:4244–8. https://doi.org/10.1016/j.vaccine.2011.03.065
4. Sala-Farré MR, Arias-Varela C, Recasens-Recasens A, Simó-Sanahuja M, Muñoz-Almagro C, Pérez-Jové J. Pertussis epidemic despite high levels of vaccination coverage with acellular pertussis vaccine. Enferm Infecc Microbiol Clin. 2015;33:27–31. https://doi.org/10.1016/j.eimc.2013.09.013
5. Sizaire V, Garrido-Estepa M, Masa-Calles J, Martinez de Aragon MV. Increase of pertussis incidence in 2010 to 2012 after 12 years of low circulation in Spain. Euro Surveill. 2014;19:20875. https://doi.org/10.2807/1560-7917.ES2014.19.32.20875
6. Hartzell JD, Blaylock JM. Whooping cough in 2014 and beyond: an update and review. Chest. 2014;146:205–14. https://doi.org/10.1378/chest.13-2942
7. Witt MA, Katz PH, Witt DJ. Unexpectedly limited durability of immunity following acellular pertussis vaccination in preadolescents in a North American outbreak. Clin Infect Dis. 2012;54:1730–5. https://doi.org/10.1093/cid/cis287
8. Clark TA. Changing pertussis epidemiology: everything old is new again. J Infect Dis. 2014;209:978–81. https://doi.org/10.1093/infdis/jiu001
9. Clark TA, Messonnier NE, Hadler SC. Pertussis control: time for something new? Trends Microbiol. 2012;20:211–3. https://doi.org/10.1016/j.tim.2012.03.003
10. Klein NP, Bartlett J, Fireman B, Rowhani-Rahbar A, Baxter R. Comparative effectiveness of acellular versus whole-cell pertussis vaccines in teenagers. Pediatrics. 2013;131:e1716–22. https://doi.org/10.1542/peds.2012-3836
11. Klein NP, Bartlett J, Rowhani-Rahbar A, Fireman B, Baxter R. Waning protection after fifth dose of acellular pertussis vaccine in children. N Engl J Med. 2012;367:1012–9. https://doi.org/10.1056/NEJMoa1200850
12. Wendelboe AM, Njamkepo E, Bourillon A, Floret DD, Gaudelus J, Gerber M, et al.; Infant Pertussis Study Group. Transmission of *Bordetella pertussis* to young infants. Pediatr Infect Dis J. 2007;26:293–9. https://doi.org/10.1097/01.inf.0000258699.64164.6d
13. Kowalzik F, Barbosa AP, Fernandes VR, Carvalho PR, Avila-Aguero ML, Goh DYT, et al. Prospective multinational study of pertussis infection in hospitalized infants and their household contacts. Pediatr Infect Dis J. 2007;26:238–42. https://doi.org/10.1097/01.inf.0000256750.07118.ee
14. Tiwari T, Murphy TV, Moran J; National Immunization Program, CDC. Recommended antimicrobial agents for the treatment and postexposure prophylaxis of pertussis: 2005 CDC Guidelines. MMWR Recomm Rep. 2005; 54(RR-14):1–16.
15. Dodhia H, Crowcroft NS, Bramley JC, Miller E. UK guidelines for use of erythromycin chemoprophylaxis in persons exposed to pertussis. J Public Health Med. 2002;24:200–6. https://doi.org/10.1093/pubmed/24.3.200
16. Altunaiji SM, Kukuruzovic RH, Curtis NC, Massie J. Antibiotics for whooping cough (pertussis) [review]. Cochrane Database Syst Rev. 2007;3:CD004404.
17. Goins WP, Edwards KM, Vnencak-Jones CL, Rock MT, Swift M, Thayer V, et al. A comparison of 2 strategies to prevent infection following pertussis exposure in vaccinated healthcare personnel. Clin Infect Dis. 2012;54:938–45. https://doi.org/10.1093/cid/cir973
18. Halperin SA, Bortolussi R, Langley JM, Eastwood BJ, De Serres G. A randomized, placebo-controlled trial of erythromycin estolate chemoprophylaxis for household contacts of children with culture-positive *bordetella pertussis* infection. Pediatrics. 1999;104:e42. https://doi.org/10.1542/peds.104.4.e42
19. Langley JM, Halperin SA, Boucher FD, Smith B; Pediatric Investigators Collaborative Network on Infections in Canada (PICNIC). Azithromycin is as effective as and better tolerated

than erythromycin estolate for the treatment of pertussis. Pediatrics. 2004;114:e96–101. https://doi.org/10.1542/peds.114.1.e96

20. Godoy P, García-Cenoz M, Toledo D, Carmona G, Caylà JA, Alsedà M, et al.; Transmission of Pertussis in Households Working Group. Factors influencing the spread of pertussis in households: a prospective study, Catalonia and Navarre, Spain, 2012 to 2013. Euro Surveill. 2016;21:24–33. https://doi.org/10.2807/1560-7917.ES.2016.21.45.30393

21. Baptista PN, Magalhães VS, Rodrigues LC. Children with pertussis inform the investigation of other pertussis cases among contacts. BMC Pediatr. 2007;7:21. https://doi.org/10.1186/1471-2431-7-21

22. Haut Conseil de la Santé Publique. Conduit â tenir devant un ou plusieurs cas de coqueluche [cited 2019 Nov 11]. http://www.sante.gouv.fr/IMG/pdf/hcspr20140710_conduitenircascoqueluche.pdf

23. Public Health England. Guidelines for the public health management of pertussis in England [cited 2019 Nov 11]. https://www.gov.uk/government/uploads/system/uploads/attachment_data/file/541694/Guidelines_for_the_Public_Health_management_of_Pertussis_in_England.pdf

24. Britton PH, Jones CA. Pertussis prophylaxis. Aust Prescr. 2012;35:82–4. https://doi.org/10.18773/austprescr.2012.036

25. The European Commission. Commission implementing decision (EU) 2018/945 of 22 June 2018 on the communicable diseases and related special health issues to be covered by epidemiological surveillance as well as relevant case definitions [cited 2020 702/09]. https://eur-lex.europa.eu/legal-content/EN/TXT/PDF/?uri=CELEX:32018D0945&from=EN#page=32

26. Pour AM, Allensworth CD, Clark TA, Liang JL, Cullison P, Messonnier ML, et al.; Centers for Disease Control and Prevention (CDC). Local health department costs associated with response to a school-based pertussis outbreak—Omaha, Nebraska, September–November 2008. MMWR Morb Mortal Wkly Rep. 2011;60:5–9.

27. Thampi N, Gurol-Urganci I, Crowcroft NS, Sander B. Pertussis post-exposure prophylaxis among household contacts: a cost-utility analysis. PLoS One. 2015;10:e0119271. https://doi.org/10.1371/journal.pone.0119271

28. Wang Z, Li Y, Hou T, Liu X, Liu Y, Yu T, et al. Appearance of macrolide-resistant *Bordetella pertussis* strains in China. Antimicrob Agents Chemother. 2013;57:5193–4. https://doi.org/10.1128/AAC.01081-13

Address for correspondence: Pere Godoy, Departament de Salut, Epidemiología Alcalde Rovira Roure 2 Lleida, Lleida 25006 Spain; email: pere.godoy@gencat.cat

Modeling Treatment Strategies to Inform Yaws Eradication

Alex Holmes, Michael J. Tildesley, Anthony W. Solomon,
David C.W. Mabey, Oliver Sokana, Michael Marks, Louise Dyson

Yaws is a neglected tropical disease targeted for eradication by 2030. To achieve eradication, finding and treating asymptomatic infections as well as clinical cases is crucial. The proposed plan, the Morges strategy, involves rounds of total community treatment (i.e., treating the whole population) and total targeted treatment (TTT) (i.e., treating clinical cases and contacts). However, modeling and empirical work suggests asymptomatic infections often are not found in the same households as clinical cases, reducing the utility of household-based contact tracing for a TTT strategy. We use a model fitted to data from the Solomon Islands to predict the likelihood of elimination of transmission under different intervention schemes and levels of systematic nontreatment resulting from the intervention. Our results indicate that implementing additional treatment rounds through total community treatment is more effective than conducting additional rounds of treatment of at-risk persons through TTT.

Yaws is an infectious disease found in South America, Asia, Africa, and Oceania. It is caused by *Treponema pallidum* subspecies *pertenue* (*1*), an organism morphologically identical to *T. pallidum* subsp. *pallidum*, which causes syphilis. Yaws can manifest as skin lesions, involvement of the bones and joints, and eventually irreversible disfigurement. It is spread by direct contact between a susceptible person and lesions of infectious persons and particularly affects persons 2–15 years of age.

In the 1950s, the World Health Organization (WHO) and UNICEF led efforts to eradicate yaws through mass treatment with benzathine benzylpenicillin (*2*),

Author affiliations: Mathematics Institute, University of Warwick, Coventry, UK (A. Holmes, M.J. Tildesley, L. Dyson); University of Warwick School of Life Sciences, Coventry (M.J. Tildesley, L. Dyson); Hospital for Tropical Diseases, London, UK (A.W. Solomon, D.C.W. Mabey, M. Marks); London School of Hygiene and Tropical Medicine, London (A.W. Solomon, D.C.W. Mabey, M. Marks); Ministry of Health and Medical Services, Honiara, Solomon Islands (O. Sokana)

reducing the number of cases worldwide by ≈95% (*3*). Yaws then fell off the public health agenda and has since resurged in several countries. Eradication efforts were renewed when, in 2012, a study (*4*) showed that treatment with a single oral dose of azithromycin was noninferior to benzathine benzylpenicillin and did not require cold chains, injection equipment, or special training to administer, thus reducing the logistic barriers to mass drug administration and potentially making eradication more feasible.

In 2012, in response to this finding, member states of WHO committed to eradicate yaws by 2020 (*5*), although more recently 2030 has been suggested as a more realistic target (*6*). The primary reason for this change was the high number of countries in which yaws is still endemic, and the even higher number of previously yaws-endemic countries whose current endemicity status is currently unknown. The current eradication strategy, known as the Morges strategy, consists of treatment with single-dose oral azithromycin in 2 modes of community-based intervention: total community treatment (TCT) and total targeted treatment (TTT) (*7*). TCT attempts to treat everyone in a given community (village or town) regardless of the number of active clinical cases, whereas TTT treats active clinical case-patients and their contacts, where contacts are those in the same household or school or are playmates of affected persons (*8*). In response to evidence from pilot studies that a single round of TCT is not sufficient to interrupt transmission, WHO has proposed revising the strategy (*9*). The revised strategy suggests that, in most circumstances, 2–3 rounds of TCT are likely to be required, followed by TTT performed at intervals of 6–12 months (*9*). TCT is designed for situations in which a large proportion of the population is infected, whereas TTT is intended to treat a small number of remaining cases once elimination of transmission (EOT) appears close.

T. pallidum subsp. *pertenue* infection can be divided into active yaws and latent yaws. Active yaws can then be split further into primary, secondary, and tertiary yaws (*10*). After an incubation period averaging

21 days (range 9–90 days), primary yaws initially manifests as a papule at the site of inoculation. The papule then enlarges, lasting for 3–6 months. Early secondary yaws lesions might appear near the initial lesion and persist >6 months. These lesions heal spontaneously, leading to a noninfectious latent period that can last the remaining lifetime of the person (*11*). However, the state of latency can end at any time by the reappearance of infectious lesions. Tertiary yaws lesions are now rarely seen (*12*), but when they do manifest, they appear years after primary yaws and are often destructive but are noninfectious.

A considerable challenge for eradicating yaws is the existence of asymptomatic persons, who together harbor a large reservoir of infection. For each active case of yaws, as many as 6–10 cases of latent yaws might exist (*13*). If we are not treating the whole community, successfully treating clinical case-patients and latently infected persons is essential. The assumption conceptually underlying TTT is that asymptomatic persons are likely to be close contacts of existing clinical case-patients.

The difficulty of diagnosing latent yaws in adults also represents a challenge for researchers attempting to understand the dynamics of transmission. Serologic testing cannot distinguish between syphilis and yaws infections; thus, only children <15 years of age typically have serologic tests performed (*3*).

In this article, we extend previous yaws modeling work by incorporating household structure and simulations of eradication strategies into the model. We evaluate the Morges strategy and variants of it for their suitability in meeting the WHO goal of yaws eradication. We investigate the likely effect of different assumptions regarding coverage during rounds of TCT on the success of a strategy and the effect systematic nonadherence could have on its effectiveness. We also consider whether regular surveillance could be an effective component of a program seeking to meet the WHO goal.

Methods

We adapted the Markov model developed by Dyson et al. (*14*). The model consists of houses, each containing several inhabitants. Persons might be classified as susceptible, infected and infectious, or asymptomatically infected but not infectious. Within each household, susceptible persons might become infected by other persons from within their household or from other households. From the infectious state, a person can either recover and reenter the susceptible state, or they can have onset of a latent infection, entering the asymptomatic state. From the asymptomatic state, persons can either recover, entering the susceptible state, or the infectious lesions can recur, causing them to reenter the infectious state. These transitions are summarized in Table 1 and Figure 1. In Dyson et al. (*14*) this model was fitted at steady state to data from the Solomon Islands (*13*), using a presumed constant rate of between-household infection. In our study, we extended the model to include a dynamic rate of between-household infection, which we assumed to be proportional to the total prevalence of infectious persons in the population at a given time (Appendix, https://wwwnc.cdc.gov/EID/article/26/11/19-1491-App1.pdf). We took parameter values from posterior distributions with maximum posterior value drawn from expert opinion and previous model-fitting to Solomon Islands data (*14*) (Table 2).

We considered a population of 5,000 households, with sizes distributed according to empirical data from the Solomon Islands (Figure 2), representing a population of ≈20,000 persons. Each treatment scheme consisted of several rounds of TCT, followed by several rounds of TTT. During TTT, we defined a contact to be anyone in the same household as an infectious person. We assumed an optimistic coverage of 100% of active case-patients and their contacts given treatment during rounds of TTT (a conservative assumption under the hypothesis that TTT is not an effective strategy), TCT coverage of 80% (*3*), and azithromycin efficacy of 95% (*10*). We considered up to 10 rounds of TCT and up to 10 rounds of TTT. Treatment rounds would be scheduled, on the basis of WHO guidelines (*9*), at 6-month intervals, with all rounds of TCT being performed before any TTT. Using the Gillespie algorithm (*15*), simulations were run to steady state before starting treatment and then run for an additional 150 months to simulate the time remaining to

Table 1. Permitted state transitions and state transition rates for steady state household model of yaws transmission*

Description	State transition	Rate
Infection, external (ε) and within-household (β)	(S,I,A) → (S-1,I+1,A)	$\varepsilon + \dfrac{\beta I}{N-1}$
Treatment/birth-death	(S,I,A) → (S+1,I-1,A)	δ
Remission	(S,I,A) → (S,I-1,A+1)	λ
Recurrence	(S,I,A) → (S,I+1,A-1)	ρ
Treatment/birth-death	(S,I,A) → (S+1,I,A-1)	δ

*Methods described in Appendix (https://wwwnc.cdc.gov/EID/article/26/11/19-1491-App1.pdf). A, asymptomatically infected (but not infectious); I, infected and infectious; S, susceptible.
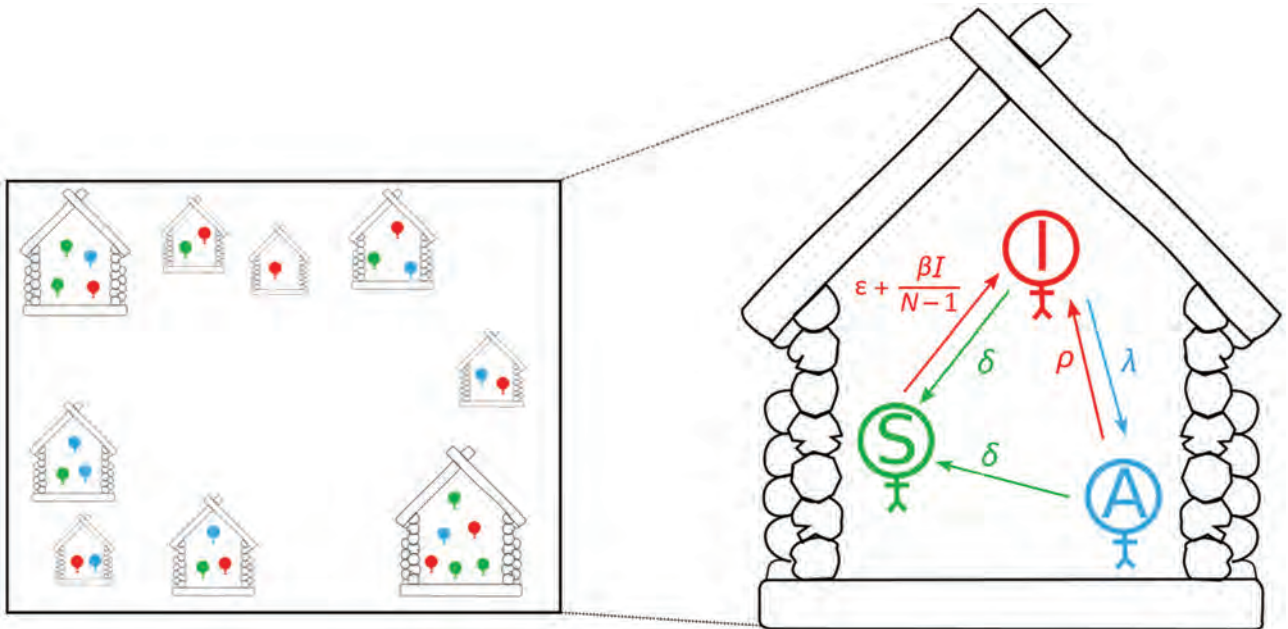
Figure 1. Graphic representation of the model being used for yaws transmission. Each house shape indicates a household, and the number of shapes inside each indicates number of persons. Each person is either susceptible (S, green), infectious (I, red), or asymptomatic (A, blue). Close-up image at right shows details of model parameters (see Tables 1, 2).

meet the 2030 deadline. We simulated each scenario 2,240 times and took the mean of the results.

We then considered the effect of population size on the probability of campaign success (i.e., whether a specific treatment campaign would be more successful in areas with greater or fewer persons). We considered population sizes ranging from 100 to 50,000 households, using 2 rounds of TCT followed by 2 rounds of TTT.

Although coverage is likely to be important in determining how successful a mass treatment campaign would be (*16*), recent modeling work has shown that the quality of coverage is also critical (*17*); for example, whether the same persons receive treatment in each round has a substantial effect on the likelihood

Table 2. Parameter values for household structured yaws transmission model, based on data collected from the Solomon Islands*

Parameter	Value	Source
β	0.0516	(*13*)
δ	0.0513	(*13*)
λ	0.185	(*14,15*)
ρ	0.0165	(*13*)
ε†	0.004	(*13*)
α‡	0.1669	Appendix

*Given parameter value is the maximum posterior value of the distribution from which each parameter is drawn, with the exception of λ which is consistent with expert opinion. Methods described in Appendix (https://wwwnc.cdc.gov/EID/article/26/11/19-1491-App1.pdf).
†Steady state external force of infection.
‡Between-household rate of infection corresponding to a steady state external force of infection ε.

of EOT. Treatment campaigns that repeatedly miss the same persons are said to have a high level of systematic nontreatment. Models of treatment campaigns usually assume that a random selection of persons receive treatment in each round. However, this likely overestimates the effectiveness of a TCT round. We therefore developed a framework, as laid out in Fitzpatrick et al. (*18*), for mass drug administration, in which we could control person-level treatment correlation between rounds (i.e., if a person is treated in 1 round, how likely are they to be treated in a subsequent round?). For the sake of illustration, we can consider the special cases in which the correlation coefficient (ρ) is 0 or 1. Where ρ = 0, treatment status in 1 treatment round is not associated with the probability of treatment in subsequent treatment rounds, which are independent events. Where ρ = 1, in each treatment round, the same persons are treated, and the same persons are not treated.

We investigated the effect of assigning different values to ρ on the modeled effectiveness of intervention. For ρ>0, we considered treatment status only at household level. So, for ρ = 1, the same households (and everyone in those households) would be treated every round, whereas for 0<ρ<1, each person in the same household has the same probability of receiving treatment, which is different to the persons in other households.

We also considered the use of more frequent, lower-intensity treatment. This could be delivered

by, for example, a volunteer offering azithromycin to persons who the volunteer thinks have yaws. We investigated whether this treatment would reduce the required number of rounds of TTT by using an estimated coverage of 5% of infectious persons and their household contacts every month, in addition to rounds of TCT/TTT every 6 months (up to 10 rounds of TCT, and up to 10 rounds of TTT).

Results

We first consider the dynamics under 3 different treatment strategies, chosen as strategies that have been previously discussed by yaws experts. These strategies, and the probability of EOT calculated for each, are summarized in Table 3. Although an extra round of treatment of either kind is beneficial, an extra round of TCT outperforms an extra round of TTT (Figure 3). In Figure 4, we plot EOT probability for up to 8 additional rounds of TCT or TTT, from a base intervention of 2 rounds of TCT and 2 rounds of TTT. Increasing the number of rounds of TCT increases the probability of EOT more rapidly than including additional rounds of TTT. In fact, an additional 4–5 TTT rounds would be required to achieve the same effect as 1 additional round of TCT.

We extend this further by comparing the effectiveness of 120 different treatment strategies, plus a control strategy in which no antibiotic treatment is provided, in a population of 5,000 households. Any strategy involving <3 rounds of TCT is unlikely to be effective in meeting the 2030 WHO goal for yaws (Figure 5). When we assume a TCT coverage of 90%, we still find that ≥3 rounds should be considered (Appendix). TTT does not directly precipitate EOT by treating all cases. Instead, multiple rounds of TTT serve to keep infection prevalence low, so that in a small population infection eventually disappears stochastically. Effective population size therefore influences the probability of EOT (i.e., infection in a smaller population is more susceptible to stochasticity). Effective population size refers to the population that interacts, so that an isolated small village will have a small population size, whereas multiple villages sharing schools with substantial between-village intermingling have a larger effective size than the individual villages.

Figure 6 shows EOT probability with changing effective population size using a fixed strategy of 2 rounds of TCT followed by 2 rounds of TTT. As the effective population size increases, the probability of EOT decreases, with the probability approaching 0 at ≈10,000 households.

As coverage becomes more systematic (so that treatments tend to be given repeatedly to the same
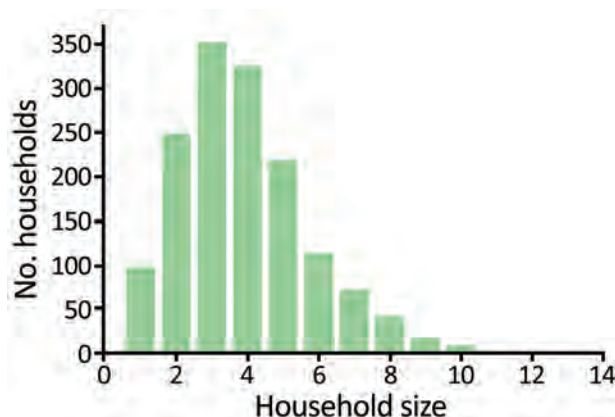

Figure 2. Distribution of household sizes in the model being used for yaws transmission, based on data collected from the Solomon Islands in 2013.

persons), the number of cases increases and the probability of EOT decreases substantially (Figure 7). Although random coverage resulted in a probability of EOT of 15%, this result fell to 2% with fully systematic coverage. Each scheme we considered consists of 2 rounds of TCT followed by 2 rounds of TTT. As the correlation between rounds of treatment increases, the probability of EOT decreases substantially, particularly for lower correlations, as we start moving away from random to more systematic treatment (Figure 8).

Since TTT primarily acts by keeping the infectious population at a sufficiently low level that stochasticity eventually leads to elimination, we hypothesize that a lower level of more frequent treatment might act as a potential replacement for TTT. We consider the strategies investigated (Table 3), this time incorporating a monthly volunteer treatment with a coverage of 5% (Table 4). Under a strategy of 2 rounds of TCT followed by 2 rounds of TTT, the probability of elimination increased from 15% to 53% when we incorporated this low-level regular treatment, an increase of 38 percentage points. Similar increases were observed for the other 2 strategies. We noted a very small increase in probability of elimination achieved when performing a third round of TTT, suggesting that TTT has very limited effect with this volunteer treatment. Extending this to the full range of strategies previously considered, we

Table 3. Summary of yaws treatment strategies*

Strategy	Rounds of TCT	Rounds of TTT	Probability of elimination
1	2	2	15%
2	3	2	57%
3	2	3	26%

*As shown in Figure 3 (https://wwwnc.cdc.gov/EID/article/26/11/19-1491-F3.htm). TCT, total community treatment; TTT, total targeted treatment.
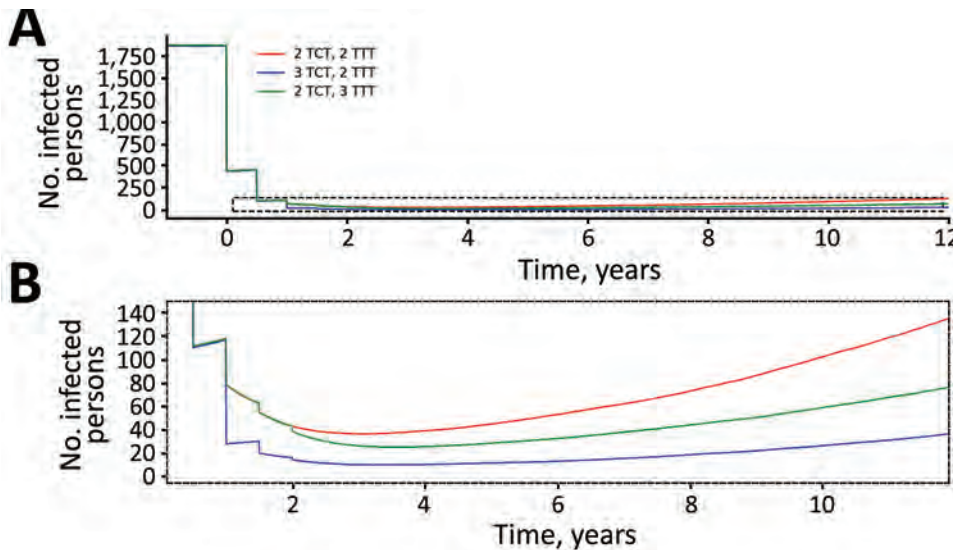
Figure 3. Dynamics of yaws transmission (clinical infectious and latent cases combined, averaged over 1,000 simulations) under 3 different treatment strategies: 2 TCT, 2 TTT (red); 3 TCT, 2 TTT (blue); 2 TCT, 3 TTT (green). A) All parameters tested; B) close-up showing detail of results. Simulations are run to steady state before starting the first round of treatment. Times given are the amount of time (in years) since the first round of treatment. Parameters are inferred from data collected from the Solomon Islands in 2013. TCT, total community treatment; TTT, total targeted treatment.

observe that additional rounds of TTT have a reduced effect compared with interventions without background treatment (Figure 9). Further reductions in impact are observed when more rounds of TCT are undertaken (Figures 10, 11). When performing 2 rounds of TCT, increasing volunteer coverage leads to increased probabilities of EOT unless >5 rounds of TTT are undertaken. When using 4 rounds of TCT, increasing the number of rounds of TTT performed results in very little increase in the probability of EOT, regardless of the number of rounds of TTT performed.
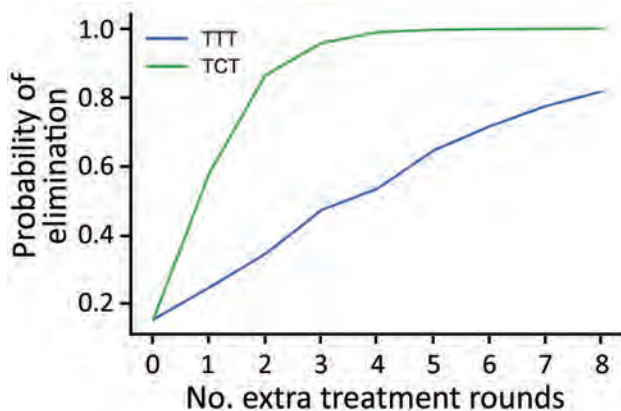
Discussion

We used a stochastic household-level model of yaws transmission to consider the likely effectiveness of various treatment strategies in the eradication of yaws. As expected, we found that more rounds of TCT and TTT led to higher probability of EOT. However, in our model, EOT was not directly achieved through treatment itself. Rather, TTT served to keep the infection prevalence low, so that yaws eventually disappeared through chance events (i.e., TCT acts to reduce the prevalence of infection to a low level, which is then maintained by TTT until elimination
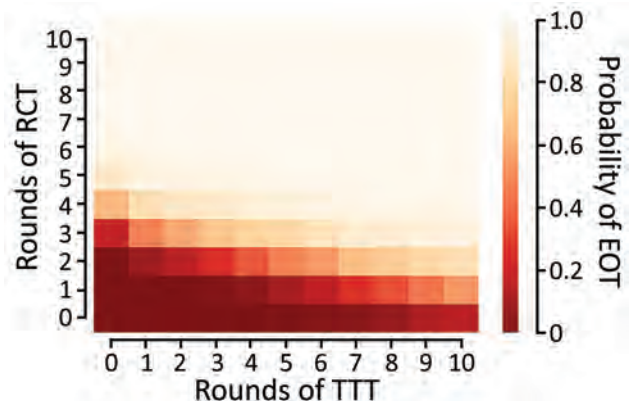

Figure 4. Probability of local elimination of transmission under different intervention strategies consisting of >2 rounds of TCT and >2 rounds of TTT, with varying numbers of additional rounds of TTT (blue) or TCT (green). Each twice-yearly round of TCT has 80% coverage, whereas TTT has 100% coverage and treatment is assumed to have 95% efficacy. All rounds of TCT are performed first before any rounds of TTT begin, which are then also performed twice yearly. Parameters are inferred from data collected from the Solomon Islands in 2013. TCT, total community treatment; TTT, total targeted treatment.

Figure 5. Probability of local elimination of transmission under different intervention strategies with varying numbers of rounds of TCT followed by rounds of TTT treating clinical case-patients and household contacts. Each rectangle in the figure represents a different strategy (consisting of some number of rounds of TCT followed by rounds of TTT). The color of the rectangle shows the probability of elimination of transmission, based on the color bar to the right. Each twice-yearly round of TCT has 80% coverage, whereas TTT has 100% coverage and treatment is assumed to have 95% efficacy. Parameters are inferred from data collected from the Solomon Islands in 2013. TCT, total community treatment; TTT, total targeted treatment.

Figure 6. Probability of local elimination of transmission for varying population sizes after 2 rounds of TCT followed by 2 rounds of TTT, 6 months apart. TCT has 80% coverage, and TTT has 100% coverage, and treatment is assumed to have 95% efficacy. Parameters are inferred from data collected from the Solomon Islands in 2013. TCT, total community treatment; TTT, total targeted treatment.
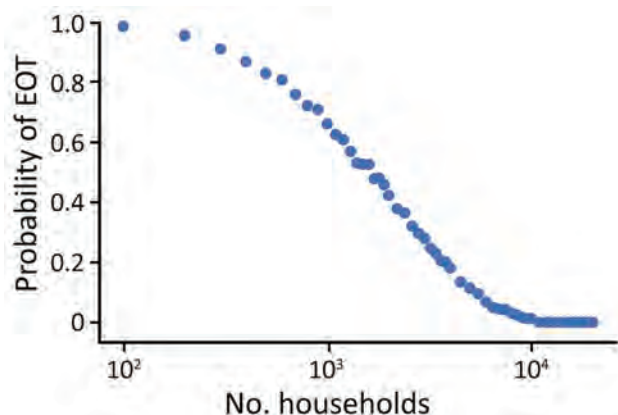

Figure 7. Dynamics of infected yaws (clinical infectious cases and latent cases) under random (red) or fully systematic (blue) coverage when implementing mass drug administration. Simulations are run to steady state before starting the first round of treatment. Times given are the amount of time since the first round of treatment. Treatment involved 2 twice-yearly rounds of TCT, followed by 2 twice-yearly rounds of TTT. TCT has a coverage of 80%, whereas TTT has a coverage of 100% of all infectious persons and their household contacts. Azithromycin efficacy is assumed to be 95%. Shaded regions denote values within 1 SD of the mean value. Parameters are inferred from data collected from the Solomon Islands in 2013. TCT, total community treatment; TTT, total targeted treatment.

occurs). As such, TCT should be considered the principal driving force for EOT. To efficiently reach elimination, according to our model, multiple rounds of TCT need to be implemented, and TTT should not be considered an effective method for reducing prevalence of infection. Indeed, it would take up to 5 rounds of TTT to achieve the same effect as 1 additional round of TCT. The original Morges strategy, in which only a single round of TCT is advised, is unlikely to enable us to meet the WHO 2030 goal. However, the revised strategy, in which 2–3 rounds of TCT are advised, is more likely to meet this goal if linked to appropriate ongoing surveillance after TCT. However, further rounds of TCT will likely be required if 90% coverage is not attained. This conclusion is consistent with the conclusions of previous modeling work (using the same data) (*14,16*), and recent empirical findings from Papua New Guinea (*19*).

Because the effect of chance events was found to be a critical factor in determining success, we next considered the effect of population size on the effectiveness of an eradication campaign. We found that, for a given treatment scheme, the size of the population had a considerable influence on the probability of EOT (i.e., a given strategy is more likely to be successful for smaller than larger populations). The corollary of this finding is that the intervention strategy used in any context should be influenced by the size of the population being treated. This conclusion should be considered in parallel with the conclusion outlined above. For stochasticity to successfully drive EOT, the prevalence of infection after completion of the rounds of TCT needs to be sufficiently small. The larger the population, the greater will be the
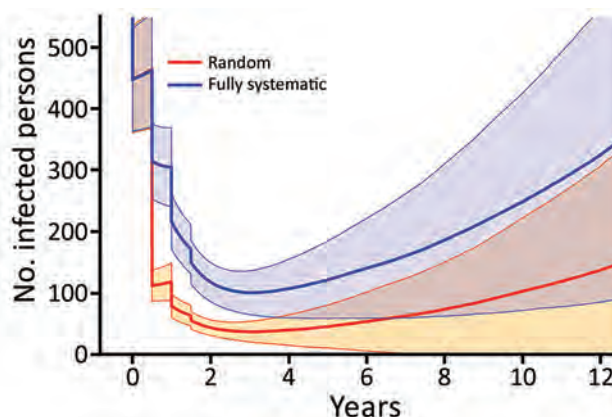
number of rounds of TCT required to reduce the infection prevalence to the appropriate threshold (Figure 6).

Although the effect of varying treatment coverage levels is widely appreciated, the critical importance of the quality of the coverage is less well understood. The effect of rounds of TCT will be modified by the
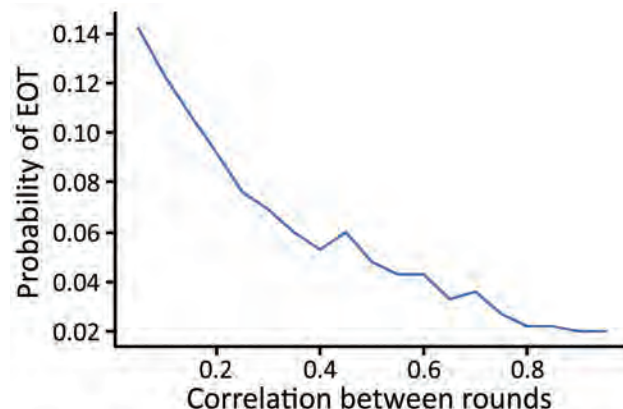
Figure 8. Probability of local elimination of transmission under intervention strategy consisting of 2 rounds of TCT, followed by 2 rounds of TTT treating clinical cases and household contacts as correlation between treatment rounds varies. 0 correlation denotes random treatment, whereas a correlation of 1 denotes fully systematic treatment. Each twice-yearly round of TCT has 80% coverage, whereas TTT has 100% coverage, and treatment is assumed to have 95% efficacy. Parameters are inferred from data collected from the Solomon Islands in 2013. TCT, total community treatment; TTT, total targeted treatment.

Table 4. Summary of yaws treatment strategies with and without regular surveillance*

Strategy	Rounds of TCT	Rounds of TTT	Volunteer treatment coverage	Probability of elimination
1a	2	2	0%	15%
1b	2	2	5%	53%
2a	3	2	0%	57%
2b	3	2	5%	71%
3a	2	3	0%	26%
3b	2	3	5%	56%

*Strategies labeled "a'" are those without any regular surveillance, whereas "b" indicates the corresponding strategy with regular surveillance. TCT, total community treatment; TTT, total targeted treatment.

coverage attained and the level of systematic nontreatment. When we assume treatment with some level of systematic nontreatment, we find that treatment is substantially less effective, given that under these schemes the same persons are treated many times, whereas others are never treated. Because any treatment campaign will likely suffer from some level of systematic nontreatment (in terms of correlation of treatment status between different treatment rounds), programs need to take this into account. As such, when undertaking a treatment campaign, maximizing not just the coverage of the campaign but also the quality of that coverage is beneficial. In short, if we always treat the same persons and miss the same persons, a perpetual reservoir of infection might be maintained, undercutting efforts to interrupt transmission.

Because TTT primarily acts by keeping the infectious population at a sufficiently low level that stochasticity eventually leads to elimination, we hypothesized

Figure 9. Probability of local elimination of transmission under different intervention strategies with varying numbers of rounds of TCT followed by rounds of TTT treating clinical case-patients and household contacts. Each rectangle in the figure represents a different strategy (consisting of some number of rounds of TCT followed by rounds of TTT). The color of the rectangle shows the probability of elimination of transmission, based on the color bar to the right. Each twice-yearly round of TCT has 80% coverage, whereas TTT has 100% coverage, and treatment is assumed to have 95% efficacy. An additional type of treatment round is administered once a month, giving treatment to 5% of infectious persons and their household contacts. Parameters are inferred from data collected from the Solomon Islands in 2013. TCT, total community treatment; TTT, total targeted treatment.

that a lower level of more frequent treatment might act as a potential replacement for TTT. This end could be accomplished through volunteers handing out azithromycin to infected persons and their household contacts on a monthly (or more frequent) basis. We found this approach to be very effective (theoretically) in increasing the probability of EOT. Once the prevalence of infection was at a sufficiently low level, 5% coverage with ongoing treatment was sufficient to maintain that prevalence until infection was eliminated because of chance. After ≥4 rounds of TCT, this finding was valid regardless of whether any TTT was performed, perhaps indicating that TTT is redundant. This finding further supports the concept that additional rounds of TCT could be prioritized over TTT, particularly if low-level background antibiotic treatment could be subsequently deployed. Strategies to support ongoing community surveillance deserve further consideration and could link with ongoing regular surveillance for other neglected tropical diseases (20,21). This approach is supported by a successful elimination campaign in India, in which cash incentives were offered to persons who identified persons with confirmed cases.

Our study has several limitations, which might be addressed in future work. First, we defined a TTT contact as a person in the same household as an infectious person. Extending this to include multiple nearby households, villages, or schools might affect model results. Treating school contacts could be particularly relevant because most new cases of yaws are found in children, which could suggest schools are important settings for transmission. Second, our model includes adults and children in a single class; however, given age-stratified data, we could model treatment effectiveness separately for adults and children, resulting in, for example, age-dependent treatment strategies, such as only treating children, which has been empirically tested for the use of azithromycin in trachoma elimination (22). Higher coverage could be more reasonably achieved in younger age groups by yaws programs if this extension of the contact definition was incorporated. Third, spatial heterogeneities might play a role in affecting the transmission of yaws. In parts of the Solomon Islands, persons generally live near the coast and rarely walk through
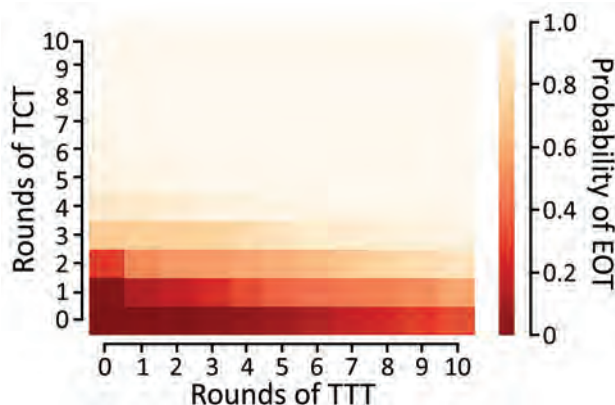
the center of the island. Because an implementation unit is likely to consist of several villages, the population's spatial distribution and movement patterns might limit the spread of infection. Including this information in our analyses could potentially more closely reflect real-world transmission dynamics.

Reintroduction of yaws from outside the implementation site, although not directly relevant to our research question (which relates to the optimal control strategy within a given area), is possible and should be kept in mind for future yaws modeling work. Similarly, recent reports suggest that nonhuman primates can be reservoirs for yaws bacteria. If further evidence that transmission from nonhuman primates to humans is found, such findings should be considered in future models.

Recent reports have shown that as with the *T. pallidum* subsp. *palldium* bacteria that cause syphilis, the *T. pallidum* subsp. *pertenue* bacteria that cause yaws can develop azithromycin resistance (*19,23*). Although penicillin would remain effective in this scenario, such resistance is an important concern for yaws eradication, and how likely implementation strategies are to generate resistance is a critical research question. Although drug resistance is currently a lesser concern than the relapse of latent infection, which is what we investigated in this study, collection of further data on drug resistance should be prioritized so that this possibility can be investigated and incorporated into future models.

In summary, we have shown that the current iteration of the Morges strategy is unlikely to help programs meet the WHO 2030 goal of global yaws eradication. We have suggested alternative strategies that might increase the likelihood of achieving this goal. In particular, we found that further rounds of TCT should be preferred to TTT. We have also shown that population size and quality of coverage can greatly affect the success of a treatment campaign and thus need to be considered in program design. Finally, further consideration should be given to strategies supporting ongoing community surveillance, which could be integrated with ongoing surveillance for other neglected tropical diseases.

Figure 10. Probability of eradication under a strategy of 2 rounds of TCT with a varying number of rounds of TTT. Additional treatment rounds have coverages of 0% (blue), 1% (yellow), 2% (green), 3% (red), 4% (purple), and 5% (brown). Low-coverage treatment of infected persons and their household contacts occurs once a month. Parameters are inferred from data collected from the Solomon Islands in 2013. TCT, total community treatment; TTT, total targeted treatment.
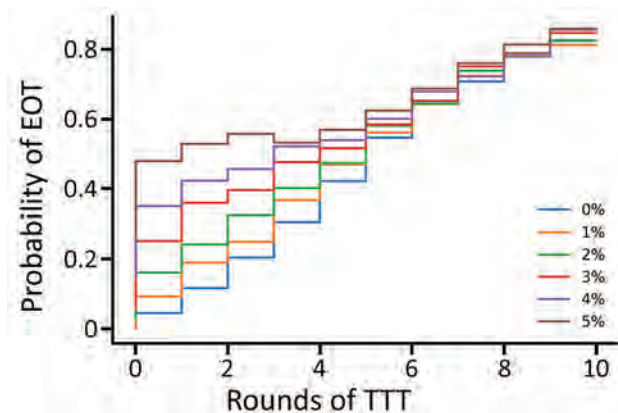
Figure 11. Probability of eradication under a strategy of 4 rounds of TCT with a varying number of rounds of TTT. Additional treatment rounds have coverages of 0% (blue), 1% (yellow), 2% (green), 3% (red), 4% (purple), and 5% (brown). Low-coverage treatment of infected persons and their household contacts occurs once a month. Parameters are inferred from data collected from the Solomon Islands in 2013. TCT, total community treatment; TTT, total targeted treatment.

About the Author

Mr. Holmes is a PhD student at the Mathematics for Real-World Systems Centre for Doctoral Training based at the University of Warwick. His primary research interests are in modeling approaches to investigate eradication strategies for yaws.

References

1. Mitjà O, Asiedu K, Mabey D. Yaws. Lancet. 2013;381:763–73. https://doi.org/10.1016/S0140-6736(12)62130-8
2. Antal GM, Causse G. The control of endemic treponematoses. Rev Infect Dis. 1985;7(Suppl 2):S220–6. https://doi.org/10.1093/clinids/7-Supplement_2.S220
3. Mitjà O, Houinei W, Moses P, Kapa A, Paru R, Hays R, et al. Mass treatment with single-dose azithromycin for yaws. N Engl J Med. 2015;372:703–10. https://doi.org/10.1056/NEJMoa1408586
4. Mitjà O, Hays R, Ipai A, Penias M, Paru R, Fagaho D, et al. Single-dose azithromycin versus benzathine benzylpenicillin for treatment of yaws in children in Papua New Guinea: an open-label, non-inferiority, randomised trial. Lancet. 2012;379:342–7. https://doi.org/10.1016/S0140-6736(11)61624-3
5. World Health Organization. Accelerating work to overcome the global impact of neglected tropical diseases: a roadmap for implementation—executive summary. 2012 [cited 2020 Apr 22]. https://apps.who.int/iris/handle/10665/70809
6. World Health Organization. NTD roadmap landscape 2021–2030. 2019 [cited 2020 Apr 22]. https://www.who.int/neglected_diseases/news/NTD-Roadmap-targets-2021-2030.pdf
7. World Health Organization. Eradication of yaws—the Morges strategy. Wkly Epidemiol Rec. 2012;87:189–94.
8. World Health Organization. Eradication strategy—the new eradication initiative [cited 2020 Apr 22]. http://www.who.int/yaws/strategy
9. World Health Organization. Eradication of yaws: a guide for programme managers. 2018 [cited 2020 Apr 22]. https://www.who.int/yaws/resources/9789241512695
10. Marks M, Mitjà O, Solomon AW, Asiedu KB, Mabey DC. Yaws. Br Med Bull. 2015;113:91–100. https://doi.org/10.1093/bmb/ldu037
11. World Health Organization. Handbook of endemic treponematoses: yaws, endemic syphilis, and pinta. 1984 [cited 2020 Apr 22]. https://w]ww.who.int/yaws/resources/9241541768
12. Marks M, Solomon AW, Mabey DC. Endemic treponemal diseases. Trans R Soc Trop Med Hyg. 2014;108:601–7. https://doi.org/10.1093/trstmh/tru128
13. Marks M, Vahi V, Sokana O, Puiahi E, Pavluck A, Zhang Z, et al. Mapping the epidemiology of yaws in the Solomon Islands: a cluster randomized survey. Am J Trop Med Hyg. 2015;92:129–33. https://doi.org/10.4269/ajtmh.14-0438
14. Dyson L, Marks M, Crook OM, Sokana O, Solomon AW, Bishop A, et al. Targeted treatment of yaws with household contact tracing: how much do we miss? Am J Epidemiol. 2018;187:837–44. https://doi.org/10.1093/aje/kwx305
15. Daniel T. Gillespie. Exact stochastic simulation of coupled chemical reactions. J Phys Chem. 1977;81:2340–61. https://doi.org/10.1021/j100540a008
16. Marks M, Mitjà O, Fitzpatrick C, Asiedu K, Solomon AW, Mabey DCW, et al. Mathematical modeling of programmatic requirements for yaws eradication. Emerg Infect Dis. 2017;23:22–8. https://doi.org/10.3201/eid2301.160487
17. Dyson L, Stolk WA, Farrell SH, Hollingsworth TD. Measuring and modelling the effects of systematic non-adherence to mass drug administration. Epidemics. 2017;18:56–66. https://doi.org/10.1016/j.epidem.2017.02.002
18. Fitzpatrick C, Asiedu K, Jannin J. Where the road ends, yaws begins? The cost-effectiveness of eradication versus more roads. PLoS Negl Trop Dis. 2014;8:e3165. https://doi.org/10.1371/journal.pntd.0003165
19. Mitjà O, Godornes C, Houinei W, Kapa A, Paru R, Abel H, et al. Re-emergence of yaws after single mass azithromycin treatment followed by targeted treatment: a longitudinal study. Lancet. 2018;391:1599–607. https://doi.org/10.1016/S0140-6736(18)30204-6
20. Mitjà O, Marks M, Bertran L, Kollie K, Argaw D, Fahal AH, et al. Integrated control and management of neglected tropical skin diseases. PLoS Negl Trop Dis. 2017;11:e0005136. https://doi.org/10.1371/journal.pntd.0005136
21. World Health Organization. Recognizing neglected tropical diseases through changes on the skin: a training guide for front-line health workers. 2018 [cited 2020 Apr 22]. https://www.who.int/neglected_diseases/resources/9789241513531
22. Amza A, Kadri B, Nassirou B, Cotter SY, Stoller NE, Zhou Z, et al. A cluster-randomized trial to assess the efficacy of targeting trachoma treatment to children. Clin Infect Dis. 2017;64:743–50.
23. Šmajs D, Paštěková L, Grillová L. Macrolide resistance in the syphilis spirochete, *Treponema pallidum* ssp. *pallidum*: can we also expect macrolide-resistant yaws strains? Am J Trop Med Hyg. 2015;93:678–83. https://doi.org/10.4269/ajtmh.15-0316

Address for correspondence: Alexander Holmes, Centre for Complexity Science, Warwick Mathematics Institute, Zeeman Building, University of Warwick, Coventry, CV4 7AL, UK; email: alexander.holmes@warwick.ac.uk

Multidrug-Resistant *Candida auris* Infections in Critically Ill Coronavirus Disease Patients, India, April–July 2020

Anuradha Chowdhary, Bansidhar Tarai, Ashutosh Singh, Amit Sharma

In New Delhi, India, candidemia affected 15 critically ill coronavirus disease patients admitted to an intensive care unit during April–July 2020. *Candida auris* accounted for two thirds of cases; case-fatality rate was high (60%). Hospital-acquired *C. auris* infections in coronavirus disease patients may lead to adverse outcomes and additional strain on healthcare resources.

The ongoing coronavirus disease (COVID-19) pandemic has overwhelmed healthcare systems worldwide. Reports from China and New York have highlighted the concern for nosocomial infections, primarily bacterial, in critically ill COVID-19 patients (*1–3*). Secondary *Candida* spp. bloodstream infections in COVID-19 patients with prolonged intensive care unit (ICU) stays have not been documented. However, a new concern coinciding with the brisk expansion of critical care facilities for COVID-19 patients is the potential for nosocomial spread of *Candida auris* infections (*4*). *C. auris* is a global health threat because of its ability to colonize skin, persist in environments, cause nosocomial outbreaks, and lead to severe disease with high mortality rates (*5,6*).

The Study

Following up on our prediction (*4*), we report bloodstream infections caused by multidrug resistant *C. auris* in 1 COVID-19 ICU in New Delhi, India. A total of 596 patients with confirmed COVID were admitted to the 65-bed ICU during April–July 2020. Of these, 420 patients required mechanical ventilation. Overall, candidemia was detected in 15 (2.5%) of the 596 ICU

Author affiliations: Vallabhbhai Patel Chest Institute of the University of Delhi, New Delhi, India (A. Chowdhary, A. Singh); Max Health Care Institute, New Delhi (B. Tarai); International Centre for Genetic Engineering and Biotechnology, New Delhi (A. Sharma)

patients; the predominant agent was *C. auris* for 10 (67%) of those patients. For the remaining 5 patients, candidemia was caused by *C. albicans* (n = 3), *C. tropicalis* (n = 1), and *C. krusei* (n = 1).

We abstracted the following data for the candidemia patients: baseline demographics, medical history, laboratory parameters, microbiological findings, concomitant antimicrobial drug use, and treatments. Isolates were identified by matrix-assisted laser desorption/ionization time-of-flight mass spectrometry (MALDI Biotyper, https://www.bruker.com). In addition, species identification was conducted by amplification and sequencing of the internal transcribed spacer region of ribosomal DNA and of the D1/D2 domain of the large subunit ribosomal DNA. Antifungal susceptibility testing was performed by using the Clinical and Laboratory Standards Institute brothmicrodilution method M27-A3/S4 (*7*). Antifungals tested were fluconazole, voriconazole, posaconazole, isavuconazole, 5-flucytosine, caspofungin, micafungin, anidulafungin, and amphotericin B.

Most of the 10 patients with *C. auris* infection were elderly (8 patients were 66–88 years of age) and male (7 patients) (Table 1, https://wwwnc.cdc.gov/EID/article/26/11/20-3504-T1.htm). *C. auris* was cultured from paired blood samples from all 10 patients and also from urine for 2 of these patients. All of the COVID-19 patients in whom *C. auris* infections developed had been hospitalized in the ICU for prolonged periods (20–60 days) and had underlying chronic conditions (e.g., hypertension, n = 7; diabetes mellitus, n = 6; and chronic kidney and liver disease, n = 2). Candidemia caused by *C. auris* developed 10–42 days after admission. Half (50%) of the patients with *C. auris* infections received mechanical ventilation as a result of severe COVID-19 pneumonia. Furthermore, all patients with candidemia had indwelling central lines and urinary catheters. Of the 15 patients, COVID-19

was hospital acquired for 2 (acquired 2 and 7 weeks after hospital admission). Severity parameters for COVID-19 were elevated for all patients with candidemia (Table 1). Among the 15 candidemia patients, 8 (53%) died; among those with *C. auris* infection, the fatality rate was 60%. Of note, 4 of the 6 patients who died experienced persistent fungemia, and despite micafungin therapy for 5 days, *C. auris* again grew in blood culture.

Antifungal susceptibility testing data for *C. auris* isolates from 10 patients showed that all isolates were resistant to fluconazole (MIC $\geq$32 mg/L) and 30% were nonsusceptible to voriconazole (MIC $\geq$2 mg/L). Furthermore, 40% were resistant to amphotericin B (MIC $\geq$2 mg/L) and 60% were resistant to 5-flucytosine (MIC $\geq$32 mg/L). Overall, 30% of *C. auris* isolates were multiazole (fluconazole + voriconazole) resistant; whereas, 70% were multidrug resistant, including 30% (n = 3) that were resistant to 3 classes of drugs (azoles + amphotericin B + 5-flucytosine) and 4 that were resistant to 2 classes of drugs (azoles + 5-flucytosine and azoles + amphotericin B). All isolates were susceptible to echinocandins (Table 2, https://wwwnc.cdc.gov/EID/article/26/11/20-3504-T2.htm).

Conclusions

Our findings highlight the role of hospital-acquired *C. auris* bloodstream infections; the patients were probably infected while hospitalized. *C. auris* can be transmitted in healthcare settings just like other multidrug-resistant organisms, such as carbapenem-resistant *Enterobacteriaceae* and methicillin-resistant *Staphylococcus aureus* (*4*). For 4 of 10 patients studied, bacteremia caused by *Enterobacter cloacae* and *Staphylococcus haemolyticus* was also noted. In patients with severe COVID-19, the rate of secondary infections was substantially higher, as has been reported by Goyal et al. (6% of cases of secondary bacterial infections in the United States) (*3*) and Zhou et al. (15% of cases of secondary bacterial infections in China) (*8*). Among fungal co-infections in France, the incidence of putative invasive pulmonary aspergillosis was high (30%) (*9*).

Several major outbreaks of bloodstream infections caused by *C. auris* have been reported in India, the United Kingdom, Colombia, South Africa, and the United States (*5,10–12*). In our report, all patients in the ICU had indwelling invasive devices such as central venous and urinary catheters, which may be the source of *C. auris* infections (i.e., candidemia and urinary tract infection). We anticipate that transmission of *C. auris* to COVID-19 patients by healthcare personnel is unlikely because of the use of personal protective equipment. However, incorrect and extended use of personal protective equipment can lead to self-contamination and transmission.

Of note, 6 of the 10 patients died, possibly because of multiple underlying health conditions. However, 67% of those who died had persistent candidemia, which may have contributed to their death. Furthermore, multidrug-resistant *C. auris* affects the choice of antifungal therapy and treatment outcomes. Most *C. auris* isolates are resistant to fluconazole, and pan-resistant isolates have been described (*13*). All *C. auris* isolates in our study were resistant to fluconazole, and 40% were resistant to amphotericin B, both of which are commonly used in resource-limited countries; therefore, resistance to both classes of drug by *C. auris* is highly concerning because use of other antifungals such as echinocandins are limited in these countries.

Candidemia affected 2.5% of the COVID-19 patients in this cohort admitted to the ICU. In a tertiary care center in New Delhi, *C. auris* was reportedly the second most common *Candida* species that caused candidemia in non-COVID patients (*14*). Extensive contamination of the hospital environment has been detected in hospitals experiencing outbreaks of *C. auris* infection, warranting adherence to strict hospital infection prevention practices, such as enhanced cleaning of rooms with chlorine-based disinfectants at high concentrations (0.5%) for highly resistant pathogens such as *C. auris*. Critically ill COVID-19 patients with *C. auris* infection tend to have concurrent conditions (e.g., diabetes mellitus, chronic kidney disease) and risk factors (e.g., need for mechanical ventilation, receipt of steroids). To reduce complications, admission times in overburdened hospitals, and death rates among COVID-19 patients, identifying and treating *C. auris* infections is vital. A recent report that investigated changes in the fecal fungal microbiomes of COVID-19 patients has shown increasing prevalence of opportunistic fungal pathogens such as *C. albicans*, *C. auris*, and *Aspergillus flavus* (*15*). These data, along with our findings, provide evidence that the ongoing COVID-19 pandemic may provide ideal conditions for outbreaks of *C. auris* in hospital ICUs (*4*). Thus, during the COVID-19 pandemic, extra caution is warranted in hospitals, regions, cities, and countries where *C. auris* is prevalent.

About the Author

Dr. Chowdhary is a clinical microbiologist and a professor at the Vallabhbhai Patel Chest Institute, New Delhi, India. Her main research interest includes fungal infections.

References

1. Ruan Q, Yang K, Wang W, Jiang L, Song J. Clinical predictors of mortality due to COVID-19 based on an analysis of data of 150 patients from Wuhan, China. Intensive Care Med. 2020;46:846–8. https://doi.org/10.1007/s00134-020-05991-x
2. He Y, Li W, Wang Z, Chen H, Tian L, Liu D. Nosocomial infection among patients with COVID-19: a retrospective data analysis of 918 cases from a single center in Wuhan, China. Infect Control Hosp Epidemiol. 2020;41:982–3.
3. Goyal P, Choi JJ, Pinheiro LC, Schenck EJ, Chen R, Jabri A, et al. Clinical characteristics of Covid-19 in New York City. N Engl J Med. 2020;382:2372–4. https://doi.org/10.1056/NEJMc2010419
4. Chowdhary A, Sharma A. The lurking scourge of multidrug resistant *Candida auris* in times of COVID-19 pandemic. J Glob Antimicrob Resist. 2020;22:175–6. https://doi.org/10.1016/j.jgar.2020.06.003
5. Cortegiani A, Misseri G, Fasciana T, Giammanco A, Giarratano A, Chowdhary A. Epidemiology, clinical characteristics, resistance, and treatment of infections by *Candida auris*. J Intensive Care. 2018;6:69. https://doi.org/10.1186/s40560-018-0342-4
6. Chowdhary A, Sharma C, Meis JF. *Candida auris*: a rapidly emerging cause of hospital-acquired multidrug-resistant fungal infections globally. PLoS Pathog. 2017;13:e1006290. https://doi.org/10.1371/journal.ppat.1006290
7. Clinical and Laboratory Standards Institute. Reference method for broth dilution antifungal susceptibility testing of yeasts: 4th informational supplement (M27–S4). Wayne (PA): The Institute; 2012.
8. Zhou F, Yu T, Du R, Fan G, Liu Y, Liu Z, et al. Clinical course and risk factors for mortality of adult inpatients with COVID-19 in Wuhan, China: a retrospective cohort study. Lancet. 2020;395:1054–62. https://doi.org/10.1016/S0140-6736(20)30566-3
9. Alanio A, Dellière S, Fodil S, Bretagne S, Mégarbane B. Prevalence of putative invasive pulmonary aspergillosis in critically ill patients with COVID-19. Lancet Respir Med. 2020;8:e48–9. https://doi.org/10.1016/S2213-2600(20)30237-X
10. Chowdhary A, Sharma C, Duggal S, Agarwal K, Prakash A, Singh PK, et al. New clonal strain of *Candida auris*, Delhi, India. Emerg Infect Dis 2013;19:1670–3.
11. Adams E, Quinn M, Tsay S, Poirot E, Chaturvedi S, Southwick K, et al.; *Candida auris* Investigation Workgroup. *Candida auris* in healthcare facilities, New York, USA, 2013–2017. Emerg Infect Dis. 2018;24:1816–24. https://doi.org/10.3201/eid2410.180649
12. Arensman K, Miller JL, Chiang A, Mai N, Levato J, LaChance E, et al. Clinical outcomes of patients treated for *Candida auris* infections in a multisite health system, Illinois, USA. Emerg Infect Dis. 2020;26:876–80. https://doi.org/10.3201/eid2605.191588
13. Chowdhary A, Prakash A, Sharma C, Kordalewska M, Kumar A, Sarma S, et al. A multicentre study of antifungal susceptibility patterns among 350 *Candida auris* isolates (2009–17) in India: role of the *ERG11* and *FKS1* genes in azole and echinocandin resistance. J Antimicrob Chemother. 2018;73:891–9. https://doi.org/10.1093/jac/dkx480
14. Mathur P, Hasan F, Singh PK, Malhotra R, Walia K, Chowdhary A. Five-year profile of candidaemia at an Indian trauma centre: high rates of *Candida auris* blood stream infections. Mycoses. 2018;61:674–80. https://doi.org/10.1111/myc.12790
15. Zuo T, Zhan H, Zhang F, Liu Q, Tso EYK, Lui GCY, et al. Alterations in fecal fungal microbiome of patients with COVID-19 during time of hospitalization until discharge. Gastroenterology. 2020 Jun 26 [Epub ahead of print]. https://doi.org/10.1053/j.gastro.2020.06.048

Address for correspondence: Pr. Anuradha Chowdhary, Department of Medical Mycology, VP Chest Institute, University of Delhi, New Delhi 110007, India; email: dranuradha@hotmail.com

Potential Role of Social Distancing in Mitigating Spread of Coronavirus Disease, South Korea

Sang Woo Park, Kaiyuan Sun, Cécile Viboud, Bryan T. Grenfell, Jonathan Dushoff

In South Korea, the coronavirus disease outbreak peaked at the end of February and subsided in mid-March. We analyzed the likely roles of social distancing in reducing transmission. Our analysis indicated that although transmission might persist in some regions, epidemics can be suppressed with less extreme measures than those taken by China.

The first coronavirus disease (COVID-19) case in South Korea was confirmed on January 20, 2020 (*1*). In the city of Daegu, the disease spread rapidly within a church community after the city's first case was reported on February 18 (*1*). Chains of transmission that began from this cluster distinguish the epidemic in South Korea from that in any other country. As of March 16, a total of 8,236 cases were confirmed, of which 61% were related to the church (*1*).

The Daegu Metropolitan Government implemented several measures to prevent the spread of COVID-19. On February 20, the Daegu Metropolitan Government recommended wearing masks in everyday life and staying indoors (*2*). On February 23, South Korea raised its national alert level to the highest level (*1*) and delayed the start of school semesters (*3*). Intensive testing and contact tracing enabled rapid identification and isolation of case-patients and reduction of onward transmission (*4*). We describe potential roles of social distancing in mitigating CO-VID-19 spread in South Korea by comparing metropolitan traffic data with transmission in 2 major cities.

The Study

We analyzed epidemiologic data describing the COVID-19 outbreak in South Korea during January

Author affiliations: Princeton University, Princeton, New Jersey, USA (S.W. Park, B.T. Grenfell); National Institutes of Health, Bethesda, Maryland, USA (K. Sun, C. Viboud, B.T. Grenfell); McMaster University, Hamilton, Ontario, Canada (J. Dushoff)

20–March 16. We transcribed daily numbers of reported cases in each municipality from Korea Centers for Disease Control and Prevention (KCDC) press releases (*1*). We also transcribed partial line lists from press releases by KCDC and municipal governments. All data and code are stored in a publicly available GitHub repository (https://github.com/parksw3/Korea-analysis).

We compared epidemiologic dynamics of COV-ID-19 from 2 major cities: Daegu (2020 population: 2.4 million) and Seoul (2020 population: 9.7 million). During January 20–March 16, KCDC reported 6,083 cases from Daegu and 248 from Seoul. The Daegu epidemic was characterized by a single large peak followed by a decrease (Figure 1, panel A); the Seoul epidemic comprised several small outbreaks (Figure 1, panel B).

We obtained the daily number of persons who boarded the subway or monorail in Daegu and Seoul during 2017–2020. For Daegu, we used data from https://data.go.kr for lines 1–3; for Seoul, we used data from https://data.seoul.go.kr for lines 1–9 (Figure 1). Soon after the first church-related case was reported, traffic volume decreased by ≈80% in Daegu and ≈50% in Seoul. To our knowledge, KCDC first recommended social distancing on February 29 (*1*), and no official guidelines existed regarding public transportation, which suggests that distancing was, at least in part, voluntary.

We reconstructed the time series of a proxy for incidence of infection I_t, representing the number of persons who became infected at time t and reported later, and estimated the instantaneous reproduction number, R_t, defined as the average number of secondary infections caused by an infected person, given conditions at time t (*5*). We adjusted the daily number of reported cases to account for changes in testing criteria and censoring bias (Appendix, https://wwwnc.cdc.gov/EID/article/26/11/20-1099-App1.pdf) and then sampled infection dates using inferred onset-to-confirmation delay distributions from the partial line list (Appendix Figure 1) and previous

estimated incubation period distribution (Table) to obtain our incidence proxy, I_t. Finally, we estimated R_t on the basis of the renewal equation (5):

$$R_t = \frac{I_t}{\sum_{k=1}^{14} I_{t-k} w_k}$$

where w_t is the generation-interval distribution randomly drawn from a prior distribution (Table). We weighted each sample of R_t using a gamma probability distribution with a mean of 2.6 and a SD ± 2 to reflect prior knowledge (S. Abbott, unpub. data, https://doi.org/10.12688/wellcomeopenres.16006.1) and took weighted quantiles to calculate medians and associated 95% credible intervals. We estimated R_t for February 2 (14 days after the first confirmed case) through March 10 (after which the effects of censoring were too strong for reliable estimates) (Appendix). All analyses were performed using R version 3.6.1 (https://www.r-project.org).

We reconstructed incidence proxy (Figure 2, panels A, B) and estimates of R_t (Figure 2, panels C, D) in Daegu and Seoul. In Daegu, incidence peaked shortly after the first case was confirmed (Figure 2, panel A). In Daegu, symptoms had developed in the first case-patient on February 7; this person had visited the church on February 9 and 16, indicating the disease probably was spreading within the church community earlier (1). Likewise, the estimates of R_t gradually decreased and eventually decreased to <1 approximately 1 week after the first case was reported, coinciding with the decrease in the metropolitan traffic volume (Figure 2, panel C). The initial decrease in R_t was likely to have been caused by our resampling method for infection times for each reported case, which oversmooths the incidence curve and the R_t estimates (K. Gostic, unpub. data, https://doi.org/10.1101/2020.06.18.20134

858). In Seoul, estimates of R_t decreased slightly but remained at ≈1 (Figure 2, panel D), which might be explained by less-intense social distancing. Stronger distancing or further intervention would have been necessary to reduce R_t to <1 by March 10.

Although we found clear, positive correlations on a daily scale between normalized traffic and the median estimates of R_t in Daegu ($r = 0.93$; 95% credible interval 0.86–0.96; Appendix Figure 2) and Seoul ($r = 0.76$; 95% credible interval 0.60–0.87; Appendix Figure 2), these correlations are conflated by time trends and by other measures that could have affected R_t. We did not find clear signatures of lags in the correlation between R_t and traffic volume (Appendix Figure 3). Patterns in R_t were similar in directly adjacent provinces (Gyeongsangbuk-do and Gyeonggi-do), demonstrating the robustness of our analysis (Appendix Figure 4).

Conclusions

The South Korea experience with COVID-19 provides evidence that epidemics can be suppressed with less extreme measures than those taken by China (9) and demonstrates the necessity of prompt identification and isolation of case-patients in preventing spread (4). Our analysis reveals the potential role of social distancing in assisting such efforts. Even though social distancing alone might not prevent spread, it can flatten the epidemic curve (compare Figure 2, panels B, D) and reduce the burden on the healthcare system (10).

Our study is not without limitations. Because of insufficient data, we could not account for differences in delay distributions or changes in testing capacity among cities; line list data were mostly derived from outside Daegu. Nonetheless, the sensitivity analyses support the robustness of our findings (Appendix
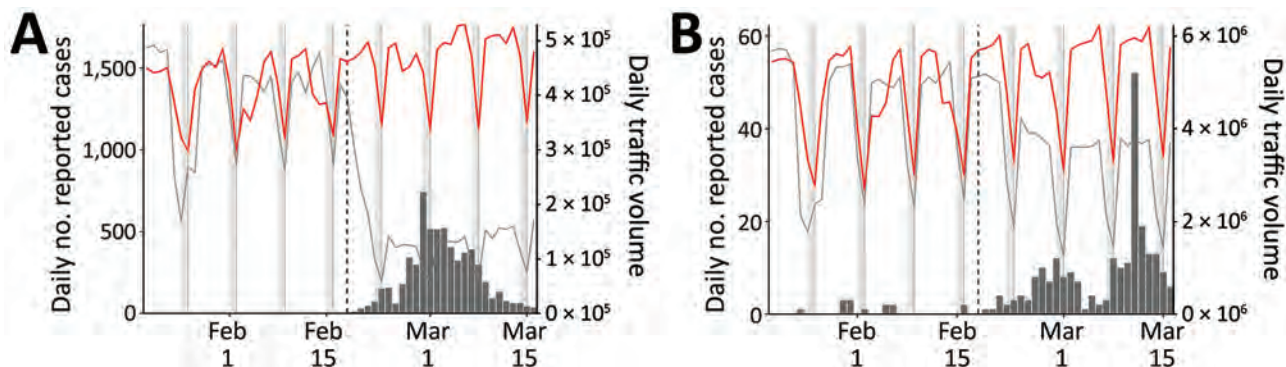
Figure 1. Comparison of daily epidemiologic and traffic data from Daegu (A) and Seoul (B) during the coronavirus disease (COVID-19) outbreak, South Korea. Black bars indicate no. COVID-19 cases; lines represent daily metropolitan traffic volume in 2020 (red) and mean daily metropolitan traffic volume during 2017–2019 (black). Daily traffic from previous years have been shifted by 1–3 days to align day of the weeks. Vertical dashed lines indicate February 18, 2020, when the first COVID-19 case was confirmed in Daegu. Gray bars indicate weekends.

Table. Assumed incubation and generation-interval distributions in an analysis of the potential role of social distancing in mitigating the spread of coronavirus disease, South Korea, 2020*

Distribution	Parameterization	Priors	Source
Incubation period distribution	Gamma (μ_I, μ^2/σ^2)	$\mu_I \approx$ gamma (6.5 d, 145); $\sigma \approx$ gamma (2.6 d, 25)	(6)
Generation-interval distribution	Negative binomial (μ_G, θ)	$\mu_G \approx$ gamma (5 d, 62); $\theta \approx$ gamma (5, 20)	(7,8)

*Gamma distributions are parameterized using its mean and shape. Negative binomial distributions are parameterized using its mean and dispersion. Priors are chosen such that the 95% quantiles of prior means and standard deviations are consistent with previous estimates.

Figures 5–8). We were unable to distinguish local and imported cases and thus might have overestimated R_t (11). Conducting a separate analysis for Seoul that accounts for imported cases did not affect our qualitative conclusions (Appendix Figure 9). Finally, although the method of resampling infection time can capture qualitative changes in R_t, estimates of R_t can be oversmoothed and should be interpreted with care (K. Gostic, unpub. data, https://doi.org/10.1101/2020.06.18.20134858). Nonetheless, our estimates of R_t are broadly consistent with previous estimates (12).

We used metropolitan traffic to quantify the degree of social distancing. The 80% decrease in traffic volume suggests that distancing measures in Daegu might be comparable to those in Wuhan, China (13). We were unable to directly estimate the effect of social distancing on population contacts or epidemiologic dynamics. Other measures, such as intensive testing and tracing of core transmission groups, are also likely to have affected transmission dynamics.

Our study highlights the importance of considering geographic heterogeneity in estimating epidemic potential. The sharp decrease in Daegu drove the number of reported cases in South Korea. Our analysis revealed that the epidemic remained close to the epidemic threshold in other regions, including Seoul and Gyeonggi-do. Relatively weak distancing might have assisted the recent resurgence of COVID-19 cases in Seoul (E. Shim, G. Chowell, unpub. data, https://doi.org/10.1101/2020.07.21.20158923).

This article was preprinted at https://www.medrxiv.org/content/10.1101/2020.03.27.20045815v1.

About the Author

Mr. Park is a PhD student in the Ecology and Evolutionary Biology Department at Princeton University. His research focuses on mathematical and statistical modeling of infectious diseases.
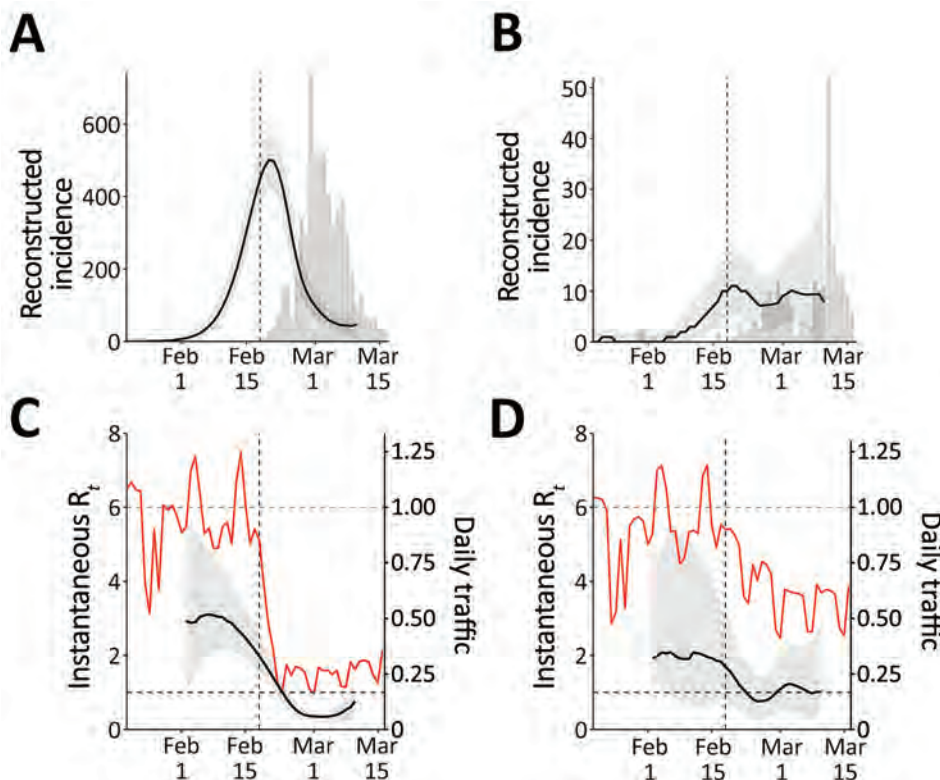
Figure 2. Comparison of reconstructed coronavirus disease incidence proxy and instantaneous reproduction number R_t in Daegu (A, C) and Seoul (B, D), South Korea. The instantaneous reproduction number R_t reflects transmission dynamics at time *t.* Black lines and gray shading represent the median estimates of reconstructed incidence (A, B) and R_t (C, D) and their corresponding 95% credible intervals. Gray bars show the number of reported cases. Red lines represent the normalized traffic volume (daily traffic, 2020, divided by the mean daily traffic, 2017–2019). Vertical dashed lines indicate February 18, 2020, when the first case was confirmed in Daegu.

References

1. Korea Centers for Disease Control and Prevention). Press release [in Korean]. Release dates 2020 Jan 20, Feb 18, Feb 19, Feb 24, Feb 29, Mar 16 [cited 2020 Jan 20–Jul 23]. https://www.cdc.go.kr/board/board.es?mid=a20501000000&bid=0015#

2. Daegu Metropolitan City Government. Press release [in Korean] [cited 2020 Jul 22]. http://152.99.22.79:8080/SynapDocViewServer/viewer/doc.html?key=2c948aed7356835e017378b583741d07&contextPath=/SynapDocViewServer/

3. Korean Ministry of Education. Press release [in Korean] [cited 2020 Jul 22]. https://www.moe.go.kr/boardCnts/view.do?boardID=294&boardSeq=79829&lev=0&searchType=null&statusYN=W&page=21&s=moe&m=020402&opType=N

4. Park YJ, Choe YJ, Park O, Park SY, Kim YM, Kim J, et al.; COVID-19 National Emergency Response Center, Epidemiology and Case Management Team. Contact tracing during coronavirus disease outbreak, South Korea, 2020. Emerg Infect Dis. 2020 Jul 16 [Epub ahead of print]. https://doi.org/10.3201/eid2610.201315

5. Fraser C. Estimating individual and household reproduction numbers in an emerging epidemic. PLoS One. 2007;2:e758. https://doi.org/10.1371/journal.pone.0000758

6. Backer JA, Klinkenberg D, Wallinga J. Incubation period of 2019 novel coronavirus (2019-nCoV) infections among travellers from Wuhan, China, 20–28 January 2020. Euro Surveill. 2020;25:25. https://doi.org/10.2807/1560-7917.ES.2020.25.5.2000062

7. Ferretti L, Wymant C, Kendall M, Zhao L, Nurtay A, Abeler-Dörner L, et al. Quantifying dynamics of SARS-CoV-2 transmission suggests epidemic control with digital contact tracing. Science. 2020;368:eabb6936.

8. Ganyani T, Kremer C, Chen D, Torneri A, Faes C, Wallinga J, et al. Estimating the generation interval for coronavirus disease (COVID-19) based on symptom onset data, March 2020. Euro Surveill. 2020;25:2000257. https://doi.org/10.2807/1560-7917.ES.2020.25.17.2000257

9. Kickbusch I, Leung G. Response to the emerging novel coronavirus outbreak. BMJ. 2020;368:m406. https://doi.org/10.1136/bmj.m406

10. Anderson RM, Heesterbeek H, Klinkenberg D, Hollingsworth TD. How will country-based mitigation measures influence the course of the COVID-19 epidemic? Lancet. 2020;395:931–4. https://doi.org/10.1016/S0140-6736(20)30567-5

11. Thompson RN, Stockwin JE, van Gaalen RD, Polonsky JA, Kamvar ZN, Demarsh PA, et al. Improved inference of time-varying reproduction numbers during infectious disease outbreaks. Epidemics. 2019;29:100356. https://doi.org/10.1016/j.epidem.2019.100356

12. Ryu S, Ali ST, Jang C, Kim B, Cowling BJ. Effect of nonpharmaceutical interventions on transmission of severe acute respiratory syndrome coronavirus 2, South Korea, 2020. Emerg Infect Dis. 2020 Jun 2 [Epub ahead of print]. https://doi.org/10.3201/eid2610.201886

13. Kraemer MUG, Yang C-H, Gutierrez B, Wu C-H, Klein B, Pigott DM, et al.; Open COVID-19 Data Working Group. The effect of human mobility and control measures on the COVID-19 epidemic in China. Science. 2020;368:493–7. https://doi.org/10.1126/science.abb4218

Address for correspondence: Sang Woo Park, Department of Ecology and Evolutionary Biology, 106A Guyot Hall, Princeton University, Princeton, NJ 08544-2016, USA; email: swp2@princeton.edu

EID SPOTLIGHT TOPIC

Coronavirus
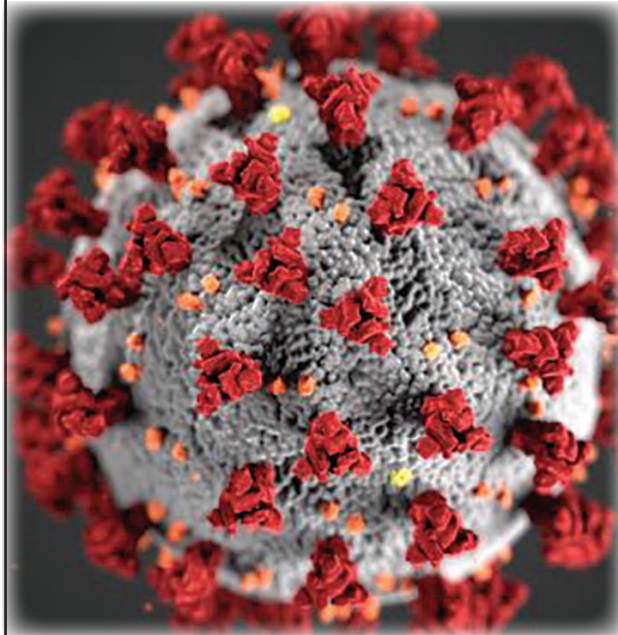
This spotlight provides articles published in *Emerging Infectious Diseases* about human coronavirus diseases, including coronavirus disease 2019 (COVID-19), severe acute respiratory syndrome (SARS), and the common cold.

https://wwwnc.cdc.gov/eid/spotlight/coronavirus

EMERGING INFECTIOUS DISEASES®

SARS-CoV-2 Virus Culture and Subgenomic RNA for Respiratory Specimens from Patients with Mild Coronavirus Disease

Ranawaka A.P.M. Perera, Eugene Tso, Owen T.Y. Tsang, Dominic N.C. Tsang, Kitty Fung, Yonna W.Y. Leung, Alex W.H. Chin, Daniel K.W. Chu, Samuel M.S. Cheng, Leo L.M. Poon, Vivien W.M. Chuang, Malik Peiris

We investigated 68 respiratory specimens from 35 coronavirus disease patients in Hong Kong, of whom 32 had mild disease. We found that severe acute respiratory syndrome coronavirus 2 and subgenomic RNA were rarely detectable beyond 8 days after onset of illness. However, virus RNA was detectable for many weeks by reverse transcription PCR.

Severe acute respiratory syndrome (SARS) coronavirus 2 (SARS-CoV-2) is causing a global pandemic and affecting global health and the world economy. Virus RNA might be detectable by reverse transcription PCR (RT-PCR) many weeks after clinical recovery (1,2), which affects the duration of isolation of patients. Similar findings were seen with SARS during 2003 (3). A large proportion of transmission occurs before and soon after onset of illness (4). However, the duration of contagiousness after the onset of clinical symptoms remains poorly understood. This duration is relevant to determining policy for discharge of patients from containment in hospitals.

Viral RNA detection by RT-PCR does not prove the presence of infectious virus; culture isolation of virus is a better indication of contagiousness. Recent studies on experimentally infected hamsters showed efficient transmission of SARS-CoV-2 to contact hamsters on day 1 after challenge when virus culture results were positive in nasal washes, but not at day 6

when nasal washes were culture negative, although viral load determined by RT-PCR was still high (>6.0 $\log_{10}$ RNA copies/mL) (5). Thus, virus culture might be a better surrogate for transmissibility.

We attempted virus isolation in 68 specimens from 35 patients in Hong Kong. Specimens were collected at different times after symptom onset to define the kinetics of virus isolation in upper respiratory specimens. Those specimens with a viral load $\geq 5 \log_{10}$ were also examined for detection of subgenomic viral RNA (sgRNA).

The Study

The study was approved by the Research Ethics Committee of the Kowloon West Cluster (reference No. KW/EX-20–039; 144–27) of the Hospital Authority of Hong Kong. We provide methods for virus nucleoprotein (N) gene copy number quantification (6), virus culture, and sgRNA detection of RT-PCR–confirmed coronavirus disease (COVID-19) patients (Appendix, https://wwwnc.cdc.gov/EID/article/26/11/20-3219-App1.pdf). Virus sgRNA was tested in specimens that had $\geq 5 \log_{10}$ N gene copies/mL.

A total of 68 specimens from 35 patients were studied (Table 1; Appendix); patients with prolonged virus shedding (10 who remained virus RNA positive for >30 days) and patients readmitted because RT-PCR positivity was detected after discharge (n = 6) were oversampled (i.e., selected to make up a larger share of the survey sample than is performed for the patient population). Patient age ranged from 17 to 75 years (median 38 years); 23 were male and 12 female (Table 1). Specimens submitted for virus culture were nasopharyngeal aspirates and throat swab specimens (n = 46), nasopharyngeal aspirates (n = 2), nasopharyngeal swab specimens and throat swab specimens (n = 4), nasopharyngeal swab specimens (n = 3), sputum (n = 11), and saliva (n = 2). The duration after

Table 1. Comparison of patients and clinical respiratory specimens that were positive or negative by culture for severe acute respiratory syndrome coronavirus 2 and duration of illness for patients with mild coronavirus disease, Hong Kong*

Characteristic	Culture positive, n = 16	Culture negative, n = 52	Total, n = 68	Statistical significance
Patients, n = 35				
Asymptomatic	1	2	3	ND
Median age (range), y	39 (21–73)	38 (17–75)	38	ND
Concurrent condition	5	4	9	ND
Clinical specimens				
Median $\log_{10}$ viral load/mL†, n = 68	7.5	3.8		p<0.0001 by Mann-Whitney test
Viral load $\log_{10}$, range, n = 68				
7.0–9.5	12 (75)	5 (10)	17 (25)	p = 0.018 by Fisher exact test
6.0–6.99	3 (19)	8 (15)	11 (16)	
5.0–5.99	1 (6)	6 (12)	7 (10)	
<5.0	0	33 (63)	33 (49)	
Days after onset of illness when sample was collected, n = 68				
1–2	8 (53)	7 (13)	15 (22)	p = 0.00001 by Fisher exact test
3–8	8 (35)	15 (29)	23 (34)	
9–67	0	30‡ (58)	30 (44)	
Days after onset of illness when sample was collected from patients without or before antiviral treatment, n = 42				
1–2	8 (50)	7 (27)	15 (36)	p = 0.01 by Fisher exact test
3–8	8 (50)	9 (35)	17 (40)	
9–67	0	10 (38)	10 (24)	

*Values are no. (%) patients unless indicated otherwise. ND, not determined.
†Viral load below limit of detection for the assay was scored as 1 $\log_{10}$/mL.
‡Six of these patients were readmissions because of detection of virus RNA after discharge from isolation.

onset of illness to specimen collection ranged from 1 to 67 days.

Virus was isolated from 16 specimens for 16 patients. The median age of the culture-positive patients was 39 years and of the culture-negative patients was 38 years. SARS-CoV-2 N gene copy number in the specimens overall ranged from 9.5 $\log_{10}$ copies/mL to undetectable (limit of detection 10 copies/mL) (Figure 1). The median viral load in culture-positive samples was 7.5 $\log_{10}$ copies/mL and in culture-negative samples was 3.8 $\log_{10}$ copies/mL (p = 0.00001) (Table 1).

Virus was isolated from 12 of 17 specimens with viral loads ≥7.0 $\log_{10}$ copies/mL, 3 of 11 specimens with viral loads 6.0–6.99 $\log_{10}$ copies/mL, 1 of 7 specimens with viral loads 5.0–5.99 $\log_{10}$ copies/mL, and 0 of 33 specimens viral loads <5 $\log_{10}$ copies/mL.

The sgRNA provides evidence of replicative intermediates of the virus, rather than residual viral RNA. Detection of virus sgRNA was attempted for 33 of the 35 the clinical specimens that had viral loads ≥5.0 $\log_{10}$ virus genome copies/mL; 2 specimens had insufficient specimen for this testing. Of 33 specimens tested for sgRNA and by virus culture, both tests showed positive results for 12 (36.4%) specimens, both tests showed negative results for 12 (36.4%), sgRNA showed positive results and culture was negative for 7 (21.2%) specimens, and culture was positive and sgRNA showed negative results for 2 (6.1%) samples (Cohen κ 0.467, p = 0.005 against κ 0) indicating a moderate agreement between virus culture and sgRNA detection. Virus

sgRNA was detectable in 18 (81.8%) of 22 specimens collected ≤8 days after symptom onset and in 1 (9.1%) of 11 specimens collected ≥9 days after onset of disease (p = 0.0003 by χ^2 test with Yates correction) (Figure 2). We also provide culture and sgRNA results stratified by specimen type (Table 2).

We conducted a subset analysis for 42 specimens collected from patients who did not receive antiviral
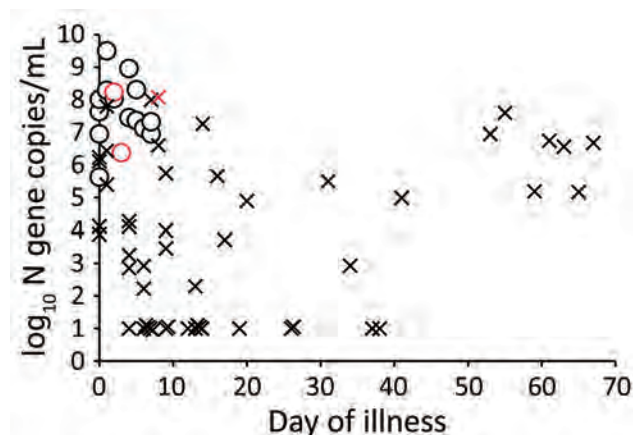
Figure 1. Severe acute respiratory syndrome coronavirus 2 RNA load, virus culture, and days after onset of illness in respiratory specimens and duration of illness for patients with mild coronavirus disease, Hong Kong. ○ indicates samples positive by virus culture and × indicates samples negative by virus culture. Red indicates 2 critically ill patients and 1 patient who died; black indicates mild, moderate, or asymptomatic infections. The limit of detection of the viral N gene RNA was 1 $\log_{10}$ copies/mL; undetectable virus load is indicated as the limit of detection. N, nucleoprotein.
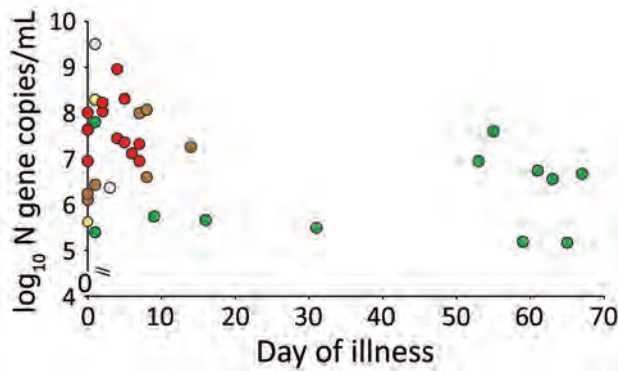
Figure 2. Severe acute respiratory syndrome coronavirus 2 viral RNA load, virus culture, and subgenomic virus RNA (sgRNA) in relation to days after onset of illness for patients with mild coronavirus disease, Hong Kong. Red indicates culture and sgRNA positive, green indicates culture and sgRNA negative, yellow indicates culture positive and sgRNA negative, brown indicates culture negative and sgRNA positive, and gray indicates culture positive and no sgRNA data (because of insufficient specimen).

Conclusions

For a cohort of patients with predominantly mild COVID-19, our findings suggest that virus isolation and sgRNA detection were positive within the first 8 days after onset of illness and mainly for specimens with ≥ 6 $\log_{10}$ virus N gene copies/mL of clinical specimen. We did not carry out serologic testing in parallel with viral culture, but data on a larger cohort of patients in Hong Kong showed that most patients had detectable virus neutralizing antibodies after day 9 of illness (*7*). Two other studies of virus culture for mildly ill or moderately ill patients showed virus culture was only successful within the first 9 days after onset of illness (*8,9*). Patients who are severely ill and immunocompromised might shed infectious virus for much longer periods (J.J.A. van Kampen, Erasmus University Medical Center, pers. comm., 2020 Jun 9), and this shedding might also be prolonged by corticosteroid therapy.

The World Health Organization has recently amended its guidelines for releasing COVID-19 patients from isolation (i.e., 10 days after symptom onset and ≥ 3 additional days without symptoms), but these guidelines do not distinguish between mild and severely ill patients (*10*). Our findings suggest that patients with mild or moderate illness might be less contagious 8 days after symptom onset. Mildly ill patients who have clinically recovered and are not immunocompromised might be discharged from containment ≥ 9 days after symptom onset, as long as they are not being discharged into settings that contain other highly vulnerable persons (e.g., old age care homes).

drugs or specimens that were collected before antiviral therapy (Table 1). This sample included all 16 specimens that were culture positive and 18 of 19 specimens that were sgRNA positive. The main conclusions remained unchanged. Median viral RNA load in culture-positive specimens was 7.54 $\log_{10}$ genome copies/mL and in culture-negative specimens was 4.0 $\log_{10}$ genome copies/mL (p<0.00001 by Mann-Whitney 2-tailed U test). Of the 16 culture positive specimens, 15 (94%) had viral RNA load ≥ 6 $\log_{10}$ copies/mL (p<0.01 by Fisher exact test). All of them were collected within the first 8 days of illness (p = 0.01 by Fisher exact test) (Table 1). However, the duration of illness in this subset of specimens was limited to 31 days. Five specimens with viral load ≥ 6 $\log_{10}$ virus N gene copies/mL collected ≥ 50 days after onset of illness were negative by virus culture and virus sgRNA, but all of these patients had received antiviral therapy.

Table 2. Culture and sgRNA results stratified by specimen type for patients with mild coronavirus disease, Hong Kong*

Specimen	Investigation	Days after onset of illness, no. positive/no. tested				
		1–2	3–8	9–14	15–21	>21
NPA + TS	Culture	8/14	2/14	0/8	0/2	0/8
	sgRNA	8/11	4/4	0/1	0/0	0/4
NPA	Culture		2/2			
	sgRNA		1/1			
NPS + TS	Culture		0/2	0/2		
	sgRNA					
NPS	Culture	1/1	1/1			0/1
	sgRNA	1/1	1/1			
Sputum	Culture		0/1	0/2	0/8	
	sgRNA		1/1	1/1	0/5	
Saliva	Culture		2/2			
	sgRNA		2/2			

*Blank cells indicate that no specimens were collected at that time point. NPA, nasopharyngeal aspirate; NPS, nasopharyngeal swab; sgRNA, subgenomic viral RNA: TS, throat swab.

About the Author

Dr. Perera is a research assistant professor at the School of Public Health, The University of Hong Kong, Hong Kong, China. His primary research interests are emerging virus infections, influenza, Middle East respiratory syndrome coronavirus, and SARS-CoV-2.

References

1. To KK, Tsang OT, Leung WS, Tam AR, Wu TC, Lung DC, et al. Temporal profiles of viral load in posterior oropharyngeal saliva samples and serum antibody responses during infection by SARS-CoV-2: an observational cohort study. Lancet Infect Dis. 2020;20:565–74. https://doi.org/10.1016/S1473-3099(20)30196-1
2. Xiao AT, Tong YX, Gao C, Zhu L, Zhang YJ, Zhang S. Dynamic profile of RT-PCR findings from 301 COVID-19 patients in Wuhan, China: a descriptive study. J Clin Virol. 2020;127:104346. https://doi.org/10.1016/j.jcv.2020.104346
3. Chan KH, Poon LL, Cheng VC, Guan Y, Hung IF, Kong J, et al. Detection of SARS coronavirus in patients with suspected SARS. Emerg Infect Dis. 2004;10:294–9. https://doi.org/10.3201/eid1002.030610
4. He X, Lau EHY, Wu P, Deng X, Wang J, Hao X, et al. Temporal dynamics in viral shedding and transmissibility of COVID-19. Nat Med. 2020;26:672–5. https://doi.org/10.1038/s41591-020-0869-5
5. Sia SF, Yan LM, Chin AW, Fung K, Choy KT, Wong AY, et al. Pathogenesis and transmission of SARS-CoV-2 in golden hamsters. Nature. 2020 May 14 [Epub ahead of print]. https://doi.org/10.1038/s41586-020-2342-5
6. Chu DK, Pan Y, Cheng SM, Hui KP, Krishnan P, Liu Y, et al. Molecular diagnosis of a novel coronavirus (2019-nCoV) causing an outbreak of pneumonia. Clin Chem. 2020;66:549–55. https://doi.org/10.1093/clinchem/hvaa029
7. Perera RA, Mok CK, Tsang OT, Lv H, Ko RL, Wu NC, et al. Serological assays for severe acute respiratory syndrome coronavirus 2 (SARS-CoV-2), March 2020. Euro Surveill. 2020;25:2000421. https://doi.org/10.2807/1560-7917.ES.2020.25.16.2000421
8. Wölfel R, Corman VM, Guggemos W, Seilmaier M, Zange S, Müller MA, et al. Virological assessment of hospitalized patients with COVID-2019. Nature. 2020;581:465–9. https://doi.org/10.1038/s41586-020-2196-x
9. Bullard J, Dust K, Funk D, Strong JE, Alexander D, Garnett L, et al. Predicting infectious SARS-CoV-2 from diagnostic samples. Clin Infect Dis. 2020 May 22 [Epub ahead of print]. https://doi.org/10.1038/s41586-020-2196-x
10. World Health Organization. Criteria for releasing COVID-19 patients from isolation, June 17, 2020 [cited 2020 Jul 4]. https://www.who.int/publications/i/item/criteria-for-releasing-covid-19-patients-from-isolation

Address for correspondence: Malik Peiris, School of Public Health, The University of Hong Kong, No. 7 Sassoon Rd, Pokfulam, Hong Kong, China; email: malik@hku.hk or malik@hkucc.hku.hkVenducias qui debit eossus quis solupta

Asymptomatic Transmission of SARS-CoV-2 on Evacuation Flight

Sung Hwan Bae, Heidi Shin, Ho-Young Koo, Seung Won Lee, Jee Myung Yang, Dong Keon Yon

We conducted a cohort study in a controlled environment to measure asymptomatic transmission of severe acute respiratory syndrome coronavirus 2 on a flight from Italy to South Korea. Our results suggest that stringent global regulations are necessary for the prevention of transmission of this virus on aircraft.

Undocumented cases of severe acute respiratory syndrome coronavirus 2 (SARS-CoV-2) infection have been common during the coronavirus disease (COVID-19) global pandemic (*1–3*). Although inflight transmission of symptomatic COVID-19 has been well established (*1,2*), the evidence for transmission of asymptomatic COVID-19 on an aircraft is inconclusive. We conducted a cohort study evaluating asymptomatic passengers on a flight that carried 6 asymptomatic patients with confirmed SARS-CoV-2 infections. The Institutional Review Board of Armed Force Medical Command approved the study protocol. The ethics commission waived written informed consent because of the urgent need to collect data on COVID-19.

The Study

On March 31, 2020, we enrolled in our study 310 passengers who boarded an evacuation flight from Milan, Italy, to South Korea. This evacuation flight was conducted under strict infection control procedures by the Korea Centers for Disease Control and Prevention (KCDC), based on the guidelines of the World

Author affiliations: Soonchunhyang University College of Medicine, Seoul, South Korea (S.H. Bae); Soonchunhyang University Seoul Hospital, Seoul (S.H. Bae); Harvard Business School, Boston, Massachusetts, USA (H. Shin); Korea University College of Medicine, Seoul (H.-Y. Koo); Sejong University College of Software Convergence, Seoul (S.W. Lee); University of Ulsan College of Medicine, Seoul (J.M. Yang); Asan Medical Center, Seoul (J.M. Yang); Armed Force Medical Command, Republic of Korea Armed Forces, Seongnam, South Korea (D.K. Yon); CHA University School of Medicine, Seongnam (D.K. Yon)

Health Organization (WHO) (*4*). When the passengers arrived at the Milan airport, medical staff performed physical examinations, medical interviews, and body temperature checks outside the airport before boarding, and 11 symptomatic passengers were removed from the flight. Medical staff dispatched from KCDC were trained in infection control under the guidance of the KCDC and complied with the COVID-19 infection protocol, which was based on WHO guidelines (*4*). N95 respirators were provided, and passengers were kept 2 m apart for physical distancing during preboarding. Most passengers wore the N95 respirators except at mealtimes and when using the toilet during the flight. After an 11-hour flight, 299 asymptomatic passengers arrived in South Korea and were immediately quarantined for 2 weeks at a government quarantine facility in which the passengers were completely isolated from one another. Medical staff examined them twice daily for elevated body temperature and symptoms of COVID-19. All passengers were tested for SARS-CoV-2 by reverse transcription PCR twice, on quarantine day 1 (April 2) and quarantine day 14 (April 15).

Asymptomatic patients were those who were asymptomatic when they tested positive and did not develop symptoms within 14 days after testing (*5*). Among the 299 passengers (median age 30.0 years; 44.1% male), 6 had a confirmed positive result for SARS-CoV-2 on quarantine day 1 and were transferred immediately to the hospital (Table). At 14 days after the positive test, the 6 patients reported no symptoms and were categorized as asymptomatic.

On quarantine day 14, a 28-year-old woman who had no underlying disease had a confirmed positive test result for COVID-19. On the flight from Milan, Italy, to South Korea, she wore an N95 mask, except when she used a toilet. The toilet was shared by passengers sitting nearby, including an asymptomatic patient. She was seated 3 rows away from the asymptomatic patient (Figure). Given that she did not go outside and had self-quarantined for 3 weeks alone at her home in Italy before the flight and did not use

Table. Baseline characteristics and quarantine day 1 SARS-CoV-2 test results for asymptomatic passengers from flight from Milan, Italy, to South Korea, March 2020*

Characteristics	All asymptomatic passengers, N = 299	Passengers testing negative for SARS-CoV-2, n = 293	Patients testing positive for SARS-CoV-2, n = 6
Median age (IQR), y	30.0 (27.0–35.0)	30.0 (27.0–35.0)	28.0 (9.9–45.0)
Sex			
M	132 (44.1)	128 (43.7)	4 (66.7)
F	167 (55.9)	165 (56.3)	2 (33.3)
Underlying conditions			
Diabetes	1 (0.3)	1 (0.3)	0 (0.0)
Hypertension	6 (2.0)	6 (2.0)	0 (0.0)
Asthma	1 (0.3)	1 (0.3)	0 (0.0)
Coronary artery disease	1 (0.3)	1 (0.3)	0 (0.0)
Cancer	3 (1.0)	3 (1.0)	0 (0.0)
Connective tissue disease	1 (0.3)	1 (0.3)	0 (0.0)
Liver disease	1 (0.3)	1 (0.3)	0 (0.0)
Thyroid disease	2 (0.7)	2 (0.7)	0 (0.0)
Current pregnancy	4 (1.4)	4 (1.4)	0 (0.0)
Charlson Comorbidity Index score			
0	287 (96.0)	281 (95.9)	6 (100.0)
1	8 (2.7)	8 (2.7)	0 (0.0)
>2	4 (1.3)	4 (1.4)	0 (0.0)

*Values are no. (%) except as indicated. IQR, interquartile range; SARS-CoV-2, severe acute respiratory syndrome coronavirus 2.

public transportation to get to the airport, it is highly likely that her infection was transmitted in the flight via indirect contact with an asymptomatic patient. She reported coughing, rhinorrhea, and myalgia on quarantine day 8 and was transferred to a hospital on quarantine day 14. The remaining 292 passengers were released from quarantine on day 15.

All crew members (n = 10) and medical staff dispatched from KCDC (n = 8) were quarantined at a government quarantine facility for 2 weeks and were tested twice for SARS-CoV-2, on quarantine days 1 and 14. All 18 members of the cabin crew and medical staff were negative for SARS-CoV-2 on both occasions.

To reinforce our results, we performed an external validation using a different dataset. Another evacuation flight of 205 passengers from Milan, Italy, to South Korea on April 3, 2020, was also conducted by KCDC under strict infection control procedures. Among the passengers on this flight were 3 asymptomatic patients who tested positive on quarantine day 1 and 1 patient who tested negative on quarantine day 1 and positive on quarantine day 14. On the basis of an epidemiologic investigation, the authors and KCDC suspect that this infection was also transmitted by inflight contact.

Conclusions

This study was one of the earliest to assess asymptomatic transmission of COVID-19 on an aircraft. Previous studies of inflight transmission of other respiratory infectious diseases, such as influenza and severe acute respiratory syndrome, revealed that sitting near a person with a respiratory infectious disease is a major risk factor for transmission (*6,7*), similar to our own findings. Considering the difficulty of airborne infection transmission inflight because of high-efficiency particulate-arresting filters used in aircraft ventilation systems, contact with contaminated surfaces or infected persons when boarding, moving, or disembarking from the aircraft may play a critical role in inflight transmission of infectious diseases (*6,7*).

Previous studies reported that viral shedding can begin before the appearance of COVID-19 symptoms (*8,9*), and evidence of transmission from presymptomatic and asymptomatic persons has been reported in epidemiologic studies of SARS-CoV-2 (*5,10,11*). Because KCDC performed strong infection control procedures during boarding; the medical staff and crew members were trained in infection control; all passengers, medical staff, and crew members were tested twice for SARS-CoV-2; and a precise epidemiologic investigation was conducted, the most plausible explanation for the transmission of SARS-CoV-2 to a passenger on the aircraft is that she became infected by an asymptomatic but infected passenger while using an onboard toilet. Other, less likely, explanations for the transmission are previous SARS-CoV-2 exposure, longer incubation period, and other unevaluated situations.

The control measures incorporated into our cohort study provide a higher level of evidence than previous studies on asymptomatic transmission (*5,10,11*). Our findings suggest the following strategies for the prevention of SARS-CoV-2 transmission on an aircraft. First, masks should be worn during the flight. Second, because contact with contaminated surfaces increases the risk for transmission of
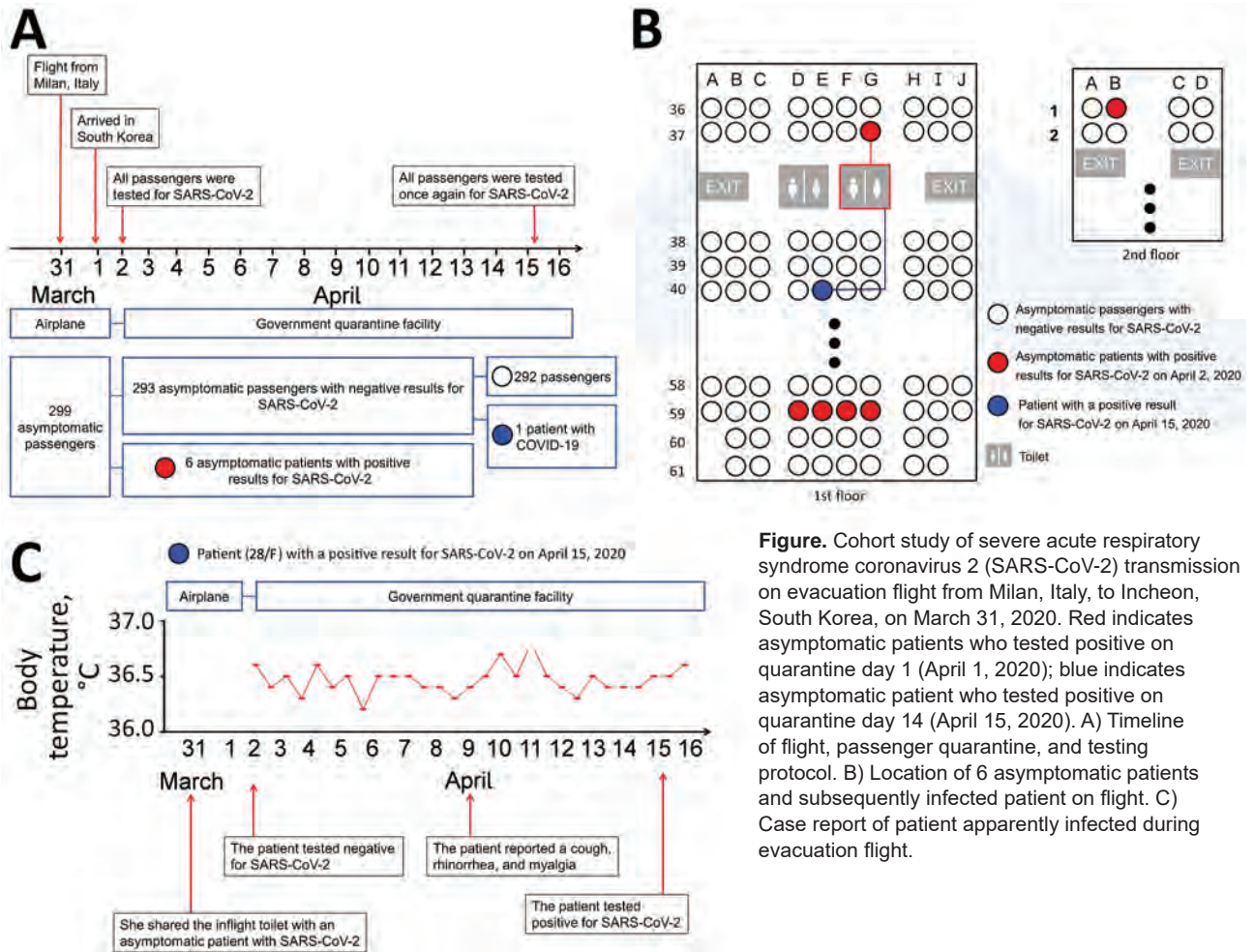
Figure. Cohort study of severe acute respiratory syndrome coronavirus 2 (SARS-CoV-2) transmission on evacuation flight from Milan, Italy, to Incheon, South Korea, on March 31, 2020. Red indicates asymptomatic patients who tested positive on quarantine day 1 (April 1, 2020); blue indicates asymptomatic patient who tested positive on quarantine day 14 (April 15, 2020). A) Timeline of flight, passenger quarantine, and testing protocol. B) Location of 6 asymptomatic patients and subsequently infected patient on flight. C) Case report of patient apparently infected during evacuation flight.

SARS-CoV-2 among passengers, hand hygiene is necessary to prevent infections. Third, physical distance should be maintained before boarding and after disembarking from the aircraft.

Our research provides evidence of asymptomatic transmission of COVID-19 on an airplane. Further attention is warranted to reduce the transmission of COVID-19 on aircraft. Our results suggest that stringent global regulations for the prevention of COVID-19 transmission on aircraft can prevent public health emergencies.

Acknowledgments

We thank the Korea Centers for Disease Control and Prevention for its support of this study.

About the Author

Dr. Bae is a physician with the Soonchunhyang University College of Medicine, Seoul, South Korea. His research interests are emerging infectious diseases and radiology.

References

1. Yang N, Shen Y, Shi C, Ma AHY, Zhang X, Jian X, et al. In-flight transmission cluster of COVID-19: a retrospective case series. Infect Dis (Lond). 2020 Jul 31:1–11.
2. Ng O-T, Marimuthu K, Chia P-Y, Koh V, Chiew CJ, De Wang L, et al. SARS-CoV-2 infection among travelers returning from Wuhan, China. N Engl J Med. 2020;382: 1476–8. https://doi.org/10.1056/NEJMc2003100
3. Lee SW, Ha EK, Yeniova AÖ, Moon SY, Kim SY, Koh HY, et al. Severe clinical outcomes of COVID-19 associated with proton pump inhibitors: a nationwide cohort study with propensity score matching. Gut. 2020;gutjnl-2020-322248. https://doi.org/10.1136/gutjnl-2020-322248
4. World Health Organization. Operational considerations for managing COVID-19 cases or outbreaks on board ships: interim guidance, 25 March 2020. World Health Organization; 2020 [cited 2020 Aug 13]. https://apps.who.int/iris/bitstream/handle/10665/331591/WHO-2019-nCoV-Ships-2020.2-eng.pdf

5. Arons MM, Hatfield KM, Reddy SC, Kimball A, James A, Jacobs JR, et al.; Public Health–Seattle and King County and CDC COVID-19 Investigation Team. Presymptomatic SARS-CoV-2 infections and transmission in a skilled nursing facility. N Engl J Med. 2020;382:2081–90. https://doi.org/10.1056/NEJMoa2008457

6. Olsen SJ, Chang H-L, Cheung TY-Y, Tang AF-Y, Fisk TL, Ooi SP-L, et al. Transmission of the severe acute respiratory syndrome on aircraft. N Engl J Med. 2003;349:2416–22. https://doi.org/10.1056/NEJMoa031349

7. Mangili A, Gendreau MA. Transmission of infectious diseases during commercial air travel. Lancet. 2005;365:989–96. https://doi.org/10.1016/S0140-6736(05)71089-8

8. He X, Lau EHY, Wu P, Deng X, Wang J, Hao X, et al. Temporal dynamics in viral shedding and transmissibility of COVID-19. Nat Med. 2020;26:672–5. https://doi.org/10.1038/s41591-020-0869-5

9. Choi S-H, Kim HW, Kang J-M, Kim DH, Cho EY. Epidemiology and clinical features of coronavirus disease 2019 in children. Clin Exp Pediatr. 2020;63:125–32. https://doi.org/10.3345/cep.2020.00535

10. Song J-Y, Yun J-G, Noh J-Y, Cheong H-J, Kim W-J. Covid-19 in South Korea—challenges of subclinical manifestations. N Engl J Med. 2020;382:1858–9. https://doi.org/10.1056/NEJMc2001801

11. Bai Y, Yao L, Wei T, Tian F, Jin D-Y, Chen L, et al. Presumed asymptomatic carrier transmission of COVID-19. JAMA. 2020;323:1406. https://doi.org/10.1001/jama.2020.2565

Address for correspondence: Dong Keon Yon, Armed Force Medical Command, Republic of Korea Armed Forces, 81 Saemaeul-ro 177, Seongnam, Gyeonggi-do, 463-040, South Korea; email: yonkkang@gmail.com
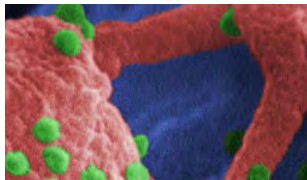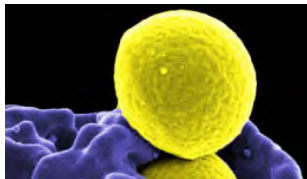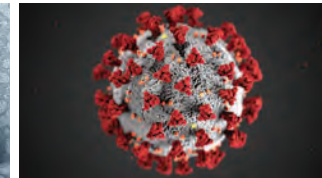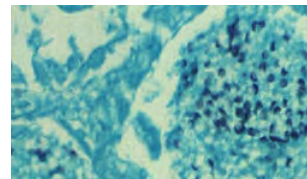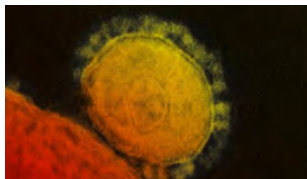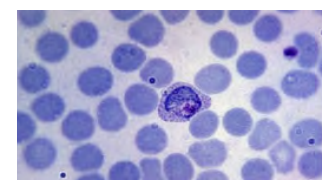
Worldwide Effects of Coronavirus Disease Pandemic on Tuberculosis Services, January–April 2020

Giovanni Battista Migliori,[1] Pei Min Thong,[1] Onno Akkerman, Jan-Willem Alffenaar, Fernando Álvarez-Navascués, Mourtala Mohamed Assao-Neino, Pascale Valérie Bernard, Joshua Sorba Biala, François-Xavier Blanc, Elena M. Bogorodskaya, Sergey Borisov, Danilo Buonsenso, Marianne Calnan, Paola Francesca Castellotti, Rosella Centis, Jeremiah Muhwa Chakaya, Jin-Gun Cho, Luigi Ruffo Codecasa, Lia D'Ambrosio, Justin Denholm, Martin Enwerem, Maurizio Ferrarese, Tatiana Galvão, Marta García-Clemente, José-María García-García, Gina Gualano, José Antonio Gullón-Blanco, Sandra Inwentarz, Giuseppe Ippolito, Heinke Kunst, Andrei Maryandyshev, Mario Melazzini, Fernanda Carvalho de Queiroz Mello, Marcela Muñoz-Torrico, Patrick Bung Njungfiyini, Domingo Juan Palmero, Fabrizio Palmieri, Pavilio Piccioni, Alberto Piubello, Adrian Rendon, Josefina Sabriá, Matteo Saporiti, Paola Scognamiglio, Samridhi Sharma, Denise Rossato Silva, Mahamadou Bassirou Souleymane, Antonio Spanevello, Eva Tabernero, Marina Tadolini, Michel Eke Tchangou, Alice Boi Yatta Thornton, Simon Tiberi, Zarir F. Udwadia, Giovanni Sotgiu, Catherine Wei Min Ong,[2] Delia Goletti[2]

Author affiliations: Istituti Clinici Scientifici Maugeri IRCCS, Tradate, Italy (G.B. Migliori, R. Centis, A. Spanevello); Yong Loo Lin School of Medicine, National University of Singapore, Singapore (P.M. Thong, C.W.M. Ong); University of Groningen, Groningen, the Netherlands (O. Akkerman); The University of Sydney, Sydney, New South Wales, Australia (J.-W. Alffenaar, J.-G. Cho); Westmead Hospital, Sydney (J.-W. Alffenaar, J.-G. Cho); Hospital Universitario San Agustín, Avilés, Spain (F. Álvarez-Navascués, J.A. Gullón-Blanco); National Tuberculosis Programme, Niamey, Niger (M.M. Assao-Neino); Centre Hospitalier Universitaire, Nantes, France (P.V. Bernard, F.-X. Blanc); Community Health Centre, Tombo, Sierra Leone (J.S. Biala); Moscow Research and Clinical Center for TB Control, Moscow, Russia (E.M. Bogorodskaya, S. Borisov); Fondazione Policlinico Universitario A. Gemelli IRCCS, Rome, Italy (D. Buonsenso); University Research Co. LLC, Manila, the Philippines (M. Calnan); Niguarda Hospital, Milan, Italy (P.F. Castellotti, L.R. Codecasa, M. Ferrarese, M. Saporiti); Kenyatta University, Nairobi, Kenya (J.M. Chakaya); Liverpool School of Tropical Medicine, Liverpool, UK (J.M. Chakaya); Parramatta Chest Clinic, Parramatta, New South Wales, Australia (J.-G. Cho); Public Health Consulting Group, Lugano, Switzerland (L. D'Ambrosio); Melbourne Health Victorian Tuberculosis Program, Melbourne, Victoria, Australia (J. Denholm); University of Melbourne, Melbourne (J. Denholm); Amity Health Consortium, Johannesburg, South Africa (M. Enwerem); Universidade Federal da Bahia, Salvador, Brazil (T. Galvão); Hospital Universitario Central de Asturias, Oviedo, Spain (M. García-Clemente); Tuberculosis Research Programme SEPAR, Barcelona, Spain (J.-M. García-García); National Institute for Infectious Diseases 'L. Spallanzani' IRCCS, Rome (G. Gualano, G. Ippolito, F. Palmieri, P. Scognamiglio, D. Goletti); Instituto Vaccarezza, Buenos Aires, Argentina (S. Inwentarz, D.J. Palmero); Royal London Hospital of Barts Health National Health Service Trust, London, UK (H. Kunst, S. Tiberi); Queen Mary University, London (H. Kunst, S. Tiberi); Northern State Medical University, Arkhangelsk, Russian Federation (A. Maryandyshev); Istituti Clinici Scientifici Maugeri IRCCS, Pavia, Italy (M. Melazzini); Instituto de Doenças do Tórax, Universidade Federal do Rio de Janeiro, Rio de Janeiro, Brazil (F.C.Q. Mello); Instituto Nacional De Enfermedades Respiratorias Ismael Cosio Villegas, Mexico City, Mexico (M. Muñoz-Torrico); Community Health Center, Hastings, Sierra Leone (P.B. Njungfiyini; M.E. Tchangou); Amedeo di Savoia Hospital, Turin, Italy (P. Piccioni); Damien Foundation, Niamey, Niger (A. Piubello, M.B. Souleymane); University Hospital of Monterrey (Universidad Autonoma de Nuevo Leon), Monterrey, Mexico (A. Rendon); Hospital Transversal Moises Broggi-HGH, Barcelona (J. Sabriá); P.D. Hinduja National Hospital and Medical Research Centre, Mumbai, India (S. Sharma, Z.F. Udwadia); Universidade Federal do Rio Grande do Sul (UFRGS), Porto Alegre, Brazil (D.R. Silva); University of Insubria, Varese-Como, Italy (A. Spanevello); Hospital de Cruces, Vizcaya, Spain (E. Tabernero); Unit of Infectious Diseases Alma Mater Studiorum University of Bologna, Bologna, Italy (M. Tadolini); Saint John of God Catholic Hospital, Mabesseneh Lunsar, Sierra Leone (A.B.Y. Thornton); University of Sassari, Sassari, Italy (G. Sotgiu); National University of Singapore, Singapore (C.W.M. Ong)

[1]These first authors contributed equally to this article.
[2]These senior authors contributed equally to this article.

Coronavirus disease has disrupted tuberculosis services globally. Data from 33 centers in 16 countries on 5 continents showed that attendance at tuberculosis centers was lower during the first 4 months of the pandemic in 2020 than for the same period in 2019. Resources are needed to ensure tuberculosis care continuity during the pandemic.

The coronavirus disease (COVID-19) pandemic has affected clinical management of tuberculosis (TB) and TB-related services (1,2). Reports of the first cohorts of patients with COVID-19 and TB have been recently published (3,4), although it may be difficult to distinguish which infection occurred first (5). The effects of COVID-19 on TB diagnostic and programmatic activities are similar (1). Almost every country has national TB programs in place, whereas national programs for COVID-19 are urgently needed (1,2).

The effect of COVID-19 on TB services is estimated to be dramatic, especially in countries where healthcare staff involved in TB management have been reassigned to the COVID-19 emergency. However, apart from local studies (6), a comprehensive, multinational description is needed.

The Global Tuberculosis Network, which conducted this study, collaborates with TB centers from 41 countries (3,4,6,7). We studied patient attendance at TB centers in 16 countries and compared the volume of TB-related healthcare activities in the first 4 months of the COVID-19 pandemic, January–April 2020, with that for the same period in 2019.

The Study

We invited 37 TB centers to participate in the study and collected data from 33 centers located in 16 countries on 5 continents (Appendix Tables 1, 2, https:// wwwnc.cdc.gov/EID/article/26/11/20-3163-App1. pdf). The participating centers received ethics clearance according to their respective center regulations (7,8). Active TB disease and latent TB infection (LTBI) were defined according to international guidelines (9,10). We recorded numbers of patients with active TB discharged from inpatient care, patients with newly diagnosed cases of active TB, patients with active TB visiting outpatient settings, and new and total outpatient visits for LTBI. We defined use of telehealth services as implementation of directly observed therapy during face-to-face virtual teleconsultations, which were considered to be equivalent to outpatient visits and were counted as such. We did not consider patient contact by telephone and emails to be telehealth. Home visits were considered outpatient visits. We also recorded national lockdown dates. If a country

reported results from >1 center, we used the sum of the attendances to generate the graphs. Quantitative variables were summarized with absolute (percentage) frequencies.

Of the 16 countries studied, data were contributed by 4 TB centers each in Italy, Russia, Spain, and Brazil; 3 each in Sierra Leone and Niger; 2 in Mexico; and 1 each in 9 other countries (Appendix Tables 1, 2). Lockdowns were imposed in all countries (Appendix Figures 1, 2). The earliest lockdown start date was February 1, 2020 (Australia); the latest was April 7, 2020 (Singapore). By the end of data collection (April 30), none of the 16 countries had reduced lockdown severity.

Data on new active TB cases were available from 32 of the 33 TB centers. Except for 5 centers (Sydney, New South Wales, Australia; San Fernando, the Philippines; Turin, Italy; Asturias, Spain; and London, UK), which each reported stable numbers or moderate increases, new active TB cases decreased in 27 (84%) of the 32 TB centers in the first 4 months of 2020 relative to the same period in 2019 (Appendix Figure 1).

Information about total outpatient TB visits was available for 29 centers but not from Groningen, the Netherlands; Mexico City, Mexico; Porto Alegre, Brazil; and Nairobi, Kenya. A total of 22 (75%) of 29 TB centers from 14 countries registered decreased outpatient visits during the lockdowns.

Active TB–associated hospital discharges differed in 2020 from 2019. Although data were not available for a few centers (Buenos Aires, Argentina; Nairobi; and the 3 centers in Niger), data for San Fernando, Singapore; Mexico City, Groningen, and London indicated minimal or no increase. Active TB–associated hospital discharges for the remaining 23 (82%) of 28 TB centers were lower during the first 4 months of 2020.

Data for LTBI outpatient visits were available from 16 of the 33 TB centers; 13 (81%) recorded decreased total outpatient visits (all except Hastings, Sierra Leone; Alvorada, Brazil; and Barcelona, Spain) (Appendix Figure 2). Data for newly diagnosed LT-BIs were available from 19 of the 33 TB centers. New LTBI outpatient visits at 18 (95%) of 19 TB centers (all except Alvorada) were fewer during the lockdown period (Appendix Figure 2).

During the first 4 months of 2020, telehealth services were used by 7 (21%) of the 33 TB centers. The number of patients using telehealth services was reported by 4 centers: Sydney; Mumbai, India; London; and Arkhangelsk, Russia. Increased use of telehealth services correlated with lockdown implementation; most uses were recorded in April 2020 (Appendix Tables 1, 2).

Conclusions

For most TB centers during their respective national lockdowns in the first 4 months of 2020, we found reductions in TB-related hospital discharges, newly diagnosed cases of active TB, total active TB outpatient visits, and new LTBI and LTBI outpatient visits. These results may be explained by a general decrease in the use of health services, including emergency services (*11*). Resources for TB service provision were reassigned to other medical services. Outpatient visit numbers may have decreased because of patients' fear of exposure to severe acute respiratory syndrome coronavirus 2 (*12*). Access to medical services may have decreased because of interruptions in or difficulty accessing public transportation, although health-related travel was permitted in most countries. In some TB centers (e.g., Mexico City), the hospital patient intake system was modified to support COVID-19 admissions, thus severely hindering TB services. In some centers, screening for LTBI was considered a lower priority than screening for active TB or COVID-19. Because of lockdowns, reactivation of active TB in persons with LTBI who did not receive preventive therapy may be expected, such as in contacts recently exposed to TB or in those who are immunocompromised (*13,14*). In England, compared with 2019, TB notifications decreased by 16.5% during April and by 37.3% during May 2020; the LTBI program was paused in response to COVID-19 on March 26 (*15*).

Lockdowns have favored the increased use of telemedicine. Telehealth is a new service offered by TB programs. In TB centers surveyed in Australia, Russia, India, and the United Kingdom, telehealth service use increased in the first 4 months of 2020.

Although our study cannot comprehensively describe all features of TB management, we found that the COVID-19 pandemic had a substantial impact on TB services worldwide. The main strength of our study is the global coverage from 33 TB centers from 16 countries on 5 continents. Limitations include lack of data from some countries. In 9 of the 16 countries, data were limited to reports from only 1 TB center, which may not have fully represented that nation's TB healthcare activities. In addition, some TB centers were located in countries with low TB incidence (e.g., Italy). The description of the changes in the TB burden over a few months did not allow for appropriate statistical inferences in these countries with low TB incidence. More information about the medium- and long-term effects of the COVID-19 pandemic on TB services after a specified time from the diagnosis of the first COVID-19 patient in each country is needed.

The COVID-19 pandemic seems to have affected TB services in all 16 countries that provided data.

At select TB centers, increased use of telehealth services during the pandemic was recorded. Resources urgently need to be channeled to ensure that TB care continues efficiently despite the ongoing COVID-19 pandemic.

About the Author

Prof. Migliori is director of the World Health Organization Collaborating Centre for Tuberculosis and Lung diseases at Istituti Clinici Scientifici Maugeri, Tradate, Italy, and chair of the Global Tuberculosis Network. Primary research interests are prevention, diagnosis, treatment, and rehabilitation of TB, including its relationship with COVID-19.

References

1. Dara M, Sotgiu G, Reichler MR, Chiang CY, Chee CBE, Migliori GB. New diseases and old threats: lessons from tuberculosis for the COVID-19 response. Int J Tuberc Lung Dis. 2020;24:544–5. https://doi.org/10.5588/ijtld.20.0151
2. Alagna R, Besozzi G, Codecasa LR, Gori A, Migliori GB, Raviglione M, et al. Celebrating World Tuberculosis Day at the time of COVID-19. Eur Respir J. 2020;55:2000650. https://doi.org/10.1183/13993003.00650-2020
3. Motta I, Centis R, D'Ambrosio L, García-García JM, Goletti D, Gualano G, et al. Tuberculosis, COVID-19 and migrants: preliminary analysis of deaths occurring in 69

patients from two cohorts. Pulmonology. 2020;26:233–40. https://doi.org/10.1016/j.pulmoe.2020.05.002

4. Tadolini M, Codecasa LR, García-García JM, Blanc FX, Borisov S, Alffenaar JW, et al. Active tuberculosis, sequelae and COVID-19 co-infection: first cohort of 49 cases. Eur Respir J. 2020;56:2001398. https://doi.org/10.1183/13993003.01398-2020

5. Tadolini M, Garcia-Garcia JM, Blanc FX, Borisov S, Goletti D, Motta I, et al. On tuberculosis and COVID-19 co-infection [cited 2020 Aug 13]. https://erj.ersjournals.com/content/early/2020/06/18/13993003.02328-2020

6. Buonsenso D, Iodice F, Sorba Biala J, Goletti D. COVID-19 effects on tuberculosis care in Sierra Leone. Pulmonology [cited 2020 Aug 13]. https://www.journalpulmonology.org/en-covid-19-effects-on-tuberculosis-care-avance-S2531043720301306

7. Borisov S, Danila E, Maryandyshev A, Dalcolmo M, Miliauskas S, Kuksa L, et al. Surveillance of adverse events in the treatment of drug-resistant tuberculosis: first global report. Eur Respir J. 2019;54:1901522. https://doi.org/10.1183/13993003.01522-2019

8. Akkerman O, Aleksa A, Alffenaar JW, Al-Marzouqi NH, Arias-Guillén M, Belilovski E, et al.; members of the International Study Group on new anti-tuberculosis drugs and adverse events monitoring. Surveillance of adverse events in the treatment of drug-resistant tuberculosis: A global feasibility study. Int J Infect Dis. 2019;83:72–6. https://doi.org/10.1016/j.ijid.2019.03.036

9. Migliori GB, Sotgiu G, Rosales-Klintz S, Centis R, D'Ambrosio L, Abubakar I, et al. ERS/ECDC Statement: European Union standards for tuberculosis care, 2017 update. Eur Respir J. 2018;51:1702678. https://doi.org/10.1183/13993003.02678-2017

10. Getahun H, Matteelli A, Abubakar I, Aziz MA, Baddeley A, Barreira D, et al. Management of latent *Mycobacterium tuberculosis* infection: WHO guidelines for low tuberculosis burden countries. Eur Respir J. 2015;46:1563–76. https://doi.org/10.1183/13993003.01245-2015

11. Lange SJ, Ritchey MD, Goodman AB, Dias T, Twentyman E, Fuld J, et al. Potential indirect effects of the COVID-19 pandemic on use of emergency departments for acute life-threatening conditions—United States, January–May 2020. MMWR Morb Mortal Wkly Rep. 2020;69:795–800. https://doi.org/10.15585/mmwr.mm6925e2

12. Min Ong CW, Migliori GB, Raviglione M, MacGregor-Skinner G, Sotgiu G, Alffenaar JW, et al. Epidemic and pandemic viral infections: impact on tuberculosis and the lung. A consensus by the World Association for Infectious Diseases and Immunological Disorders (WAidid), Global Tuberculosis Network (GTN) and members of ESCMID Study Group for Mycobacterial Infections (ESGMYC). Eur Respir J. 2020;2001727. https://doi.org/10.1183/13993003.01727-2020

13. Esmail H, Cobelens F, Goletti D. Transcriptional biomarkers for predicting development of tuberculosis: progress and clinical considerations. Eur Respir J. 2020;55:1901957. https://doi.org/10.1183/13993003.01957-2019

14. Goletti D, Petrone L, Ippolito G, Niccoli L, Nannini C, Cantini F. Preventive therapy for tuberculosis in rheumatological patients undergoing therapy with biological drugs. Expert Rev Anti Infect Ther. 2018;16:501–12. https://doi.org/10.1080/14787210.2018.1483238

15. TB Surveillance in the COVID-19 epidemic: national monthly report (provisional data): 1 January 2019 to 31 May 2020 [cited 2020 Jul 23]. https://www.gov.uk/government/statistics/tuberculosis-in-england-quarterly-reports

Address for correspondence: Catherine Ong, National University of Singapore, Division of Infectious Diseases, Department of Medicine, Yong Loo Lin School of Medicine, 1E Kent Ridge Rd, 10th Fl Tower Block, Singapore 119228; email: catherine_wm_ong@nuhs.edu.sg

EID SPOTLIGHT TOPIC: Tuberculosis

World TB Day, falling on March 24th each year, is designed to build public awareness that tuberculosis today remains an epidemic in much of the world, causing the deaths of nearly one-and-a-half million people each year, mostly in developing countries. It commemorates the day in 1882 when Dr Robert Koch astounded the scientific community by announcing that he had discovered the cause of tuberculosis, the TB bacillus. At the time of Koch's announcement in Berlin, TB was raging through Europe and the Americas, causing the death of one out of every seven people. Koch's discovery opened the way towards diagnosing and curing TB.

Click on the link below to access *Emerging Infectious Diseases* articles and podcasts, and to learn more about the latest information and emerging trends in TB.

EMERGING INFECTIOUS DISEASES® **http://wwwnc.cdc.gov/eid/page/world-tb-day**

In-Flight Transmission of Severe Acute Respiratory SARS-CoV-2

Edward M. Choi, Daniel K.W. Chu, Peter K.C. Cheng, Dominic N.C. Tsang, Malik Peiris,
Daniel G. Bausch, Leo L.M. Poon, Deborah Watson-Jones

Four persons with severe acute respiratory syndrome coronavirus 2 infection had traveled on the same flight from Boston, Massachusetts, USA, to Hong Kong, China. Their virus genetic sequences are identical, unique, and belong to a clade not previously identified in Hong Kong, which strongly suggests that the virus can be transmitted during air travel.

In 2019, severe acute respiratory syndrome coronavirus 2 (SARS-CoV-2) emerged in China, ultimately causing the coronavirus disease (COVID-19) pandemic. Many persons with SARS-CoV-2 infection have since flown into and out of COVID-19–affected areas (*1*). Some countries quarantine arriving passengers. Airports are also screening passenger body temperatures before boarding and after arrival. Recent investigations have shown that SARS-CoV-2 can be transmitted before symptom onset, posing a challenge to outbreak control (*2*). Although risks for SARS-CoV-2 transmission have been extensively investigated, in-flight transmission of the virus has not been formally confirmed. Airline staff members have voiced concerns over acquisition of SARS-CoV-2 infection (*3*). Given that flights are still departing to and from COVID-19–affected countries, determining whether in-flight transmission of SARS-CoV-2 occurs is essential.

The Study

We examined public records for 1,110 persons with laboratory-confirmed COVID-19 in Hong Kong, Chi-

Author affiliations: London School of Hygiene & Tropical Medicine, London, UK (E.M. Choi, D.G. Bausch, D. Watson-Jones); The University of Hong Kong, Hong Kong, China (D.K.W. Chu, M. Peiris, L.L.M. Poon); Department of Health, The Government of Hong Kong Special Administrative Region, Hong Kong (P.K.C. Cheng, D.N.C. Tsang); Public Health England, London (D.G. Bausch); National Institute for Medical Research, Mwanza, Tanzania (D. Watson-Jones)

na, recorded from January 23 through June 13, 2020; we used Centre for Health Protection (CHP) public records and the Vote4HK COVID-19 in HK database for case-patients who had traveled before diagnosis (*4*,*5*). At the time, the Hong Kong government had yet to introduce mandatory quarantine and airport screening (*6*). We identified a cluster of 4 persons with COVID-19 (henceforth referred to as patients A–D) associated with a commercial flight that departed from Boston, Massachusetts, USA, on March 9 and arrived in Hong Kong on March 10, 2020. The airplane, a Boeing 777-300ER, flew for ≈15 hours and carried a maximum of 294 passengers. The cluster comprised 2 passengers and 2 cabin crew members. Although these persons did not fulfill the criteria for SARS-CoV-2 testing at the time of arrival, results of reverse transcription PCR conducted in local healthcare settings within 5–11 days of arrival were positive. All 4 case-patients subsequently recovered (Appendix Figure 1, https://wwwnc.cdc.gov/EID/article/26/11/20-3254-App1.pdf).

Patients A and B were a married couple. Patient A was a 58-year-old man with underlying disease who sat in a window seat in business class on the airplane (Appendix Figure 2). On March 10, fever and productive cough developed; on March 13, he had mild abdominal discomfort, followed by diarrhea 2 days later. His 61-year-old wife, patient B, also had underlying illness. She sat directly in front of him in a business class window seat. On March 10, she had a sore throat. One day later, fever and cough developed. As their symptoms evolved, they sought healthcare and were hospitalized on March 14. On March 15, respiratory samples (collected March 14 for patient A and March 15 for patient B) were positive for SARS-CoV-2. No public record indicates what their underlying diseases were or whether these 2 passengers were symptomatic during the flight. Before the flight and within the 14-day incubation period, they visited

Toronto, Ontario, Canada (February 15–March 2); New York, New York, USA (March 2–5); and Boston (March 5–9). CHP classified the couple as imported cases into Hong Kong.

Patient C was an asymptomatic 25-year-old man identified through contact tracing by the Hong Kong government and the airline as a close contact of patients A and B. He was a Hong Kong–based business class flight attendant who served patients A and B during the flight. After patients A and B received their diagnoses, the airline informed patient C, and he attended an outpatient clinic on March 16. He was positive for SARS-CoV-2 on March 17

and was subsequently quarantined and hospitalized. Patient C stayed in Boston during March 5–9. Patient D was a 51-year-old female Hong Kong–based flight attendant on the same flight. Fever and cough developed on March 18, SARS-CoV-2 test result was positive on March 21, and patient D was hospitalized. There is no publicly available information of her travel history before the flight or her contacts with the other patients on or after the flight. Descriptions of the disease experienced by patients C and D were unavailable. CHP categorized patients C and D as close contacts of a person with an imported case.
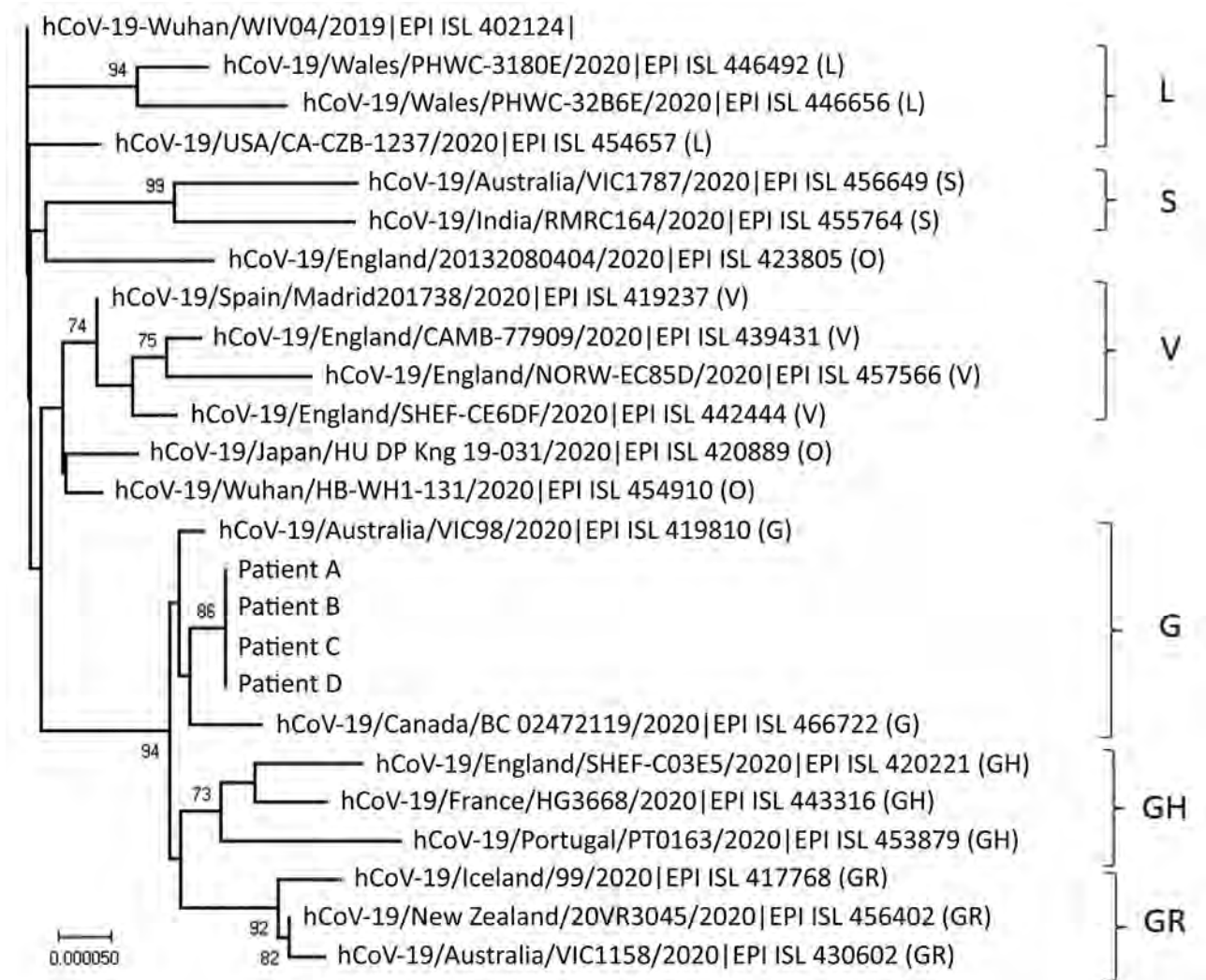
Figure. Phylogenetic tree of the severe acute respiratory syndrome coronavirus 2 (SARS-CoV-2) viruses isolated from passengers and airline crew members who traveled on the same flight from Boston, Massachusetts, USA, to Hong Kong, China. Human SARS-CoV-2 WIV04 is selected to be the root of this phylogenetic tree. The tree was constructed by using the neighbor-joining method. Only bootstrap values >80 are shown. Representative viruses from clades L, S, V, G, GH, GR, and O (others) are included in the analysis. Virus sequences from patients A–D reported in this study are grouped to clade G (GISAID [http://platform.gisaid.org] accession nos. EPI_ISL_476801 to EPI_ISL_476804). EPI ISL accession nos. for sequences retrieved in GISAID (http://platform.gisaid.org) are provided. Scale bar indicates estimated genetic distance.

Table. Single nucleotide polymorphisms in the SARS-CoV-2 virus sequences from 4 patients on the same flight from Boston, Massachusetts, USA, to Hong Kong, China*

GISAID accession no.	Source	Sample collection date	Nucleotide positions†						Nucleotide difference‡
			241	3037	9857	11083	14408	23403	
402124	Reference sequence WIV04†	2019 Dec 30	C	C	C	G	C	A	6
476802	Patient A	2020 Mar 14	T	T	T	T§	T¶	G#	0
476801	Patient B	2020 Mar 15	T	T	T	T§	T¶	G#	0
476803	Patient C	2020 Mar 17	T	T	T	T§	T¶	G#	0
476804	Patient D	2020 Mar 19	T	T	T	T§	T¶	G#	0
460471	Massachusetts, USA	2020 Mar 27	T	T	C	G	T¶	G#	2
427528	New York, USA	2020 Mar 12	T	T	C	G	T¶	G#	2
418354	Ontario, Canada	2020 Mar 15	T	T	C	G	T¶	G#	2

*These 4 viral genomes are unique among the sequences deposited into the GISAID database (http://platform.gisaid.org) January 10–June 13, 2020. They contain 6 polymorphisms compared with the WIV04 reference sequence of SARS-CoV-2, 3 of which are nonconservative. SARS-CoV-2 genomes that differ from these by 2 nt had been reported from Massachusetts, USA; New York, USA; and Ontario, Canada, in March 2020. SARS-CoV-2, severe acute respiratory syndrome coronavirus 2.
†A 2019 reference sequence from a patient in Wuhan, China (hCoV-19/Wuhan/WIV04/2019). The nucleotide positions shown are relative to this reference sequence (GISAID accession ID EPL_ISL_402124).
‡No. nucleotide differences relative to the virus genomes of patients A–D.
§Nonconservative polymorphism at nucleotide position 11083, which corresponds to a Leu (TTG) to Phe (TTT), L37F, amino acid change in the NSP6 protein.
¶Nonconservative polymorphism at nucleotide position 14408, which corresponds to a Pro (CCT) to Leu (CTT), P323L, amino acid change in the NSP12 protein.
#Nonconservative polymorphism at nucleotide position 23403, which corresponds to an Asp (GAT) to Gly (GGT), D614G, amino acid change in the spike protein.

To generate genetic evidence for transmission between the 4 patients, we sequenced their viruses. Samples were collected under public health authority, and individual patient identities are known to CHP. Retrospective analysis of leftover samples without individual consent was permitted under local regulations and approved by the institutional review board of the University of Hong Kong/Hospital Authority West Cluster (reference UW 20-168) and the London School of Hygiene & Tropical Medicine Ethics Committee (reference 22384). Stored upper respiratory samples were sent to a World Health Organization reference laboratory at the University of Hong Kong. We deduced near full-length genomes (sequence length ≥29,760 nt) by using the Illumina sequencing method and previously described primers and protocol (7). All deduced sequences had a minimum coverage of 100. While sequencing and analyzing the specimens, we were blinded to patient status as passenger or crew.

The near full-length viral genomes from all 4 patients were 100% identical and phylogenetically grouped to clade G (Figure). Other than these 4, none of the 189 viral sequences deduced from samples collected in Hong Kong (January 21–May 12, 2020; GISAID, http://platform.gisaid.org), belong to this clade (data not shown) (K.S. Leung et al., unpub. data, https://www.medrxiv.org/content/10.1101/2020.03.30.20045740v2). Conversely, in March 2020, virus sequences related to those of patients A–D with only 2 nt differences were isolated in Toronto, New York City, and Massachusetts (Table), making it plausible that patients A and B acquired a similar virus dur-

ing their visit. Worldwide during January 10–June 13, ≈30,000 complete SARS-CoV-2 genomes with high coverage were deposited into the GISAID database. None shares 100% identity with the sequences of the viruses in the cluster reported here.

Conclusions

Given the case histories and sequencing results, the most likely sequence of events is that one or both of passengers A and B contracted SARS-CoV-2 in North America and transmitted the virus to flight attendants C and D during the flight. The only location where all 4 persons were in close proximity for an extended period was inside the airplane. Passengers and cabin crew do not generally go through the same check-in process at airports before boarding. Although we cannot completely rule out the possibility that patients C and D were infected before boarding, the unique virus sequence and 100% identity across the whole virus genome from the 4 patients makes this scenario highly unlikely. Patient D may have acquired infection from patient C, but because their test results were positive within 1 incubation period, it is more likely that patient D was infected by patient A or B. We therefore conclude that these 4 patients belong to the same in-flight transmission chain.

Our results strongly suggest in-flight transmission of SARS-CoV-2. No other COVID-19 cases associated with this flight have been identified. We were unable to quantify the virus attack rate on this flight because not all passengers were tested.

Previous reports of probable in-flight transmissions of SARS-CoV-2 lack genetic evidence (8,9).

During January–March 2020, the International Air Transport Association received 3 reports of suspected in-flight transmission (*10*). Contact tracing of 2 passengers who flew from China to Canada has yielded no indication of secondary infections from the flight (*11*). Nonetheless, SARS-CoV-2 test results have been positive for hundreds of flight attendants and pilots; at least 2 have died (*12,13*). Our results demonstrate that SARS-CoV-2 can be transmitted on airplanes. To prevent transmission of the virus during travel, infection control measures must continue.

About the Author

Dr. Choi is an assistant professor at the London School and Hygiene & Tropical Medicine. His research interests include viral infections and vaccine development.

References

1. Ng O-T, Marimuthu K, Chia P-Y, Koh V, Chiew CJ, De Wang L, et al. SARS-CoV-2 infection among travelers returning from Wuhan, China. N Engl J Med. 2020;382: 1476–8. https://doi.org/10.1056/NEJMc2003100
2. Furukawa NW, Brooks JT, Sobel J. Evidence supporting transmission of severe acute respiratory syndrome coronavirus 2 while presymptomatic or asymptomatic. Emerg Infect Dis. 2020 May 4 [Epub ahead of print]. https://doi.org/10.3201/eid2607.201595
3. Burridge T. BA cabin crew virus fears after long-haul flights [cited 2020 Jun 24]. https://www.bbc.co.uk/news/business-52126661
4. The Government of Hong Kong Special Administrative Region. Latest local situation of COVID-19 [cited 2020 Jun 15]. https://www.coronavirus.gov.hk/eng/index.html
5. COVID-19 in HK [cited 2020 Jun 15]. https://wars.vote4.hk/en/cases
6. Saiidi U. Hong Kong is putting electronic wristbands on arriving passengers to enforce coronavirus quarantine [cited 2020 Jun 24]. https://www.cnbc.com/2020/03/18/hong-kong-uses-electronic-wristbands-to-enforce-coronavirus-quarantine.html
7. Sit THC, Brackman CJ, Ip SM, Tam KWS, Law PYT, To EMW, et al. Infection of dogs with SARS-CoV-2. Nature. 2020 May 14 [Epub ahead of print]. https://doi.org/10.1038/s41586-020-2334-5
8. Qian GQ, Yang NB, Ding F, Ma AHY, Wang ZY, Shen YF, et al. Epidemiologic and clinical characteristics of 91 hospitalized patients with COVID-19 in Zhejiang, China: a retrospective, multi-centre case series. QJM. 2020;113:474–81. https://doi.org/10.1093/qjmed/hcaa089
9. Eldin C, Lagier JC, Mailhe M, Gautret P. Probable aircraft transmission of Covid-19 in-flight from the Central African Republic to France. Travel Med Infect Dis. 2020;35:101643. https://doi.org/10.1016/j.tmaid.2020.101643
10. International Air Transport Association. Restarting aviation following COVID-19 [cited 2020 Jun 24]. https://www.iata.org/contentassets/f1163430bba94512a583eb6d6b24aa56/covid-medical-evidence-for-strategies-200508.pdf
11. Schwartz KL, Murti M, Finkelstein M, Leis JA, Fitzgerald-Husek A, Bourns L, et al. Lack of COVID-19 transmission on an international flight. CMAJ. 2020;192:E410. PubMed https://doi.org/10.1503/cmaj.75015
12. Wallace G. 100 American Airlines flight attendants have coronavirus, union says [cited 2020 Jun 24]. https://edition.cnn.com/2020/04/07/business/american-airlines-flight-attendants-coronavirus/index.html
13. Mutua K. Covid-19: KQ hero pilot Daudi Kibati laid to rest in Kitui [cited 2020 Jun 24]. https://www.nation.co.ke/kenya/counties/kitui/covid-19-kq-hero-pilot-daudi-kibati-laid-to-rest-in-kitui-284590

Address for correspondence: Leo L.M. Poon, School of Public Health, The University of Hong Kong, 7 Sassoon Rd, Hong Kong, China; email: llmpoon@hku.hk; and Deborah Watson-Jones, London School of Hygiene & Tropical Medicine, Keppel St, London WC1E 7HT, UK; email: deborah.watson-jones@lshtm.ac.uk

Preventing Vectorborne Transmission of Zika Virus Infection During Pregnancy, Puerto Rico, USA, 2016–2017[1]

Katherine Kortsmit, Beatriz Salvesen von Essen, Lee Warner, Denise V. D'Angelo,
Ruben A. Smith, Carrie K. Shapiro-Mendoza, Holly B. Shulman, Wanda Hernández Virella,
Aspy Taraporewalla, Leslie Harrison, Sascha Ellington, Wanda D. Barfield, Denise J. Jamieson,
Shanna Cox, Karen Pazol, Patricia Garcia Díaz, Beatriz Rios Herrera, Manuel Vargas Bernal

We examined pregnant women's use of personal protective measures to prevent mosquito bites during the 2016–2017 Zika outbreak in Puerto Rico. Healthcare provider counseling on recommended measures was associated with increased use of insect repellent among pregnant women but not with wearing protective clothing.

During 2016–2017, Puerto Rico had active transmission of Zika virus (ZIKV). During January 27, 2016–June 10, 2017, the Puerto Rico Department of Health (PRDH) reported 40,357 confirmed cases of ZIKV infection, including 3,833 cases among pregnant women (*1–3*). Because of the severity of adverse birth outcomes (e.g., brain and eye abnormalities, microcephaly, other birth defects) linked to maternal ZIKV infection (*4,5*), the Centers for Disease Control and Prevention (CDC) (*6–9*) and PRDH (*10*) released guidance for preventing ZIKV. In areas where ZIKV transmission was active, pregnant women were advised to prevent mosquito bites by wearing protective clothing (long-sleeved shirts and long pants), and by using Environmental Protection Agency (EPA)–registered insect repellent (*6–10*).

The Study

The Pregnancy Risk Assessment Monitoring System–Zika Postpartum Emergency Response Study (PRAMS-ZPER) was conducted in Puerto Rico by PRDH and CDC to assess women's use of measures to prevent ZIKV infection during pregnancy (*11*). PRAMS-ZPER, a hospital-based survey of women with a recent live birth, was implemented island-wide in 2 phases: August 28–December 3, 2016, and November 1–December 19, 2017. Hospitals with ≥100 births in the year before the study period were eligible to participate. In 2016, all 36 eligible hospitals participated; in 2017, a total of 30 of 31 eligible hospitals with operating maternity wards during the study period participated.

Delivery dates were randomly sampled for each hospital, and delivery logs were used to identify women who delivered on the sampled dates. Eligibility criteria are described elsewhere (*12,13*). In 2016, women were approached 24–36 hours after their infants were delivered (*12*). In 2017, because the environment after Hurricane Maria resulted in early hospital discharges, women were approached within 24 hours postdelivery unless hospital staff recommended otherwise (e.g., mothers who had not yet recuperated). Response rates were 80.6% in 2016 and 94.4% in 2017.

In previous research, we reported 2016 PRAMS-ZPER data on maternal use of ZIKV prevention measures (*12*) and on the association between provider counseling on condom use to prevent ZIKV infection and self-reported use of condoms with sex partners

Author affiliations: Centers for Disease Control and Prevention, Atlanta, Georgia, USA (K. Kortsmit, B. Salvesen von Essen, L. Warner, D.V. D'Angelo, R.A. Smith, C.K. Shapiro-Mendoza, H.B. Shulman, A. Taraporewalla, L. Harrison, S. Ellington, W.D. Barfield, S. Cox, K. Pazol); Puerto Rico Department of Health, San Juan, Puerto Rico, USA (W. Hernández Virella, P. Garcia Díaz, B. Rios Herrera, M. Vargas Bernal); Emory University School of Medicine, Atlanta (D.J. Jamieson)

[1]Presented in part at the 2018 CityMatCH Leadership and MCH Epidemiology Conference, Portland, Oregon, September 12–14, 2018.

during pregnancy (*13*). In this analysis, we report on the association between counseling from prenatal care providers and women wearing protective clothing and using insect repellent during pregnancy to prevent ZIKV infection using data from 2016 and 2017. We assessed the prevalence of wearing protective clothing and using repellent overall and by select maternal characteristics (e.g., education level, marital status; Table 1). We constructed separate multivariable, survey-weighted, logistic regression models for each study year to examine maternal characteristics associated with receiving provider counseling on wearing protective clothing and using repellent to prevent mosquito bites. We constructed separate multivariable models to examine associations between factors identified a priori, including receiving provider counseling, with wearing protective clothing daily and using repellent frequently (defined as use every day in 2016 and use always in 2017) when outside during pregnancy. Each model was further adjusted for maternal characteristics, health district region, and delivery month.

Among 3,806 combined respondents in 2016–2017, nearly all, 99.4%, received prenatal care. Among those who received prenatal care, 87.8% participated in the Special Supplemental Nutrition Program for Women, Infants, and Children (WIC) during pregnancy, 79.0% were 20–34 years of age, 69.5% had >high school education, and 68.6% were unmarried.

Most women reported receiving provider counseling during pregnancy to wear protective clothing in 2016 (87.1%) and 2017 (79.8%) (Table 1); however, few women reported wearing protective clothing daily during either year (11.3% in 2016 and 7.9% in 2017) (Table 2). In 2016, the prevalence of wearing protective clothing was lower among women ≤19 years (7.8%; adjusted prevalence ratio [aPR] 0.46, 95% CI 0.27–0.77) and 20–34 years (11.1%; aPR 0.65, 95% CI 0.46–0.94) compared with those ≥35 years (17.0%) of age and higher among women with less than a high school diploma (20.2%; aPR 2.03, 95% CI 1.38–2.99) and a high school diploma (13.2%; aPR 1.33, 95% CI 1.01–1.73) compared with those who had more than a high school education (9.9%). In 2017, the prevalence of wearing protective clothing was lower among women 20–34 years compared with ≥35 years of age (7.1% vs 13.5%; aPR 0.52, 95% CI 0.36–0.76) and higher among women with a high school diploma compared with those with more than a high school education (10.9% vs 7.0%; aPR 1.55, 95% CI 1.13–2.14). Although receiving provider counseling varied by age and WIC participation in 2016–2017 (Table 1), wearing protective clothing did not differ by receiving provider counseling during either study year (Table 2). The most common reason women reported for not wearing protective clothing was that it was too hot (>75%).

Most women also reported receiving provider counseling during pregnancy about repellent use in

Table 1. Adjusted weighted prevalence estimates and prevalence ratios of receiving provider counseling on personal protective measures during pregnancy to prevent vectorborne transmission of Zika virus by maternal characteristics, PRAMS-ZPER, Puerto Rico, USA, 2016–2017*

Maternal characteristics	Received provider counseling on types of clothes to wear to prevent mosquito bites				Received provider counseling about using mosquito repellent			
	2016, n = 2,241†		2017, n = 1,375†		2016, n = 2,244†		2017, n = 1,382†	
	%‡	aPR (95% CI)‡	%‡	aPR (95% CI)‡	%‡	aPR (95% CI)‡	%‡	aPR (95% CI)‡
Total§	87.1	NA	79.8	NA	92.0	NA	90.2	NA
Age, y								
≤19	90.0	1.09 (1.02–1.17)¶	82.2	0.97 (0.89–1.06)	91.5	1.00 (0.96–1.05)	95.9	1.03 (0.99–1.08)
20–34	87.3	1.06 (1.00–1.13)	78.7	0.93 (0.88–0.98)¶	92.1	1.01 (0.97–1.05)	88.9	0.96 (0.93–1.00)
≥35	82.4	Referent	84.4	Referent	91.3	Referent	92.6	Referent
Education level								
<HS diploma	86.7	0.99 (0.94–1.06)	77.2	0.97 (0.88–1.06)	93.4	1.02 (0.98–1.05)	84.2	0.93 (0.85–1.01)
HS diploma	86.7	0.99 (0.96–1.03)	80.8	1.01 (0.96–1.07)	92.1	1.00 (0.98–1.03)	89.9	0.99 (0.96–1.03)
>HS	87.2	Referent	79.7	Referent	91.8	Referent	90.6	Referent
Marital status during pregnancy								
Unmarried	86.6	0.99 (0.95–1.02)	79.5	0.99 (0.95–1.04)	92.1	1.00 (0.98–1.03)	90.0	0.99 (0.96–1.02)
Married	87.9	Referent	80.3	Referent	91.8	Referent	90.6	Referent
Prenatal WIC participation								
Yes	88.0	1.11 (1.03–1.19)¶	81.0	1.11 (1.03–1.20)¶	92.3	1.04 (0.99–1.10)	90.7	1.04 (1.00–1.09)
No	79.5	Referent	73.0	Referent	88.7	Referent	87.1	Referent

*On the 2016 PRAMS-ZPER survey, women were asked about receiving counseling from a healthcare provider about using mosquito repellent on their skin only. On the 2017 PRAMS-ZPER survey, the question was expanded to ask about mosquito repellent on their skin or clothing. aPR, adjusted prevalence ratio; HS, high school; NA, not applicable; PRAMS-ZPER, Pregnancy Risk Assessment Monitoring System–Zika Postpartum Emergency Response Study; WIC, Special Supplemental Nutrition Program for Women, Infants, and Children.
†Unweighted sample size; sample size varies because of missing responses.
‡Prevalence and prevalence ratio estimates adjusted for maternal age, education, marital status, prenatal WIC participation, infant birth month, and health district region (Aguadilla, Arecibo, Bayamon, Caguas, Fajardo, Mayaguez, Metro, or Ponce).
§Unadjusted prevalence estimates.
¶Statistically significant result.

Table 2. Adjusted weighted prevalence estimates and prevalence ratios of self-reported use of personal protective measures to prevent vectorborne transmission of Zika virus during pregnancy by maternal characteristics and provider counseling, PRAMS-ZPER, Puerto Rico, USA, 2016–2017*

Maternal characteristics	Wore long sleeves and long pants every day				Frequent mosquito repellent use†			
	2016, n = 2,238‡		2017, n = 1,365‡		2016, n = 2,241‡		2017, n = 1,375‡	
	%§	aPR (95% CI)§	%§	aPR (95% CI)§	%§	aPR (95% CI)§	%§	aPR (95% CI)§
Total¶	11.3	NA	7.9	NA	45.4	NA	56.9	NA
Age, y								
≤19	7.8	0.46 (0.27–0.77)#	8.3	0.62 (0.35–1.08)	47.6	0.82 (0.68–0.99)#	53.3	0.87 (0.73–1.04)
20–34	11.1	0.65 (0.46–0.94)#	7.1	0.52 (0.36–0.76)#	43.5	0.75 (0.67–0.85)#	56.6	0.93 (0.84–1.03)
≥35	17.0	Referent	13.5	Referent	57.9	Referent	61.1	Referent
Education level								
<HS diploma	20.2	2.03 (1.38–2.99)#	8.0	1.14 (0.63–2.08)	47.7	1.07 (0.90–1.26)	60.3	1.09 (0.93–1.27)
HS diploma	13.2	1.33 (1.01–1.73)#	10.9	1.55 (1.13–2.14)#	46.4	1.04 (0.93–1.15)	60.6	1.09 (1.00–1.20)
>HS	9.9	Referent	7.0	Referent	44.8	Referent	55.5	Referent
Marital status during pregnancy								
Unmarried	10.8	0.88 (0.68–1.14)	8.6	1.31 (0.92–1.86)	45.6	1.02 (0.92–1.12)	57.4	1.03 (0.95–1.12)
Married	12.3	Referent	6.5	Referent	44.8	Referent	55.8	Referent
Prenatal WIC participation								
Yes	11.2	0.93 (0.63–1.36)	8.1	1.15 (0.73–1.81)	46.6	1.29 (1.07–1.57)#	58.4	1.20 (1.07–1.35)#
No	12.1	Referent	7.0	Referent	36.0	Referent	48.5	Referent
Receipt of provider counseling on types of clothes to wear to prevent mosquito								
Yes	11.3	0.99 (0.73–1.35)	8.2	1.15 (0.79–1.68)	NA	NA	NA	NA
No	11.4	Referent	7.1	Referent	NA	NA	NA	NA
Receipt of provider counseling on using mosquito repellent								
Yes	NA	NA	NA	NA	46.1	1.23 (1.05–1.46)#	58.9	1.52 (1.29–1.78)#
No	NA	NA	NA	NA	37.3	Referent	38.8	Referent

*On the 2016 PRAMS-ZPER survey, women were asked about receiving counseling from a healthcare provider about using mosquito repellent on their skin only. On the 2017 PRAMS-ZPER survey, the question was expanded to ask about mosquito repellent on their skin or clothing. aPR, adjusted prevalence ratio; HS, high school; NA, not applicable; PRAMS-ZPER, Pregnancy Risk Assessment Monitoring System–Zika Postpartum Emergency Response Study; WIC, Special Supplemental Nutrition Program for Women, Infants, and Children.
†Defined as every day use in 2016 and always use in 2017.
‡Unweighted sample size; sample size varies because of missing responses.
§Prevalence and prevalence ratio estimates adjusted for maternal age, education, marital status, prenatal WIC participation, receipt of provider counseling, infant birth month, and health district region (Aguadilla, Arecibo, Bayamon, Caguas, Fajardo, Mayaguez, Metro, or Ponce).
¶Unadjusted prevalence estimates.
#Statistically significant result.

2016 (92.0%) and 2017 (90.2%); receiving counseling did not differ by maternal characteristics. Frequent repellent use was reported by 45.4% of women in 2016 and 56.9% in 2017. In 2016, frequent repellent use was lower among women ≤19 years (47.6%; aPR 0.82, 95% CI 0.68–0.99) and 20–34 years (43.5%; aPR 0.75, 95% CI 0.67–0.85) compared with those ≥35 years of age (57.9%). During 2016–2017, frequent repellent use was higher among women receiving WIC (46.6%; aPR 1.29, 95% CI 1.07–1.57 in 2016; 58.4%; aPR 1.20, 95% CI 1.07–1.35 in 2017) compared with those not receiving WIC (36.0% in 2016 and 48.5% in 2017). Women who received provider counseling on using repellent were also more likely to report frequent repellent use compared with women not receiving counseling in both 2016 (46.1% vs. 37.3%; aPR 1.23, 95% CI 1.05–1.46) and 2017 (58.9% vs. 38.8%; aPR 1.52, 95% CI 1.29–1.78). The most common reason women reported for not using repellent was forgetting to apply or reapply it (>50%).

Conclusions

Most women reported being counseled by a prenatal healthcare provider during pregnancy on using repellent and wearing protective clothing to prevent ZIKV infection from mosquito bites. Provider counseling about repellent use was associated with a higher prevalence of frequent repellent use. This finding is consistent with our previous analysis of PRAMS-ZPER data, which showed receiving provider counseling was associated with a higher prevalence of condom use to prevent sexual transmission of ZIKV infection during pregnancy (13). In contrast, no significant association was found between receiving provider counseling and wearing protective clothing. Efforts to improve use of other risk-reduction strategies to prevent mosquito bites (e.g., repellent use, removal of standing water, screens on windows) may be beneficial, particularly when barriers, such as hot tropical climates, make wearing protective clothing less feasible. In 2017, the questionnaire was modified to include a question about using repellent on clothing in addition to exposed skin. In addition, changes in conditions after Hurricane Maria may have contributed to the increase in reported repellent use. During the ZIKV outbreak, WIC also implemented efforts to provide participants with targeted education on ZIKV prevention strategies and a prevention

kit containing condoms, repellent, a bed net, and larvicide (*14*), which may partially explain increased use of repellent among WIC participants in our analysis. We found a significant association between WIC participation and frequent use of repellent but were unable to further assess the frequency or type of prenatal education WIC recipients received regarding repellent use. Of note, during 2016 only, women were asked whether they received a WIC Zika prevention kit; 77% reported receiving a kit, demonstrating the broad reach of WIC services related to ZIKV prevention among this study sample.

During prenatal care visits, healthcare providers can help prevent ZIKV infection by counseling pregnant women and their partners about risk-reduction strategies. Provider counseling on repellent and condom use were both associated with increased adoption of practices that reduce the risk of ZIKV infection (*13*). Findings from this study can be applied more broadly to the prevention of other vectorborne diseases among pregnant women, such as dengue, chikungunya, and malaria (*7*).

About the Author

Dr. Kortsmit is an epidemiologist at the Centers for Disease Control and Prevention in Atlanta, Georgia, USA. Her primary research interest is women, children, and family health.

References

1. Departamento de Salud de Puerto Rico. Weekly report on arbovirus diseases (ArboV) of the Puerto Rico Department of Health, 2016 Jan 27 [in Spanish] [cited 2019 Oct 24]. http://www.salud.gov.pr/Estadisticas-Registros-y-Publicaciones/Informes%20Arbovirales/Reporte%20ArboV%20semana%202-2016.pdf
2. Departamento de Salud de Puerto Rico. Weekly report on arbovirus diseases (ArboV) of the Puerto Rico Department of Health, 2016 Jun 23 [in Spanish] [cited 2019 Oct 10]. http://www.salud.gov.pr/Estadisticas-Registros-y-Publicaciones/Informes%20Arbovirales/Reporte%20ArboV%20semana%2023-2017.pdf
3. Shapiro-Mendoza CK, Rice ME, Galang RR, Fulton AC, VanMaldeghem K, Valencia Prado M, et al. Zika Pregnancy and Infant Registries Working Group. Pregnancy outcomes after maternal Zika virus infection during pregnancy—U.S. territories, January 1, 2016–April 25, 2017. MMWR Morb Mortal Wkly Rep. 2017;66:615–21. https://doi.org/10.15585/mmwr.mm6623e1
4. Rasmussen SA, Jamieson DJ, Honein MA, Petersen LR. Zika virus and birth defects–reviewing the evidence for causality. N Engl J Med. 2016;374:1981–7. https://doi.org/10.1056/NEJMsr1604338
5. Centers for Disease Control and Prevention. Congenital Zika syndrome and other birth defects. 2018 [cited 2019 Jan 2]. https://www.cdc.gov/pregnancy/zika/testing-follow-up/zika-syndrome-birth-defects.html
6. Petersen EE, Staples JE, Meaney-Delman D, Fischer M, Ellington SR, Callaghan WM, et al. Interim guidelines for pregnant women during a Zika virus outbreak—United States, 2016. MMWR Morb Mortal Wkly Rep. 2016;65:30–3. https://doi.org/10.15585/mmwr.mm6502e1
7. Centers for Disease Control and Prevention. Avoid bug bites. 2019 [cited 2019 Sep 5]. https://wwwnc.cdc.gov/travel/page/avoid-bug-bites
8. Oduyebo T, Igbinosa I, Petersen EE, Polen KND, Pillai SK, Ailes EC, et al. Update: interim guidance for health care providers caring for pregnant women with possible Zika virus exposure—United States, July 2016. MMWR Morb Mortal Wkly Rep. 2016;65:739–44. https://doi.org/10.15585/mmwr.mm6529e1
9. Oduyebo T, Polen KD, Walke HT, Reagan-Steiner S, Lathrop E, Rabe IB, et al. Update: interim guidance for health care providers caring for pregnant women with possible Zika virus exposure—United States (including U.S. territories), July 2017. MMWR Morb Mortal Wkly Rep. 2017;66:781–93. https://doi.org/10.15585/mmwr.mm6629e1
10. Departamento de Salud de Puerto Rico. Zika virus—pregnancies [Spanish]. 2016 [cited 2019 Nov 13]. http://www.salud.gov.pr/Sobre-tu-Salud/Pages/Zika-Embarazadas.aspx
11. Puerto Rico Pregnancy Risk Assessment Monitoring System – Zika Postpartum Emergency Response. PRAMS-ZPER 2.0 protocol 2017 [cited 2019 Jan 2]. https://www.cdc.gov/prams/special-projects/zika/docs/pdf/english/PRAMS_ZPER-2.0_Protocol_FINAL_508tagged.pdf
12. D'Angelo DV, Salvesen von Essen B, Lamias MJ, Shulman H, Hernandez-Virella WI, Taraporewalla AJ, et al. Measures taken to prevent Zika virus infection during pregnancy—Puerto Rico, 2016. MMWR Morb Mortal Wkly Rep. 2017;66:574–8. https://doi.org/10.15585/mmwr.mm6622a2
13. Salvesen von Essen B, Kortsmit K, Warner L, D'Angelo DV, Shulman HB, Virella WH, et al., Puerto Rico Department of Health, Women's Health and Fertility Branch, Division of Reproductive Health, National Center for Chronic Disease Prevention and Health Promotion, Centers for Disease Control and Prevention. Preventing sexual transmission of Zika virus infection during pregnancy, Puerto Rico, USA, 2016. Emerg Infect Dis. 2019;25:2115–9. https://doi.org/10.3201/eid2511.190915
14. Earle-Richardson G, Prue C, Turay K, Thomas D. Influences of community interventions on Zika prevention behaviors of pregnant women, Puerto Rico, July 2016–June 2017. Emerg Infect Dis. 2018;24:2251–61. https://doi.org/10.3201/eid2412.181056

Address for Correspondence: Katherine Kortsmit, Centers for Disease Control and Prevention, 4770 Buford Highway, Mailstop S107-2, Chamblee, GA 30341, USA; email: nlv2@cdc.gov

Multidrug-Resistant Hypervirulent Group B *Streptococcus* in Neonatal Invasive Infections, France, 2007–2019

Céline Plainvert, Constantin Hays,[1] Gérald Touak, Caroline Joubrel-Guyot,[2] Nicolas Dmytruk, Amandine Frigo, Claire Poyart, Asmaa Tazi

We analyzed group B *Streptococcus* (GBS) neonatal invasive infections reported during 2007–2019 in France. The hypervirulent clonal complex (CC) 17 GBS was responsible for 66% (827/1,262) of cases. The role of CC17 GBS increased over time (p for trend = 0.0001), together with the emergence of a multidrug-resistant CC17 GBS sublineage.

Group B *Streptococcus* (GBS; *Streptococcus agalactiae*) is the leading cause of neonatal invasive infections worldwide (*1*). Despite appropriate antimicrobial drug therapy, the global burden of GBS neonatal infections remains substantial, with up to 10% mortality and 30% neurologic sequelae in surviving infants (*2*). Two GBS-associated syndromes are distinguished in neonates: early-onset disease (EOD), which occurs during the first week of life, and late-onset disease (LOD), which occurs after the first week (*1*). In EOD, the neonate is infected by GBS-contaminated maternal secretions during parturition; thus, strategies based on intrapartum antibiotic prophylaxis have drastically diminished its incidence. In contrast, the pathophysiology of LOD remains elusive, and its incidence remains stable (*3*,*4*). Thus, LOD has become the main GBS-associated syndrome in France and other countries in Europe and in North America (*4*,*5*). LOD is largely attributable to a particular GBS clone of serotype III, designated the hypervirulent clonal complex (CC) 17 GBS (*3*,*6*,*7*). Recent epidemiologic data from Canada, China, and Portugal reported the emergence of a multidrug-resistant (MDR) sublineage of CC17 GBS that exhibits acquired nonsusceptibility to 4 antimicrobial categories, namely tetracyclines, aminoglycosides, macrolides, and lincosamides (*8*–*10*). We analyzed neonatal invasive GBS diseases reported to the French National Reference Center for Streptococci during 2007–2019 and investigated the role of the hypervirulent clone over this period.

The Study

GBS isolates were sent to the National Reference Center by correspondents located throughout the national territory on a voluntary basis. Only invasive infections, such as GBS isolated from a normally sterile site, were considered for this study. A total of 1,262 neonatal invasive infections (EOD, n = 394, 31%; LOD, n = 868, 69%) were reported during 2007–2019. The annual number of cases increased significantly over time as a result of a marked rise in LOD cases since 2013 (Appendix Figure 1, https://wwwnc.cdc.gov/EID/article/26/11/20-1669-App1.pdf). Bacteremia without focus was the main clinical presentation during both EOD and LOD (Table 1). Meningitis represented a frequent complication and was more common in LOD, in which it affected nearly half of infants (p<0.0001; Table 1). The proportion of meningitis during LOD dropped significantly over time, from 69% (95% CI 51%–83%) in 2007 to 33% (95% CI 25%–43%) in 2019 (p for trend = 0.008; Appendix Figure 2). The French recommendations for lumbar puncture indication in neonates did not change during the study period. This observation, together with the increased annual number of cases, suggests a better reporting

Author affiliations: Assistance Publique–Hôpitaux de Paris Centre Université de Paris, Paris, France (C. Plainvert, C. Hays, C. Joubrel-Guyot, N. Dmytruk, A. Frigo, C. Poyart, A. Tazi); Institut Cochin, Paris (C. Plainvert, G. Touak, C. Poyart, A. Tazi); FHU Prema, Paris (C. Plainvert, C. Poyart, A. Tazi); Université de Paris, Paris (C. Hays, C. Joubrel-Guyot, C. Poyart, A. Tazi)

[1]Current affiliation: APHP-Nord (St. Louis) Université de Paris, Paris, France.

[2]Current affiliation: Le Raincy Hospital, Montfermeil, France.

of bacteremia and a better representativeness of our collection over time.

Molecular capsular typing of the 1,262 GBS isolates was performed (*11*) (Table 1). Serotype III was overrepresented, especially in LOD, accounting for 57% (95% CI 52%–62%; n = 223/394) of EOD cases and 82% (95% CI 79%–84%; n = 712/868) of LOD cases. Identification of the hypervirulent CC17 GBS, a highly homogenous CC that includes the sequence type (ST) 17, was performed using a specific PCR (*12*) and showed that it caused 66% (95% CI 63%–68%; n = 827/1,262) of GBS neonatal invasive disease. CC17 GBS prevalence was particularly overwhelming in LOD (74%, 95% CI 71%–77%) compared with EOD (48%, 95% CI 43%–53%; p<0.0001) and, during EOD, in cases of meningitis compared with bacteremia (68%, 95% CI 59%–77% vs. 41%, 95% CI 36%–47%; p<0.0001). Furthermore, CC17 GBS prevalence increased by ≈50% over the study period, rising from 53% (95% CI 40%–65%) in 2007 to 76% (95% CI 68%–82%) in 2019 (p for trend = 0.0001; Figure 1). This evolution was linked with its prevalence in LOD, which gradually increased from 59% (95% CI 41%–75%) to 85% (95% CI 77%–91%) of the cases during 2007–2019 (p for trend = 0.025).

We determined the susceptibility of the 1,262 GBS isolates to antimicrobial drugs and performed the detection of resistance genes as previously described (*13*). All isolates were susceptible to penicillin, amoxicillin, and vancomycin. Resistance to tetracyclines did not vary through the study period and concerned 91% (95% CI 89%–92%) of the strains, owing to the genetic determinant *tet*(M) in 92% of the cases (data not shown). Only 3 isolates (0.2%, 95% CI 0.1%–0.7%) showed high-level resistance to gentamicin, but high-level resistance to amikacin increased from 0% (95% CI 0%–7%) in 2007 to 18% (95% CI 12%–26%) in 2019 (p for trend <0.0001; Table 2).

Table 1. Clinical manifestations, serotypes, and CC17 prevalence of group B *Streptococcus* neonatal invasive infections, France, 2007–2019*

Clinical manifestation	EOD, no. (%)	LOD, no. (%)	p value
Bacteremia	298 (75.6)	442 (50.9)	<0.0001#
Ia	69 (23.2)	45 (10.2)	<0.0001**
Ib	13 (4.4)	8 (1.8)	
II	30 (10.1)	6 (1.4)	
III	149 (50.0)	359 (81.2)	
IV	6 (2.0)	6 (1.4)	
V	26 (8.7)	18 (4.1)	
Others†	3 (1.0)	0	
CC17	122 (40.9)	334 (75.6)	<0.0001#
Meningitis‡	95 (24.1)	397 (45.7)	<0.0001#
Ia	15 (15.8)	39 (9.8)	0.33**
Ib	2 (2.1)	12 (3.0)	
II	0	7 (1.8)	
III	74 (77.9)	329 (74.4)	
IV	2(2.1)	2 (0.5)	
V	2 (2.1)	8 (2.0)	
CC17	65 (68.4)	285 (71.8)	0.52#
Others§	1 (0.3)	29 (3.3)	<0.0001#
III	0	24 (82.8)	
Others¶	1	5 (17.2)	
CC17	0	21 (72.4)	
Total	394 (100)	868 (100)	

*CC, clonal complex; EOD, early-onset disease; LOD, late-onset disease.
†Including serotypes VI (2 isolates) and VIII (1 isolate).
‡GBS recovered from cerebrospinal fluid (470 cases) or GBS bacteremia associated with a cellular reaction in the cerebrospinal fluid (>20 leukocytes/mm^3) and consistent clinical findings (4 EOD and 18 LOD cases).
§Including bone and joint and skin and soft tissue infections.
¶Including serotypes Ia (3 isolates), Ib (2 isolates), and V (1 isolate).
#χ^2 test for the distribution of the clinical manifestations in EOD and LOD.
**χ^2 test for serotype distribution or CC17 proportion in EOD and LOD during either bacteremia or meningitis.

Similarly, resistance to erythromycin increased from 22% (95% CI 13%–34%) to 30% (95% CI 23%–38%; p for trend = 0.019). Resistance to erythromycin was mostly the result of modifications of the ribosomes that confer cross resistance to lincosamides and are encoded by the genetic determinants *erm*(B) (64%), *erm*(A/TR) (13%), or *erm*(T) (1%), and in 22% of the cases were the result of an efflux mechanism encoded by the genetic determinant *mef*.
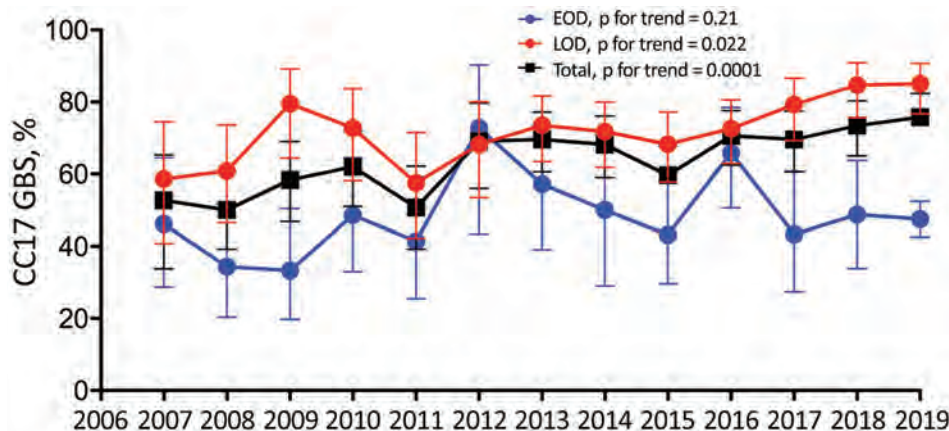

Figure 1. Increasing responsibility of the hypervirulent CC17 clone in GBS neonatal invasive diseases, France, 2007–2019. The annual proportion of infections caused by CC17 GBS during EOD (blue line), LOD (red line), and overall (black line) are represented. Results are expressed as percentage of total GBS isolates per syndrome and per year. Error bars indicate 95% CIs. Evolutionary trends were analyzed using 2-tailed nonparametric Spearman correlation. CC, clonal complex; EOD, early-onset disease; GBS, group B *Streptococcus*; LOD, late-onset disease.

Table 2. Resistance to erythromycin and high-level resistance to amikacin of GBS neonatal isolates, France, 2007–2019*

Year	Total GBS isolates, resistance, % (95% CI)		CC17 GBS, resistance, % (95% CI)	
	Erythromycin	Amikacin	Erythromycin	Amikacin
2007	21.8 (13.0–34.4)	0.0 (0.0–6.5)	17.2 (7.6–34.6)	0.0 (0.0–11.7)
2008	9.0 (4.4–17.4)	1.3 (0.2–6.9)	5.1 (1.4–16.9)	0.0 (0.0–7.7)
2009	19.4 (12.0–30.0)	1.4 (0.3–7.5)	7.1 (2.5–19.0)	0.0 (0.0–9.0)
2010	21.5 (13.9–31.8)	2.5 (0.7–8.8)	16.3 (8.5–29.0)	0.0 (0.0–8.0)
2011	21.7 (13.6–32.8)	1.5 (0.3–7.8)	8.6 (3.0–22.4)	0.0 (0.0–8.8)
2012	10.9 (5.1–21.8)	3.6 (1.0–12.3)	5.3 (1.5–17.3)	2.3 (0.4–11.8)
2013	17.4 (11.6–25.3)	3.5 (1.4–8.6)	10.0 (5.2–18.5)	0.0 (0.0–4.2)
2014	19.1 (12.8–27.4)	11.8 (7.0–19.2)	10.7 (5.5–19.7)	6.5 (3.0–13.5)
2015	25.6 (18.8–33.7)	14.7 (9.6–21.9)	23.4 (15.3–34.0)	10.6 ((5.7–18.9)
2016	18.4 (12.8–25.7)	11.8 (7.4–18.3)	20.8 (13.9–30.0)	8.4 (4.3–15.7)
2017	25.9 (18.7–34.7)	9.8 (5.6–16.7)	20.5 (13.0–30.8)	9.8 (5.0–18.1)
2018	33.1 (25.4–41.7)	16.9 (11.4–24.5)	29.7 (21.3–39.7)	22.4 (14.8–32.3)
2019	29.7 (22.5–38.1)	18.0 (12.3–25.5)	28.6 (20.6–38.2)	14.1 (9.1–21.1)
p for trend†	0.019	<0.0001	0.0042	<0.0001

*CC, clonal complex; GBS, group B *Streptococcus*.
†Evolutionary trends were analyzed using 2-tailed nonparametric Spearman correlation.

Next, we specifically investigated CC17 GBS resistance to erythromycin and amikacin and found an increase over the study period from 17% (95% CI 8%–35%) to 29% (95% CI 21%–38%; p for trend = 0.0042) for erythromycin resistance and from 0% (95% CI 0%–11%) to 14% (95% CI 9%–21%; p for trend <0.0001) for amikacin resistance (Table 2). We postulated that these evolutionary trends were attributable to the emergence of the MDR CC17 GBS sublineage, which exhibits resistance to tetracyclines, macrolides, lincosamides, and amikacin as a result of the replacement of the pilus island 1 genetic locus by mobile genetic elements carrying the resistance determinants *tet*(O), *erm*(B), and *aphA-3* (*8,9*). The proportion of CC17 GBS harboring *tet*(O), *erm*(B), and *aphA-3* among neonatal GBS isolates increased from 0% (95% CI 0%–6%) in 2007 to 14% (95% CI 9%–21%) in 2019 (p for trend <0.0001; Figure 2). Whole-genome sequencing of 8 of these MDR CC17 GBS (Appendix Table) confirmed the replacement of

the pilus island 1 locus by large integrative and conjugative elements (ICEs) similar to those previously described in China and Canada (*8,9*). Interrogation of the ICEberg database (http://db-mml.sjtu.edu. cn/ICEberg/) showed that these ICEs displayed the highest sequence similarity (92%–98%; Appendix Figure 3), with the GBS ICE*Sag*37 described in a CC10 isolate responsible for a neonatal bacteremia in China (*14*).

Conclusions

We analyzed a total of 1,262 neonatal invasive infections over a 13-year study period in France, which represents ≈30% of the total national estimated cases (*4*). A selection bias toward the more severe cases cannot be excluded. However, the proportions of EOD and LOD and the associated clinical manifestations described here are very close to the national estimations. Thus, we can assume that our study reflects the national epidemiology without major discrepancies.

Figure 2. Increasing prevalence of MDR CC17 GBS among neonatal invasive isolates, France, 2007–2019. The annual proportion of infections caused by MDR CC17 GBS, such as those harboring the determinants *tet*(O), *erm*(B), and *aphA-3,* during EOD (blue line), LOD (red line) and overall (black line) are represented. Results are expressed as percentage of total GBS isolates per syndrome and per year. Error bars indicate 95% CIs. Evolutionary trends were analyzed using 2-tailed nonparametric Spearman correlation. CC, clonal complex; EOD, early-onset disease; GBS, group B *Streptococcus*; LOD, late-onset disease; MDR, multidrug-resistant.
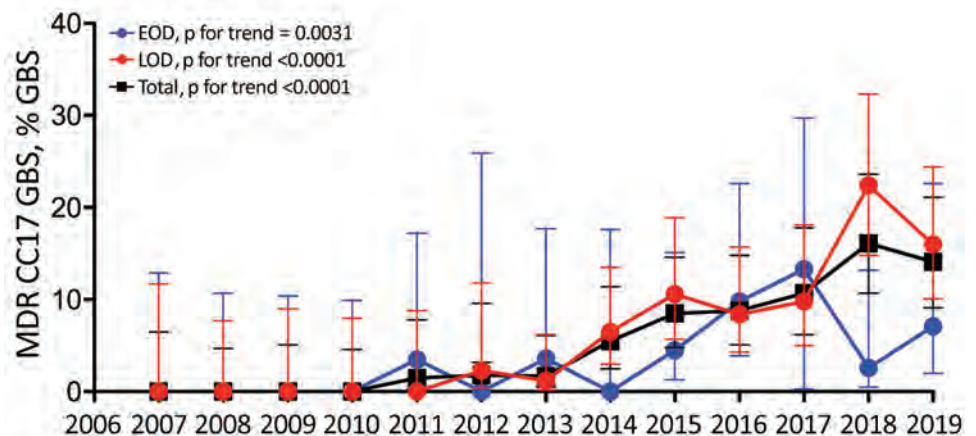
We observed a higher reporting of LOD in contrast to EOD over the 13-year study period. This trend mirrors the data from the surveillance network in France, which show a continuous increase in LOD incidence with an overall 65% rise over the past 20 years (*4*). We describe a growing prevalence of the hypervirulent CC17 GBS and of its MDR sublineage in LOD, which might account for the increasing incidence of this syndrome. Whether these trends are the result of a higher tropism of the MDR sublineage for neonatal infections or merely of its selection and clonal expansion as a result of antibiotic selection pressure requires further investigation. Given the worldwide expanding burden of GBS LOD, the adaptability of GBS to its environment through horizontal gene transfer (*15*), and the resulting potential reduction of the therapeutic arsenal against this major neonatal pathogen, our results reinforce the need for a continued surveillance of GBS diseases and for the development of alternative preventive strategies.

Acknowledgments

About the Author

Dr. Plainvert works at the French National Reference Center for Streptococci within the University Hospitals Paris Centre, Paris, France. Her main research interests focus on the epidemiology and pathogenicity of group A and group B *Streptococcus*.

References

1. Edwards MS, Nizet V, Baker CJ. Group B streptococcal infections. In: Infectious diseases of the fetus and newborn infant. 7th ed. Remington JS, Klein JO, Wilson CB, Nizet V, Maldonado Y, editors. Philadelphia: Elsevier; 2011. p. 419–69.
2. Libster R, Edwards KM, Levent F, Edwards MS, Rench MA, Castagnini LA, et al. Long-term outcomes of group B streptococcal meningitis. Pediatrics. 2012;130:e8–15. https://doi.org/10.1542/peds.2011-3453
3. Bekker V, Bijlsma MW, van de Beek D, Kuijpers TW, van der Ende A. Incidence of invasive group B streptococcal disease and pathogen genotype distribution in newborn babies in the Netherlands over 25 years: a nationwide surveillance study. Lancet Infect Dis. 2014;14:1083–9. https://doi.org/10.1016/S1473-3099(14)70919-3
4. Santé Publique France. Bulletin of the bacterial invasive infections surveillance network 2018 [cited 2020 Jan 30]. http://invs.santepubliquefrance.fr/Dossiers-thematiques/ Maladies-infectieuses/Maladies-a-prevention-vaccinale/ Infections-invasives-d-origine-bacterienne-Reseau-EPIBAC/ Bulletin-du-reseau-de-surveillance-des-infections-invasives-bacteriennes
5. Madrid L, Seale AC, Kohli-Lynch M, Edmond KM, Lawn JE, Heath PT, et al. Infant group B streptococcal disease incidence and serotypes worldwide: systematic review and meta-analyses. Clin Infect Dis. 2017;65(suppl2):S160–72. https://doi.org/10.1093/cid/cix656
6. Joubrel C, Tazi A, Six A, Dmytruk N, Touak G, Bidet P, et al. Group B *Streptococcus* neonatal invasive infections, France 2007–2012. Clin Microbiol Infect. 2015;21:910–6. https://doi.org/10.1016/j.cmi.2015.05.039
7. Teatero S, McGeer A, Low DE, Li A, Demczuk W, Martin I, et al. Characterization of invasive group B *Streptococcus* strains from the greater Toronto area, Canada. J Clin Microbiol. 2014;52:1441–7. https://doi.org/10.1128/ JCM.03554-13
8. Campisi E, Rosini R, Ji W, Guidotti S, Rojas-López M, Geng G, et al. Genomic analysis reveals multi-drug resistance clusters in group B *Streptococcus* CC17 hypervirulent isolates causing neonatal invasive disease in southern mainland China. Front Microbiol. 2016;7:1265. https://doi.org/ 10.3389/fmicb.2016.01265
9. Teatero S, Ramoutar E, McGeer A, Li A, Melano RG, Wasserscheid J, et al. Clonal complex 17 group B *Streptococcus* strains causing invasive disease in neonates and adults originate from the same genetic pool. Sci Rep. 2016;6:20047. https://doi.org/10.1038/srep20047
10. Martins ER, Pedroso-Roussado C, Melo-Cristino J, Ramirez M; Portuguese Group for the Study of Streptococcal Infections. *Streptococcus agalactiae* causing neonatal infections in Portugal (2005–2015): Diversification and emergence of a CC17/PI-2b multidrug resistant sublineage. Front Microbiol. 2017;8:499. https://doi.org/10.3389/fmicb.2017.00499
11. Imperi M, Pataracchia M, Alfarone G, Baldassarri L, Orefici G, Creti R. A multiplex PCR assay for the direct identification of the capsular type (Ia to IX) of *Streptococcus agalactiae*. J Microbiol Methods. 2010;80:212–4. https://doi.org/10.1016/j.mimet.2009.11.010
12. Lamy M-C, Dramsi S, Billoët A, Réglier-Poupet H, Tazi A, Raymond J, et al. Rapid detection of the "highly virulent" group B *Streptococcus* ST-17 clone. Microbes Infect. 2006;8:1714–22. https://doi.org/10.1016/j.micinf.2006.02.008
13. Hays C, Louis M, Plainvert C, Dmytruk N, Touak G, Trieu-Cuot P, et al. Changing epidemiology of group B *Streptococcus* susceptibility to fluoroquinolones and aminoglycosides in France. Antimicrob Agents Chemother. 2016;60:7424–30. https://doi.org/10.1128/AAC.01374-16
14. Zhou K, Xie L, Han L, Guo X, Wang Y, Sun J. ICESag37, a novel integrative and conjugative element carrying antimicrobial resistance genes and potential virulence factors in *Streptococcus agalactiae*. Front Microbiol. 2017;8:1921. https://doi.org/10.3389/fmicb.2017.01921
15. Da Cunha V, Davies MR, Douarre P-E, Rosinski-Chupin I, Margarit I, Spinali S, et al.; DEVANI Consortium. *Streptococcus agalactiae* clones infecting humans were selected and fixed through the extensive use of tetracycline. Nat Commun. 2014;5:4544. https://doi.org/10.1038/ ncomms5544

Address for correspondence: Asmaa Tazi, Service de Bactériologie, Hôpital Cochin, 27 rue du Faubourg Saint-Jacques, 75014 Paris, France; email: asmaa.tazi@aphp.fr

Epileptic Seizure after Use of Moxifloxacin in Man with *Legionella longbeachae* Pneumonia

Jin-Yong Wang,[1] Xing Li,[1] Jian-Yong Chen,[2] Bo Tong[2]

Legionellosis caused by *Legionella longbeachae* is diagnosed mainly by PCR. We report a case of *L. longbeachae* infection in mainland China, which was diagnosed by metagenomic next-generation sequencing, in a man who developed an epileptic seizure after using moxifloxacin. Metagenomic next-generation sequencing may be a useful tool to detect *Legionella* spp.

We describe a case of *Legionella longbeachae* infection in mainland China that was diagnosed by metagenomic next-generation sequencing (mNGS). The patient developed an epileptic seizure after he underwent treatment with moxifloxacin and had a prolonged corrected QT interval at a later stage of treatment.

Case Report

In June 2019, a 56-year-old man came to the pneumonia department of People's Hospital Affiliated to Nanchang University with a 2-day history of nonproductive cough and fever. He had undergone a deceased-donor kidney transplant 19 years earlier for end-stage renal disease and had received regular hemodialysis for the previous 2 years. His medications included tacrolimus capsule (1.0 mg 2×/d), mycophenolate capsule (0.25 mg 2×/d), and prednisone (10 mg/d). He had recently done gardening activities, using potting mixes. On physical examination, his temperature was 39.6°C, heart rate 95 beats/min, oxygen saturation 96% while breathing ambient air. Pulmonary auscultation revealed wet rales in the right lung. The rest of the examination results were unremarkable.

The patient's leukocyte count was 10.54×10^9 cells/L (reference range $4–10×10^9$ cells/L), with 95% neutrophils; his C-reactive protein (CRP) level was 200 mg/L (reference range 0–15 mg/L). Computed tomography (CT) of the chest revealed extensive consolidation in the right upper and middle lobes (Figure 1, panel A).

We treated the patient with 5 g of intravenous piperacillin every 12 hours. However, the patient's symptoms did not improve. Cultures of bronchoalveolar lavage fluid (BALF) samples were negative. Results of a T-SPOT.TB test (Oxford Immunotec, https://www.tspot.com) were negative. We began intravenous meropenem (2,000 mg/d) and withdrew piperacillin. The patient's temperature decreased but was still elevated. We performed another BAL 8 days later; cultures were still negative.

We sent a BALF sample to BGI-Wuhan (formerly Beijing Genomic Institute; Wuhan, China) for pathogenic detection by mNGS. Qualified libraries were sequenced by BGI-Wuhan's BGISEQ-50 platform. The classification reference databases were downloaded from the National Center of Biotechnology Information (ftp://ftp.ncbi.nlm.nih.gov/genomes), whose RefSeq database contains 4,189 whole-genome sequences of viral taxa, 2,328 bacterial genomes or scaffolds, 199 fungi related to human infection, and 135 parasites associated with human diseases.

On the patient's 14th day in the hospital, the results of mNGS were positive for *L. longbeachae* (Figure 2). We began treatment with intravenous moxifloxacin (400 mg/d) and oral azithromycin (500 mg/d); meropenem was withdrawn. The patient was afebrile and his cough diminished.

On his 25th day in the hospital, the patient had an epileptic seizure. The CT of skull and chest revealed that the brain was normal, and the lungs had a smaller consolidation than before (Figure 1, panel B). After considering the side effects of moxifloxacin, we discontinued treatment. The seizure did not recur. Six days later, the patient developed another cough with a low-grade fever. We performed a new BAL and cultures were still negative. We started treatment again with 400 mg of intravenous moxifloxacin daily, and the patient's symptoms improved.

[1]These authors contributed equally to this article.

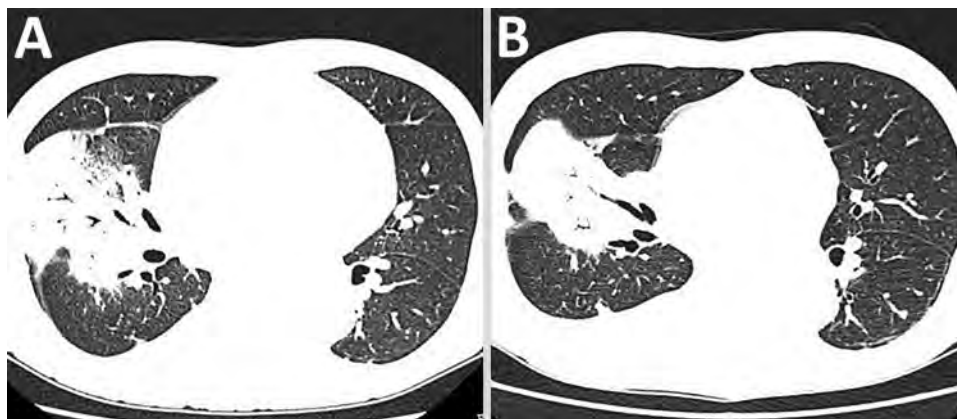[2]These authors contributed equally to this article.

Figure 1. Computed tomographic scan of the chest of a patient hospitalized with *Legionella longbeachae*. A) On day 14 of the patient's hospital stay, extensive consolidation was present in the right upper and middle lobe. B) On day 25 of the patient's hospital stay, the consolidation was smaller than before.

On his 36th day in the hospital, the patient had another seizure. Intravenous moxifloxacin was discontinued again and 400 mg oral moxifloxacin daily was started. An electrocardiogram (ECG) revealed a prolonged corrected QT interval. After considering the cardiologic side effects of azithromycin, we withdrew the azithromycin. However, the patient experienced a fever again and the sputum cultures showed no growth. The epilepsy did not improve despite pumping depakin continuously.

On the patient's 39th day in the hospital, we began treatment with intravenous ciprofloxacin and tigecycline because of his worsening condition. The following day, he had a temperature of ≤41°C. Oxygen saturation was 93% while he was on 28% fraction of inspired oxygen. That night, the patient suffered cardiac arrest and died. The patient's family refused to have an autopsy performed.

Since *L. longbeachae* was first identified as a new species in 1981 (*1*), legionellosis caused by *L. longbeachae* has been reported in many countries, including Australia, New Zealand, Netherlands, Japan, and Canada (*2–6*). However, to our knowledge, there are no relevant reports from countries such as mainland China, Russia, South Korea, and India. Some reasons may explain the discrepancy. On one hand, *L. longbeachae* is commonly isolated from compost and potting mixes (*7*). The composition of commercial potting mix used in different countries is different (*8*). On the other hand, the PCR technique for *L. longbeachae* is immature in many regions, so the urinary antigen test is used, which detects only *L. pneumophila* serogroup 1 (*9*). Even in countries with low incidence rates for *L. longbeachae* infection, when the cultures and urine antigen test are negative, a high index of suspicion must be maintained for patients with immunosuppression and a personal history of gardening activities.

Detection by culture techniques is insensitive for *Legionella* spp. (*10*). At present, in some countries with high incidence of *L. longbeachae* infection, such as Australia and New Zealand, PCR is the most commonly used tool to detect *Legionella* spp. (*8,9*). In most areas of China, PCR technique for *L. longbeachae* is still immature. However, mNGS is rapidly moving from research to clinical practice (*11*). As of November 2019, >100 case reports
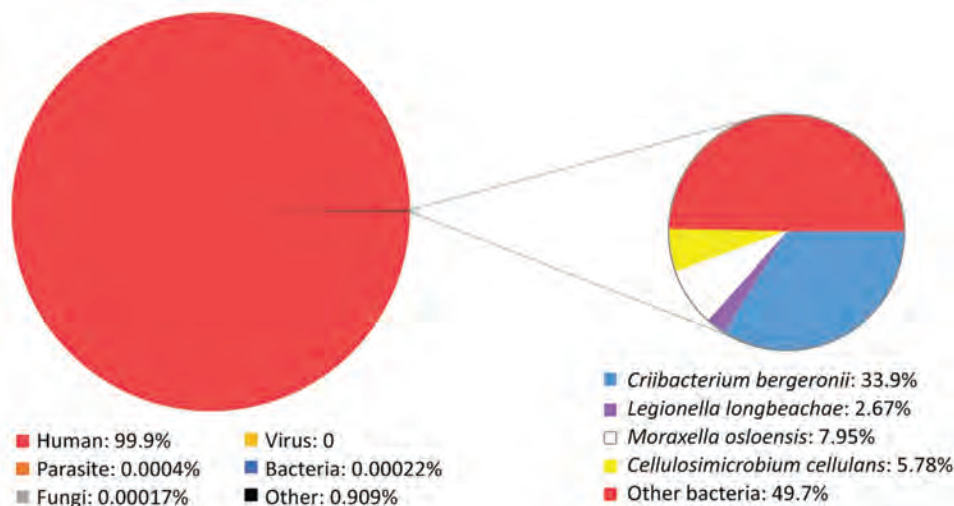

Figure 2. Analysis of metagenomic next-generation sequencing result from a patient with *Legionella longbeachae*. Total reads distribution is on the left; percentage distribution of bacterial reads is shown on the right.

■ Human: 99.9%   ■ Virus: 0
■ Parasite: 0.0004%   ■ Bacteria: 0.00022%
■ Fungi: 0.00017%   ■ Other: 0.909%

■ *Criibacterium bergeronii*: 33.9%
■ *Legionella longbeachae*: 2.67%
□ *Moraxella osloensis*: 7.95%
■ *Cellulosimicrobium cellulans*: 5.78%
■ Other bacteria: 49.7%

or clinical studies have indicated that mNGS has been successfully applied in dozens of sample types, such as respiratory secretions, cerebrospinal fluid, urine, and blood (*12*), but it is rarely reported that *L. longbeachae* infection is diagnosed by mNGS. In this case, using a novel mNGS platform, we were able to detect *L. longbeachae* in a BALF sample and finally confirm the etiology of the patient's pneumonia. The result indicated that mNGS may be a useful tool for detecting *Legionella* spp.

Antimicrobial susceptibility testing of *L. longbeachae* has demonstrated that quinolones, macrolides, and rifampin were most sensitive to it (*13*). However, there are few relevant reports of developing side effects after using quinolones for patients with *L. longbeachae* infection. Unfortunately, our patient not only had a seizure after using moxifloxacin but also had a prolonged QT interval at the later stage of therapy. Therefore, the available antimicrobial drugs were very limited. Looking back to the therapy process of the patient, our treatment regimen had some deficiencies. First, considering that other quinolones may also cause seizure, we did not switch to other types of quinolones, and ciprofloxacin was used until the day before the patient died. Second, considering that other types of macrolide drugs were not as effective as azithromycin and also had the possibility of prolonging the QT interval, dosage of the macrolide drugs had not been adjusted. We possibly should have switched to intravenous erythromycin while closely monitoring ECG changes. Third, given the relatively weak efficacy of rifampin, we did not try to add rifampin. In fact, rifampin could have been added when seizures were repeatedly caused by moxifloxacin. However, the patient died of sudden cardiac arrest and ECG was not performed in time. The cause of cardiac arrest may have been that ciprofloxacin or deteriorating pneumonia aggravated the patient's arrhythmia. More treatment experience and reports are needed for such patients.

Conclusions

In summary, even in countries with low incidence rates for *L. longbeachae* infection, when the cultures and urine antigen test are negative, *L. longbeachae* infection must be highly suspected for patients with immunosuppression and a personal history of gardening activities. This case indicated that mNGS may be a useful tool to diagnose *L. longbeachae* infection. For patients with *L. longbeachae* infection, antimicrobial drugs should be changed in time when patients develop adverse side effects after using moxifloxacin and azithromycin; more treatment experience and reports are needed for such patients.

About the Author

Dr. Wang is a resident doctor at Jiangxi Provincial People's Hospital Affiliated to Nanchang University, Nanchang, Jiangxi, China. His main research interest is nosocomial infectious diseases.

References

1. McKinney RM, Porschen RK, Edelstein PH, Bissett ML, Harris PP, Bondell SP, et al. *Legionella longbeachae* species nova, another etiologic agent of human pneumonia. Ann Intern Med. 1981;94:739–43. https://doi.org/10.7326/0003-4819-94-6-739
2. Dugar M, Rankin WA, Rowe E, Smith MD. "My foot hurts": a flare of rheumatoid arthritis? Med J Aust. 2009;190:392–3. https://doi.org/10.5694/j.1326-5377.2009.tb02459.x
3. Heriot WJ, Mack HG, Stawell R. Ocular involvement in a patient with *Legionella longbeachae* 1 infection. Clin Experiment Ophthalmol. 2014;42:497–9. https://doi.org/10.1111/ceo.12335
4. Kubota M, Tomii K, Tachikawa R, Harada Y, Seo R, Kaji R, et al. Legionella longbeachae pneumonia infection from home garden soil [in Japanese]. Nihon Kokyuki Gakkai Zasshi. 2007;45:698–703.
5. Leggieri N, Gouriet F, Thuny F, Habib G, Raoult D, Casalta JP. *Legionella longbeachae* and endocarditis. Emerg Infect Dis. 2012;18:95–7. https://doi.org/10.3201/eid1801.110579
6. Wright AJ, Humar A, Gourishankar S, Bernard K, Kumar D. Severe Legionnaire's disease caused by *Legionella longbeachae* in a long-term renal transplant patient: the importance of safe living strategies after transplantation. Transpl Infect Dis. 2012;14:E30–3. https://doi.org/10.1111/j.1399-3062.2012.00755.x
7. Bacigalupe R, Lindsay D, Edwards G, Fitzgerald JR. Population genomics of *Legionella longbeachae* and hidden complexities of infection source attribution. Emerg Infect Dis. 2017;23:750–7. https://doi.org/10.3201/eid2305.161165
8. Whiley H, Bentham R. *Legionella longbeachae* and legionellosis. Emerg Infect Dis. 2011;17:579–83. https://doi.org/ 10.3201/eid1704.100446
9. Isenman HL, Chambers ST, Pithie AD, MacDonald SLS, Hegarty JM, Fenwick JL, et al. Legionnaires' disease caused by *Legionella longbeachae*: clinical features and outcomes of 107 cases from an endemic area. Respirology. 2016;21:1292–9. https://doi.org/10.1111/resp.12808.
10. Fields BS, Benson RF, Besser RE. Legionella and Legionnaires' disease: 25 years of investigation. Clin Microbiol Rev. 2002; 15:506–26. https://doi.org/10.1128/CMR.15.3.506-526.2002
11. Miao Q, Ma Y, Wang Q, Pan J, Zhang Y, Jin W, et al. Microbiological diagnostic performance of metagenomic next-generation sequencing when applied to clinical practice. Clin Infect Dis. 2018;67(suppl_2):S231–40. https://doi.org/10.1093/cid/ciy693
12. Han D, Li Z, Li R, Tan P, Zhang R, Li J. mNGS in clinical microbiology laboratories: on the road to maturity. Crit Rev Microbiol. 2019;45:668–85. https://doi.org/10.1080/1040841X.2019.1681933
13. Nimmo GR, Bull JZ. Comparative susceptibility of *Legionella pneumophila* and *Legionella longbeachae* to 12 antimicrobial agents. J Antimicrob Chemother. 1995;36:219–23. https://doi.org/10.1093/jac/36.1.219

Address for correspondence: Bo Tong and Jianyong Chen, Department of Internal Medicine, Jiangxi Provincial People's Hospital Affiliated to Nanchang University, 152 Aiguo Rd, Nanchang 330006, Jiangxi, China; email: ncdxwjy@163.com and cjyktz@163.com

Two New Cases of Pulmonary Infection by *Mycobacterium shigaense*, Japan

Shiomi Yoshida,[1] Tomotada Iwamoto,[1] Takehiko Kobayashi,[1] Ryohei Nomoto,
Yoshikazu Inoue, Kazunari Tsuyuguchi, Katsuhiro Suzuki

We report 2 case-patients in Japan with *Mycobacterium shigaense* pulmonary infections. One patient was given aggressive treatment and the other conservative treatment, according to distinctive radiologic evidence. A close phylogenetic relationship based on whole-genome sequencing was found between strain from the conservatively treated patient and a reference strain of cutaneous origin.

Nontuberculous mycobacteria (NTM) are ubiquitous organisms whose pathogenicity might vary according to the immune status of the host (*1*). An increase in incidence of pulmonary NTM infections among immunocompetent patients in recent years is an emerging public health concern (*2*).

The most predominant pulmonary *Mycobacterium avium–intracellulare* complex (MAC) disease has 2 possible radiologic patterns: a fibrocavitary (FC) type, which results in progressive radiographic abnormalities associated with a difficult-to-treat outcome; and a nodular bronchiectasis (NB) type, which is stable, often associated with chronic bronchiectasis (BE). International guidelines suggest slightly different multidrug treatment regimens for these types: conservative nonchemical treatment or intermittent oral therapy for NB-type and daily treatment for FC-type (*3*). Clinical and radiographic features of pulmonary disease caused by infection with rare NTM resemble those of MAC.

M. shigaense is a unique species of the *M. simiae* complex reported in 2012 (*4*). This slow-growing mycobacteria, UN-152^T (JCM 32072^T and DSM 46748^T), caused cutaneous disease in an immunosuppressed patient (*4*). Since then, 5 cases of

patients with *M. shigaense* infection have been reported, in the form of skin or disseminated diseases associated with cellular immunodeficiency (*5*). In 2014, another case of *M. shigaense* infection was reported in a respiratory sample of a patient in Japan (*6*). To date, *M. shigaense* has been found in eastern Asia, China, and Japan (*5*,*6*), but its transmission routes and sources have not been identified.

We isolated *M. shigaense* from 2 patients, 1 with FC-type disease and 1 with NB-type disease. We summarize clinical features and drug regimens (Appendix, https://wwwnc.cdc.gov/EID/article/26/11/20-0315-App1.pdf) for these patients and describe genomic comparison of strains associated with different treatments for infection with *M. shigaense*.

The Study

This retrospective study was approved by the Institutional Review Board of the Kinki-Chuo Chest Medical Center (approval code 689) and has been performed in accordance with the ethical standards in the 1964 Declaration of Helsinki and its later amendments or comparable ethical standards. We required that all patients provide written informed consent before information was collected.

Case-patient 1 was an 88-year-old HIV-negative man admitted to our hospital in 2018. He had complications from stable interstitial pneumonia and an increased productive cough and fever. Chest radiograph and transverse computed tomography showed left-side consolidation.

Two months later, sputum cultures were positive for *M. shigaense*, identified by partial DNA sequences of the 16S rRNA, *hsp65*, and *rpoB* genes. Thereafter, multidrug treatment was orally administered for 12 months. After ≈1 month of treatment, his sputum was culture negative and negative for acid-fast bacilli (AFB). The patient showed

Author affiliations: National Hospital Organization Kinki-chuo Chest Medical Center, Sakai, Osaka, Japan (S. Yoshida, T. Kobayashi, Y. Inoue, K. Tsuyuguchi, K. Suzuki); Kobe Institute of Health, Kobe, Japan (T. Iwamoto, R. Nomoto)

[1]These authors contributed equally to this article.

clinical improvement and decreased symptoms. He has remained culture negative for >1 year (Figure 1, panel A).

Case-patient 2 was a 78-year-old HIV-negative woman referred for an evaluation of previously diagnosed

chronic BE since 2016. She had an NB-type radiologic pattern. AFB smear and culture test results were negative on 3 consecutive sputum samples.

This patient was not initially given antimicrobial drugs and was evaluated by expectorated

Figure 1. Radiographic and therapeutic drug monitoring for 2 patients with pulmonary disease caused by *Mycobacterium shigaense*. Each panel shows the timeline at the top (X, initial hospitalization period for *M. shigaense* disease) with smear results and chest radiograph (top) and chest CT (bottom) images below. The chemotherapy regimen is provided (Appendix, https://wwwnc.cdc.gov/EID/article/26/11/20-0315-App1.pdf). A) Case 1, patient with FC-type disease. a) Chest radiograph shows abnormal nodular shadows and a small calcification in the right upper and middle lung fields on day 60 before initial hospitalization. b) Chest radiograph taken 2 months later showed a more indistinct bilateral contour of the lung; there was increased consolidation of a cavitary lesion in the right upper lobe and a centrilobular nodule with branching in the left upper lobe on transverse chest CT. Lesions including progressive cavities are shown in the right upper and middle lung fields. c) Chest CT shows reduction in cavities and consolidation in the left lobe on day 199. B) Case 2, patient with NB-type disease. a) Chest CT showed a small nodular shadow in the right lower lung field. Image showed bronchiectasis in the left middle lobe and the lingular segment of the right upper lobe. There was peribronchiectasic consolidation and multiple small nodules suggesting bronchiolitis in both lungs. b) After 24 months, chest CT showed a stable extent of scattered small nodules including bronchiectasis just beneath the pleura and pleural thickening in the right middle lobe. c) Chest CT showed bronchiectasis in the right middle lobe. According to the number of AFB seen by Ziehl-Neelsen method for acid-fast staining, smear results were classified as 3+, 2+, 1+, or ±. –, negative; +, positive. AFB, acid-fast bacilli; AFB culture result –, culture negative; +, culture positive.
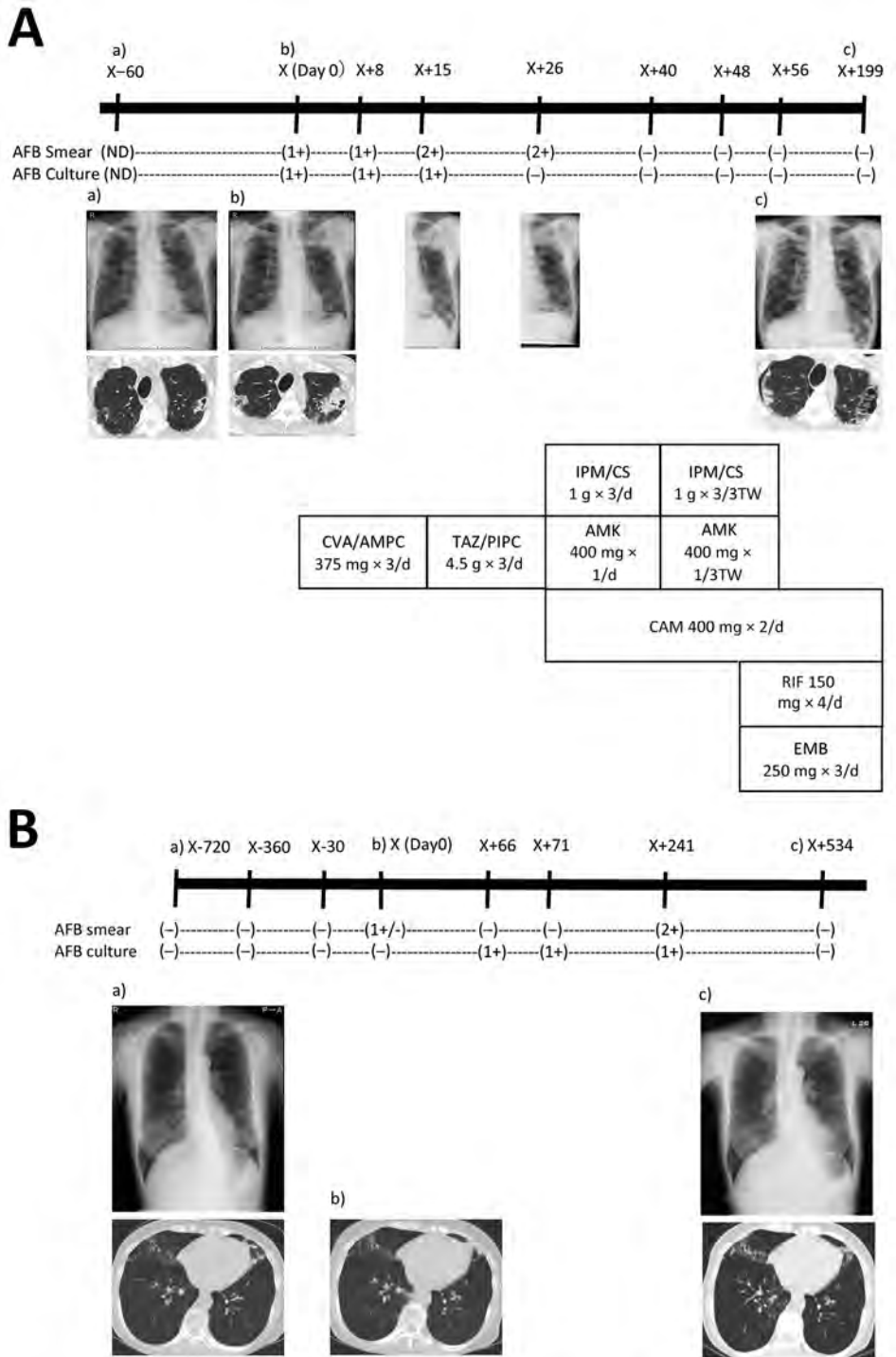
AMK, amikacin; CAM, clarithromycin; CVA/AMPC, clavulanic acid/amoxicillin; CT, computed tomography; EMB, ethambutol; FC, fibrocavitary; IPM/CS, imipenem/cilastatin; NB, nodular bronchiectasis; ND, no data; RIF, rifampin; TAZ/PIPC, tazobactam/piperacillin.

Table 1. Nucleotide identities of *Mycobacterium species* calculated by using average nucleotide identity BLAST ANI analysis*

Strain	Case 2, NB-type, KC354	Case 1, FC-type, KC8	*M. shigaense* JCM 32072[T]†	*M. shigaense* SCY‡	*M. triplex* DSM 4426[T]	*M. simiae* DSM 44165[T]
Case 2, NB-type, KC354	100.00	99.72	99.98	98.79	85.16	84.49
Case 1, FC-type, KC8	99.72	100.00	99.97	99.76	85.16	84.48
M. shigaense JCM 32072[T]†	99.98	99.97	100.00	99.81	85.17	84.50
M. shigaense SCY‡	99.79	99.76	99.81	100.00	85.18	84.49
M. triplex DSM 44626[T]	85.16	85.16	85.17	85.18	100.00	85.31
M. simiae DSM 44165[T]	84.49	84.48	84.50	84.19	85.31	100.00

*Values are percentages. ANI, average nucleotide identity; FC, fibrocavitary; NB, nodular bronchiectasis.
†*M. shigaense* JCM 32072[T] was obtained from a skin biopsy specimen of a Japanese man
‡*M. shigaense* SCY was isolated from a skin biopsy specimen of a Chinese woman.

sputum examinations at follow-up. After 2 years, *M. shigaense* was isolated from subsequent sputum samples on 3 occasions. Because there were no respiratory symptoms, the patient was not initially given antimicrobial drugs after diagnosis. Spontaneous culture conversion was found after 3 consecutive negative sputum cultures, and the negative status was maintained during the follow-up period of >1 year (Figure 1, panel B).

We performed drug susceptibility testing considering MAC breakpoints and using broth microdilution according to Clinical and Laboratory Standards Institute guidelines (*7*). Testing showed that isolates of both patients were susceptible to clarithromycin, amikacin, moxifloxacin, and linezolid.

Whole-genome sequencing was performed on an initial isolate from each case-patient (strain KC8 from case-patient 1 and strain KC354 from case-patient 2). DNA sequence libraries were prepared by using the QIAseq FX DNA Library Kit (QIAGEN, https://www.qiagen.com) using 50 ng *M. tuberculosis* genomic DNA, followed by paired-end sequencing using Illumina MiSeq Reagent Kit version 3 (600 cycles) (Illumina, https://www.illumina.com).

We conducted average nucleotide identity basic local sequence alignment tool analysis by using JSpecies version 1.2.1 (*8*). Average nucleotide identity values for strains KC8 and KC354 clearly indicated that these 2 patients were infected by *M. shigaense* (Table 1). Identification of single-nucleotide polymorphisms (SNPs) in these isolates, compared with those in *M. shigaense* JCM 32072[T], was conducted by using the BactSNP pipeline (*9*). KC354 had 19 SNPs, whereas KC8 had 6,826 SNPs (Table 2).

A core genes phylogenetic tree for genome sequences of 19 *M. simiae* complex and *M. avium* 104 was reconstructed by using Roary version 3.11.2 (*10*) (Figure 2). *M. shigaense* strains were most closely related to *M. rhizamassiliense* (*11*); KC8 was less related to *M. shigaense* JCM 32072[T] than to *M. shigaense* SCY. Raw sequence reads of *M. shigaense* KC8 and *M. shigaense* KC354 were deposited in the DNA Data Bank of Japan Sequence Read Archive (DNA Sequence Read Archive, https://www.ddbj.nig.ac.jp/dra/index.html) under study accession no. DRA009490.

Conclusions

NB-type infection with *M. shigaense* is considered sufficiently indolent that careful longitudinal appraisal without therapy is safe and poses little risk for rapid progression (*12,13*). The previously reported case-patient with NB-type pulmonary *M. shigaense* disease did not have a history of immunosuppressive therapy or clinical symptoms but was treated successfully (*6*). Clinical data, including the presence or absence of underlying BE as a concurrent condition, was insufficient (*6*). Our NB-type patient with chronic BE was considered not to have a clinically serious condition and required no treatment. In contrast, the patient with progressive FC-type infection was given chemotherapy that resulted in improvement observed by computed tomography (Figure 1). We showed that clinical features of *M. shigaense* disease resemble those of MAC disease, but radiographic differences indicated that MAC disease was more serious.

We also observed genomic diversity of *M. shigaense*. Our comparative genomic analysis showed that strain KC354 obtained from the NB-type patient was closely related to *M. shigaense* JCM 32071[T]. In contrast, strain KC8 obtained from the FC-type patient showed a large number of SNPs when compared

Table 2. SNP detection using *Mycobacterium shigaense* JCM 32072[T] as reference genome for 2 strains isolated*

Strain no.	No. SNPs	Mapped region to reference genome†		Pseudogenome by BactSNP, bases
		Length, bases	Coverage ratio	
Case 2, NB-type, KC354	19	5,232,622	0.99999	5,182,569
Case 1, FC-type, KC8	6,826	5,200,032	0.99376	5,138,016

*SNPs called by BactSNP pipeline (*9*). FC, fibrocavitary; NB, nodular bronchiectasis; SNP, single-nucleotide polymorphism.
†Coverage depth is >5 at each position of the reference genome (5,232,660).

with the type strain. This result might explain the increased virulence of strain KC8.

More than 50% of stable pulmonary MAC disease patients have spontaneous sputum conversion without treatment (*3,14*). Bacterial genotypic comparison between patients with spontaneous sputum conversion and those with serial sputum-positive cultures might identify patients who are likely to profit from antimicrobial drug therapy. Our next-generation sequencing findings indicated that differences in the genetic background of the pathogens might aid physicians with clinical decisions regarding therapy

initiation. We believe that accumulation of genomic data for clinical strains should be helpful for future comparative studies and will probably lead to diagnosis of more cases. Further studies of this relatively new pathogen with larger sample sets are needed to identify clear, reliable, and clinical markers that predict the virulence of *M. shigaense*.

Current treatment for pulmonary mycobacterial disease recommends ethambutol, rifampin and macrolides (*1,13*). Little is known regarding response of antimicrobial agents and clinical outcome for this rare species. Therefore, a better understanding of drug
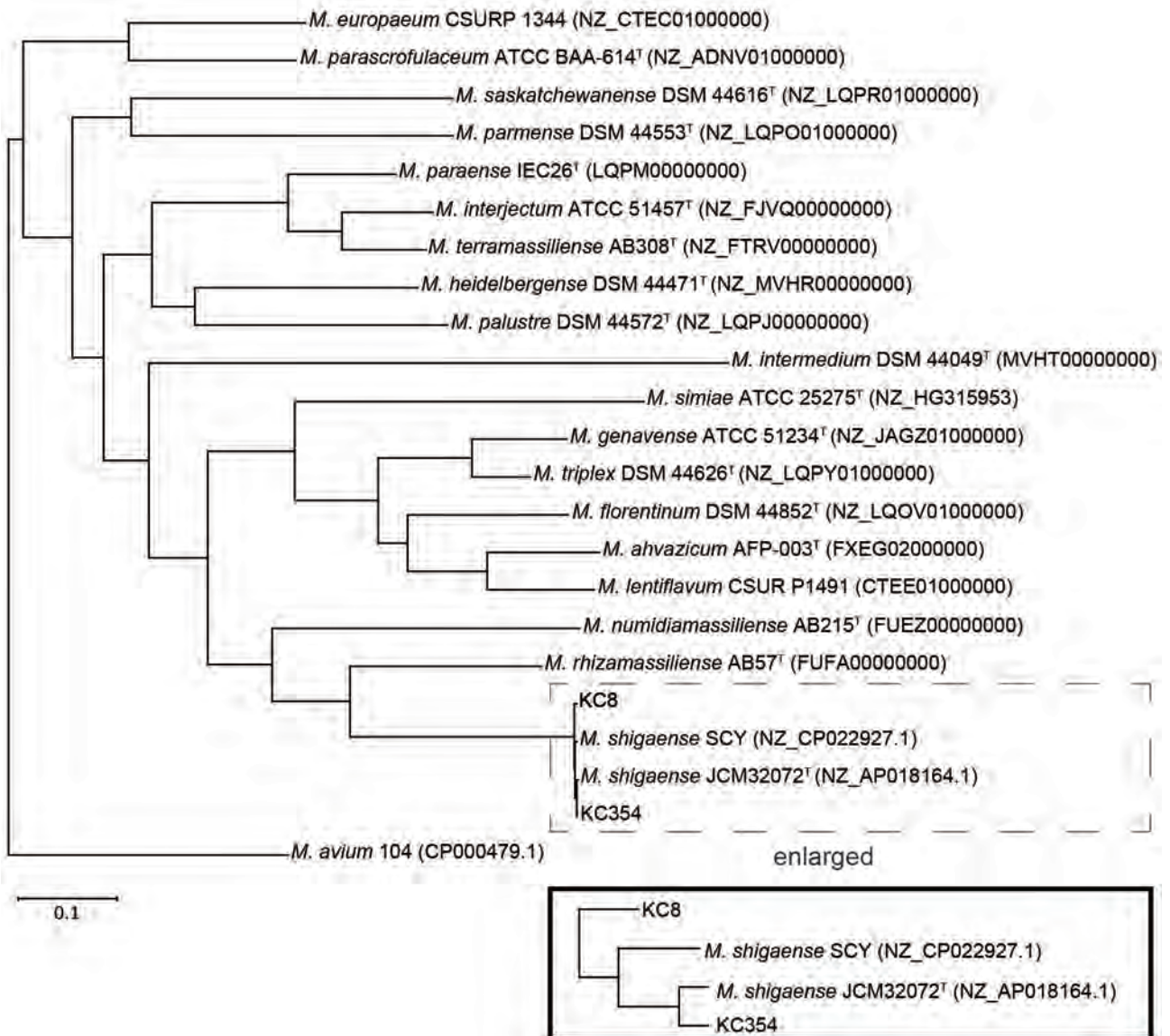

Figure 2. Phylogenetic tree based on whole-genome sequence data of 19 species in the *Mycobacterium simiae* complex and *M. avium* 104 from the GenBank database. The tree was constructed by using concatenated alignments of the 1,399 core genes with Roary, the pan genome pipeline (https://sanger-pathogens.github.io/Roary), and displayed by using Dendroscope (https://www.dendroscope.org). Box at the bottom shows an enlarged version of the branch of *M. shigaense* in the tree. Scale bar indicates nucleotide substitutions per site.

susceptibility of the pathogen is necessary to provide suitable treatment. Most patients reported with *M. shigaense* disease were given multiple agents: 4 patients showed improvement after receiving a clarithromycin-based treatment for 4–12 months (no data were available for linezolid) (*6,15*). In comparison to previous cases of *M. shigaense* disease (*5*), for which the pathogen was susceptible to clarithromycin and moxifloxacin, our isolates showed susceptibility to amikacin. We believe that a synergistic response of antimicrobial drugs against *M. shigaense* requires further evaluation.

In summary, we found that the NB-type *M. shigaense* pulmonary strain was closely related to the cutaneous reference strain, but the more pathogenic FC-type strain differed considerably. Our results for this rare species open possibilities for further investigation into this neglected NTM disease and provide indications for the need for therapy.

About the Author

Dr. Yoshida is a microbiology research scientist at the Clinical Research Center, National Hospital Organization Kinki-chuo Chest Medical Center, Osaka, Japan. Her primary research interests are tuberculosis, nontuberculous mycobacteria, and antimicrobial agents.

References

1. Griffith DE, Aksamit T, Brown-Elliott BA, Catanzaro A, Daley C, Gordin F, et al.; ATS Mycobacterial Diseases Subcommittee; American Thoracic Society; Infectious Disease Society of America. An official ATS/IDSA statement: diagnosis, treatment, and prevention of nontuberculous mycobacterial diseases. Am J Respir Crit Care Med. 2007;175:367–416. https://doi.org/10.1164/rccm.200604-571ST
2. Hoefsloot W, van Ingen J, Andrejak C, Ängeby K, Bauriaud R, Bemer P, et al.; Nontuberculous Mycobacteria Network European Trials Group. The geographic diversity of nontuberculous mycobacteria isolated from pulmonary samples: an NTM-NET collaborative study. Eur Respir J. 2013;42:1604–13. https://doi.org/10.1183/09031936.00149212
3. Hwang JA, Kim S, Jo KW, Shim TS. Natural history of *Mycobacterium avium* complex lung disease in untreated patients with stable course. Eur Respir J. 2017;49:1600537. https://doi.org/10.1183/13993003.00537-2016
4. Nakanaga K, Hoshino Y, Wakabayashi M, Fujimoto N, Tortoli E, Makino M, et al. *Mycobacterium shigaense* sp. nov., a novel slowly growing scotochromogenic mycobacterium that produced nodules in an erythroderma patient with severe cellular immunodeficiency and a history of Hodgkin's disease. J Dermatol. 2012;39:389–96. https://doi.org/10.1111/j.1346-8138.2011.01355.x
5. Fukano H, Yoshida M, Kazumi Y, Fujiwara N, Katayama K, Ogura Y, et al. *Mycobacterium shigaense* sp. nov., a slow-growing, scotochromogenic species, is a member of the *Mycobacterium simiae* complex. Int J Syst Evol Microbiol. 2018;68:2437–42. https://doi.org/10.1099/ijsem.0.002845
6. Fukano H, Hiranuma O, Matsui Y, Tanaka S, Hoshino Y. The first case of chronic pulmonary *Mycobacterium shigaense* infection in an immunocompetent patient. New Microbes New Infect. 2019;33:100630. https://doi.org/10.1016/j.nmni.2019.100630
7. Clinical and Laboratory Standards Institute. Woods GL, Wengenack NL, Lin G, Brown-Elliott BA, Cirillo DM, Conville PS, et al. Performance standards for susceptibility testing of *Mycobacteria, Nocardia* spp., and other aerobic Actinomycetes, 2018. M62, 1st ed. Wayne (PA): The Institute, 2018.
8. Richter M, Rosselló-Móra R, Oliver Glöckner F, Peplies J. JSpeciesWS: a web server for prokaryotic species circumscription based on pairwise genome comparison. Bioinformatics. 2016;32:929–31. https://doi.org/10.1093/bioinformatics/btv681
9. Yoshimura D, Kajitani R, Gotoh Y, Katahira K, Okuno M, Ogura Y, et al. Evaluation of SNP calling methods for closely related bacterial isolates and a novel high-accuracy pipeline: BactSNP. Microb Genom. 2019;5:e000261. https://doi.org/10.1099/mgen.0.000261
10. Page AJ, Cummins CA, Hunt M, Wong VK, Reuter S, Holden MT, et al. Roary: rapid large-scale prokaryote pan genome analysis. Bioinformatics. 2015;31:3691–3. https://doi.org/10.1093/bioinformatics/btv421
11. Bouam A, Armstrong N, Levasseur A, Drancourt M. *Mycobacterium terramassiliense, Mycobacterium rhizamassiliense* and *Mycobacterium numidiamassiliense* sp. nov., three new *Mycobacterium simiae* complex species cultured from plant roots. Sci Rep. 2018;8:9309. https://doi.org/10.1038/s41598-018-27629-1
12. Shu C-C, Lee C-H, Hsu C-L, Wang J-T, Wang J-Y, Yu C-J, et al.; TAMI Group. Clinical characteristics and prognosis of nontuberculous mycobacterial lung disease with different radiographic patterns. Hai. 2011;189:467–74. https://doi.org/10.1007/s00408-011-9321-4
13. Aksamit TR, Philley JV, Griffith DE. Nontuberculous mycobacterial (NTM) lung disease: the top ten essentials. Respir Med. 2014;108:417–25. https://doi.org/10.1016/j.rmed.2013.09.014
14. Griffith DE, Philley JV. The new "hesitation blues": initiating *Mycobacterium avium* complex lung disease therapy. Eur Respir J. 2017;49:1700110. https://doi.org/10.1183/13993003.00110-2017
15. Koizumi Y, Shimizu K, Shigeta M, Minamiguchi H, Hodohara K, Andoh A, et al. *Mycobacterium shigaense* causes lymph node and cutaneous lesions as immune reconstitution syndrome in an AIDS patient: the third case report of a novel strain non-tuberculous *Mycobacterium*. Intern Med. 2016;55:3375–81. https://doi.org/10.2169/internalmedicine.55.6996

Address for correspondence: Shiomi Yoshida, Clinical Research Center, National Hospital Organization Kinki-chuo Chest Medical Center, Japan, 1180 Nagasone-cho, Kita-ku, Sakai, Osaka, 591-8555, Japan; email: yoshida.shiomi.vg@mail.hosp.go.jp

Thresholds versus Anomaly Detection for Surveillance of Pneumonia and Influenza Mortality

Timothy L. Wiemken, Ana Santos Rutschman, Samson L. Niemotka, Daniel Hoft

Computational surveillance of pneumonia and influenza mortality in the United States using FluView uses epidemic thresholds to identify high mortality rates but is limited by statistical issues such as seasonality and autocorrelation. We used time series anomaly detection to improve recognition of high mortality rates. Results suggest that anomaly detection can complement mortality reporting.

Lower respiratory tract infections, including pneumonia and influenza (P&I), are the leading cause of infectious disease–related death worldwide (*1*). Annually, up to 95,000 persons might die from P&I in the United States alone (*2*). Ongoing surveillance of risk factors for influenza acquisition, incident influenza disease, and clinical outcomes of influenza infection are a global public health priority (*3*). Ensuring that public health professionals and the public at large are informed about the incidence and severity of disease in the community is an important benefit of these surveillance programs. To fulfill surveillance needs in the United States, the Centers for Disease Control and Prevention maintains FluView (*4*), a public-facing web interface providing detailed results of their influenza surveillance program. Reports maintained on FluView range from spatial analytics of influenza-like illness to virologic surveillance, virus characterization, hospitalization rates, and P&I mortality. Each report is useful for focused interventions and planning at a personal, local, state, regional, and national level.

Mortality reporting in FluView is a particularly critical public health endpoint for P&I because early interventions can lessen these catastrophic outcomes. Currently, mortality is monitored and reported as epidemic if the percentage of total deaths is above a value termed the epidemic threshold. This threshold is defined at a P&I death rate 1.645 SDs above the seasonal

baseline mortality (*5*) as measured by the National Center for Health Statistics mortality surveillance system. These statistics are useful but limited in their ability to detect abnormally high death rates because they do not rigorously account for common statistical issues inherent in influenza surveillance data, such as within- and between-season seasonality and autocorrelation (*6*). Without accounting for the complex temporal fluctuations (seasonality) and nonindependence of period-to-period data points (autocorrelation), traditional statistical methodologies might provide spurious results, leading to inappropriate conclusions. Because an essential aspect of surveillance is ensuring that robust statistical methods are used to provide a valid view of the state of disease or outcome, the exploration of innovative methods for computational surveillance of P&I outcomes is warranted. The objective of our study was to evaluate the utility of a novel anomaly detection algorithm for P&I mortality surveillance.

The Study

For our study, we obtained national P&I mortality data from FluView for a 350-week period ranging from week 40 of 2013 through week 24 of 2020. First, we recreated the current FluView P&I mortality plot, shading areas above the epidemic threshold to more easily delineate mortality rates higher than this limit. Next, we used Twitter's time-series decomposition and the generalized extreme studentized deviate anomaly detection algorithm to identify anomalous P&I mortality rates (*7*,*8*). For anomaly detection, default α (0.05) and maximum anomalies (20%) were used as options. Anomaly plots identify anomalies using red dots. We analyzed data using R version 4.0.1 (R Foundation for Statistical Computing, https://www.r-project.org).

Using current epidemic threshold methodologies, we found that 72 (20.6%) of weekly P&I mortality rates were beyond the epidemic threshold (Figure, panel A). P&I mortality rates spiked above the epidemic threshold in approximately the same weeks
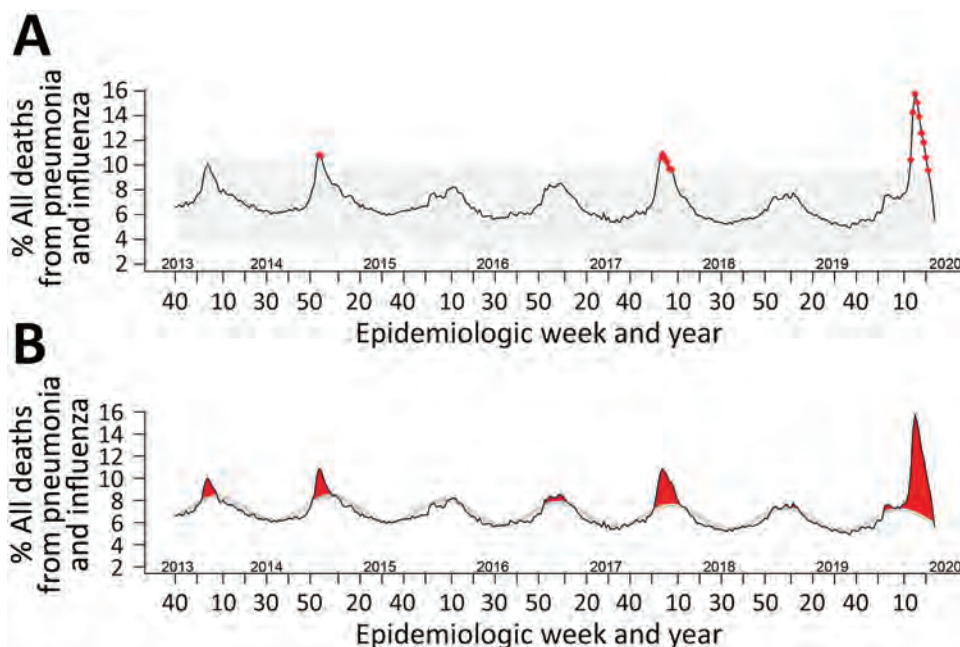
Figure. Pneumonia and influenza mortality surveillance using anomaly detection analysis versus threshold method, United States. A) Line chart representing anomaly detection analysis of surveillance. Red points indicate anomalous data points. B) Line chart representing the pneumonia and influenza mortality data using the standard FluView (*4*) threshold method. Gray areas indicate values between expected (baseline seasonal mortality) and the epidemic threshold. Red areas indicate areas beyond expected or epidemic threshold values.

every year since week 40 of 2013. Anomaly detection identified 17 (4.9%) P&I mortality rates as abnormally high (Figure, panel B). To ensure that this methodology can be continually used into the future, we also created a free, open-source, web-based application to recreate both figures on demand as data are updated (https://surveillance.shinyapps.io/fluview). Once loaded, the current national data are pulled from FluView and analyzed on the first tab. The anomaly plot and the updated current FluView P&I mortality surveillance plots are then displayed. For this web application, we included the options to modify some basic functionality of the anomaly detection algorithm with brief discussions of how they can be used (*7,8*). A second tab was created to enable upload of state-level P&I mortality data from FluView Interactive (https://gis.cdc.gov/grasp/fluview/mortality.html), providing the same anomaly detection plot.

Conclusions

The current epidemic threshold for documenting P&I mortality in the United States cannot differentiate characteristic mortality rates during peak influenza season from unusually high mortality attributable to P&I. An important benefit of mortality surveillance is the identification of periods where rates are beyond a reasonable expectation such that adequate interventions can be developed to lower death rates in the community. Currently, P&I mortality rates are compared with a basic SD statistic obtained and averaged over seasonal baseline mortality estimates. This traditional approach does not account for seasonality or autocorrelative functions

within and across influenza seasons (*6*). Given the advancements in computational power and the development of easy-to-interpret algorithms capable of filtering out these biases, alternative approaches for surveillance of P&I mortality at a national level should be considered to complement the current FluView methods. Our approach is one such alternative. Others such as the European EuroMoMo modeling (https://www.euromomo.eu) might also be applicable methods for bolstering our understanding of P&I mortality.

Although this particular anomaly detection might underestimate the frequency of abnormally high mortality rates, our approach is also likely to produce an additional, more focused message for public health professionals. Currently, P&I mortality peaks above the epidemic threshold at approximately the same time each year. Therefore, the existing approach might have a limited ability to provide public health professionals with the reports necessary to make informed interventions to limit mortality, such as through recalibrating targeted screening and preventative approaches, and to more accurately develop focused interventions such as vaccination campaigns. To accomplish this task, a computational method motivated by identifying outlying mortality rates should be used, with the caveat that mortality data must be reported in near real-time. Our approach provides such an outcome and might be useful for public health professionals in their quest to prevent and control P&I-related death. Our approach might also be useful for computational surveillance of other respiratory diseases, such as coronavirus.

About the Author

Dr. Wiemken is an associate professor at Saint Louis University School of Medicine, Department of Health and Clinical Outcomes Research, and Department of Medicine, Division of Infectious Diseases, Allergy, and Immunology, and is the director of The AHeaD Institute Systems Infection Prevention Center. His primary research interests include emerging infectious diseases, influenza, vaccinology, healthcare-associated infections, and data science.

References

1. World Health Organization. Top 10 causes of death 2016 [cited 2020 Aug 24]. https://www.who.int/en/news-room/fact-sheets/detail/the-top-10-causes-of-death
2. Centers for Disease Control and Prevention. Influenza (flu): burden of influenza [cited 2020 Aug 24]. https://www.cdc.gov/flu/about/burden/index.html
3. Bresee J, Fitzner J, Campbell H, Cohen C, Cozza V, Jara J, et al.; WHO Working Group on the Burden of Influenza Disease. Progress and remaining gaps in estimating the global disease burden of influenza. Emerg Infect Dis. 2018;24:1173–7. https://doi.org/10.3201/eid2407.171270
4. Centers for Disease Control and Prevention. Influenza (flu) weekly U.S. influenza surveillance report (FluView) [cited 2020 Aug 24]. https://www.cdc.gov/flu/weekly/index.htm
5. Centers for Disease Control and Prevention. Influenza surveillance considerations [cited 2020 Aug 24]. https://www.cdc.gov/flu/weekly/overview.htm#anchor_1539281356004
6. Schanzer DL, Langley JM, Dummer T, Aziz S. The geographic synchrony of seasonal influenza: a waves across Canada and the United States. PLoS One. 2011;6:e21471. https://doi.org/10.1371/journal.pone.0021471
7. Wiemken TL, Furmanek SP, Mattingly WA, Wright MO, Persaud AK, Guinn BE, et al. Methods for computational disease surveillance in infection prevention and control: statistical process control versus Twitter's anomaly and breakout detection algorithms. Am J Infect Control. 2018;46:124–32. https://doi.org/10.1016/j.ajic.2017.08.005
8. Vallis O, Hochenbaum J, Kejariwal A. A novel technique for long-term anomaly detection in the cloud [cited 2020 Aug 24]. https://www.usenix.org/system/files/conference/hotcloud14/hotcloud14-vallis.pdf

Address for correspondence: Timothy L Wiemken, Saint Louis University School of Medicine, 3545 Lafayette Ave #411, St. Louis, MO 63130, USA; email: timothy.wiemken@health.slu.edu

Multiple Introductions of *Salmonella enterica* Serovar Typhi H58 with Reduced Fluoroquinolone Susceptibility into Chile

Mailis Maes,[1] Zoe A. Dyson,[1] Ellen E. Higginson, Alda Fernandez, Pamela Araya, Sharon M. Tennant, Stephen Baker, Rosanna Lagos, Myron M. Levine, Juan Carlos Hormazabal,[2] Gordon Dougan[2]

Salmonella enterica serovar Typhi H58, an antimicrobial-resistant lineage, is globally disseminated but has not been reported in Latin America. Genomic analysis revealed 3 independent introductions of *Salmonella* Typhi H58 with reduced fluoroquinolone susceptibility into Chile. Our findings highlight the utility of enhanced genomic surveillance for typhoid fever in this region.

*S*almonella enterica serovars Typhi, Paratyphi A, and Paratyphi B are the etiologic agents of typhoid and paratyphoid fever. Each year, ≈11–21 million cases and 128,000–161,000 typhoid-related deaths occur, making typhoid a continued health concern in many low- and middle-income countries, particularly among populations without access to clean water or improved sanitation (*1*). *Salmonella* Typhi H58 lineage, genotype 4.3.1, commonly is associated with multidrug resistance, including resistance to chloramphenicol, ampicillin, and trimethoprim/sulfamethoxazole. In addition, isolates exhibiting resistance to fluoroquinolones have been linked to emergent clades of genotype 4.3.1 in South Asia (*2*), the spread of which could cause major challenges for disease management.

Salmonella Typhi H58 4.3.1 is the dominant genotype in many parts of Southeast and South Asia and in East Africa (*3*) and has spread globally but has not been reported in Latin America. Recent data on typhoid fever in South America are limited, and little is known about the population structure and antimicrobial susceptibility profiles of *Salmonella* Typhi on the continent. However, a report of 402 *Salmonella* Typhi isolates collected in Colombia during 2012–2015 showed that only 2.2% were resistant to fluoroquinolones (*4*). In 2016, Colombia reported collecting 204 *Salmonella* Typhi isolates, 12.7% of which exhibited decreased susceptibility to fluoroquinolones (*5*). Because these reports did not include whole-genome sequencing (WGS) data, determining whether isolates were genotype 4.3.1 is not possible.

Before the 1970s, typhoid fever was endemic in parts of South America and hyperendemic in Chile. However, water quality and sanitation improvements across the continent, partly in response to a major cholera epidemic in 1991, likely have contributed to a steep decline in the incidence of typhoid fever (*6*). During 1982–1992, Chile implemented interventions to reduce typhoid fever, including immunizing schoolchildren, prohibiting use of untreated sewage to irrigate crops, and detecting and treating chronic carriers. These interventions drastically reduced transmission and typhoid incidence has declined to 0.2 cases/100,000 persons (*7*), including in the greater Santiago metropolitan region (*8*).

Chile's epidemiologic surveillance system tracks suspected typhoid fever. Two thirds of cases are confirmed by pathogen isolation from ordinarily sterile body fluids, such as blood or bone marrow. *Salmonella* Typhi isolates from Chile typically are susceptible

Author affiliations: University of Cambridge, Cambridge, UK (M. Maes, Z.A. Dyson, E.E. Higginson, S. Baker, G. Dougan); Monash University, Melbourne, Victoria, Australia (Z.A. Dyson); London School of Hygiene & Tropical Medicine, London, UK (Z.A. Dyson); Instituto de Salud Publica de Chile, Santiago, Chile (A. Fernandez, P. Araya, J.C. Hormazabal); University of Maryland School of Medicine, Baltimore, Maryland, USA (S.M. Tennant, M. M. Levine); Hospital de Niños de Santiago, Santiago, Chile (R. Lagos)

[1]These first authors contributed equally to this work.

[2]These authors contributed equally to this work.

to antimicrobial agents, but ciprofloxacin resistance has been reported. Among isolates collected during 2009–2016, nearly 2% were ciprofloxacin resistant and 14% displayed intermediate resistance (*9*). We used WGS and bioinformatic analyses to characterize *Salmonella* Typhi isolates from Chile to determine if antimicrobial-resistant H58 4.3.1 isolates have been introduced into South America.

The Study

We used a HiSeq WGS platform (Illumina, https://www.illumina.com) to generate 150 bp paired-end reads from *Salmonella* Typhi isolates collected during 2011–2017 by Chile's National Typhoid Surveillance System. We assigned sequences to previously

defined genotypes and identified 7 genotype 4.3.1 isolates (Appendix 1, https://wwwnc.cdc.gov/EID/article/26/11/20-1676-App1.pdf). Isolates were obtained from clinical cases in the Santiago metropolitan region: 1 in 2012, 5 in 2015, and 1 in 2016. For global context, we analyzed these 7 genomes and 2,386 publicly available sequences (Appendix 2 Table 1, https://wwwnc.cdc.gov/EID/article/26/11/20-1676-App2.xlsx). Among publicly available sequences, 2,326 were genotype 4.3.1 and 60 were non–4.3.1 genotypes (Appendix 1 Table 2). We used the non–4.3.1 genotypes and a *Salmonella* Paratyphi A sequence as an outgroup for phylogenetic tree rooting. We produced clean and filtered SNP alignments (Appendix 1) and used these alignments to
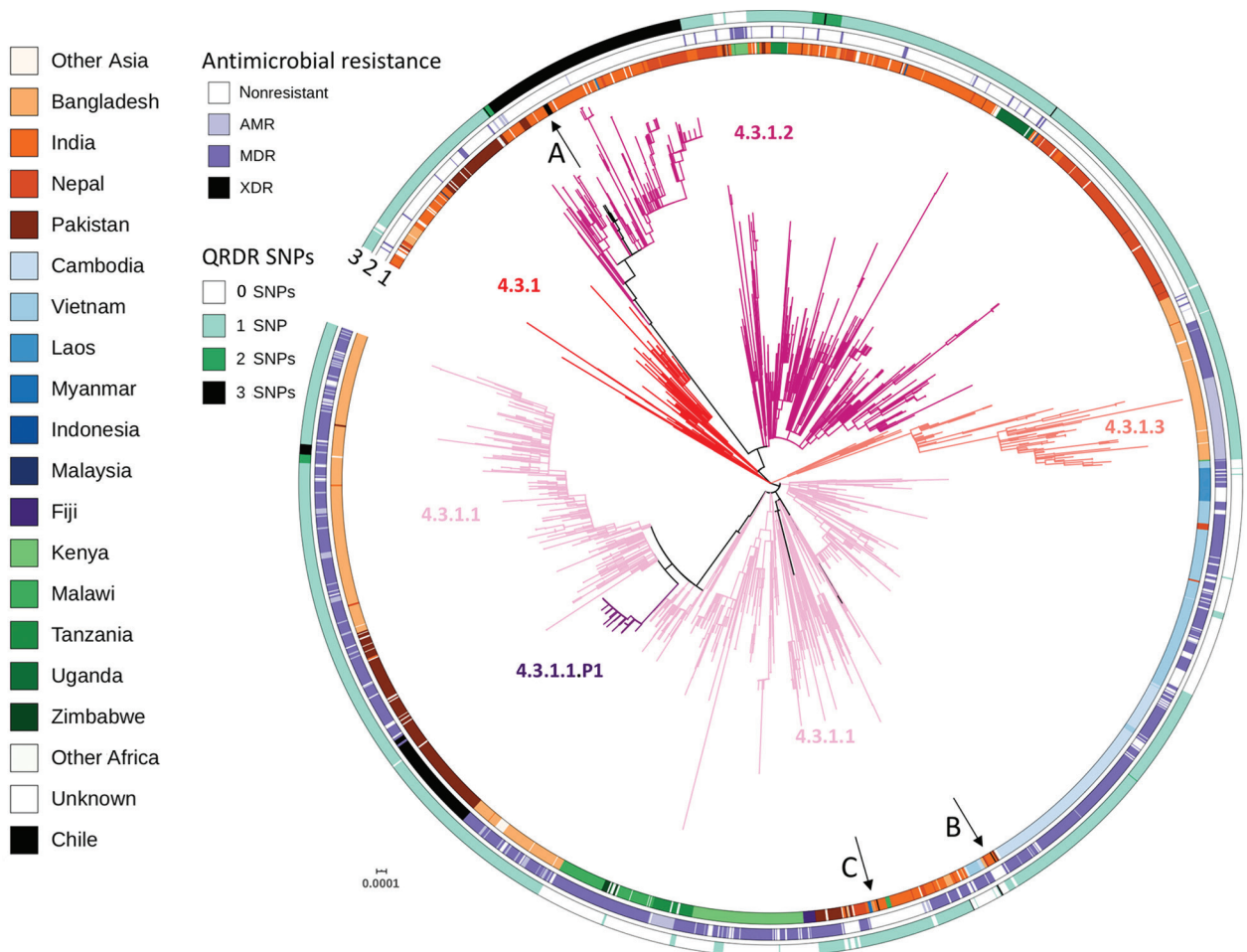

Figure 1. Global context of *Salmonella enterica* serovar Typhi genotype 4.3.1 from Chile. *Salmonella* Typhi H58 genotype 4.3.1-based phylogenetic tree. Branches are colored by genotypes labeled in the tree. A, B, and C arrows indicate isolates from the Chile and the 3 independent introductions. The inner circle indicates country of isolation. The middle circle indicates AMR, excluding reduced susceptibility to fluoroquinolones caused by QDRD SNPs; MDR, including resistance to chloramphenicol, ampicillin, and trimethoprim-sulfamethoxazole; or XDR, multidrug resistance plus resistance to third-generation cephalosporins and reduced susceptibility to fluoroquinolones. The outer circle indicates number of SNPs, 0, 1, 2 or 3, in the quinolone resistance determining region of *gyrA* and *parC* genes. Scale bar indicates nucleotide substitutions per site. AMR, antimicrobial resistance; MDR, multidrug-resistant; QRDR, quinolone-resistance determining region; SNP, single-nucleotide polymorphism; XDR, extremely drug-resistant.

Figure 2. Nearest-neighbor calculations of *Salmonella enterica* serovar Typhi of genotype 4.3.1 and maximum-likelihood phylogenetic trees for 3 introductions of *Salmonella* Typhi genotype 4.3.1 into Chile in the context of their closest *Salmonella* Typhi isolate neighbors. A) Isolate collected during 2012–2014 resembles isolates from South Asia. B) Isolate collected during 2015 resembles isolates from India. C) Isolate collected in 2016 is closely related to a cluster of sequences from India and Bangladesh. Accession numbers, genotypes, countries, and years of isolation are shown. Stars indicate mutations in the quinolone resistance determining region of genes *gyrA*, *gyrA*-S83F and *gyrA*-D87N, and *parC*-S80I. Scale bars indicate SNP distance. SNP, single-nucleotide polymorphism.

infer maximum likelihood phylogenies and specified a generalized time-reversible model and a Gamma distribution to model site-specific rate variation by using GTRGAMMA in RAxML version 8.2.9 (https://github.com/stamatak/standard-RAxML) and 100 bootstrap pseudoreplicates to assess branch support. SNP distances were calculated by using snp-dists (https://github.com/tseemann/snp-dists; Appendix 2). Raw Illumina reads were assembled by using either Velvet version 1.2 (European Bioinformatics Institute, https://www.ebi.ac.uk/~zerbino/velvet) or Unicycler version 0.4.7 (*10*). Assembled reads were input into Pathogenwatch (https://pathogen.watch) to detect nonsynonymous mutations in the quinolone-resistance determining region of *gyrA* and *parC* genes responsible for reduced fluoroquinolone susceptibility. We also used this approach to look for known antimicrobial resistance (AMR) genes. We further screened the sequences from Chile and close genetic relatives to determine molecular determinants of AMR and known plasmid replicon genes (Appendix 1 Table).

Phylogenomic and SNP analyses confirmed 7 *Salmonella* Typhi genotype 4.3.1 isolates from Chile. Contact tracing implies that 4/5 isolates from 2015 were part of a localized outbreak. We found that the 7 isolates were members of 2 different sublineages, lineage I (4.3.1.1) and lineage II (4.3.1.2), suggesting multiple introductions into Chile. The 2 isolates of lineage I carried a single *gyrA*-S83F mutation predicted to confer reduced susceptibility to fluoroquinolones. The 5 lineage II isolates carried 3 quinolone-resistance determining region mutations, 2 in *gyrA* genes, S83F and D87N, and 1 in *parC*-S80I. Genotype 4.3.1 triple mutants were predicted to be resistant to fluoroquinolones, and isolates of this sublineage with identical mutations have been observed on the subcontinent of India and have been associated with treatment failure (*2,11,12*). None of the lineage II triple mutants in Chile carried detectable horizontally acquired AMR genes.

To provide a global contextualization of *Salmonella* Typhi genotype 4.3.1 in Chile, we analyzed the novel sequences alongside 2,326 existing sequences from 31 countries (Figure 1). The 4.3.1.2 triple

mutants from Chile formed a closely related phylogenetic cluster (median distance 2 SNPs) with sequences that have the same antimicrobial susceptibility profile isolated from India during 2012–2014, indicating an introduction from South Asia (Figure 2, panel A).

The two 4.3.1.1 isolates from 2015 and 2016 in Chile were in distinct subclades of the tree and were separated by 19 SNPs, suggestive of 2 separate introductions. Of these, 1 introduction was closely related to a 2015 isolate from India (5 SNPs apart) (Figure 2, panel B) and the other was nested in a cluster of sequences from Southeast and South Asia and most closely related (median distance of 20 SNPs) to sequences from India and Bangladesh (Figure 2, panel C).

Conclusions

Our study confirmed *Salmonella* Typhi H58 genotype 4.3.1 in South America. Phylogenomic and SNP analyses indicate ≥3 separate genotype introductions into Chile; 5/7 isolates carried 3 distinct mutations, 2 in the *gyrA* gene, at D87N and S83F, and 1 in the *parC* gene at S80I, which are associated with ciprofloxacin resistance. For a high-income country with adequate surveillance, like Chile, the presence of fluoroquinolone-resistant genotype 4.3.1 *Salmonella* Typhi has no immediate implications. However, if this genotype is transferred to low- or middle-income countries in South America, it could have major consequences. Therefore, these data should be of concern to other countries in the region where potential typhoid fever transmission remains high and adequate sanitation might be lacking (*5,6,10*). Ciprofloxacin is a first-line drug for typhoid fever in much of Latin America, and fluoroquinolone-resistant genotype 4.3.1 would reduce its long-term efficacy.

Most diagnostic laboratories across South America are using pulsed-field gel electrophoresis to study *Salmonella* Typhi epidemiology (*13*), but efforts are underway to implement WGS for epidemiologic surveillance in several countries (*14,15*). However, WGS-based approaches for detecting genotype 4.3.1 and understanding trends in genotype population, circulating lineages, and AMR dynamics have not been adopted widely across the region. Our work highlights the need for a uniform WGS platform for global *Salmonella* Typhi monitoring and the need to elucidate the current epidemiology of typhoid fever in South America.

Acknowledgments

About the Author

Ms. Maes is a PhD student at the University of Cambridge. Her research interests include the intracellular pathogen *Salmonella* Typhi, phylogenetics of *Salmonella* Typhi in Latin America, and the behavior of *Salmonella* Typhi in macrophages and the gallbladder.

References

1. World Health Organization. Typhoid [cited 2020 Apr 16]. https://www.who.int/health-topics/typhoid
2. Wong VK, Baker S, Pickard DJ, Parkhill J, Page AJ, Feasey NA, et al. Phylogeographical analysis of the dominant multidrug-resistant H58 clade of *Salmonella* Typhi identifies inter- and intracontinental transmission events. Nat Genet. 2015;47:632–9. https://doi.org/10.1038/ng.3281
3. Park SE, Pham DT, Boinett C, Wong VK, Pak GD, Panzner U, et al. The phylogeography and incidence of multi-drug resistant typhoid fever in sub-Saharan Africa. Nat Commun. 2018;9:5094. https://doi.org/10.1038/s41467-018-07370-z
4. Diaz-Guevara P, Montaño LA, Duarte C, Zabaleta G, Maes M, Martinez Angarita JC, et al. Surveillance of *Salmonella enterica* serovar Typhi in Colombia, 2012-2015. PLoS Negl Trop Dis. 2020;14:e0008040. https://doi.org/10.1371/journal.pntd.0008040
5. Pan American Health Organization. Epidemiological alert, *Salmonella enterica* serovar Typhi haplotype H58, 18 October 2018 [cited 2020 Apr 16]. https://iris.paho.org/handle/10665.2/50533
6. Marco C, Delgado I, Vargas C, Muñoz X, Bhutta ZA, Ferreccio C. Typhoid fever in Chile 1969–2012: Analysis of an epidemic and its control. Am J Trop Med Hyg. 2018;99 (3_Suppl):26–33. https://doi.org/10.4269/ajtmh.18-0125
7. Government of Chile, Department of Epidemiology. Quarterly epidemiological bulletin 2015 Jan 13 [in Spanish] [cited 2020 Apr 16]. http://epi.minsal.cl/wp-content/uploads/2016/01/FT_BET2_2015.pdf
8. Gauld JS, Hu H, Klein DJ, Levine MM. Typhoid fever in Santiago, Chile: insights from a mathematical model utilizing venerable archived data from a successful disease control program. PLoS Negl Trop Dis. 2018;12:e0006759. https://doi.org/10.1371/journal.pntd.0006759
9. Ministerio de Salud, Chile; Instituto de Salud Pública. Antimicrobial resistance bulletin 2018 [in Spanish] [cited

2020 Apr 16]. http://www.ispch.cl/sites/default/files/BoletinRam2018-08012019A.pdf
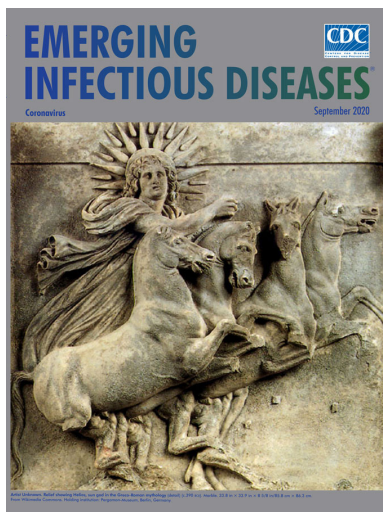10. Wick RR, Judd LM, Gorrie CL, Holt KE. Unicycler: resolving bacterial genome assemblies from short and long sequencing reads. PLOS Comput Biol. 2017;13:e1005595. https://doi.org/10.1371/journal.pcbi.1005595
11. Wong VK, Baker S, Connor TR, Pickard D, Page AJ, Dave J, et al.; International Typhoid Consortium. An extended genotyping framework for *Salmonella enterica* serovar Typhi, the cause of human typhoid. Nat Commun. 2016;7:12827. https://doi.org/10.1038/ncomms12827
12. Pham Thanh D, Karkey A, Dongol S, Ho Thi N, Thompson CN, Rabaa MA, et al. A novel ciprofloxacin-resistant subclade of H58 *Salmonella* Typhi is associated with fluoroquinolone treatment failure. eLife. 2016; 5:e14003. https://doi.org/10.7554/eLife.14003
13. Campos J, Pichel M, Vaz TMI, Tavechio AT, Fernandes SA, Muñoz N, et al. Building PulseNet Latin America and Caribbean *Salmonella* regional database: first conclusions of genetic subtypes of *S.* Typhi, *S.* Typhimurium and *S.* Enteritidis circulating in six countries of the region. Food Res Int. 2012;45:1030–6. https://doi.org/10.1016/j.foodres.2011.10.020
14. Baker KS, Campos J, Pichel M, Della Gaspera A, Duarte-Martínez F, Campos-Chacón E, et al. Whole genome sequencing of *Shigella sonnei* through PulseNet Latin America and Caribbean: advancing global surveillance of foodborne illnesses. Clin Microbiol Infect. 2017;23:845–53. https://doi.org/10.1016/j.cmi.2017.03.021
15. Chinen I, Campos J, Dorji T, Pérez Gutiérrez E. PulseNet Latin America and the Caribbean network: present and future. Foodborne Pathog Dis. 2019;16:489–97. https://doi.org/10.1089/fpd.2018.2587

Address for correspondence: Mailis Maes, Cambridge Institute of Therapeutic Immunology & Infectious Disease Medicine, University of Cambridge, Puddicombe Way, Cambridge, Cambridgeshire CB2 0AW, UK; email: mm2032@medschl.cam.ac.uk

September 2020
Coronavirus

- Disparate Effects of Invasive Group A Streptococcus on Native Americans
- Seroepidemiologic Study Designs for Determining SARS-COV-2 Transmission and Immunity
- Polyclonal *Burkholderia cepacia* Complex
- Outbreak in Peritoneal Dialysis Patients Caused by Contaminated Aqueous Chlorhexidine
- Severe Acute Respiratory Syndrome Coronavirus 2 Prevalence, Seroprevalence, and Exposure among Evacuees from Wuhan, China, 2020
- Pathology and Pathogenesis of SARS-CoV-2 Associated with Fatal Coronavirus Disease, United States
- Encephalopathy and Encephalitis Associated with Cerebrospinal Fluid Cytokine Alterations and Coronavirus Disease, Atlanta, Georgia, USA, 2020
- Invasive Infections with *Nannizziopsis obscura* Species Complex in 9 Patients from West Africa, France, 2004–2020
- *Saprochaete clavata* Outbreak Infecting Cancer Center through Dishwasher
- Retrospective Description of Pregnant Women Infected with Severe Acute Respiratory Syndrome Coronavirus 2, France

- Q Fever Osteoarticular Infection in Children
- Updated Estimates of Chronic Conditions Affecting Risk for Complications from Coronavirus Disease, United States
- Web-Based Interactive Tool to Identify Facilities at Risk of Receiving Patients with Multidrug-Resistant Organisms
- Isolation, Sequence, Infectivity, and Replication Kinetics of Severe Acute Respiratory Syndome Coronavirus 2

- Evaluation of World Health Organization– Recommended Hand Hygiene Formulations
- Heterogeneity of Dengue Illness in Community-Based Prospective Study, Iquitos, Peru
- Association of Biosecurity and Hygiene Practices with Environmental Contamination with Influenza A Viruses in Live Bird Markets, Bangladesh
- Costs Associated with Nontuberculous Mycobacteria Infection, Ontario, Canada, 2001–2012
- No Change in Risk for Antibiotic– Resistant Salmonellosis from Beef, United States, 2002-2010
- Detection of H1 Swine Influenza A Virus Antibodies in Human Serum Samples by Age Group
- Incidence and Seroprevalence of Avian Influenza in a Cohort of Backyard Poultry Growers, Egypt, August 2015–March 2019
- Risk-Based Estimate of Human Fungal Disease Burden, China
- Molecular Description of a Novel Orientia Species Causing Scrub Typhus in Chile
- Large Outbreak of Coronavirus Disease among Wedding Attendees, Jordan

To revisit the September 2020 issue, go to:
https://wwwnc.cdc.gov/eid/articles/issue/26/9/table-of-contents

Chikungunya Virus Infection in Blood Donors and Patients During Outbreak, Mandalay, Myanmar, 2019

Aung Kyaw Kyaw,[1] Mya Myat Ngwe Tun,[1] Takeshi Nabeshima, Aung Min Soe, Khin Mya Mon, Thida, Thet Htoo Aung, Thein Thein Htwe, Su Su Myaing, Tu Tu Mar, Thida Aung, Khin Moh Moh Win, Khin Mar Myint, Ei Phyu Lwin, Hlaing Myat Thu, Corazon C Buerano, Kyaw Zin Thant, Kouichi Morita

In 2019, an outbreak of chikungunya virus infection occurred in Mandalay, Myanmar, and 3.2% of blood donors and 20.5% of patients who were children were confirmed as being infected. The prevalence rate was up to 6.3% among blood donors. The East Central/South African genotype was predominantly circulating during this outbreak.

Chikungunya (CHIK) is an emerging tropical disease caused by CHIK virus (CHIKV; family *Togaviridae*, genus *Alphavirus*), of which there are 3 genotypes: Asian, East/Central/South African (ECSA), and West African (*1*). This virus was detected in Asia during 1954 and has been observed to continuously circulate in countries in southern and Southeast Asia (*2–5*). In Myanmar, the first case of CHIKV infection was confirmed serologically in 1973 (*6*), and the CHIKV ECSA genotype was observed in patients during 2010 (*7*).

The signs and symptoms (e.g., fever, rash, and severe joint pain) caused by CHIKV are similar to those caused by dengue virus. Although deaths from CHIK are rare, this disease can cause neurologic manifestations (*8*). The asymptomatic infection rate for CHIKV is 10%–25%. There is a risk for CHIKV transmission by blood transfusion (*9*), but no transfusion-transmitted infections have been documented. In many countries, including Myanmar, CHIKV screening is not routinely performed for blood donors.

We aimed to determine the proportion of blood donors who had CHIKV IgM and CHIKV RNA. Because our study was conducted during the outbreak of CHIKV infection in Myanmar in 2019, proportions of virus-positive children with acute febrile illness during routine dengue surveillance were also determined. We also sought to identify the CHIKV genotype for CHIKV RNA-positive samples.

The Study

An outbreak of CHIKV infection occurred in Mandalay, Myanmar, during 2019. A cross-sectional descriptive study was conducted among blood donors at the Blood Bank of Mandalay General Hospital and patients at the Mandalay Children Hospital. A total of 500 blood donors and 151 patients who had acute febrile illness but were negative for dengue virus nonstructural protein 1 (NS1) were enrolled. Approximately 20–25 blood donors/week were enrolled, and their blood samples were collected once per week by using saturation method during the peak season of arboviral infection (June–September). Children (<13 years of age) with acute febrile illness were also enrolled.

Blood samples (2 mL) from blood donors and patients in the acute phase of disease were collected after hospital admission. Individual serum samples were tested by using the QuickProfile Chikungunya

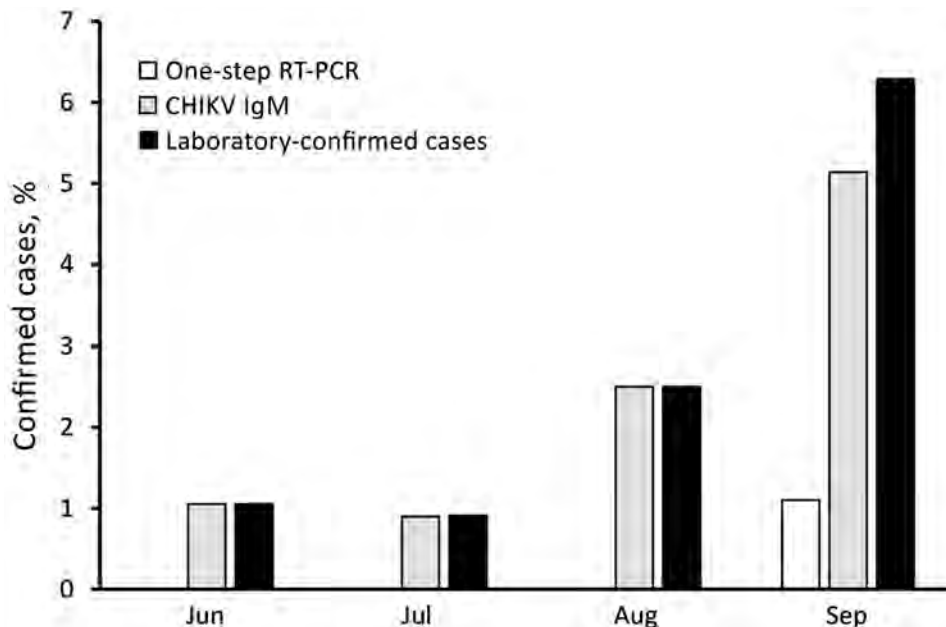[1]These authors contributed equally to this article.

Figure 1. Distribution of laboratory-confirmed cases of infection with CHIKV among blood donors, Myanmar, June–September, 2019. Laboratory confirmed cases were defined as RT-PCR or CHIKV IgM positive. CHIKV, chikungunya virus; RT-PCR, reverse transcription PCR.

IgG/IgM Combo Rapid Diagnostic Test Kit (LumiQuick, https://lumiquick.co). IgM-positive samples were confirmed by using an in-house CHIKV IgM capture ELISA (7).

Viral RNA was extracted from pooled serum samples (15–20 samples/pool) of blood donors and from individual samples of patients by using the Viral RNA Extraction Kit (QIAGEN, https://www.qiagen.com). Conventional 1-step RT-PCR was performed by using the Invitrogen 1-step RT-PCR Kit (Thermofisher Scientific, https://www.thermofisher.com). For reverse transcription PCR (RT-PCR)–positive pooled samples, viral RNA was extracted again from individual samples and checked by using conventional RT-PCR. A case of laboratory-confirmed CHIKV infection was defined as a case with positive results by RT-PCR or CHIKV IgM ELISA.

Sequencing of envelope protein 1 (E1) (402 bp) and NS1 1 (262 bp) gene regions of CHIKV was performed by using Sanger method with a 3500 Genetic Analyzer (Thermofisher Scientific). We used the maximum-likelihood method by using PHYML version 3.0.1 (http://www.atgc-montpellier.fr). Phylogenetic trees were constructed on the basis of partial nucleotides sequences of 2 gene regions for CHIKV strains. The substitution model was selected by using jmodeltest-2.1.7 (https://github.com), and generalized time reversible plus l was chosen as the model with bootstrap values after 1,000 replications. Trees were drawn by using Fig tree software version 1.4.2 (10). Sequences of the strains in this study were submitted to GenBank (accessions nos. MN552427–41).

Data entry was performed by using Microsoft Excel (https://www.microsoft.com), and analysis was performed by using R software version 3.4.4 (https://www.r-project.org). Our protocol was approved (Ethics/DMR/2019/082) by the Institutional Review Board of the Department of Medical Research, Ministry of Health and Sports, Myanmar.

Of 500 blood donors, 14 (2.8%, 95% C 1.7%–4.6%) were positive for CHIKV IgM, 135 (27.0%, 95% CI 23.2%–31.1%) for CHIKV IgG, 2 (0.4%, 95% CI 0.05%–1.4%) for CHIKV RNA. A total of 16 of 500 blood donors (3.2%, 95% CI 2.0%–5.1%) were confirmed as having CHIKV infection. All IgM-positive blood donors were negative for CHIKV RNA, and blood donors positive for CHIKV RNA were negative by serologic analysis. Of 151 patients with acute febrile illness, 26 (17.2%) were positive for CHIKV RNA, 4 (2.6%) for CHIKV IgM, 1 (0.7%) for CHIKV RNA and CHIKV IgM, and 9 (5.9%) for CHIKV IgG. Using these data, we confirmed that 31 (20.5%, 95% CI 14.1%–26.9%) had CHIKV infection.

Table 1. Clinical manifestations of blood donors and patients with acute febrile illness who were confirmed as having chikungunya virus infection, Myanmar

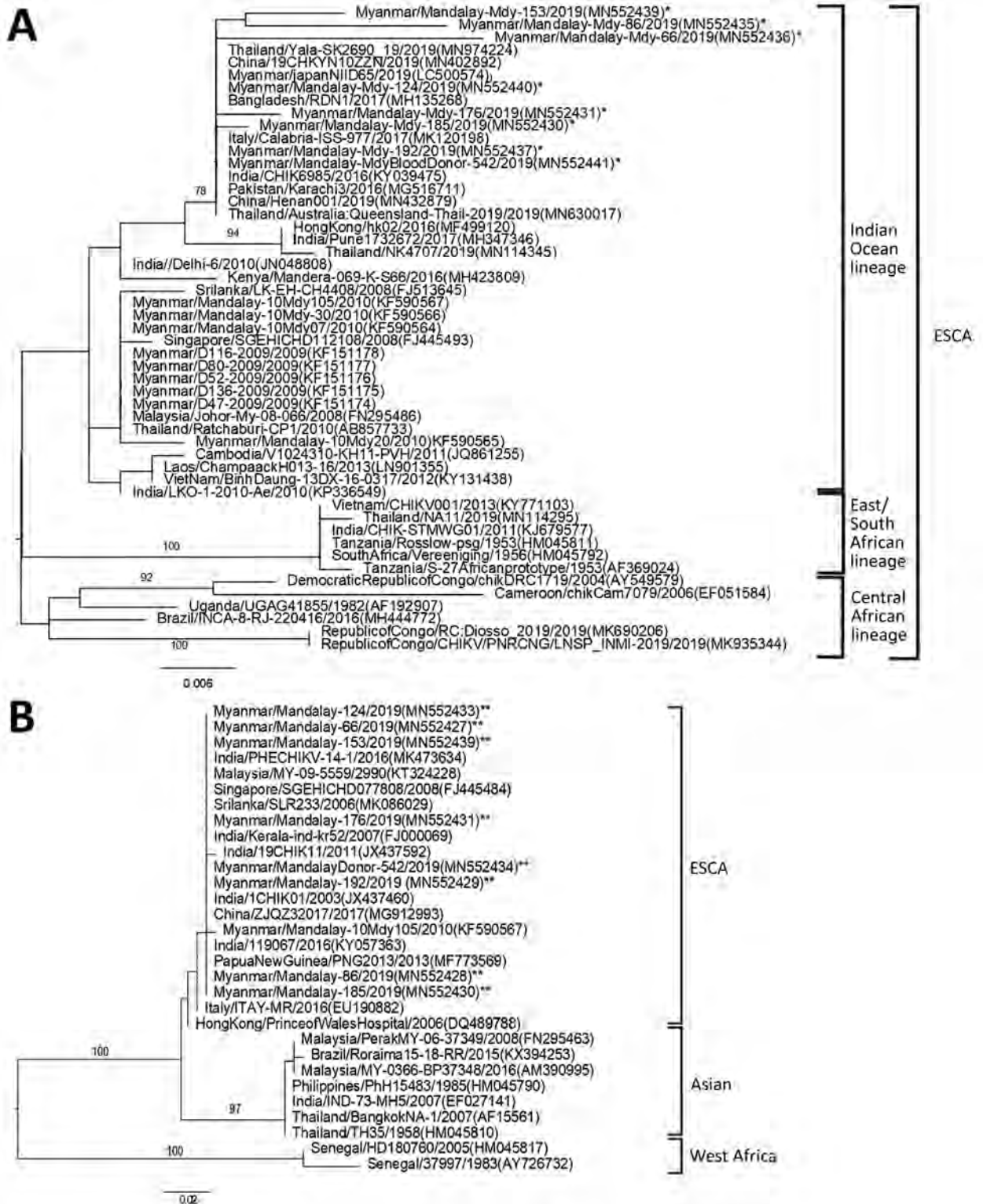| Group	No. positive/ no. tested (%)
Blood donors	16/500 (3.2)
Asymptomatic	16/16 (100.0)
Patients with acute febrile illness	31/151 (20.5)
Acute viral infection	19/31 (61.3)
Meningitis	2/31 (6.5)
Viral encephalitis	2/31 (6.5)
Dengue virus infection	5/31 (16.1)
Chikungunya virus infection	1/31 (3.2)
Febrile convulsion	2/31 (6.5)

Figure 2. Phylogenetic trees constructed on the basis of partial nucleotide sequences of CHIKV to show the relationships of CHIKV strains from different sources, including strains detected in Myanmar during 2019 (asterisks). A) Envelope protein 1 gene; B) nonstructural protein 1 gene. Numbers along branches are bootstrap values. Representative strains of each genotype obtained from GenBank are named by country of origin, strain name, year of isolation, and GenBank accession number. Scale bars indicate nucleotide substitutions per site. ESCA, East/Central South African.

The proportion of confirmed CHIKV cases among blood donors had an increasing trend from June through September: prevalence rates were 1.1% in June, 0.9% in July, 2.5% in August, and 6.3% in September (p = 0.02) (Figure 1). Among infected patients, 19 had an acute viral infection and 4 had neurologic manifestations, and all blood donors were asymptomatic (Table 1).

Amino acid sequences of the partial E 1 protein of the infecting 2019 CHIKV strains in this study showed no E1:A226V mutation (Table, https://wwwnc.cdc.gov/EID/article/26/11/20-1824-T2.htm). However, the E1:K211E mutation, which was not observed in strains isolated in Myanmar during 2010 having the E1:A226V mutation, was present. Phylogenetic trees for partial E1 and NS1 genes (*11*) showed that our virus strains belonged to the Indian Ocean clade of the ECSA genotype and were similar to those circulating in India and Thailand and previously circulating in Myanmar (Figure 2).

Conclusions

We showed that 3.2% of blood donors and 20.5% of children had CHIKV infections during the CHIK outbreak in Myanmar in 2019. During 2019 in Puerto Rico, USA, 2.1% of blood donors was found to be positive with CHIKV RNA (*12*). CHIKV can be detected up to 7 days after symptom onset. IgM can appear on day 4 after symptom onset, peak at day 7, and can persist for 2–3 months. Thus, if blood donors are positive for CHIKV IgM but not viremic, there is a low risk for transfusion-transmitted infection (*13*). However, the World Health Organization recommends deferment of blood donations by persons with confirmed CHIKV infections for >6 months (*14*). To avoid risks of transfusion-transmitted infection, molecular testing for CHIKV infection must be conducted for blood donors (*11*). Detection of CHIKV IgM and IgG indicates recent (IgM) and past (IgG) infections with CHIKV. The blood donors positive for CHIKV infection in this study did not have symptoms of CHIKV infection. Thus, verbal questions about the history of infections of blood donors are not sufficient for donor screening in disease-endemic countries.

Previous studies showed that genotypes from Asia and the ECSA genotype were circulating in Southeast Asia (*11*). In Thailand, Indian Ocean and South African clades of the ECSA genotype were detected during the outbreak in 2019 (*2*). The Indian Ocean lineage of ECSA genotype has been introduced in SEA countries since 2007 (*11*). In our study, the virus strains detected in the 2019 outbreak in Myanmar belonged to Indian Ocean lineage of ECSA genotype and had close similarity to the strains circulating in 2019 in Thailand, which could be the source of CHIKV in Myanmar. The CHIKV strains seen in 2010 in Myanmar also belonged to the same clade of ECSA genotype. However, the E1:A226V mutation in these strains (*7*) was not present in the 2019 CHIKV strains. Both E1:A226V mutant and nonmutant strains were isolated in Thailand during 2019 (*2*). Furthermore, the CHIKV strains in this study had the E1: K211E mutation with an E1:226A background. A previous study reported that CHIKV strains with the E1:K211E mutation with an E1:226A background increased virus infectivity and transmission compared with nonmutant parenteral E1:226A CHIKV virus (*15*). Our study highlights the need to strengthen infection prevention control measure activities and blood donor screening during CHIK outbreaks.

About the Author

Dr. Kyaw is a research scientist in the Virology Research Division, Department of Medical Research, Pyin Oo Lwin, Myanmar. His primary research interest is arboviral infectious diseases, including dengue, Japanese encephalitis, chikungunya, and Zika fever.

References

1. Powers AM, Brault AC, Tesh RB, Weaver SC. Re-emergence of chikungunya and o'nyong-nyong viruses: evidence for distinct geographical lineages and distant evolutionary relationships. J Gen Virol. 2000;81:471–9. https://doi.org/10.1099/0022-1317-81-2-471
2. Intayot P, Phumee A, Boonserm R, Sor-Suwan S, Buathong R, Wacharapluesadee S, et al. Genetic characterization of chikungunya virus in field-caught *Aedes aegypti* mosquitoes collected during the recent outbreaks in 2019, Thailand. Pathogens. 2019;8:E121. https://doi.org/10.3390/pathogens8030121

3. Agarwal A, Gupta S, Yadav AK, Nema RK, Ansari K, Biswas D. Molecular and phylogenetic analysis of chikungunya virus in central India during 2016 and 2017 outbreaks reveal high similarity with recent New Delhi and Bangladesh strains. Infect Genet Evol. 2019;75:103940. https://doi.org/10.1016/j.meegid.2019.103940

4. Kularatne SA, Gihan MC, Weerasinghe SC, Gunasena S. Concurrent outbreaks of chikungunya and dengue fever in Kandy, Sri Lanka, 2006–07: a comparative analysis of clinical and laboratory features. Postgrad Med J. 2009;85:342–6. https://doi.org/10.1136/pgmj.2007.066746

5. Pulmanausahakul R, Roytrakul S, Auewarakul P, Smith DR. Chikungunya in Southeast Asia: understanding the emergence and finding solutions. Int J Infect Dis. 2011;15:e671–6. https://doi.org/10.1016/j.ijid.2011.06.002

6. Thaung U, Ming CK, Thein M. Dengue haemorrhagic fever in Burma. Southeast Asian J Trop Med Public Health. 1975;6:580–91.

7. Tun MM, Thant KZ, Inoue S, Nabeshima T, Aoki K, Kyaw AK, et al. Detection of east/central/south African genotype of chikungunya virus in Myanmar, 2010. Emerg Infect Dis. 2014;20:1378–81. https://doi.org/10.3201/eid2008.131431

8. Rampal SM, Sharda M, Meena H. Neurological complications in chikungunya fever. J Assoc Physicians India. 2007;55:765–9.

9. Sharp TM, Roth NM, Torres J, Ryff KR, Pérez Rodríguez NM, Mercado C, et al.; Centers for Disease Control and Prevention (CDC). Chikungunya cases identified through passive surveillance and household investigations—Puerto Rico, May 5–August 12, 2014. MMWR Morb Mortal Wkly Rep. 2014;63:1121–8.

10. Guindon S, Dufayard JF, Lefort V, Anisimova M, Hordijk W, Gascuel O. New algorithms and methods to estimate maximum-likelihood phylogenies: assessing the performance of PhyML 3.0. Syst Biol. 2010;59:307–21. https://doi.org/10.1093/sysbio/syq010

11. Wimalasiri-Yapa BM, Stassen L, Huang X, Hafner LM, Hu W, Devine GJ, et al. Chikungunya virus in Asia–Pacific: a systematic review. Emerg Microbes Infect. 2019;8:70–9. https://doi.org/10.1080/22221751.2018.1559708

12. Simmons G, Brès V, Lu K, Liss NM, Brambilla DJ, Ryff KR, et al. High incidence of chikungunya virus and frequency of viremic blood donations during epidemic, Puerto Rico, USA, 2014. Emerg Infect Dis. 2016;22:1221–8. https://doi.org/10.3201/eid2207.160116

13. Chusri S, Siripaitoon P, Silpapojakul K, Hortiwakul T, Charernmak B, Chinnawirotpisan P, et al. Kinetics of chikungunya infections during an outbreak in southern Thailand, 2008–2009. Am J Trop Med Hyg. 2014;90:410–7. https://doi.org/10.4269/ajtmh.12-0681

14. World Health Organization. Guidelines on assessing donor suitability for blood donation. Geneva: The Organization; 2012.

15. Agarwal A, Sharma AK, Sukumaran D, Parida M, Dash PK. Two novel epistatic mutations (E1:K211E and E2:V264A) in structural proteins of chikungunya virus enhance fitness in *Aedes aegypti*. Virology. 2016;497:59–68. https://doi.org/10.1016/j.virol.2016.06.025

Address for correspondence: Mya Myat Ngwe Tun or Kouichi Morita, Department of Virology, Institute of Tropical Medicine, Nagasaki University, 1-12-4 Sakamoto, Nagasaki City, 852-8523, Japan; email: myamyat@tm.nagasaki-u.ac.jp or moritak@nagasaki-u.ac.jp

KPC-3–Producing *Serratia marcescens* Outbreak between Acute and Long-Term Care Facilities, Florida, USA

Adriana Jimenez, Lilian M. Abbo, Octavio Martinez, Bhavarth Shukla,
Kathleen Sposato, Alina Iovleva, Erin Louise Fowler, Christi Lee McElheny, Yohei Doi

We describe an outbreak caused by *Serratia marcescens* carrying bla_{KPC-3} that was sourced to a long-term care facility in Florida, USA. Whole-genome sequencing and plasmid profiling showed involvement of 3 clonal lineages of *S. marcescens* and 2 bla_{KPC-3}-carrying plasmids. Determining the resistance mechanism is critical for timely implementation of infection control measures.

Serratia marcescens has been linked to healthcare-associated outbreaks, particularly after use of colistin, which is intrinsically resistant to polymyxins (*1,2*). Outbreaks of carbapenemase-producing *Enterobacteriaceae* (CPE) in long-term care facilities (LTCF) have been well described (*3,4*); outbreaks of the closely related carbapenemase-producing (CP)–*S. marcescens* are unusual. We describe an outbreak in 2 hospitals in Florida, USA, of *S. marcescens* producing *Klebsiella pneumoniae* carbapenemase (KPC). Subsequent investigation identified a local LTCF as the source.

The Study

In June 2018, a 382-bed hospital that is part of a large hospital health system network in Miami, Florida, identified an increase of CP–*S. marcescens*. A retrospective search for more cases included all patients admitted to any facility in the 4-hospital network during October 2017–June 2018 using the automatic

Author affiliations: Jackson Health System, Miami, Florida, USA (A. Jimenez, L. M. Abbo, K. Sposato); Florida International University Robert Stempel College of Public Health and Social Work, Miami (A. Jimenez); University of Miami Miller School of Medicine, Miami (L. M. Abbo, O. Martinez, B. Shukla); University of Pittsburgh School of Medicine, Pittsburgh, Pennsylvania, USA (A. Iovleva, E. L. Fowler, C. L. McElheny, Y. Doi)

surveillance system (VigiLanz; VigiLanz Corporation, https://vigilanzcorp.com) with interface to the electronic medical record (EMR).

We defined cases as patients with carbapenem-resistant *S. marcescens* by Clinical and Laboratory Standards Institute (CLSI) breakpoints (*5*) isolated from any source, including clinical or surveillance cultures, during October 2017–December 2018. Based on Centers for Disease Control and Prevention guidelines, community-onset events (CO) were those cases identified <3 days after hospital admission; hospital-onset (HO) were those for which the specimens were collected >4 days after hospital admission (*6*).

In response to the outbreak, and in addition to interventions in place to prevent hospital-acquired infections (Appendix Table 1, https://wwwnc.cdc.gov/EID/article/26/11/20-2203-App1.pdf), all possible cases were prospectively identified upon admission to any of the network facilities via automatic surveillance system. Transfer forms and regular communication with the local Department of Health (DOH) notified hospitals when a known case-patient was transferred from the LTCF. All patients admitted from the source LTCF were placed in contact precautions at admission and screened for CPE. If positive, patients were placed in enhanced contact precautions (Appendix Table 1) for the duration of their stay. Miami-Dade DOH provided infection prevention and control education and support to the LTCF.

We performed matrix-assisted laser desorption/ionization time-of-flight (MALDI-TOF) mass spectrometry (bioMérieux, https://www.biomerieux-diagnostics.com) and Biofire BCID panel (bioMérieux) for bacterial identification. We conducted susceptibility testing using Vitek2 (bioMérieux) following CLSI guidelines. We tested carbapenemase production with CarbaNP test (Hardy Diagnostics,

Table 1. Characteristics of patients with KPC-3–producing *Serratia marcescens* infection, Miami, Florida, USA*

Characteristic	Value, N = 14
Sex	
M	5 (35)
F	9 (65)
Median age	63 (22–89)
Median total length of stay, d	23 (3–74)
Hospital onset	5 (36)
Community onset	9 (64)
Median length of stay to positive culture, d	9 (0–73)
Hemodialysis dependent	7 (50)
Ventilator dependent (tracheostomy)	14 (100)
PEG tube	14 (100)
Positive clinical culture source	
Respiratory tract	13 (93)
Blood	3 (21)
Clinical infection	10 (71)
Pneumonia	9 (90)
Bloodstream infection	4 (40)
Colonized	4 (29)
Other MDR-GNR isolated	
Carbapenem-resistant *Pseudomonas aeruginosa*	11 (79)
KPC-producing *Klebsiella pneumoniae*	1 (7)
Carbapenem-resistant *Acinetobacter baumannii*	2 (14)
Concurrent condition	
Diabetes	5 (36)
Congestive heart failure	3 (21)
Myocardial infarction	1 (7)
ESRD	7 (50)
Dementia	1 (21)
COPD	2 (14)
CVA	8 (57)
Chronic respiratory failure	7 (50)
Hypertension	9 (64)
Discharged disposition	
Died	3 (21)
Home with home-healthcare	2 (14)
Back to source LTCF	6 (43)
Other LTCF	3 (21)

*Values are no. (%) except as indicated. COPD, chronic obstructive pulmonary disease; CVA, cerebrovascular accident; ESRD, end-stage renal disease; KPC, *Klebsiella pneumoniae* carbapenemase; LTCF, long-term care facility; MDR-GNR, multidrug resistant gram-negative rods; PEG, percutaneous endoscopic gastrostomy.

https://hardydiagnostics.com). We processed active surveillance testing (AST) using a 10 µg meropenem disk on MacConkey plate after broth enrichment; possible CPE colonies were identified and tested for carbapenemase production.

We subjected 1 isolate per patient to whole-genome sequencing on NextSeq500 (Illumina, https://www.illumina.com). We assembled sequences by SPAdes version 3.13 (https://github.com/ablab/spades) and annotated them by prokka version 1.14 (https://github.com/tseemann/prokka). Snippy version 4.4.0 (https://github.com/tseemann/snippy) was used to identify SNPs. We used ResFinder 3.2 (https://cge.cbs.dtu.dk/services/ResFinder) and PlasmidFinder 2.0 (https://cge.cbs.dtu.dk/services/PlasmidFinder) to identify antimicrobial resistance genes and plas-

mid replicons. We generated a SNP phylogenetic tree with RAxMLversion 8.2.11 (https://github.com/stamatak/standard-RAxML) and visualized it using Interactive Tree of Life (iTOL) version 5 (https://itol.embl.de) (*7*). We sequenced isolates 505 and 514 using the MinION platform (Oxford Science Park, UK, https://nanoporetech.com/products/minion) to define the bla_{KPC}-harboring plasmids. We used Unicycler version 0.4.8-β (https://github.com/rrwick/Unicycler) for hybrid assembly of Illumina and MinION reads; we confirmed the presence of identified plasmids by aligning Illumina reads to the identified plasmid sequences.

We purified plasmids by alkaline-lysis method and used them to transform *Escherichia coli* TOP10 by electroporation (*8*). We selected transformants harboring bla_{KPC-3} on lysogenic agar with ampicillin, and confirmed acquisition of plasmids by PCR. The plasmids were extracted from the *E. coli* transformants, digested (*Eco*RI or *Hin*dIII), and run on 0.7% gel to obtain restriction patterns.

During October 2017–December 2018, a total of 14 patients with CP–*S. marcescens* were identified in our hospitals (Figure 1); all patients resided at a neighboring LTCF (Table 1). Five cases (36%) were HO, but 4 were detected ≤15 days after admission and did not coincide in location or time with the other cases. Transmission within the hospital was not suspected; those patients were possibly colonized at admission but undetected due to low sensitivity of AST protocols. The fifth patient had long length-of-stay and previous bloodstream infection (BSI) with KPC-producing *Klebsiella pneumoniae*.

Ten patients had ≥1 rectal AST; all were negative. Twelve patients had ≥1 tracheal aspirate AST; 2 were positive for CP–*S. marcescens* (suceptibilities in Table 2; Appendix Table 2). Ten cases had clinical infections by CP–*S. marcescens* including pneumonia (n = 9) and bloodstream infection (n = 4). Most cases were treated empirically with piperacillin/tazobactam, cefepime, and vancomycin. Targeted treatments included ceftazidime/avibactam. Four cases were colonized without signs or symptoms of CP-*S. marcescens* infection during hospital admission. Three patients died (21% in-hospital mortality); these deaths were not associated with infection by CP-*S.marcescens*.

During June 2018–January 2019, the 67 notifications of admissions from the source LTCF were related to 30 individual patients. In 7 cases (23%), CP–*S. marcescens* was present at admission.

We performed molecular testing on 12 isolates, 1 per patient. Core genome analysis demonstrated the presence of 3 clonal lineages of bla_{KPC-3}-carrying
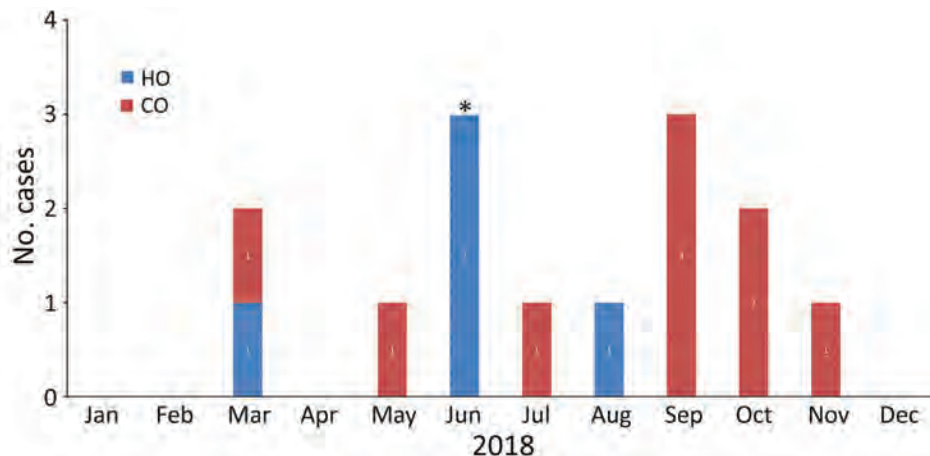
Figure 1. Epidemic curve of carbapenemase-producing *Serratia marcescens* infections by month in 2 hospitals of a large healthcare system in Miami, Florida, USA, 2018. Asterisk (*) indicates the implementation of new interventions in response to the outbreak. CO, community-onset; HO, hospital-onset.

S. marcescens involving >1 patient, and 1 outlier (Figure 2). Eleven isolates belonging to the 3 lineages shared a 43-kb FII-type bla_{KPC-3}-harboring plasmid, which had >99% sequence identity with pKPC_Kp46 plasmid previously described in *K. pneumoniae* (GenBank accession no. KX348146.1) (*9*); confirmation was by an identical plasmid restriction profile. Lineage 1 isolates shared a 19-kb ColRNAI-type bla_{KPC-3}-harboring plasmid, 99% identical to previously reported pNJST258C2 from *K. pneumoniae* (GenBank accession no. CP006919.1), except for the absence of the transposable element containing aminoglycoside resistance genes *aacA1* and *aacA4* (*10*). The outlying isolate, 520, only contained a pNJST258C2-like bla_{KPC-3}-harboring plasmid identical to that found in lineage 1. The bla_{KPC-3} sequence was identical between the 2 plasmids and was located on *Tn4401b*-like elements, which were identical except for a 70-bp deletion in *tnpA* leading to frameshift and premature stop in the pNJST258C2-like plasmid. This deletion did not seem to affect KPC expression; isolate 520, carrying only the pNJST258C2-like plasmid, was still resistant to carbapenems. In addition to bla_{KPC-3}, the pKPC_Kp46–like plasmid contained bla_{TEM-1}, Δbla_{OXA-9}, and *qnrB19*. The pNJST258C2-like plasmid did not contain additional antimicrobial resistance genes; however, it contained an operon encoding production of colicin, an antimicrobial substance that is lethal against related strains that lack it (*11*). Isolate 520 was from the patient with a history of KPC-producing *K. pneumoniae*, suggesting that the bla_{KPC-3}-harboring plasmid was transferred to *S. marcescens* in the patient in a separate event from the infection of the other 11 cases.

Conclusions

Use of an automatic surveillance system enabled retrospective and prospective detection of cases and identification of their common exposure in an LTCF on the basis of shared address. Prospective identification of residents of the source LTCF enabled screening at point of entry and implementation of interventions to prevent hospital transmission. Direct communication between the infection control department and the LTCF was difficult and relied upon the local DOH to share information about known cases. Unfortunately, a regional registry of patients with CPE is not available in Florida (*12,13*).

The pKPC-KP4–like plasmid shared among the 3 clonal lineages involved in the outbreak, and the pNJST258C2-like plasmid, shared between lineage 1 and the outlier isolate, were the vehicles of bla_{KPC-3} in this polyclonal outbreak. However, it is unclear why lineage 1 isolates contained both bla_{KPC-3}-harboring plasmids. It is possible that in addition to antimicrobial resistance, factors such as colicin production facilitated dissemination within the LTCF.

Table 2. Susceptibility profiles of KPC-producing *Serratia marcescens* isolates, Miami, Florida, USA*

Drug	Total no. isolates tested	No. (%) susceptible	No. (%) intermediate	No. (%) resistant
ATM	14	0	0	14 (100)
CFZ	14	0	0	14 (100)
FEP	14	0	0	14 (100)
CAZ	14	0	0	14 (100)
CRO	14	0	0	14 (100)
LVX	14	5 (36)	1 (7)	8 (57)
MEM	14	0	0	14 (100)
AMK	14	14 (100)	0	0
GEN	14	0	13 (93)	1 (7)
TOB	14	0	0	14 (100)
SXT	14	14 (100)	0	0
TET	14	2 (14)	8 (57)	4 (28)
TGC	12	12 (100)	0	0
CZA	3	3 (100)	0	0

*AMK, amikacin; ATM, aztreonam; CAZ, ceftazidime; CFZ, cefazolin; CRO, ceftriaxone; CZA, ceftazidime/avibactam; FEP, cefepime; GEN, gentamicin; LVX, levofloxacin; MEM, meropenem; SXT, trimethoprim/sulfamethoxazole; TET, tetracycline; TGC, tigecycline; TOB, tobramycin.
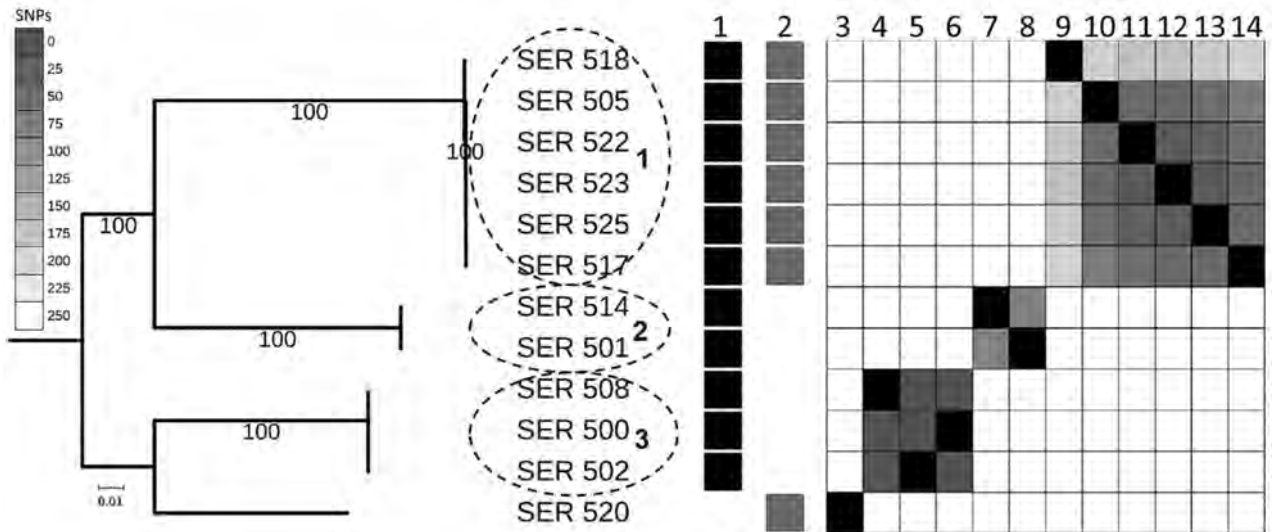
Figure 2. Core-genome SNP phylogeny of 12 *Serratia marcescens* isolates involved in outbreak in Miami, Florida, USA, 2018, depicted with KPC plasmid presence/absence matrix. Dotted circles indicate 3 major lineages involved in the outbreak. Nodes supported by bootstrap values of 100 are shown. A heat map of core genome SNP differences between strains involved in the outbreak shows genome similarity as measured by SNP distance; dark gray indicates higher similarity and lighter gray lower similarity. 1, pKP46-like; 2, pnJST258C2-like; 3, SER_520; 4, SER_508; 5, SER_502; 6, SER_500; 7, SER_514; 8, SER_501; 9, SER_518; 10, SER_505; 11, SER_522; 12, SER_523; 13, SER_525; 14, SER_517. Scale bar indicates number of differences between sequences. KPC, *Klebsiella pneumoniae* carbapenemase; SNP, single-nucleotide polymorphisms.

In summary, our investigation of this CP–*S. marcescens* outbreak in 2 hospitals in Florida identified a local LTCF as the source. Early identification, communication, and implementation of preventive measures within healthcare facilities and cooperation with local public health authorities are pivotal in preventing transmission of multidrug-resistant organisms among vulnerable populations.

About the Author

Ms. Jimenez is an infection preventionist at Jackson Health System in Miami, Florida, and a doctoral candidate at Robert Stempel School of Social Work and Public Health, Epidemiology Department of Florida International University in Miami, Florida. Her primary research interest is the epidemiology of multidrug-resistant bacilli and the prevention of hospital-acquired infections.

References

1. Weinstein RA, Gaynes R, Edwards JR, Edwards JR; National Nosocomial Infections Surveillance System. Overview of nosocomial infections caused by gram-negative bacilli. Clin Infect Dis. 2005;41:848–54. https://doi.org/10.1086/432803
2. Merkier AK, Rodríguez MC, Togneri A, Brengi S, Osuna C, Pichel M, et al.; Serratia marcescens Argentinean Collaborative Group. Outbreak of a cluster with epidemic behavior due to *Serratia marcescens* after colistin administration in a hospital setting. J Clin Microbiol. 2013;51:2295–302. https://doi.org/10.1128/JCM.03280-12
3. Legeay C, Hue R, Berton C, Cormier H, Chenouard R, Corvec S, et al. Control strategy for carbapenemase-producing Enterobacteriaceae in nursing homes: perspectives inspired from three outbreaks. J Hosp Infect. 2019;101:183–7. https://doi.org/10.1016/j.jhin.2018.10.020
4. Kelly AM, Mathema B, Larson EL. Carbapenem-resistant Enterobacteriaceae in the community: a scoping review. Int J Antimicrob Agents. 2017;50:127–34. https://doi.org/10.1016/j.ijantimicag.2017.03.012
5. Clinical and Laboratory Standards Institute. Performance standards for antimicrobial susceptibility testing, 28th edition (supplement M100). Wayne (PA): The Institute; 2018.
6. Centers for Disease Control and Prevention. National Healthcare Safety Network (NHSN) patient safety component manual. 2018 January [cited 2020 Sep 28]. https://www.cdc.gov/nhsn/pdfs/validation/2018/pcsmanual_2018-508.pdf
7. Letunic I, Bork P. Interactive Tree of Life (iTOL) v4: recent updates and new developments. Nucleic Acids Res. 2019;47(W1):W256–9. https://doi.org/10.1093/nar/gkz239
8. Sidjabat HE, Paterson DL, Qureshi ZA, Adams-Haduch JM, O'Keefe A, Pascual A, et al. Clinical features and molecular epidemiology of CMY-type β-lactamase–producing *Escherichia coli*. Clin Infect Dis. 2009;48:739–44. https://doi.org/10.1086/597037
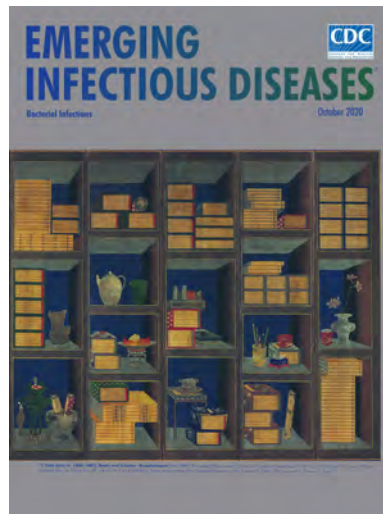
9. Kim JO, Song SA, Yoon EJ, Shin JH, Lee H, Jeong SH, et al. Outbreak of KPC-2-producing Enterobacteriaceae caused by clonal dissemination of *Klebsiella pneumoniae* ST307 carrying an IncX3-type plasmid harboring a truncated Tn*4401a*. Diagn Microbiol Infect Dis. 2017;87:343–8. https://doi.org/10.1016/j.diagmicrobio.2016.12.012

10. Deleo FR, Chen L, Porcella SF, Martens CA, Kobayashi SD, Porter AR, et al. Molecular dissection of the evolution of carbapenem-resistant multilocus sequence type 258 *Klebsiella pneumoniae.* Proc Natl Acad Sci U S A. 2014;111:4988–93. https://doi.org/10.1073/pnas.1321364111

11. Cascales E, Buchanan SK, Duché D, Kleanthous C, Lloubès R, Postle K, et al. Colicin biology. Microbiol Mol Biol Rev. 2007;71:158–229. https://doi.org/10.1128/MMBR.00036-06

12. Clarivet B, Pantel A, Morvan M, Jean Pierre H, Parer S, Jumas-Bilak E, et al. Carbapenemase-producing Enterobacteriaceae: use of a dynamic registry of cases and contacts for outbreak management. J Hosp Infect. 2016;92:73–7. https://doi.org/10.1016/j.jhin.2015.07.007

13. Lee BY, Bartsch SM, Hayden MK, Welling J, DePasse JV, Kemble SK, et al. How introducing a registry with automated alerts for carbapenem-resistant Enterobacteriaceae (CRE) may help control CRE spread in a region. Clin Infect Dis. 2020;70:843–9.

Address for correspondence: Adriana Jimenez, Department of Infection Prevention and Control, Jackson Health System, 1611 NW 12th Ave, Park Plaza West L-301, Miami, FL 33136, USA; email: adriana.jimenez@jhsmiami.org

October 2020
Bacterial Infections

EMERGING INFECTIOUS DISEASES®

To revisit the October 2020 issue, go to:
https://wwwnc.cdc.gov/eid/articles/issue/26/10/table-of-contents

Isolation Cocoon, May 2020

After Zhuangzi's Butterfly Dream

Ron Louie

Spinning, what you will, in heeding that swarm of guidance, creating
your own shell, then transforming, as you will, within that isolation,
still seems like an almost unconvincing, almost unnecessary nuisance.

You had chosen this situation, if it is fair to say there was a choice,
when there was no viable alternative. Your cocoon can feel so safe,
an illusion perhaps, but reality provides nothing less vulnerable.

The walls are thin enough to allow you to breathe, and to vaguely hear
or feel vibrations, even though their meaning cannot be known.
Light penetrates, and darkness, too; the changes remain obscure.

Ruminating on that former lifestyle, you can digest time thoroughly,
like those last memorable green leaves of Springtime, then so succulent,
and satisfying, but to what end you know not; not all cocoons survive.

Time, space, being, identity, the interpreted past, the fancied future
can all be consumed within your insatiable capsule. Chrysalis or cocoon,
distinctions no longer matter; each benefits from a covering and distancing.

Complacency or contentment allows a concentration on one's only
certainty, the presentness right now, in this cell-like confinement,
because emergence would require several just preposterous miracles.

About the Author

Dr. Louie is a clinical professor in Pediatrics (Hematology–Oncology) at the University of Washington, Seattle. His professional interests include clinical trials, dementia care, and writing the blog AlzheimerGadfly.net.

Address for correspondence: Ron Louie, Pediatric Hematology–Oncology, Mary Bridge Children's Health Center, MB-1, 311 S "L" St, Tacoma, WA 98405, USA; email: ronlouie@uw.edu

Author affiliations: University of Washington, Seattle, Washington, USA; Mary Bridge Children's Hospital and Health Center, Tacoma, Washington, USA

Abrupt Subsidence of Seasonal Influenza after COVID-19 Outbreak, Hong Kong, China

Ngai-Sze Wong, Chi-Chiu Leung, Shui-Shan Lee

Author affiliations: The Chinese University of Hong Kong, Hong Kong, China (N.-S. Wong, S.-S. Lee); Hong Kong Tuberculosis, Chest and Heart Diseases Association, Hong Kong (C.-C. Leung)

The onset of the 2019–20 winter influenza season in Hong Kong coincided with the emergence of the coronavirus disease epidemic in neighboring mainland China. After widespread adoption of large-scale social distancing interventions in response to the impending coronavirus disease outbreak, the influenza season ended abruptly with a decrease to a low trough.

Seasonality is a distinctive feature of influenza epidemics, the pattern of which is shaped by host, virus, and environmental factors (1). An influenza season typically lasts for an average of 13 weeks (https://www.cdc.gov/flu/pastseasons/1112season.htm) in the United States, and seasons might range from 6.5 to 21.4 weeks, as reported in a study in Europe (2). Seasonal influenza in Hong Kong, China, which is located in the Northern Hemisphere, is characterized by dual peaks: a winter peak frequently occurring within the first 2 months of the year, followed by a less prominent summer peak in August or September of the same year. Toward the end of December 2019, emergence of severe acute respiratory syndrome coronavirus 2 (SARS-CoV-2) was reported in Wuhan (3), the timing of which coincided with the onset of the 2019–20 winter influenza season in Hong Kong.

Using surveillance data accessed from the Hong Kong Government Centre for Health Protection (https://www.chp.gov.hk/en/resources/29/304.html), we assessed the epidemic pattern of the concurrent winter influenza season and explored its temporal relationship with prevailing interventions. We found that the 2019–20 winter season had its onset in late November, reaching its peak 7 weeks later, and decreasing precipitously to a trough after 1 month (Figure).

Compared with the winter seasons in the preceding 6 years, the 2019–20 winter season was shorter (13 weeks vs. median 22 weeks, interquartile range [IQR] 14–25 weeks), had a relatively small peak (18.8% vs. median 26.5%, IQR 18.8%–31.4%), and decreased to a much lower postseason trough on its subsidence (0.4% vs median 4.3%, IQR 0.8%–5.5%) (Table). The decrease was abrupt and had a peak-to-trough median interval of 6 weeks versus 14 weeks (IQR 6–17 weeks). The median weekly number of respiratory specimens tested during the 2019–20 winter season was also higher (5,711 vs. 4,104, IQR 3,640–5,711).

This pattern contrasted with that for the United States, in which increased influenza-like illness activity was first noted in November 2019 (4). Influenza activity remained increased for >4 months, through March 2020, without any sign of abrupt subsidence in the United States. Influenza A(H1N1)pdm09 was the dominant virus for the 2019–20 season in Hong Kong (https://www.chp.gov.hk/files/pdf/fluexpress_week2_16_1_2020_eng.pdf) and the United States (4). However, the second most common virus was H3N2 subtype virus in Hong Kong but influenza B/Victoria virus in United States.

To explain the unique epidemic pattern of the 2019–20 winter influenza season, we matched the epidemic curve with the corresponding milestones related to the emergence of SARS-CoV-2 in Hong Kong (Figure). From the last week of January 2020 (influenza surveillance calendar week 4), the government had implemented school closure and mandated work-from-home arrangements for civil servants immediately after the Lunar New Year Holiday. This implementation was followed by closure of most borders with mainland China during the first week of February 2020. The effect was dramatic because vacating of workplaces affected not only the government staff force of 170,000 but also employees of statutory bodies, nongovernment organizations, and major businesses. Universities, secondary and primary schools, and kindergartens were closed and were not expected to reopen by late April. Mass gatherings, including the Lunar New Year celebration, and sports events were cancelled; church services had largely ceased; and the overcrowded public transportation system had eased substantially. Another common sight was mass masking, which has occurred as an adopted precaution voluntarily by most local citizens as a result of panic and as advocated by the medical profession (5). The phenomenon might have played a supplemental role in reducing the opportunity of virus exposure, although its precise effect has yet to be confirmed.

The early plateauing and abrupt decrease of influenza activities toward the end of January 2020 was temporally correlated with the extended social
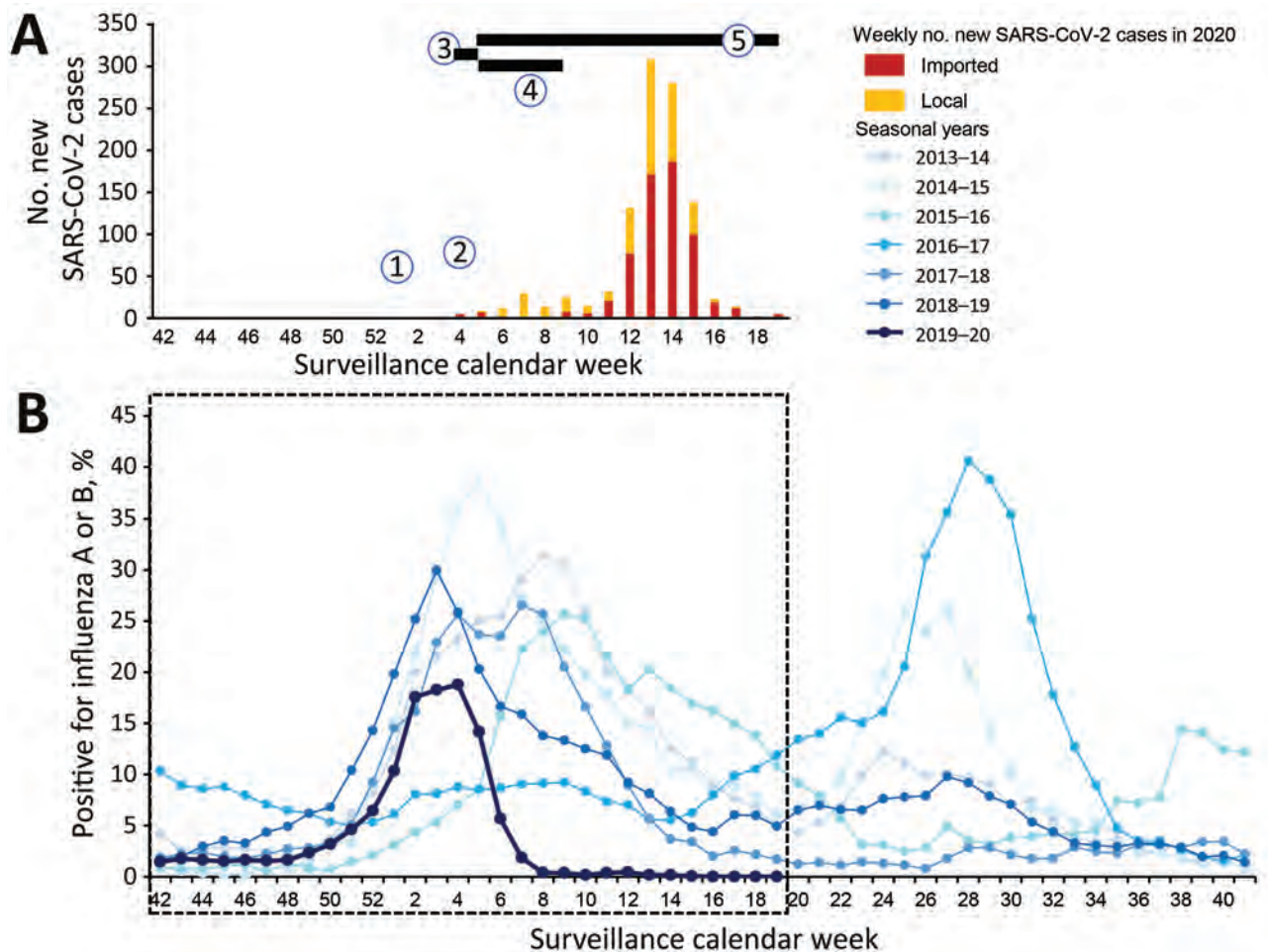
Figure. Epidemic curve showing number of reported SARS-CoV-2 cases (A) in Hong Kong, China, and abrupt subsidence during the corresponding 2019–20 winter influenza season (B) compared with 6 preceding years between 2013 and 2019, as derived from the percentage of respiratory specimens tested that were positive for influenza A or B viruses. Onset of winter influenza season is defined as the first week that had an increase in percentage of respiratory samples tested that were positive for influenza A or B viruses, followed by a consecutive increase for ≥4 weeks. End of the season is defined as the last week that had a decrease of the same percentage, followed by a consecutive decrease for ≥2 weeks, compared with the previous week. SARS-CoV-2 timelines: 1, on December 30, 2019, the Wuhan Municipal Health Committee issued an urgent notice on treatment for pneumonia of unknown cause; 2, on January 25, 2020, the World Health Organization declared a Public Health Emergency of International Concern; 3, during January 25–28, 2020, the Lunar New Year public holiday occurred; 4, during January 29–March 1, 2020, civil servants made special work arrangements; 5, during January 29–May 26, 2020, schools were closed. SARS-CoV-2, severe acute respiratory syndrome coronavirus 2.

distancing effects of the government's SARS-CoV-2 mitigation strategy. Overall, the abrupt subsidence of influenza activities and suppressed postseason trough were unique characteristics of the 2019–20 influenza season, differing substantially from the continually high peak of the parallel season in the United States.

Table. Characteristics of winter influenza seasons, Hong Kong, China, 2013–14 through 2019–20*

Seasonal year	Onset week	Duration, weeks	Peak level, %	Postseason trough, %	Peak to trough, wk	Weekly no. tests, median (IQR)
2013–14	49	22	31.4	4.3	13	2,423 (2,191–2,588)
2014–15	49	21	38.6	6.1	15	3,640 (3,029–4,230)
2015–16	51	25	25.7	2.5	17	4,017 (3,292–4,537)
2016–17	52	14	9.2	5.5	6	4.104 (3,890–4,216)
2017–18	47	30	26.5	0.8	20	4,426 (4,100–6,335)
2018–19	47	23	29.9	4.4	14	6,073 (5,439–6,475)
2019–20	48	13	18.8	0.4	6	5,711 (5,327–6,318)

*IQR, interquartile range.

We acknowledge that our assessment could be limited by the application of retrospective and descriptive methods involving analyses of publicly available surveillance data. It is possible that the temporal relationship between the seasonal influenza pattern and social distancing strategy implementation had occurred coincidentally by chance because heterogeneity of influenza seasons is a well-known phenomenon. Previous research suggested that despite the marked fluctuations of peak amplitudes and peak times, epidemic duration is often conserved (2). However, occurrence of a deformed seasonal pattern in the setting of the outbreak of infection with SARS-CoV-2 served as a natural experiment for supporting the evaluation of the impacts of social distancing in mitigating influenza virus transmission (6,7).

Acknowledgment

We thank the Li Ka Shing Institute of Health Sciences, Hong Kong, for providing technical support during the study.

About the Author

Dr. Wong is a research assistant professor at the Stanley Ho Centre for Emerging Infectious Diseases, the Chinese University of Hong Kong, Hong Kong, China. Her primary research interests are epidemiology, HIV/AIDS, and spatial–temporal analyses.

References

1. Moorthy M, Castronovo D, Abraham A, Bhattacharyya S, Gradus S, Gorski J, et al. Deviations in influenza seasonality: odd coincidence or obscure consequence? Clin Microbiol Infect. 2012;18:955–62. https://doi.org/10.1111/j.1469-0691.2012.03959.x
2. Domenech de Cellès M, Arduin H, Varon E, Souty C, Boëlle PY Lévy-Bruhl D, et al. Characterizing and comparing the seasonality of influenza-like illnesses and invasive pneumococcal diseases using seasonal waveforms. Am J Epidemiol. 2018;187:1029–39. https://doi.org/10.1093/aje/kwx336
3. Hui DS, I Azhar E, Madani TA, Ntoumi F, Kock R, Dar O, et al. The continuing 2019-nCoV epidemic threat of novel coronaviruses to global health: the latest 2019 novel coronavirus outbreak in Wuhan, China. Int J Infect Dis. 2020;9 1:264–6. https://doi.org/10.1016/j.ijid.2020.01.009
4. Dawood FS, Chung JR, Kim SS, Zimmerman RK, Nowalk MP, Jackson ML, et al. Interim estimates of 2019–20 seasonal influenza vaccine effectiveness—United States, February 2020. MMWR Morb Mortal Wkly Rep. 2020;69:177–82. https://doi.org/10.15585/mmwr.mm6907a1
5. Ahmed F, Zviedrite N, Uzicanin A. Effectiveness of workplace social distancing measures in reducing influenza transmission: a systematic review. BMC Public Health. 2018;18:518. https://doi.org/10.1186/s12889-018-5446-1
6. Fong MW, Gao H, Wong JY, Xiao J, Shiu EY, Ryu S, et al. Nonpharmaceutical measures for pandemic influenza in nonhealthcare settings—social distancing measures. Emerg Infect Dis. 2020;26:976–84. https://doi.org/10.3201/eid2605.190995
7. Leung CC, Lam TH, Cheng KK. Mass masking in the COVID-19 epidemic: people need guidance. Lancet. 2020;395:945. https://doi.org/10.1016/S0140-6736(20)30520-1

Address for correspondence: Shui-Shan Lee, Stanley Ho Centre for Emerging Infectious Diseases, The Chinese University of Hong Kong, 2/F Postgraduate Education Centre, Prince of Wales Hospital, 32 Ngan Shing St, Shatin, Hong Kong, China; email: sslee@cuhk.edu.hk

Three Patients with COVID-19 and Pulmonary Tuberculosis, Wuhan, China, January–February 2020

Zhi Yao,[1] Junbo Chen,[1] Qianli Wang,[1] Weiyong Liu,[1] Qi Zhang,[1] Jing Nan, Hai Huang, Yuying Wu, Lan Li, Lu Liang, Lei You, Yingle Liu,[2] Hongjie Yu[2]

Author affiliations: Wuhan Pulmonary Hospital, Wuhan, China (Z. Yao, J. Nan, H. Huang, Y. Wu, L. Li); School of Public Health, Fudan University, Key Laboratory of Public Health Safety, Ministry of Education, Shanghai, China (J. Chen, Q. Wang, L. You, H. Yu); Tongji Hospital, Tongji Medical College, Huazhong University of Science and Technology, Wuhan (W. Liu); Wuhan University, State Key Laboratory of Virology, Wuhan (Q. Zhang, Y. Liu); Sichuan University, Chengdu, China (L. Liang)

During January–February 2020, coronavirus disease (COVID-19) and tuberculosis were diagnosed for 3 patients in Wuhan, China. All 3 patients had COVID-19 pneumonia. One severely ill patient died after acute respiratory distress syndrome developed. Clinicians and public health officials should be aware of underlying chronic infections such as tuberculosis in COVID-19 patients.

The leading cause of death from a single infectious agent is tuberculosis (TB) (1). Globally, an estimated 1.7 billion persons are infected with *Mycobacterium*

---

[1]These first authors contributed equally to this article.

[2]These senior authors contributed equally to this article.

tuberculosis (*2*), and a country with one of the highest TB burdens in the world is China (*2,3*). Co-infection with severe acute respiratory syndrome coronavirus (*4,5*) or Middle East respiratory syndrome coronavirus (*6*) and *M. tuberculosis* has been associated with intensive care unit admission. As severe acute respiratory syndrome coronavirus 2 (SARS-CoV-2) emerges, we report 2 patients with COVID-19 and laboratory-confirmed TB and 1 with COVID-19 and clinically diagnosed TB in China.

Patient 1 was a 50-year-old man who became ill with fever and productive cough on December 25, 2019. Pulmonary TB had been diagnosed for this patient 20 years ago, for which he received anti-TB treatment for 6 months (Table; Appendix Figure 1, https://wwwnc.cdc.gov/EID/article/26/11/20-1536-App1.pdf). At hospital admission, chest auscultation detected bilateral rhonchi and wet rales. While hospitalized, the patient experienced continuous fever, respiratory distress, and hypoxia. A computed tomography (CT) scan of his chest showed bilateral emphysema, bullous cysts, and right pleural effusion. The pleural effusion contained elevated concentrations of adenosine deaminase (ADA) and lactate dehydrogenase (LDH), and results of a Rivalta test for pleural effusion and *M. tuberculosis* DNA tests were positive. Sputum samples were positive for acid-fast bacilli (AFB) and for *M. tuberculosis* DNA and RNA. On January 28, 2020, a chest CT scan showed progression of bilateral patchy ground-glass opacities (Appendix Figure 2). The diagnosis was severe pneumonia, laboratory-confirmed active pulmonary TB, anemia, and hypoproteinemia. The patient received anti-TB and corticosteroid treatments and oxygen therapy. The patient's dyspnea gradually deteriorated; subsequently, acute respiratory distress syndrome developed. On January 29, he died of respiratory and circulatory failure; a throat swab sample taken that day was positive for SARS-CoV-2 RNA.

Patient 2 was a 44-year-old man who became ill with fever, fatigue, headache, and dry cough on January 16. Chest CT scan showed bilateral patchy ground-glass opacities and pleural effusion (Appendix Figure 3). On February 14, a chest CT scan showed signs of cavitation, which according to the patient's medical records were new, and a throat swab sample tested positive for SARS-CoV-2 RNA. At admission, the patient had tachycardia. A TB purified protein derivative skin test showed an induration of 7 × 10 mm. Rivalta test was positive for pleural effusion, which contained elevated concentrations of C-reactive protein, LDH, and ADA (35.1 U/L) and was infiltrated with lymphocytes. Sputum and pleural effusion AFB smears were negative. The clinical diagnosis was active pulmonary TB, tuberculous pleuritis, and pleural effusion. While hospitalized, the patient received antiviral drugs and a fixed-dose combination of isoniazid, rifampicin, pyrazinamide and ethambutol. After admission, the patient was found to have type 2 diabetes mellitus, for which acarbose and metformin were prescribed. His signs and symptoms improved after treatment, and he was discharged on March 3 with anti-TB treatment to be continued.

Patient 3 was a 57-year-old man with a 3-year history of diabetes mellitus who on January 16 became ill with cough. In 2001, pulmonary TB had been diagnosed and considered cured. On January 27, 2020, according to the patient's medical records, a chest CT scan showed signs of TB. On February 3, another CT scan showed bilateral patchy ground-glass opacities (Appendix Figure 4). On February 5, the patient was transferred to Wuhan Pulmonary Hospital, Wuhan, China, where a test for SARS-CoV-2 was positive. At admission, the patient had tachypnea and a peripheral capillary oxygen saturation of 90%. His sputum was positive for *M. tuberculosis* DNA. The diagnosis was severe COVID-19 pneumonia and latent pulmonary TB. While hospitalized, the patient received antibiotics, antiviral drugs, corticosteroids, and oxygen support. On February 7, a chest CT scan showed progression of the ground-glass opacities. Immunoglobulin was administered. Additional CT scans showed gradual improvement, and the patient was discharged on March 2.

All 3 patients with SARS-CoV-2 infection and pulmonary TB had COVID-19 pneumonia; illness was moderate for 1 patient and severe for the other 2. The patient in whom acute respiratory distress syndrome developed died of respiratory and circulatory failure.

In consideration of the high disease burden of TB and the rapid spread of COVID-19, the potential effects of a possible interaction between the 2 infections requires attention (*7*; P. Glaziou, unpub. data, https://www.medrxiv.org/content/10.1101/2020.04.28.20079582v1). As for general COVID-19 patients, the spectrum of disease for COVID-19 patients with TB can vary from moderate to severe respiratory illness and even death. Underlying conditions including chronic obstructive pulmonary disease, diabetes, hypertension, and malignancy have been associated with more severe outcomes in COVID-19 patients (*8*). However, in our study, the outcome for 1 of the 3 co-infected patients was severe despite his having no other known conditions thought to predispose him to severe COVID-19. Clinicians and public health officials should remain aware of heightened risks caused by chronic infections such as TB in COVID-19 patients.

Table. Clinical characteristics and laboratory results for 3 patients with COVID-19 and TB, Wuhan, China, January–February 2020*

Characteristics	Patient 1	Patient 2	Patient 3
Age, y	50	44	57
Smoker	+	+	−
Underlying medical conditions†	−	+	+
Signs and symptoms‡			
Fever	+	+	+
Cough	+	+	+
Fatigue	+	+	+
Wheeze	+	+	+
Chills	−	+	−
Weight loss	+	+	+
Night sweats	NA	+	−
Vomiting	−	−	−
Diarrhea	−	−	−
Tachycardia	−	+	−
Tachypnoea	+	−	+
Laboratory findings§			
Leukocyte count, × 10^9 cells/L (reference range 3.5–9.5 × 10^9 cells/L)	10.4 (↑)	6.86	8.86
Neutrophil count, ×10^9 cells/L (reference range 1.8–6.3 × 10^9 cells/L)	8.74 (↑)	4.35	7.74 (↑)
Lymphocyte count ×10^9 cells/L (reference range 1.1–3.2 × 10^9 cells/L)	0.73 (↓)	1.75	0.74 (↓)
T-cell count, cells/μL (reference range 690–2,540 cells/μL)	NA	1,092.92	282.12 (↓)
CD4+ T-cell percentage (reference range 40%–57%)	NA	25.3 (↓)	25.91 (↓)
CD4+ T-cell count, cells/μL (reference range 410–1,590 cells/μL)	NA	415.51	138.91 (↓)
CD8+ T-cell percentage (reference range 8%–37%)	NA	36.67	19.37
CD8+ T-cell count, cells/μL (reference range 190–1,140 cells/μL)	NA	602.14	103.8 (↓)
CD4+ to CD8+ T-cell count ratio (reference range 0.71–2.78)	NA	0.69 (↓)	1.34
Hemoglobin, g/L (reference range 130–175 g/L)	83 (↓)	127 (↓)	134
Platelet count, ×10^9/L (reference range 125–350 10^9/L)	430 (↑)	280	218
Activated partial thromboplastin time, s (reference range 27–45 s)	45.5 (↑)	36.4	30.8
Prothrombin time, s (reference range 11–16 s)	18.4 (↑)	13.3	16.29
International normalized ratio (reference range 0.8–1.3)	1.44 (↑)	1.03	1
Fibrinogen, g/dL (reference range 2–4 g/dL)	8.01 (↑)	4.5 (↑)	5.07 (↑)
D–dimer, μg/L (reference range 0–0.5 μg/L)	1.58 (↑)	3.7 (↑)	NA
Alanine aminotransferase, U/L (reference range 9–50 U/L)	9	12	52 (↑)
Aspartate aminotransferase, U/L (reference range 15–40 U/L)	3 (↓)	11 (↓)	45 (↑)
Albumin, g/L (reference range 35–55 g/L)	29.9 (↓)	36.7	35.6
Bilirubin, μmol/L (reference range 0–21 μmol/L)	2.56	5	4.15
Creatinine, μmol/L (reference range 44–115 μmol/L)	38 (↓)	NA	64
Lactate dehydrogenase, U/L (reference range 106–245 U/L)	170	NA	367 (↑)
Creatine kinase, U/L (reference range 24.0–194.0 U/L)	31	24.7	45.1
Creatine kinase isoenzyme, U/L (reference range 0–24 U/L)	9	12.6	22.6
Bicarbonate, mmol/L (reference range 22–27 mmol/L)	21.4	29.9 (↑)	29.8 (↑)
C-reactive protein, mg/L (reference range 0.0–5.0 mg/L)	293.8 (↑)	3.99	44.4 (↑)
Procalcitonin, ng/mL (reference range 0.00–0.25 ng/mL)	0.14	0.04	0.04
Erythrocyte sedimentation rate, mm/h (reference range 0–15 mm/h)	123 (↑)	81 (↑)	53 (↑)
Chest CT findings			
Ground-glass opacities	+	+	+
Pleural effusion	+	+	−
Treatment			
Antibiotics	+	+	+
Anti-TB therapy	+	+	−
Lopinavir/ritonavir	−	+	+
Umifenovir hydrochloride	−	+	−
Interferon–α	−	+	+
Corticosteroid	+	−	+
Immunoglobulin	−	−	+
Oxygen support	+	−	+
Duration of hospitalization, d	22	26	27
Time from illness onset to discharge or death, d	35	47	46
Clinical severity	Severe	Moderate	Severe
Outcome	Died	Survived	Survived

*All patients were male. COVID-19, coronavirus disease; CT, computed tomography; NA, not available; TB, tuberculosis; ↑, values higher than reference range; ↓, values lower than reference range.; +, positive; −, negative.
†Patients 2 and 3 had type 2 diabetes mellitus.
‡At admission to the original hospital.
§Test results after transfer to the Wuhan Pulmonary Hospital.

About the Author

Dr. Yao is a physician at the Wuhan Pulmonary Hospital, Wuhan, China. His research focuses on respiratory infections and critical care medicine.

References

1. World Health Organization. Global tuberculosis report 2019 [cited 2020 Jun 11]. https://www.who.int/tb/publications/global_report
2. Houben RM, Dodd PJ. The global burden of latent tuberculosis infection: a re-estimation using mathematical modelling. PLoS Med. 2016;13:e1002152. https://doi.org/10.1371/journal.pmed.1002152
3. Zhao Y, Xu S, Wang L, Chin DP, Wang S, Jiang G, et al. National survey of drug-resistant tuberculosis in China. N Engl J Med. 2012;366:2161–70. https://doi.org/10.1056/NEJMoa1108789
4. Low JG, Lee CC, Leo YS, Low JG, Lee CC, Leo YS. Severe acute respiratory syndrome and pulmonary tuberculosis. Clin Infect Dis. 2004;38:e123–5. https://doi.org/10.1086/421396
5. Liu W, Fontanet A, Zhang PH, Zhan L, Xin ZT, Tang F, et al. Pulmonary tuberculosis and SARS, China. Emerg Infect Dis. 2006;12:707–9. https://doi.org/10.3201/eid1204.050264
6. Alfaraj SH, Al-Tawfiq JA, Altuwaijri TA, Memish ZA. Middle East respiratory syndrome coronavirus and pulmonary tuberculosis coinfection: implications for infection control. Intervirology. 2017;60:53–5. https://doi.org/10.1159/000477908
7. World Health Organization. World Health Organization (WHO) information note: tuberculosis and COVID-19 [cited 2020 Jun 11]. https://www.who.int/docs/default-source/documents/tuberculosis/infonote-tb-covid-19.pdf
8. Guan WJ, Liang WH, Zhao Y, Liang HR, Chen ZS, Li YM, et al.; China Medical Treatment Expert Group for COVID-19. Comorbidity and its impact on 1590 patients with COVID-19 in China: a nationwide analysis. Eur Respir J. 2020;55:2000547. https://doi.org/10.1183/13993003.00547-2020

Address for correspondence: Hongjie Yu, School of Public Health, Fudan University, Key Laboratory of Public Health Safety, Ministry of Education, Shanghai, China; email: yhj@fudan.edu.cn; and Yingle Liu, State Key Laboratory of Virology, Modern Virology Research Center, College of Life Sciences, Wuhan University, Wuhan, China; email: mvlwu@whu.edu.cn

Detection of SARS-CoV-2 in Hemodialysis Effluent of Patient with COVID-19 Pneumonia, Japan

Ayako Okuhama, Masahiro Ishikane, Daisuke Katagiri, Kohei Kanda, Takato Nakamoto, Noriko Kinoshita, Naoto Nunose, Takashi Fukaya, Isao Kondo, Harutaka Katano, Tadaki Suzuki, Norio Ohmagari, Fumihiko Hinoshita

Author affiliations: National Center for Global Health and Medicine, Tokyo, Japan (A. Okuhama, M. Ishikane, D. Katagiri, K. Kanda, T. Nakamoto, N. Kinoshita, N. Nunose, T. Fukaya, I. Kondo, N. Ohmagari, F. Hinoshita); National Institute of Infectious Diseases, Tokyo (H. Katano, T. Suzuki)

DOI: https://doi.org/10.3201/eid2611.201956

We report detection of severe acute respiratory syndrome coronavirus 2 RNA in hemodialysis effluent from a patient in Japan with coronavirus disease and prolonged inflammation. Healthcare workers should observe strict standard and contact precautions and use appropriate personal protective equipment when handling hemodialysis circuitry from patients with diagnosed coronavirus disease.

Since December 2019, coronavirus disease (COVID-19), caused by severe acute respiratory syndrome coronavirus 2 (SARS-CoV-2), has been a major health threat worldwide (1). Reports have been published on COVID-19 among patients receiving hemodialysis (2), but none have evaluated whether HD effluent is infectious. In addition, handling of hemodialysis circuitry is not mentioned in US Centers for Disease Control and Prevention (CDC) guidelines for COVID-19 infection control and prevention in dialysis facilities (3). We report detection of SARS-CoV-2 RNA in hemodialysis effluent from a patient with COVID-19 pneumonia and prolonged inflammation.

The patient, a 79-year-old man with end-stage renal disease (ESRD) due to IgA nephritis, had been receiving maintenance hemodialysis 3 times per week for 12 years. Six days before admission, he started having a fever and cough. Four days later, he had a nasal swab test for SARS-CoV-2 RNA. Quantitative reverse transcription PCR (qRT-PCR) (4) of the patient's specimen was positive, and he was admitted to the hospital. At admission, his body temperature was 37.7°C and oxygen saturation was 98% on room air. Multiple bilateral patchy ground glass opacities (GGO) were observed on the patient's chest computed tomography (CT) scan (Figure, panel A). Blood test results showed C-reactive protein (CRP) of 8.8 mg/dL and leukocyte count of 4,470 cells/µL. Although we started him on hydroxychloroquine (200 mg 2 ×/d) and azithromycin (500 mg, 1 ×/d), he had a fever (>38.0°C) on day 2 of his hospitalization. A follow-up chest CT on hospitalization day 5 showed worsening COVID-19 pneumonia and expanding GGO areas (Figure, panel B).

During the patient's hospitalization, we administered hemodialysis by using a polysulfone membrane dialyzer in a private depressurized room with dedicated machines. We tested hemodialysis effluent for SARS-CoV-2 on day 2. PCR results showed SARS-CoV-2 RNA of 157.9 copies/µL with cycle threshold (C_t) values of 38.3 at 1 hour after starting hemodialysis but were negative on effluent collected at 2 hours. Because the patient's fever persisted and CRP levels remained high, on hospitalization days 9, 11, and 15 we performed direct hemoperfusion by using a β2 microglobulin adsorbent column (Lixelle-DHP) to absorb cytokine. On hospitalization day 10, the patient became afebrile and CRP began decreasing until it reached 5.9 mg/dL on hospitalization day 15. On hospitalization day 16, chest CT showed markedly improved pneumonia (Figure, panel C), and the patient was discharged (Table).

Our case highlights 3 things. First, inflammation and clinical symptoms of COVID-19 can persist in patients on hemodialysis. COVID-19 is thought to progress in a 2-stage manner: viral replication and hyperinflammation (1). Hyperinflammation starts 7–10 days after symptom onset and involves extensive lung areas. This patient's fever persisted for >13 days, with pneumonia and CRP worse at 11 days after fever onset. Hyperinflammation appeared to progress slower and be maintained longer than in patients who are not receiving hemodialysis, which might be related to immune system dysfunction in patients with ESRD (5). Second, although SARS-CoV-2 RNA has been detected in various clinical specimens (6,7), our case demonstrates it also can be detected in hemodialysis effluent, even though we did not detect SARS-CoV-2 RNA in blood, as

Figure. Chest computed tomography (CT) scan of a patient on hemodialysis diagnosed with positive reverse transcription PCR for severe acute respiratory syndrome coronavirus 2 in hemodialysis effluent, Japan. A) Chest CT at day 1 of hospitalization showing bilateral patchy ground glass opacities (GGO). B) Chest CT from day 5 of hospitalization showing worsening coronavirus disease 2019 (COVID-19) pneumonia with GGO expansion. C) Chest CT on hospitalization day 16 showing improvement of COVID-19 pneumonia; the patient was discharged on this day. A, anterior; P, posterior.

Table. Clinical course and quantitative reverse transcription PCR results for severe acute respiratory syndrome coronavirus 2 RNA in patient receiving hemodialysis, Japan*

Day after symptom onset	Hospitalization, d	Temperature, °C	Event	Medication† AZM	Medication† Hydroxy	CRP, mg/dL	Dialysis	Nasal swab	Blood	Effluent, time collected 1 h	Effluent, time collected 2 h
1		37.3									
2		37.2									
3		37.3									
4		37.3	Clinic					18.8 (NA‡)			
5		37.7									
6		39.0									
7	1	38.8	Chest CT	N	N	8.8	–				
8	2	38.4		Y	Y	9.0	Y	29.6 (1,080.6)§	ND§	38.3 (157.91)	ND
9	3	38.7		Y	Y	–	–	–			
10	4	38.7		Y	Y	14.0	–	–			
11	5	37.4	Chest CT	N	Y	15.0	Y	–			
12	6	37.0		N	Y	–	–	–			
13	7	37.2		N	Y	–	–	–			
14	8	37.0		N	Y	–	–	–			
15	9	36.9		N	Y	14.4	Lixelle-DHP	–			
16	10	37.0		N	N	–	–	34.3 (NA‡)			
17	11	36.9		N	N	–	Lixelle-DHP	ND			
18	12	36.9		N	N	13.7	–	ND			
19	13	36.8		N	N	–	–	–			
20	14	36.6		N	N	–	–	–			
21	15	36.7		N	N	5.9	Lixelle-DHP	–			
22	16	36.7	Chest CT, discharge	N	N	–	–	–			

*AZM, azithromycin; CRP, C-reactive protein; CT, computed tomography; Hydroxy, hydroxychloroquine; Lixelle-DHP, direct hemoperfusion using a β2 microglobulin adsorbent column; NA, not available; ND, not detected; qRT-PCR, quantitative reverse transcription-PCR; –, not done.
†We prescribed azithromycin, 500 mg 2 times/d from day 1 to 3 because it was 1 of the potentially effective treatment regimens at the time. We also prescribed hydroxychloroquine 200 mg 2 times/d and initially planned to use it for 10 d in total, but the patient's liver function tests (LFTs) became elevated during the course. We suspected side effects of hydroxychloroquine and stopped it on day 9. His LFTs returned to normal afterwards.
‡Results for SARS-CoV-2 shown as cycle threshold values (Viral load, copies/μL). Viral loads were not available because PCR was performed at an outside commercial laboratory where they did not report these results. The same PCR method was used (*4*) at both National Institute of Infectious Diseases (NIID), Japan, and the outside laboratory. HD effluent was collected at 1 hr and 2 hr into hemodialysis.
§PCR test was performed at NIID, Japan where they report viral loads.

noted in a previous case (*6*). We hypothesized that only a small amount of fragmented RNA might pass through the dialysis membrane at the start of hemodialysis, but no marked fragments remain in the blood as a session progresses. Third, our case suggests Lixelle-DHP can have therapeutic effects for patients on hemodialysis. Although we did not measure the patient's predialysis and postdialysis cytokine levels, use of a blood purification technique might alleviate the effects of cytokine in COVID-19 pathophysiology due to its proven effect in reducing plasma cytokine levels in general (*8*).

Our report has several limitations. First, we did not confirm the duplicability of PCR results of hemodialysis effluent. We performed PCR only once and did not reevaluate the same specimen, even though the C_t was high. Second, the infectiousness of hemodialysis effluent is unclear. Its viability should be quantified by endpoint titration on authorized cell lines, as previously reported (*9*). Third, this is a single case report. Despite these limitations, we cannot underestimate the infectiousness of hemodialysis effluent. We performed dialysis in a private room with dedicated machines. We also conducted strict standard and contact precautions when handling HD circuitry, following CDC recommendations for preventing transmission of hepatitis B virus infection among patients on HD (*10*).

In conclusion, we report positive qRT-PCR results for SARS-CoV-2 RNA from hemodialysis effluent in a patient receiving renal dialysis. The clinical course of our patient was characteristic of the persistent inflammation of COVID-19 and shows the potential effectiveness of Lixelle-DHP as a treatment in patients on hemodialysis. Our case indicates that strict standard and contact precautions are essential when handling hemodialysis circuitry of patients with COVID-19. As more patients on hemodialysis contract SARS-CoV-2,

we expect further studies on infection control and prevention in dialysis facilities and on the effectiveness of Lixelle-DHP in treating patients with COVID-19.

About the Author
Dr. Okuhama is a clinical senior resident at the Disease Control and Prevention Center, National Center for Global Health and Medicine, Tokyo, Japan. Her research interests include emerging infectious diseases and public health.

References
1. Huang C, Wang Y, Li X, Ren L, Zhao J, Hu Y, et al. Clinical features of patients infected with 2019 novel coronavirus in Wuhan, China. Lancet. 2020;395:497–506. https://doi.org/10.1016/S0140-6736(20)30183-5
2. Wang R, Liao C, He H, Hu C, Wei Z, Hong Z, et al. COVID-19 in hemodialysis patients: A report of 5 cases. Am J Kidney Dis. 2020;76:141–3. https://doi.org/10.1053/j.ajkd.2020.03.009
3. US Centers for Disease Control and Prevention. Interim guidance for infection prevention and control recommendations for patients with suspected or confirmed COVID-19 in outpatient hemodialysis facilities 2020 Apr 21 [cited 2020 Apr 22]. https://www.cdc.gov/coronavirus/2019-ncov/healthcare-facilities/dialysis.html
4. Shirato K, Nao N, Katano H, Takayama I, Saito S, Kato F, et al. Development of genetic diagnostic methods for novel coronavirus 2019 (nCoV-2019) in Japan. Jpn J Infect Dis. 2020;73:304–7. PubMed https://doi.org/10.7883/yoken.JJID.2020.061
5. Lisowska KA, Dębska-Ślizień A, Jasiulewicz A, Heleniak Z, Bryl E, Witkowski JM. Hemodialysis affects phenotype and proliferation of CD4-positive T lymphocytes. J Clin Immunol. 2012;32:189–200. https://doi.org/10.1007/s10875-011-9603-x
6. Katagiri D, Ishikane M, Ogawa T, Kinoshita N, Katano H, Suzuki T, et al. Continuous renal replacement therapy for a patient with severe COVID-19. Blood Purif. 2020;11:1–3. https://doi.org/10.1159/000508062
7. Wang W, Xu Y, Gao R, Lu R, Han K, Wu G, et al. Detection of SARS-CoV-2 in different types of clinical specimens. JAMA. 2020;323:1843–4. https://doi.org/10.1001/jama.2020.3786
8. Tsuchida K, Yoshimura R, Nakatani T, Takemoto Y. Blood purification for critical illness: cytokines adsorption therapy. Ther Apher Dial. 2006;10:25–31. https://doi.org/10.1111/j.1744-9987.2006.00342.x
9. van Doremalen N, Bushmaker T, Morris DH, Holbrook MG, Gamble A, Williamson BN, et al. Aerosol and surface stability of SARS-CoV-2 as compared with SARS-CoV-1. N Engl J Med. 2020;382:1564–7. https://doi.org/10.1056/NEJMc2004973
10. US Centers for Disease Control and Prevention. Recommendations for preventing transmission of infections among chronic hemodialysis patients. MMWR Recomm Rep. 2001 Apr 27;50(RR-5):1–43.

Seroprevalence of SARS-CoV-2–Specific Antibodies, Faroe Islands

Maria Skaalum Petersen, Marin Strøm, Debes Hammershaimb Christiansen, Jógvan Páll Fjallsbak, Eina Hansen Eliasen, Malan Johansen, Anna Sofía Veyhe, Marnar Fríðheim Kristiansen, Shahin Gaini, Lars Fodgaard Møller, Bjarni á Steig, Pál Weihe

Author affiliations: University of the Faroe Islands, Tórshavn, Faroe Islands (M.S. Petersen, M. Strøm, E.H. Eliasen, M. Johansen, A.S. Veyhe, M.F. Kristiansen, S. Gaini, P. Weihe); The Faroese Hospital System, Tórshavn (M.S. Petersen, E.H. Eliasen, M. Johansen, A.S. Veyhe, P. Weihe); Faroese Food and Veterinary Authority, Tórshavn, (D.H. Christiansen, J.P. Fjallsbak); National Hospital of the Faroe Islands, Tórshavn, (M.F. Kristiansen, S. Gaini, B. Steig); COVID-19 Task Force, Ministry of Health, Tórshavn (M.F. Kristiansen, B. Steig); Odense University Hospital, Odense, Denmark (S. Gaini); University of Southern Denmark, Odense (S. Gaini); Chief Medical Officer Office, Tórshavn (L.F. Møller)

We conducted a nationwide study of the prevalence of severe acute respiratory syndrome coronavirus 2 infection in the Faroe Islands. Of 1,075 randomly selected participants, 6 (0.6%) tested seropositive for antibodies to the virus. Adjustment for test sensitivity and specificity yielded a 0.7% prevalence. Our findings will help us evaluate our public health response.

The magnitude of the coronavirus disease (CO-VID-19) pandemic is unknown because of a relatively large proportion of presumably asymptomatic persons (1–3). Reported infection rates, which mostly rely on PCR-based testing of symptomatic persons, may underestimate underlying infection rates. Analysis of severe acute respiratory syndrome coronavirus 2 (SARS-CoV-2)–specific antibodies is required to

more accurately guide COVID-19 response and calibrate public health efforts.

In the Faroe Islands, a geographic isolate of 52,154 inhabitants, the first COVID-19 case occurred on March 3, 2020. From early in the pandemic, the Faroe Islands adhered to the official recommendations by the World Health Organization of an active suppression strategy with high numbers of testing, contact tracing, and quarantine of infected persons and close contacts (M.F. Kristiansen et al., unpub. data). We aimed to estimate the population prevalence of SARS-CoV-2 infection by serotesting for antibodies in a nationwide sample of randomly selected inhabitants of the Faroe Islands (Appendix, https://wwwnc.cdc.gov/EID/article/26/11/20-2736-App1.pdf).

From the Faroese Population Registry, we randomly sampled 1,500 persons and invited them by letter to a clinical visit at 1 of 6 study sites around the islands mainly during week 18 (April 27–May 1, 2020) independently of previous positive PCR test result. To persons unable to attend a testing site, we offered home visits. Nonresponders received a follow-up phone call. We obtained informed consent from all participants; parents signed the consent form for their children <18 years of age. The Faroese Ethical Committee and the Data Protection Agency approved the study.

We conducted SARS-CoV-2–specific antibody (IgG, IgM) analyses on serum samples by using the commercial Wantai SARS-CoV-2 Ab ELISA kit (Beijing Wantai Biologic Pharmacy Enterprise, http://www.ystwt.cn), according to the manufacturer's instructions. We estimated the 95% CI for crude prevalence using exact binomial models and for prevalence

adjusted for test performance as reported by the producer (sensitivity (94.4% [95% CI 90.9–96.8]) and specificity (100% [95% CI 98.8–100.0]) using bootstrap methods (4). We used SPSS Statistics 25 (IBM, Inc., https://www.ibm.com) for the analysis.

Of 1,500 persons invited to the study, 1,141 (76.1%) provided consent and 1,075 (71.7%) were tested (Figure). Mean age of participants was 42.1 years (SD ± 23.1, range 0–100 years); 50% were women (Table). The study sample was representative of the entire population (Table) regarding geography, sex, and age; the representativeness of the youngest (0–9 years) participants and participants 60–69 years of age was slightly less. Nonparticipants were more often men and significantly younger than participants (32.6 [SD ± 26.7] vs. 42.9 years [SD ± 23.2]; p<0.01), and geographic distribution was comparable (p = 0.7).

Six persons (3 women, 3 men) tested positive for SARS-CoV-2–specific antibodies (0.6% [exact binomial 95% CI 0.2%–1.2%]). One of the 6 positive persons had previously confirmed infection by PCR; the others had not been tested, although 2 reported symptoms. After adjustment for test sensitivity and specificity, the prevalence of SARS-CoV–2- specific antibodies was 0.7% (bootstrap 95% CI 0.3%–1.3%).

The crude seroprevalence of SARS-CoV-2 antibodies (0.6% [adjusted 0.7%]) in our randomly selected population-based sample corresponds to 313 SARS-CoV-2–seropositive persons in the population, which is somewhat higher than the number of confirmed infections (187 cases [crude prevalence 0.4%]) in the Faroe Islands on June 6 (5). The number of active COVID-19 cases peaked on March 23 when the prevalence was 196 cases/100,000 persons, and the last locally transmitted case was diagnosed April 22. The low number of undetected cases found in this study supports the effectiveness of the extensive testing regime, contact tracing, and quarantining in mitigating the virus. The exact seroprevalence levels from the few published studies included in a recent meta-analysis are highly region-dependent; levels ranged from 2.8% to 31.5% (J. Levesque, D.W. Maybury, unpub data, https://doi.org/10.1101/2020.05.03.20089201). Contrary to the other studies, the participants in our study sample were unselected and representative of the background population with respect to age, sex, and geographic area, making selection bias an unlikely explanation of our results.

Major strengths of our study include the high participation rate and the representativeness of

Figure. Study participation and reasons for dropout in a seroprevalence analysis of severe acute respiratory syndrome coronavirus 2–specific antibodies, Faroe Islands, 2020.

Flowchart text:
1,500 persons 0–100 years of age received invitation letter

199 declined participation (62 children, 33 abroad)
14 letter returned/unknown address
146 unreachable by telephone

1,141 accepted the invitation

37 did not show up
11 in quarantine
18 not available weeks 18 and 19
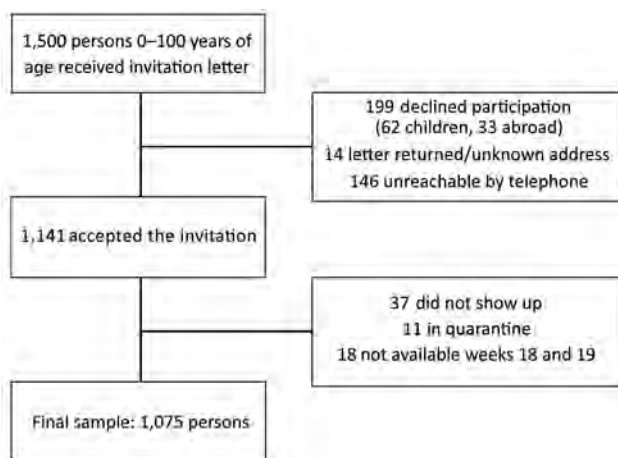
Final sample: 1,075 persons

Table. Comparison of study participants and the entire population in a seroprevalence analysis of severe acute respiratory syndrome coronavirus 2–specific antibodies, Faroe Islands, April 27–May 1, 2020

Characteristic	No. (%)	Population distribution, no. (%)	No. seropositive	Crude prevalence for antibody % (exact binomial 95%CI)
Entire sample	1,075	52,154	6	0.6 (0.1–1.2)
Sex				
M	538 (50.2)	26,987 (51.7)	3	0.6 (0.1–1.6)
F	537 (49.8)	25,167 (48.3)	3	0.6 (0.1–1.6)
Age group, y				
0–9	92 (8.6)	7,164 (13.7)*	0	0
10–19	150 (14.0)	7,335 (14.1)	1	0.7 (0.0–3.7)
20–29	116 (10.8)	5,966 (11.4)	1	0.9 (0.0–4.7)
30–39	126 (11.7)	6,298 (12.1)	0	0
40–49	148 (13.8)	6,522 (12.5)	0	0
50–59	154 (14.3)	6,718 (12.9)	1	0.6 (0.0–3.6)
60–69	151 (14.0)	5,665 (10.9)*	1	0.7 (0.0–3.6)
70–79	98 (9.1)	4,201 (8.1)	2	2.0 (0.2–7.2)
80–89	30 (2.8)	1,848 (3.5)	0	0
≥90	10 (0.9)	437 (0.8)	0	0
Geographic area				
Streymoy	530 (49.3)	24,926 (47.8)	3	0.6 (0.1–1.6)
Eysturoy	251 (23.3)	11,782 (22.6)	1	0.4 (0.0–2.2)
Norðoyggjar	114 (10.6)	6,206 (11.9)	0	0
Vágar	74 (6.9)	3,366 (6.5)	1	1.4 (0.0–7.3)
Sandoy og Suðuroy	106 (10.0)	5,874 (11.2)	1	0.9 (0.0–5.1)
*Significant difference, p<0.05.				

the randomly selected study sample, although the youngest children were slightly underrepresented. Rather than a flow immunoassay test, we used the ELISA that performed best of 9 commercial SARS-CoV-2 immunoassays (R. Lassaunière et al., unpub. data, https://doi.org/10.1101/2020.04.09.20056325). However, we acknowledge that our estimates could change with new information about test accuracy of kits used, and cross-reactivity with other infections might be a challenge in antibody testing, but evidence on serologic testing is limited. Although antibodies might be undetected during early stages of the disease (6), our sample collection occurred 5–10 days after the last case in the Faroe Islands was detected, which makes this possibility unlikely in explaining the low proportion tested seropositive.

Our findings will help us evaluate the effect of public health efforts in the Faroe Islands. In addition, our findings will help guide the COVID-19 response moving forward, ensuring the previously held belief that few undetected cases were present in the Faroe Islands.

Acknowledgments

About the Author

Dr. Petersen is an associate professor at the University of the Faroe Islands, senior researcher at The Faroese Hospital System, and head of Centre of Health Sciences, University of the Faroe Islands. Her primary research interests include epidemiologic and COVID-19 research.

References

1. Gudbjartsson DF, Helgason A, Jonsson H, Magnusson OT, Melsted P, Norddahl GL, et al. Spread of SARS-CoV-2 in the Icelandic population. N Engl J Med. 2020;382:2302–15. https://doi.org/10.1056/NEJMoa2006100
2. Mizumoto K, Kagaya K, Zarebski A, Chowell G. Estimating the asymptomatic proportion of coronavirus disease 2019 (COVID-19) cases on board the Diamond Princess cruise ship, Yokohama, Japan, 2020. Euro Surveill. 2020;25:2000180. https://doi.org/10.2807/1560-7917.ES.2020.25.10.2000180
3. Zhu J, Ji P, Pang J, Zhong Z, Li H, He C, et al. Clinical characteristics of 3,062 COVID-19 patients: a meta-analysis. J Med Virol. 2020 Apr 15 [Epub ahead of print]. https://doi.org/10.1002/jmv.25884
4. Speybroeck N, Devleesschauwer B, Joseph L, Berkvens D. Misclassification errors in prevalence estimation: Bayesian handling with care. Int J Public Health. 2013;58: 791–5. https://doi.org/10.1007/s00038-012-0439-9
5. The Government of the Faroe Islands. Coronavirus in the Faroe Islands—statistics [cited 2020 Jun 6]. https://corona.fo/statistics
6. Zhao J, Yuan Q, Wang H, Liu W, Liao X, Su Y, et al. Antibody responses to SARS-CoV-2 in patients of novel coronavirus disease 2019. Clin Infect Dis 2020;ciaa344.

Address for correspondence: Maria Skaalum Petersen, Department of Occupational Medicine and Public Health, The Faroese Hospital System, Sigmundargøta 5, 100 Tórshavn, Faroe Islands; email: maria@health.fo

Four Patients with COVID-19 and Tuberculosis, Singapore, April–May 2020

Sai Meng Tham, Wei Yang Lim, Chun Kiat Lee, Jerold Loh, Arthi Premkumar, Benedict Yan, Adrian Kee, Louis Chai, Paul Anantharajah Tambyah, Gabriel Yan

Author affiliation: National University Health System, Singapore

Coronavirus disease (COVID-19) and tuberculosis (TB) developed in 4 foreign workers living in dormitories in Singapore during April–May 2020. Clinical manifestations and atypical radiographic features of COVID-19 led to the diagnosis of TB through positive interferon-gamma release assay and culture results. During the COVID-19 pandemic, TB should not be overlooked.

As the world focuses on the coronavirus disease (COVID-19) pandemic, caution must be taken to not overlook tuberculosis (TB). COVID-19 was first diagnosed in Singapore in January 2020, after cases were imported from Wuhan, China. Subsequent sustained community transmission of the virus followed a wave of imported cases from local residents returning from abroad (1). The outbreak in Singapore is being driven by spread within migrant worker dormitories. As of June 28, 2020, Singapore reported 43,459 confirmed cases of COVID-19, of which 41,010 were in dormitory residents (1). TB is endemic to Singapore; annual incidence rate is »40 cases/100,000 population (2), and a large proportion of cases are in nonpermanent residents.

We describe migrant workers in Singapore dormitories who were co-infected with severe acute respiratory syndrome virus 2 (SARS-CoV-2) and *Mycobacterium tuberculosis*. For all 4 patients, TB was diagnosed by positive interferon-gamma release assay (IGRA) (QIAGEN, https://www.qiagen.com); *M. tuberculosis* was isolated from pleural fluid culture from patient 4 only (Table).

Patient 1 was a 32-year-old man from India with a 2-day history of fever and cough. He was positive for SARS-CoV-2 by reverse transcription PCR (RT-PCR) of a nasopharyngeal swab sample. Radiographs showed bilateral cavitary lung lesions (Figure 1, panel A). Sputum samples were smear negative and culture negative for acid-fast bacilli (AFB) and negative by molecular testing for *M. tuberculosis* nucleic acids (Cepheid Xpert MTB/RIF, https://www.cepheid.com).

The IGRA for TB result was positive. In consideration of the clinical manifestations and risk factors, anti-TB therapy (ATT) was started, and interval radiographic imaging showed resolution.

Patient 2 was a 33-year-old man from India with an 8-day history of fever and cough and a 1-month history of weight loss (3 kg). He was positive for SARS-CoV-2 by RT-PCR of a nasopharyngeal swab sample. Radiographs showed a right-sided pleural effusion (Figure 1, panel B). Pleural fluid analysis revealed a lymphocytic exudative effusion with an adenosine deaminase (ADA) level of 130 U/L (reference range <40 U/L), but the fluid was negative for SARS-CoV-2 by RT-PCR. Sputum and pleural fluid were smear negative for AFB and *M. tuberculosis* nucleic acid negative by molecular testing; culture results are pending. IGRA was positive for TB, and ATT was started with subsequent clinical improvement.

Patient 3 was a 22-year old man from India with a 10-day history of fever and cough (associated with exertional dyspnea) and pleuritic chest pain. He was positive for SARS-CoV-2 by RT-PCR of a nasopharyngeal swab sample. Radiographs showed a right-sided pleural effusion (Figure 1, panel C). Pleural fluid analysis revealed a lymphocytic exudative effusion with an ADA level of 112 U/L and interleukin-6 (IL-6) level of >1,000 pg/mL, but the fluid was negative for SARS-CoV-2 by RT-PCR. Sputum and pleural fluid were smear negative for AFB and negative for *M. tuberculosis* nucleic acids by molecular testing; culture results are pending. IGRA was positive for TB and ATT was started; symptoms subsequently resolved.

Patient 4 was a 40-year old man from Bangladesh with a 3-day history of fever and cough. He was positive for SARS-CoV-2 by RT-PCR from a nasopharyngeal swab sample. Radiographs showed a left-sided pleural effusion with bilateral consolidation (Figure 1, panel D). Pleural fluid analysis revealed a lymphocytic exudative effusion with an ADA level of 62 U/L and an IL-6 level of >1,000 pg/mL, but the fluid was negative for SARS-CoV-2 by RT-PCR. Sputum and pleural fluid were smear negative for AFB and negative for *M. tuberculosis* nucleic acids by molecular testing, but the IGRA for TB was positive. ATT was started, and pleural fluid cultures were subsequently positive for *M. tuberculosis*.

All 4 patients were workers who resided in dormitories and had COVID-19 but atypical radiographic features; typical radiographic features for COVID-19 patients include ground-glass opacities, multifocal patchy consolidation, and peripheral interstitial changes (3). Despite confirmed diagnoses of COVID-19,

Table. Epidemiologic and clinical features for 4 patients with coronavirus disease and tuberculosis, Singapore*

Pt no.	Age, y/sex, nationality	Initial signs/symptoms	Radiologic findings	Pleural fluid analysis	Sputum analysis	Microbiological findings	IGRA for TB	Outcome
1†	32/M, India	Fever, productive cough	CXR: right upper zone and left lower zone cavitary lesions; chest CT: irregular opacifications with central cavitation	NA	AFB smear negative; molecular TB analysis negative	Sputum AFB culture negative	+	Symptoms resolved; repeat CXR after starting ATT demonstrated resolution of cavitary lesions at 2 mo of treatment
2	33/M, India	Fever, nonproductive cough; 3-kg weight loss over 1 mo	CXR: right-sided pleural effusion; chest CT: loculated right-sided effusion with adjacent collapse/consolidation	Lymphocytic exudative effusion; ADA 130 U/L; SARS-CoV-2 PCR negative	AFB smear negative; molecular TB analysis negative	Sputum and pleural fluid AFB cultures pending	+	Symptoms resolved with interval improvement of CXR
3†	22/M, India	Fever, nonproductive cough; exertional dyspnea, pleuritic chest pain	CXR: right-sided pleural effusion with adjacent compressive atelectasis	Lymphocytic exudative effusion; ADA 112 U/L; SARS-CoV-2 PCR negative	AFB smear negative; molecular TB analysis negative	Sputum and pleural fluid AFB cultures pending	+	Symptoms resolved with interval improvement of CXR
4	40/M, Bangladesh	Fever, productive cough; reduced effort tolerance	CXR: large left-sided pleural effusion; Chest CT: left-sided pleural effusion, bilateral patchy consolidative changes with ground-glass opacities and interlobular septal thickening	Lymphocytic exudative effusion; ADA 69 U/L; SARS-CoV-2 PCR negative	AFB smear negative; molecular TB analysis negative	Sputum AFB culture negative; pleural fluid AFB culture positive for *Mycobacterium tuberculosis* complex	+	Symptoms resolved with interval improvement of CXR

*ADA, adenosine deaminase; AFB, acid-fast bacilli; ATT, anti-TB therapy; CT, computed tomography image; CXR, plain chest radiograph; IGRA, interferon gamma release assay; NA, not applicable; Pt, patient; SARS-CoV-2, severe acute respiratory syndrome coronavirus 2; TB, tuberculosis; +, positive.
†These patients reside in the same dormitory.

the 4 patients' pulmonary radiologic findings were more consistent with those for TB, highlighting the value of considering other pulmonary pathologic conditions for patients with COVID-19.

Risk factors for TB include low socioeconomic status and overcrowded living conditions (*4*). Of note, patients 1 and 3 resided in the same dormitory. Migrant worker dormitories are often inadequately ventilated and crowded, resulting in residents being more susceptible to infectious diseases, including dengue, Zika, and varicella (*5,6*). The same working and living conditions have served
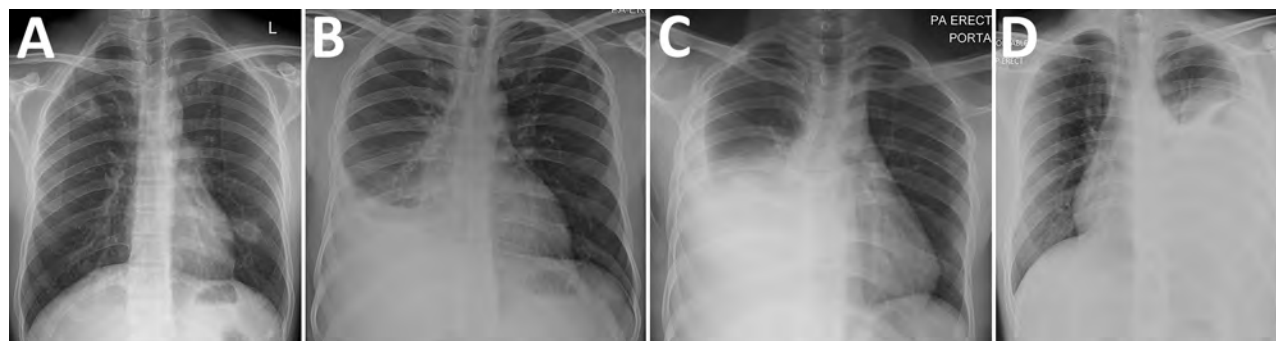
Figure. Plain chest radiographs of 4 patients with severe acute respiratory syndrome coronavirus 2 and *Mycobacterium tuberculosis* co-infection, Singapore. A) Patient 1, showing bilateral cavitary lesions; B) patient 2, showing a large right-sided loculated pleural effusion and adjacent consolidation; C) patient 3, showing a large right-sided pleural effusion with adjacent compressive atelectasis; D) patient 4, showing a large left-sided pleural effusion with adjacent consolidation.

as a catalyst for the rapid transmission of SARS-CoV-2, and potentially TB, in this population. Improving screening processes and living conditions and implementing routine vaccination strategies for this population may prevent future infectious disease outbreaks.

As the COVID-19 pandemic continues, care for patients with TB may be compromised as additional strains are placed on essential services. The 4 cases we report highlight a serious public health issue. Precautionary measures must be undertaken to be vigilant of an epidemic within the ongoing pandemic—TB. To ensure that care is not compromised, clinicians treating these at-risk populations should be aware of possible co-infection with *M. tuberculosis* and SARS-CoV-2 in patients with atypical radiographic features of COVID-19.

About the Author

Dr. Tham is an infectious diseases senior resident in the Department of Medicine at the National University Hospital of Singapore. His research interests include virology and public health.

References

1. Ministry of Health Singapore. COVID-19 situation report [cited 2020 Jun 29]. https://covidsitrep.moh.gov.sg
2. Ministry of Health Singapore. Communicable diseases surveillance in Singapore [cited 2020 May 15]. https://www.moh.gov.sg/docs/librariesprovider5/diseases-updates/communicable-diseases-surveillance-in-singapore-2018210c9a3beaa94db49299c2da53322dce.pdf
3. Shi H, Han X, Jiang N, Cao Y, Alwalid O, Gu J, et al. Radiological findings from 81 patients with COVID-19 pneumonia in Wuhan, China: a descriptive study. Lancet Infect Dis. 2020;20:425–34. https://doi.org/10.1016/S1473-3099(20)30086-4
4. Narasimhan P, Wood J, Macintyre CR, Mathai D. Risk factors for tuberculosis. Pulm Med. 2013;2013:828939. https://doi.org/10.1155/2013/828939
5. Sadarangani SP, Lim PL, Vasoo S. Infectious diseases and migrant worker health in Singapore: a receiving country's perspective. J Travel Med. 2017;24:1–9. https://doi.org/10.1093/jtm/tax014
6. Ho ZJM, Hapuarachchi HC, Barkham T, Chow A, Ng LC, Lee JMV, et al.; Singapore Zika Study Group. Outbreak of Zika virus infection in Singapore: an epidemiological, entomological, virological, and clinical analysis. Lancet Infect Dis. 2017;17:813–21. https://doi.org/10.1016/S1473-3099(17)30249-9

Address for correspondence: Gabriel Yan, Division of Infectious Diseases, Department of Medicine, National University Health System, NUHS Tower Block, 1E Kent Ridge Rd, 119228, Singapore; email: gabriel_zherong_yan@nuhs.edu.sg

Seroprevalence of SARS-CoV-2 and Infection Fatality Ratio, Orleans and Jefferson Parishes, Louisiana, USA, May 2020

Amy K. Feehan, Daniel Fort, Julia Garcia-Diaz, Eboni G. Price-Haywood, Cruz Velasco, Eric Sapp, Dawn Pevey, Leonardo Seoane

Author affiliations: Ochsner Clinic Foundation, New Orleans, Louisiana, USA (A.K. Feehan, D. Fort, J. Garcia-Diaz, E.G. Price-Haywood, C. Velasco, D. Pevey, L. Seoane); University of Queensland Ochsner Clinical School, New Orleans (A.K. Feehan, J. Garcia-Diaz, E.G. Price-Haywood, L. Seoane); Public Democracy, Arlington, Virginia, USA (E. Sapp); Louisiana State University Health Science Center–Shreveport, Shreveport, Louisiana, USA (L. Seoane)

Using a novel recruitment method and paired molecular and antibody testing for severe acute respiratory syndrome coronavirus 2 infection, we determined seroprevalence in a racially diverse municipality in Louisiana, USA. Infections were highly variable by ZIP code and differed by race/ethnicity. Overall census-weighted seroprevalence was 6.9%, and the calculated infection fatality ratio was 1.61%.

Seroprevalence studies around the world have estimated the spread of severe acute respiratory syndrome coronavirus 2 (SARS-CoV-2) to range from 1.79% (*1*) in Boise, Idaho, USA, to 25% in Breves, Brazil (P. Hallal, unpub. data, https://doi.org/10.1101/2020.05.30.20117531). Coronavirus disease (COVID-19) has also been reported to disproportionately affect Black patients, but we do not know the infection fatality ratio (IFR), which requires knowing how many persons are at risk (i.e., infected). We estimated SARS-CoV-2 infections in Orleans and Jefferson Parishes, Louisiana, USA, and determined the COVID-19–related IFR by race.

The protocol was approved by the Ochsner Clinic Foundation Institutional Review Board (New Orleans, LA, USA) and designed to enroll and test up to 3,000 persons at 10 sites during May 9–15, 2020. To recruit a representative sample for this high-throughput method, a novel 2-step system developed by Public Democracy (https://www.publicdemocracy.io) considered >50 characteristics, including social determinants of health and US Census population

Table. Prevalence of SARS-CoV-2 infection and COVID-19–related IFR after 7 weeks of an active stay-at-home order, by race/ethnicity, 10 sites in Orleans and Jefferson Parishes, Louisiana, USA, May 9–15, 2020*

Value	Total	White	Black	Asian	Native American	Pacific Islander	Multiracial or other	Hispanic†
Positive, no./total no. (%)	183/2,640 (100)	79/1,607 (60.9)	90/828 (31.4)	9/130 (4.9)	0/14 (0.5)	0/3 (0.1)	5/58 (2.2)	18/293 (11.1)
Orleans/Jefferson Parish residents, no. (%)	825,057 (100)	419,800 (50.8)	356,925 (43.2)	29,740 (3.6)	4,088 (0.5)	495 (0.1)	14,009 (1.7)	86,289 (10.5)
Unadjusted exposure‡	6.9 (6.0–8.0)	4.9 (3.9–6.1)	10.9 (8.8–13.2)	6.9 (3.2–12.7)	0	0	8.6 (2.9–19.0)	6.1 (3.7–9.5)
Weighted exposure§	7.8 (7.8–7.9)	5.9 (5.8–5.9)	10.3 (10.2–10.4)	6.4 (6.1–6.7)	0	0	9.4 (9.0–10.0)	7.5 (7.3– 7.7)
Weighted point prevalence¶	1.0 (0.6–1.3)	1.3 (0.8–1.9)	0.5 (0–1.0)	0.9 (0–2.6)	0	0	2.2 (0–5.9)	2.2 (0.5–3.8)
Weighted seroprevalence#	6.9 (6.8–6.9)	4.5 (4.4–4.6)	9.8 (9.7–9.9)	5.5 (5.2–5.7)	0	0	7.1 (6.7–7.6)	5.3 (5.2–5.5)
No. presumed recovered**	56,578	18,975	34,973	1,629	–	–	1,001	4,582
No. deaths as of May 16, 2020	925	299	600	10	0	2	14	Unknown
IFR††	1.61 (1.5–1.7)	1.55 (1.4–1.7)	1.69 (1.6–1.8)	0.61 (0.3–1.1)‡‡	–	–	1.38 (0.8–2.3)	–

*Values are % (95% CI) except as indicated. The 2018 population estimates and deaths by race reported by the Louisiana Department of Public Health (*4*). Deaths are deemed to be COVID-19–related and have an associated confirmed PCR-positive test. Probable COVID-19 deaths without a positive PCR test were not included in these counts. By May 16, a total of 13,666 state-aggregated, confirmed cases had been reported in both parishes. COVID-19, coronavirus disease; IFR, infection fatality ratio; SARS-CoV-2, severe acute respiratory syndrome coronavirus 2; –, calculated value would be unreliable given low sample.
†Hispanic ethnicity is a separate analysis and numbers were not subtracted from race. Hispanic deaths were not being reported as of May 16, 2020 (*4*).
‡Percentage of the sample with a PCR-positive test, an IgG-positive test, or both.
§Census-weighted percentage of a PCR-positive test, an IgG-positive test, or both calculated to match 2018 racial demographics by parish and then combined.
¶Census-weighted percentage of PCR-positive and IgG-postive tests calculated to match 2018 racial demographics by parish and then combined.
#Census-weighted percentage of IgG-positive tests calculated to match 2018 racial demographics by Parish and then combined.
**Number of residents multiplied by weighted seroprevalence (IgG-positive tests).
††IFR equals the number of deaths per number of persons presumed recovered from SARS-CoV-2 infection plus deaths.
‡‡Significantly lower than White (p = 0.0034), Black (p = 0.0013), and multiracial or other (p = 0.0467) persons.

data, to establish a pool of potential participants reflective of the demographics of the parishes, from which a randomized subset of 150,000 was selected. Of these, >25,000 volunteers were recruited through dynamic, cross-device digital advertisements, supplemented by television advertisements and a call-in number to register (Appendix, https://wwwnc.cdc. gov/EID/article/26/11/20-3029-App1.pdf). This volunteer pool was stratified by the same attributes and then randomly issued a text message inviting them to private testing locations. Invitations were adjusted daily on the basis of response rates to achieve a representative sample. Volunteers checked in with a digital code to discourage unsolicited walk-ins. We did not turn uninvited persons away but excluded them from analysis if they did not fit criteria. Housemates of participants (n = 234) or persons from ineligible ZIP codes (n = 34) were excluded. Six people withdrew consent. All study materials were created in English, Spanish, and Vietnamese. Participants were offered free transportation if needed. Verbal consent was electronically documented, and participants were asked a short list of questions followed by a blood draw and nasopharyngeal swab.

Tests approved by the US Food and Drug Administration's Emergency Use Authorization were used. Real-time reverse transcription PCR tests of nasopharyngeal swabs were performed on the Abbott *m*2000 Real*Time* System (Abbott, https://www. abbott.com) and qualitative IgG blood tests on the ARCHITECT *i*2000*SR* (Abbott). The IgG test meets criteria described by the Centers for Disease Control and Prevention as yielding high positive predictive value, which was validated by a laboratory at Ochsner Health and others (*1,2*). Study participants for whom either or both tests were positive were considered to be infected with SARS-CoV-2.

US Census values, weighted by race and parish of residence, were divided by the total sample for exposure (a PCR-positive test, an IgG-positive test, or both), point prevalence (PCR-positive only), and seroprevalence (IgG-positive tests regardless of PCR test result). The positive-testing population included persons with early-stage infections (PCR-positive only) and persons recovering (PCR-positive and IgG-positive) and recovered (IgG-positive only). Early-stage infections were excluded from IFR estimation because their outcomes would not yet be registered as deaths. Therefore, weighted seroprevalence was used to calculate persons presumed to be recovered (*3*). IFR was calculated by dividing cumulative deaths by race (*4*) by the number
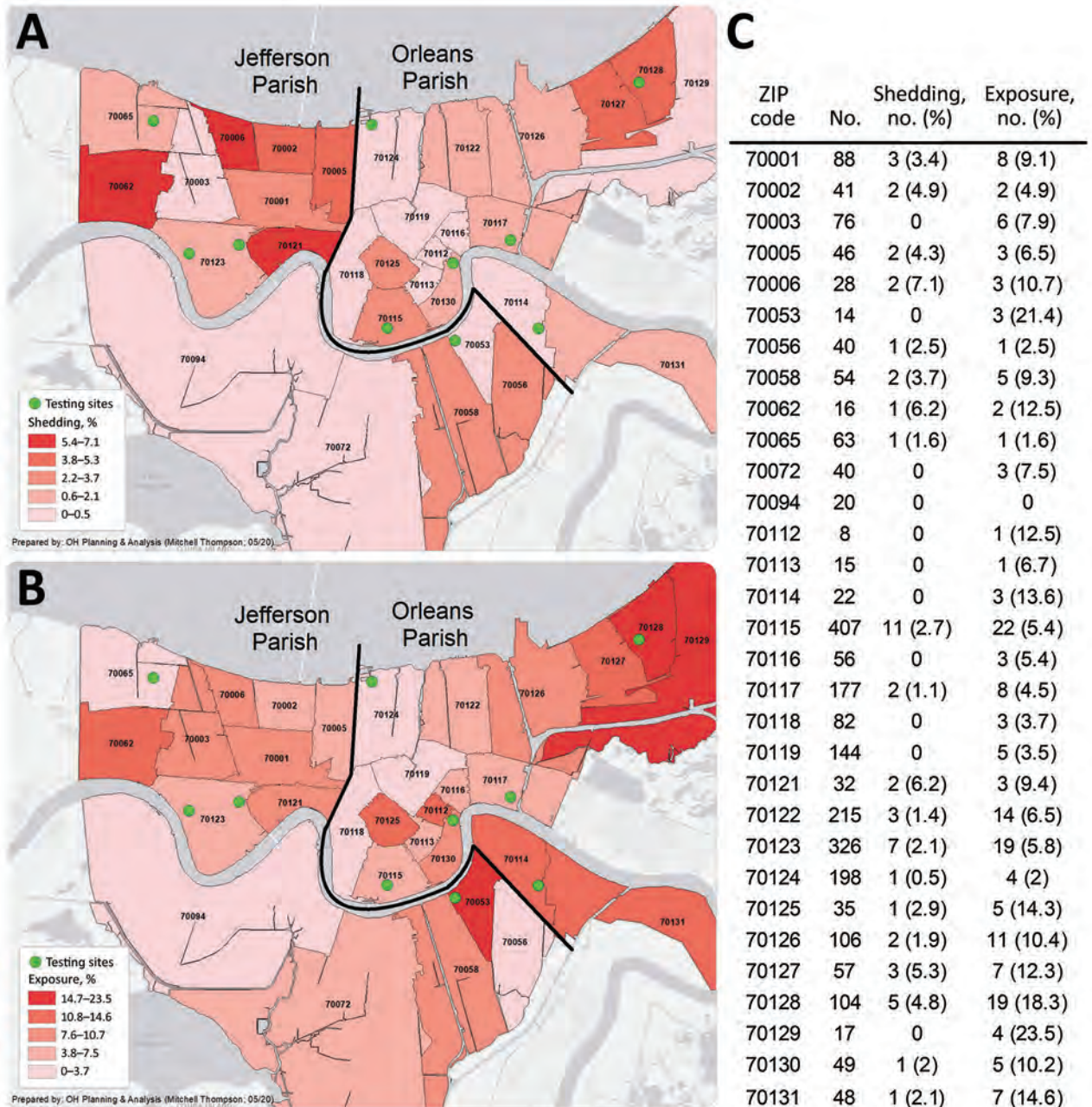
Figure. Heat maps of current and past severe acute respiratory syndrome coronavirus 2 infections after 7 weeks of an active stay-at-home order, 10 sites in Orleans and Jefferson Parishes, Louisiana, USA, May 9–15, 2020. A) Viral shedding, as indicated by PCR-positive test. B) Exposure to virus, as indicated by PCR-positive test, IgG-positive test, or both. C) Number and percentage of persons who were tested in each ZIP code, who were shedding virus (PCR-positive), and who had past or current infection (having a PCR-positive test, IgG-positive test, or both).

ZIP code	No.	Shedding, no. (%)	Exposure, no. (%)
70001	88	3 (3.4)	8 (9.1)
70002	41	2 (4.9)	2 (4.9)
70003	76	0	6 (7.9)
70005	46	2 (4.3)	3 (6.5)
70006	28	2 (7.1)	3 (10.7)
70053	14	0	3 (21.4)
70056	40	1 (2.5)	1 (2.5)
70058	54	2 (3.7)	5 (9.3)
70062	16	1 (6.2)	2 (12.5)
70065	63	1 (1.6)	1 (1.6)
70072	40	0	3 (7.5)
70094	20	0	0
70112	8	0	1 (12.5)
70113	15	0	1 (6.7)
70114	22	0	3 (13.6)
70115	407	11 (2.7)	22 (5.4)
70116	56	0	3 (5.4)
70117	177	2 (1.1)	8 (4.5)
70118	82	0	3 (3.7)
70119	144	0	5 (3.5)
70121	32	2 (6.2)	3 (9.4)
70122	215	3 (1.4)	14 (6.5)
70123	326	7 (2.1)	19 (5.8)
70124	198	1 (0.5)	4 (2)
70125	35	1 (2.9)	5 (14.3)
70126	106	2 (1.9)	11 (10.4)
70127	57	3 (5.3)	7 (12.3)
70128	104	5 (4.8)	19 (18.3)
70129	17	0	4 (23.5)
70130	49	1 (2)	5 (10.2)
70131	48	1 (2.1)	7 (14.6)

of persons presumed to be recovered. Methodology and symptoms observed have been described elsewhere (A. Feehan, unpub. data, https://ssrn.com/abstract=3633166).

Among the 2,640 persons in the sample, 63.5% were female and 60.9% were White; average age was 50.6 years, and average household size was 2.55 persons. Among the 183 participants who tested positive, 49% were Black. The unadjusted exposure rate of SARS-CoV-2 in the sample population was 6.9% (7.8%, census-weighted); 0.9% were positive for active viral shedding but had no detectable antibody. By race, seroprevalence was highest (9.8%) in Black participants, followed by multiracial (7.1%),

Asian (5.5%), and White (4.5%) participants. Hispanic participants had 5.3% seroprevalence. We multiplied 2018 population estimates by weighted seroprevalence to generate the number of persons presumed to be recovered (Table). Reported deaths (4) were divided by number of persons presumed to be recovered plus deaths to calculate the IFR, which was 1.61% overall. The IFR was statistically similar for White (1.55%), Black (1.69%), and multiracial (1.38%) persons but was significantly lower for Asian persons (0.61%). No COVID-19–related data on Hispanic persons were collected by the Louisiana Department of Public Health during the study period.

The prevalence of viral shedding (PCR-positive) and overall SARS-CoV-2 exposure (PCR-positive, IgG-positive, or both) were listed and mapped by ZIP code across the 2 parishes (Figure). Prevalence was highly variable across the map and in some areas exceeded 20%.

Prevalence studies help to understand infection spread, especially when testing resources are limited. Our study found the overall SARS-CoV-2 exposure rate in this area to be 7.8% and confirmed a recent report of overrepresentation of Black persons with COVID-19 in the New Orleans area (5). Multiracial, Hispanic, and Asian persons also had higher seroprevalence than White persons. The overall IFR was 1.63%, which is higher than IFRs found in other seroprevalence studies (0.5%–1.2%) (6; M. Emmenegger, unpub. data, https://doi.org/10.1101/2020.05.31.201 18554; P. Hallal, unpub. data, https://doi.org/10.110 1/2020.05.30.20117531). The similar IFR among most racial groups indicates that viral spread at least partially explains the increased number of deaths among minority populations.

About the Author

Dr. Feehan is a research scientist at the Ochsner Clinic Foundation's Infectious Disease Clinical Research Department. Her research focuses on the gut microbiome as a treatment modality for neurologic disease, but more immediately on the SARS-CoV-2 pandemic that has greatly impacted the New Orleans area.

References

1. Bryan A, Pepper G, Wener MH, Fink SL, Morishima C, Chaudhary A, et al. Performance characteristics of the Abbott Architect SARS-CoV-2 IgG assay and seroprevalence in Boise, Idaho. J Clin Microbiol. 2020;58:e00941–20. https://doi.org/10.1128/JCM.00941-20
2. Centers for Disease Control and Prevention. Interim guidelines for COVID-19 antibody testing. 2020 [cited 2020 May 15]. https://www.cdc.gov/coronavirus/2019-ncov/lab/resources/antibody-tests-guidelines.html
3. Wilson N, Kvalsvig A, Barnard LT, Baker MG. Case-fatality risk estimates for COVID-19 calculated by using a lag time for fatality. Emerg Infect Dis. 2020;26:1339–441. https://doi.org/10.3201/eid2606.200320
4. Louisiana Department of Public Health. COVID-19. 2020 [cited 2020 May 16]. http://ldh.la.gov/coronavirus
5. Price-Haywood EG, Burton J, Fort D, Seoane L. Hospitalization and mortality among Black patients and white patients with Covid-19. N Engl J Med. 2020;382:2534–43. https://doi.org/10.1056/NEJMsa2011686
6. Pollán M, Pérez-Gómez B, Pastor-Barriuso R, Oteo J, Hernán MA, Pérez-Olmeda M, et al.; ENE-COVID Study Group. Prevalence of SARS-CoV-2 in Spain (ENE-COVID): a nationwide, population-based seroepidemiological study. [Epub ahead pf print]. Lancet. 2020 Jul 3 Epub ahead of print]. https://doi.org/10.1016/S0140-6736(20)31483-5

Address for correspondence: Amy K. Feehan, Ochsner Health, 1st floor AT, Infectious Diseases, 1514 Jefferson Hwy, New Orleans, LA 70121, USA; email: amy.feehan@ochsner.org

Saliva Alternative to Upper Respiratory Swabs for SARS-CoV-2 Diagnosis

Rachel L. Byrne, Grant A. Kay,
Konstantina Kontogianni, Ghaith Aljayyoussi,
Lottie Brown, Andrea M. Collins, Luis E. Cuevas,
Daniela M. Ferreira, Tom Fletcher, Alice J. Fraser,
Gala Garrod, Helen Hill, Grant L. Hughes,
Stefanie Menzies, Elena Mitsi, Sophie I. Owen,
Edward I. Patterson, Stacy Todd,
Christopher T. Williams, Angela Hyder-Wright,
Emily R. Adams, Ana I. Cubas-Atienzar

Author affiliations: Liverpool School of Tropical Medicine,
Liverpool, UK (R.L. Byrne, G.A. Kay, K. Kontogianni, G. Aljayyoussi,
L. Brown, A.M. Collins, L.E. Cuevas, D.M. Ferreira, T. Fletcher,
A.J. Fraser, G. Garrod, H. Hill, G.L. Hughes, S. Menzies, E. Mitsi,
S.I. Owen, E.I. Patterson, S. Todd, C.T. Williams, A. Hyder-Wright,
E.R. Adams, A.I. Cubas-Atienzar); National Institute for Health
Research, Leeds, UK (A.M. Collins, A. Hyder-Wright); Liverpool
University Hospitals National Health Services Foundation Trust,
Liverpool (A.M. Collins, T. Fletcher, A. Hyder-Wright S. Todd)

PCR of upper respiratory specimens is the diagnostic standard for severe acute respiratory syndrome coronavirus 2 infection. However, saliva sampling is an easy alternative to nasal and throat swabbing. We found similar viral loads in saliva samples and in nasal and throat swab samples from 110 patients with coronavirus disease.

Quantitative reverse transcription PCR (qRT-PCR) is the diagnostic standard for severe acute respiratory syndrome coronavirus 2 (SARS-CoV-2), the causative agent of coronavirus disease (COVID-19) (1). Testing usually is conducted on upper respiratory specimens collected using swabs (1–3). However, this method requires multiple samples and has a low sensitivity (4). Swab sampling can cause patients to cough or sneeze, uncomfortable reactions that might also increase transmission risks to healthcare workers (A. Wyllie et al., unpub. data, https://doi.org/10.1101/2020.04.16.20067835). Sampling technique proficiency also varies, especially during self-sampling (A. Wyllie et al., unpub. data, https://doi.org/10.1101/2020.04.16.20067835), which can result in false negatives. Furthermore, shortages of swabs, transport media, and personal protective equipment limit healthcare capacity to conduct SARS-CoV-2 tests that rely on swab sampling.

Saliva sampling is a noninvasive alternative to upper respiratory swabbing. We compared paired self-collected saliva samples with healthcare worker–collected nasal and throat swab specimens from 110 patients with suspected SARS-CoV-2 infection. This analysis was part of a prospective study (Facilitating a SARS CoV-2 Test for Rapid Triage) at the Royal Liverpool University and Aintree University Hospitals (Liverpool, UK). We recruited participants who had provided written informed consent and had COVID-19 symptoms. The National Health Service Research Ethics Committee (20/SC/0169) approved the study under Integrated Research Application System no. 282147.

Within 24 hours after patient consent, we collected nasal and throat swab specimens containing 1.0 mL of Amies transport medium (COPAN Diagnostics, https://www.copanusa.com). We also asked participants to funnel their saliva into a sterile cryotube (SARSTEDT, https://www.sarstedt.com). We immediately extracted RNA from the swab samples; we stored saliva samples at –80°C until processing. We extracted viral RNA using the QIAamp Viral RNA Mini Kit (QIAGEN, https://www.qiagen.com) and tested 8 μL of extracted RNA using the genesig Real-Time Coronavirus COVID-19 PCR (genesig, https://www.genesig.com). We quantified viral loads using the manufacturer's positive control (1.67×10^5 copies/μL) as reference.

Of the 110 adults recruited from April through June 2020, a total of 61 (55.5%) were women. Most participants were hospitalized; 21 (19.1%) were discharged to home directly from the emergency department. Overall, 12 (10.9%) saliva and 14 (12.7%) nasal and throat swab specimens of 110 paired samples tested positive for
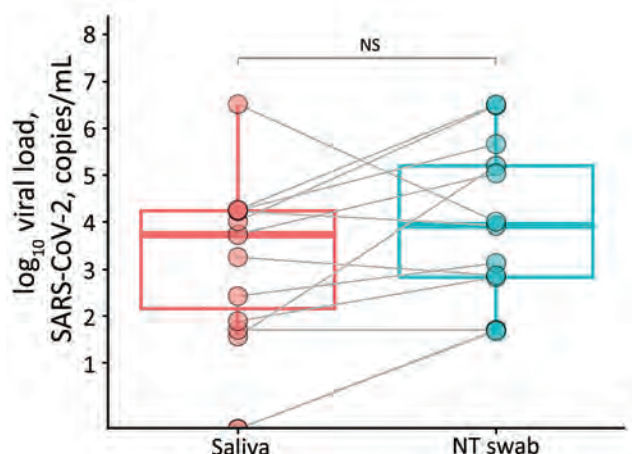

Figure. Viral load (copies/mL) of SARS-CoV-2 RNA recovered from paired saliva samples and nasal and throat swab specimens from 14 patients with coronavirus disease, United Kingdom, 2020. Viral loads are shown on a logarithmic scale. NS, not significant; NT, nasal and throat; SARS-CoV-2, severe acute respiratory syndrome coronavirus 2.

SARS-CoV-2 RNA. Viral loads for all samples ranged from 36 to 3.3×10^6 copies/mL. Overall viral loads were similar among all positive samples (Figure).

Insignificant viral load discrepancies existed among all positive samples (p = 0.1955 by Wilcoxon signed-rank paired test). Two patients tested positive (<10 copies/mL) on nasal and throat swab samples and negative on saliva samples; the discrepancies might have resulted from the different processing times of the 2 specimens because freeze-thawing can reduce the stability of RNA (5,6).

Saliva sampling can improve SARS-CoV-2 diagnostic techniques. Saliva samples are easier to collect than nasal and throat samples; the technique is noninvasive, presumably preferred by the participant, and does not require sampling proficiency. In addition, saliva sampling does not require swabs and transport media, which have limited availability during the pandemic. Our technique uses a funnel which, although helpful, might not be necessary for sample collection. Our study focused on symptomatic hospitalized participants; further research is needed on saliva sampling for patients with mild and asymptomatic SARS-CoV-2 infection.

Further studies should document the effects of storage and transport on RNA and viral loads. Rapid processing of saliva samples might benefit patients in low- and middle-income countries, where the pandemic is still accelerating and swab availability is limited (7). Furthermore, high-income countries can establish a cold chain for sample transportation. A cold chain could enable home sampling and screening of children who have rejected swabbing. It could also streamline research studies that require repeat sampling.

As rates of SARS-CoV-2 infection increase, we must continue to investigate efficient diagnostic strategies. Easy and effective diagnostic techniques, such as saliva sampling, should be evaluated in certified clinical laboratories.

This article was preprinted at https://www.medrxiv.org/content/10.1101/2020.07.09.20149534v1.

About the Author
Ms. Byrne is a doctoral candidate at the Liverpool School of Tropical Medicine, Liverpool. Her primary research interest is the application of new molecular diagnostics for the detection of emerging infectious diseases.

References
1. World Health Organization. Laboratory testing strategy recommendations for COVID-19. 2020 [cited 2020 July 1]. https://www.who.int/publications/i/item/laboratory-testing-strategy-recommendations-for-covid-19-interim-guidance
2. Centers for Disease Control and Prevention. Interim guidelines for collecting, handling, and testing clinical specimens from persons for coronavirus disease 2019 (COVID-19). 2020 [cited 2020 Jun 22]. https://www.cdc.gov/coronavirus/2019-ncov/lab/guidelines-clinical-specimens.html
3. To KKW, Tsang OTY, Leung WS, Tam AR, Wu TC, Lung DC, et al. Temporal profiles of viral load in posterior oropharyngeal saliva samples and serum antibody responses during infection by SARS-CoV-2: an observational cohort study. Lancet Infect Dis. 2020;20:565–74. https://doi.org/10.1016/S1473-3099(20)30196-1
4. Zhang W, Du RH, Li B, Zheng XS, Yang XL, Hu B, et al. Molecular and serological investigation of 2019-nCoV infected patients: implication of multiple shedding routes. Emerg Microbes Infect. 2020;9:386–9. https://doi.org/10.1080/22221751.2020.1729071
5. Ji X, Wang M, Li L, Chen F, Zhang Y, Li Q, et al. The impact of repeated freeze–thaw cycles on the quality of biomolecules in four different tissues. Biopreserv Biobank. 2017;15:475–83. https://doi.org/10.1089/bio.2017.0064
6. Kuang J, Yan X, Genders AJ, Granata C, Bishop DJ. An overview of technical considerations when using quantitative real-time PCR analysis of gene expression in human exercise research. PLoS One. 2018;13:e0196438. https://doi.org/10.1371/journal.pone.0196438
7. Gilbert M, Pullano G, Pinotti F, Valdano E, Poletto C, Boëlle PY, et al. Preparedness and vulnerability of African countries against importations of COVID-19: a modelling study. Lancet. 2020;395:871–7. https://doi.org/10.1016/S0140-6736(20)30411-6

Address for correspondence: Emily R. Adams, Centre for Drugs and Diagnostics, Liverpool School of Tropical Medicine, Pembroke Place, Liverpool L3 5QA, UK; email: emily.adams@lstmed.ac.uk

COVID-19 Outbreak, Senegal, 2020

Ndongo Dia,[1] Ndeye Aïssatou Lakh,[1]
Moussa Moise Diagne, Khardiata Diallo Mbaye,
Fabien Taieb, Ndeye Maguette Fall,
Mamadou Alioune Barry, Daye Ka, Amary Fall,
Viviane Marie Pierre Cisse Diallo, Oumar Faye,
Mamadou Malado Jallow, Idrissa Dieng,
Mamadou Ndiaye, Mamadou Diop,
Abdoulaye Bousso, Cheikh Ioucoubar,
Marie Khemesse Ngom Ndiaye,
Christophe Peyreffite, Louise Fortes,
Amadou Alpha Sall, Ousmane Faye,[1] Moussa Seydi[1]

Author affiliations: Institut Pasteur, Dakar, Senegal (N. Dia,
M.M. Diagne, F. Taieb, M.A. Barry, A. Fall, Oumar Faye,
M.M. Jallow, I. Dieng, M. Diop, C. Ioucoubar, C. Peyreffite,
A.A. Sall, Ousmane Faye, M. Seydi); Service des Maladies
infectieuses de l'hôpital Fann, Dakar (N.A. Lakh, K.D. Mbaye,
N.M. Fall, D. Ka, V.M.P.C. Diallo, L. Fortes); Ministère de la Santé
et de l'Action Sociale (MSAS), Dakar (M. Ndiaye, A. Bousso,
M.K.N. Ndiaye)

The spread of severe acute respiratory syndrome coronavirus 2 began later in Africa than in Asia and Europe. Senegal confirmed its first case of coronavirus disease on March 2, 2020. By March 4, a total of 4 cases had been confirmed, all in patients who traveled from Europe.

The spread of severe acute respiratory syndrome coronavirus 2 (SARS-CoV-2) was delayed in Africa and Latin America. The earliest recorded case of coronavirus disease (COVID-19) in Africa was identified in Egypt 7 weeks after the beginning of the outbreak (1). On February 28, 2020, Nigeria declared the first confirmed case in sub-Saharan Africa (2). On March 2, Senegal confirmed an imported case, then 2 additional imported cases the next day, and a fourth on March 4.

In Senegal, the Ministry of Health coordinated all standard operating procedures (SOPs) for the detection, notification, case management, and transport of persons with suspected COVID-19 cases from entry points (e.g., airport, harbor), healthcare centers, or locality to the referral service, using the initial WHO case definition (3). A nasopharyngeal swab specimen was collected from any symptomatic suspected case-patient or person in contact with confirmed case-patients for SARS-CoV-2–

specific real-time RT-PCR testing at the Institut Pasteur Dakar (IPD) (Appendix, https://wwwnc.cdc.gov/EID/article/26/11/20-2615-App1.pdf). Samples were accompanied by a standardized investigation form collecting demographical information, clinical details, and history of exposure (contact with a confirmed case or history of travel).

In the case of a positive diagnosis of SARS-CoV-2 infection, an active surveillance of contacts or co-exposed persons was initiated immediately around the index case. The nasopharyngeal swabs of positive patients were used for the next-generation sequencing.

Senegal experienced its first COVID-19 suspected case on February 26. During February 26–March 4, a total of 26 suspected case-patients (14 female and 12 male) were tested for a possible SARS-CoV-2 infection. Patient age range was 3–80 years (mean 35.16 years; median 33 years). Of the 26 suspected case-patients, 2 male and 2 female were confirmed as SARS-CoV-2 infected; they were 34 (patient 1), 82 (patient 2), 68 (patient 3), and 33 (patient 4) years of age. Because all were probably infected outside of the country, they were reported as imported cases. They all arrived by airplane, 3 from France and 1 from England. One case-patient had traveled manifesting symptoms undetected by the crew members. Patients 2 and 3, a married couple, traveled together; both had diabetes and hypertension, and both experienced mild clinical symptoms. All 4 patients were admitted to the Isolation and treatment Center (ITC) established by the Ministry of Health (MoH) in Dakar, Senegal. They all were apyretic the first day of hospitalization; they required mild supportive care but not oxygen therapy. In the adopted protocol, discharge of a patient from ITC required 2 consecutive negative tests for SARS-CoV-2 taken 48 hours apart. Patient 1 was discharged after 4 days, and patient 4 after 7 days, whereas patients 2 and 3 stayed for 16 days. Indeed, the viral shedding lasted longer with patients 2 and 3, the oldest. Patients 1 and 4 represented a moderate risk for dissemination of the disease, but patients 2 and 3 represented a high risk for diffusion. Investigations of contact cases and swabbing of high-risk contact cases have not to date identified any secondary cases.

We successfully obtained the complete genome sequences from the 4 SARS-CoV-2–positive patients' samples. The 4 complete genomes were nearly identical across the whole genome; sequence identity was >99%. Outside of the stretch of 44 undetermined nucleotides (19360–19403) in the genome of the strain from patient 1, only 1 nucleotide difference was mapped in open reading frame 8 of patient 4's virus isolate genome, at position 28259 with a T→C

synonymous substitution in virus isolate genomes from patients 1, 2, and 3. All genome sequences have been deposited in GISAID database (https://www.gisaid.org; accession nos. EPI_ISL_418206–9).

Phylogenetic analyses revealed that SARS-CoV-2 strains from Senegal clustered with strains from diverse origins (Europe, Asia, Latin America, and Africa).

Of note, they were close to the hCoV-19 Netherlands Haarlem 1363688 2020 EPI ISL 413572 and hCoV-19 Taiwan NTU03 2020 EPI ISL 413592 strains. The strains from Senegal clustered together, as shown by the phylogenetic branch with a high bootstrap value of 99% (Figure). All strains from Senegal belong to the ORF8-L isoform.

Figure. Phylogeny of 4 severe acute respiratory syndrome coronavirus 2 strains isolated from Senegal (green dots). Whole-genome nucleotide sequences were compared with 56 other genome sequences from the coronavirus disease pandemic retrieved from GenBank and GISAID (https://www.gisaid.org) databases. Sequences were aligned with MAFFT (https://mafft.cbrc.jp/alignment/server). We generated the phylogenetic tree by the maximum-likelihood method under the HKY85-gamma nucleotide substitution model using IQ-TREE (http://www.cibiv.at/software/iqtree). We assessed robustness of tree topology with 1,000 replicates; bootstrap values >75% are shown on the branches of the consensus trees. Phylogenetic analyses revealed that strains from Senegal clustered with strains from diverse origins (Europe, Asia, Latin America, and Africa). CoV, coronavirus; hCoV, human coronavirus.

The diagnosis of these cases showed the surveillance system of Senegal's capacity to quickly detect, isolate, and investigate those cases to take adequate control measures. Our findings indicate that the earliest cases in Senegal or sub-Saharan Africa were imported from Europe, implying that the particularly high volume of direct flights from Europe was a key factor in the spread of the virus in West Africa. However, we cannot exclude the possibility that a few COVID-19 cases were missed at that time in Senegal, including paucisymptomatic or asymptomatic cases (*4,5*). Our study emphasizes the imperative need for efficient epidemiologic investigations to identify the cases and characterize the transmission modes to prevent, control, and stop the spread of COVID-19.

Acknowledgments

We thank the Ministry of Health for COVID-19 surveillance coordination. We thank the healthcare workers and the IPD staff for its unwavering efforts in testing and tracing.

About the Author

Dr. Dia is a virologist and head of the Reference Center for influenza and other respiratory viruses at Pasteur Institute Dakar. His primary research interests are the genetic and antigenic dynamics of influenza viruses in Senegal.

References

1. World Health Organization Regional Office for the Eastern Mediterranean. Update on COVID-19 in the Eastern Mediterranean Region, 16 February 2020 [cited 2020 Sep 8]. http://www.emro.who.int/media/news/update-on-covid-19-in-the-eastern-mediterranean-region.html
2. World Health Organization Regional Office for Africa. COVID-19 situation update for WHO African region, 4 March 2020 [cited 2020 Sep 8]. https://apps.who.int/iris/bitstream/handle/10665/331330/SITREP_COVID-19_WHOAFRO_20200304-eng.pdf
3. World Health Organization. Global surveillance for human infection with novel coronavirus (2019-nCoV): interim guidance, 21 January 2020 [cited 2020 Sep 16]. https://www.ephi.gov.et/images/20200121-global-surveillance-for-2019-ncov.pdf
4. Rothe C, Schunk M, Sothmann P, Bretzel G, Froeschl G, Wallrauch C, et al. Transmission of 2019-nCoV infection from an asymptomatic contact in Germany. N Engl J Med. 2020;382:970–1. https://doi.org/10.1056/NEJMc2001468
5. Spiteri G, Fielding J, Diercke M, Campese C, Enouf V, Gaymard A, et al. First cases of coronavirus disease 2019 (COVID-19) in the WHO European Region, 24 January to 21 February 2020. Euro Surveill. 2020;25. https://doi.org/10.2807/1560-7917.ES.2020.25.9.2000178

Address for correspondence: Ndongo Dia, Institut Pasteur, Virology, 36 Avenue Pasteur, Dakar 220, Senegal; email: ndia@pasteur.sn

Burkholderia pseudomallei in Soil, US Virgin Islands, 2019

Nathan E. Stone, Carina M. Hall, A. Springer Browne, Jason W. Sahl, Shelby M. Hutton, Ella Santana-Propper, Kimberly R. Celona, Irene Guendel, Cosme J. Harrison, Jay E. Gee, Mindy G. Elrod, Joseph D. Busch, Alex R. Hoffmaster, Esther M. Ellis, David M. Wagner

Author affiliations: Northern Arizona University, Flagstaff, Arizona, USA (N.E. Stone, C.M. Hall, J.W. Sahl, S.M. Hutton, E. Santana-Propper, K.R. Celona, J.D. Busch, D.M. Wagner); US Virgin Islands Department of Health, Charlotte Amalie, US Virgin Islands, USA (A.S. Browne, I. Guendel, C.J. Harrison, E.M. Ellis); Centers for Disease Control and Prevention, Atlanta, Georgia, USA (A.S. Browne, J.E. Gee, M.G. Elrod, A.R. Hoffmaster)

The distribution of *Burkholderia pseudomallei* in the Caribbean is poorly understood. We isolated *B. pseudomallei* from US Virgin Islands soil. The soil isolate was genetically similar to other isolates from the Caribbean, suggesting that *B. pseudomallei* might have been introduced to the islands multiple times through severe weather events.

Burkholderia pseudomallei is a gram-negative soil-dwelling bacterium and the causative agent of melioidosis (*1*). *B. pseudomallei* is endemic to tropical regions around the world (*1*), but its environmental distribution in the Caribbean remains poorly understood. Although it is rare but ecologically established in Puerto Rico (*2,3*), it has not been isolated from the environment in the neighboring US Virgin Islands (USVI). After the 2017 Caribbean hurricane season, melioidosis developed in 3 persons in the USVI (*4*), 2 in St. Thomas and 1 in St. John. We aimed to determine whether, as this cluster suggests, *B. pseudomallei* might be endemic to the USVI.

We collected 480 soil and 100 freshwater samples from 29 sites (24 terrestrial and 5 freshwater) on the 3 main USVI islands (i.e., St. Thomas, St. John, and St. Croix) during January 20–April 17, 2019. We selected study sites to maximize geographic distribution across the islands and epidemiologic connection to melioidosis cases in humans (Appendix Figure 1, https://wwwnc.cdc.gov/EID/article/26/11/19-1577-App1.pdf). These efforts followed consensus guidelines for environmental sampling of *B. pseudomallei* (*5*) and

methods previously reported (*2*) with 4 modifications: we collected 20 samples per site; we collected soil samples in 2 linear transects of 10 samples each; we collected 150 mL water per sample; and we used half of each sample for our analysis (the other half was archived). Although we strove for a sampling depth of 30 cm in soil, this was impossible at some sites because of rocks and debris (Appendix Table 1). We placed environmental samples in Ashdown's liquid media for *Burkholderia* spp. enrichment (*2*). After enrichment, we extracted DNA using QiaAmp kits (QIAGEN, https://www.qiagen.com) and screened it using a *B. pseudomallei*–specific TaqMan assay (ThermoFisher Scientific, https://www.thermofisher.com)

(*6,7*). We cultured samples to isolate pure *B. pseudomallei* and generate whole-genome sequences (WGSs). We conducted a phylogenetic analysis as previously described (*2*) and conducted genetic typing on these WGSs, WGSs from the 3 patients with melioidosis from USVI in 2017, and 43 additional *B. pseudomallei* WGSs available in GenBank from the Caribbean, the Americas, and Africa (Appendix Table 2).

We isolated *B. pseudomallei* from only 1 (≈4%) of 24 soil sites, a prevalence resembling that of nearby Puerto Rico (*2*), where another study isolated *B. pseudomallei* from 2 soil samples collected at only 1 (2%) of 50 sampled sites. We obtained the *B. pseudomallei*–positive sample from site 122 (Appendix Figure 1),
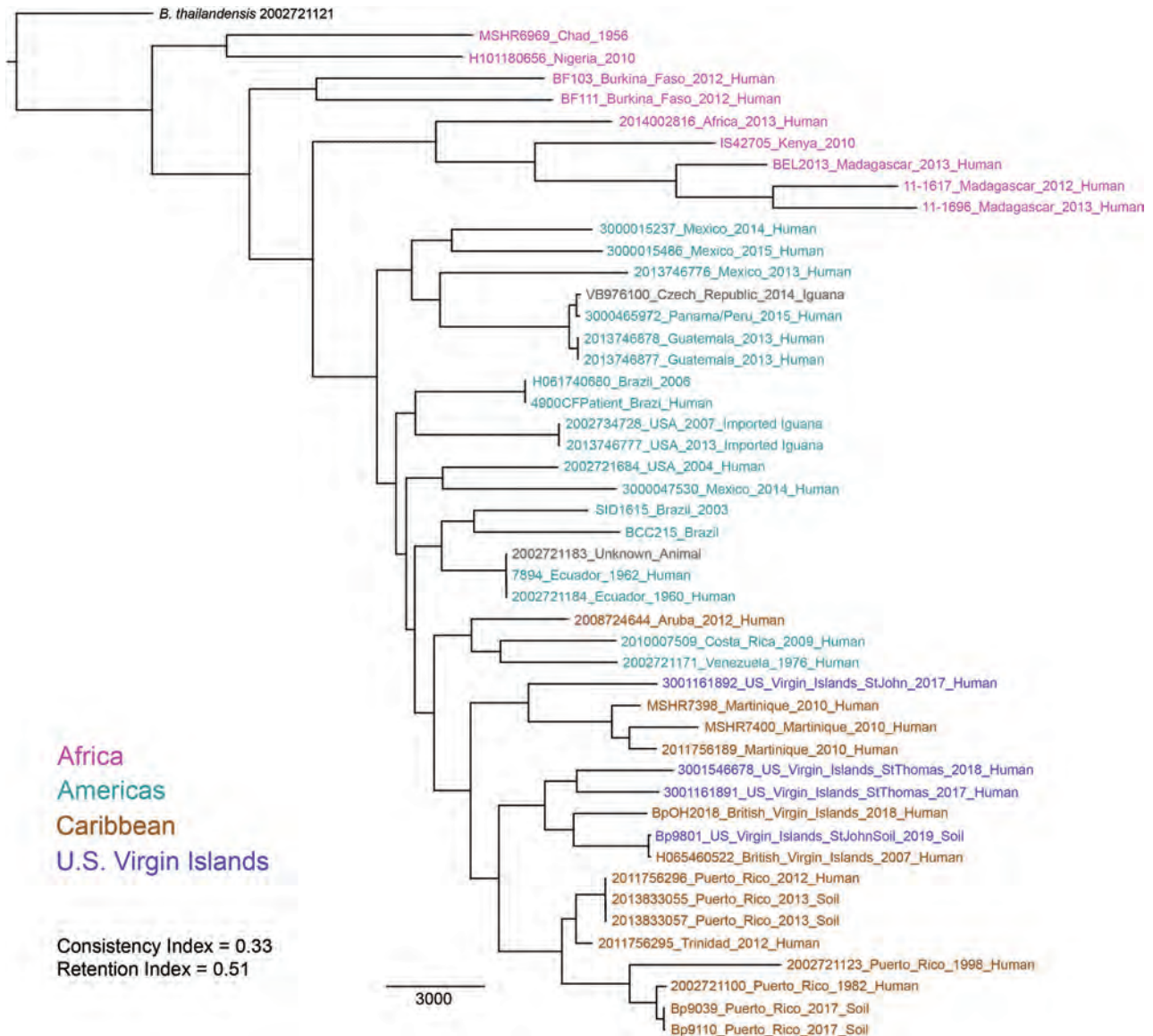

Figure. Maximum-likelihood phylogeny of *Burkholderia pseudomallei* isolates from patients and the environment in the US Virgin Islands and reference isolates available in GenBank from other countries in the Americas, Africa, and the Caribbean.

which was adjacent to a paved roadway 76 meters above sea level on eastern St. John. We collected the soil sample, which was composed of dry gravelly loam and had a pH of 6.9, from a depth of 30 cm (*8*) (Appendix; Appendix Table 1, Figure 2).

Our phylogenetic analysis assigned the 4 isolates (3 from patients, 1 from the environment) from the USVI to a monophyletic clade with all other *B. pseudomallei* isolates from the Caribbean (except 1 from Aruba) (Figure). However, none of the 4 isolates from the USVI were close genomic matches. These isolates differed by 6,355–10,115 single-nucleotide polymorphisms (SNPs) in the core genome, exhibiting more genomic diversity than *B. pseudomallei* isolates within Puerto Rico and Martinique (Figure). The 2019 soil and 2017 human isolates from St. John were not closely related (differing by 10,115 core genome SNPs), suggesting multiple introductions of *B. pseudomallei* to this island. The closest genomic match to the St. John soil isolate (differing by 170 core genome SNPs) was a 2007 isolate from Road Town, Tortola, British Virgin Islands (*9*). Although the dispersal mechanism of *B. pseudomallei* to this region is unknown, a dispersal event between these 2 locations (≈11 km) might have been caused by aerosolization of *B. pseudomallei* during an extreme weather event, such as a hurricane (*10*). This mechanism of long-distance dispersal might also explain why the 2017 isolate from St. John is more closely related to isolates from Martinique than to the other isolates from USVI; this patient from the USVI was infected shortly after hurricane Maria (*4*). We placed the 2 isolates, despite differing by 6,355 core genome SNPs, from patients on St. Thomas in a single subclade; this pattern might suggest long-term endemicity on this island. However, these scenarios are based on an analysis of a relatively small number of *B. pseudomallei* WGSs from the Caribbean.

Our findings demonstrate that *B. pseudomallei* is rare in the environment in the USVI. The 2017 cases of melioidosis and the soil isolate from St. John indicate this bacterium might be ecologically established in the USVI. Additional environmental sampling will determine the environmental distribution of *B. pseudomallei* in the USVI, aiding the development of public health strategies to mitigate the risk for melioidosis.

Acknowledgments

About the Author

Mr. Stone is a research project coordinator in the Pathogen and Microbiome Institute at Northern Arizona University. His research interests include molecular genetics and ecology of infectious diseases, population genetics of disease vectors, and public health.

References

1. Currie BJ. Melioidosis: evolving concepts in epidemiology, pathogenesis, and treatment. Semin Respir Crit Care Med. 2015;36:111–25. https://doi.org/10.1055/s-0034-1398389

2. Hall CM, Jaramillo S, Jimenez R, Stone NE, Centner H, Busch JD, et al. *Burkholderia pseudomallei*, the causative agent of melioidosis, is rare but ecologically established and widely dispersed in the environment in Puerto Rico. PLoS Negl Trop Dis. 2019;13:e0007727. https://doi.org/10.1371/journal.pntd.0007727

3. Doker TJ, Sharp TM, Rivera-Garcia B, Perez-Padilla J, Benoit TJ, Ellis EM, et al. Contact investigation of melioidosis cases reveals regional endemicity in Puerto Rico. Clin Infect Dis. 2015;60:243–50. https://doi.org/10.1093/cid/ciu764

4. Guendel I, Ekpo LL, Hinkle MK, Harrison CJ, Blaney DD, Gee JE, et al. Melioidosis after hurricanes Irma and Maria, St. Thomas/St. John District, US Virgin Islands, October 2017.Emerg Infect Dis. 2019;25:1952–5. https://doi.org/10.3201/eid2510.180959

5. Limmathurotsakul D, Dance DA, Wuthiekanun V, Kaestli M, Mayo M, Warner J, et al. Systematic review and consensus guidelines for environmental sampling of *Burkholderia pseudomallei*. PLoS Negl Trop Dis. 2013;7:e2105. https://doi.org/10.1371/journal.pntd.0002105

6. Wiersinga WJ, Virk HS, Torres AG, Currie BJ, Peacock SJ, Dance DAB, et al. Melioidosis. Nat Rev Dis Primers. 2018;4:17107. https://doi.org/10.1038/nrdp.2017.107

7. Novak RT, Glass MB, Gee JE, Gal D, Mayo MJ, Currie BJ, et al. Development and evaluation of a real-time PCR assay targeting the type III secretion system of *Burkholderia pseudomallei*. J Clin Microbiol. 2006;44:85–90. https://doi.org/10.1128/JCM.44.1.85-90.2006

8. US Department of Agriculture. Web Soil Survey. 2018 [cited 2019 Sept 16]. https://websoilsurvey.sc.egov.usda.gov

9. Corral DM, Coates AL, Yau YC, Tellier R, Glass M, Jones SM, et al. *Burkholderia pseudomallei* infection in a cystic fibrosis patient from the Caribbean: a case report. Can Respir J. 2008;15:237–9. https://doi.org/10.1155/2008/290412

10. Cheng AC, Jacups SP, Gal D, Mayo M, Currie BJ. Extreme weather events and environmental contamination are associated with case-clusters of melioidosis in the Northern Territory of Australia. Int J Epidemiol. 2006;35:323–9. https://doi.org/10.1093/ije/dyi271

Address for correspondence: David M. Wagner, Northern Arizona University, PO Box 4073, Flagstaff, AZ 86011, USA; email: dave.wagner@nau.edu

Nontuberculous Mycobacterial Pulmonary Disease from *Mycobacterium hassiacum*, Austria

Helmut J.F. Salzer, Bakari Chitechi, Doris Hillemann, Michael Mandl, Christian Paar, Monika Mitterhumer, Bernd Lamprecht, Florian P. Maurer

Author affiliations: Kepler University Hospital, Linz, Austria (H.J.F. Salzer, B. Chitechi, C. Paar, M. Mitterhumer, M. Mandl, B. Lamprecht); National and WHO Supranational Reference Centre for Mycobacteria–Borstel, Borstel, Germany (D. Hillemann, F.P. Maurer)

The clinical relevance of newly described nontuberculous mycobacteria is often unclear. We report a case of pulmonary infection caused by *Mycobacterium hassiacum* in an immunocompetent patient in Austria who had chronic obstructive pulmonary disease. Antimicrobial drug susceptibility testing showed low MICs for macrolides, aminoglycosides, fluoroquinolones, tetracyclines, imipenem, and linezolid.

Currently, >170 species of nontuberculous mycobacteria (NTM) are recognized (1), most considered nonpathogenic to humans. However, some NTM can cause severe pulmonary disease. We recently observed a case of NTM pulmonary disease (NTM-PD) in Austria that was caused by *Mycobacterium hassiacum*.

In January 2019, a 62-year-old man was admitted to the outpatient clinic at Kepler University Hospital in Linz, Austria, having had dry cough and progressive dyspnea for several months. No weight loss or night sweats were reported. He had a medical history of chronic obstructive pulmonary disease with severe emphysema because of cigarette smoking. The patient had no history of tuberculosis or NTM-PD and was unaware of any contact with persons with mycobacterial infections.

Chest radiograph showed new consolidations in the right and left upper lung lobes compared with images obtained 1 year before. We performed a high-resolution computed tomography scan of the chest and an 18F-fluorodeoxyglucose positron emission tomography (18F-FDG PET) scan that indicated metabolic activity consistent with an inflammatory process (Figure). In addition, results of tests for serum lung cancer biomarkers, including CA 19-9, CEA (carcinoembryonic antigen), CYFRA 21-1, and NSE (neuron-specific enolase), and for HIV-1 and HIV-2 were negative. Transbronchial catheter aspiration from the posterior lung segment of the right upper lung lobe showed no microscopic evidence of bacteria, acid-fast bacilli, or fungi. The result from a PCR assay (*Mycobacterium tuberculosis* PCR kit; Geneproof, https://www.geneproof.com) for *M. tuberculosis* complex DNA was negative. Results from bacterial and fungal cultures were unremarkable. Because the patient was at high risk for developing pneumothorax due to severe emphysema, no transbronchial biopsy was taken during initial bronchoscopy.
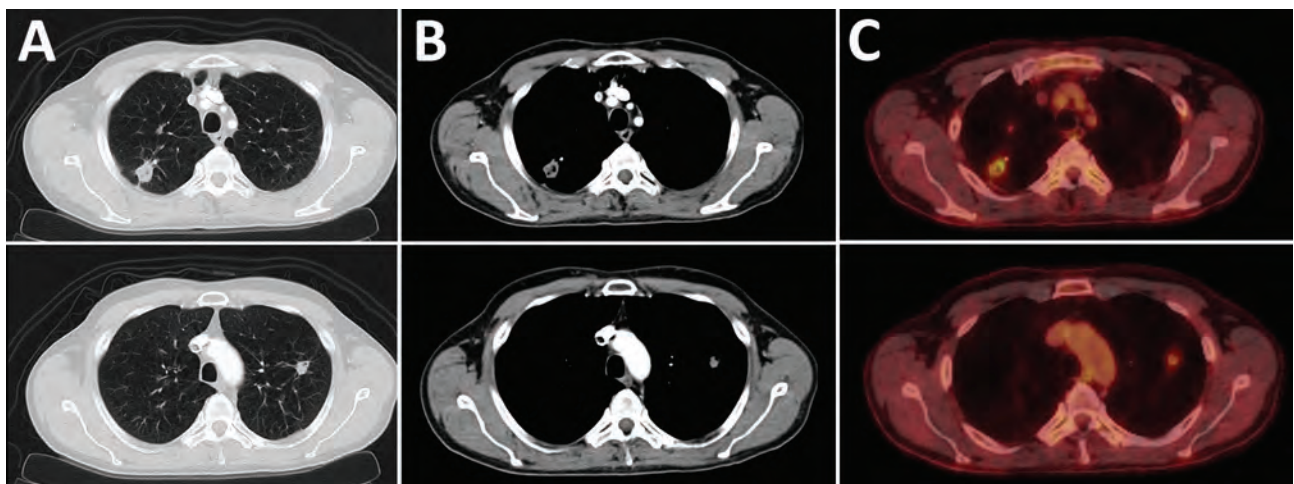

Figure. High-resolution computed tomography and 18F-fluorodeoxyglucose positron emission tomography scans of the chest showing pulmonary lesions caused by *Mycobacterium hassiacum* in a 62-year-old man, Austria. A and B) Computed tomography scans of the chest showing a subpleural thick-walled cavitary lesion in the posterior segment of the right upper lung lobe with associated pleural thickening and a smaller adjacent partly calcified solitary nodule. Another solid nodule of 13 mm diameter was found in the left upper lung lobe. C) Positron emission tomography scan showing a tracer uptake in both lesions with a standardized uptake values of 5 (top image) and 1.9 (bottom image).

Mycobacterial culture results of the transbronchial catheter aspirate were negative after 8 weeks of incubation. Consequently, we performed a computed tomography–guided needle biopsy of the cavitary lesion in the right upper lung lobe. Histological results showed granulomatous inflammation with focal eosinophilic necrosis. We detected no atypical cells, acid-fast bacilli, or fungal hyphae and subsequent immunohistochemistry testing revealed no evidence of malignant disease.

Results of a PCR of formalin-fixed, paraffin-embedded lung tissue revealed no DNA of *M. tuberculosis* (MTB Nested ACE Detection Kit, Seegene, http://www.seegene.com) or of 13 different NTM species (MYCO Direct 1.7 LCD-Array Kit; Chipron, https://www.chipron.com). However, native lung tissue was used to set up both liquid (MGIT 960 system, Becton Dickinson, https://www.bd.com) and solid mycobacterial cultures (Löwenstein-Jensen and Middlebrook agar), which showed growth after 21 days of incubation at 37°C. 16S rRNA gene sequence analysis identified *M. hassiacum* (GenBank accession no. AF547933.1).

We analyzed the samples by DNA sequencing of the first 500 bp of the 5′ region of the 16S rRNA gene (*2*,*3*). The analyzed DNA fragment showed 500-bp identity with the *M. hassiacum* type strain 3849 16S ribosomal RNA (sequence identification NR_026011.1). More than 25 mismatches were found with the type strains of *M. thermoresistibile* strain NCTC10409, *M. goodii* strain ATCC 700504, and *M. celeriflavum* strain AFPC-000207. Antimicrobial susceptibility testing by broth microdilution method according to Clinical and Laboratory Standards Institute guidelines (*4*,*5*) showed low MICs for clarithromycin (≤0.06 µg/mL), amikacin (≤1 µg/mL), tobramycin (≤1 µg/mL), linezolid (≤1.0 µg/mL), moxifloxacin (≤0.25 µg/mL), ciprofloxacin (0.25 µg/mL), doxycycline (≤0.12 µg/mL), minocycline (≤1 µg/mL), tigecycline (0.25 µg/mL), imipenem (≤2.0 µg/mL), and trimethoprim/sulfamethoxazole (4.75 µg/mL) (*4*,*5*). Comparably high MIC values were observed for cefoxitin (32 µg/mL), ceftriaxone (>64 µg/mL), and cefepime (>32 µg/mL). Antimycobacterial treatment, including clarithromycin (500 mg orally 2×/d), moxifloxacin (400 mg orally 1×/d), and minocycline (100 mg orally 2×/d), was initiated. On first follow-up visit, the patient indicated that the treatment had been well tolerated.

Since *M. hassiacum* was described as a new species in 1997, 3 cases of suspected infections caused by *M. hassiacum* have been reported in the medical literature (*6*). So far, *M. hassiacum* has been reported as the causative agent for peritonitis and cystitis (*7*,*8*). In addition, *M. hassiacum* was recently isolated from a respiratory sample in a patient in Germany with exacerbation of chronic obstructive pulmonary disease (*9*). However, that patient likely did not have NTM-PD because *M. hassiacum* was isolated in only 1 of 3 sputum samples, he showed no NTM-specific radiological abnormalities in a chest radiograph, and his clinical condition improved rapidly without any antimycobacterial treatment.

In contrast, the patient we report fulfills 3 diagnostic criteria of NTM-PD: 1) an NTM-specific radiologic pattern characterized by new nodules in both upper lung lobes in a high-resolution computed tomography scan of the chest, 2) a positive culture result from a sterile computed tomography–guided needle biopsy, as well as typical mycobacterial histopathologic features including granulomatous inflammation, and 3) exclusion of other disorders including pulmonary tuberculosis or lung cancer (*10*).

In conclusion, detection of *M. hassiacum* in patients fulfilling the criteria for NTM-PD should be considered a potentially relevant finding. Further studies are needed to evaluate the precise role of *M. hassiacum* as an emerging mycobacterial pathogen.

About the Author

Dr. Salzer works as a senior physician in the Department of Pulmonary Medicine at the Kepler University Hospital in Linz, Austria. His primary research interests include chronic pulmonary infections, especially nontuberculous mycobacterial pulmonary diseases and chronic pulmonary aspergillosis.

References

1. Fedrizzi T, Meehan CJ, Grottola A, Giacobazzi E, Fregni Serpini G, Tagliazucchi S, et al. Genomic characterization of nontuberculous mycobacteria. Sci Rep. 2017;7:45258. https://doi.org/10.1038/srep45258
2. Richter E, Niemann S, Gloeckner FO, Pfyffer GE, Rüsch-Gerdes S. *Mycobacterium holsaticum* sp. nov. Int J Syst Evol Microbiol. 2002;52:1991–6. https://doi.org/10.1099/00207713-52-6-1991
3. Böddinghaus B, Rogall T, Flohr T, Blöcker H, Böttger EC. Detection and identification of mycobacteria by amplification of rRNA. J Clin Microbiol. 1990;28:1751–9. https://doi.org/10.1128/JCM.28.8.1751-1759.1990
4. Clinical and Laboratory Standards Institute. Susceptibility testing of mycobacteria, *Nocardia* spp., and other aerobic actinomycetes, 3rd edition (standard M24). Wayne (PA): The Institute; 2018.
5. Clinical and Laboratory Standards Institute. Performance standards for susceptibility testing of mycobacteria, *Nocardia*

spp., and other aerobic actinomycetes, 3rd edition (standard M62). Wayne (PA): The Institute; 2018.

6. Schröder KH, Naumann L, Kroppenstedt RM, Reischl U. *Mycobacterium hassiacum* sp. nov., a new rapidly growing thermophilic mycobacterium. Int J Syst Bacteriol. 1997; 47:86–91. https://doi.org/10.1099/00207713-47-1-86

7. Jiang SH, Roberts DM, Clayton PA, Jardine M. Non-tuberculous mycobacterial PD peritonitis in Australia. Int Urol Nephrol. 2013;45:1423–8. https://doi.org/10.1007/s11255-012-0328-4

8. Tortoli E, Reischl U, Besozzi G, Emler S. Characterization of an isolate belonging to the newly described species *Mycobacterium hassiacum*. Diagn Microbiol Infect Dis. 1998;30:193–6. https://doi.org/10.1016/S0732-8893(97)00242-3

9. Deinhardt-Emmer S, Höring S, Mura C, Hillemann D, Hermann B, Sachse S, et al. First time isolation of *Mycobacterium hassiacum* from a respiratory sample. Clin Med Insights Circ Respir Pulm Med. 2018;12:1179548417747529. https://doi.org/10.1177/1179548417747529

10. Griffith DE, Aksamit T, Brown-Elliott BA, Catanzaro A, Daley C, Gordin F, et al.; ATS Mycobacterial Diseases Subcommittee. An official ATS/IDSA statement: diagnosis, treatment, and prevention of nontuberculous mycobacterial diseases. Am J Respir Crit Care Med. 2007;175:367–416. Erratum in Am J Respir Crit Care Med. 2007 Apr 1;175:744–5. https://doi.org/10.1164/rccm.200604-571ST

Address for correspondence: Helmut J.F. Salzer, Department of Pulmonary Medicine, Kepler University Hospital, Krankenhausstrasse 9, 4021 Linz, Austria; email: helmut.salzer@kepleruniklinikum.at

Large Outbreak of Guillain-Barré Syndrome, Peru, 2019

César V. Munayco, Ronnie G. Gavilan,
Gladys Ramirez, Manuel Loayza, Maria L. Miraval,
Erin Whitehouse, Radhika Gharpure, Jesus Soares,
Hans Vasquez Soplopuco, James Sejvar

Author affiliations: Centro Nacional de Epidemiología
Prevención y Control de Enfermedades, Lima, Peru
(C.V. Munayco, G. Ramirez, M. Loayza); Instituto Nacional de
Salud, Lima (R.G. Gavilan, M.L. Miraval, H.V. Soplopuco); Centers
for Disease Control and Prevention, Atlanta, Georgia, USA
(E. Whitehouse, R. Gharpure, J. Soares, J. Sejvar)

Outbreaks of Guillain-Barré syndrome (GBS) are uncommon. In May 2019, national surveillance in Peru detected an increase in GBS cases in excess of the expected incidence of 1.2 cases/100,000 population. Several clinical and epidemiologic findings call into question the suggested association between this GBS outbreak and *Campylobacter*.

Guillain-Barré syndrome (GBS) is the most common form of acute flaccid paralysis worldwide (*1*). It is characterized by motor weakness, areflexia, sensory abnormalities, and cytoalbuminologic dissociation in cerebrospinal fluid (*2*). An upper respiratory or gastrointestinal illness typically precedes GBS (*3*). *Campylobacter jejuni* infection is the most frequently identified precipitant of GBS and usually is associated with the acute motor axonal neuropathy form of GBS (*4*).

During the week of May 26, 2019, the Peruvian Ministry of Health surveillance system detected several cases of suspected GBS that exceeded the expected incidence of 1.2 cases/100,000 persons/year (i.e., 29 cases/year) (*1*). Since 2016, hospitals in Peru have reported suspected GBS cases to a passive surveillance system (https://www.dge.gob.pe/portal/index.php?option=com_content&view=article&id=653). In early May 2019, when the system was modified to an active surveillance system because of increasing incidence, the National Center of Epidemiology, Prevention, and Disease Control solicited cases. Examining physicians classified cases in accordance with the Brighton Collaboration case definition for GBS (*5*). The Instituto Nacional de Salud tested serum, urine, nasal swab samples, and feces for infectious pathogens using molecular panels for multipathogen detection (bioMérieux, https://www.biomerieux-diagnostics.com) and conventional microbiology assays.

During May 20–July 27, 2019, we identified 683 suspected or confirmed GBS cases in Peru. The largest outbreaks of GBS have involved ≈30–50 cases, except for large GBS outbreaks associated with Zika virus infection; thus, this outbreak was extremely unusual because of its size. Of the cases, 32 (6.9%) were Brighton level 1, 188 (27.5%) were Brighton level 2, and 463 (67.7%) were Brighton level 3. We classified Brighton levels 1 and 2 cases as confirmed, and Brighton level 3 cases as suspected (Figure; Appendix Figures 1, 2, https://wwwnc.cdc.gov/EID/article/26/11/20-0127-App1.pdf). Nine of Peru's 24 departments reported GBS cases, which resulted in an annualized incidence of 30.9 cases/100,000 persons/year (Table).

Of the 683 GBS patients, 287 (42.0%) had descending muscle weakness and 446 (65.3%) had ascending muscle weakness. Of 530 patients for whom data on
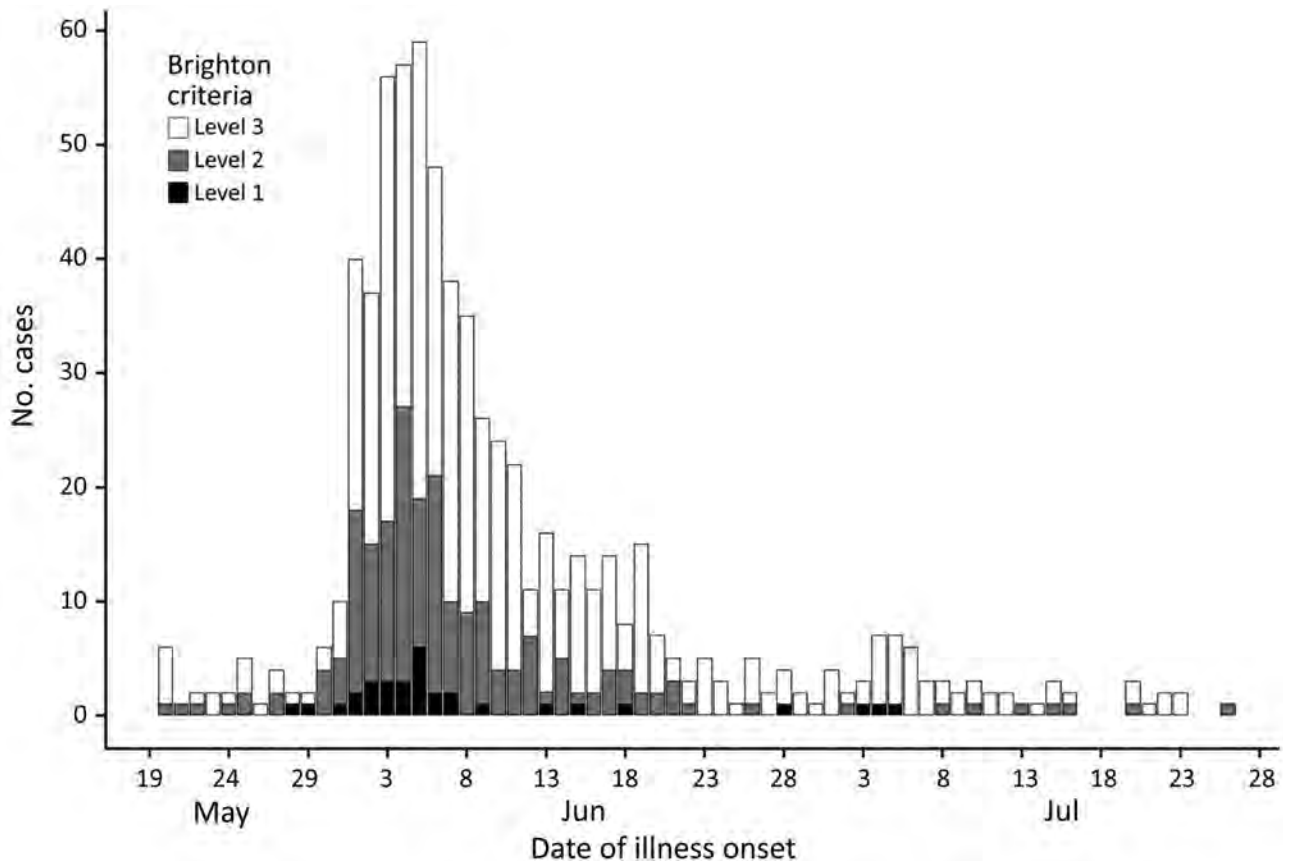
Figure. Cases of Guillain-Barré syndrome classified by Brighton Collaboration criteria (5) and date of illness onset, Peru, May–July 2019.

antecedent illness were complete in the 4 weeks before neurologic symptom onset, 219 (41.3%) reported respiratory and gastrointestinal infections, 195 (36.8%) reported only a respiratory infection, 3 (0.6%) reported only a gastrointestinal infection, and 113 (21.3%) did not report any infection. Of 426 patients for whom hospitalization data were available, 64 (15.0%) required mechanical ventilation. Of 147 patients who had an electrodiagnostic exam, 100 (68.0%) had acute motor axonal neuropathy.

Clinical samples received by Instituto Nacional de Salud were as follows: serum (622 samples), urine (191), cerebrospinal fluid (230), nasal and pharyngeal swab samples (394), and feces (362) (Appendix Tables 1–3). We detected *Campylobacter* spp. in 19 (5.2%) fecal samples. Fecal cultures yielded 8 isolates confirmed as *C. jejuni* biotype I by Gram stain (6). Isolates were highly related by core-genome multilocus sequence typing and were sequence type 2993, Penner serotype HS:41.

This GBS outbreak was unusual because of the large number of cases. The incidence rate was nearly 25 times higher than expected (1) and higher than previously described GBS outbreaks. The rapid increase in numbers, followed by an equally precipitous decrease, might suggest a point-source exposure. The outbreak affected many geographically disparate

Table. General characteristics of persons with Guillain-Barré syndrome, Peru, 2019

Characteristic	No. cases	Population	Cases/100,000 population
Sex			
M	401	10,416,496	3.85
F	282	10,882,518	2.59
Age, y			
0–11	48	4,321,980	1.11
12–17	45	2,223,271	2.02
18–29	118	4,498,823	2.62
30–59	333	7,870,813	4.23
>60	139	2,384,127	5.83
Area			
Junín	132	1,389,850	9.50
Piura	115	1,901,896	6.05
Cajamarca	53	1,543,104	3.43
La Libertad	57	1,956,389	2.91
Lambayeque	31	1,300,720	2.38
Lima	247	10,458,367	2.36
Callao	25	1,067,815	2.34
Huancavelica	10	509,117	1.96
Ancash	13	1,171,756	1.11
Total	683	21,299,014	3.21
Peru, total	709	32,526,084	2.18

regions, including some that differed substantially in geoclimatic properties.

General demographic features, such as slight male predominance and greater incidence with increased age, are typical for GBS (*7*). However, in many patients, a descending, rather than the more common ascending, paralysis developed (*8*). The clinical significance of this observation is unclear. Electrophysiologically, most cases appeared to have the acute motor axonal neuropathy phenotype of GBS, which has been closely associated with antecedent *C. jejuni* infection (*9*).

PCR and culture detected the *C. jejuni* outbreak reported here. Genetic analysis confirmed the clonality of these isolates recovered from affected regions of Peru and identified genotype sequence type 2993, which has been associated with GBS outbreaks in China (*10*). These results support the hypothesis that this unprecedented GBS outbreak was related to an antecedent *Campylobacter* outbreak with point source. However, diarrheal illnesses shortly before or during the GBS outbreak were not reported; previous GBS outbreaks associated with *Campylobacter* mostly have occurred in the context of larger outbreaks of symptomatic diarrheal illness (*10*). Because of the wide distribution of outbreaks in many geographically separated regions, we questioned how all areas were exposed to *C. jejuni* within a short time frame.

Limitations of our investigation included nonsystematic testing of samples and incomplete data on variables, such as hospitalization and clinical features. Epidemiologic investigations are ongoing to determine the potential antigenic source of the presumed infection, testing for *Campylobacter*-specific IgM and antiganglioside antibodies, additional isolate sequencing, and active surveillance for new cases.

About the Author

Dr. Munayco is a physician, researcher, and epidemiologist at the Uniformed Services University of the Health Sciences; director of the unit of epidemiological research and evaluation of sanitary interventions at Centro Nacional de Epidemiología, Prevención y Control de Enfermedades, Ministry of Health; and professor in the School of Medicine at Universidad Peruana de Ciencias Aplicadas. His primary research interests include public health, mathematical modeling of communicable and noncommunicable diseases, health economics, social determinants and inequality, and monitoring and evaluation of health interventions and public policies.

References

1. Sejvar JJ, Baughman AL, Wise M, Morgan OW. Population incidence of Guillain-Barré syndrome: a systematic review and meta-analysis. Neuroepidemiology. 2011;36:123–33. https://doi.org/10.1159/000324710
2. Ansar V, Valadi N. Guillain-Barré syndrome. Prim Care. 2015;42:189–93. https://doi.org/10.1016/j.pop.2015.01.001
3. Govoni V, Granieri E. Epidemiology of the Guillain-Barré syndrome. Curr Opin Neurol. 2001;14:605–13. https://doi.org/10.1097/00019052-200110000-00009
4. Nachamkin I, Arzarte Barbosa P, Ung H, Lobato C, Gonzalez Rivera A, Rodriguez P, et al. Patterns of Guillain-Barré syndrome in children: results from a Mexican population. Neurology. 2007;69:1665–71. https://doi.org/10.1212/01.wnl.0000265396.87983.bd
5. Sejvar JJ, Kohl KS, Gidudu J, Amato A, Bakshi N, Baxter R, et al.; Brighton Collaboration GBS Working Group. Guillain-Barré syndrome and Fisher syndrome: case definitions and guidelines for collection, analysis, and presentation of immunization safety data. Vaccine. 2011;29:599–612. https://doi.org/10.1016/j.vaccine.2010.06.003
6. Lior H. New, extended biotyping scheme for *Campylobacter jejuni*, *Campylobacter coli*, and "*Campylobacter laridis*". J Clin Microbiol. 1984;20:636–40. https://doi.org/10.1128/JCM.20.4.636-640.1984
7. Hughes RA, Cornblath DR. Guillain-Barré syndrome. Lancet. 2005;366:1653–66. https://doi.org/10.1016/S0140-6736(05)67665-9
8. Hughes RA, Rees JH. Clinical and epidemiologic features of Guillain-Barré syndrome. J Infect Dis. 1997;176(Suppl 2):S92–8. https://doi.org/10.1086/513793
9. Zhang M, He L, Li Q, Sun H, Gu Y, You Y, et al. Genomic characterization of the Guillain-Barré syndrome-associated *Campylobacter jejuni* ICDCCJ07001 isolate. PLoS One. 2010;5:e15060. https://doi.org/10.1371/journal.pone.0015060
10. Zhang M, Li Q, He L, Meng F, Gu Y, Zheng M, et al. Association study between an outbreak of Guillain-Barré syndrome in Jilin, China, and preceding *Campylobacter jejuni* infection. Foodborne Pathog Dis. 2010;7:913–9. https://doi.org/10.1089/fpd.2009.0493

Address for correspondence: Cesar V. Munayco, Calle Daniel Olaechea 199, Jesus Maria, Lima, Peru; email: cmunayco@dge.gob.pe; James Sejvar, Centers for Disease Control and Prevention, 1600 Clifton Rd NE, Mailstop H24-12, Atlanta, GA 30329-4027, USA; email: zea3@cdc.gov

Osteomyelitis Due to *Mycobacterium goodii* in an Adolescent, United States

Alejandro Diaz, Monica I. Ardura, Huanyu Wang, Stella Antonara, Christopher P. Ouellette

Author affiliations: Nationwide Children's Hospital and The Ohio State University, Columbus, Ohio, USA (A. Diaz, M.I. Ardura, H. Wang, C.P. Ouellette); Riverside Methodist Hospital, Columbus (S. Antonara)

Osteomyelitis is a rare clinical manifestation of infection with nontuberculous mycobacteria (NTM). We report an adolescent with femoral osteomyelitis associated with prosthetic material due to an emerging pathogen, *Mycobacterium goodii*. Application of *secA1* and 16S ribosomal RNA gene sequencing reliably determined the NTM species, enabling targeted antimicrobial therapy.

Nontuberculous mycobacteria (NTM) are an emerging cause of human infections, likely because of improved detection methods and an increasing high-risk population (*1–3*). Conventional methods to identify NTM species rely on phenotypic characteristics to differentiate the most common species, but these labor-intensive and time-consuming methods delay final identification and appropriate therapy (*2*). Sequencing of 16S rRNA and *secA1* (essential secretory protein SecA1) genes provides an accurate and cost-effective method for NTM identification, offering a turnaround time of 1–2 days compared with 2–6 weeks for results from conventional methods (*4*).

M. goodii is a rapidly growing mycobacterium that can be nonpigmented or late-pigmented. Before 1999, the original classification of the 3 species in the *M. smegmatis* group identified 28 isolates of *M. goodii*, which most often were associated with posttraumatic wound infections (*5*). Since then, *M. goodii* has been implicated in infections related to prosthetic devices and penetrating trauma. Three recent reports detail 19 cases of *M. goodii* infections in patients with a mean age of 60 years (range 6–85 years). Types of infection included prosthetic device or pocket infection (n = 12), wound infection (n = 3), endocarditis (n = 1), pneumonia (n = 2), and endophthalmitis (n = 1) (*6–8*). We noted only 3 pediatric cases in the literature: 2 cases of pneumonia, 1 in a 15-year-old girl and 1 in a 7-week-old infant; and 1 soft tissue infection in a 6-year-old boy (*6,9,10*).

We report a 15-year-old male patient with severe bilateral knee flexion contractures who underwent bilateral femoral extension osteotomies with hardware implantation. Two months later, he had intermittent low-grade fevers, right thigh pain, and surgical wound dehiscence with discharge. Initial laboratory results showed elevated leukocyte count, erythrocyte sedimentation rate, and C-reactive protein (Figure). An incision and drainage was performed but the femoral hardware was retained; 4 days later, a second incision and drainage was performed with primary closure.

Acid-fast bacillus (AFB) cultures were obtained; after 22 days, NTM growth was identified. Empiric therapy was initiated with intravenous (IV) amikacin (15 mg/kg 1×/d), IV cefoxitin (3,000 mg every 8 h), oral azithromycin (250 mg 1×/d), and oral ciprofloxacin (500 mg every 12 h). Two weeks later, the patient underwent a third incision and drainage and hardware was removed because of recrudescent fever and surgical site discharge. AFB tissue cultures from bone again grew NTM. Sequencing of the *secA1* and 16S genes from all NTM isolates identified *M. goodii* (Appendix Figure, https://wwwnc.cdc.gov/EID/article/26/11/20-0206-App1.pdf). The patient's therapy was modified to oral trimethoprim/sulfamethoxazole (TMP/SMX; 320 mg 2×/d, 6 mg/kg/dose based on TMP component), with continued IV amikacin and oral ciprofloxacin. Antimicrobial susceptibility testing results confirmed susceptibility to TMP/SMX, ciprofloxacin, amikacin, and doxycycline but noted resistance to clarithromycin and cefoxitin. Amikacin was discontinued after a total of 36 days of therapy.

Five months after his last surgical intervention, the patient had clear discharge from his right thigh. A small superficial skin abscess was noted on magnetic resonance imaging. Fine needle aspiration of the fluid collection was performed from which AFB cultures were sterile but universal bacterial 16S rDNA PCR detected *M. goodii*. Given the potential for antimicrobial resistance, oral doxycycline (100 mg 2×/d) was added to the patient's antimicrobial drug regimen. The 3-drug regimen was continued for an additional 4 months. Repeat imaging at the end of therapy showed no evidence of fluid reaccumulation, and the patient has not had an infection relapse for 10 months after discontinuation of antimicrobial drug therapy. No other *M. goodii* infections have been identified at our institution since this case.

NTM osteomyelitis treatment can be challenging. Management strategies include prolonged antimicrobial drug therapy, surgical debridement, and removal of foreign material (*2*). *M. goodii* usually is susceptible to TMP/SMX, amikacin, ciprofloxacin,
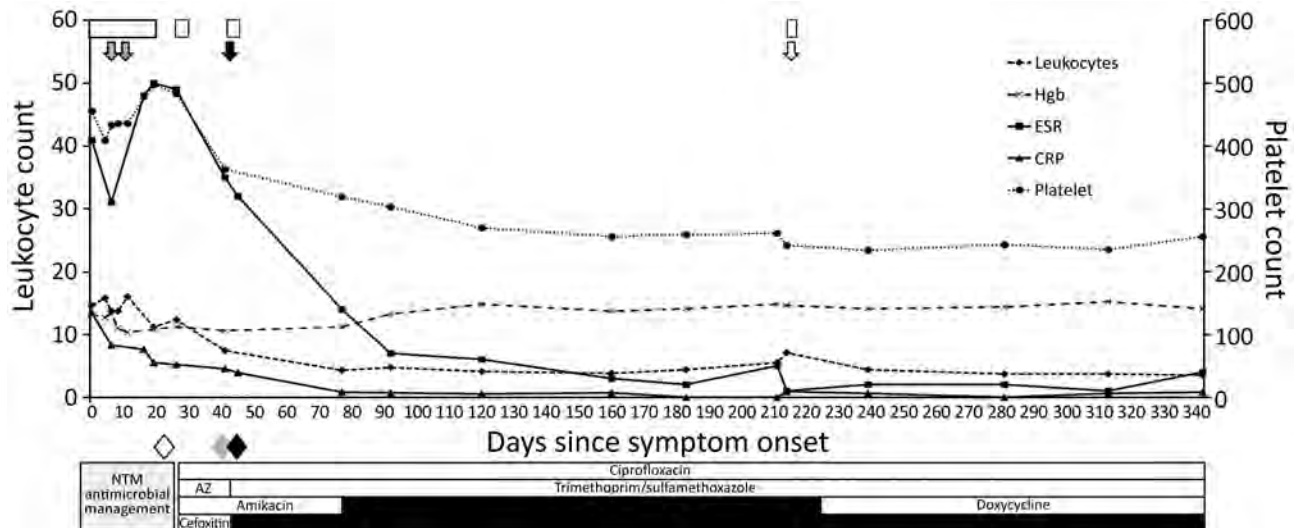
Figure. Timeline of laboratory values, surgical interventions, notification of pertinent culture results, and antimicrobial drug therapy in a case of osteomyelitis due to *Mycobacterium goodii* in an adolescent, United States. White boxes represent periods of hospitalization. Gray arrows indicate dates of surgical intervention with cultures obtained and femoral hardware retained. Solid black arrow indicates surgical intervention with cultures obtained and femoral hardware removed. Shaded arrow indicates interventional radiology aspiration of subcutaneous fluid collection with cultures obtained. Shaded diamond indicates first notification of nontuberculous mycobacterium growth. Solid gray diamond indicates first notification of *M. goodii* by 16S and *secA1* sequencing. Solid black diamond indicates first notification of susceptibility results for *M. goodii.* AZ, azithromycin; CRP, C-reactive protein; ESR, erythrocyte sedimentation rate; Hgb, hemoglobin; NTM, nontuberculous mycobacteria.

imipenem, and doxycycline (*5*). However, *M. goodii* is intrinsically resistant to macrolides and rifampin, which commonly are used for empirical therapy of NTM infections; early species identification is crucial to ensuring effective and timely treatment (*2*,*5*,*6*). Optimal treatment is unknown, but a combination of ≥ 2 active drugs, for a minimum of 6 months, combined with surgical debridement and hardware removal, is recommended to ensure clinical and bacteriological cure and prevent antimicrobial resistance (*2*,*6*).

Our case shows similarities to prior adult reports, specifically prosthetic-associated *M. goodii* infection, and further highlights the emergence of this pathogen in the pediatric population. Given the repeated culture-positive results from our patient, we do not believe this case was the result of an environmental contaminant. In addition, no other cases of *M. goodii* infection have been identified at our institution to suggest nosocomial infection, but we cannot definitively exclude this mode of acquisition.

In conclusion, our case highlights *M. goodii* as an emerging pediatric NTM pathogen. These findings underscore the use of *secA1* and 16S rRNA sequencing for rapid species identification to enable timely and effective antimicrobial drug therapy.

About the Author

Dr. Diaz is a pediatric infectious disease fellow at Nationwide Children's Hospital, Columbus, Ohio, USA. His research interests include antibiotic stewardship and antimicrobial resistance.

References

1. Brown-Elliott BA, Wallace RJ Jr. Clinical and taxonomic status of pathogenic nonpigmented or late-pigmenting rapidly growing mycobacteria. Clin Microbiol Rev. 2002;15:716–46. https://doi.org/10.1128/CMR.15.4.716-746.2002
2. Griffith DE, Aksamit T, Brown-Elliott BA, Catanzaro A, Daley C, Gordin F, et al.; ATS Mycobacterial Diseases Subcommittee; American Thoracic Society; Infectious Disease Society of America. An official ATS/IDSA statement: diagnosis, treatment, and prevention of nontuberculous mycobacterial diseases. Am J Respir Crit Care Med. 2007;175:367–416. https://doi.org/10.1164/rccm.200604-571ST
3. Tebruegge M, Pantazidou A, MacGregor D, Gonis G, Leslie D, Sedda L, et al. Nontuberculous Mycobacterial Disease in Children - Epidemiology, Diagnosis & Management at a Tertiary Center. PLoS One. 2016; 11:e0147513. https://doi.org/10.1371/journal.pone.0147513
4. Cook VJ, Turenne CY, Wolfe J, Pauls R, Kabani A. Conventional methods versus 16S ribosomal DNA sequencing for identification of nontuberculous mycobacteria: cost analysis. J Clin Microbiol. 2003;41:1010–5. https://doi.org/10.1128/JCM.41.3.1010-1015.2003
5. Brown BA, Springer B, Steingrube VA, Wilson RW, Pfyffer GE, Garcia MJ, et al. *Mycobacterium wolinskyi* sp. nov.

and *Mycobacterium goodii* sp. nov., two new rapidly growing species related to *Mycobacterium smegmatis* and associated with human wound infections: a cooperative study from the International Working Group on Mycobacterial Taxonomy. Int J Syst Bacteriol. 1999;49:1493–511. https://doi.org/10.1099/00207713-49-4-1493

6. Salas NM, Klein N. *Mycobacterium goodii:* an emerging nosocomial pathogen: a case report and review of the literature. Infect Dis Clin Pract (Baltim Md). 2017;25:62–5. https://doi.org/10.1097/IPC.0000000000000428

7. Harper G, Ong JL, Costanigro L. Oh Goody! Two additional *Mycobacterium goodii* infections. Open Forum Infectious Diseases. 2015;2(suppl_1):576. https://doi.org/10.1093/ofid/ofv133.450

8. Parikh RB, Grant M. *Mycobacterium goodii* endocarditis following mitral valve ring annuloplasty. Ann Clin Microbiol Antimicrob. 2017;16:14. https://doi.org/10.1186/s12941-017-0190-4

9. Goussard P, Rabie H, Morrison J, Schubert PT. Superinfection with *Mycobacteria goodii* in a young infant with exogenous lipoid pneumonia. Pediatr Pulmonol. 2019;54:1345–7. https://doi.org/10.1002/ppul.24355

10. Hougas JE III, Bruneteau RJ, Varman M. *Mycobacterium goodii* infection of skin graft in an immunocompetent child. Infect Dis Clin Pract. 2011;19:146–7. https://doi.org/10.1097/IPC.0b013e3182002df1

Address for correspondence: Christopher Ouellette, Division of Infectious Diseases and Host Defense Program, Nationwide Children's Hospital, 700 Children's Dr, Rm C5C-J5432, Columbus, OH 43205, USA; email: christopher.ouellette@nationwidechildrens.org

Sporotrichosis Cases in Commercial Insurance Data, United States, 2012–2018

Kaitlin Benedict, Brendan R. Jackson

Author affiliation: Centers for Disease Control and Prevention, Atlanta, Georgia, USA

The geographic distribution of sporotrichosis in the United States is largely unknown. In a large commercial health insurance database, sporotrichosis was rare but most frequently occurred in southern and south-central states. Knowledge about where sporotrichosis is most likely to occur is essential for increasing clinician awareness of this rare fungal disease.

Sporotrichosis is an infection caused by the fungus *Sporothrix*. The infection typically follows cutaneous inoculation and involves the skin, subcutaneous tissue, and lymph nodes; pulmonary or disseminated disease occurs less frequently and usually affects immunocompromised persons (*1*). *Sporothrix* exists nearly worldwide in soil and decaying plant matter, but many unanswered questions remain about its precise ecologic niche (*2*). In the United States, its geographic distribution is poorly understood. Knowledge about where sporotrichosis is most likely to occur can help healthcare providers recognize and treat it earlier and help public health officials focus prevention messages.

We used the MarketScan Research Databases (IBM, https://www.ibm.com) to examine the geographic distribution of sporotrichosis in the United States. These databases comprise health insurance claims data from outpatient visits, prescriptions, and hospitalizations for employees, dependents, and retirees throughout the United States. In 2018, the databases contained records for ≈27 million persons. MarketScan data are fully de-identified; thus, the Centers for Disease Control and Prevention institutional review board did not need to approve this study.

To query the database, we used Treatment Pathways (IBM), a web-based platform, that comprises data from persons with health insurance plans that contributed prescription drug information to the MarketScan databases. We used data from February 1, 2012–December 31, 2018, to identify sporotrichosis patients using code 117.1 from the International Classification of Diseases (ICD), Ninth Revision, Clinical Modification and code B42 from the ICD, 10th Revision, Clinical Modification (ICD-10-CM). We used the primary beneficiary's state of residence to calculate average annual state-specific rates per 1 million MarketScan enrollees. We evaluated underlying conditions on or in the month before sporotrichosis diagnosis, demographic features, and type of sporotrichosis.

Of ≈76 million unique patients during 2012–2018, 1,322 had a sporotrichosis diagnosis code. For 1,236 (93.5%) of those, information was available about state of residence. The average annual rate of sporotrichosis cases per 1 million enrollees was highest in Oklahoma (6.1), Michigan (3.9), Kansas (3.5), and Kentucky (3.5) (Figure). Nationwide, the average annual rate was 2.0 cases/1 million enrollees.

For the 1,252 patients continuously enrolled during the month before their diagnosis, median age was 54 years; most (62%) patients were female (Table). The most common underlying conditions we evaluated were diabetes (7%), immune-mediated inflammatory disease (3%), and chronic obstructive pulmonary

disease (2%). Among 514 patients with sporotrichosis ICD-10-CM codes, specific types included lymphocutaneous in 13% and unspecified forms in 69%. Thirty-seven (3%) patients were hospitalized at diagnosis.

Although sporotrichosis occurred rarely in this large sample of privately insured patients, it was most common in the southern and south-central United States. The US geographic distribution of sporotrichosis has not been well described since the 1940s, when most cases were observed in the Mississippi River basin, with the highest frequencies in North Dakota, Nebraska, Wisconsin, Kansas, and Missouri (3). Reasons for the low rates we found in North Dakota and Wisconsin and the high rates in Michigan are unknown. Historically, Wisconsin-grown sphagnum moss has been the most common source of sporotrichosis outbreaks. At least 8 published outbreaks implicated Wisconsin moss shipped to other states for use in topiaries or packing material for tree seedlings (4,5). Since the late 1990s, sporotrichosis outbreaks appeared absent from published literature (4). Industry changes in harvesting sources or processing methods might play a role in the absence of outbreaks (5). Public health officials might not detect or investigate these outbreaks, as no routine surveillance for sporotrichosis exists. Our observation of higher sporotrichosis rates in Oklahoma and Kansas is consistent with past outbreaks linked to contaminated hay in those states (6–8).

In our analysis, sporotrichosis more frequently affected older women. These results possibly reflected differences in care-seeking behavior or exposures.

Underlying conditions were uncommon, suggesting that most cases occurred in previously healthy persons. This finding was consistent with lymphocutaneous disease resulting from traumatic inoculation.

Our findings are subject to several limitations. The primary limitation was that patients' states of residence might not represent the exposure location or the original environmental source of *Sporothrix*. Undetected cases and potential case misclassification are inherent limitations of administrative data. Diagnosis codes might substantially underestimate the true number of cases because affected persons might not seek care for self-limiting sporotrichosis. In addition, sporotrichosis might not have been correctly diagnosed or coded. Furthermore, administrative data often lack detail (i.e., differentiating between different sporotrichosis forms is not possible in ICD's Ninth Revision, Clinical Modification, and was not frequently used in ICD-10-CM). However, MarketScan is one of the few data sources large enough to provide a sufficient number of sporotrichosis cases to analyze at a subregional level.

Knowledge about where sporotrichosis is most likely to occur is essential for increasing clinician awareness of this rare disease. Increased awareness might lead to faster diagnosis and treatment with antifungal medication, which most sporotrichosis patients need (1). Understanding the distribution of sporotrichosis is also essential for understanding emerging sources of infection. Parts of Latin America are experiencing a large and growing epidemic of severe sporotrichosis caused by cat-transmitted
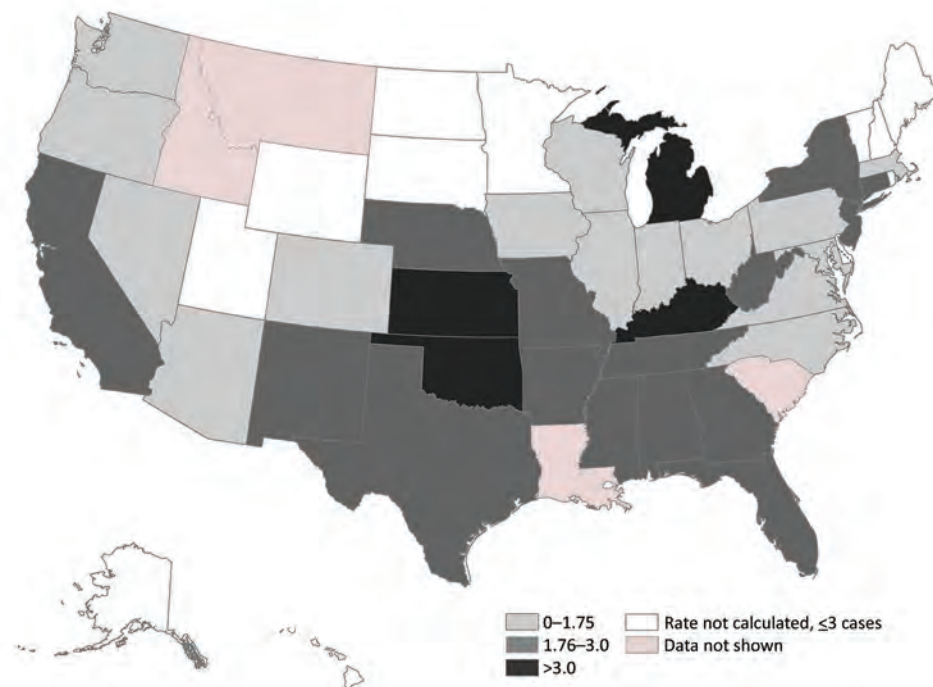

Figure. Average annual sporotrichosis rate per 1 million MarketScan enrollees, United States, 2012–2018. MarketScan (IBM, https://www.ibm.com) data are a subset of privately insured persons in the United States and are not necessarily representative of persons with other types of health insurance or of persons without insurance. To avoid potentially unreliable estimates, the rates for states with ≤3 cases were not calculated. MarketScan does not permit state-level analyses for certain states.

0–1.75   Rate not calculated, ≤3 cases
1.76–3.0 Data not shown
>3.0

Table. Characteristics of 1,252 patients with sporotrichosis, United States, 2012–2018*

Characteristic	No. (%)
Age group, y†	
0–17	46 (4)
18–34	153 (12)
35–44	154 (12)
45–54	305 (24)
55–64	402 (32)
≥65	192 (15)
Sex	
F	774 (62)
M	478 (38)
Residence in a rural area	184 (15)
Type of sporotrichosis	
Lymphocutaneous‡	68 (13)
Pulmonary§	27 (5)
Other forms¶	71 (14)
Unspecified#	357 (69)
Underlying conditions on or in the month before sporotrichosis diagnosis	
Alcohol related disorders**	9 (0.7)
Immune-mediated inflammatory disease††	39 (3)
Chronic obstructive pulmonary disease‡‡	26 (2)
Diabetes§§	90 (7)
HIV disease¶¶	5 (0.4)
Solid organ or stem cell transplant##	5 (0.4)
Hematologic malignancy***	7 (0.6)

*Diagnosis codes for sporotrichosis are as follows: ICD-9-CM code 117.1 and ICD-10-CM B42. ICD-9-CM, International Classification of Diseases, Ninth Revision, Clinical Modification; ICD-10-CM, International Classification of Diseases, 10th Revision, Clinical Modification.
†Median age 54 y (range 0–93 y).
‡ICD-10-CM code B42.1.
§ICD-10-CM code B42.0.
¶ICD-10-CM codes B42.7, B42.81, B42.82, B42.89.
#ICD-10-CM code B42.9.
**ICD-9-CM codes 291, 303, 305.0, 571.0–571.3; ICD-10-CM codes F10, K70.
††ICD-9-CM codes 555, 556, 696.0, 696.1, 696.8, 714.0, 714.2; ICD-10-CM codes K50, K51, L40, M023, M05, M06, M08, M33, M352, M45.
‡‡ICD-9-CM codes 490–492, 494, 496; ICD-10-CM codes J41–J44.
§§ICD-9-CM codes 249–250; ICD-10 codes E08–E11.
¶¶ICD-9-CM code 042; ICD-10-CM code B20.
##ICD-9-CM codes V42 (excluding V42.3–V42.5), 996.8; ICD-10-CM codes T86, Z94 (excluding Z94.5– Z94.7).
***ICD-9-CM codes 200–208; ICD-10-CM codes C81–C86, C88, C90–C96.

S. brasiliensis (*9*). This emerging infection provides further evidence of the need for ongoing monitoring.

Acknowledgments

About the Author

Ms. Benedict is an epidemiologist in the Mycotic Diseases Branch, Division of Foodborne, Waterborne, and Environmental Diseases, National Center for Emerging and Zoonotic Infectious Diseases, CDC. Her research interests include the epidemiology and prevention of fungal infections.

References

1. Kauffman CA, Bustamante B, Chapman SW, Pappas PG; Infectious Diseases Society of America. Clinical practice guidelines for the management of sporotrichosis: 2007 update by the Infectious Diseases Society of America. Clin Infect Dis. 2007;45:1255–65. https://doi.org/10.1086/522765
2. Chakrabarti A, Bonifaz A, Gutierrez-Galhardo MC, Mochizuki T, Li S. Global epidemiology of sporotrichosis. Med Mycol. 2015;53:3–14. https://doi.org/10.1093/mmy/myu062
3. Gastineau F, Spolyar L, Haynes E. Sporotrichosis: report of six cases among florists. J Am Med Assoc. 1941;117:1074–7. https://doi.org/10.1001/jama.1941.02820390016005
4. Hajjeh R, McDonnell S, Reef S, Licitra C, Hankins M, Toth B, et al. Outbreak of sporotrichosis among tree nursery workers. J Infect Dis. 1997;176:499–504. https://doi.org/10.1086/514070
5. Coles FB, Schuchat A, Hibbs JR, Kondracki SF, Salkin IF, Dixon DM, et al. A multistate outbreak of sporotrichosis associated with sphagnum moss. Am J Epidemiol. 1992;136:475–87. https://doi.org/10.1093/oxfordjournals.aje.a116521
6. Dooley DP, Bostic PS, Beckius ML. Spook house sporotrichosis. A point-source outbreak of sporotrichosis associated with hay bale props in a Halloween haunted-house. Arch Intern Med. 1997;157:1885–7. https://doi.org/10.1001/archinte.1997.00440370135014
7. Centers for Disease Control (CDC). Sporotrichosis among hay-mulching workers—Oklahoma, New Mexico. MMWR Morb Mortal Wkly Rep. 1984;33:682–3.
8. Dahl BA, Silberfarb PM, Sarosi GA, Weeks RJ, Tosh FE. Sporotrichosis in children. Report of an epidemic. JAMA. 1971;215:1980–2. https://doi.org/10.1001/jama.1971.03180250072022
9. Gremião IDF, Oliveira MME, Monteiro de Miranda LH, Saraiva Freitas DF, Pereira SA. Geographic expansion of sporotrichosis, Brazil. Emerg Infect Dis. 2020;26:621–4. https://doi.org/10.3201/eid2603.190803

Address for correspondence: Kaitlin Benedict, Centers for Disease Control and Prevention, 1600 Clifton Rd NE, Mailstop H24-9, Atlanta, GA 30329-4027, USA; email: jsy8@cdc.gov

Sociodemographic Predictors of SARS-CoV-2 Infection in Obstetric Patients, Georgia, USA

Naima T. Joseph, Kaitlyn K. Stanhope,
Martina L. Badell, John P. Horton, Sheree L. Boulet,
Denise J. Jamieson

Author affiliation: Emory University School of Medicine, Atlanta,
Georgia, USA

We conducted a cohort study to determine sociodemographic risk factors for severe acute respiratory syndrome coronavirus 2 infection among obstetric patients in 2 urban hospitals in Atlanta, Georgia, USA. Prevalence of infection was highest among women who were Hispanic, were uninsured, or lived in high-density neighborhoods.

Data from New York, New York, USA, have high-lighted the disproportionate burden of coronavirus disease (COVID-19) in minority and low socioeconomic status communities in the United States (1), yet data are lacking from southeastern states, which are home to a large share of the nation's racial and ethnic minority populations (2,3). The information is imperative in states like Georgia, which has average of 3,000–4,000 new cases daily and an urgent need for improved public health mitigation and containment strategies (4). The objective of this study was to determine associated sociodemographic and neighborhood risk factors for infection in an obstetric cohort undergoing testing for severe acute respiratory syndrome coronavirus 2 (SARS-CoV-2) in 2 urban hospitals in Atlanta, Georgia. Emory University School of Medicine Institutional Review Board and Grady Memorial Hospital Research Oversight Committee approved the study.

Universal testing for SARS-CoV-2 was initiated on all parturients admitted to labor and delivery at Grady Memorial Hospital, a safety-net hospital in Atlanta, starting on April 20, 2020, and at Emory University Hospital Midtown, an academic hospital in Atlanta, starting on April 24. Both hospitals serve a diverse, predominantly minority population; the safety-net hospital captures a larger proportion of uninsured and Medicaid patients (5). The safety-net hospital performs ≈2,500 and the academic hospital ≈5,000 deliveries annually. We abstracted test results, age, race, and ZIP code from electronic medical records and validated the data for all deliveries at both hospitals through July 29, 2020. Patient residential ZIP code was linked with data from the US Census Bureau to estimate median household income, proportion of households below federal poverty limit, use of public transit to travel to work, average household size, proportion of crowded households (>1 person per room), population density per square mile, neighborhood deprivation index, and proportion minority (nonwhite) residents (2). Data on neighborhood characteristics were derived from American Community Survey 5-year estimates for 2014–2018. Characteristics were calculated at the census tract level and linked to patient resident address using a validated ZIP code to tract crosswalk (6). To calculate the neighborhood deprivation index, we conducted principal components analysis using data for all census tracts in Georgia on 8 sociodemographic indicators, framed around domains of income, education, employment, and housing quality, producing a summary score ranging from –1.85 to 3.87, centered at 0; higher values indicated higher deprivation or more disadvantage.

We examined distributions of sociodemographic (age, race/ethnicity, and insurance status) and neighborhood characteristics by delivery hospital; we then combined data from both institutions to calculate prevalence rates and 95% CIs. For prevalence calculations, we dichotomized median income, proportion nonwhite residents, proportion below federal poverty limit, use of public transit, household crowding, neighborhood density, and neighborhood deprivation index by <50th percentile and ≥50th percentile. We performed data analysis using R (https://www.r-project.org); p values <0.05 were considered statistically significant.

We captured data on 1,882 women after delivery who had available test results, out of a total of 2,196 deliveries (Table; Appendix Figure, https://wwwnc.cdc.gov/EID/article/26/11/20-3091-App1.pdf). Overall SARS-COV-2 infection rate was 4.1% (77/1,882); prevalence was higher at the safety net hospital (9.4%, 58/616) than at the academic hospital (1.5%, 19/1,266). The study population was predominantly non-Hispanic Black (81.1%, 1,526/1,882) and publicly insured (43.9%, 826/1,882).

The prevalence of SARS-CoV-2 was highest among women who were Hispanic (15.8%, 95% CI 9.8–21.9; p<0.001) or uninsured (10.1%, 95% CI 5.5–14.6; p<0.001). Prevalence was also higher for women living in census tracts with smaller average household size (5.2%, 95% CI 3.8–6.6. vs. 3.0%, 95% CI 1.9–4.1; p = 0.02), increased neighborhood density (5.1%, 95% CI 3.7–6.5, vs. 3.1%, 95% CI 2.0–4.2; p = 0.03). We observed non–statistically significant increases in prevalence in census tracts with lower average household income, increased proportion of households below the federal poverty limit, and more neighborhood deprivation.

Table. Sociodemographic and neighborhood characteristics associated with increased prevalence of severe acute respiratory syndrome coronavirus 2 infection in laboring women, Georgia, USA*

Demographics	No. patients, N = 1,882	Total tested positive	Prevalence, % (95% CI)†	p value
Patient				
Age, y				0.34
<20	108	7	6.5 (1.8–11.12)	
20–35	1,393	57	4.1 (3.1–5.1)	
>35	381	13	3.4 (1.6–5.2)	
Race/ethnicity				<0.001
Non-Hispanic Black	1,353	52	3.8 (2.8–4.9)	
Non-Hispanic White	226	0	0	
Hispanic	139	22	15.8 (9.8–21.9)	
Asian/other	164	3	1.8 (−0.2 to 3.9)	
Insurance type				<0.001
Commercial	698	11	1.6 (0.7–2.5)	
Medicaid/Medicare	1,015	49	4.8 (3.5–6.1)	
Uninsured	169	17	10.1 (5.5–14.6)	
Neighborhood†				
Median household income				0.06
Lower average income	934	47	5.0 (3.6–6.4)	
Higher average income	939	30	3.2 (2.1–4.3)	
Below federal poverty limit				0.20
Lower poverty	924	32	3.5 (2.3–4.6)	
Higher poverty	949	45	4.7 (3.4–6.1)	
Use of public transit				0.25
Less transit use	950	34	3.6 (2.4–4.8)	
More transit use	923	43	4.7 (3.3–6.0)	
Proportion non-White				0.73
Lower percent minority	944	37	3.9 (2.7–5.2)	
Greater percent minority	929	40	4.3 (3.0–5.6)	
Household crowding				0.02
Small household size	944	49	5.2 (3.8–6.6)	
Large household size	929	28	3.0 (1.9–4.1)	
Neighborhood density				0.03
Less dense	911	28	3.1 (2.0–4.2)	
More dense	958	49	5.1 (3.7–6.5)	
Neighborhood deprivation index				0.64
Less deprived	935	36	3.9 (2.6–5.1)	
More deprived	938	41	4.4 (3.1–5.7)	

*Lower/less/small categories indicate <50th percentile; higher/more/large categories indicate ≥50th percentile. IQR, interquartile range; NDI, neighborhood deprivation index; Pr., proportion.
†Prevalence is for entire cohort. Nine women provided out-of-state zip codes and were excluded from the neighborhood analysis; all 9 tested negative.

This study leveraged a universal SARS-COV-2 testing program in an obstetric cohort to determine sociodemographic and neighborhood risk factors for infection. Infection was significantly associated with Hispanic ethnicity, uninsured status, high neighborhood density. The counterintuitive findings for household size may be due to chance or the narrow range of average household size across included neighborhoods (1.5–3.8 persons/household) (*1*).

This study has several limitations, including retrospective data collection and limited generalizability. However, its strengths include reporting of rates during a period of universal testing in an area outside of New York, and the use of census data to approximate neighborhood factors associated with increased risk for infection.

These data suggest that concentrated socioeconomic and neighborhood disadvantage, such as race/ethnicity, uninsured status, and neighborhood density, account for some of the disparate burden of COVID-19 illness in pregnant patients, a unique population at increased risk for perinatal illness (*7*). Research that considers specific features of neighborhood is needed to inform community-targeted mitigation strategies if viral containment is to be achieved.

About the Author

Dr. Joseph is a clinical fellow in the Division of Maternal Fetal Medicine in Department of Gynecology and Obstetrics at Emory University School of Medicine.

Her current research investigates the impact of Social Determinants of Health needs and interventions on severe maternal morbidity and maternal mortality in an attempt to improve parity in maternal/neonatal health outcomes.

References

1. Emeruwa UN, Ona S, Shaman JL, Turitz A, Wright JD, Gyamfi-Bannerman C, et al. Associations between built environment, neighborhood socioeconomic status, and SARS-CoV-2 infection among pregnant women in New York City. JAMA. 2020;324:390–392 https://doi.org/10.1001/jama.2020.11370
2. United States Census Bureau. American community survey, 2012–2016. [cited 2020 May 23]. https://www.census.gov/programs-surveys/acs/
3. Moore JT, Ricaldi JN, Rose CE, Fuld J, Parise M, Kanget GJ et al. Disparities in incidence of COVID-19 among underrepresented racial/ethnic groups in counties identified as hotspots during June 5–18, 2020 — 22 states, February–June 2020. MMWR Morb Mortal Wkly Rep. https://www.cdc.gov/mmwr/volumes/69/wr/mm6933e1.htm
4. Georgia Department of Public Health. COVID-19 daily status report. 2020 [cited 2020 May 23]. https://dph.georgia.gov/covid-19-daily-status-report
5. Jamieson DJ, Haddad LB. What obstetrician-gynecologists should know about population health. Obstet Gynecol.2018;131:1145–52. https://doi.org/10.1097/AOG.0000000000002638
6. Wilson R, Din A. Understanding and enhancing the U.S. Department of Housing and Urban Development's ZIP code crosswalk files. Cityscape: J Policy Dev Res. 2018;20:277–94 [cited 2020 Sep 23]. https://www.huduser.gov/portal/periodicals/cityscpe/vol20num2/ch16.pdf
7. Ellington S, Strid P, Tong VT, Woodworth K, Galang RR, Zambrano LD, et al. Characteristics of women of reproductive age with laboratory-confirmed SARS-CoV-2 infection by pregnancy status—United States, January 22–June 7, 2020. MMWR Morb Mortal Wkly Rep. 2020;69:769–75. https://doi.org/10.15585/mmwr.mm6925a1

Address for correspondence: Naima T. Joseph, Department of Gynecology and Obstetrics, Emory University School of Medicine, 69 Jesse Hill Jr. Dr SE, 4th Fl, Glenn Building, Atlanta, GA 30303, USA; email: ntjose2@emory.edu

COMMENT LETTERS

Nocardia ignorata Infection in Heart Transplant Patient

Victoria A. Muggia, Yoram A. Puius

Author affiliations: Albert Einstein College of Medicine, Bronx, NY, USA; Montefiore Medical Center, Bronx

To the Editor: We read with interest the recent description of pulmonary *Nocardia ignorata* infection (*1*). We report a similar infection in an orthotopic heart transplant recipient, which likely began as a pulmonary infection with dissemination to soft tissue, without known exposure. Risk factors included tacrolimus, steroids, older age, and posttransplant intensive care unit admission (*2*).

The patient was a 66-year-old African American man with a history of ischemic cardiomyopathy. After implantation of a left ventricular assist device, infectious complications included *Enterococcus faecalis* device infection and extended spectrum β-lactamase–producing (ESBL) *Klebsiella* urosepsis. The course after left ventricular assist device explantation and orthotopic heart transplant was complicated by tamponade requiring a pericardial window and an ESBL *Klebsiella* urinary tract infection treated with meropenem. Because of leukopenia, *Pneumocystis* prophylaxis was changed from trimethoprim/sulfamethoxazole to atovaquone 2 weeks posttransplant. ESBL *Klebsiella* bacteremia recurred 6 weeks later, again treated with meropenem.

The patient returned 6 months posttransplant with 10 days of cough and dyspnea. Chest computed tomography demonstrated bilateral nodules with cavitation, bronchiectasis, and spiculation. We initially treated the patient with meropenem and doxycycline. Results from severe acute respiratory syndrome coronavirus 2 swab test, respiratory pathogen panel, fungal studies, and sputum culture were nondiagnostic. We obtained no additional pulmonary samples.

Due to severe left calf pain, venous duplex was performed, revealing a nonvascular mass. The patient reported no trauma, soil contact, or recent travel. The abscess was aspirated, demonstrating branching gram-positive beaded rods. The isolate was identified by a reference laboratory (Mycobacteria and Nocardia Laboratory, University of Texas Health Center at Tyler, Tyler, TX, USA) by partial 16S rRNA sequencing as a 99.51% match with *Nocardia ignorata*, with susceptibilities identical to the isolate in Rahdar et al. (*1*). Brain magnetic resonance imaging results were unremarkable. The patient's respiratory status and leg pain quickly

improved and he was discharged on long-term trimethoprim/sulfamethoxazole and doxycycline. Because of renal insufficiency, trimethoprim/sulfamethoxazole was switched to moxifloxacin after 2 weeks. Chest radiograph results were improving 3 months later.

References

1. Rahdar HA, Gharabaghi MA, Bahador A, Shahraki-Zahedani S, Karami-Zarandi M, Mahmoudi S, et al. Pulmonary *Nocardia ignorata* infection in gardener, Iran, 2017. Emerg Infect Dis. 2020;26:610–1. https://doi.org/10.3201/eid2603.180725
2. Coussement J, Lebeaux D, van Delden C, Guillot H, Freund R, Marbus S, et al.; European Study Group for Nocardia in Solid Organ Transplantation. *Nocardia* infection in solid organ transplant recipients: a multicenter European case-control study. Clin Infect Dis. 2016;63:338–45. https://doi.org/10.1093/cid/ciw241

Address for correspondence: Yoram A. Puius, Division of Infectious Diseases, Montefiore Medical Center, 111 East 210th Street, Bronx, NY 10467, USA; e-mail: ypuius@montefiore.org

etymologia

Nocardia [no-kahr′ e-əm]

Christoffel J. Opperman

The genus *Nocardia* is named in honor of Edmond Isidore Etienne Nocard (1850–1903), a French veterinarian and microbiologist who discovered the bacteria in 1888 from a bovine farcy case. He named this filamentous, branching bacteria *Streptothrix farcinica* (Greek *streptós*- "twisted" and *thrix* "hair"). Farcy (old French *farcin*), is a form of cutaneous glanders, characterized by superficial lymph node swelling and ulcerating nodule formation under the skin (Late Latin *farcīminum* "glanders," from Latin *farcīmen* "a sausage," from *farcīre* "to stuff").

One year later, Trevisan characterized and termed the bacteria *Nocardia farcinica*, creating the genus *Nocardia*. In 1890, Eppinger isolated a similar organism from a brain abscess and called it *Cladothrix asteroides* (Greek *kládos*- "branch" and *-thrix* "hair") because of its star-shaped colonies (Greek *asteroeidēs* "starlike"). Blanchard renamed the organism *Nocardia asteroides* in 1896. Additional taxonomic work in 1962 resulted in *Nocardia asteroides* replacing *Nocardia farcinica* as the type species for the genus *Nocardia*.
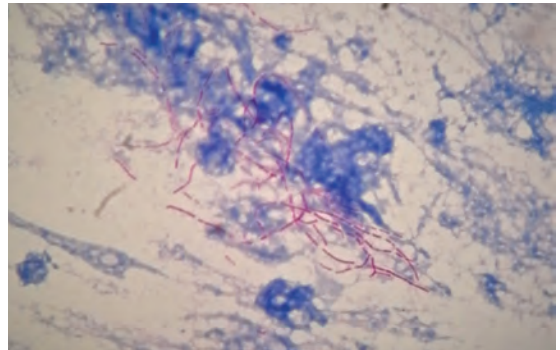

Figure. Twisted hair bacteria (*Nocardia* spp.) described by Edmond Nocard, from a bronchial alveolar lavage sample. Nocardiosis is an opportunistic infection, commonly associated with pulmonary disease. *Nocardia* are partially acid-fast, filamentous, branching bacilli (modified Kinyoun acid-fast stain using weak acid [0.5% sulfuric acid] for decolorization and methylene blue counterstain, original magnification x1,000.) Photograph courtesy of the author.

Sources

1. Blanchard R. 1896. Plant pests excluding bacteria [in French]. In: Bouchard C, editor. Treatise of general pathology. Volume II. Paris: Mason. p. 811–926.
2. Gordon RE, Mihm JM. The type species of the genus *Nocardia*. J Gen Microbiol. 1962;27:1–10. https://doi.org/10.1099/00221287-27-1-1
3. Nocard E. Note on the disease of oxen from Guadeloupe known as farcin [in French]. Ann Inst Pasteur (Paris). 1888;2:293–302.
4. Saubolle MA, Sussland D. Nocardiosis: review of clinical and laboratory experience. J Clin Microbiol. 2003;41:4497–501. https://doi.org/10.1128/JCM.41.10.4497-4501.2003
5. Trevisan V. 1889. Genera and species of the batteries [in Italian]. Milan: Zanaboni and Gabuzzi; 1889.

Address for correspondence: Christoffel J. Opperman, National Health Laboratory Service, Department of Medical Microbiology, University of Cape Town and Groote Schuur Hospital, Cape Town, South Africa.; email: stefanopperman1@gmail.com

COVID-19 Outbreak Associated with Air Conditioning in Restaurant, Guangzhou, China, 2020

Ana M. Rule

Author affiliation: Johns Hopkins Bloomberg School of Public Health, Baltimore, Maryland, USA

To the Editor: In the research letter by J. Lu et al. (*1*), the authors claim that "The air outlet and the return air inlet for the central air conditioner were located above table C (Figure, panel B)." This sentence does not describe the actual layout depicted in the Figure, in which the air conditioner is located by table C and the exhaust fan is between tables B and D.

Furthermore, the authors do not provide evidence of why "Virus transmission in this outbreak cannot be explained by droplet transmission alone." Their discussion does not mention the possibility that persons move around and may have been infected by touching surfaces, going to the restroom at the same time, or engaging in other close contact.

It is hard to understand how the authors conclude that "… strong airflow from the air conditioner could have propagated droplets from table C to table A, then to table B, and then back to table C." According to the figure, air flows from table C to the exhaust fan (tables B–D). The authors do not provide evidence that the exhaust fan was not working; they ignored its presence. A simple measurement of air flow would answer this question.

The fact that "… none of the staff or other diners in restaurant X were infected" is another indication that the air conditioner was probably working. Also puzzling is the authors' conclusion that "… the smear samples from the air conditioner were all nucleotide negative." This finding is less consistent with aerosol transmission."

The authors' conclusion that "… in this outbreak, droplet transmission was prompted by air-conditioned ventilation" is not supported by the data provided. They further conclude that "The key factor for infection was the direction of the airflow" but do not follow the airflow to the exhaust fan.

Reference

1. Lu J, Gu J, Li K, Xu C, Su W, Lai Z, et al. COVID-19 outbreak associated with air conditioning in restaurant, Guangzhou, China, 2020. Emerg Infect Dis. 2020;26:1628–31. https://doi.org/10.3201/eid2607.200764

Address for correspondence: Ana M. Rule, Johns Hopkins Bloomberg School of Public Health Department of Environmental Health and Engineering, 615 N. Wolfe St. E6614, Baltimore, MD 21205; USA; email: arule1@jhu.edu

Jianyun Lu, Zhicong Yang

Author affiliation: Guangzhou Center for Disease Control and Prevention, Guangzhou, China

In Response: We thank Prof. Rule (*1*) for her comments on our letter (*2*). We welcome the opportunity to offer additional information on several of the points made.

We wish to explain that although she stated that, "'The air outlet and the return air inlet for the central air conditioner were located above table C (Figure, panel B)' does not describe the actual layout depicted in the Figure, in which the air conditioner is located by table C and the exhaust fan is between tables B and D" (*1*). In fact, the air outlet and the return air inlet for the central air conditioner were located above table C (Figure 1). The central air conditioner is constructed in 2 parts: air outlet and air inlet, indicating no discrepancy between the text and the figure.

We agree that virus transmission in this outbreak could be explained by droplet transmission and the possibility that persons move around, touch surfaces, go to the restroom, or engage in other close contact. We con-

Figure 1. Inlet and outlet of air conditioner described in study of COVID-19 outbreak associated with air conditioning in restaurant, Guangzhou, China, 2020 (*2*).
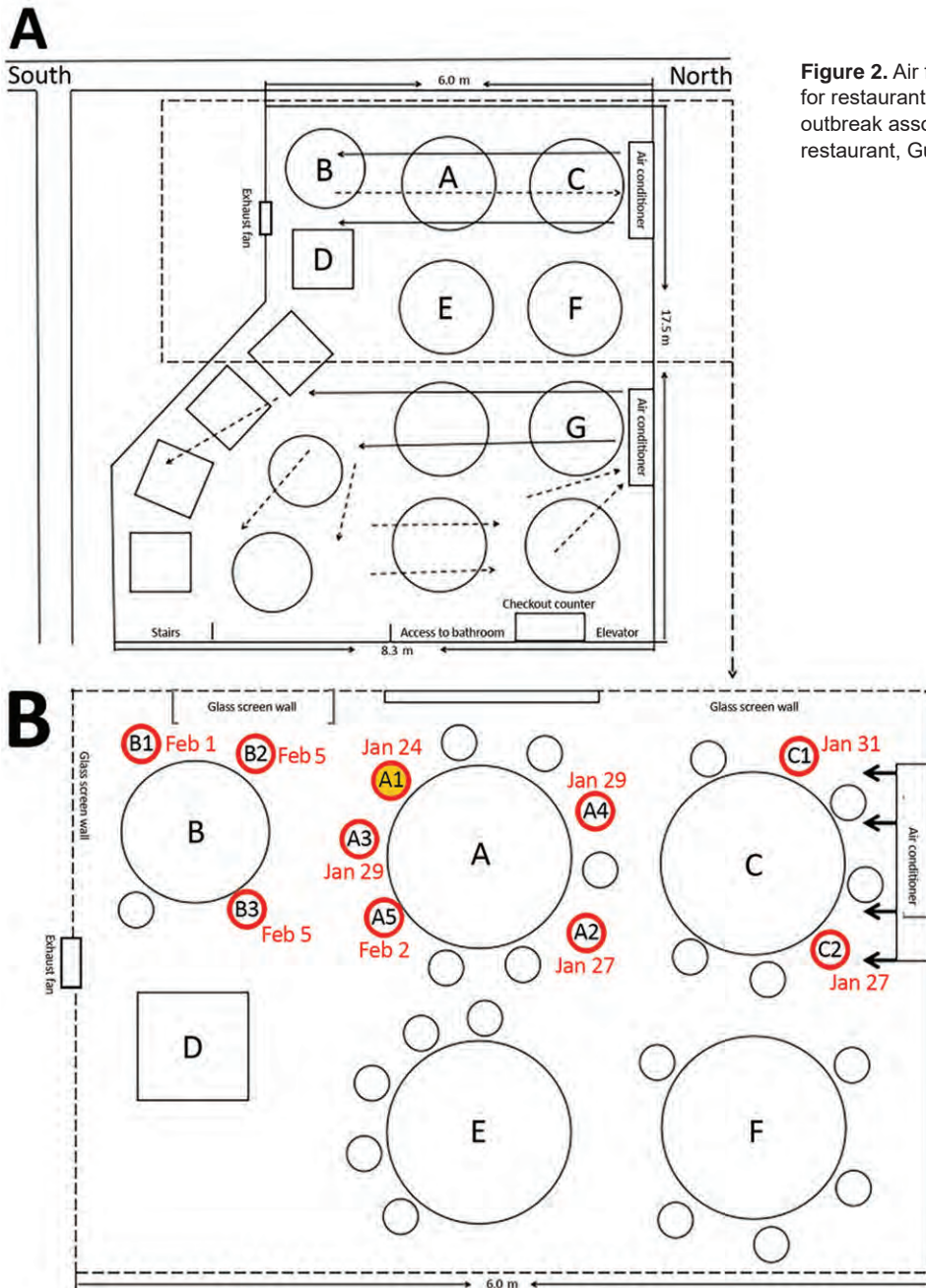
Figure 2. Air flow (A) and seating diagram (B) for restaurant described in study of COVID-19 outbreak associated with air conditioning in restaurant, Guangzhou, China, 2020 (*2*).

sidered these scenarios but omitted their mention in the research letter. Instead, we reported what we considered to be the most likely scenario, which is that the droplet transmission was prompted by the air blown from right to left and then across tables C, A, and B successively. The air movement facilitated dispersion of droplets containing severe acute respiratory syndrome coronavirus 2 (SARS-COV-2) from patient A1 to the 3 patients at table B. After the air had passed over tables C, A, and B, patients C1 and C2 acquired the infection from droplets mixed with SARS-COV-2 as they returned to the air

inlet over table C. None of the 62 persons at the other 12 tables were infected, which suggests that the alternate scenarios (touching surfaces or going to the restroom at the same time) were less likely. Furthermore, some diners and waitresses also went to the restroom and were not infected. In addition, closed-circuit television tapes did not show that the patients in our study had gone to the restroom at the same time. The tapes showed that patient C1 walked in and out several times and passed table A on the way, which might be one of the reasons for the infection of patient C1.

We did not describe the exhaust fan in the text, but we drew an exhaust fan between tables B and D in the figure. To point out the exhaust fan, we drew it bigger than actual measurements, which were only 12 × 12 inches (305 mm × 305 mm); the fan was not strong enough to remove all air produced by the central air conditioner. After the initial publication, we revised the figure to show the appropriate size of the exhaust fan and added details about its size, emphasizing that the ventilation system was not well designed (Figure 2). The main air flow is discharged from the central air conditioning outlet and then returned to the air inlet. Because of the weak exhaust system, the ventilation in the restaurant was not good. We did not ignore the presence of the exhaust fan.

We conclude that the air conditioner prompted transmission of SARS-CoV-2; the customers in the airflow were at high risk for infection with SARS-CoV-2 in the poorly ventilated environment. Because the staff and other diners were not exposed to the airflow mixed with SARS-CoV-2 transmitted by patient A1, their risk for infection was lower.

We excluded the possibility of aerosol transmission (2). It has been reported that aerosols (<5 mm) can remain in the air and disperse long distances (>1 m) (3). The potential for aerosol transmission has been reported for severe acute respiratory syndrome coronavirus (4) and Middle East respiratory syndrome coronavirus (5,6). However, in our study, none of the 62 persons at the other 12 tables were infected. Moreover, the smear samples from the air conditioner were all negative by reverse transcription PCR.

We believe that the most likely scenario for SARS-CoV-2 transmission in the restaurant was droplet transmission prompted by the air conditioning, although other scenarios are possible. The exhaust fan was not strong enough to modify the ventilation; the main mode of air circulation was the central air conditioning outlet with air returned to the air conditioning inlet. Because of the weak exhaust system, ventilation in the restaurant was poor. We recommend that air handling systems be sufficiently powered and maintained.

References

1. Rule AM. COVID-19 outbreak associated with air conditioning in restaurant, Guangzhou, China, 2020. Emerg Infect Dis. 2020;26:xxx. https://doi.org/10.3201/eid2611.202948
2. Lu J, Gu J, Li K, Xu C, Su W, Lai Z, et al. COVID-19 outbreak associated with air conditioning in restaurant, Guangzhou, China, 2020. Emerg Infect Dis. 2020;26:1628–31. https://doi.org/10.3201/eid2607.200764
3. Fernstrom A, Goldblatt M. Aerobiology and its role in the transmission of infectious diseases. J Pathogens. 2013;2013:493960. https://doi.org/10.1155/2013/493960
4. Lee N, Hui D, Wu A, Chan P, Cameron P, Joynt GM, et al. A major outbreak of severe acute respiratory syndrome in Hong Kong. N Engl J Med. 2003;348:1986–94. https://doi.org/10.1056/NEJMoa030685
5. Kim SH, Chang SY, Sung M, Park JH, Bin Kim H, Lee H, et al. Extensive viable Middle East Respiratory Syndrome (MERS) coronavirus contamination in air and surrounding environment in MERS isolation wards. Clin Infect Dis. 2016;63:363–9. https://doi.org/10.1093/cid/ciw239
6. Tong ZD, Tang A, Li KF, Li P, Wang HL, Yi JP, et al. Potential presymptomatic transmission of SARS-CoV-2, Zhejiang Province, China, 2020. Emerg Infect Dis. 2020;26:1052–4. https://doi.org/10.3201/eid2605.200198

Address for correspondence: Zhicong Yang, Center for Disease Control and Prevention, Baiyun District, Jiahe St, Qide Rd No. 1, Guangzhou, Guangdong 510440, China; email: gdgzcdc@163.com

John William Waterhouse (1849–1917), *A Tale from The Decameron*, **1916.** Oil on canvas, 39.7 in x 62.5 in/101 cm x 159 cm. Lady Lever Art Gallery, National Museums Liverpool, Liverpool, UK.

Social Distancing and Artful Pandemic Survival

Terence Chorba

"Social distancing" is a relatively novel term, recently popularized in strategies for disrupting transmission of newly identified airborne pathogens, including influenza virus variants, Ebola virus, and coronaviruses. An American cultural anthropologist, Edward T. Hall, Jr., coined the term "social distance" in 1963 to describe a zone of space customarily adopted in many cultures to minimize visual, olfactory, auditory, and tactile stimulation when meeting strangers or mere acquaintances. A PubMed search by term indicates that social distancing as an infectious disease intervention first appeared in a 2005 article about strategies for containing an emerging influenza pandemic. However, awareness of distancing oneself from others as a prevention tool against infection dates to biblical times. Reference to removing persons with leprosy from the community was recorded in the Bible (Lev. 13:46, New Jerusalem Version) during the 6th–4th centuries BCE. Later, for both plague and smallpox, avoiding contact between diseased and healthy persons became a method for disrupting disease transmission. Beginning in the 14th century, Italian port cities began isolating ships and travelers suspected of carrying plague for periods of 30 days (*trentino*) and later for 40 days (*quarantino*), thus, the English term "quarantine."

History is replete with examples of artistic genius creatively flourishing in the face of an epidemic. Shakespeare took advantage of London's intermittent lockdowns in response to plague during 1603–1613 to

Author affiliation: Centers for Disease Control and Prevention, Atlanta, Georgia, USA

dedicate time to writing some of his greatest masterpieces; in 1605–1606 alone, when the Globe and other London theaters were closed, he completed *King Lear*, *Macbeth*, *Anthony and Cleopatra, and Timon of Athens*. Earlier, in the mid-1300s, Italian literature was graced with *The Decameron*, a narrative that contains many shorter stories. A humanist writer and poet, Giovanni Boccaccio started the work in 1347 at the beginning of the Black Death, the global epidemic of bubonic plague that peaked in Europe until 1351; he completed the work in 1353. The fictitious tale describes 10 young noble women and men who isolate themselves as a group in a secluded Tuscan villa just outside Florence. This exercise in social distancing is an effort to escape the plague that killed half the Florentine population. Daily, over the course of a fortnight, each group member takes a turn as the storyteller, telling a story that follows a specific theme. In all, *The Decameron* is composed of a hundred novellas, many stories within stories.

In *A Tale from The Decameron*, the painting on this month's cover, we see the group in a bucolic setting, devoid of any hint of the devastating plague in nearby Florence. The painting is in the collection of the Lady Lever Art Gallery in Liverpool, known for its Victorian paintings that include works of the Pre-Raphaelite Brotherhood. Pre-Raphaelites were a 19th-century group of English painters who revered medieval culture and the early Renaissance and were prolific in portraying realistic scenes of bygone cultures. *A Tale from The Decameron* was created in 1916 by a realist painter associated with the Pre-Raphaelites, John William Waterhouse (1849–1917). In the painting, Waterhouse depicts five of the young women seated comfortably on cushioned

ground, listening to a story being told by one of two young men seated above them on steps. The storyteller, in a red skullcap, is intently speaking, and across his lap lies a mandolin-type instrument that may have some role in the storytelling itself. In the background, two others are strolling together in the villa's ornate garden. Despite being gathered together, the group members are neither wearing facial masks nor practicing social distancing among themselves. A similar scene from *The Decameron* is portrayed in a painting by Raffaello Sorbi (1844–1931), which features a young woman storyteller (Figure); Sorbi, a contemporary of Waterhouse, was a Florentine realist painter, also popular in 19th-century Britain. In both paintings, the opulent surroundings and clothing show the circumstances of a wealthy emerging merchant class in Florence; their resources gave them access to such villas and distance from the urban squalor with its rodents, principally brown rats, which served as a reservoir for fleas that transmitted the epidemic's pathogen, *Yersinia pestis*.

Whether those living in rural villas rather than in urban settings were any less exposed to the ravages of the Black Death is unknown. However, the perception of the wealthy was that urban flight was a preventive alternative to living in crowded environments where the dead and dying were far more concentrated, where in Boccaccio's words, people were "*non come uomini ma quasi come bestie morieno*" [dying more like animals than like humans]. Such escape also served a therapeutic psychological purpose, restoring a vision of order, away from the horror and chaos of plague-ridden Florence. In the limited understanding of the 14th century, such escape warded off bad humors that would otherwise increase one's susceptibility to plague.

In the present pandemic circumstances, we can appreciate that the impacts of communicable diseases on social behavior are somewhat conflicting: increasing altruism and within-group cohesion but decreasing social interactions if there are associated risks for infection. Although much remains for study of combinations of social distancing measures, many observational studies from influenza pandemics have found positive effects of isolating sick persons; quarantining exposed persons; and implementing school and workplace closures, workplace measures to reduce disease transmission, and measures to reduce population density. Early plateauing and abrupt decrease of influenza reports have also been correlated temporally with social distancing efforts in response to SARS-CoV-2 infection.

Fortunately, respiratory spread of *Yersinia* bacteria, principally by coughing or vomiting, occurs only after the disease has progressed. For Boccaccio's characters, an appreciation of the concept of respiratory

Figure. Painting by Raffaello Sorbi (1844–1931), *Decamerone*, 1876. Public domain image. Private collection.

transmission of diseases was still a half a millennium away, so the listeners in his masterpiece are portrayed as comfortably sitting closely together without masks. Unfortunately, with the current spread of coronavirus disease via respiratory secretions, we cannot dispense with respiratory protection. However, as with past pandemics, lovers of art, music, and literature hope that necessary measures to avoid infection, including staying at home and engaging in self-isolation and social distancing, will again yield or inspire masterpieces that will enrich our culture and our world.

Bibliography

1. Alchon SA. A pest in the land: new world epidemics in a global perspective. Albuquerque (NM): University of New Mexico Press; 2003.
2. Chambers EK. William Shakespeare: a study of facts and problems, Vol. I. Oxford: Clarendon; 1930. p. 270–1.
3. Fenner F, Henderson DA, Arita I, Jezek Z, Ladnyi ID. Smallpox and its eradication. 1988 [cited 2020 Aug 31]. https://apps.who.int/iris/handle/10665/39485
4. Ferguson NM, Cummings DA, Cauchemez S, Fraser C, Riley S, Meeyai A, et al. Strategies for containing an emerging influenza pandemic in Southeast Asia. Nature. 2005;437:209–14. https://doi.org/10.1038/nature04017
5. Fong MW, Gao H, Wong JY, Xiao J, Shiu EYC, Ryu S, et al. Nonpharmaceutical measures for pandemic influenza in nonhealthcare settings—social distancing measures. Emerg Infect Dis. 2020;26:976–84. https://doi.org/10.3201/eid2605.190995
6. Gerlitt J. The development of quarantine. Ciba Found Symp. 1940;2:566–72.
7. Hall ET. A system for the notation of proxemic behavior. Am Anthropol. 1963;65:1003–6. https://doi.org/10.1525/aa.1963.65.5.02a00020
8. Olson G. Literature as recreation in the later Middle Ages. Ithaca (NY): Cornell University Press; 1986. p. 164–83.
9. Trippi PJ. J.W. Waterhouse. London: Phaidon Press; 2002.
10. Wong N-S, Leung C-C, Lee S-S. Abrupt subsidence of seasonal influenza after coronavirus disease outbreak, Hong Kong, China. Emerg Infect Dis. 2020;26:2753–55. https://doi.org/10.3201/eid2611.200861

Address for correspondence: Terence Chorba, Centers for Disease Control and Prevention, 1600 Clifton Rd NE, Mailstop US 12-4, Atlanta, GA 30329-4027, USA; email: tlc2@cdc.gov

EMERGING INFECTIOUS DISEASES®

Upcoming Issue

Complete list of articles in the December issue at http://www.cdc.gov/eid/upcoming.htm

Earning CME Credit

To obtain credit, you should first read the journal article. After reading the article, you should be able to answer the following, related, multiple-choice questions. To complete the questions (with a minimum 75% passing score) and earn continuing medical education (CME) credit, please go to http://www.medscape.org/journal/eid. Credit cannot be obtained for tests completed on paper, although you may use the worksheet below to keep a record of your answers.

You must be a registered user on http://www.medscape.org. If you are not registered on http://www.medscape.org, please click on the "Register" link on the right hand side of the website.

Only one answer is correct for each question. Once you successfully answer all post-test questions, you will be able to view and/or print your certificate. For questions regarding this activity, contact the accredited provider, CME@medscape.net. For technical assistance, contact CME@medscape.net. American Medical Association's Physician's Recognition Award (AMA PRA) credits are accepted in the US as evidence of participation in CME activities. For further information on this award, please go to https://www.ama-assn.org. The AMA has determined that physicians not licensed in the US who participate in this CME activity are eligible for AMA PRA Category 1 Credits™. Through agreements that the AMA has made with agencies in some countries, AMA PRA credit may be acceptable as evidence of participation in CME activities. If you are not licensed in the US, please complete the questions online, print the AMA PRA CME credit certificate, and present it to your national medical association for review.

Article Title

Phage-Mediated Immune Evasion and Transmission of Livestock-Associated Methicillin-Resistant *Staphylococcus aureus* in Humans

CME Questions

1. You are advising a public health department about the likelihood of livestock-associated methicillin-resistant *Staphylococcus aureus* (LA-MRSA) transmission. According to the whole-genome sequencing and epidemiologic study by Sieber and colleagues, which of the following statements about the impact of immune evasion cluster (IEC)- and *tarP*-harboring phages on household transmission of LA-MRSA in the North Denmark Region during 2004–2011 is correct?

A. *tarP*, but not IEC, facilitates household transmission of LA-MRSA CC398
B. The proportion of secondary cases was significantly higher in IEC-negative than in IEC-positive households
C. Secondary transmission occurred more often in IEC-positive than in IEC-negative households, but the difference was not statistically significant (80% vs 32%; p = 0.064)
D. *tarP*-204–positive vs *tarP*-negative households had significantly greater secondary transmission and proportion of secondary cases

2. According to the analysis by Sieber and colleagues of all Danish patients who had an episode of LA-MRSA infection during 2007–2018, which of the following statements about the association of IEC- and *tarP*-harboring phages in LA-MRSA in the North Denmark Region during 2004–2011 with spread in the general population is correct?

A. Horizontal acquisition of IEC in the human host was associated with increased household transmission of LA-MRSA CC398 and spillover into the community and healthcare settings

B. The findings suggest that IEC-positive LA-MRSA isolates have become self-sustainable in the general population
C. Proportion of IEC-positive isolates was highest in cases with direct livestock contact and lowest in cases with healthcare-onset (HO) or healthcare-associated community-onset (HACO) infection
D. The prevalence ratio of IEC-positive isolates among patients with CO and HO/HACO infections increased over time

3. According to the genetic and epidemiologic study by Sieber and colleagues, which of the following statements about clinical and public health implications of the effect of IEC- and *tarP*-harboring phages on household transmission of LA-MRSA in the North Denmark Region during 2004–2011, and of their association with spread into the general population, is correct?

A. The findings suggest that all LA-MRSA CC398 isolates have the same ability to acquire ΦSa3int phages
B. Acquisition of IEC by LA-MRSA CC398 rarely occurs through transfer of ΦSa3int phages from human *S aureus* donors circulating in the respective households
C. *TarP*-mediated protection against anti-wall teichoic acid (WTA) antibodies increased household transmission of LA-MRSA CC398
D. Changing *S aureus* genome evolution and host adaptability mandate ongoing human-animal surveillance to detect evolutionary and epidemiologic changes that may affect public health